UCLA
UCLA Electronic Theses and Dissertations

**Title**
Harnessing Heterocyclic Arynes & Amides as Synthetic Building Blocks

**Permalink**
https://escholarship.org/uc/item/6135d837

**Author**
Shah, Tejas K.

**Publication Date**
2016

Peer reviewed|Thesis/dissertation

eScholarship.org Powered by the California Digital Library
University of California

UNIVERSITY OF CALIFORNIA

Los Angeles

# Harnessing Heterocyclic Arynes & Amides as Synthetic Building Blocks

A dissertation submitted in partial satisfaction of the

requirements for the degree Doctor of Philosophy

in Chemistry

by

Tejas Shah

2016

© Copyright by

Tejas Shah

2016

ABSTRACT OF THE DISSERTATION

Harnessing Heterocyclic Arynes & Amides as Synthetic Building Blocks

by

Tejas Shah

Doctor of Philosophy in Chemistry

University of California, Los Angeles, 2016

Professor Neil Kamal Garg, Chair

This dissertation describes the study of two synthetic building blocks, heterocyclic arynes and amides, and their applications in synthetic organic chemistry. Heterocyclic arynes are highly reactive intermediates that act as electrophilic arene surrogates. In contrast, amides are tradionally considered to be robust functional groups. However, recently the acyl–nitrogen bond of amides have been activated under mild transition metal-catalysis to act as acyl electrophiles and form C–heteroatom and C–C bonds.

Chapter One reviews the field of heterocyclic arynes from a historial perspective with an emphasis on pyridyne and indolyne methodologies. Moreover, this chapter highlights the use of pyridynes, indolynes, and related strained intermediates in the synthesis of natural products.

Chapter Two describes the total syntheses of (–)-indolactam V and its C7-substituted natural product derivatives, (–)-pendolmycin, (–)-lyngbyatoxin A, and (–)-teleocidin A-2. The C4–N linkage is constructed with a distortion-controlled indolyne functionalization. The total

synthesis of (–)-indolactam V provides a platform for the divergent syntheses of the other three natural products via a palladium-catalyzed cross-coupling to functionalize C7 and introduce a quaternary center.

Chapter Three pertains to accessing two new oxacyclic strained intermediates, the 4,5-benzofuranyne and the 3,4-oxacyclohexyne. In situ trapping of these intermediates affords an array of heterocyclic scaffolds and the experimentally-determined ratio of regioisomers are consistent with predictions made using the distortion/interaction model. In addition, oxygen-containing strained intermediates were found to provide access to greater selectivities from trapping experiments compared to their corresponding nitrogen-containing counterparts.

Chapter Four illustrates the synthesis of six new indole-based conjugated trimers and their photophysical properties. These conjugated trimers are generated using highly reactive indolyne intermediates in the presence of a palladium catalyst. In addition, this reactivity could provide access to a variety of trimeric cores, which could have further applications in new materials.

Chapter Five depicts the activation of the carbon–nitrogen bond of amides under nickel catalysis and the utility of amides as electrophilic acyl cross-coupling partners. We first investigated the conversion of amides to esters, which is a challenging and underdeveloped transformation. Density functional theory calculations provide insight into the thermodynamics and catalytic cycle of the amide-to-ester transformation. This report provides a way to harness amides as synthons and has led to the further use of amides in the construction of carbon–heteroatom or carbon–carbon bonds under nickel-catalysis.

The dissertation of Tejas Shah is approved.

Miguel A. García-Garibay

Andrea M. Kasko

Neil Kamal Garg, Committee Chair

University of California, Los Angeles

2016

*"Be humble in everything you do…"*

*– Drew Calvo, circa 2007*

*For my parents and brother: Kapil, Taruna and Kayur Shah*

TABLE OF CONTENTS

ABSTRACT OF THE DISSERTATION ..... ii

COMMITTEE PAGE ..... iv

DEDICATION PAGE ..... v

TABLE OF CONTENTS ..... vi

LIST OF FIGURES ..... xii

LIST OF SCHEMES ..... xxv

LIST OF TABLES ..... xxvii

LIST OF ABBREVIATIONS ..... xxix

ACKNOWLEDGEMENTS ..... xxxiv

BIOGRAPHICAL SKETCH ..... xli

CHAPTER ONE: Pyridynes and Indolynes as Building Blocks for Functionalized Heterocycles and Natural Products ..... 1

1.1 Abstract ..... 1

1.2 Introduction and Historical Perspective ..... 1

1.3 Hetaryne Experimental Results ..... 5

1.3.1 Pyridyne Methodology ..... 6

1.3.2 Indolyne Methodology ..... 12

1.4 Use of Hetarynes in Total Synthesis ..... 17

1.5 Conclusions ..... 30

1.6 Notes and References ..... 30

CHAPTER TWO: Total Syntheses of Indolactam Alkaloids (–)-Indolactam V, (–)-Pendolmycin, (–)-Lyngbyatoxin A, and (–)-Teleocidin A-2 ..... 39

2.1 Abstract ..... 39

2.2 Introduction ..... 40

2.3 Results and Discussion ..... 43

2.3.1 Optimization of the Total Synthesis of Indolactam V (**2.1**) ..... 43

2.3.2 Cross-Coupling to Introduce the C7 $sp^2$–$sp^3$ Linkage and the Key Quaternary Carbon ..... 44

2.3.3 Total Synthesis of (–)-Pendolmycin (**2.2**) ..... 46

2.3.4 Total Synthesis of (–)-Lyngbyatoxin A (**2.3**) and (–)-Teleocidin A-2 (**2.4**) 48

2.4 Conclusion ..... 51

2.5 Experimental Section ..... 51

2.5.1 Materials and Methods ..... 51

2.5.2 Experimental Procedures ..... 53

2.5.2.1 Optimization of the Total Synthesis of Indolactam V (**2.1**) ..... 53

2.5.2.2 Cross-Coupling to Introduce the C7 $sp^2$–$sp^3$ Linkage ..... 61

2.5.2.3 Total Synthesis of (–)-Pendolmycin (**2.2**) ..... 63

2.5.2.4 Total Syntheses of (–)-Lyngbyatoxin A (**2.3**) and (–)-Teleocidin A-2 (**2.4**) ..... 68

2.6 Spectra Relevant to Chapter Two: ..... 79

2.7 Notes and References ..... 108

CHAPTER THREE: Expanding the Strained Alkyne Toolbox: Generation and Utility of Oxygen-Containing Strained Alkynes ..... 115

3.1 Abstract ..... 115

3.2 Introduction ..... 116

3.3 Results and Discussion ..... 118

3.3.1 Prediction of Regioselectivities Based on the Distortion / Interaction Model ..... 118

3.3.2 Synthesis of Silyl Triflate Precursors ..... 120

3.3.3 Generation & Trapping of 4,5-Benzofuranyne ..... 121

3.3.4 Generation & Trapping of 3,4-Oxacyclohexyne (**3.5**) ..... 124

3.3.5 Comparison of Regioselectivities for *N*- and *O*-Containing Strained Alkynes ..... 127

3.4 Conclusion ..... 129

3.5 Experimental Section ..... 130

3.5.1 Materials and Methods ..... 130

3.5.2 Experimental Procedures. ..... 131

3.5.2.1 Synthesis of 3,4-Benzofuranyne Precursor ..... 131

3.5.2.2 Synthesis of 3,4-Oxacyclohexyne Precursor ..... 134

3.5.2.3 4,5-Benzofuranyne Trapping Experiments ..... 135

3.5.2.4 Oxacyclohexyne Trapping Experiments ..... 148

3.5.3 Computational Methods. ..... 159

3.5.3.1 Cartesian Coordinates of Strained Alkynes ..... 159

3.5.3.2 Energies of Strained Alkynes ..... 160

3.6 Spectra Relevant to Chapter Three: ..... 161

3.7 Notes and References ..... 238

CHAPTER FOUR: A New Class of Conjugated Trimeric Scaffolds Accessible Using Indolyne Cyclotrimerizations ..... 245

4.1 Abstract ..... 245

4.2 Introduction ..... 246

4.3 Results and Discussion ..... 247

4.3.1 Optimization of 4,5-Indolyne Cyclotrimerization ..... 247

4.3.2 Cyclotrimerization of 5,6- and 6,7-Indolynes ..... 249

4.3.3 Photophysical Properties of Trimers ..... 250

4.3.4 Structural Analysis ..... 252

4.4 Conclusion ..... 254

4.5 Experimental Section ..... 255

4.5.1 Materials and Methods ..... 255

4.5.2 Experimental Procedures ..... 256

4.5.2.1 Cyclotrimerization of Indolyne Precursors ..... 256

4.5.3 Photophysical Properties ..... 260

4.5.3.1 UV-Vis and Fluorescence Spectra ..... 260

4.5.3.2 Cyclic Voltammetry Spectra ..... 261

4.6 Spectra Relevant to Chapter Four: ..... 262

4.7 Notes and References ..... 275

CHAPTER FIVE: Conversion of Amides to Esters by the Nickel-Catalyzed Activation of Amide C–N Bonds ..... 280
5.1 Abstract ..... 280
5.2 Introduction ..... 281
5.3 Optimization and Substrate Scope ..... 284
5.4 Computational Studies ..... 289
5.5 Selective Amide Bond Activation ..... 292
5.6 Conclusion ..... 293
5.7 Experimental Section ..... 294
5.7.1 Materials and Methods ..... 294
5.7.2 Experimental Procedures ..... 296
5.7.2.1 Syntheses of Amide Substrates ..... 296
5.7.2.2 Methanolysis Control Experiments ..... 301
5.7.2.3 Screening of Amide Substrates ..... 302
5.7.2.4 Comparison of Ligands and Relevant Control Experiments ..... 303
5.7.2.5 Scope of Methodology ..... 305
5.7.2.6 Selective Cleavage of Tertiary over Secondary Amide ..... 316
5.7.2.7 Selective Cleavage of Aryl Amide Over Alkyl Amide ..... 318
5.7.2.8 Selective Cleavage of Aryl Amide in the Presence of an Ester .. 322
5.7.3 Verification of Enantiopurity ..... 325
5.7.3.1 Racemic Compound Syntheses ..... 325
5.7.3.2 Chiral SFC Assays ..... 327
5.7.4 Computational Methods ..... 333

5.7.4.1 Complete Reference of Gaussian 09 ..... 333

5.7.4.2 Transition State Structures for Decarbonylation Pathway ..... 334

5.7.4.3 Comparison of Acyl C–N and Aryl C–N Bond Activation Pathway ..... 334

5.7.4.4 Analysis of Amides Derived from Alkyl Carboxylic Acids ..... 335

5.7.4.5 Analysis of *N*-Me,Boc Amide Esterification ..... 336

5.7.4.6 Free Energy and Enthalpy of Amide and Ester Formation ..... 338

5.7.4.7 Energies, Enthalpies, and Free Energy of the Calculated Structures ..... 340

5.7.4.8 Cartesian Coordinates for the Optimized Structures. ..... 341

5.8 Spectra Relevant to Chapter Five: ..... 342

5.9 Notes and References ..... 394

LIST OF FIGURES

CHAPTER ONE

***Figure 1.1.*** Examples of Arynes....2

***Figure 1.2.*** Initial Proposal of 2,3-Benzofuranyne Formation....3

***Figure 1.3.*** Competing Aryne and Non-Aryne Mechanisms....4

***Figure 1.4.*** Early ortho-Benzyne Studies....5

***Figure 1.5.*** Pyridyne Isomers and Methods of Generation....7

***Figure 1.6.*** Examples of 3,4-Pyridyne Studies....9

***Figure 1.7.*** Our laboratory's 3,4-Pyridyne Studies....10

***Figure 1.8.*** Examples of 2,3-Pyridyne Studies....12

***Figure 1.9.*** Indolyne Isomers and Seminal Indolyne Example....13

***Figure 1.10.*** Silyltriflates as Indolyne Precursors....14

***Figure 1.11.*** Sample Reactivity of Indolyne Intermediates....15

***Figure 1.12.*** Recent Examples of Indolyne Reactivity and Indolinyne Generation....16

***Figure 1.13.*** 2,3-Indolyne and other 5-Membered Hetarynes....17

***Figure 1.14.*** Natural Products Synthesized using Heterocyclic Arynes....18

***Figure 1.15.*** Representative Indolactam Alkaloids **1.101**–**1.104**....21

***Figure 1.16.*** Synthesis of C7 Substituted Indolactam Alkaloids....24

***Figure 1.17.*** [4.3.1]-Bicyclic Welwitindolinone Natural Products....25

***Figure 1.18.*** Tubingensins A and B....28

CHAPTER TWO

***Figure 2.1.*** Representative Indolactam Alkaloids **2.1**–**2.4** .....41

APPENDIX ONE

***Figure A1.1.*** $^{1}$H NMR (500 MHz, $CDCl_3$) of compound **2.14**. .....80

***Figure A1.2.*** Infrared spectrum of compound **2.14**. .....81

***Figure A1.3.*** $^{13}$C NMR (125 MHz, $CDCl_3$) of compound **2.14**.....81

***Figure A1.4.*** $^{1}$H NMR (500 MHz, $CDCl_3$) of compound **2.16b**.....82

***Figure A1.5.*** Infrared spectrum of compound **2.16b**. .....83

***Figure A1.6.*** $^{13}$C NMR (125 MHz, $CDCl_3$) of compound **2.16b**. .....83

***Figure A1.7.*** $^{1}$H NMR (500 MHz, $CDCl_3$) of compound **2.16c** .....84

***Figure A1.8.*** Infrared spectrum of compound **2.16c**.....85

***Figure A1.9.*** $^{13}$C NMR (125 MHz, $CDCl_3$) of compound **2.16c**.....85

***Figure A1.10.*** $^{1}$H NMR (500 MHz, $CDCl_3$) of compound **2.24** .....86

***Figure A1.11.*** Infrared spectrum of compound **2.24**. .....87

***Figure A1.12.*** $^{13}$C NMR (125 MHz, $CDCl_3$) of compound **2.24**.....87

***Figure A1.13.*** $^{1}$H NMR (500 MHz, $CDCl_3$) of compound **2.25** .....88

***Figure A1.14.*** Infrared spectrum of compound **2.25**. .....89

***Figure A1.15.*** $^{13}$C NMR (125 MHz, $CDCl_3$) of compound **2.25**.....89

***Figure A1.16.*** $^{1}$H NMR (500 MHz, $CDCl_3$) of compound **2.26** .....90

***Figure A1.17.*** $^{1}$H NMR (500 MHz, $CDCl_3$) of compound **2.27** .....91

***Figure A1.18.*** Infrared spectrum of compound **2.27**. .....92

***Figure A1.19.*** $^{13}$C NMR (125 MHz, $CDCl_3$) of compound **2.27**.....92

***Figure A1.20.*** $^{1}$H NMR (500 MHz, $CDCl_3$) of compound **2.2** .....93

***Figure A1.21.*** $^{1}$H NMR (500 MHz, $CDCl_3$) of compound **2.29** .....94

***Figure A1.22.*** Infrared spectrum of compound **2.29**. .....95

***Figure A1.23.*** $^{13}$C NMR (125 MHz, $CDCl_3$) of compound **2.29**.....95

***Figure A1.24.*** $^{1}$H NMR (500 MHz, $CDCl_3$) of compound **2.31** .....96

***Figure A1.25.*** Infrared spectrum of compound **2.31**. .....97

***Figure A1.26.*** $^{13}$C NMR (125 MHz, $CDCl_3$) of compound **2.31**.....97

***Figure A1.27.*** $^{1}$H NMR (500 MHz, $CDCl_3$) of compound **2.33** .....98

***Figure A1.28.*** $^{1}$H NMR (500 MHz, $CDCl_3$) of compound **2.34** .....99

***Figure A1.29.*** Infrared spectrum of compound **2.34**. ..... 100

***Figure A1.30.*** $^{13}$C NMR (125 MHz, $CDCl_3$) of compound **2.34**..... 100

***Figure A1.31.*** $^{1}$H NMR (500 MHz, $CDCl_3$) of compound **2.3** ..... 101

***Figure A1.32.*** $^{1}$H NMR (500 MHz, $CDCl_3$) of compound **2.32** ..... 102

***Figure A1.33.*** Infrared spectrum of compound **2.32**. ..... 103

***Figure A1.34.*** $^{13}$C NMR (125 MHz, $CDCl_3$) of compound **2.32**..... 103

***Figure A1.35.*** $^{1}$H NMR (500 MHz, $CDCl_3$) of compound **2.46** ..... 104

***Figure A1.36.*** $^{1}$H NMR (500 MHz, $CDCl_3$) of compound **2.47** ..... 105

***Figure A1.37.*** Infrared spectrum of compound **2.47**. ..... 106

***Figure A1.38.*** $^{13}$C NMR (125 MHz, $CDCl_3$) of compound **2.47**..... 106

***Figure A1.39.*** $^{1}$H NMR (500 MHz, $CDCl_3$) of compound **2.4** ..... 107

CHAPTER THREE

***Figure 3.1.*** Well studied *N*-containing cyclic alkynes **3.1**–**3.3**, *O*–containing strained alkynes **3.4** and **3.5** (present study), and representative drugs and natural products ..... 118

***Figure 3.2.*** Geometry optimized structures of **3.4**–**3.7** ..... 120

APPENDIX TWO

***Figure A2.1.*** $^{1}$H NMR (500 MHz, $CDCl_3$) compound **3.10** ..... 162

***Figure A2.2.*** Infrared spectrum of compound **3.10** ..... 163

***Figure A2.3.*** $^{13}$C NMR (125 MHz, $CDCl_3$) of compound **3.10** ..... 163

***Figure A2.4.*** $^{1}$H NMR (500 MHz, $C_6D_6$) compound **3.13** ..... 164

***Figure A2.5.*** Infrared spectrum of compound **3.13** ..... 165

***Figure A2.6.*** $^{13}$C NMR (125 MHz, $C_6D_6$) of compound **3.13** ..... 165

***Figure A2.7.*** $^{1}$H NMR (500 MHz, $C_6D_6$) compound **3.14** ..... 166

***Figure A2.8.*** Infrared spectrum of compound **3.14** ..... 167

***Figure A2.9.*** $^{13}$C NMR (125 MHz, $C_6D_6$) of compound **3.14** ..... 167

***Figure A2.10.*** $^{1}$H NMR (500 MHz, $CDCl_3$) compound **3.27** ..... 168

***Figure A2.11.*** Infrared spectrum of compound **3.27** ..... 169

***Figure A2.12.*** $^{13}$C NMR (125 MHz, $CDCl_3$) of compound **3.27** ..... 169

***Figure A2.13.*** $^{1}$H NMR (500 MHz, $CDCl_3$) compound **3.28** ..... 170

***Figure A2.14.*** Infrared spectrum of compound **3.28** ..... 171

***Figure A2.15.*** $^{13}$C NMR (125 MHz, $CDCl_3$) of compound **3.28** ..... 171

***Figure A2.16.*** $^{1}$H NMR (500 MHz, $CDCl_3$) compound **3.29** ..... 172

***Figure A2.17.*** Infrared spectrum of compound **3.29** ..... 173

***Figure A2.18.*** $^{13}C$ NMR (125 MHz, $CDCl_3$) of compound **3.29** ..... 173

***Figure A2.19.*** $^{1}H$ NMR (500 MHz, $CD_3CN$) compound **3.30** ..... 174

***Figure A2.20.*** Infrared spectrum of compound **3.30** ..... 175

***Figure A2.21.*** $^{13}C$ NMR (125 MHz, $CD_3CN$) of compound **3.30** ..... 175

***Figure A2.22.*** $^{1}H$ NMR (500 MHz, $CDCl_3$) compound **3.31** ..... 176

***Figure A2.23.*** Infrared spectrum of compound **3.31** ..... 177

***Figure A2.24.*** $^{13}C$ NMR (125 MHz, $CDCl_3$) of compound **3.31** ..... 177

***Figure A2.25.*** $^{1}H$ NMR (500 MHz, $CDCl_3$) compound **3.32** ..... 178

***Figure A2.26.*** Infrared spectrum of compound **3.32** ..... 179

***Figure A2.27.*** $^{13}C$ NMR (125 MHz, $CDCl_3$) of compound **3.32** ..... 179

***Figure A2.28.*** $^{1}H$ NMR (500 MHz, $CDCl_3$) compound **3.33** ..... 180

***Figure A2.29.*** Infrared spectrum of compound **3.33** ..... 181

***Figure A2.30.*** $^{13}C$ NMR (125 MHz, $CDCl_3$) of compound **3.33** ..... 181

***Figure A2.31.*** $^{1}H$ NMR (500 MHz, $CD_3CN$) compound **3.34** ..... 182

***Figure A2.32.*** Infrared spectrum of compound **3.34** ..... 183

***Figure A2.33.*** $^{13}C$ NMR (125 MHz, $CDCl_3$) of compound **3.34** ..... 183

***Figure A2.34.*** $^{1}H$ NMR (500 MHz, $CDCl_3$) compound **3.35** ..... 184

***Figure A2.35.*** Infrared spectrum of compound **3.35** ..... 185

***Figure A2.36.*** $^{13}C$ NMR (125 MHz, $CDCl_3$) of compound **3.35** ..... 185

***Figure A2.37.*** $^{1}H$ NMR (500 MHz, $CDCl_3$) compounds **3.36** & **3.37** ..... 186

***Figure A2.38.*** Infrared spectrum of compounds **3.36** & **3.37** ..... 187

***Figure A2.39.*** $^{13}C$ NMR (125 MHz, $CDCl_3$) of compounds **3.36** & **3.37** ..... 187

***Figure A2.40.*** $^{1}H$ NMR (500 MHz, $CDCl_3$) compounds **3.38** & **3.39** ..... 188

***Figure A2.41.*** Infrared spectrum of compound **3.38** & **3.39** ..... 189

***Figure A2.42.*** $^{13}C$ NMR (125 MHz, $CDCl_3$) of compound **3.38** ..... 189

***Figure A2.43.*** $^{1}H$ NMR (500 MHz, $CDCl_3$) compound **3.40** ..... 190

***Figure A2.44.*** Infrared spectrum of compound **3.40** ..... 191

***Figure A2.45.*** $^{13}C$ NMR (125 MHz, $CDCl_3$) of compound **3.40** ..... 191

***Figure A2.46.*** $^{1}H$ NMR (500 MHz, $CDCl_3$) compound **3.41** ..... 192

***Figure A2.47.*** Infrared spectrum of compound **3.41** ..... 193

***Figure A2.48.*** $^{13}C$ NMR (125 MHz, $CDCl_3$) of compound **3.41** ..... 193

***Figure A2.49.*** $^{1}H$ NMR (500 MHz, $CD_3CN$) compound **3.42** ..... 194

***Figure A2.50.*** Infrared spectrum of compound **3.42** ..... 195

***Figure A2.51.*** $^{13}C$ NMR (125 MHz, $CD_3CN$) of compound **3.42** ..... 195

***Figure A2.52.*** $^{1}H$ NMR (500 MHz, $CD_3CN$) compound **3.43** ..... 196

***Figure A2.53.*** Infrared spectrum of compound **3.43** ..... 197

***Figure A2.54.*** $^{13}C$ NMR (125 MHz, $CD_3CN$) of compound **3.43** ..... 197

***Figure A2.55.*** $^{1}H$ NMR (500 MHz, $CDCl_3$) compound **3.44** ..... 198

***Figure A2.56.*** Infrared spectrum of compound **3.44** ..... 199

***Figure A2.57.*** $^{13}C$ NMR (125 MHz, $CDCl_3$) of compound **3.44** ..... 199

***Figure A2.58.*** $^{1}H$ NMR (500 MHz, $CDCl_3$) compound **3.45** ..... 200

***Figure A2.59.*** Infrared spectrum of compound **3.45** ..... 201

***Figure A2.60.*** $^{13}C$ NMR (125 MHz, $CDCl_3$) of compound **3.45** ..... 201

***Figure A2.61.*** $^{1}H$ NMR (500 MHz, $CDCl_3$) compound **3.46** ..... 202

***Figure A2.62.*** Infrared spectrum of compound **3.46** ..... 203

***Figure A2.63.*** $^{13}C$ NMR (125 MHz, $CDCl_3$) of compound **3.46** ..... 203

***Figure A2.64.*** $^{1}$H NMR (500 MHz, $CDCl_3$) compound **3.47** ..... 204

***Figure A2.65.*** Infrared spectrum of compound **3.47** ..... 205

***Figure A2.66.*** $^{13}$C NMR (125 MHz, $CDCl_3$) of compound **3.47** ..... 205

***Figure A2.67.*** $^{1}$H NMR (500 MHz, $CDCl_3$) compound **3.48** ..... 206

***Figure A2.68.*** Infrared spectrum of compound **3.48** ..... 207

***Figure A2.69.*** $^{13}$C NMR (125 MHz, $CDCl_3$) of compound **3.48** ..... 207

***Figure A2.70.*** $^{1}$H NMR (500 MHz, $CDCl_3$) compound **3.49** ..... 208

***Figure A2.71.*** Infrared spectrum of compound **3.49** ..... 209

***Figure A2.72.*** $^{13}$C NMR (125 MHz, $CDCl_3$) of compound **3.49** ..... 209

***Figure A2.73.*** $^{1}$H NMR (500 MHz, $CDCl_3$) compound **3.50** ..... 210

***Figure A2.74.*** Infrared spectrum of compound **3.50** ..... 211

***Figure A2.75.*** $^{13}$C NMR (125 MHz, $CDCl_3$) of compound **3.50** ..... 211

***Figure A2.76.*** $^{1}$H NMR (500 MHz, $CDCl_3$) compound **3.51** ..... 212

***Figure A2.77.*** Infrared spectrum of compound **3.51** ..... 213

***Figure A2.78.*** $^{13}$C NMR (125 MHz, $CDCl_3$) of compound **3.51** ..... 213

***Figure A2.79.*** $^{1}$H NMR (500 MHz, $CDCl_3$) compound **3.52** ..... 214

***Figure A2.80.*** Infrared spectrum of compound **3.52** ..... 215

***Figure A2.81.*** $^{13}$C NMR (125 MHz, $CDCl_3$) of compound **3.52** ..... 215

***Figure A2.82.*** $^{1}$H NMR (500 MHz, $CDCl_3$) compound **3.53** ..... 216

***Figure A2.83.*** Infrared spectrum of compound **3.53** ..... 217

***Figure A2.84.*** $^{13}$C NMR (125 MHz, $CDCl_3$) of compound **3.53** ..... 217

***Figure A2.85.*** $^{1}$H NMR (500 MHz, $C_6D_6$) compound **3.54** ..... 218

***Figure A2.86.*** Infrared spectrum of compound **3.54** ..... 219

***Figure A2.87.*** $^{13}$C NMR (125 MHz, $C_6D_6$) of compound **3.54** ..... 219

***Figure A2.88.*** $^{1}$H NMR (500 MHz, $CDCl_3$) compound **3.55** ..... 220

***Figure A2.89.*** Infrared spectrum of compound **3.55** ..... 221

***Figure A2.90.*** $^{13}$C NMR (125 MHz, $CDCl_3$) of compound **3.55** ..... 221

***Figure A2.91.*** $^{1}$H NMR (500 MHz, $CDCl_3$) compound **3.56** ..... 222

***Figure A2.92.*** Infrared spectrum of compound **3.56** ..... 223

***Figure A2.93.*** $^{13}$C NMR (125 MHz, $C_6D_6$) of compound **3.56** ..... 223

***Figure A2.94.*** $^{1}$H NMR (500 MHz, $CDCl_3$) compound **3.57** & **3.58** ..... 224

***Figure A2.95.*** Infrared spectrum of compound **3.57** & **3.58** ..... 225

***Figure A2.96.*** $^{13}$C NMR (125 MHz, $CDCl_3$) of compound **3.57** & **3.58** ..... 225

***Figure A2.97.*** $^{1}$H NMR (500 MHz, $CDCl_3$) compound **3.59** ..... 226

***Figure A2.98.*** Infrared spectrum of compound **3.59** ..... 227

***Figure A2.99.*** $^{13}$C NMR (125 MHz, $CDCl_3$) of compound **3.59** ..... 227

***Figure A2.100.*** $^{1}$H NMR (500 MHz, $C_6D_6$) compound **3.60** ..... 228

***Figure A2.101.*** Infrared spectrum of compound **3.60** ..... 229

***Figure A2.102.*** $^{13}$C NMR (125 MHz, $C_6D_6$) of compound **3.60** ..... 229

***Figure A2.103.*** $^{1}$H NMR (500 MHz, $CDCl_3$) compounds **3.61** & **3.62** ..... 230

***Figure A2.104.*** Infrared spectrum of compounds **3.61** & **3.62** ..... 231

***Figure A2.105.*** $^{13}$C NMR (125 MHz, $CDCl_3$) of compounds **3.61** & **3.62** ..... 231

***Figure A2.106.*** $^{1}$H NMR (500 MHz, $CDCl_3$) compound **3.63** ..... 232

***Figure A2.107.*** Infrared spectrum of compound **3.63** ..... 233

***Figure A2.108.*** $^{13}$C NMR (125 MHz, $CDCl_3$) of compound **3.63** ..... 233

***Figure A2.109.*** $^{1}$H NMR (500 MHz, $CDCl_3$) compound **3.64** ..... 234

***Figure A2.110.*** Infrared spectrum of compound **3.64** ..... 235

***Figure A2.111.*** $^{13}C$ NMR (125 MHz, $CDCl_3$) of compound **3.64**..... 235

***Figure A2.112.*** $^{1}H$ NMR (500 MHz, $CDCl_3$) compounds **3.65** & **3.66** ..... 236

***Figure A2.113.*** Infrared spectrum of compounds **3.65** & **3.66**..... 237

***Figure A2.114.*** $^{13}C$ NMR (125 MHz, $C_6D_6$) of compounds **3.65** & **3.66** ..... 237

CHAPTER FOUR

***Figure 4.1.*** Previously studied conjugated trimers **4.1–4.3** and indole trimer (present study) ..... 247

***Figure 4.2.*** Trimerization of indolyne precursors **4.9** and **4.12**. ..... 250

***Figure 4.3.*** UV-Vis absorbance and fluorescence emission spectra for trimers **4.7**, **4.8**, **4.10**, **4.11**, **4.13**, and **4.14** in methylcyclohexane. ..... 252

***Figure 4.4.*** Geometry-optimized structures and computed energies of trimers. ..... 254

APPENDIX THREE

***Figure A3.1.*** $^{1}H$ NMR (500 MHz, $CD_3CN$) compound **4.7** ..... 263

***Figure A3.2.*** Infrared spectrum of compound **4.7** ..... 264

***Figure A3.3.*** $^{13}C$ NMR (125 MHz, $CD_3CN$) of compound **4.7**..... 264

***Figure A3.4.*** $^{1}H$ NMR (500 MHz, $CD_3CN$) compound **4.8** ..... 265

***Figure A3.5.*** Infrared spectrum of compound **4.8** ..... 266

***Figure A3.6.*** $^{13}C$ NMR (125 MHz, $CD_2Cl_2$) of compound **4.8** ..... 266

***Figure A3.7.*** $^{1}H$ NMR (500 MHz, $CD_3CN$) compound **4.10** ..... 267

***Figure A3.8.*** Infrared spectrum of compound **4.10** ..... 268

***Figure A3.9.*** $^{13}$C NMR (125 MHz, $CD_3CN$) of compound **4.10** ..... 268

***Figure A3.10.*** $^{1}$H NMR (500 MHz, $CD_3CN$) compound **4.11** ..... 269

***Figure A3.11.*** Infrared spectrum of compound **4.11** ..... 270

***Figure A3.12.*** $^{13}$C NMR (125 MHz, $CD_2Cl_2$) of compound **4.11** ..... 270

***Figure A3.13.*** $^{1}$H NMR (500 MHz, $CD_2Cl_2$) compound **4.12** ..... 271

***Figure A3.14.*** Infrared spectrum of compound **4.13** ..... 272

***Figure A3.15.*** $^{13}$C NMR (125 MHz, $CD_2Cl_2$) of compound **4.13** ..... 272

***Figure A3.16.*** $^{1}$H NMR (500 MHz, $CD_3CN$) compound **4.14** ..... 273

***Figure A3.17.*** Infrared spectrum of compound **4.14** ..... 274

***Figure A3.18.*** $^{13}$C NMR (125 MHz, $CD_3CN$) of compound **4.14** ..... 274

CHAPTER FIVE

***Figure 5.1.*** Amide-bond cleavage using transition-metal catalysis ..... 283

***Figure 5.2.*** Computational study of catalytic cycle ..... 291

***Figure 5.3.*** Selective amide-bond cleavage processes ..... 293

***Figure 5.4.*** Analysis of Competing Pathways for Esterification of *N*-Me,Boc Substrate **5.95** ..... 336

***Figure 5.5.*** Substitution Effects on Equilibrium of Amide Esterification ..... 338

APPENDIX FOUR

***Figure A4.1.*** $^{1}$H NMR (500 MHz, $CDCl_3$) of compound **5.31** ..... 343

***Figure A4.2.*** Infrared spectrum of compound **5.31** ..... 344

***Figure A4.3.*** $^{13}$C NMR (125 MHz, $CDCl_3$) of compound **5.31** ..... 344

***Figure A4.4.*** $^{1}$H NMR (400 MHz, $CDCl_3$) of compound **5.33** ..... 345

***Figure A4.5.*** Infrared spectrum of compound **5.33** ..... 346

***Figure A4.6.*** $^{13}$C NMR (125 MHz, $CDCl_3$) of compound **5.33** ..... 346

***Figure A4.7.*** $^{1}$H NMR (300 MHz, $CDCl_3$) of compound **5.35** ..... 347

***Figure A4.8.*** Infrared spectrum of compound **5.35** ..... 348

***Figure A4.9.*** $^{13}$C NMR (75 MHz, $CDCl_3$) of compound **5.35** ..... 348

***Figure A4.10.*** $^{1}$H NMR (500 MHz, $CDCl_3$) of compound **5.37** ..... 349

***Figure A4.11.*** Infrared spectrum of compound **5.37** ..... 350

***Figure A4.12.*** $^{13}$C NMR (125 MHz, $CDCl_3$) of compound **5.37** ..... 350

***Figure A4.13.*** $^{1}$H NMR (300 MHz, $CDCl_3$) of compound **5.39** ..... 351

***Figure A4.14.*** Infrared spectrum of compound **5.39** ..... 352

***Figure A4.15.*** $^{13}$C NMR (125 MHz, $CDCl_3$) of compound **5.39** ..... 352

***Figure A4.16.*** $^{1}$H NMR (300 MHz, $CDCl_3$) of compound **5.8** ..... 353

***Figure A4.17.*** $^{1}$H NMR (400 MHz, $CDCl_3$) of compound **5.40** ..... 354

***Figure A4.18.*** $^{1}$H NMR (300 MHz, $CDCl_3$) of compound **5.42** ..... 355

***Figure A4.19.*** $^{1}$H NMR (400 MHz, $CDCl_3$) of compound **5.44** ..... 356

***Figure A4.20.*** $^{1}$H NMR (400 MHz, $CDCl_3$) of compound **5.46** ..... 357

***Figure A4.21.*** $^{1}$H NMR (500 MHz, $CDCl_3$) of compound **5.48** ..... 358

***Figure A4.22.*** $^{1}$H NMR (500 MHz, $CDCl_3$) of compound **5.49** ..... 359

***Figure A4.23.*** $^{1}$H NMR (500 MHz, $CDCl_3$) of compound **5.51** ..... 360

***Figure A4.24.*** $^{1}$H NMR (500 MHz, $CDCl_3$) of compound **5.53** ..... 361

***Figure A4.25.*** $^{1}$H NMR (300 MHz, $CDCl_3$) of compound **5.54** ..... 362

***Figure A4.26.*** $^{1}$H NMR (400 MHz, $CDCl_3$) of compound **5.55** ..... 363

***Figure A4.27.*** $^{1}$H NMR (300 MHz, $CDCl_3$) of compound **5.56**..... 364

***Figure A4.28.*** $^{1}$H NMR (500 MHz, $CDCl_3$) of compound **5.64**..... 365

***Figure A4.29.*** $^{1}$H NMR (500 MHz, $CDCl_3$) of compound **5.66**..... 366

***Figure A4.30.*** $^{1}$H NMR (500 MHz, $CDCl_3$) of compound **5.68**..... 367

***Figure A4.31.*** $^{1}$H NMR (600 MHz, $CDCl_3$) of compound **5.70**..... 368

***Figure A4.32.*** Infrared spectrum of compound **5.70** ..... 369

***Figure A4.33.*** $^{13}$C NMR (150 MHz, $CDCl_3$) of compound **5.70**..... 369

***Figure A4.34.*** $^{1}$H NMR (500 MHz, $CDCl_3$) of compound **5.72**..... 370

***Figure A4.35.*** $^{1}$H NMR (300 MHz, $(CD_3)_2SO$) of compound **5.21** ..... 371

***Figure A4.36.*** $^{1}$H NMR (500 MHz, $CDCl_3$) of compound **5.74**..... 372

***Figure A4.37.*** $^{1}$H NMR (500 MHz, $CDCl_3$) of compound **5.76**..... 373

***Figure A4.38.*** Infrared spectrum of compound **5.76** ..... 374

***Figure A4.39.*** $^{13}$C NMR (125 MHz, $CDCl_3$) of compound **5.76**..... 374

***Figure A4.40.*** $^{1}$H NMR (500 MHz, $CDCl_3$) of compound **5.78**..... 375

***Figure A4.41.*** Infrared spectrum of compound **5.78** ..... 376

***Figure A4.42.*** $^{13}$C NMR (125 MHz, $CDCl_3$) of compound **5.78**..... 376

***Figure A4.43.*** $^{1}$H NMR (500 MHz, $CDCl_3$) of compound **5.80**..... 377

***Figure A4.44.*** Infrared spectrum of compound **5.80** ..... 378

***Figure A4.45.*** $^{13}$C NMR (125 MHz, $CDCl_3$) of compound **5.80**..... 378

***Figure A4.46.*** $^{1}$H NMR (400 MHz, $CDCl_3$) of compound **5.19**..... 379

***Figure A4.47.*** Infrared spectrum of compound **5.19** ..... 380

***Figure A4.48.*** $^{13}$C NMR (125 MHz, $CDCl_3$) of compound **5.19**..... 380

***Figure A4.49.*** $^{1}$H NMR (500 MHz, $(CD_3)_2SO$) of compound **5.22** ..... 381

***Figure A4.50.*** Infrared spectrum of compound **5.22** ..... 382

***Figure A4.51.*** $^{13}$C NMR (125 MHz, $(CD_3)_2SO$) of compound **5.22** ..... 382

***Figure A4.52.*** $^{1}$H NMR (500 MHz, $CDCl_3$) of compound **5.83** ..... 383

***Figure A4.53.*** $^{1}$H NMR (500 MHz, $CDCl_3$) of compound **5.85** ..... 384

***Figure A4.54.*** Infrared spectrum of compound **5.85** ..... 385

***Figure A4.55.*** $^{13}$C NMR (125 MHz, $CDCl_3$) of compound **5.85** ..... 385

***Figure A4.56.*** $^{1}$H NMR (500 MHz, $CDCl_3$) of compound **5.23** ..... 386

***Figure A4.57.*** Infrared spectrum of compound **5.23** ..... 387

***Figure A4.58.*** $^{13}$C NMR (125 MHz, $CDCl_3$) of compound **5.23** ..... 387

***Figure A4.59.*** $^{1}$H NMR (500 MHz, $CDCl_3$) of compound **5.24** ..... 388

***Figure A4.60.*** Infrared spectrum of compound **5.24** ..... 389

***Figure A4.61.*** $^{13}$C NMR (125 MHz, $CDCl_3$) of compound **5.24** ..... 389

***Figure A4.62.*** $^{1}$H NMR (500 MHz, $CDCl_3$) of compound **5.26** ..... 390

***Figure A4.63.*** Infrared spectrum of compound **5.26** ..... 391

***Figure A4.64.*** $^{13}$C NMR (125 MHz, $CDCl_3$) of compound **5.26** ..... 391

***Figure A4.65.*** $^{1}$H NMR (500 MHz, $CDCl_3$) of compound **5.25** ..... 392

***Figure A4.66.*** Infrared spectrum of compound **5.25** ..... 393

***Figure A4.67.*** $^{13}$C NMR (125 MHz, $CDCl_3$) of compound **5.25** ..... 393

LIST OF SCHEMES

CHAPTER ONE

***Scheme 1.1.*** Singh's Synthesis of Perlolidine (**1.89**) .....19

***Scheme 1.2.*** Guitián's Synthesis of Ellipticine (**1.87**).....20

***Scheme 1.3.*** Julia's Formal Synthesis of Lysergic Acid (**1.80**) .....20

***Scheme 1.4.*** Total Synthesis of (–)-Indolactam V (**1.101**).....22

***Scheme 1.5.*** Total Synthesis of Welwitindolinone Alkaloids.....27

***Scheme 1.6.*** Total Synthesis of (+)-Tubingensin A (**1.84**) .....29

CHAPTER TWO

***Scheme 2.1.*** Synthetic Strategy Toward **2.1** and C7 Substituted Indolactam Alkaloids **2.2**–**2.4** .....42

***Scheme 2.2.*** Optimized Synthesis of Indolactam V (**2.1**) and **2.14** .....44

***Scheme 2.3.*** C7 Functionalization of **2.14** and Introduction of Key $sp^2$–$sp^3$ Linkage with a Quaternary Carbon Substituent.....47

***Scheme 2.4.*** Total Synthesis of (–)-Pendolmycin (**2.2**) .....48

***Scheme 2.5.*** Synthesis of Morpholine Amide **2.29** and Cross-Coupling to Access Diastereomeric Adducts **2.31** and **2.32** Possessing the Necessary All-Carbon Quaternary Stereocenters.....49

***Scheme 2.6.*** Total Synthesis of (–)-Lyngbyatoxin A (**2.3**) .....50

***Scheme 2.7.*** Total Synthesis of (–)-Teleocidin A-2 (**2.4**) .....50

CHAPTER THREE

***Scheme 3.1.*** Syntheses of Silyl Triflates **3.10** and **3.14** ..... 121

LIST OF TABLES

CHAPTER TWO

***Table 2.1.*** C7 $sp^2$–$sp^3$ Cross-Coupling on Model Substrate **2.15**.....46

CHAPTER THREE

***Table 3.1.*** Diels–Alder Cycloadditions of 4,5-Benzofuranyne (**3.4**) ..... 122

***Table 3.2.*** Reactions of Silyl Triflate **3.10** with Nucleophiles and Cycloaddition Partners ..... 124

***Table 3.3.*** Diels–Alder Cycloadditions of 3,4-Oxacyclohexyne (**3.5**)..... 125

***Table 3.4.*** Reactions of Silyl Triflate **3.14** with Nucleophiles and Cycloaddition Partners ..... 127

***Table 3.5.*** Comparison of 4,5-Indolyne and 4,5-Benzofuranyne Regioselectivities..... 128

***Table 3.6.*** Comparison of Oxacyclohexyne and Piperidyne Regioselectivities..... 129

CHAPTER FOUR

***Table 4.1.*** Optimization of Cyclotrimerization ..... 249

CHAPTER FIVE

***Table 5.1.*** Experimental and computational study of amide-bond activation during the conversion of benzamides **5.7** to methyl benzoate **5.8a** ..... 286

***Table 5.2.*** Scope of our methodology..... 289

***Table 5.3.*** Attempted Conversion of Amide **5.7g** to Methyl Benzoate **5.8a** ..... 301

***Table 5.4.*** Survey of Amide Substrates ..... 302

***Table 5.5.*** Ligand Screening for Nickel-Catalyzed Esterification[a] ..... 304

***Table 5.6.*** Comparison of Aryl vs. Alkyl Amide Substrates..... 335

***Table 5.7.*** Energies, enthalpies, and free energies of the structures calculated at the M06/SDD, 6-311+G(d,p)($SMD^{toluene}$)//B3LYP/LANL2DZ,6-31G(d) ..... 340

LIST OF ABBREVIATIONS

| | |
|---|---|
| Å | angstrom |
| $[\alpha]_D$ | specific rotation at wavelength of sodium D line |
| Ac | acetyl, acetate |
| AcOH | acetic acid |
| α | alpha |
| app. | apparent |
| aq. | aqueous |
| atm | atmosphere |
| Bn | benzyl |
| br | broad |
| Boc | *tert*-butoxycarbonyl |
| Bu | butyl |
| *n*-Bu | butyl (linear) |
| *t*-Bu | *tert*-butyl |
| *s*-Bu | *sec-butyl* |
| *c* | concentration for specific rotation measurements |
| °C | degrees Celsius |
| calcd | calculated |
| cat. | catalytic |
| Cbz | carboxybenzyl |

| | |
|---|---|
| COD | 1,5-cyclooctadiene |
| CSA | camphorsulfonic acid |
| Cy | cyclohexyl |
| d | doublet |
| DABCO | 1,4-diazabicyclo[2.2.2]octane |
| dba | dibenzylideneacetone |
| DCE | 1,2-dichloroethane |
| DIC | *N,N*′-diisopropylcarbodiimide |
| DMAP | 4-dimethylaminopyridine |
| DME | dimethoxyethane |
| DMF | *N*,*N*-dimethylformamide |
| DMI | 1,3-dimethyl-2-imidazolidinone |
| DMSO | dimethyl sulfoxide |
| dppe | 1,2-bis(diphenylphosphino)ethane |
| dppf | 1,1′-bis(diphenylphosphino)ferrocene |
| ee | enantiomeric excess |
| equiv | equivalent |
| ESI | electrospray ionization |
| Et | ethyl |
| g | gram(s) |
| h | hour(s) |
| HMDS | hexamethyldisilane |

| | |
|---|---|
| HRMS | high resolution mass spectroscopy |
| Hz | hertz |
| IR | infrared (spectroscopy) |
| IMes | 1,3-bis(2,4,6-trimethylphenyl)imidazol-2-ylidene |
| IPr | 1,3-bis(2,6-di-i-propylphenyl)imidazol-2-ylidene |
| *i*-Pr | iso-propyl |
| *J* | coupling constant |
| L | liter |
| LDA | lithium diisopropylamide |
| M | molecular mass |
| m | multiplet or milli |
| *m* | meta |
| *m/z* | mass to charge ratio |
| μ | micro |
| Me | methyl |
| MHz | megahertz |
| min | minute(s) |
| mol | mole(s) |
| mp | melting point |
| MS | molecular sieves |
| NBS | *N*-bromosuccinimide |
| NMR | nuclear magnetic resonance |

| | |
|---|---|
| *o* | ortho |
| *p* | para |
| PPA | polyphosphoric acid |
| PCC | pyridinium chlorochromate |
| Ph | phenyl |
| pH | hydrogen ion concentration in aqueous solution |
| PhH | benzene |
| ppm | parts per million |
| *i*-Pr | isopropyl |
| PSI | Pounds per square inch |
| pyr | pyridine |
| q | quartet |
| rt | room temperature |
| $R_f$ | retention factor |
| s | singlet |
| sat. | saturated |
| SIMes | 1,3-bis(2,4,6-trimethylphenyl)-4,5-dihydroimidazol-2-ylidene |
| SIPr | 1,3-bis(2,6-di-i-propylphenyl)-4,5-dihydroimidazol-2-ylidine |
| t | triplet |
| TBAF | tetrabutylammonium fluoride |

| | |
|---|---|
| TBAI | tetrabutylammonium iodide |
| TBS | *tert*-butyldimethylsilyl |
| TBSCl | *tert*-butyldimethylsilyl chloride |
| TES | triethylsilyl |
| Tf | trifluoromethanesulfonyl (trifyl) |
| TFA | trifluoroacetic acid |
| THF | tetrahydrofuran |
| TLC | thin layer chromatography |
| TMEDA | tetramethylethylenediamine |
| TMS | trimethylsilyl |
| TMSCl | trimethylsilyl chloride |
| TMSOTf | trimethylsiyl triflate |
| Ts | *p*-toluenesulfonyl (tosyl) |
| UV | ultraviolet |
| λ | wavelength |

# ACKNOWLEDGEMENTS

My doctoral degree would not have been possible without the guidance, persistence, and general compassion from Professor Neil K. Garg. I appreciate being part of Neil's lab for a number of reasons but two have always stood out to me: 1. Neil wasn't just a doctoral advisor but also a professional mentor and friend. Throughout my five years, he has taught me how to the best possible chemist in the laboratory and a polished individual in life. In between his chemistry tips, he has shared numerous life lessons and showed us how old he is through his 80's references. Neil has truly shaped the person I am today and I am tremendously thankful for being part of his laboratory. 2. Hard work achieves greatness. From the first day in the laboratory, he has pushed me day after day because he knew I could always do better and I'm truly grateful for it. I appreciate Neil for not just pushing me to work harder but for tireless working along side his students. Whether it is finishing a BACON tutorial, reviewing a fellowship application, or editing a manuscript (for a thesis ☺), Neil has taught me to work as hard as you want people to work for you and be a role model to younger students. I am deeply indebted to him for allowing me to be apart of the Garg Lab Family, shaping the scientist and person I am today, and for countless other things that I can't begin to write because that would require another chapter.

Additional, I would like to acknowledge Professor Miguel Garcia-Garibay for serving on my doctoral committee and being an advisor for the Organization for Cultural Diversity in Science (OCDS). It was a true honor to be the co-president of this organization and I hope to see it grow under your tutelage. I am also thankful to Professors Andrea Kasko and Louis Bouchard for taking the time to serve on my doctoral committee and advising me in my professional ambitions.

I have to thank a number of teachers, mentors, and friends who have guided me toward and through graduate school. First, I'd like to thank my undergraduate research advisor, Professor Daniel Seidel, for taking me into his research group after interviewing me for only ten minutes! I'm so grateful to him for allowing me to work in his laboratory and earn my first two publications, which changed my career path from a M.D. to a Ph.D. Of course my graduate mentor and role model in the Seidel group, Dr. Eric Klauber, had an enormous impact on me. He taught me the ropes and showed me how to be a leader in a research group. Our numerous column chromatography races and Giants vs. Jets bets were some of my fondest memories. My hoodmate, now Dr. Marlena Konieczynaska was always a constant source of encouragement. We will always be "The Babes"! I'm grateful to the rest of the Seidel lab, in particular Dr. Chandra Kante De, Dr. Nisha Mittal, Dr. Deepankar Das, and Dr. Indu Deb, for their friendship and for making my research experience so memorable. In addition, I must give a huge shout out to my high school teachers, Mrs. Ruth Tinverin, Mr. Nicolas Hunter, and Mr. Drew Calvo, whom I have looked up to and value for their opinions and advice.

The research in this dissertation would not have been possible without the great coworkers and friends I've made in the Garg group. When I joined the lab I was mentored by Dr. Sarah Bronner, who is a very interesting, intelligent, and intense (at times) mentor. I learned so much from her about cats and chemistry! I will always appreciate her for taking me under her wing and making me her little chemistry kitten ☺.

Then there was my unofficial mentor, little conscience, and friend, Dr. Adam Goetz whom I've grown to admire and I hope one day can be half the chemist/man he is today. Adam is a no "BS" kind of guy but always willing to help anyone in need! I really have to attribute Adam

for helping me pass my cumulative exams and develop as a scientist. Regardless the number of times I screwed up, Adam would be there to lend a hand. Thank you Big Playa G!

Dr. Noah Fine Nathel has been my longest project partner and a consistent source of curious conversations. Noah has helped me conquer natural products and nickel-catalysis but also has taught me so much about physical organic chemistry. The work in this dissertation would LITERALLY not be possible without him! Outside the lab, he's been an incredible friend and I will miss your movie nights and our fancy dinners and drinks.

My work-wife, project partner, and friend forever, Dr. Liana Hie has always been there for me over the last five years. Even though she was intimidating our first year, I've grown to love her like a sister! She has been one of the few people I can always count on for anything, personal or professional, and her opinions are always something I've trusted. I'm so happy we survived five long years together and I wouldn't want anyone else by my side. Thank you for being an amazing friend and letting me lean on you for inspiration and encouragement. Working next to her the last two years has brought us even closer together and I know we will have many more wonderful adventures and memories to come (including approving my future wife!).

I've had the privilege of overlapping with the first four classes of graduates from the Garg Laboratory whom all have taught me something essential to my education and development. When I first started out in the lab, Dr. Tehetena Mesganaw gave me some tough love but she was a true sweetheart inside. She is one of the most encouraging individuals I have ever met and her perfectionism is a trait I'm still jealous of! Along with Mrs. Kanya West, I had the joy of working around some older gifted chemists, Drs. Kyle Quasdorf, Ben Boal, Alex Schammel, and Alex Huters. Kyle was a shy and quiet guy but I sincerely enjoyed his chemistry insights and his hilarious behavior after numerous group outings. Ben was also a quiet chemist

but had a unique taste in rap music. Schammel and Huters were both individuals whom always had suggestions for me on how to solve the challenges I encountered in my first year.

Dr. Grace Chiou was the first person I talked to in California and we've been best friends every since! During the beginning of my doctoral degree she was the person who would give me the blunt truth and would be a "Tiger Mom" whenever I needed it. I have come to miss our cooking, wine, Walking Dead nights, but I know we will still be great friends for many years to come. Dr. Stephen Ramgen is a character to say the least. I have learned more about the glove box from Stephen then I ever asked for. But I thank Stephen for always challenging me and making me a better scientist. Although I did not interact with Dr. Amanda Silberstein on a daily basis, she always impressed me with her witty sense of humor and uncanny ability to find typos. I wish her good luck in her academic career. It was a pleasure to work and live with Dr. Evan Styduhar. Although he hated my music selections in 5235, Adam, Evan and I could always agree on Christmas dubstep! Thank you for helping me through my second year talk, candidacy exam, and being an overall good friend.

I've also had the opportunity to witness a number of younger graduate students develop into intelligent, distinguished scientists. My roommate for the last three years and loyal friend, Jesus Moreno has been a huge part of my life inside and outside the lab. I'm truly grateful to have met him and will miss our unforgettable nights out. I'm excited to see him go off into the pharmaceutical industry and discover the next anti-cancer drug! I have also had the chance to get to know Mike Corsello, Jose Medina, and Nick Weires in my time in the Garg group. These three individuals are a constant source of entertainment and fun and it has been a pleasure to overlap with them. Emma Baker is a sweet girl whom I enjoy conversing about food, Los Angeles, and dating lives. Of course there is Junyong Kim aka JunPuppy aka JunBug who has an

Adele-like singing voice or so he thinks. I will miss our hectic, sleep-deprived BACON days. Over the last two years, I've gotten to know Elias Picazo, a guy that will never stop smiling or take a sick day! I have always adored his 'go-get'em' attitude and his positivity in chemistry and his personal life.

There is a number of budding first and second years I'd like to acknowledge. Joyann Barber always has a smile on her face and could brighten anyone's day. Lucas Morrill has a special singing voice that could wake anyone up (2/3 of the MSB 5234 choir)! I also will miss our Patriots/Jets banter during the Fall season. Bryan Simmons is a witty and funny individual whom I'm jealous of his so eloquent presentation style. In my last year, I was able to meet Robert Susick, a cheesey, happy-go-lucky guy whom I had the opportunity to mentor. Although he left me, I enjoyed our time together and I'm anxiously waiting to see the brilliant scientist that graduates in 2020! Besides Robert, I was able to interact with two crazy comedians named Jacob Dander and Michael Yamano.

In addition to the graduate students, I have interacted with two postdoctoral scholars. First there is Dr. Travis McMahon whom always had a different prespective on solving challenging chemistry problems but also was a levelheaded individual you could count on.

In my last nine months, I've had the privilege of interacting with a gifted postdoctoral scholar named Dr. Marie Hoffmann. Marie, in her short time, has taught me an assortment of topics ranging from NMR tricks and gold catalysis to French culture and partying. In addition, she is one of the most caring, genuine, and intelligent people I have ever met! I thank her for her friendship and will visit soon! I wish all the graduate students and postdoctoral fellows of the Garg Lab the best of luck on their research and professional aspirations.

I had the chance to get to know a number of undergraduates in the Garg Lab including Sonam Kumar, Josh Melamed, Jordan Cisneros, Josh Demeo, Ashley Pournamdari, Sarah Anthony, and JJ Hwang, I wish Sonam, Josh M., Jordan, Ashley good luck on their futures in their respective medical fields. To Josh D., Sarah, and JJ, I wish them all the best in their chemistry ambitions.

My best friends, Timothy Yiu, Lindsey Stevens, and Robin Rubinstein, have been back home in Jersey for last five years but have never left my side. For over twenty-two years, you three have believed in me and supported in all my crazy desires (e.g. like moving across the country after never traveling passed Ohio!). Even though I'd be crazy busy or stressed, seeing a text from any one of you would put a smile on my face.

Finally, I'd like to thank my family for their unconditional love and support. I am certain I would not be where I am today without their wisdom and support. Thank you to my mother for her unwavering care and concern for me. Also, of course, the endless fifty pound packages of food every six months even when I said NO! My father, I thank him for his never-ending encouragement and allowing me to pursue anything I believed in. In addition, I'd like to thank my brother for always being there for me, regardless of our ideological differences. He would come help me from across the country in a heartbeat. Lastly, I would like to thank my grandfather for always looking out for me and inspiring me through his stories.

Chapter One is a version of Goetz, A. E.; Shah, T. K.; Garg, N. K. *Chem. Commun.* **2015**, *51*, 34–45. Goetz, Shah, and Garg were responsible for writing the manuscript.

Chapter Two is a version of Fine Nathel, N. F.[†]; Shah, T. K.[†]; Bronner, S. M.; Garg, N. K. *Chem. Sci.* **2014**, *5*, 2184–2190. Fine Nathel, Shah, and Bronner were responsible for experimental work.

Chapter Three is a version of Shah, T. K.;[†] Medina, J. M.;[†] Garg, N. K. *J. Am. Chem. Soc.* **2016**, *138*, 4948–4954. Shah and Medina were responsible for experimental work.

Chapter Four is a version of Shah, T. K; Lin, J.; Goetz, A. E.; Houk, K. N.; Garg, N. K. *manuscript in preparation*. Shah and Goetz were responsible for experimental work. Lin was responsible for computional work.

Chapter Five is a version of Hie, L.; Fine Nathel, N. F.; Shah, T. K.; Baker, E. L.; Hong, X.; Yang, Y.-F.; Liu, P.; Houk, K. N.; Garg, N. K. *Nature* **2015**, *524*, 79-83. Hie, Fine Nathel, Shah and Baker were responsible for experimental work. Hong, Yang, and Liu were responsible for computational work.

BIOGRAPHICAL SKETCH

## Education:

**University of California, Los Angeles, CA**

- Ph.D. in Organic Chemistry, anticipated Spring 2016
- Graduate Research Assistant, August 2011 to present
- Cumulative GPA: 3.8/4.0

**Rutgers University, New Brunswick, NJ**

- B.A. Degree in Chemistry and Molecular Biology & Biochemistry, May 2011
- Cumulative GPA: 3.4/4.0

## Professional and Academic Experience:

**Graduate Research Assistant -** University of California, Los Angeles, CA

- July 2011 to present, studying in the laboratory of Professor Neil K. Garg
- Completed the total synthesis of indolactam alkaloids: (–)-indolactam V, (–)-pendolmycin, (–)-lyngbyatoxin A, and (–)-teleocidin A-2.
- Synthesized a new hetaryne, the 4,5-benzofuranyne, and demonstrated its utility as a synthetic building block.
- Discovered the first catalytic activation of amide C–N bonds using nickel-catalysis, which allowed for the conversion of amides to esters.
- Synthesized novel small molecule organic photovoltaics using hetarynes methodology for application in organic solar cell devices.

**Educational Content Developer -** University of California, Los Angeles, CA

- January 2014 to Present
- Created "BACON AT UCLA: Biology And Chemistry, Online Notes And Tutorials, UCLA" in collaboration with Professor Neil K. Garg.
- Introduced online weekly tutorials to over 5000 students that connect organic chemistry with topics in health, the real world, and pop culture.
- Aided in securing funding from the UCLA Office of Instructional Development and crowdfunding sources.

**Teaching Assistant -** University of California, Los Angeles, CA

- Undergraduate organic chemistry for life science majors and physical science majors. (Winter 2012, Spring 2012, Fall 2012, and Spring 2013)
- Senior level undergraduate biochemistry laboratory (Fall 2011)

**Undergraduate Research Assistant -** Rutgers University, New Brunswick, NJ

- May 2009 to July 2011
- Investigated the kinetic resolution of propargylic and allylic amines through anion binding catalysis under the guidance of Professor Daniel Seidel.
- Assisted in synthesizing a large scope of thiourea-type hydrogen bonding catalysts for a number of organocatalytic reactions.

**Undergraduate Research Assistant** - Rutgers University, New Brunswick, NJ

- May 2008 to July 2010
- Studied the excitation of carbon monoxide molecules on a copper surface via helium beam scattering methodology under the direction of Professor Barbara J. Hinch
- Created a LabView program to automatically analyze thousands of helium beam scattering data files.

## Honors and Awards:

- Hanson-Dow Award for Excellence in Teaching, 2015
- UCLA Excellence in Chemical Research Fellowship, 2015
- Christopher S. Foote Graduate Fellowship in Organic Chemistry, 2014–2016
- Rutgers University - Highest Honors in Research Award, 2011
- Henry Rutgers Research Scholarship, 2011
- Jerome and Lorraine Aresty Research Scholarship, 2010
- Aresty Undergraduate Research Grant, 2008–2011
- Dean's List, 2008–2011

## Publications:

8. **A New Class of Conjugated Trimeric Scaffolds Accessible Using Indolyne Cyclotrimerizations.** Tejas K. Shah, Janice Lin, Adam E. Goetz, K. N. Houk, and Neil K. Garg**,** *Manuscript in preparation.*

7. **Expanding the Strained Alkyne Toolbox: Generation and Utility of Oxygen-containing Strained Alkynes.** Tejas K. Shah,[†] Jose Medina,[†] and Neil K. Garg. *J. Am. Chem. Soc.* **2016**, *138*, 4948–4954. ([†] indicates joint first authorship) )(Highlighted in *J. Am. Chem. Soc.* **2016**, *138*, 5171.)

6. **Conversion of Amides to Esters by the Nickel-Catalyzed Activation of Amide C–N Bonds.** Liana Hie, Noah F. Fine Nathel, Tejas K. Shah, Emma Baker, Xin Hong, Yun-Fang Yang, Peng Liu, K. N. Houk, and Neil K. Garg. *Nature* **2015**, *524*, 79–83. (Highlighted in *C&EN* **2015**, *93*, 9; *Nat. Chem.* **2015**, *7*, 682; *Angew. Chem. Int. Ed.* **2015**, *54*, 13856–13858; *Synform* **2016**, A3–A8.)

5. **Pyridynes and Indolynes as Building Blocks for Functionalized Heterocycles and Natural Products**. Adam E. Goetz, Tejas K. Shah, and Neil K. Garg. *Chem. Commun. (Feature Article)* **2015**, *51*, 34–45.

4. **Total Syntheses of Indolactam Alkaloids (–)-Indolactam V, (–)-Pendolmycin, (–)-Lyngbyatoxin A, and (–)-Teleocidin A-2**. Noah F. Fine Nathel,[†] Tejas K. Shah,[†] Sarah M. Bronner, and Neil. K. Garg. *Chem. Sci.* **2014**, *5*, 2184–2190. ([†] indicates joint first authorship)

3. **A Dual-Catalysis/Anion-Binding Approach to the Kinetic Resolution of Allylic Amines**. Eric G. Klauber, Nisha Mittal, Tejas K. Shah, Daniel Seidel, *Org. Lett.* **2011***, 13,* 2464–2467. (Highlighted in *Synfacts* **2011**, 675.)

2. **Merging Nucleophilic and Hydrogen Bonding Catalysis: An Anion Binding Approach to the Kinetic Resolution of Propargylic Amines**. Eric G. Klauber, Chandra Kanta De, Tejas K. Shah, Daniel Seidel, *J. Am. Chem. Soc.* **2010**, *132*, 13624–13626. (Highlighted in *Synfacts* **2010**, 1426.)

1. **Isolation of an mRNA from Artemia franciscana for sarcoplasmic calcium-binding protein.** Pratik Padooru, Tejas K. Shah, Andrew K. Vershon, Marty E. Nemeroff. NCBI, December 19, 2007. Accession # EU358113.1.

# CHAPTER ONE

## Pyridynes and Indolynes as Building Blocks for Functionalized Heterocycles and Natural Products

Adam E. Goetz, Tejas K. Shah, and Neil K. Garg

*Chem. Commun.* **2015**, *51*, 34–45.

### 1.1 Abstract

Heterocyclic arynes, or hetarynes, have been studied for over 100 years. However, challenges associated with observing these reactive species, as well as developing synthetically useful methods for their generation and trapping, have limited their use. This review provides a brief historical perspective on the field of hetarynes, in addition to a discussion of pyridyne and indolyne methodologies. Moreover, this review highlights the use of pyridynes, indolynes, and related strained intermediates in natural product synthesis.

### 1.2 Introduction and Historical Perspective

The importance of heterocyclic compounds in modern chemistry cannot be overstated. Methods for the synthesis of functionalized heterocyclic compounds are highly prized because of their applications in pharmaceutical chemistry, materials chemistry, natural products synthesis, organometallic chemistry, and many other fields. Among the various methods for functionalizing heterocycles, the use of highly reactive heterocyclic arynes, or hetarynes,[1] offers a strategically different approach compared to many conventional methods. Arynes have a rich history, and

despite being studied experimentally for over 60 years, many of these species are still treated as scientific curiosities rather than as useful synthetic intermediates. The majority of studies related to arynes focus on carbocyclic arynes, such as *ortho*-benzyne (**1.1**),[2] rather than heterocyclic arynes (e.g., **1.2**–**1.6**, Figure 1.1).

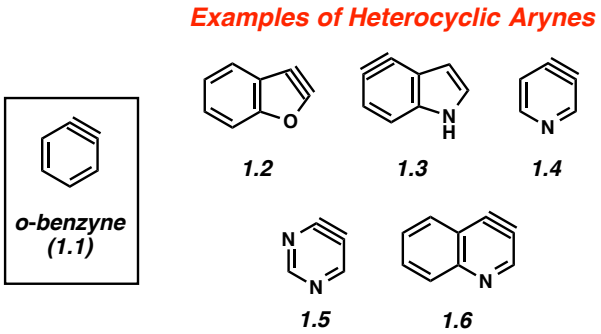


***Figure 1.1.*** Examples of Arynes

The first appearance of any type of aryne in the literature comes from Stoermer and Kahlert's 1902 report invoking 2,3-benzofuranyne (**1.2**) as an intermediate (Figure 1.2).[3] The authors proposed that treatment of 3-bromobenzofuran (**1.7**) with sodium ethoxide led to hetaryne **1.2**, which was trapped by excess ethoxide to give **1.8**. This proposal, despite its influence on the field of aryne chemistry, has been called into question.[1b] In the original report, compound **1.8** was not isolated, but rather was inferred based on the formation of **1.9a** and **1.9b**, which were thought to arise from ring opening of **1.8**. Alternative proposals suggest that contamination of precursor **1.7** with the isomeric 2-bromobenzofuran (**1.11**) would readily give the proposed intermediate **1.8** through an $S_NAr$ pathway.[1b] Given that bromide **1.7** was prepared through elimination of dibromide **1.10**, the alternate mechanism is certainly plausible.

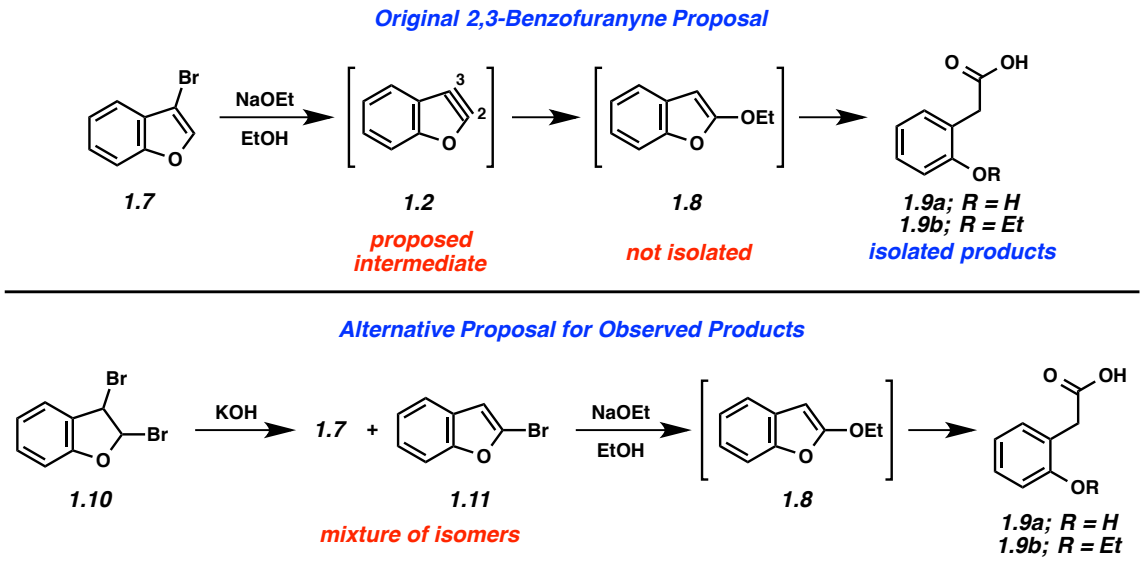


***Figure 1.2.*** Initial Proposal of 2,3-Benzofuranyne Formation

This example highlights one of the inherent challenges with the study of arynes and hetarynes; specifically, the fact that they cannot be readily observed. Typically, the strongest evidence for the presence of an aryne intermediate is the identity of the products obtained. However, even this can lead to incorrect conclusions. As shown in Figure 1.3, it is possible to arrive at so-called "aryne products" through pathways that do not involve aryne formation. This possibility is especially relevant when strong bases, which are also nucleophilic, are employed to generate arynes through dehydrohalogenation, as is demonstrated using pyridine **1.12**. In what is termed the addition/elimination pathway, nucleophilic attack by the amide on the electrophilic C4 position generates stabilized adduct **1.13**, which then undergoes ejection of the leaving group to give product **1.14**. This is in contrast to the elimination/addition pathway. In this route, pyridine **1.12** can undergo deprotonation at C3 followed by elimination of the leaving group to generate 3,4-pyridyne (**1.4**). Attack on this species by a nucleophile at C4 followed by protonation then provides product **1.14**. Additionally, it is also possible that both aryne and non-aryne mechanisms are operating competitively in a given reaction. Since many of the early aryne

studies relied on this method of aryne generation, not all claims of aryne generation are likely accurate, and care must be taken in interpretation of results. Previous reviews have sought to identify certain aryne precursors that are prone to favor one mechanism over the other.[1]

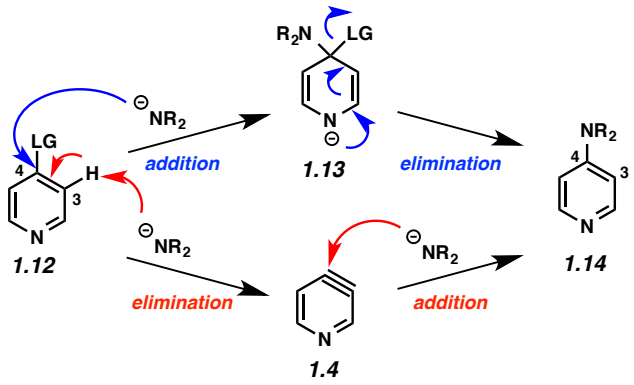


***Figure 1.3.*** Competing Aryne and Non-Aryne Mechanisms

Despite uncertainty over the generation of arynes such as **1.2**, solid evidence for the intermediacy of these highly reactive species was obtained in the 1950s. Following several reports of unexplained "rearrangements" in reactions of halobenzenes with amide bases,[4] Roberts demonstrated that treatment of $^{14}$C-labeled chlorobenzene (**1.15**) with potassium amide gave an equimolar mixture of products **1.16a** and **1.16b** (Figure 1.4).[5] This was rationalized by the presence of the symmetrical "benzyne" (**1.1**) intermediate. Shortly thereafter, Huisgen demonstrated that treating either 2- or 3-fluoroanisole (**1.17a** or **1.17b**) with phenyllithium followed by $CO_2$ led to the isolation of compounds **1.19a** and **1.19b** with a strong preference for **1.19a** (Figure 1.4).[6] Similar to Roberts' reasoning, Huisgen noted that since the two isomeric starting materials gave the same major product with similar ratios, a common intermediate, **1.18**, was likely involved. He also noted that the π-system of the proposed intermediate **1.18** would be orthogonal to the aromatic system. Finally, Wittig demonstrated that treatment of dihalobenzene **1.20** with lithium amalgam in furan led to the isolation of cycloadduct **1.21**, which further

suggested the intermediacy of benzyne (**1.1**).[7] These three studies represent the first solid evidence for the intermediacy of any aryne and inspired the development of much of the hetaryne chemistry reported since.

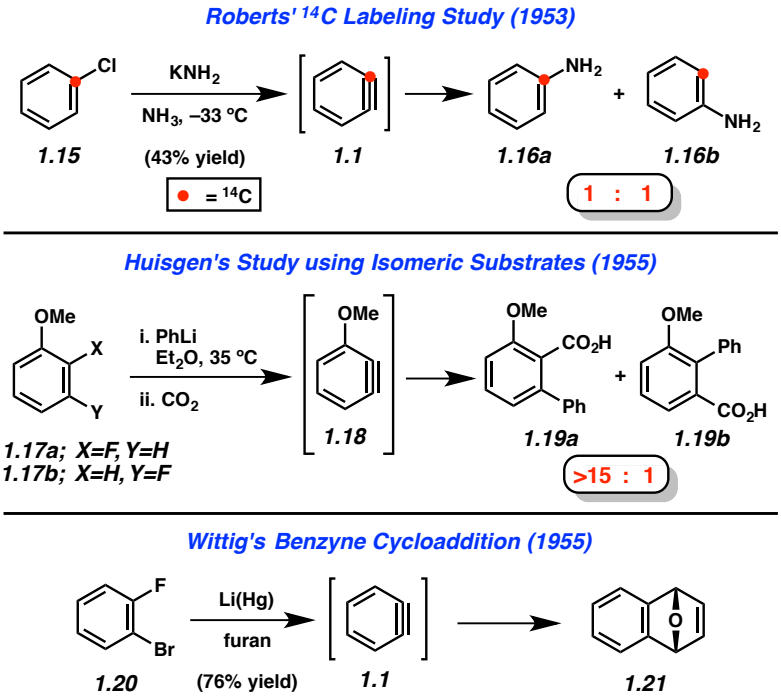


***Figure 1.4.*** Early ortho-Benzyne Studies

## 1.3 Hetaryne Experimental Results

Throughout the years, many heterocyclic arynes have been proposed as intermediates. As discussed above, it is likely that some of the reported reactions do not actually involve the reported aryne as an intermediate.[1] Additionally, aryne reactions frequently give low yields of products, likely due to a combination of the high instability of these intermediates, as well as the harsh conditions that have been traditionally used to generate these species. As a result, the following sections focus on the aryne derivatives of pyridines and indoles, two of the most well-studied classes of hetarynes. Both of these families of hetarynes have undergone an evolution

from their initial discovery to their current uses as versatile intermediates for organic synthesis. Emphasis is placed on developments that have sought to address key challenges related to the utility of these species. This article also highlights the application of hetarynes in the total synthesis of natural products, including our own laboratory's recent syntheses of tubingensin A, the [4.3.1]-bicyclic welwitindolinones, and several indolactam alkaloids.

### 1.3.1 Pyridyne Methodology

Considering all classes of heterocyclic arynes, pyridynes have been the most intensely studied over the past 60 years. Of the three pyridyne isomers shown in Figure 1.5, 3,4-pyridyne (**1.4**) is suggested computationally[8] to be the most stable, followed by 2,3-pyridyne (**1.22**). Attempts to study 1,2-pyridyne (**1.23**, alternatively represented as the 2-pyridyl cation) in solution have been unsuccessful,[9] however, studies in the gas phase have shown evidence of this species.[10] All of these isomers have long been recognized as promising intermediates for the preparation of substituted pyridines and, collectively, have been the target of much synthetic effort.[11,12]

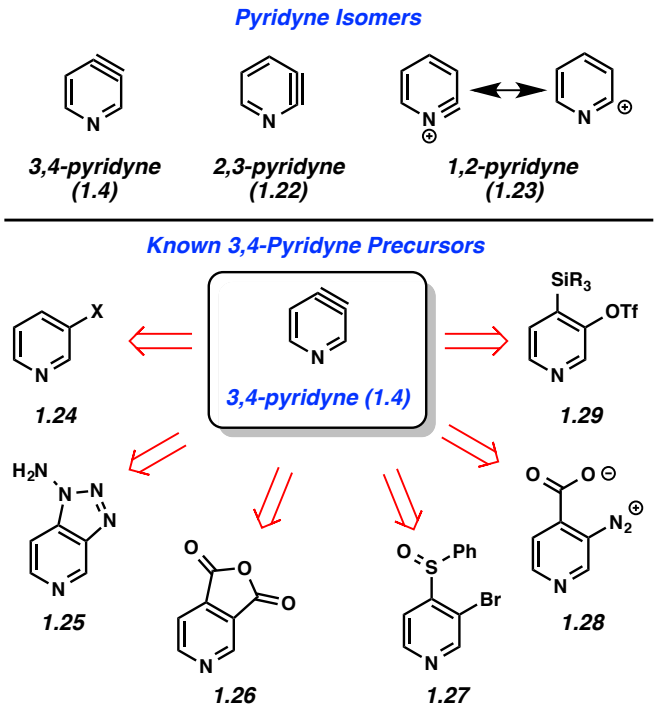


***Figure 1.5.*** Pyridyne Isomers and Methods of Generation

The 3,4-pyridyne can be used to illustrate the wide range of methods typically used to generate arynes. Most of the methods are derived from analogous precursors to *o*-benzyne, illustrating that similar strategies could be applicable for the generation of other hetarynes. For example, 3,4-pyridyne (**1.4**) is accessible from 3-halopyridines upon treatment with strong base (**1.24** → **1.4**),[13] oxidation of aminotriazoles with $Pb(OAc)_4$ (**1.25** → **1.4**),[14] photolysis of anhydrides (**1.26** → **1.4**),[15] magnesium-sulfur exchange followed by elimination (**1.27** → **1.4**),[16] thermolysis of diazonium carboxylates (**1.28** → **1.4**),[17] or fluoride-induced elimination of *ortho*-trialkylsilyl pyridyl triflates (**1.29** → **1.4**).[18] Of note, this latter method, which was first pioneered by Kobayashi for *o*-benzyne generation,[19] has demonstrated the most functional group tolerance in terms of both the trapping agents that can be utilized and the substituents present on the precursors. Although there is always the possibility that some precursors may react through non-

aryne mechanisms, the isolation of pyridyne **1.4** in an $N_2$ matrix and subsequent characterization by IR spectroscopy[20] demonstrated that pyridyne **1.4** is a valid intermediate.

The 3,4-pyridyne has been demonstrated to be useful for the preparation of 3- and 4-substituted pyridines as well as 3,4-disubstituted derivatives.[21] Leake and Levine reported the first generation of 3,4-pyridyne (**1.4**) utilizing 3-bromopyridine (**1.30**),[22] which upon treatment with acetophenone and sodium amide in liquid ammonia gave low yields of 4-aminopyridine (**1.31**) and adduct **1.32**, the latter of which arises from attack by the enolate of acetophenone (Figure 1.6). Many early studies that relied on dehydrohalogenation for pyridyne generation were limited in the scope of the trapping agent employed. In order to minimize the byproducts resulting from attack by the base used for pyridyne generation, strongly nucleophilic groups such as alkoxides, amide salts, and thiolates were often employed. In an example of the latter reported by Zoltewicz, treatment of bromopyridine **1.30** with sodium methanethiolate and sodium amide led to an equimolar mixture of adducts **1.33a** and **1.33b**.[23] This lack of regioselectivity is characteristic of pyridyne **1.4**, and has limited the synthetic utility of this intermediate.

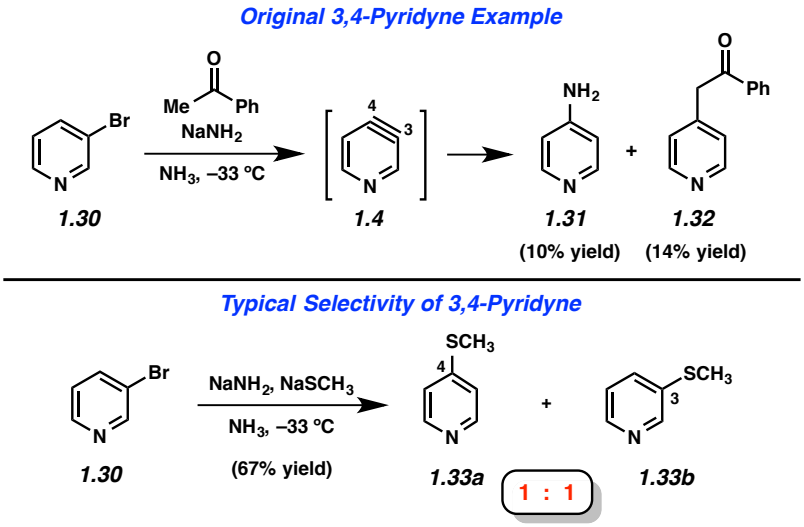


***Figure 1.6.*** Examples of 3,4-Pyridyne Studies

Several studies have focused on the development of methods to control regioselectivity in reactions of 3,4-pyridynes,[18, 24] and include a report by our laboratory in 2013, which systematically explored the use of substituents to control selectivity via aryne distortion.[25] We prepared three pyridyne precursors, **1.34**, **1.36**, and **1.38**, and then performed a series of pyridyne generation and trapping experiments (Figure 1.7). For example, using 3,4-pyridyne precursor **1.34** in a nitrone cycloaddition yielded products **1.35a** and **1.35b** in a 1.9 to 1 ratio. However, by employing the sulfamoylated precursor **1.36** in the corresponding reaction, higher regioselectivity could be achieved favoring attack at C4. In a complementary sense, selectivity could be reversed by use of the brominated precursor **1.38** in the aryne trapping experiment to now favor attack at C3. Of note, after performing aryne trapping experiments of silyltriflates **1.36** and **1.38**, the sulfamate and bromides remaining may be used in Ni- or Pd-catalyzed cross-coupling experiments.[26,27] For example, after performing pyridyne trapping experiments with 1,3-dimethyl-2-imidazolidinone,[28] similar to trapping experiments recently report by Sato and

coworkers,[29] **1.40** and **1.41** were obtained using catalytic C–C and C–N bond forming processes. Pyridyne precursors **1.34** and **1.38** are now available commercially.[30]

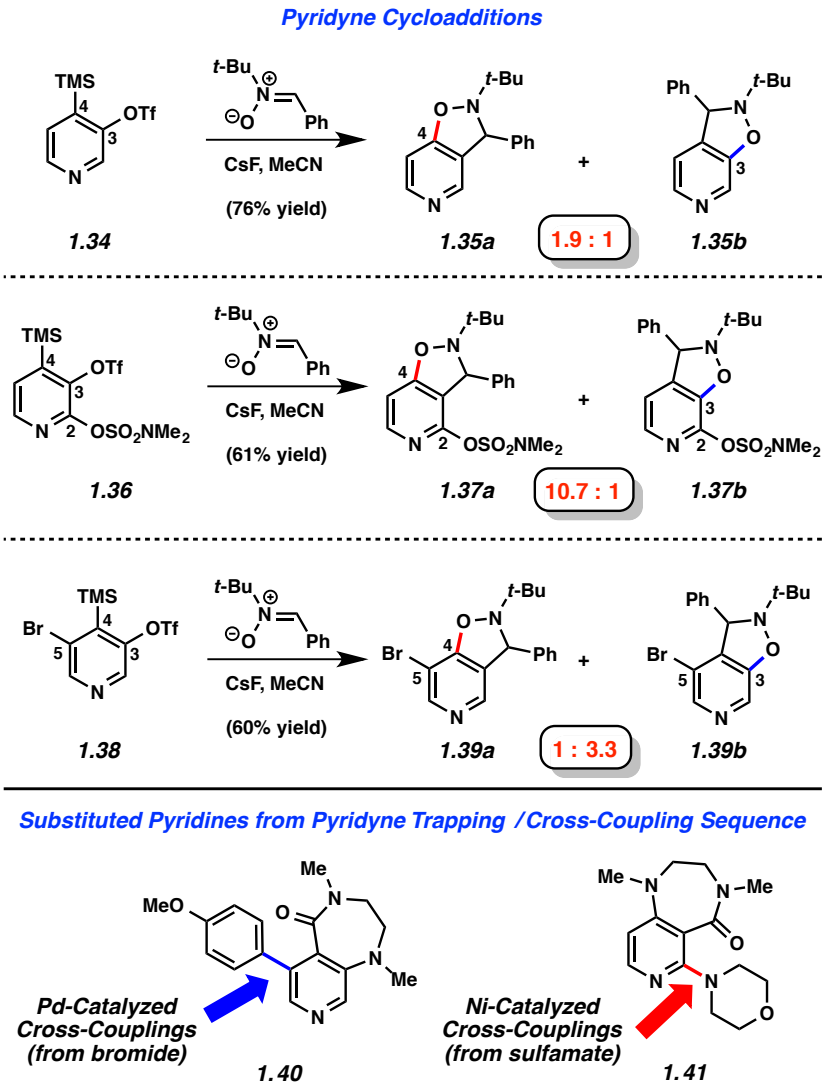


***Figure 1.7.*** Our laboratory's 3,4-Pyridyne Studies

Early attempts to generate the 2,3-pyridyne (**1.22**) were more ambiguous than those targeting the 3,4-pyridyne (Figure 1.8). Dehydrohalogenation cannot be easily utilized, as 3-halopyridine precursors (e.g., **1.30**, Figure 1.6) have been shown to lead to formation of the 3,4-pyridyne (**1.4**) selectively,[13] and the use of 2-halopyridines makes it difficult to determine whether products arise through an aryne pathway or through an $S_NAr$ pathway. However, in

1962, Martens and den Hertog demonstrated that treatment of dihalide **1.42** with lithium amalgam in the presence of furan led to the isolation of quinoline (**1.44**) in moderate yield.[31] The formation of this product was rationalized by a pathway involving 2,3-pyridyne (**1.22**) formation, cycloaddition to give **1.43**, followed by reduction. The development of silyltriflate precursor **1.45**, which is now commercially available,[30] has allowed for a reliable means of generating the 2,3-pyridyne under mild conditions[32] and can be used to demonstrate the high regioselectivity that is typically observed in these reactions. Treatment of precursor **1.45** with CsF leads to aryne **1.22**, which undergoes attack by *N*-Me-aniline to exclusively give the 2-amino product **1.46**.[33] The high selectivity typically obviates the need to separate isomeric products, and can be used to form 2,3-disubstituted pyridines. Additionally, **1.50** was obtained through a formal C–N bond insertion reaction between pyridyne **1.49** into carbamate **1.48**.[29]

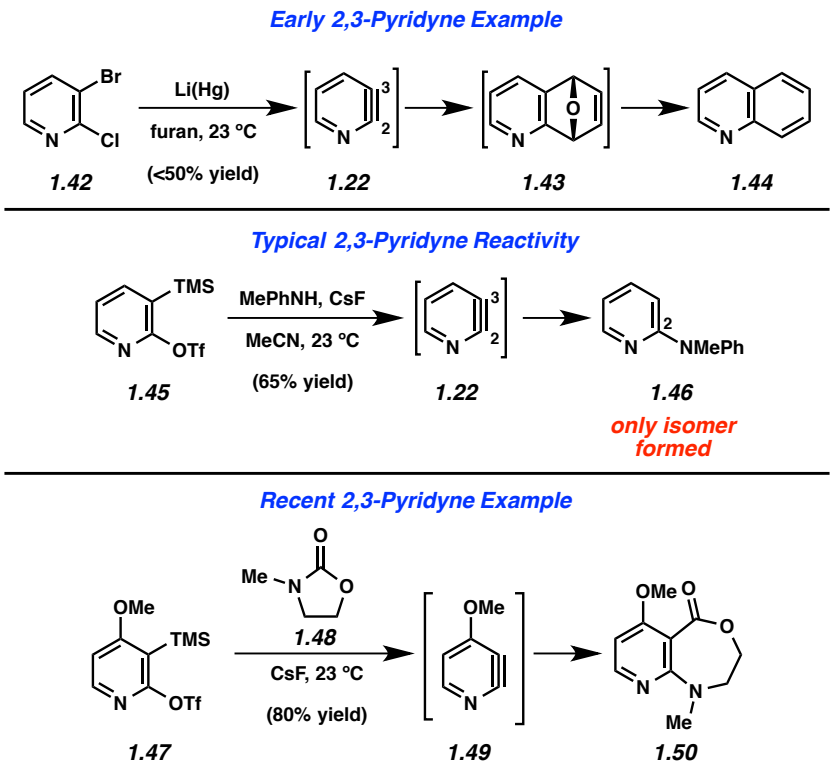


***Figure 1.8.*** Examples of 2,3-Pyridyne Studies

### 1.3.2 Indolyne Methodology

Given the importance of the indole heterocycle, attempts to utilize the corresponding indolyne to prepare substituted indole derivatives has received significant attention. Of the four possible indolyne isomers, three contain the reactive triple bond within the benzenoid ring (**1.3**, **1.51**, and **1.52**, Figure 1.9), whereas the 2,3-indolyne (**1.53**) contains the triple bond in the pyrrole ring. The first report concerning indolynes came from Julia and coworkers, who in 1967 showed that treatment of 5-bromoindole (**1.54**) with potassium amide led to a mixture of 4- and 5-aminoindole products (**1.56a** and **1.56b**), likely arising through indolyne intermediate **1.55**.[34] Despite the promise demonstrated by this early work,[35] indolynes saw little attention over the

subsequent 40 years.[36] In a series of reports beginning in 2007, Buszek and co-workers reported elegant studies of indolyne Diels–Alder reactions.[37]

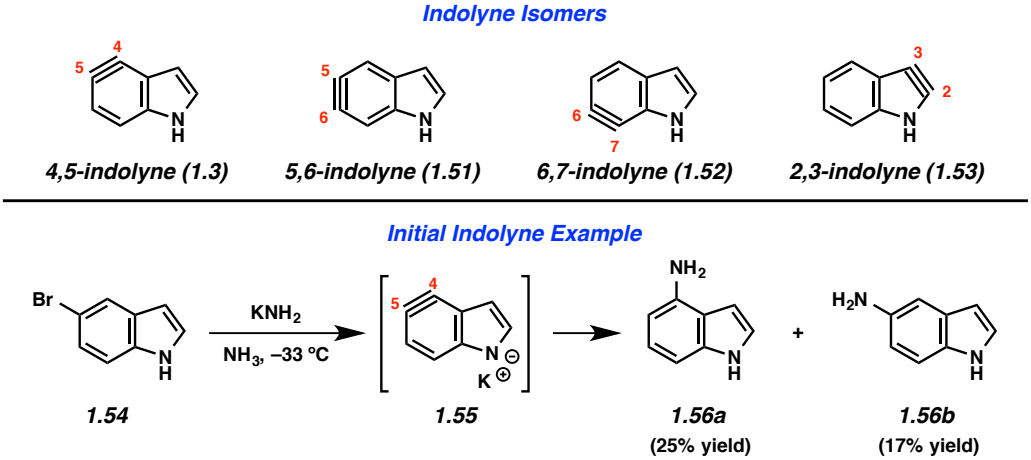


***Figure 1.9.*** Indolyne Isomers and Seminal Indolyne Example

Our laboratory has focused on mild methods for indolyne generation and trapping, with the hope that indolynes could be better exploited by synthetic chemists. We have shown that 4,5-, 5,6-, and 6,7-indolynes **1.57**–**1.59** can be generated from silyltriflate precursors **1.60**–**1.62**, respectively (Figure 1.10).[38] These precursors were accessible as *N*-Me, *N*-Boc, or *N*-H variants for each indolyne isomer and also left C3 available for later functionalization.[38c] Indolyne formation could be achieved upon treatment of the indolyne precursors with fluoride sources such as TBAF or CsF. Buszek has also reported an alternative strategy for the preparation of similar silyltriflate precursors that contain a phenyl substituent at C3.[37b]

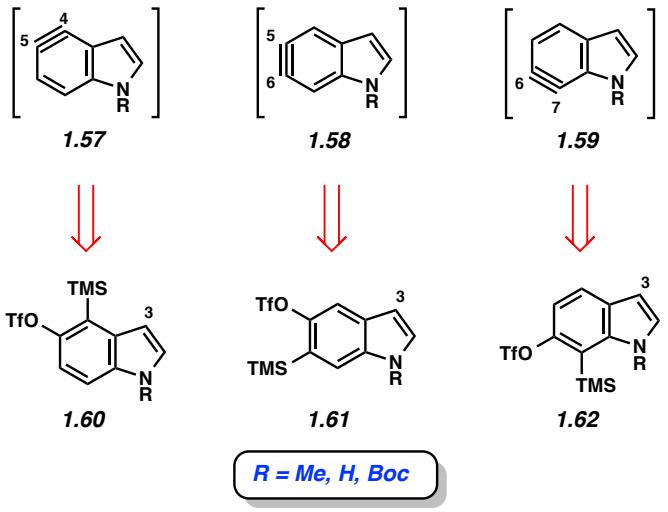


***Figure 1.10.*** Silyltriflates as Indolyne Precursors

The mild fluoride-based conditions for indolyne generation allowed for the scope of trapping agents to be significantly expanded compared to prior indolyne studies. As seen in Figure 1.11, treatment of 4,5-indolyne precursor **1.64** with CsF in the presence of aniline led to the formation of C5 adduct **1.63** preferentially over the formation of the corresponding C4-substituted product in a ratio of 12.5:1. Trapping of the same indolyne with benzyl azide demonstrated the compatibility of cycloaddition reactions and provided triazole product **1.65** and its regioisomer in a 2.4:1 ratio. Further demonstrations of the scope of indolyne reactions can be seen in products **1.66**–**1.69**. The regioselectivity observed in the formation of products **1.63**, **1.65**, **1.68**, and **1.69** was explained using the Aryne Distortion Model.[38b,38c, 39] Generally speaking, both the 4,5- and 5,6-indolynes preferentially give products resulting from initial attack at C5, while the 6,7-indolyne typically gives products resulting from attack at C6.

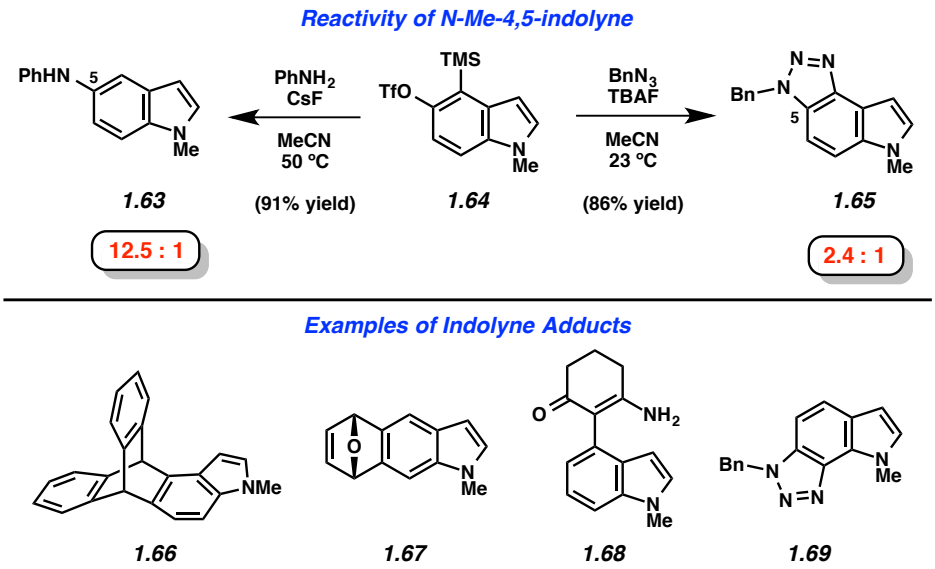


***Figure 1.11.*** Sample Reactivity of Indolyne Intermediates

Recent reports of indolynes and related species have further demonstrated the utility of these hetarynes for the assembly of complex indole derivatives. Lautens and coworkers reported that treatment of bromoindole **1.70** with LDA led to the generation of 6,7-indolyne **1.71** (Figure 1.12). This species was found to undergo an intramolecular ene reaction involving the homoprenyl group on the indole nitrogen to afford tricyclic product **1.72**.[40] Interestingly, the observed regioselectivity is due to the fact that the homoprenyl group is tethered to the indole nitrogen.

The Hoye group has recently reported a novel method for the generation of arynes in which a molecule containing three alkynes undergoes a "Hexadehydro Diels–Alder (HDDA) Reaction" to provide the reactive intermediate.[41] The authors demonstrated that molecules such as tri-yne **1.73** could be used to form indolinyne **1.74**, which further reacted to furnish product **1.75** (Figure 1.12).[41a] Of note, this reaction can be used to prepare indoline systems in which the benzenoid ring is fully substituted. Almost simultaneously, Lee and coworkers have reported a

nearly identical strategy for the generation of indolinynes and explored a variety of reactions of these species.[42]

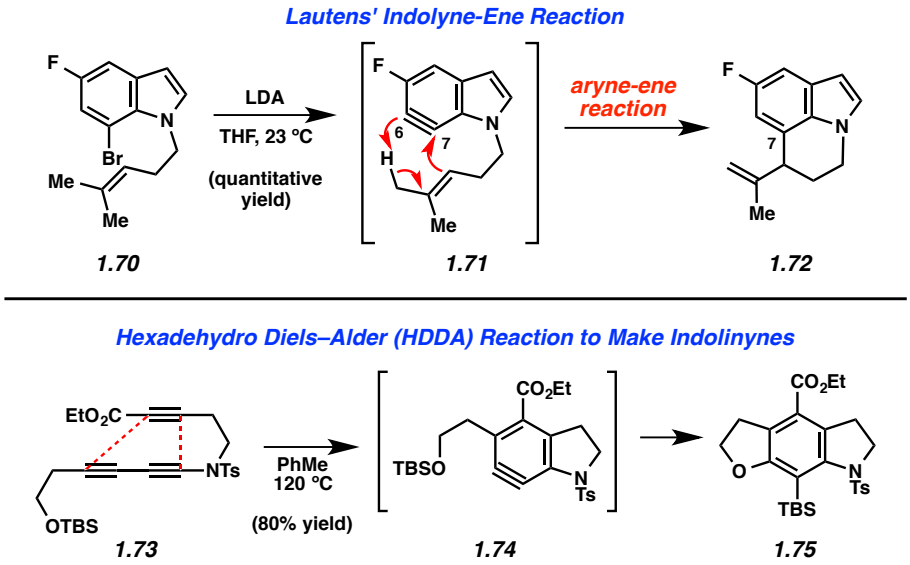


***Figure 1.12.*** Recent Examples of Indolyne Reactivity and Indolinyne Generation

In contrast to the benzenoid indolyne isomers discussed above, the 2,3-indolyne (**1.53**, Figure 1.13) likely experiences extreme strain due to the presence of the triple bond within the five-membered ring. Gribble has reported an extensive study of unsuccessful attempts to generate **1.53**[43] and, while there are claims of this intermediate being involved in reactions,[44] unambiguous evidence has yet to be offered. In fact, there have been many attempts over the years to generate various 5-membered hetarynes, however, most claims are lacking in conclusive proof.[1b] In addition to the 2,3-indolyne (**1.53**), attempts to generate the 3,4-pyrrolyne (**1.76**) have been made, resulting only in < 5% yield of any products suggestive of an aryne mechanism.[45] The strongest case for formation of any of the 5-membered hetarynes can be made for thiophynes **1.77**–**1.79**, especially the 3,4-thiophyne (**1.78**).[46] It was suggested that the longer C–S bond would help relieve some of the strain present in these molecules compared to other 5-

membered hetarynes. Unfortunately, isolated yields of cycloadducts suggestive of **1.78** are ≤ 30%. Thus, although these species may be accessible, their synthetic utility is currently limited.

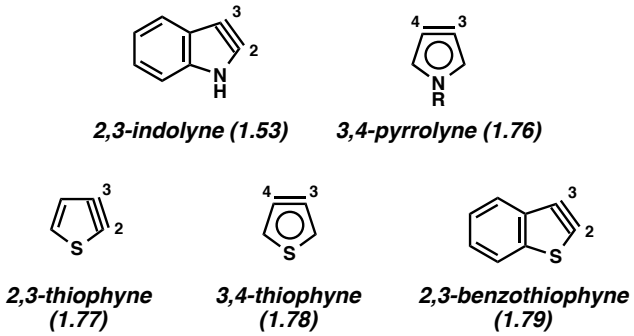


***Figure 1.13.*** 2,3-Indolyne and other 5-Membered Hetarynes

## 1.4 Use of Hetarynes in Total Synthesis

Despite early limitations, hetarynes are now useful tools for the total synthesis of complex molecules. Many of the targets that have been accessed using hetaryne chemistry are shown in Figure 1.14. Indolynes (or related species) have found use in the synthesis of C4-substituted indole derivatives,[47] including lysergic acid (**1.80**),[35c] various makaluvamines (**1.81**),[36] and members of the welwitindolinone (**1.82**)[48] and indolactam (**1.83**)[49] alkaloid families. All of these syntheses utilize the electrophilic nature of the indolyne to functionalize C4 of the indole ring, a position that is often difficult to access. Additionally, the indole diterpenoid, tubingensin A (**1.84**) was prepared by our laboratory using a related carbazolyne intermediate.[50] Finally, indolynes have been utilized as cycloaddition partners for the synthesis of *cis*-trikentrin A (**1.85**) and herbindole B (**1.86**).[37c,e] Pyridynes have found use mainly as cycloaddition partners for the synthesis of molecules such as ellipticine (**1.87**)[24b,d,51] and macrostomine (**1.88**),[52] but also for intramolecular arylation reactions to build perlolidine (**1.89**)[53] and eupolauramine (**1.90**).[54]

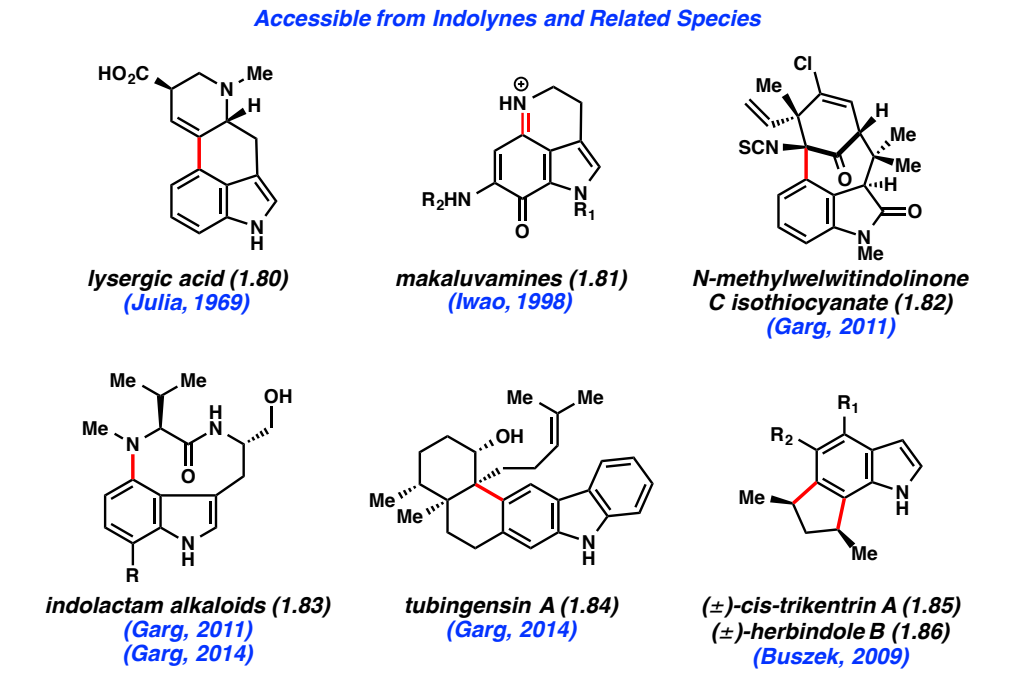


***Figure 1.14.*** Natural Products Synthesized using Heterocyclic Arynes

Pyridynes have a rich history in total synthesis dating back to the seminal report by Singh and coworkers in 1976 on the synthesis of the grass alkaloid perlolidine (**1.89**, Scheme 1.1).[53] Starting from readily available 2-amino-3-methylpyridine (**1.91**), the authors were able to quickly access compound **1.92**. Exposure of this compound to standard aryne-forming conditions resulted in formation of the biaryl linkage to provide **1.94** in good yield. It is proposed that the aniline ring in compound **1.92** undergoes a Friedel–Crafts type intramolecular arylation reaction

with the highly reactive tethered pyridyne (see transition structure **1.93**). Compound **1.94** was successfully elaborated to perlolidine (**1.89**) by oxidation, followed by benzyl ether cleavage.

***Scheme 1.1.*** Singh's Synthesis of Perlolidine (**1.89**)

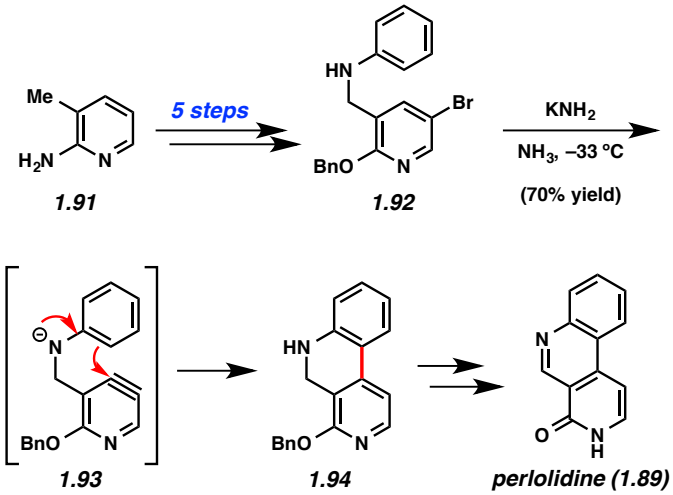


Another prominent example utilizing pyridynes in total synthesis comes from studies of ellipticine (**1.87**), which has been targeted by multiple groups.[24b,d,51] In an exciting approach, Guitián examined the effect of employing substituted 3,4-pyridynes as the dienophile with a variety of dienes (Scheme 1.2).[24b,d] Although other substituted pyridynes showed variable levels of selectivity depending on the diene present, when 2-chloro-3,4-pyridyne precursor **1.95** was reacted with CsF and decorated furan **1.96**, the desired regioisomer **1.97** was formed as the major product.[55] Compound **1.97** was then elaborated to ellipticine (**1.87**).

***Scheme 1.2.*** Guitián's Synthesis of Ellipticine (**1.87**)

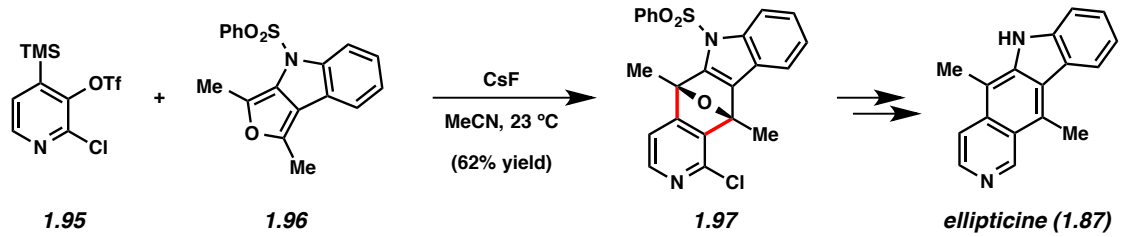


Likewise, indolynes and related intermediates have been judiciously exploited in total synthesis. A seminal example was reported by Julia and coworkers in their formal synthesis of lysergic acid (**1.80**) in 1969 (Scheme 1.3).[35c] The authors found that treatment of 5-bromoindoline **1.98** with $NaNH_2$ led to cyclized product **1.100** in a modest 15% yield. Tetracycle **1.100** presumably arises from attack of the vinylogous enolate onto the C4 position of the indolinyne (see transition structure **1.99**), where the regiochemistry is controlled by geometrical constraints. Of note, the authors reported that the use of C3-*epi*-**1.108** did not provide any of the corresponding product when reacted under the same conditions. Tetracycle **1.110** could be elaborated to the natural product following the procedure reported by Woodward and coworkers.[56] Despite the low yield in the key aryne step, this synthesis validated the notion that indolyne-type intermediates could be used to build complex heterocyclic compounds.

***Scheme 1.3.*** Julia's Formal Synthesis of Lysergic Acid (**1.80**)

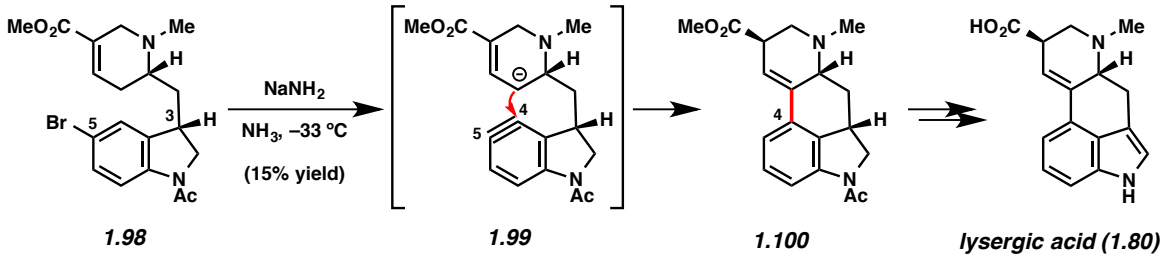

As mentioned earlier, our laboratory has been interested in the development of indolyne methodology, and we have recently employed these intermediates in several total syntheses. One class of compounds that appeared ideally suited for a test of indolyne methodology was the indolactam alkaloids (e.g., Figure 1.15, **1.101**–**1.104**).[57] These compounds have been widely studied for decades because of their interesting structures and pharmacological properties. Although these compounds are most well known for their use in studies aimed at better understanding tumor growth, indolactam V (**1.101**) is also known to function as a stem cell differentiator.[58] Structurally, these alkaloids are characterized by several unique features including a conformationally-flexible 9-membered lactam and a 3,4-disubstituted indole core. Additionally, compounds **1.102**–**1.104** possess $sp^2$–$sp^3$ linkages at C7, which present a significant challenge for synthesis.

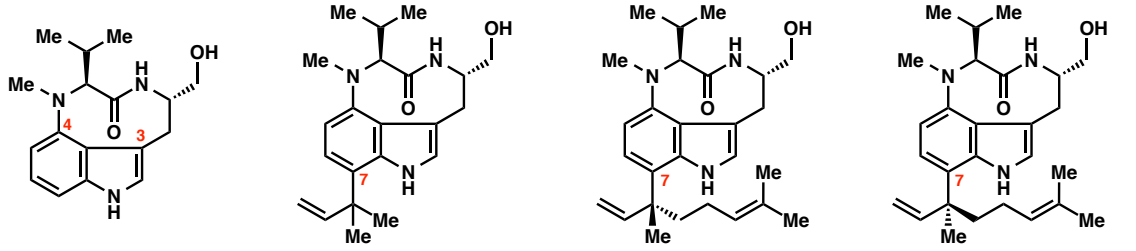


***Figure 1.15.*** Representative Indolactam Alkaloids **1.101**–**1.104**

With the goal of accessing the four natural products **1.101**–**1.104** through common late-stage intermediates, we first pursued an efficient means to assemble the common core of these targets (Scheme 1.4).[49] Beginning from commercially available 5-benzyloxyindole (**1.105**), we were able to access multi-gram quantities of bromosilyltriflate **1.106**. Of note, this efficient

conversion proceeded in 7 steps with an overall yield of 62%. With silyltriflate **1.106** in hand, we were poised to build the C4–N linkage using indolyne chemistry. We found that exposure of silyltriflate **1.106** to CsF and peptide **1.107** furnished adduct **1.109** in 75% yield, presumably by way of 4,5-indolyne intermediate **1.108**. Although 4,5-indolynes typically react to give products of C5 substitution, the presence of the C6 bromide in **1.108** overturns the usual preference by perturbing the distortion of the aryne.[49a] Indolyne adduct **1.109** could be elaborated to the natural product **1.101** in several steps including reductive removal of the aryl bromide and ring closure at C3.

***Scheme 1.4.*** Total Synthesis of (–)-Indolactam V (**1.101**)

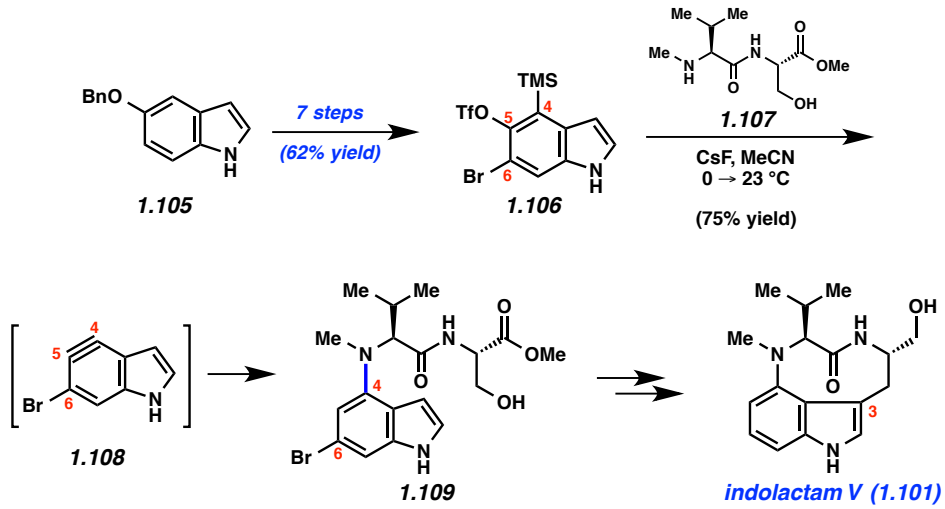


Having synthesized indolactam V (**1.101**) using indolyne methodology, we used **1.101** as a stepping-stone toward indolactam alkaloids **1.102**–**1.104** (Figure 1.16).[49b] To access pendolymycin (**1.102**), **1.101** was elaborated to bromide **1.110** using a simple two-step sequence. We then surveyed a variety of reaction conditions to assemble the critical $sp^2$–$sp^3$ linkage at C7. We were delighted to find that bromide **1.110** underwent coupling with zinc enolate **1.111** to

furnish **1.112** in 61% yield using Hartwig's enolate coupling methodology.[59] It is notable that this complexity-generating reaction proceeds smoothly, despite the presence of a tertiary amine and the free NHs present in **1.110**. From **1.112**, a three-step sequence involving amide reduction with Schwartz's reagent, olefination of the resulting aldehyde, and deprotection of the primary alcohol furnished pendolmycin (**1.112**). An analogous approach was used to prepare lyngbyatoxin A (**1.113**), in addition to its congener teleocidin A-2 (**1.114**) as suggested in Figure 1.16.

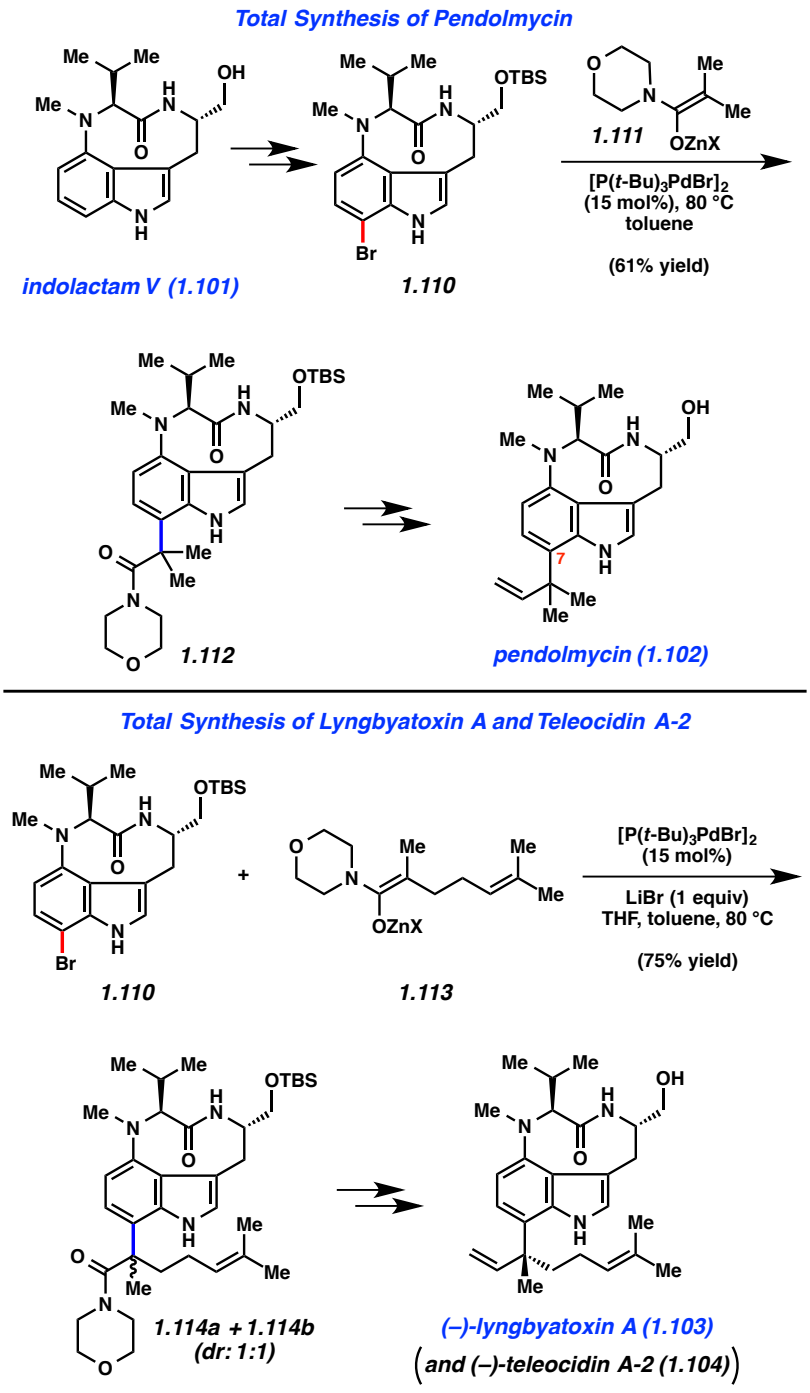


***Figure 1.16.*** Synthesis of C7 Substituted Indolactam Alkaloids

In a more recent example, our laboratory has reported what is arguably one of the most complex aryne cyclizations to date while pursuing the welwitindolinone alkaloids that bear a

bicyclic [4.3.1] core (e.g., **1.82** and **1.115–1.119**, Figure 1.17). The isolation of these compounds was reported by Moore and co-workers through two publications in 1994 and 1999.[60] Although the structures of these compounds are relatively compact, these natural products bear highly functionalized cores that pose tremendous challenges to synthetic chemists. Over the past two decades, at least fifteen laboratories have reported approaches toward these captivating natural products[61] and several recent total syntheses have been reported.[62,63,48]

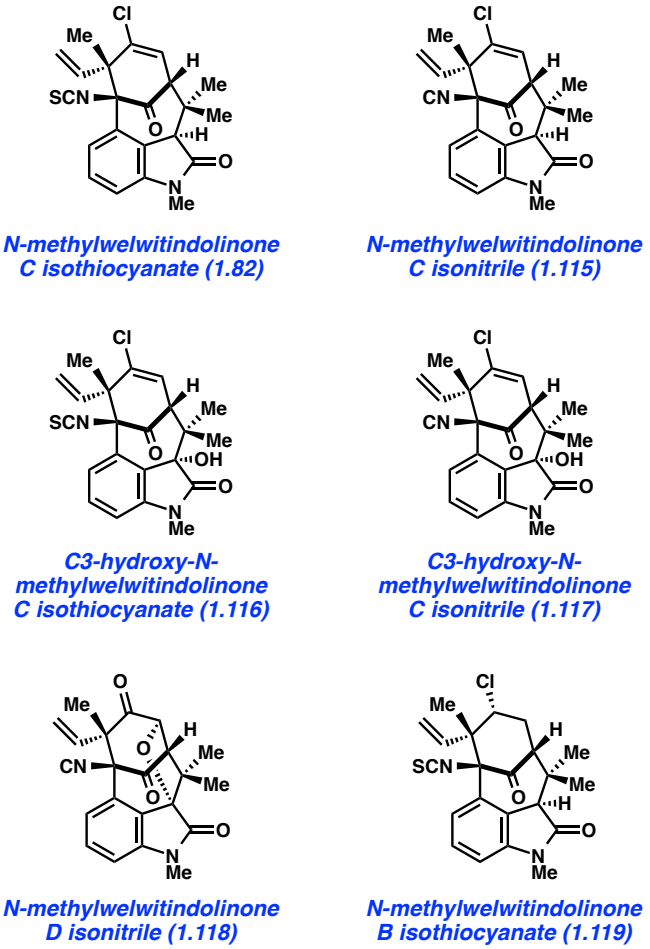


***Figure 1.17.*** [4.3.1]-Bicyclic Welwitindolinone Natural Products

As shown in Scheme 5, our synthesis began from known enone **1.120**, which is prepared using a modification of Natsume's five-step procedure reported in the enantiomeric series.[64]

Cleavage of the pivalate ester, followed by iodine-catalyzed conjugate addition of 5-bromo-*N*-methylindole provided indole **1.121** in 54% yield over two steps. Silyl protection of the alcohol then furnished TBS ether **1.122**, the key substrate for constructing the complex [4.3.1]-bicyclic core. Exposure of bromoindole **1.122** to the complex base conditions first developed by Caubere[65] led to generation of intermediate **1.123**, which contains both an enolate and 4,5-indolyne. Cyclization led to the desired *C*-arylated product **1.124** in 33% yield, as well as the corresponding *O*-arylated product in 13% yield. Product **1.124** possesses the necessary tetracyclic core, including the congested linkage at C4 of the indole ring. This intermediate was successfully converted to the elusive natural product *N*-methylwelwitindolinone C isothiocyanate (**1.82**).[48] The indolyne cyclization was subsequently utilized for the synthesis of a number of related family members including isonitrile derivative **1.115** and the C3-hydroxy derivatives **1.116** and **1.117**.[48b] Additionally, indolyne cyclization product **1.124** has been converted to another family member, *N*-methylwelwitindolinone D isonitrile (**1.118**),[48d] which contains an additional ethereal linkage.

***Scheme 1.5.*** Total Synthesis of Welwitindolinone Alkaloids

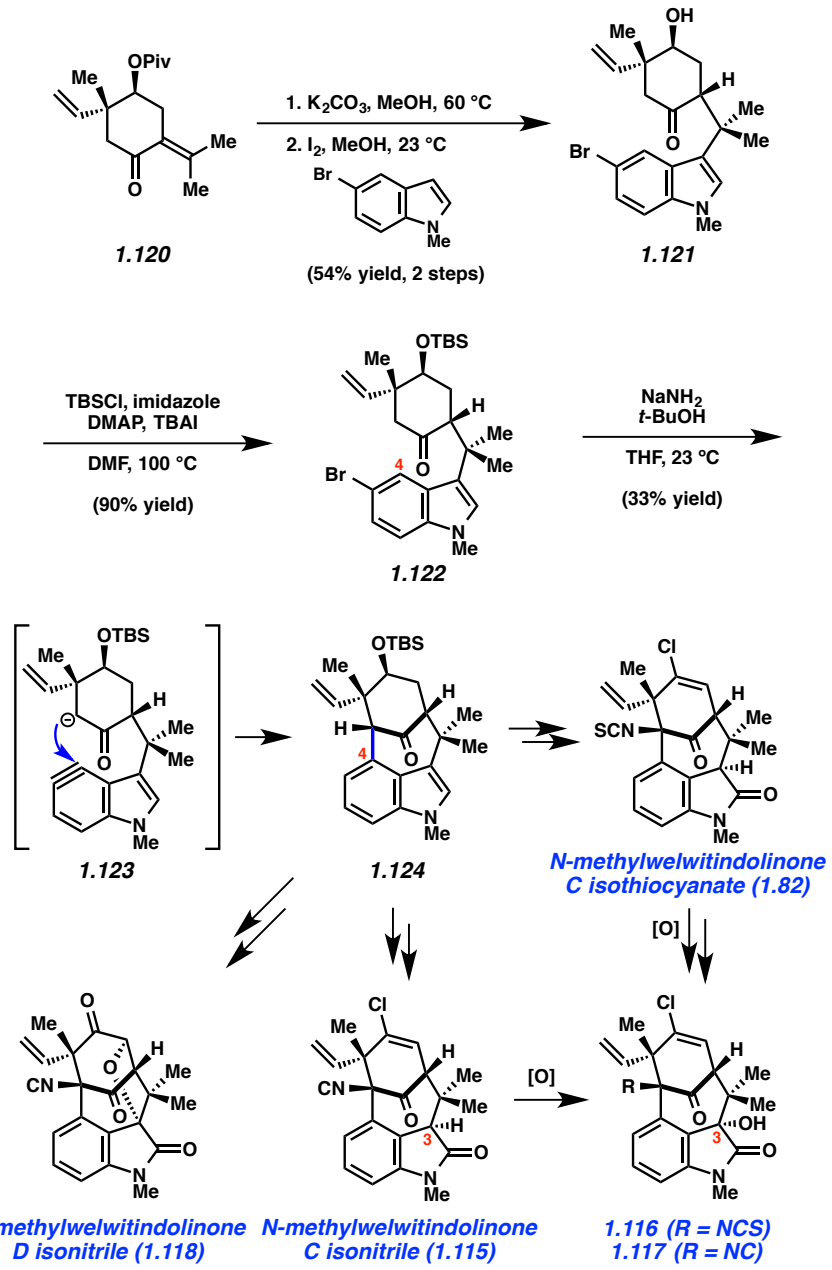


Most recently, we have further tested the viability of using heterocyclic arynes to construct complex scaffolds in our pursuit of the tubingensin natural products (**1.84** and **1.125**, Figure 1.18). Both tubingensins A and B were isolated in 1989 by Gloer and co-workers from the fungus *Aspergillus tubingensis*.[66,67] In addition to possessing interesting biological activities

(e.g., antiviral, anticancer properties), these compounds have unique and challenging structures. For example, tubingensin A (**1.84**) contains a densely functionalized cis-decalin scaffold, appended to a disubstituted carbazole unit. The decalin contains four stereogenic centers, all of which are contiguous and two of which are vicinal and quarternary. Although arynes have not previously been used to assemble vicinal quaternary stereocenters, we envisioned the use of a 'carbazolyne' intermediate to achieve this goal and ultimately establish the tubingensin A skeleton.[50,68]

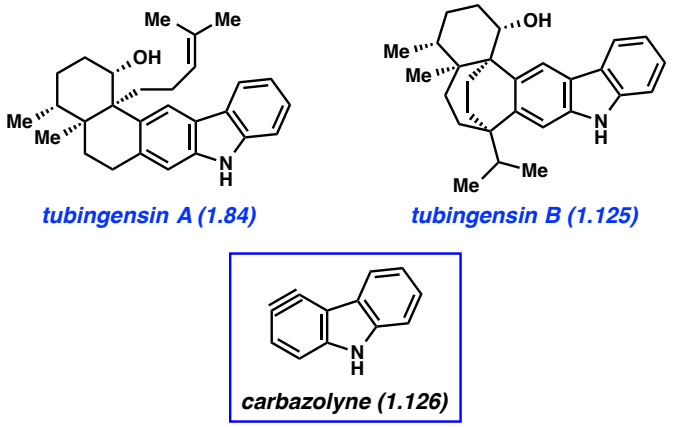


***Figure 1.18.*** Tubingensins A and B

Our concise total synthesis of tubingensin A (**1.84**) is summarized in Scheme 1.6. Beginning from silyl enol ether **1.127**, which was readily obtained from (+)-dihydrocarvone, we implemented a hydroboration β-alkyl Suzuki–Miyaura coupling sequence. Thus, **1.127** was first treated with 9-BBN to generate the requisite alkyl boron intermediate. Subsequent coupling with bromotriflate **1.128** in the presence of catalytic $Pd(PPh_3)_4$ furnished product **1.129** in 64% yield. Of note, neither the bromide or silyl enol ether were disturbed in this transformation. With the C12–C13 linkage intact, **1.129** was elaborated to silyl enol ether **1.130** in three steps. In the critical carbazolyne cyclization (see transition structure **1.131**), exposure of **1.130** to $NaNH_2$/*t*-

BuOH delivered the desired product **1.132** in 84% yield. The transformation proceeds with complete diastereoselectivity and, importantly, introduces the challenging vicinal quaternary stereocenters of the natural product. Finally, a deprotection / reduction sequence furnished the natural product **1.84**. The total synthesis of tubingensin A (**1.84**) requires only 9 steps (longest linear sequence), beginning from known compounds, and highlights the efficiency by which heterocyclic arynes may be used to build stereocenter-rich architectures.

***Scheme 1.6.*** Total Synthesis of (+)-Tubingensin A (**1.84**)

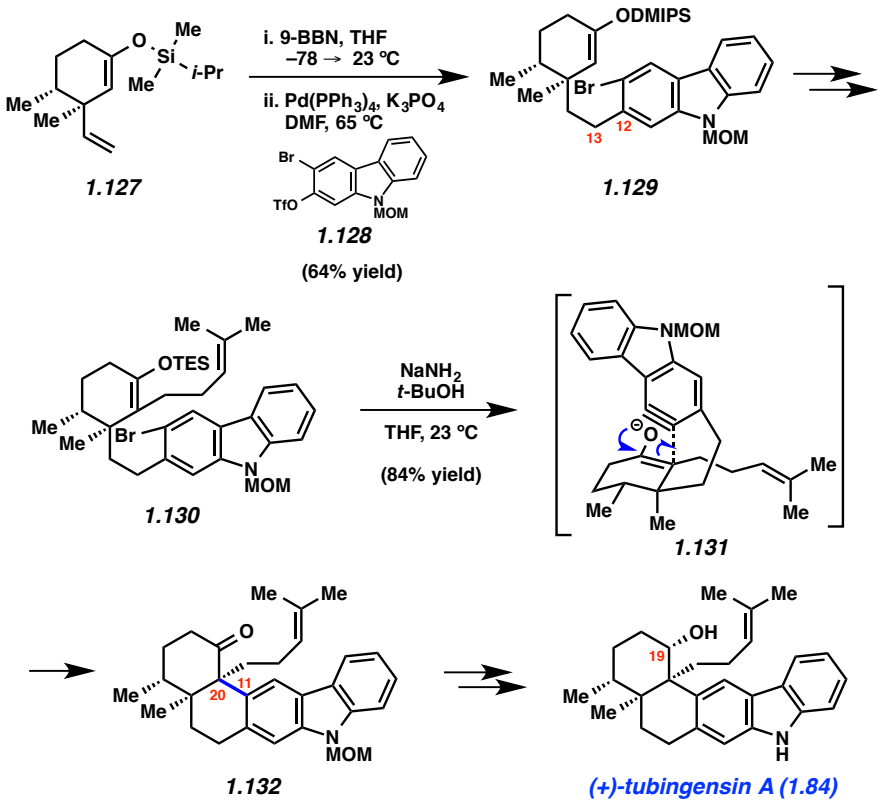

## 1.5 Conclusions

Over the last 60 years, the chemistry of heterocyclic arynes has lagged behind that of their all-carbon counterparts such as *ortho*-benzyne. Although many of the early claims were questionable regarding the generation of these reactive intermediates, more recent studies have demonstrated that these species are not only accessible, but offer a unique alternative for the synthesis of substituted heterocycles. The increasing popularity of easy-to-handle precursors, such as *o*-trimethylsilyl triflates, allow for the generation of hetarynes under mild conditions that allow for a significantly expanded scope of trapping agents to be employed. In fact, some heterocyclic aryne silyltriflate precursors are now commercially available. Additionally, the high reactivity of hetarynes can be exploited for the construction of complex motifs that would otherwise be difficult to access. It is envisioned that the development of even more exotic heterocyclic arynes and trapping agents will be seen in the future, along with more challenging applications in the synthesis of drugs and natural products.

## 1.6 Notes and References


[1] For reviews of hetarynes, see: (a) Kauffmann, T. *Angew. Chem. Int. Ed.* **1965**, *4*, 543–618. (b) Reinecke, M. G. *Tetrahedron* **1982**, *38*, 427–498. (c) Bronner, S. M.; Goetz, A. E. Garg, N. K. *Synlett* **2011**, 2599–2604. (d) Goetz, A. E.; Garg, N. K. *J. Org. Chem.* **2014**, *79*, 846–851.

[2] For reviews of *ortho*-benzyne, see: (a) Dubrovskiy, A. V.; Markina, N. A.; Larock, R. C. *Org. Biomol. Chem.* **2013**, *11*, 191–218. (b) Tadross, P. M.; Stoltz, B. M. *Chem. Rev.* **2012**, *112*, 3550–3577. (c) Gampe C. M.; Carreira, E. M. *Angew. Chem. Int. Ed.* **2012**,

*51*, 3766–3778; (d) Bhunia, A.; Yetra S. R.; Biju, A. T. *Chem. Soc. Rev.* **2012**, *41*, 3140–3152. (e) Sanz, R. *Org. Prep. Proced. Int.* **2008**, *40*, 215–291. (f) Pellisier, H.; Santelli, M. *Tetrahedron* **2003**, *59*, 701–730.

[3] Stoermer R.; Kahlert, B. *Ber.* **1902**, *35*, 1633–1640.

[4] (a) Gilman, H.; Avakian, S. *J. Am. Chem. Soc.* **1945**, *67*, 349–351. (b) Gilman H.; Kyle, R. H. *J. Am. Chem. Soc.* **1948**, *70*, 3945–3946. (c) Benkeser, R. A.; Severson, R. G. *J. Am. Chem. Soc.* **1949**, *71*, 3838–3839. (d) Benkeser, R. A.; Buting, W. E. *J. Am. Chem. Soc.* **1952**, *74*, 3011–3014.

[5] Roberts, J. D.; Simmons, Jr., H. E.; Carlsmith, L. A.; Vaughan, C. W. *J. Am. Chem. Soc.* **1953**, *75*, 3290–3291.

[6] (a) Huisgen R.; Rist, H. *Naturwissenschaften* **1954**, *41*, 358–359. (b) Huisgen, R.; Rist, H. *Justus Liebigs Ann. Chem.* **1955**, *594*, 137–158.

[7] Wittig, G.; Pohmer, L. *Angew. Chem.* **1955**, *67*, 348.

[8] (a) Nam, H. H.; Leroi, G. E.; Harrison, J. F. *J. Phys. Chem.* **1991**, *95*, 6514–6519. (b) Debbert, S. L.; Cramer, S. L. *Int. J. Mass Spectrom.* **2000**, *201*, 1–15. (c) Mariet, N.; Ibrahim-Ouali, M.; Parrain, J.-L.; Santelli, M. *J. Mol. Struct.: THEOCHEM* **2004**, *679*, 53–58. (d) Rau, N. J.; Wenthold, P. G. *J. Phys. Chem. A* **2011**, *115*, 10353–10362. (e) Sánchez-Sanz, G.; Alkorta, I.; Trujillo, C.; Elguero, J. *Tetrahedron* **2012**, *68*, 6548–6556.

[9] Bunnett J. F.; Singh, P. *J. Org. Chem.* **1981**, *46*, 4567–4569.

[10] (a) Gozzo, F. C.; Eberlin, M. N. *J. Org. Chem.* **1999**, *64*, 2188–2193. (b) Sparrapan, R.; Mendes, M. A.; Carvalho, M.; Eberlin, M. N. *Chem. Eur. J.* **2000**, *6*, 321–326.

[11] For the corresponding 2,3- and 3,4-pyridyne-*N*-oxides, see: (a) Kato, T.; Niitsuma, T. *Chem. Pharm. Bull.* **1965**, *13*, 963–968. (b) Martens, R. J.; den Hertog, H. J. *Recl. Trav. Chim. Pays–Bas* **1967**, *86*, 655–669. (c) Kato, T. Niitsuma, T. *Heterocycles* **1973**, *1*, 233–236.

[12] For studies pertaining to the related quinolynes, see references 29, 33, and the following: (a) Kauffmann, T.; Boettcher, F.-P.; Hansen, J. *Justus Liebigs Ann. Chem.* **1962**, *659*, 102–109. (b) Grig-Alexa, I.-C.; Garnier, E.; Finaru, A.-L.; Ivan, L.; Jarry, C.; Léger, J.-M.; Caubère, P.; Guillaumet, G. *Synlett* **2004**, 2000–2004. (c) Collis, G. E.; Burrell, A. K. *Tetrahedron Lett.* **2005**, *46*, 3653–3656. (d) Pangamte, H. N.; Lyngdoh, R. H. D. *J. Phys. Chem. A* **2010**, *114*, 2710–2726.

[13] Treatment of 3-halopyridines has been demonstrated to selectively generate 3,4-pyridyne (**1.4**) over 2,3-pyridyne (**1.22**), see: Zoltewicz, J. A.; Smith, C. L. *Tetrahedron* **1969**, *25*, 4331–4337.

[14] Fleet, G. W. J. Fleming, I. *J. Chem. Soc. C* **1969**, 1758–1763.

[15] Kramer, J. Berry, R. S. *J. Am. Chem. Soc.* **1972**, *94*, 8336–8347.

[16] Furukawa, N.; Shibutani, T.; Fujihara, H. *Tetrahedron Lett.* **1987**, *28*, 2727–2730.

[17] Kauffmann, T.; Boettcher, F.-P. *Chem. Ber.* **1962**, *95*, 949–955.

[18] Tsukazaki, M.; Snieckus, V. *Heterocycles* **1992**, *33*, 533–536.

[19] Himeshima, Y.; Sonoda, T.; Kobayashi, H. *Chem. Lett.* **1983**, *12*, 1211–1214.

[20] Pyridyne **1.4** showed a strong absorbance at 2085 $cm^{-1}$, similar to the signal observed at 2082 $cm^{-1}$ for *o*-benzyne (**1.1**), which is attributed to the C–C triple bond; see: Nam, H.-H.; Leroi, G. E. *J. Am. Chem. Soc.* **1988**, *110*, 4096–4097.

[21] For metal-catalyzed [2+2+2] cycloadditions involving 3,4-pyridynes, see: (a) Iwayama, T.; Sato, Y. *Chem. Commun.* **2009**, 5245–5247. (b) Sato, Y.; Iwayama, T. *Heterocycles* **2010**, *80*, 917–924.

[22] Levine, R.; Leake, W. W. *Science* **1955**, *121*, 780.

[23] Zoltewicz, J. A.; Nisi, C. *J. Org. Chem.* **1969**, *34*, 765–766.

[24] (a) Vinter-Pasquier, K.; Jamart-Grégoire, B.; Caubère, P. *Heterocycles* **1997**, *45*, 2113–2129. (b) Díaz, M. T.; Cobas, A.; Guitián, E.; Castedo, L. *Synlett* **1998**, 157–158. (c) Wang, A.; Tandel, S.; Zhang, H.; Huang, Y.; Holdeman, T. C.; Biehl, E. R. *Tetrahedron* **1998**, *54*, 3391–3400. (d) Díaz, M. T.; Cobas, A.; Guitián, E.; Castedo, L. *Eur. J. Org. Chem.* **2001**, 4543–4549.

[25] Goetz, A. E.; Garg, N. K. *Nat. Chem.* **2013**, *5*, 54–60.

[26] For recent reviews of nickel-catalyzed couplings involving C–O bonds, see: (a) Rosen, B. M.; Quasdorf, K. W.; Wilson, D. A.; Zhang, N.; Resmerita, A.-M.; Garg, N. K.; Percec, V. *Chem. Rev.* **2011**, *111*, 1346–1416. (b) Li, B.-J.; Yu, D.-G.; Sun, C.-L.; Shi, Z.-J. *Chem. Eur. J.* **2011**, *17*, 1728–1759. (c) Mesganaw, T.; Garg, N. K. *Org. Process Res. Dev.* **2013**, *17*, 29–39. (d) Yamaguchi, J.; Muto, K.; Itami, K. *Eur. J. Org. Chem.* **2013**, 19–30.

[27] For the Ni-catalyzed amination of aryl sulfamates, see: (a) Ramgren, S. D.; Silberstein, A. L.; Yang, Y.; Garg, N. K. *Angew. Chem. Int. Ed.* **2011**, *50*, 2171–2173. (b) Mesganaw, T.; Silberstein, A. L.; Ramgren, S. D.; Fine Nathel, N. F.; Hong, X.; Liu, P.; Garg, N. K. *Chem. Sci.* **2011**, *2,* 1766–1771. (c) Hie, L.; Ramgren, S. D.; Mesganaw, T.; Garg, N. K.; *Org. Lett.* **2012**, *14*, 4182–4185.

[28] Yoshida, H.; Shirakawa, E.; Honda, Y.; Hiyama, T. *Angew. Chem. Int. Ed.* **2002**, *41*, 3247–3249.

[29] Saito, N.; Nakamura, K.-i.; Shibano, S.; Ide, S.; Minami, M.; Sato, Y. *Org. Lett.* **2013**, *15*, 386–389.

[30] Several silyltriflate hetaryne precursors are available from Aldrich Chemical Co., Inc. The precursors and their product numbers are as follows: 3,4-pyridyne precursor **1.34**: L511633; bromopyridyne precursor **1.38**: L511641; 2,3-pyridyne precursor **1.45**: L511668; **1.60** (R=H) 4,5-indolyne precursor: L511625.

[31] Martens, R. J.; den Hertog, H. J. *Tetrahedron Lett.* **1962**, *3*, 643–645.

[32] Walters, M. A.; Shay, J. J. *Synth. Commun.* **1997**, *27*, 3573–3579.

[33] Fang, Y.; Larock, R. C. *Tetrahedron* **2012**, *68*, 2819–2826.

[34] Julia, M.; Huang, Y.; Igolen, J. *C. R. Acad. Sci., Ser. C* **1967**, *265*, 110–112.

[35] (a) Julia, M.; Le Goffic, F.; Igolen, J.; Baillarge, M. *C. R. Acad. Sci., Ser. C* **1967**, *264*, 118–120. (b) Igolen, J.; Kolb, A. *C. R. Acad. Sci., Ser. C* **1969**, *269*, 54–56. (c) Julia, M.; Le Goffic, F.; Igolen, J.; Baillarge, M. *Tetrahedron Lett.* **1969**, *10*, 1569–1572. (d) Julia, M.; Igolen, J.; Kolb, A. *C. R. Acad. Sci., Ser. C* **1971**, *273*, 1776–1777.

[36] One exception is the work of Iwao and coworkers in the synthesis of a variety of Makaluvamine natural products: Iwao, M.; Motoi, O.; Fukuda, T.; Ishibashi, F. *Tetrahedron* **1998**, *54*, 8999–9010.

[37] (a) Buszek, K. R.; Luo, D.; Kondrashov, M.; Brown, N.; VanderVelde, D. *Org. Lett.* **2007**, *9*, 4135–4137. (b) Brown, N.; Luo, D.; VanderVelde, D.; Yang, S.; Brassfield, A.; Buszek, K. R. *Tetrahedron Lett.* **2009**, *50*, 63–65. (c) Buszek, K. R.; Brown, N.; Luo, D.

*Org. Lett.* **2009**, *11*, 201–204. (d) Garr, A. N.; Luo, D.; Brown, N.; Cramer, C. J.; Buszek, K. R.; VanderVelde, D. *Org. Lett.* **2010**, *12*, 96–99. (e) Brown, N.; Luo, D.; Decapo, J. A.; Buszek, K. R. *Tetrahedron Lett.* **2009**, *50*, 7113–7115. (f) Thornton, P. D.; Brown, N.; Hill, D.; Neuenswander, B.; Lushington, G. H.; Santini, C.; Buszek, K. R. *ACS Comb. Sci.* **2011**, *13*, 443–448. (g) Nerurkar, A.; Chandrasoma, N.; Maina, L.; Brassfield, A.; Luo, D.; Brown, N.; Buszek, K. R. *Synthesis* **2013**, *45*, 1843–1852.

[38] (a) Bronner, S. M.; Bahnck, K. B.; Garg, N. K. *Org. Lett.* **2009**, *11*, 1007–1010. (b) Cheong, P. H.-Y.; Paton, R. S.; Bronner, S. M.; Im, G-Y. J.; Garg, N. K.; Houk, K. N. *J. Am. Chem. Soc.* **2010**, *132*, 1267–1269. (c) Im, G-Y. J.; Bronner, S. M.; Goetz, A. E.; Paton, R. S.; Cheong, P. H.-Y.; Houk, K. N.; Garg, N. K. *J. Am. Chem. Soc.* **2010**, *132*, 17933–17944.

[39] For additional references regarding the aryne distortion model, see references 1c, 1d, 25, and the following: Bronner, S. M.; Mackey, J. L.; Houk, K. N.; Garg, N. K. *J. Am. Chem. Soc.* **2012**, *134*, 13966–13969.

[40] Candito, D. A.; Dobrovolsky, D.; Lautens, M. *J. Am. Chem. Soc.* **2012**, *134*, 15572–15580.

[41] (a) Hoye, T. R.; Baire, B.; Niu, D.; Willoughby, P. H.; Woods, B. P. *Nature* **2012**, *490*, 208–212. (b) Niu, D.; Willoughby, P. H.; Woods, B. P.; Baire, B.; Hoye, T. R. *Nature* **2013**, *501*, 531–534. (c) Chen, J.; Baire, B.; Hoye, T. R. *Heterocycles* **2014**, *88*, 1191–1200. (d) Niu, D.; Hoye, T. R. *Nat. Chem.* **2014**, *6*, 34–40. (e) Hoye, T. R.; Baire, B.; Wang, T. *Chem. Sci.* **2014**, *5*, 545–550. (f) Niu, D.; Wang, T.; Woods, B. P.; Hoye, T. R. *Org. Lett.* **2014**, *16*, 254–257.

[42] (a) Yun, S. Y.; Wang, K.-P.; Lee, N.-K.; Mamidipalli, P.; Lee, D. *J. Am. Chem. Soc.* **2013**, *135*, 4668–4671. (b) Wang, K.-P.; Yun, S. Y.; Mamidipalli, P.; Lee, D. *Chem. Sci.* **2013**, *4*, 3205–3211. (c) Karmakar, R.; Mamidipalli, P.; Yun, S. Y.; Lee, D. *Org. Lett.* **2013**, *15*, 1938–1941. (d) Karmakar, R.; Yun, S. Y.; Wang, K.-P.; Lee, D. *Org. Lett*. **2014**, *16*, 6–9.

[43] Conway, S. C.; Gribble, G. W. *Heterocycles* **1992**, *34*, 2095–2108.

[44] (a) Muller, H. Dissertation, University of Heidelberg, **1964**. (b) Bergman, J.; Eklund, N. *Tetrahedron* **1980**, *36*, 1439–1443.

[45] Liu, J.-H.; Chan, H.-W.; Xue, F.; Wang, Q.-G.; Mak, T. C. W.; Wong, H. N. C. *J. Org. Chem.* **1999**, *64*, 1630–1634.

[46] (a) Ye, X.-S.; Li, W.-K.; Wong, H. N. C. *J. Am. Chem. Soc.* **1996**, *118*, 2511–2512. (b) Reinecke, M. G.; Newsom, J. G.; Chen, L.-J. *J. Am. Chem. Soc.* **1981**, *103*, 2760–2769.

[47] A recent Reaxys search showed >700 natural products contain a C4-substituted indole motif.

[48] (a) Huters, A. D.; Quasdorf, K. W.; Styduhar, E. D.; Garg, N. K. *J. Am. Chem. Soc.* **2011**, *133*, 15797–15799. (b) Quasdorf, K. W.; Huters, A. D.; Lodewyk, M. W.; Tantillo, D. J.; Garg, N. K. *J. Am. Chem. Soc.* **2012**, *134*, 1396–1399. (c) Styduhar, E. D.; Huters, A. D.; Weires, N. A.; Garg, N. K. *Angew. Chem. Int. Ed.* **2013**, *52*, 12422–12425.

[49] (a) Bronner, S. M.; Goetz, A. E.; Garg, N. K. *J. Am. Chem. Soc.* **2011**, *133*, 3832–3835. (b) Fine Nathel, N. F.; Shah, T. K.; Bronner, S. M.; Garg, N. K. *Chem. Sci.* **2014**, *5*, 2184–2190.

[50] Goetz, A. E.; Silberstein, A. L.; Corsello, M. A.; Garg, N. K. *J. Am. Chem. Soc.* **2014**, *136*, 3036–3039.

[51] (a) May, C.; Moody, C. J. *J. Chem. Soc. Chem. Commun.* **1984**, 926–927. (b) Gribble, G. W.; Saulnier, M. G.; Sibi, M. P.; Obaza-Nutaitis, J. A. *J. Org. Chem.* **1984**, *49*, 4518–4523. (c) May, C.; Moody, C. J. *J. Chem. Soc. Perkin Trans. 1* **1988**, 247–250. (d) Sha, C.-K.; Yang, J.-F. *Tetrahedron* **1992**, *48*, 10645–10654.

[52] Enamorado, M. F.; Ondachi, P. W.; Comins, D. L. *Org. Lett.* **2010**, *12*, 4513–4515.

[53] (a) Kessar, S. V.; Gupta, Y. P.; Pahwa, P. S.; Singh, P. *Tetrahedron Lett.* **1976**, *17*, 3207–3208. (b) Kessar, S. V.; Singh, P. *Indian J. Chem., Sec. B* **2001**, *40B*, 1129–1131.

[54] Hoarau, C.; Couture, A.; Cornet, H.; Deniau, E.; Grandclaudon, P. *J. Org. Chem.* **2001**, *66*, 8064–8069.

[55] A mixture of cycloaddition adducts was obtained in a 2.4:1 ratio.

[56] Kornfeld, E. C.; Fornefeld, E. J.; Kline, G. B.; Mann, M. J.; Morrison, D. E.; Jones, R. G.; Woodward, R. B. *J. Am. Chem. Soc.* **1956**, *78*, 3087–3114.

[57] For pertinent reviews on (–)-indolactam V isolation, tumor-promoting activity, and derivatives, see: (a) Irie, K.; Koshimizu, K. *Mem. Coll. Agric. Kyoto Univ.* **1988**, *132*, 1–59. (b) Irie, K.; Koshimizu, K. *Comments Agric. Food Chem.* **1993**, *3*, 1–25. (c) Irie, K. *Nippon Nogei Kagaku Kaishi* **1994**, *68*, 1289–1296. (d) Irie, K.; Nakagawa, Y.; Ohigashi, H. *Curr. Pharm. Des.* **2004**, *10*, 1371–1385. (e) Irie, K.; Nakagawa, Y.; Ohigashi, H. *Chem. Rec.* **2005**, *5*, 185–195.

[58] Chen, S.; Borowiak, M.; Fox, J. L.; Maehr, R.; Osafune, K.; Davidow, L.; Lam, K.; Peng, L. F.; Schreiber, S. L.; Rubin, L. L.; Melton, D. *Nat. Chem. Biol.* **2009**, *5*, 258–265.

[59] Hama, T.; Culkin, D. A.; Hartwig, J. F. *J. Am. Chem. Soc.* **2006**, *128*, 4976–4985.

[60] (a) Stratmann, K.; Moore, R. E.; Bonjouklian, R.; Deeter, J. B.; Patterson, G. M. L.; Shaffer, S.; Smith, C. D.; Smitka, T. A. *J. Am. Chem. Soc.* **1994**, *116*, 9935–9942. (b) Jimenez, J. L.; Huber, U.; Moore, R. E.; Patterson, G. M. L. *J. Nat. Prod.* **1999**, *62*, 569–572.

[61] Huters, A. D.; Styduhar, E. D.; Garg, N. K. *Angew. Chem. Int. Ed.* **2012**, *51*, 3758–3765 and see references therein.

[62] For formal total syntheses, see: (a) Fu, T.-h.; McElroy, W. T.; Shamszad, M.; Martin, S. F. *Org. Lett.* **2012**, *14*, 3834–3837. (b) Fu, T.-h.; McElroy, W. T.; Shamszad, M.; Heidebrecht, Jr., R. W.; Gulledge, B.; Martin, S. F. *Tetrahedron* **2013**, *69*, 5588–5603.

[63] (a) Bhat, V.; Allan, K. M.; Rawal, V. H. *J. Am. Chem. Soc.* **2011**, *133*, 5798–5801. (b) Allan, K. M.; Kobayashi, K.; Rawal, V. H. *J. Am. Chem. Soc.* **2012**, *134*, 1392–1395.

[64] Sakagami, M.; Muratake, H.; Natsume, M. *Chem. Pharm. Bull.* **1994**, *42*, 1393–1398.

[65] Caubere, P. *Acc. Chem. Res.* **1974**, *7*, 301–308.

[66] TePaske, M. R.; Gloer, J. B.; Wicklow, D. T.; Dowd, P. F. *J. Org. Chem.* **1989**, *54*, 4743–4746.

[67] TePaske, M. R.; Gloer, J. B.; Wicklow, D. T.; Dowd, P. F. *Tetrahedron Lett.* **1989**, *30*, 5965–5968.

[68] For an elegant total synthesis of **1.84**, see: Bian, M.; Wang, Z.; Xiong, X.; Sun, Y.; Matera, C.; Nicolaou, K. C.; Li, A. *J. Am. Chem. Soc.* **2012**, *134*, 8078–8081.

# CHAPTER TWO

## Total Syntheses of Indolactam Alkaloids (–)-Indolactam V, (–)-Pendolmycin, (–)-Lyngbyatoxin A, and (–)-Teleocidin A-2

Noah F. Fine Nathel, Tejas K. Shah, Sarah M. Bronner, and Neil K. Garg.

*Chem. Sci.* **2014**, *5*, 2184–2190.

### 2.1 Abstract

We report the total syntheses of (–)-indolactam V and the C7-substituted indolactam alkaloids (–)-pendolmycin, (–)-lyngbyatoxin A, and (–)-teleocidin A-2. The strategy for preparing indolactam V relies on a distortion-controlled indolyne functionalization reaction to establish the C4–N linkage, in addition to an intramolecular conjugate addition to build the conformationally-flexible nine-membered ring. The total synthesis of indolactam V then sets the stage for the divergent synthesis of the other targeted alkaloids. Specifically, late-stage $sp^2$–$sp^3$ cross-couplings on an indolactam V derivative are used to introduce the key C7 substituents and the necessary quaternary carbons. These challenging couplings, in addition to other delicate manipulations, all proceed in the presence of a basic tertiary amine, an unprotected secondary amide, and an unprotected indole. Thus, our approach not only enables the enantiospecific total syntheses of four indolactam alkaloids, but also serves as a platform for probing complexity-generating and chemoselective transformations in the context of alkaloid total synthesis.

## 2.2 Introduction

Natural products belonging to the family of indolactam alkaloids[1] (e.g., **2.1**–**2.4**, Figure 2.1) have been widely studied for their pharmacological properties. The most well-known of these compounds is indolactam V (**2.1**), which was first isolated in 1984.[2] Indolactam V (**2.1**) functions as an efficient tumor promoter as a result of its ability to bind to protein kinase C (PKC). Accordingly, **2.1** has been used in a variety of studies to better understand mammalian tumor growth.[3,4] Similarly, C7-substituted indolactams **2.2**–**2.4** have been valued for their tumor-promoting abilities. It should be noted that each of **2.1**–**2.4** and their derivatives exhibit biological functions which range from stem-cell differentiation[5] to anti-bacterial,[6] anti-malarial[7] and anti-cancer[8] activities.

The attractive biological profiles of indolactam alkaloids have prompted numerous synthetic investigations. These efforts have led to several total syntheses of **2.1**,[9,10] as well as completed syntheses of **2.2**–**2.4**.[11,12] A central challenge to accessing each of these alkaloids involves assembly of the parent 3,4-disubstituted indole framework possessing a conformationally-flexible[13] 9-membered lactam. To this end, most strategies to access the medium-sized ring have involved amide bond formation as the key step.[9] With regard to **2.2**–**2.4**, introduction of the C7 $sp^2$–$sp^3$ linkage presents an additional challenge. The few successful approaches to **2.2**–**2.4** all involve early introduction of the C7-linked quaternary carbon, followed by assembly of the indole core.[11,12]

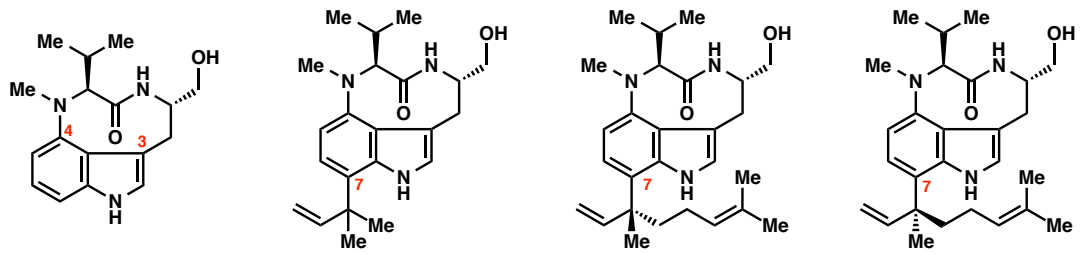


***Figure 2.1.*** Representative Indolactam Alkaloids **2.1**–**2.4**

We envisioned a strategically distinct approach to indolactam V (**2.1**) and related C7-substituted alkaloids **2.2**–**2.4**, which is summarized in Scheme 2.1. Specifically, the 9-membered ring would be introduced through two key steps from an appropriate indole building block: namely, intermolecular assembly of the C4–N bond and ring closure at C3. This would be implemented in practice by accessing an indolyne *in situ*,[14,15,16] which would undergo selective C4-trapping by an amine nucleophile (**2.5** → **2.6**). Elaboration of adduct **2.6** to ester **2.7** would be followed by a challenging conjugate addition at C3 to forge the 9-membered ring en route to **2.1**. We hypothesized that **2.1** could be used as a precursor to the C7-substituted indolactam alkaloids, without the use of *N*-protecting groups. Our divergent strategy would require the use of efficient cross-couplings to build the $sp^2$–$sp^3$ C–C linkages and introduce the quaternary carbons (**2.1** → **2.8** → **2.2**–**2.4**). Achieving alkylative cross-couplings at C7 of indoles can be difficult, and only a few such examples are known in the presence of unprotected indole nitrogens.[17] Moreover, to our knowledge, there are no examples of $sp^2$–$sp^3$ cross-couplings to introduce quaternary C7 substituents on indole substrates in the literature.

***Scheme 2.1.*** Synthetic Strategy Toward **2.1** and C7 Substituted Indolactam Alkaloids **2.2**–**2.4**

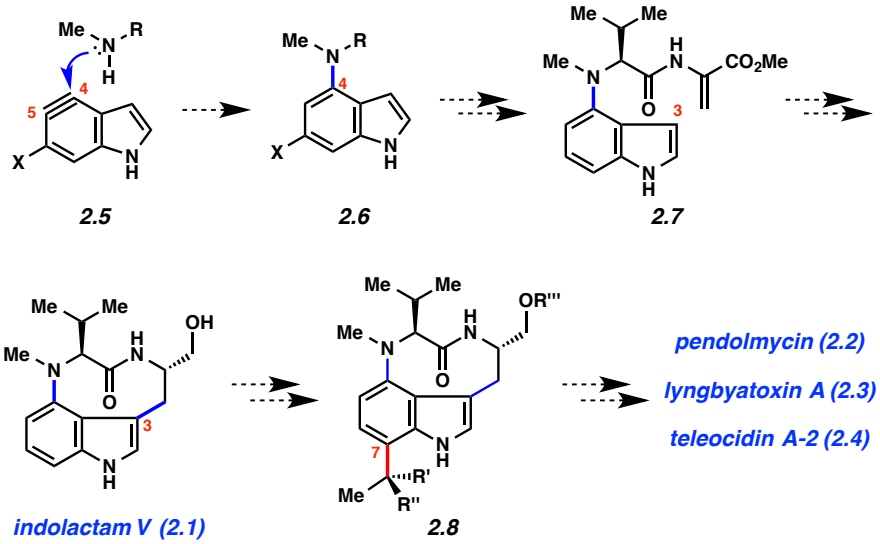


We herein describe the enantiospecific total syntheses of indolactam alkaloids **2.1**–**2.4**. As we have previously reported a formal total synthesis of **2.1**,[10] aside from a brief discussion of optimization of key steps, this manuscript focuses on C7 functionalization studies and the divergent total syntheses of the less well-studied targets **2.2**–**2.4**. This study not only leads to the generation of several natural products enantiospecifically, but also serves as an exercise aimed at probing complexity-generating and chemoselective transformations in alkaloid total synthesis.

## 2.3 Results and Discussion

### 2.3.1 Optimization of the Total Synthesis of Indolactam V (2.1)

Although our previous studies toward **2.1** validated our approach, we sought to improve several key steps of our formal synthesis[10] and render the route suitable for scale-up (Scheme 2.2). We first optimized the synthesis of indolyne precursor **2.9**, which can now be obtained in 7 steps from commercially available materials in 62% overall yield (previously 27% yield, over 7 steps).[18] Next, treatment of silyltriflate **2.9** with peptide **2.10** in the presence of CsF in acetonitrile efficiently furnished indolyne adduct **2.11** and established the key C4–N linkage.[19,20] The regioselectivity in the indolyne trapping is governed by aryne distortion,[15a,b] which arises from the presence of the inductively-withdrawing C6 bromide substituent.[10] After elaborating **2.11** to α,β-unsaturated ester **2.7**, $ZrCl_4$-mediated cyclization[21] provided **2.12** as a single diastereomer in 90% yield.[22] As **2.12** possesses the undesired stereochemical configuration at C9, we developed optimal conditions to facilitate its epimerization based on the protocol reported by Nakatsuka.[9c] Treatment of **2.12** with $NaHCO_3$ in MeOH at 40 °C delivered a separable mixture of recovered **2.12** and the desired epimer **2.13**. Reduction of **2.13** delivered indolactam V (**2.1**), which was subsequently protected to give silyl ether **2.14** in 90% yield over two steps. Using our optimized route, we have prepared over 500 mg of **2.14** for use in subsequent functionalization efforts.

***Scheme 2.2.*** Optimized Synthesis of Indolactam V (**2.1**) and **2.14**

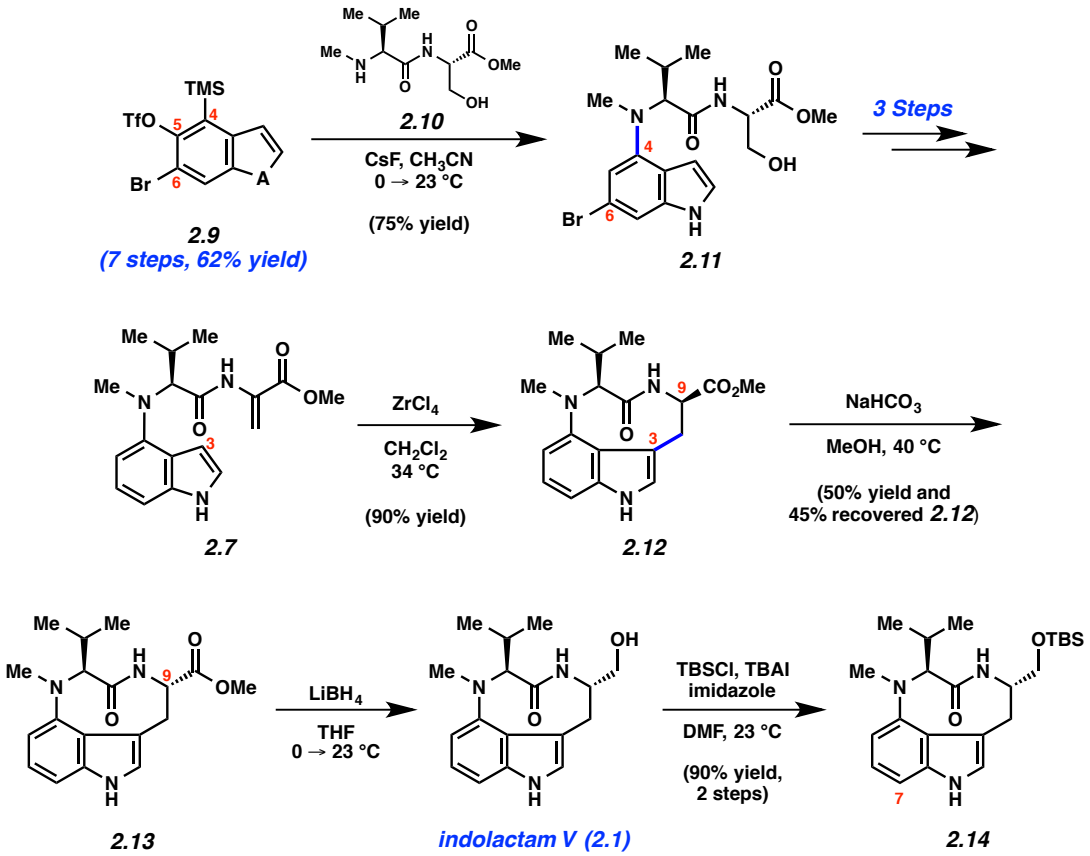


### 2.3.2 Cross-Coupling to Introduce the C7 $sp^2$–$sp^3$ Linkage and the Key Quaternary Carbon

With access to late-stage compound **2.14**, we turned our attention to the previously unexplored divergent approach to alkaloids **2.2**–**2.4**. One of the most challenging aspects of this strategy involves functionalization of C7. Importantly, the methodology would have to build a new $sp^2$–$sp^3$ C–C linkage, containing a quaternary center, on an unprotected indole. In general, $sp^2$–$sp^3$ couplings are far less common compared to their $sp^2$–$sp^2$ counterparts and, as mentioned previously, no examples of such couplings to introduce quaternary carbons at C7 of indoles are available.

We tested the viability of our alkylative coupling strategy using readily available unprotected bromoindole substrate **2.15** (Table 2.1). Enolate precursors **2.19**–**2.22** were examined, as the carbonyls in the presumed products could plausibly be elaborated to the olefins present in **2.2**–**2.4**. Unfortunately, attempts to use isobutyraldehyde (**2.19**) as the coupling partner[23] led predominantly to the recovery of starting material **2.15** with or without formation of desbromo indole **2.17** (entries 1[24] and 2, respectively). We also tested ester **2.20** as a coupling partner,[25] but only observed recovered substrate **2.15** (entries 3 and 4). Next, silylketene acetal **2.21** was employed in the desired coupling.[26] To our delight, using 1 mol% $Pd(dba)_2$, some of the desired product **2.16b** was formed, albeit with recovered substrate **2.15** (entry 5). By simply increasing the catalyst loading to 5 mol%, full conversion to product **2.16b** was observed (entry 6). Zinc enolate **2.22**, which was generated in situ from the corresponding a-bromoamide, was also evaluated as a potential coupling partner using Hartwig's methodology.[27] Although no reaction was observed using literature conditions (entry 7), we found that the desired product **2.16c** could be obtained under more forcing conditions (i.e., 15 mol% Pd and 80 °C) (entry 8). It should be noted that desbromo compound **2.17** and dimer **2.18** were also formed in minor quantities. To our knowledge, the successful formation of **2.16b** and **2.16c** represents the first simultaneous formation of an $sp^2$–$sp^3$ bond and quaternary center at the C7 position of an indole with an unprotected nitrogen.

***Table 2.1.*** C7 $sp^2$–$sp^3$ Cross-Coupling on Model Substrate **2.15**

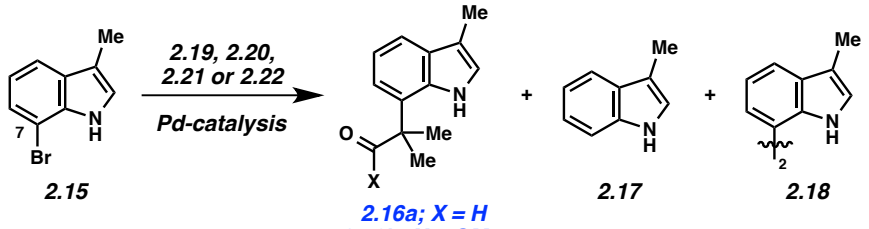


| entry | cross-coupling partner | conditions[a] | ratio[b] 5.15 : 5.16 : 5.17 : 5.18 |
|---|---|---|---|
| 1 | 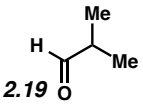 2.19 | 2 mol% $Pd(OAc)_2$, Ligand 2.23[c] $Cs_2CO_3$, dioxane, 80 °C | 3.7 : 0 : 1 : 0 |
| 2 | | 2 mol% $Pd(OAc)_2$, Ligand 2.23[c] $LiNCy_2$, dioxane, 80 °C | 1 : 0 : 0 : 0 |
| 3 | 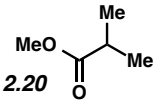 2.20 | 1 mol% $Pd(dba)_2$, P(*t*-Bu)$_3$ $LiNCy_2$, toluene, 23 °C | 1 : 0 : 0 : 0 |
| 4 | | 5 mol% $Pd(dba)_2$, P(*t*-Bu)$_3$ $LiNCy_2$, toluene, 23 °C | 1 : 0 : 0 : 0 |
| 5 | 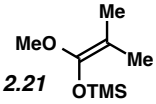 2.21 | 1 mol% $Pd(dba)_2$, P(*t*-Bu)$_3$ $ZnF_2$, DMF, 80 °C | 1 : 3 : 0 : 0 |
| 6 | | 5 mol% $Pd(dba)_2$, P(*t*-Bu)$_3$ $ZnF_2$, DMF, 80 °C | 0 : 1 : 0 : 0 |
| 7 | 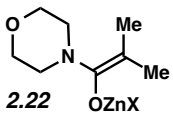 2.22 | 2.5 mol% $[P(t\text{-Bu})_3PdBr]_2$ toluene, 23 °C | 1 : 0 : 0 : 0 |
| 8 | | 15 mol% $[P(t\text{-Bu})_3PdBr]_2$ toluene, 80 °C | 0 : 11.3 : 2.1 : 1 |

[a] For detailed reaction conditions, see the experimental procedures. [b] Ratios determined by $^1$H NMR analysis of the crude reaction mixtures. [c] Ligand **2.23** = diisopropyl[2'-methoxy-1,1'-binaphthalen]-2-yl.

### 2.3.3 Total Synthesis of (–)-Pendolmycin (2.2)

Our promising results for the cross-coupling on the model system prompted us to shift our efforts to the complex indolactam scaffold (Scheme 2.3). Treatment of **2.14** with NBS led to C7 bromination to furnish **2.24**.[28] Next, the critical coupling reactions using the aforementioned conditions (see Table 2.1, entries 6 and 8) were tested. Despite our previous success in coupling silylketene acetal **2.21**, attempts to effect the corresponding coupling on indolylbromide **2.24** led

to no reaction. However, the coupling of bromide **2.24** with zinc enolate **2.22** delivered cross-coupled product **2.25** in 61% yield. As this complexity-generating transformation proceeds on an advanced late-stage intermediate in the presence of two free NHs and a tertiary amine to introduce an $sp^2$–$sp^3$ linkage with a quaternary carbon, its success demonstrates the exceptional tolerance and utility of Hartwig's parent methodology.[59]

***Scheme 2.3.*** C7 Functionalization of **2.14** and Introduction of Key $sp^2$–$sp^3$ Linkage with a Quaternary Carbon Substituent

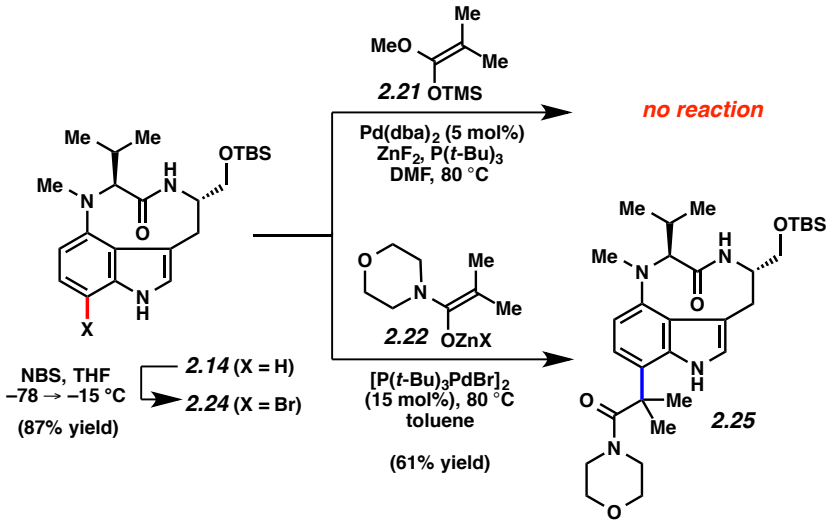


Having installed the necessary C7 substituent and the key quaternary carbon, we were able to complete the total synthesis of pendolmycin (**2.2**), as shown in Scheme 2.4. The morpholine amide of **2.25**, which neighbors the sterically-congested quaternary carbon, was selectively reduced with the Schwartz reagent (i.e., $Cp_2Zr(H)Cl$)[29] to furnish aldehyde **2.26**. Of note, competitive reduction of the secondary amide was not observed.[30] Subsequent Wittig olefination of **2.26** provided the penultimate compound **2.27**. Finally, exposure of **2.27** to TBAF in THF revealed the primary alcohol to deliver (–)-pendolmycin (**2.2**). This three-step sequence

provides a concise means to convert amide **2.25** to the natural product (**2.2**), without the use of *N*-protecting groups.

***Scheme 2.4.*** Total Synthesis of (–)-Pendolmycin (**2.2**)

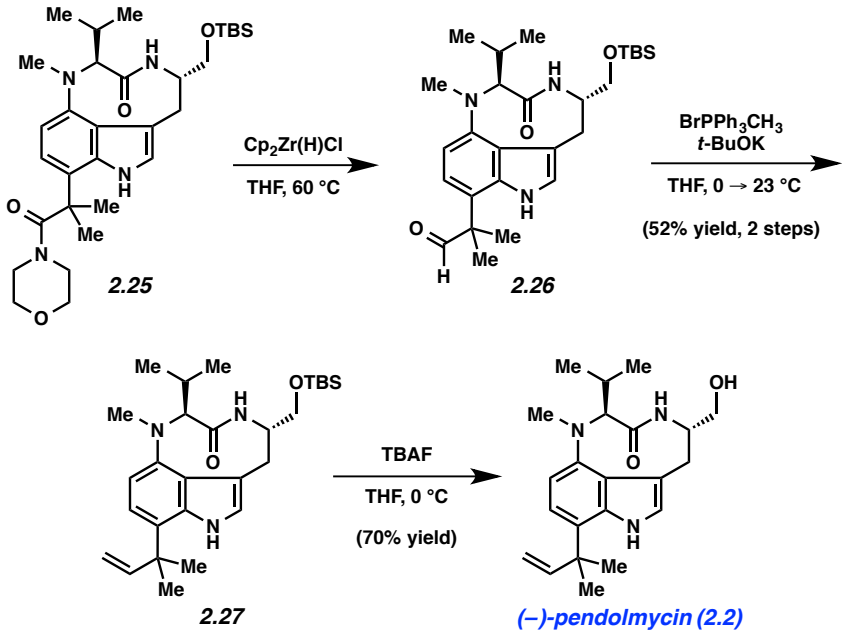


### 2.3.4 Total Synthesis of (–)-Lyngbyatoxin A (2.3) and (–)-Teleocidin A-2 (2.4)

Although structurally similar to pendolmycin (**2.2**), lyngbyatoxin A (**2.3**) and teleocidin A-2 (**2.4**) present additional degrees of complexity. Specifically, the sidechains appended to C7 of the indole each contain a quaternary stereocenter, in addition to an electron-rich olefin. We envisioned that both natural products **2.3** and **2.4** could be obtained from bromoindole **2.24** (see Scheme 2.3) and a prochiral cross-coupling partner.

To enable this approach, we prepared amide **2.29** and tested the key cross-coupling reaction (Scheme 2.5). Ester **2.28**, which was obtained from commercial sources, first underwent α-bromination under standard conditions.[31] Subsequent saponification,[32] followed by CDI-

mediated coupling with morpholine, afforded amide **2.29**.[33] Reaction of amide **2.29** with Zn metal resulted in conversion to the corresponding zinc enolate **2.30**. Gratifyingly, treatment of bromoindole **2.24** with in situ-generated enolate **2.30** under Pd-catalyzed coupling conditions gave the desired diastereomeric products **2.31** and **2.32** in 75% combined yield (d.r. = 1:1 by $^1$H NMR analysis).[34] Isomers **2.31** and **2.32** were separable by silica gel chromatography.[35] The formation of **2.31** and **2.32** represents the first implementation of Hartwig's amide enolate coupling methodology in the assembly of stereogenic quaternary carbons.[59]

***Scheme 2.5.*** Synthesis of Morpholine Amide **2.29** and Cross-Coupling to Access Diastereomeric Adducts **2.31** and **2.32** Possessing the Necessary All-Carbon Quaternary Stereocenters

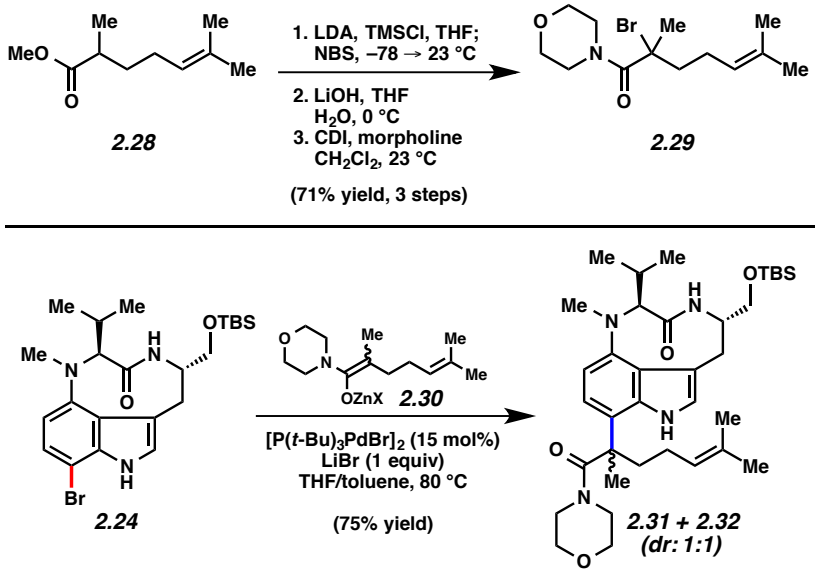


With coupled products **2.31** and **2.32** in hand, we completed the total syntheses of (–)-lyngbyatoxin A (**2.3**) and (–)-teleocidin A-2 (**2.4**), respectively (Schemes 2.6 and 2.7). Amide **2.31** was reduced to aldehyde **2.33**, which in turn, underwent Wittig homologation to give **2.34** (Scheme 2.6). To complete the total synthesis of (–)-lyngbyatoxin (**2.3**), it was necessary to deprotect the primary alcohol. Although attempts to employ TBAF led to decomposition, we

found that exposure of **2.34** to $LiBF_4$ and camphorsulfonic acid (CSA) in THF at ambient temperature afforded natural product **2.3**.[28,36] We were delighted to find that the analogous 3-step reaction sequence facilitated the conversion of diastereomer **2.32** to (–)-teleocidin A-2 (**2.4**) as summarized in Scheme 2.7. Spectral data for our synthetic samples of natural products **2.2**–**2.4** matched literature reports.[11,12]

***Scheme 2.6.*** Total Synthesis of (–)-Lyngbyatoxin A (**2.3**)

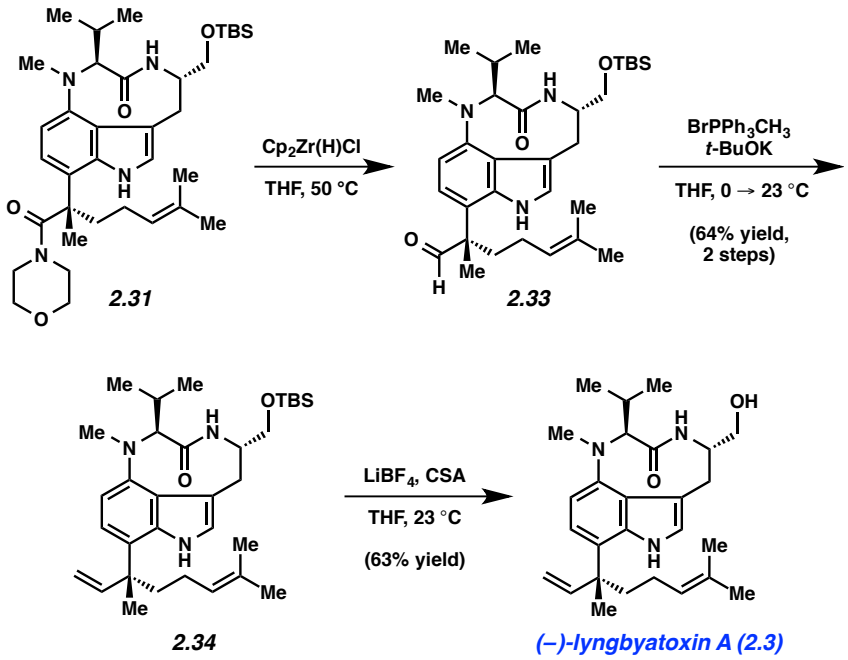


***Scheme 2.7.*** Total Synthesis of (–)-Teleocidin A-2 (**2.4**)

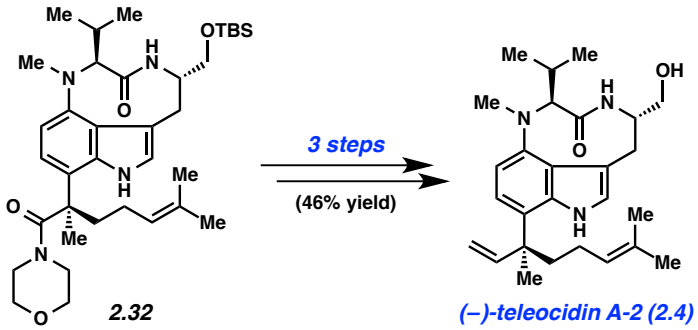

## 2.4 Conclusion

We have completed the total syntheses of four indolactam alkaloids: (–)-indolactam V, (–)-pendolmycin, (–)-lyngbyatoxin A, and (–)-teleocidin A-2. Our approach to these alkaloids features a number of key steps, including: a) a distortion-controlled indolyne functionalization reaction to assemble a key C–N bond; b) a Lewis acid-mediated cyclization to assemble the nine-membered lactam; and specifically, for the divergent syntheses of **2.2**–**2.4**; c) late-stage $sp^2$–$sp^3$ cross-couplings to introduce the C7 sidechains and the challenging quaternary carbons; and d) a series of delicate functional group manipulations in the absence of *N*-protecting groups. Our studies demonstrate that indolynes serve as valuable electrophilic indole surrogates and provide an unconventional tactic for use in total synthesis. Moreover, these efforts showcase a series of complexity-generating (e.g., $sp^2$–$sp^3$ cross-couplings) and chemoselective transformations in the context of alkaloid synthesis.

## 2.5 Experimental Section

### 2.5.1 Materials and Methods

Unless stated otherwise, reactions were conducted in flame-dried glassware under an atmosphere of nitrogen using anhydrous solvents (either freshly distilled or passed through activated alumina columns). All commercially obtained reagents were used as received unless otherwise specified. 6-Benzyloxyindole was obtained from Combi-Blocks, Inc. Cesium fluoride (CsF), tris(dibenzylideneacetone)dipalladium ($Pd(dba)_2$), di-μ-bromobis(tri-*tert*-butylphosphino)-dipalladium(I) ($[P(t\text{-}Bu)_3PdBr]_2$), and bis(cyclopentadienyl)zirconium(IV) chloride hydride (Schwartz's reagent) were purchased from Strem Chemicals. Tri-*tert*-butylphosphine and methyl trimethyl dimethylketene acetal was purchased from Sigma-Aldrich. The following reagents

were distilled prior to use: chlorotrimethylsilane (TMSCl), *tert*-butyldimethylsilyl trifluoromethanesulfonate (TBSOTf), and tetramethylethylenediamine (TMEDA); 1,2-dibromoethane was passed over basic Brockman Grade I 58 Å activated alumina and then stirred over 4 Å molecular sieves for 7 h before distillation. Diethylamine ($Et_2NH$) was stirred over KOH for 1 h and then passed over basic Brockman Grade I 58 Å activated alumina prior to use. DBU was stirred over 4 Å molecular sieves for 3 h and then passed over basic Brockman Grade I 58 Å. *N*-pentane was dried over $MgSO_4$. *N*-bromosuccinamide (NBS) was purified by recrystallization from deionized water. Reaction temperatures were controlled using an IKAmag temperature modulator, and unless stated otherwise, reactions were performed at room temperature (rt, approximately 23 °C). Melting points were determined using a MEL TEMP II melting point apparatus. Thin-layer chromatography (TLC) was conducted with EMD gel 60 F254 pre-coated plates (0.25 mm) and visualized using a combination of UV, anisaldehyde, iodine, vanillin, ninhydrin, and potassium permanganate staining. Silicycle Siliaflash P60 (particle size 0.040–0.063 mm) was used for flash column chromatography. $^1$H NMR spectra were recorded on Bruker spectrometers (at 500 MHz or 600 MHz) and are reported relative to deuterated solvent signals. Data for $^1$H NMR spectra are reported as follows: chemical shift (δ ppm), multiplicity, coupling constant (Hz) and integration. $^{13}$C NMR spectra were recorded on Bruker Spectrometers (at 125 or 150 MHz). Data for $^{13}$C NMR spectra are reported in terms of chemical shift. IR spectra were recorded on a Perkin-Elmer 100 spectrometer and are reported in terms of frequency of absorption ($cm^{-1}$). Optical rotations were measured with a Rudolf Autopol III Automatic Polarimeter. High-resolution mass spectra were obtained from the UC Irvine Mass Spectrometry Facility and the UCLA Molecular Instrumentation Center.

### 2.5.2 Experimental Procedures

#### 2.5.2.1 Optimization of the Total Synthesis of Indolactam V (2.1)

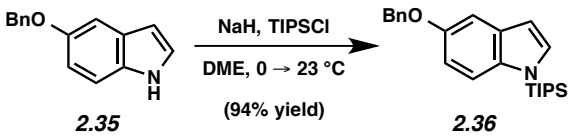


*2.35* *2.36*

***N*-TIPS benzyloxyindole 2.36.** To a flask containing NaH (60% dispersion in mineral oil, 0.700 g, 17.5 mmol, 1.3 equiv) at 0 °C was added a solution of 5-benzyloxyindole **2.35** (3.00 g, 13.5 mmol) in 1,2-dimethoxyethane (40 mL). The resulting solution was stirred at 0 °C for 20 min, then TIPSCl (4.34 mL, 20.3 mmol, 1.5 equiv) was added dropwise over 5 min. The resulting mixture was removed from the 0 °C bath and allowed to warm to 23 °C. After stirring for an additional 90 min, the reaction was quenched with $H_2O$ (2 mL). The biphasic mixture was concentrated under reduced pressure, then further diluted with $Et_2O$ (50 mL) and $H_2O$ (10 mL). The layers were separated, and then the aqueous layer was extracted with $Et_2O$ (2 × 50 mL). The combined organic layers were dried over $MgSO_4$. Evaporation of the solvent under reduced pressure afforded the crude product, which was further purified by flash chromatography (3:1 Hexanes:$CH_2Cl_2$) to afford known **2.36**[15b] (4.82 g, 94% yield) as a white solid.

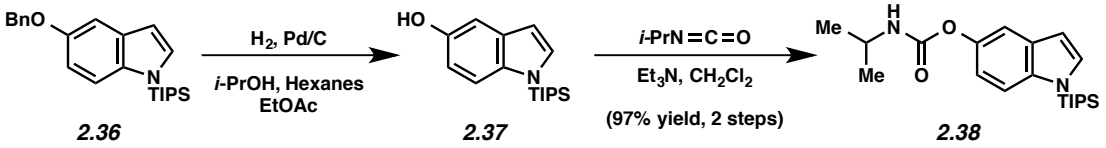


*2.36* *2.37* *2.38*

***N*-TIPS carbamate 2.38.** Carbamate **2.38** was prepared following the general procedure described by Igarashi.[37] To a solution of *N*-TIPS benzyloxyindole (4.72 g, 12.4 mmol) in 1:1:1 *i*-PrOH:Hexanes:EtOAc (108 mL) was added 5% Pd/C (0.67 g, 0.32 mmol, 2.6 mol% Pd). The

mixture was placed under an atmosphere of hydrogen (double-balloon), stirred for 2.5 h at 23 °C, and then filtered over celite (EtOAc eluent). Evaporation of the solvent under reduced pressure afforded crude **2.37** as a pink solid, which was used in the subsequent step without further purification.

To a solution of crude **2.37** in $CH_2Cl_2$ (60.0 mL) and $Et_3N$ (0.518 mL, 3.72 mmol, 0.3 equiv), was added *i*-PrNCO (3.64 mL, 37.2 mmol, 3 equiv. The solution was stirred at 23 °C for 24 h, then concentrated to dryness under reduced pressure. Purification by flash chromatography (2:1 Hexanes:$Et_2O$) provided known *N*-TIPS carbamate **2.38**[15b] (4.48 g, 97% yield, 2 steps) as a white solid.

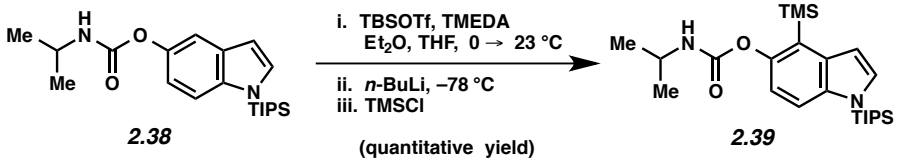


***N*-TIPS silylcarbamate 2.39.** Silyl carbamate **2.39** was prepared following the general procedure described by Hoppe and Snieckus for *o*-lithiation of isopropyl carbamates, with minor modifications.[38,39] To a solution of *N*-TIPS carbamate **2.38** (4.48 g, 11.98 mmol) and TMEDA (2.51 mL, 16.8 mmol, 1.4 equiv) in 3:1 $Et_2O$:THF (120 mL) at 0 °C was added a solution of TBSOTf in *n*-pentane (1.30 M, 17.3 mL, 14.4 mmol, 1.2 equiv). After stirring for 5 min, the white suspension was allowed to warm to 23 °C over 30 min. TMEDA (6.28 mL, 41.9 mmol, 3.5 equiv) was added, and the mixture was cooled to –78 °C. A solution of *n*-BuLi in hexanes (1.43 M, 29.3 mL, 41.9 mmol, 3.5 equiv) was added dropwise over 55 min. The mixture was stirred at –78 °C for 3 h, then neat TMSCl (10.6 mL, 83.9 mmol, 7 equiv) was added dropwise over 1 h. The resulting mixture was stirred at –78 °C for 1 h, quenched with 1 M $NaHSO_4$ (50 mL), and

allowed to warm to 23 °C over 45 min with vigorous stirring. The biphasic mixture was further diluted with $Et_2O$ (50 mL), the layers were separated, and then the aqueous layer was extracted with $Et_2O$ (2 × 50 mL). The combined organic layers were dried over $MgSO_4$. Evaporation of the solvent under reduced pressure afforded the crude product, which was further purified by flash chromatography (2:1 Hexanes:$Et_2O$) to afford known silylcarbamate **2.39**[15b] (2.33 g, quantitative yield) as a white solid.

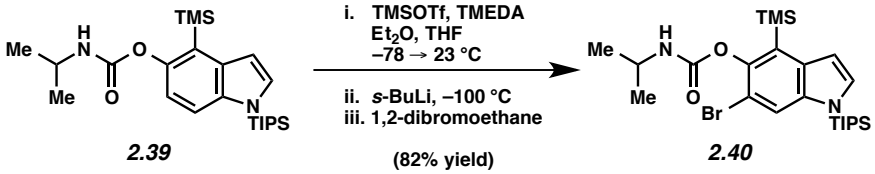


**6-Bromo silylcarbamate 2.40.** 6-Bromo silylcarbamate **2.40** was prepared following the general procedure described by Snieckus for *o*-lithiation, with modifications.[40] To a solution of silylcarbamate **2.39** (2.19 g, 4.90 mmol) in 3:1 $Et_2O$:THF (69.6 mL) at –78 °C was added TMEDA (1.02 mL, 6.86 mmol, 1.4 equiv), followed by a solution of TMSOTf in *n*-pentane (1.30 M, 3.91 mL, 5.90 mmol, 1.2 equiv). After stirring for 5 min, the white suspension was allowed to warm to 23 °C over 28 min, by which time TMEDA·TfOH had formed as an oil on the bottom of the flask. The mixture was placed in a hexanes and liquid nitrogen bath at –100 °C and TMEDA (2.56 mL, 17.2 mmol, 3.5 equiv) was added. A solution of *sec*-BuLi in cyclohexane (1.18 M, 37.4 mL, 44.1 mmol, 9 equiv) was added dropwise over 1.2 h. The mixture was stirred at –100 °C for 4.5 h, then neat 1,2-dibromoethane (5.09 mL, 58.8 mmol, 12.0 equiv) was added dropwise over 10 min. The resulting mixture was stirred at –100 °C for 3 h, quenched with 0.5 M aqueous $NaHSO_4$ (50 mL), and warmed to 23 °C over 40 min with vigorous stirring. The layers were separated, and the organic layer was washed successively with 1 M aqueous $NaHSO_4$ (50 mL)

and brine (50 mL), then dried over $MgSO_4$. Evaporation under reduced pressure afforded the crude product, which was purified by flash chromatography (5:1 Benzene:$CH_2Cl_2$) to afford known 6-bromo silylcarbamate **2.40**[10] (2.12 g, 82% yield) as a white solid.

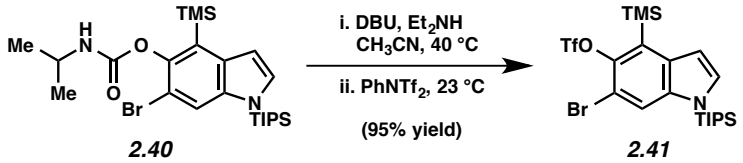

*2.40* *2.41*

***N*-TIPS 6-bromo silyltriflate 2.41.** To a solution of 6-bromo silylcarbamate **2.40** (0.636 g, 1.21 mmol) in MeCN (24 mL) were added DBU (0.427 mL, 3.03 mmol, 2.5 equiv) and $Et_2NH$ (0.187 μL, 1.82 mmol, 1.5 equiv). The resulting mixture was placed in a heating bath maintained at 40 °C for 15 min, then allowed to cool to 23 °C. Next, a solution of $PhNTf_2$ (0.650 g, 1.82 mmol, 1.5 equiv) in MeCN (2.1 mL) was added. After stirring for 25 min, the reaction mixture was passed over a plug of silica gel (EtOAc eluent). Evaporation under reduced pressure afforded the crude product, which was further purified by flash chromatography (30:1 Hexanes:$Et_2O$) to provide known *N*-TIPS 6-bromo silyltriflate **2.41**[10] (0.654 g, 95% yield) as a white solid.

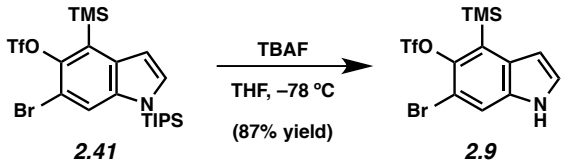

*2.41* *2.9*

***N*-H 6-bromo silyltriflate 2.9.** To a solution of *N*-TIPS 6-bromo silyltriflate **2.41** (0.143 g, 0.250 mmol) in THF (9.4 mL) at –78 °C was added a solution of TBAF in THF (1.0 M, 250 μL, 0.250 mmol, 1 equiv) dropwise over 3 min. The solution was stirred for 15 min, then quenched with $H_2O$ (12 mL). The biphasic mixture was further diluted with EtOAc (12 mL). The layers were

separated, and then the aqueous layer was extracted with EtOAc (2 × 12 mL). The combined organic layers were dried over $MgSO_4$. Evaporation under reduced pressure afforded the crude product, which was further purified by flash chromatography (2.5:1 Hexanes:$CH_2Cl_2$) to provide known bromo silyltriflate **2.9**[10] (90.9 mg, 87% yield) as a white solid.

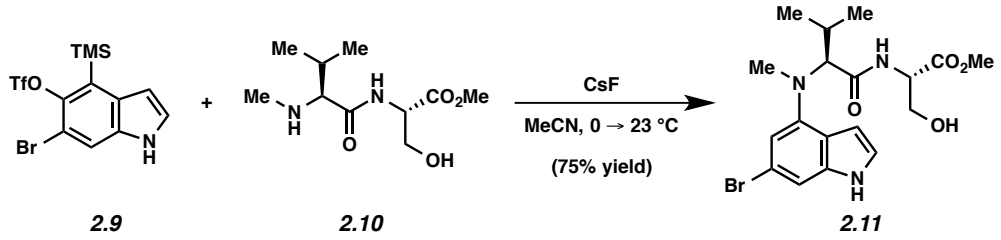


*2.9* *2.10* *2.11*

**Indolyne adduct 2.11.** To a stirred solution of *N*-H 6-bromo silyltriflate **2.9** (52.1 mg, 0.125 mmol) and peptide **2.10**[10] (87.1 mg, 0.375 mmol, 3 equiv) in MeCN (1.25 mL) was placed in a 0 °C bath and added CsF (38.0 mg, 0.250 mmol, 2 equiv). The reaction mixture was stirred at 0 °C for 12 h, and was then allowed to warm to 23 °C. After stirring for an additional 12 h, the reaction mixture was filtered over silica gel (EtOAc eluent). Evaporation under reduced pressure afforded the crude product, which was further purified by flash chromatography (1:0.7:0.7 Hexanes:$CH_2Cl_2$:$Et_2O$) to provide known indolyne adduct **2.11**[10] (40.0 mg, 75% yield) as a clear oil.

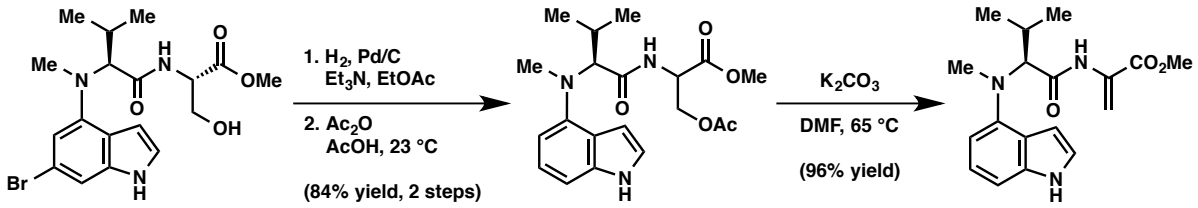


*2.11* *2.42* *2.7*

**Unsaturated ester 2.7.** Indolyne adduct **2.11** was converted to **2.42** in 84% yield using our previously reported two-step procedure.[10] To a solution of **2.42** (98.2 mg, 0.252 mmol) in DMF

(2.5 mL) was added $K_2CO_3$ (69.7 mg, 0.504 mmol, 2 equiv). The resulting mixture was placed in a heating bath maintained at 65 °C for 10 h, then allowed to cool to 23 °C. The reaction mixture was passed over a plug of cotton (EtOAc eluent). Evaporation at 60 °C under reduced pressure afforded the crude product, which was further purified by flash chromatography (5:1 Hexanes:EtOAc) to provide known ester **2.7**[10] (79.7 mg, 96% yield) as a white solid.

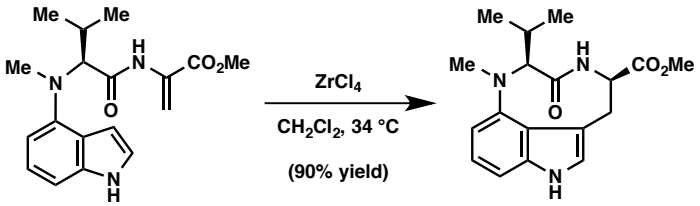

*2.7* *2.12*

**Tricycle 2.12.** A modification of Piersanti's procedure for alkylation of indoles was employed to construct the desired 9-membered ring.[21] Inside a glove box, $ZrCl_4$ (336.5 mg, 1.45 mmol, 15 equiv) and then $CH_2Cl_2$ (0.96 mL) were added to a vial containing **2.7** (31.7 mg, 0.096 mmol). The reaction vessel was placed into an aluminum block maintained at 34 °C. After 16 h, the vial was transferred out of the glove box and the reaction mixture was added dropwise to saturated aqueous $NaHCO_3$ (15 mL) at 0 °C. The resulting solids were removed by filtration over celite (EtOAc eluent). The layers were separated and the aqueous layer was extracted with EtOAc (15 mL). The combined organic layers were dried over $Na_2SO_4$. Evaporation under reduced pressure afforded the crude product, which was further purified by flash chromatography (5:1 → 2:1 Hexanes:EtOAc) to afford known tricycle **2.12**[10] (28.5 mg, 90% yield) as a white solid.

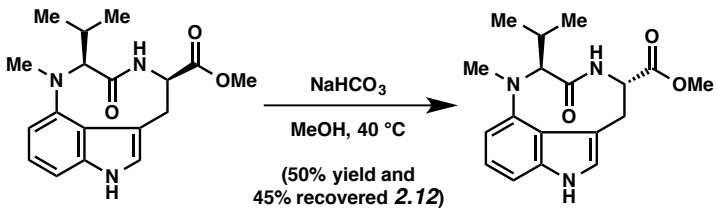


*2.12* *2.13*

**Ester 2.13.** Tricycle **2.12** was epimerized following the protocol described by Nakatsuka, with modifications.[9d] To a solution of **2.12** (42.1 mg, 0.128 mmol) in MeOH (8.5 mL) was added $NaHCO_3$ (294.4 mg, 3.5 mmol, 27.4 equiv). The resulting mixture was placed in a heating bath maintained at 40 °C for 3 d, then allowed to cool to 23 °C. The reaction mixture was concentrated and diluted with EtOAc (50 mL) and $H_2O$ (50 mL). The organic layer was separated, and then the organic layer was washed with brine (50 mL), and dried over $MgSO_4$. Evaporation under reduced pressure afforded the crude mixture, which was purified by flash chromatography (95:5 → 90:10 Benzene:$CH_3CN$) to afford known ester **2.13**[9d] (21.0 mg, 50% yield) and recovered epimer **2.12**[9d] (19.0 mg, 45% yield) as a white solid.

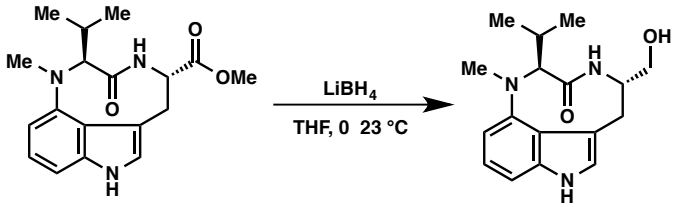


*2.13* *indolactam V (2.1)*

**Indolactam V (2.1).** Ester **2.13** was reduced following the protocol described by Nakatsuka, with modifications.[9d] Inside a glove box, a vial was charged with **2.13** (125.4 mg, 0.381 mmol), $LiBH_4$ (54.8 mg, 2.515 mmol, 6.6 equiv) and THF (0.381 mL). The vial was removed from the glove box and allowed to stir for 2 h at 23 °C. After 2 h, the reaction mixture was poured into ice water (5 mL). The mixture was then extracted with $CH_2Cl_2$ (50 mL). The organic layers were

combined, washed with brine (15 mL), and dried over $MgSO_4$. Evaporation of the solvent under reduced pressure afforded crude indolactam V (**2.1**), which was used in the subsequent step without further purification. Spectral data match those previously reported.[9d]

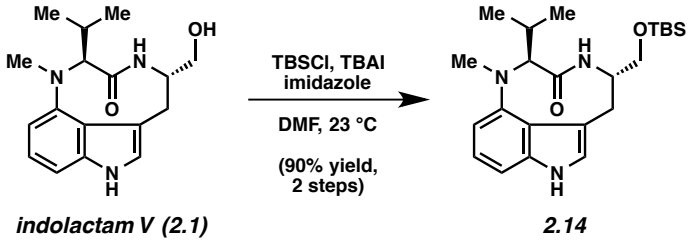

*indolactam V (2.1)* *2.14*

**Silylether 2.14.** Indolactam V (**2.1**) was silyl protected following the protocol described by Kishi.[36] To a stirred solution of indolactam V (**2.1**) (41.7 mg, 0.317 mmol) in DMF (1.4 mL) was added TBSCl (20.6 mg, 0.137 mmol, 1.0 equiv), imidazole (46.5 mg, 0.684 mmol, 5.0 equiv), and TBAI (5.0 mg, 0.014 mmol, 0.1 equiv). The resulting mixture was allowed to stir at 23 °C. After 12 h, the reaction was quenched with saturated aqueous $NH_4Cl$ (5 mL) and diluted with EtOAc (10 mL). The organic layer was separated, and then the organic layer was washed with brine (50 mL), and dried over $Na_2SO_4$. Evaporation under reduced pressure afforded the crude product, which was purified by flash chromatography (4:1 Hexane:EtOAc) to afford known silylether **2.14** (118.5 mg, 90% yield over two steps) as a white solid. Silylether **2.14**: Mp = 192-195 °C; $R_f$ 0.65 (1:1 Hexanes:EtOAc); $^1$H NMR (500 MHz, $CDCl_3$): δ 8.05 (br s, 1H), 7.08 (t, $J$ = 7.9, 1H), 6.91 (d, $J$ = 8.0, 1H), 6.89 (s, 1H), 6.52 (d, $J$ = 7.7, 1H), 6.19 (br s, 1H), 4.38 (d, $J$ = 10.2, 1H), 4.24 (d, $J$ = 3.9, 1H), 3.65 (dd, $J$ = 10.1, 4.3, 1H), 3.48 (t, $J$ = 9.5, 1H), 3.17 (d, $J$ = 17.4, 1H), 2.95–2.88 (m, 4H), 2.65–2.61 (m, 1H), 0.94 (d, $J$ = 6.4, 3H), 0.91 (s, 3H), 0.89 (s, 9H), 0.64 (d, $J$ = 6.7, 3H), 0.06 (s, 3H) 0.04 (s, 3H); $^{13}$C NMR (125 MHz, $CDCl_3$): δ 173.1, 148.0, 139.5, 123.0, 121.4, 118.1, 114.7, 106.4, 104.0, 71.3, 65.5, 55.2, 34.2, 33.0, 28.7, 26.0,

21.7, 19.6, 18.4, -5.2, -5.3; IR (film): 3320, 2928, 1643, 1251 $cm^{-1}$; HRMS-ESI (*m/z*) $[M + Na]^+$ calculated for $C_{23}H_{37}N_3O_2SiNa$, 438.2553; found, 438.2554; $[\alpha]^{20}_D$ –124.00° (c = 0.100, $CH_2Cl_2$).

### 2.5.2.2 Cross-Coupling to Introduce the C7 $sp^2$–$sp^3$ Linkage

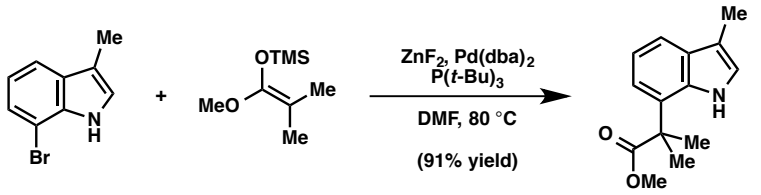


*2.15* *2.21* *2.16b*

**Ester 2.16b.** Ester **2.16b** was prepared following the general coupling protocol described by Hartwig for the cross-coupling of silyl ketene acetals with aryl bromides, with modifications.[26] A flame-dried vial under $N_2$, containing 7-bromoskatol (**2.15**)[41] (9.9 mg, 0.047 mmol), was transferred to a glovebox. A magnetic stir bar was added, followed by P(*t*Bu)$_3$ (4.7 µl, 4.7 µmol, 0.1 equiv), $ZnF_2$ (2.5 mg, 0.025 mmol, 0.5 equiv), and a solution of $Pd(dba)_2$ (1.4 mg, 2.4 µmol, 0.05 equiv) in DMF (0.47 mL). Trimethylsilyldimethylketene (**2.21**) (14.4 µl, 0.071 mmol, 1.5 equiv) was added and the vial was sealed with a teflon-coated cap and removed from the glovebox. The reaction was stirred at 80 °C for 12 h, cooled to 23 °C, and then filtered over silica (100% EtOAc eluent) and concentrated in vacuo. The crude residue was purified by preparative thin layer chromatography (3:1:1 Hexanes:$CH_2Cl_2$:$EtO_2$) to afford ester **2.16b** (9.9 mg, 91%) as an amorphous tan solid. Ester **2.16b**: $R_f$ 0.6 (3:1:1 Hexanes:$CH_2Cl_2$:$EtO_2$); $^1$H NMR (500 MHz, $CDCl_3$): δ 8.63 (br s, 1H), 7.52 (ddd, *J* = 7.8, 1.0, 1.0, 1H), 7.19 (dd, *J* = 7.5, 1.0 1H), 7.12 (dd, *J* = 7.8, 7.5 1H), 6.96 (ddd, *J* = 1.0, 1.0, 1.0, 1H), 3.61 (s, 3H), 2.32 (d, *J* = 1.0, 3H), 1.71 (s, 6H),; $^{13}$C NMR (125 MHz, $CDCl_3$): δ 178.7, 134.1, 129.2, 126.5, 121.9, 119.2, 118.4,

117.9, 111.4, 52.8, 45.3, 25.2, 9.8; IR (film): 3428, 2950, 1713, 1434, 1264, 1152 $cm^{-1}$; HRMS-ESI (*m/z*) $[M + H]^+$ calculated for $C_{14}H_{18}NO_2$, 232.1332; found, 232.1328.

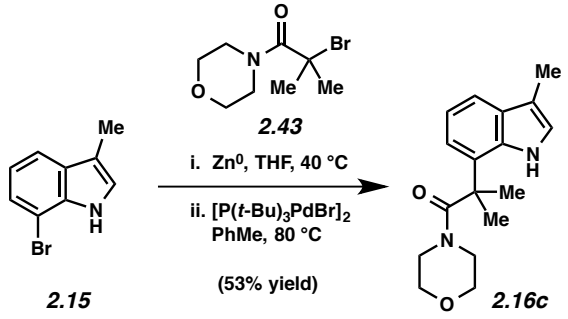


**Morpholine amide 2.16c.** Amide **2.16c** was prepared following the general protocol for the cross-coupling of α-bromoamides with aryl bromides described by Hartwig, with modifications.[59] Inside a glove box, a vial was charged with morpholine amide **2.43** (390.0 mg, 1.65 mmol, 5 equiv), activated zinc dust (112.0 mg, 1.71 mmol, 5.2 equiv) and THF (1.4 mL). The vial was sealed and placed into a heating block maintained at 40 °C for 4 h. This heterogeneous solution was removed from the heat and immediately added to a solution of 7-bromoskatol **2.15**[41] (69.0 mg, 0.33 mmol) and $[P(t\text{-Bu})_3PdBr]_2$ (38.3 mg, 0.05 mmol, 0.15 equiv) in toluene (3.2 mL). The resulting solution was stirred at 80 °C for 12 h. After cooling to 23 °C, the reaction mixture was loaded directly onto a silica gel column and separated by flash chromatography (5:1 Hexane:EtOAc) to afford morpholine amide **2.16c** (50.3 mg, 53% yield) as a clear oil. Morpholine Amide **2.16c**: $R_f$ 0.08 (5:1 Hexanes:EtOAc); $^1H$ NMR (500 MHz, $CDCl_3$): δ 8.35 (br s, 1H), 7.51–7.46 (m, 1H), 7.12–7.08 (m, 2H), 6.95–6.93 (m, 1H), 3.89–2.45 (br m, 8H), 2.32 (d, $J$ = 1.1, 3H), 1.67 (s, 6H); $^{13}C$ NMR (125 MHz, $CDCl_3$): δ 176.2, 133.7, 129.3, 128.1, 121.9, 119.6, 118.0, 116.1, 111.6, 67.1, 65.8, 47.5, 45.3, 43.7, 9.8; IR (film): 3365, 2920, 1619, 1426, 1245, 1112 $cm^{-1}$; HRMS-ESI (*m/z*) $[M - H]^-$ calculated for $C_{17}H_{21}N_2O_2$, 285.1609; found, 285.1610.

### 2.5.2.3 Total Synthesis of (–)-Pendolmycin (2.2)

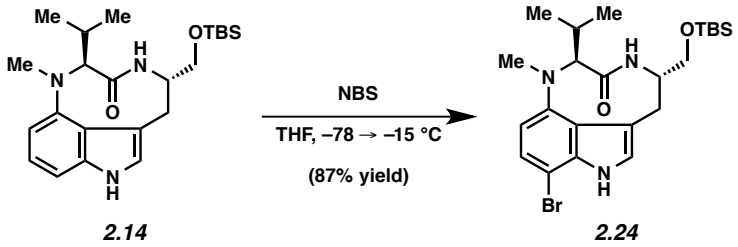


*2.14* *2.24*

**Bromoindole 2.24.** Silylether **2.14** was functionalized following the general protocol described by Kishi, with modification.[28] To a stirred solution of silylether **2.14** (9.5 mg, 0.023 mmol) in THF (2.3 mL) at –78 °C was added *N*-bromosuccinimide (4.1 mg, 0.023 mmol, 1.0 equiv) in THF (2.3 mL). After 10 min, the reaction warmed to –15 °C and stirred for an additional 10 min. The reaction was quenched with water (1 mL), diluted with EtOAc (10 mL) and then washed sequentially with water (10 mL), and brine (5 mL). The organic layers were combined and dried over $Na_2SO_4$. Evaporation under reduced pressure afforded the crude product, which was purified by flash chromatography (3:1 Hexane:EtOAc) to afford bromoindole **2.24** (6.8 mg, 87% yield) as a white solid. Bromoindole **2.24**: Mp: 188–190 °C; $R_f$ 0.6 (2:1 Hexanes:EtOAc); $^1$H NMR (500 MHz, $CDCl_3$): δ 8.20 (br s, 1H), 7.18 (d, $J$ = 8.3, 1H), 6.94 (t, $J$ = 1.8, 1H), 6.41 (d, $J$ = 8.3, 1H), 6.16 (s, 1H), 4.30 (d, $J$ = 10.2, 1H), 4.18–4.14 (m, 1H), 3.65 (dd, $J$ = 10.2, 4.4, 1H), 3.48 (dd, $J$ = 10.0, 9.1 1H), 3.17–3.10 (m, 1H), 2.93–2.87 (m, 4H), 2.66–2.55 (m, 1H) 0.93 (d, $J$ = 6.3, 3H), 0.90–0.88 (m, 9H), 0.62 (d, $J$ = 6.8, 3H), 0.04 (d, $J$ = 11.9, 6H); $^{13}$C NMR (125 MHz, $CDCl_3$): δ 172.7, 147.6, 137.3, 125.1, 121.8, 119.1, 116.1, 107.6, 95.9, 71.5, 65.4, 55.0, 34.1, 33.0, 28.7, 26.0, 21.7, 19.7, 18.4, -5.2, -5.3; IR (film): 3369, 3325, 2928, 2857, 1647, 1502, 1251, 1104 cm$^{-1}$; HRMS-ESI (*m/z*) $[M + Na]^+$ calculated for $C_{23}H_{36}BrN_3O_2SiNa$, 516.1658; found, 516.1659; $[\alpha]^{20}_D$ –384.00° (c = 0.100, $CH_2Cl_2$).

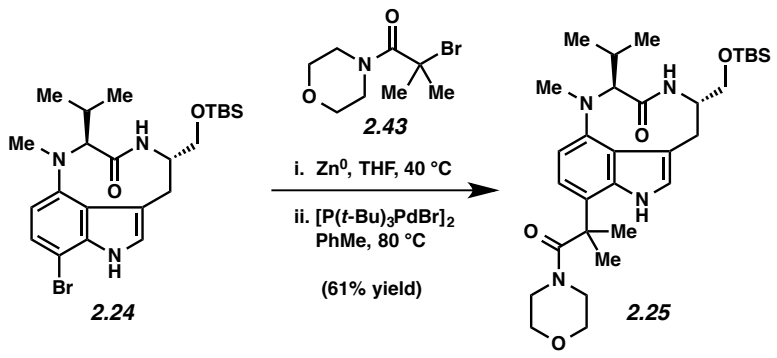


**Morpholine amide 2.25.** Amide **2.25** was prepared following the general protocol described by Hartwig for the cross-coupling of α-bromoamides with aryl bromides, with modifications.[59] Inside a glove box, a vial was charged with morpholine amide **2.43** (19.1 mg, 0.081 mmol, 10.0 equiv), activated zinc dust (5.5 mg, 0.084 mmol, 10.4 equiv) and THF (0.3 mL). The vial was sealed and placed into a heating block maintained at 40 °C for 4 h. This heterogeneous solution was removed from the heat and immediately added to a solution of bromoindole **2.24** (4.0 mg, 8 μmol) and $[P(t\text{-Bu})_3PdBr]_2$ (0.9 mg, 1 μmol, 15 mol%) in toluene (0.2 mL). The resulting solution was stirred at 80 °C for 12 h. After cooling to 23 °C, the reaction mixture was loaded directly onto a silica gel column and separated by flash chromatography (1:1 Hexane:EtOAc) to afford morpholine amide **2.25** (2.8 mg, 61% yield) as a light yellow oil. Morpholine amide **2.25**: $R_f$ 0.4 (1:1 Hexanes:EtOAc); $^1$H NMR (500 MHz, $CDCl_3$): δ 8.52 (br s, 1H), 6.96 (d, $J$ = 8.0, 1H), 6.86 (s, 1H), 6.49 (d, $J$ = 8.0, 1H), 6.16 (br s, 1H), 4.33 (d, $J$ = 10.0, 1H), 4.25–4.16 (m, 1H), 3.70–3.56 (m, 4H), 3.47 (t, $J$ = 10.0, 1H), 3.39–3.20 (m, 3H), 3.14 (d, $J$ =17.4, 3H), 2.66–2.55 (m, 1H), 1.70 (s, 3H), 1.42 (s, 3H), 1.10 (d, $J$ = 6.6, 3H), 0.93 (d, $J$ = 6.6, 4H), 0.88 (s, 9H), 0.55 (d, $J$ = 6.6, 3H), 0.05 (d, $J$ = 12.5, 6H); $^{13}$C NMR (125 MHz, $CDCl_3$): δ 176.6, 172.9, 170.9, 147.0, 136.7, 122.0, 120.5, 118.7, 117.2, 114.3, 106.3, 71.2, 65.5, 56.7, 55.0, 44.8, 36.4, 34.1, 32.9, 28.7, 26.0, 23.4, 21.7, 20.7, 19.7, 18.4 -5.2, -5.3; IR (film): 3375, 2956, 2928, 2857, 1665,

1620, 1508 $cm^{-1}$; HRMS-ESI (*m/z*) $[M + Na]^+$ calculated for $C_{31}H_{50}N_4O_4SiNa$, 593.3498; found, 593.3499; $[\alpha]^{22}_D$ 317.80° (c = 0.100, $CH_2Cl_2$).

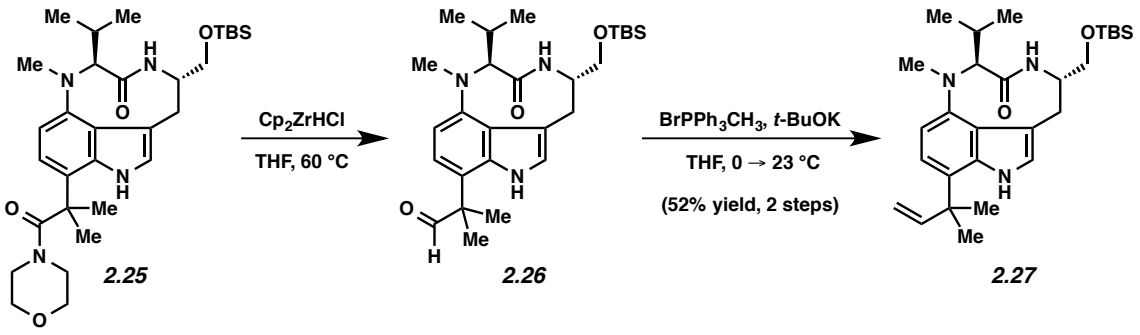


**Olefin 2.27.** Aldehyde **2.26** was prepared following the general protocol described by Georg for the reduction of tertiary amides, with modifications.[29] Inside a glove box, $Cp_2ZrHCl$ (33.9 mg, 0.131 mmol, 5 equiv) and THF (0.7 mL) were added to a vial containing **2.25** (15.0 mg, 0.026 mmol). The reaction vessel was placed in an aluminum block maintained at 60 °C. After stirring for 2 h, the vial was transferred out of the glove box and the reaction mixture was quenched with $H_2O$ (5 mL) and EtOAc (5 mL). The layers were separated and the aqueous layer was extracted with EtOAc (3 x 15 mL). The combined organic layers were washed with brine (15 mL) and dried over $Na_2SO_4$. Evaporation under reduced pressure afforded the crude product, which was used in the subsequent step without further purification. Aldehyde **2.26**: $R_f$ 0.8 (1:1 Hexanes:EtOAc); $^1$H NMR (500 MHz, $CDCl_3$): δ 9.33 (s, 1H), 8.39 (br s, 1H), 7.07 (d, *J* = 8.2, 1H), 6.85 (s, 1H), 6.56 (d, *J* = 8.2, 1H), 6.15 (s, 1H), 4.33 (d, *J* = 10.1, 1H), 4.21–4.12 (m, 1H), 3.62 (dd, *J* = 10.1, 4.2, 1H), 3.45 (t, *J* = 10.1, 1H), 3.17–3.10 (m, 1H), 2.92 (s, 3H), 2.90–2.86 (m, 1H), 2.66–2.57 (m, 1H) 1.56 (s, 3H), 0.93 (d, *J* = 6.3, 3H), 0.87 (s, 9H), 0.62 (d, *J* = 6.7, 3H), 0.09–0.0 (m, 9H).

To a solution of methyl triphenylphosphonium bromide (48.8 mg, 0.137 mmol, 12 equiv) in THF (0.29 mL) at 0 °C was added potassium *tert*-butoxide (15.3 mg, 0.137 mmol, 12 equiv). The resulting mixture was stirred at 0 °C for 30 min then warmed 23 °C. After 30 min the vial was cooled to 0 °C and a solution of aldehyde **2.26** (5.5 mg, 0.011 mmol) in THF (0.29 mL) was added. After 1 h, the reaction was warmed to 23 °C for 2 h. The reaction is quenched with water (5 mL) and diluted with EtOAc (10 mL). The layers were separated, and then the aqueous layer was extracted with EtOAc (3 × 20 mL). The combined organic layers were washed with brine (5 mL) and dried over $MgSO_4$. Evaporation under reduced pressure afforded the crude product, which was further purified by flash chromatography (4:1 Hexanes:EtOAc + 2% $Et_3N$) to provide olefin **2.27** (2.9 mg, 52% yield) as a light yellow oil. Olefin **2.27**: $R_f$ 0.3 (5:1 Hexanes:EtOAc); $^1$H NMR (500 MHz, $CDCl_3$): 8.47 (br s, 1H), 7.01 (d, $J$ = 8.0, 1H), 6.85–6.79 (m, 1H), 6.53–6.46 (m, 1H), 6.24–6.10 (m, 2H), 5.33 (dd, $J$ = 17.8, 1.2, 1H), 5.22 (dd, $J$ = 10.5, 1.2 1H), 4.32 (d, $J$ = 10.5, 1H) 4.29–4.21 (m, 1H) 3.63 (dd, $J$ = 10.5, 4.2, 1H), 3.49–3.41 (m, 1H), 3.15 (app d, $J$ = 17.8, 1H), 2.91 (s, 3H), 2.89–2.72 (m, 1H), 2.68–2.57 (m, 1H), 1.51 (s, 3H), 1.48 (s, 3H), 0.95–0.90 (m, 3H), 0.87 (s, 9H), 0.65 (d, $J$ = 6.5, 3H), 0.05 (s, 3H), 0.02 (s, 3H). $^{13}$C NMR (125 MHz, $CDCl_3$): δ 173.2, 149.8, 146.8, 137.6, 122.8, 121.2, 119.2, 118.8, 114.3, 111.4, 106.5, 71.3, 65.5, 55.1, 40.3, 34.1, 33.1, 28.7, 27.4, 26.9, 26.0, 21.7, 19.7, 18.4, -5.2, -5.3; IR (film): 3452, 3380, 2956, 2929, 2858, 1656, 1507 $cm^{-1}$; HRMS-ESI (*m/z*) $[M + Na]^+$ calculated for $C_{28}H_{45}N_3O_2SiNa$, 506.3179; found, 506.3182; $[\alpha]^{20}_D$ –126.00° (c = 0.100, $CH_2Cl_2$).

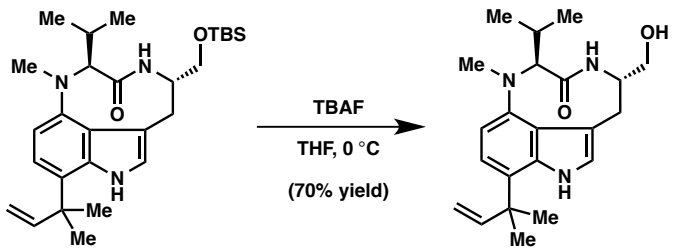


*2.27* *pendolmycin (2.2)*

**Pendolmycin (2.2).** To a solution of olefin **2.27** (6.7 mg, 0.014 mmol) in THF (0.276 mL) at 0 °C was added a solution of TBAF in THF (1.0 M, 138 μL, 0.138 mmol, 10 equiv) dropwise over 3 min. The solution was stirred for 15 min, and then quenched with $H_2O$ (2 mL). The biphasic mixture was further diluted with EtOAc (10 mL) and $H_2O$ (5 mL). The layers were separated, and then the aqueous layer was extracted with EtOAc (3 × 15 mL). The combined organic layers were dried over $MgSO_4$. Evaporation under reduced pressure afforded the crude product, which was further purified by flash chromatography (5:1 $CH_2Cl_2$:$CH_3OH$) to provide pendolmycin (**2.2**) (3.6 mg, 70% yield) as a viscous oil. Spectral data for synthetic **2.2** was consistent with literature reports.[11] Pendolmycin (**2.2**): $R_f$ 0.2 (5:1 $CH_2Cl_2$:$CH_3OH$); $^1H$ NMR (500 MHz, $CDCl_3$): Major conformer: δ 8.48 (br s, 1H), 7.01 (d, *J* = 8.0, 1H), 6.86–6.82 (m, 1H), 6.48 (d, *J* = 8.0, 1H), 6.19 (dd, *J* = 17.8, 10.5, 1H), 5.32 (dd, *J* = 17.8, 1.4, 1H), 5.21 (dd, *J* = 10.5, 1.0, 1H), 4.34 (d, *J* = 10.0, 1H), 4.36–4.29 (m, 1H), 3.74 (app d, *J* = 12.0, 1H), 3.62–3.39 (m, 2H), 3.39–3.32 (m, 1H), 3.17 (app d, *J* = 17.0, 1H), 3.08 (dd, *J* = 17.0, 4.0, 1H), 2.9 (s, 3H), 2.65–2.55 (m, 1H) 1.51 (s, 3H), 1.48 (s, 3H), 0.92 (d, *J* = 7.0, 3H), 0.64 (d, *J* = 7.0, 3H); Minor conformer [26/31 protons were discernable]: δ 8.72 (br s, 1H), 7.12 (d, *J* = 7.8, 1H), 7.02 (d, *J* = 7.8, 1H), 6.97 (d, *J* = 2.0, 1H), 6.21 (dd, 17.8, 10.5, 1H), 5.37 (dd, *J* =17.8, 1.4, 1H), 5.27 (dd, *J* =10.5, 1.4, 1H), 4.48–4.39 (m, 1H), 3.43 (app d, *J* =7.2, 1H), 3.44–3.39 (dd, *J* =1.8, 1.4, 1H), 2.99 (d, *J* =10.5, 1.4, 1H), 2.80 (dd, *J* = 15.0, 2.0, 1H), 2.73 (s, 3H), 2.44–2.31 (m, 1H), 1.53 (s, 3H), 1.52 (s, 3H), 1.25 (d, *J* =6.7, 1H), 0.94 (d, *J* =6.7, 3H).

### 2.5.2.4 Total Syntheses of (–)-Lyngbyatoxin A (2.3) and (–)-Teleocidin A-2 (2.4)

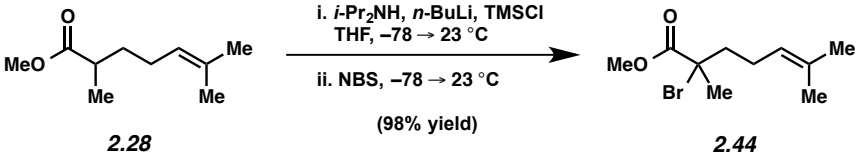


**Bromo ester 2.44.** α-Bromo methyl ester **2.44** was prepared following the known protocol described by Webber for the α-bromination of esters, with modifications.[31] A flask containing THF (33.4 mL) and diisopropylamine (2.81 mL, 20.03 mmol, 2.4 equiv) was cooled to –78 °C and then a solution of *n*-BuLi (8.8 mL, 2.55 M in hexanes, 2.7 equiv) was added dropwise over 5 min. The reaction was stirred for an additional 10 min at –78 °C and then warmed to 23 °C over 1 h. The mixture was cooled to –78 °C and TMSCl (2.8 mL, 21.8 mmol, 2.61 equiv) was added dropwise over 5 min. To the resulting clear solution was added ester **2.28** (1.42 g, 8.35 mmol) as a solution in THF (41.7 mL) over 10 min. The resulting yellow solution was stirred at –78 °C for 20 min and *N*-bromosuccinamide (3.86 g, 21.7 mmol, 2.6 equiv) was added quickly under a stream of nitrogen. The flask was purged with nitrogen for 1 min and allowed to warm to 23 °C in the absence of light over 2.5 h. The reaction was quenched with saturated aqueous $NH_4Cl$ (30 mL) and further diluted with water (200 mL) and $Et_2O$ (200 mL). The layers were separated and the aqueous layer was extracted with $Et_2O$ (3 × 200 mL). The organics were combined, washed with brine (50 mL), and dried over $MgSO_4$. Evaporation under reduced pressure provided a crude light yellow oil, which was purified by flash chromatography (60:1 Hexane:$Et_2O$) to afford bromo ester **2.44** (2.03 g, 98% yield) as a yellow oil. Bromo ester **2.44**: $^1$H NMR (600 MHz, $CDCl_3$): δ 5.12–5.06 (m, 1H), 3.78 (s, 3H), 2.18–1.96 (m, 4H), 1.91 (s, 3H), 1.68 (s, 3H), 1.61 (s, 3H).

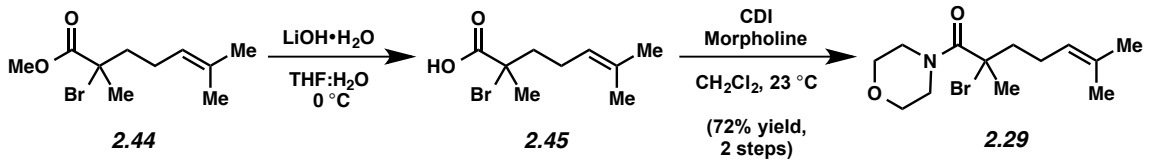


**α-Bromo amide 2.29.** Carboxylic acid **2.45** was prepared following the general protocol by Xia for the saponification of methyl esters, with modifications.[42] To a stirred solution of α-bromo methyl ester **2.44** (12.50 g, 50.1 mmol) in THF (157 mL) at –15 °C was added a solution of lithium hydroxide monohydrate (3.13 g, 74.6 mmol, 1.4 equiv) in $H_2O$ (133 mL) dropwise via syringe pump. After 7 h, the reaction was quenched with 1 M HCl (100 mL) and then diluted with EtOAc (100 mL). The layers were separated, and the aqueous layer was extracted with EtOAc (3 × 100 mL). The combined organic layers were dried over $MgSO_4$. Evaporation of the solvent under reduced pressure afforded crude **2.45**, which was used in the subsequent step without further purification.

Amide **2.29** was prepared from crude **2.45** following a general protocol for the coupling of esters to amines using 1,1'-carbonyldiimidazole, with modifications.[33] To a solution of crude **2.45** in $CH_2Cl_2$ (250 mL) was added 1,1'-carbonyldiimidazole (12.99 g, 80.16 mmol, 1.6 equiv). After stirring for 15 min, morpholine (10.83 mL, 125.25 mmol, 2.5 equiv) was added and the reaction was allowed to stir for 6 h. The reaction was quenched with 5% citric acid (400 mL), concentrated in vacuo, and then diluted with $H_2O$ (150 mL) and $Et_2O$ (150 mL). The organic layer was separated, washed with brine (50 mL), and then dried over $MgSO_4$. Evaporation under reduced pressure afforded the crude product, which was purified by flash chromatography (5:1 Hexanes:EtOAc) to afford α-bromo amide **2.29** (11.0 g, 72% yield, over two steps) as a yellow oil. α-bromo amide **2.29**: $R_f$ 0.7 (1:1 Hexanes:EtOAc); $^1$H NMR (500 MHz, $CDCl_3$): δ 5.11–5.05 (m, 1H), 4.00–3.66 (m, 8H), 2.30–1.90 (m, 7H), 1.68 (s, 3H), 1.61 (s, 3H); $^{13}$C NMR (125 MHz,

$CDCl_3$): δ 168.6, 133.1, 122.3, 66.6, 61.4, 43.0, 30.5, 25.7, 24.7, 17.7; IR (neat): 2967, 2916, 2855, 1635, 1418 $cm^{-1}$; HRMS-ESI (*m/z*) $[M + H]^+$ calculated for $C_{13}H_{22}BrNO_2$, 304.0907; found, 304.0901.

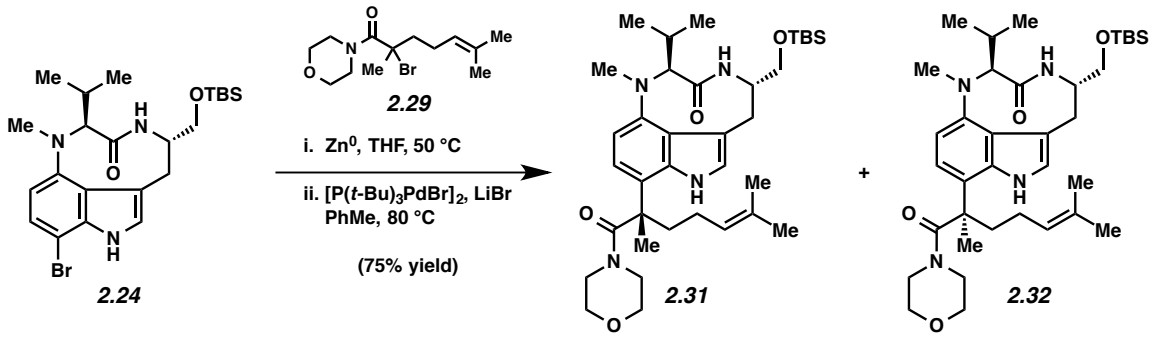


**Morpholine amides 2.31 and 2.32.** Amides **2.31** and **2.32** were prepared following the general protocol described by Hartwig for the cross-coupling of α-bromoamides with aryl bromides, with modifications.[59] Inside a glove box, a vial was charged with a magnetic stir bar, α-bromo amide **2.29** (41.2 mg, 0.135 mmol, 10 equiv), activated zinc dust (8.8 mg, 0.134 mmol, 9.9 equiv), and THF (0.32 mL). The vial was sealed and placed into a heating block maintained at 50 °C for 12 h. This clear, pale yellow solution was removed from the heat and immediately added to a solution of bromoindole **2.24** (6.7 mg, 0.0135 mmol), LiBr (1.2 mg, 0.0135 mmol, 1.0 equiv) and $[P(t\text{-}Bu)_3PdBr]_2$ (1.6 mg, 2 μmol, 15 mmol%) in toluene (0.2 mL). The resulting solution was stirred at 80 °C for 12 h. The reaction mixture was passed through a silica gel plug (EtOAc eluent) and concentrated in vacuo. The crude residue was separated by preparatory thin layer chromatography (2:1 Hexane:EtOAc) to afford two separate diastereomeric amides **2.31** (1.8 mg, 43% yield) and **2.32** (2.4 mg, 32% yield) as light yellow viscous oils. Morpholine amide **2.31**: $R_f$ 0.7 (2:1 Hexanes:EtOAc); $^1H$ NMR (500 MHz, $CDCl_3$): δ 8.52 (br s, 1H), 6.89 (d, $J$ = 8.2, 1H), 6.82 (br s, 1H), 6.46 (d, $J$ = 8.2, 1H), 6.13 (br s, 1H), 4.40–4.00 (m, 1H), 4.31 (d, $J$ = 10.2, 1H),

4.28–4.20 (m, 1H), 3.65 (dd, $J$ = 10.2, 4.3, 2H), 3.48 (t, $J$ = 9.9, 1H), 3.39–2.70 (m, 14H), 2.69–2.50 (m, 1H), 2.45–1.66 (m, 10H), 0.94–0.91 (m, 4H), 0.88 (s, 9H), 0.54 (br s, 3H), 0.04 (s, 3H), 0.02 (s, 3H); $^{13}$C NMR (125 MHz, $CDCl_3$): δ 172.9, 146.9, 136.8, 124.5, 121.8, 118.7, 114.1, 106.2, 71.3, 67.2, 65.9, 65.6, 61.6, 55.1, 54.5, 47.5, 46.0, 43.7, 38.8, 34.1, 32.9, 29.9, 28.7, 26.0, 25.8, 23.2, 21.7, 20.3, 19.7, 17.6, -5.2, -5.3; IR (film): 3383, 2928, 1664, 1508, 1115 cm$^{-1}$; HRMS-ESI (*m/z*) $[M + H]^+$ calculated for $C_{36}H_{59}N_4O_4Si$, 639.4305; found, 639.4301; $[\alpha]^{22}_D$ – 108.00 (c 0.10 $CH_2Cl_2$). Morpholine amide **2.32**: $R_f$ 0.7 (2:1 Hexanes:EtOAc); $^1$H NMR (500 MHz, $CDCl_3$): δ 8.53 (br s, 1H), 6.95 (d, $J$ = 8.2, 1H), 6.84 (br s, 1H), 6.46 (d, $J$ = 8.2, 1H), 6.14 (br s, 1H), 5.25–5.00 (m, 1H), 4.32 (d, $J$ = 10.0, 1H), 4.24–4.16 (br m, 1H), 3.70–3.42 (m, 1H) 3.64 (dd, $J$ = 10.0, 4.1, 2H), 3.46 (t, $J$ = 9.9, 1H), 3.40–3.0 (m, 6H), 2.90 (dd, $J$ = 17.9, 4.1, 1H) 2.90 (s, 3H), 2.66–2.51 (m, 1H), 2.35–1.81 (m, 5H), 1.79–1.58 (m, 8H), 0.96–0.89 (m, 4H), 0.87 (s, 9H), 0.52 (d, $J$ = 6.6, 3H), 0.05 (s, 3H), 0.03 (s, 3H); $^{13}$C NMR (125 MHz, $CDCl_3$) [28/36 carbons were discernable]: δ 175.5, 172.9, 171.3, 147.0, 136.6, 118.7, 114.2, 106.2, 71.2, 67.2, 65.9, 65.5, 60.6, 55.0, 47.5, 34.2, 32.9, 29.8, 29.4, 28.8, 26.0, 21.7, 21.2, 19.7, 18.4, 14.4, -5.2, -5.3; IR (film): 3375, 2928, 1666, 1508, 1115 cm$^{-1}$; HRMS-ESI (*m/z*) $[M - H]^-$ calculated for $C_{36}H_{57}N_4O_4Si$, 637.4149; found, 637.4147; $[\alpha]^{22}_D$ –106.00 (c = 0.100, $CH_2Cl_2$).

*Note: $^1$H NMR and $^{13}$C NMR integrations and peaks were complicated by the presence of major and minor conformers.[13] Empirical data is therefore reported for compounds **2.31**–**2.34**, **2.46** and **2.47**. Absolute stereochemical configuration for amides **2.31** and **2.32** were determined by subjecting each compound to the subsequent synthetic steps and matching each resulting compound to known spectral data for the natural products **2.3** and **2.4**.*

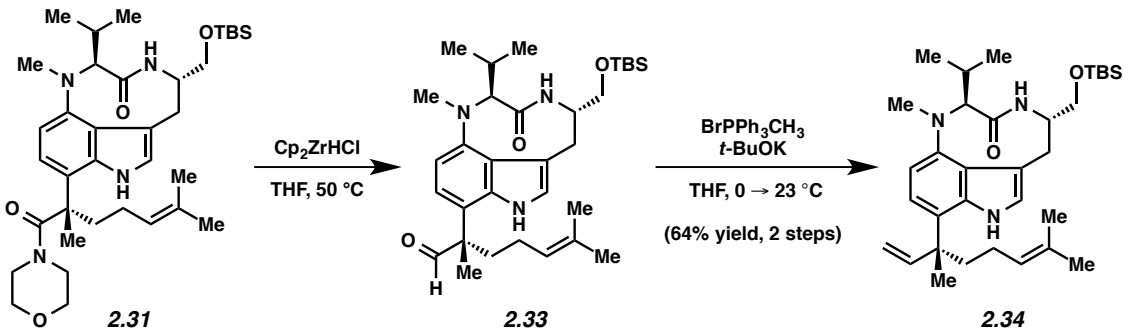


**Olefin 2.34.** Aldehyde **2.33** was prepared following the general protocol described by Georg for the reduction of tertiary amides, with modifications.[29] Inside a glove box, $Cp_2ZrHCl$ (7.3 mg, 0.03 mmol, 10 equiv) and THF (0.3 mL) were added to a vial containing **2.31** (1.8 mg, 3 μmol). The reaction vessel was placed into an aluminum block maintained at 50 °C. After stirring for 12 h, the vial was transferred out of the glove box. The reaction mixture was quenched with silica gel (10.0 mg) and EtOAc with 2% $Et_3N$ (1.0 mL), and then stirred for 1 h. The mixture was eluted through a plug of silica gel (EtOAc with 2% $Et_3N$ eluent). Evaporation under reduced pressure afforded crude **2.33**, which was used in the subsequent step without further purification. Aldehyde **2.33**: $R_f$ 0.9 (1:1 Hexanes:EtOAc); $^1$H NMR (500 MHz, $CDCl_3$): δ 9.33 (s, 1H), 8.5 (br s, 1H), 7.05 (d, $J$ = 8.2, 1H), 6.83 (b s, 1H), 6.55 (d, $J$ = 8.2, 1H), 6.16 (s, 1H), 5.18–5.01 (m, 1H), 4.33 (d, $J$ = 9.9, 1H), 4.26–4.08 (m, 1H), 3.78–3.68 (m, 1H), 3.63 (dd, $J$ = 10.9, 4.8, 1H), 3.45 (t, $J$ = 9.9, 1H), 3.11–3.06 (m, 1H), 2.91 (s, 3H), 2.79–2.49 (m, 2H), 2.43–1.76 (m, 5H), 1.65 (s, 2H), 1.63 (s, 2H), 1.42–1.40 (m, 1H), 0.94–0.88 (m, 9H), 0.86–0.80 (m, 3H), 0.82 (dd, $J$ = 9.9, 6.7, 2H)  0.58 (d, $J$ = 6.7, 3H), 0.05 (s, 3H), 0.02 (s, 3H).

A vial was charged with methyl triphenylphosphonium bromide (266.5 mg, 0.746 mmol, 265 equiv) and placed in a 0 °C bath. To this vial was added a solution of potassium *tert*-butoxide (79.0 mg, 0.704 mmol, 250 equiv) in THF (1.0 mL) dropwise over 2 min, and the resulting yellow mixture was allowed to warm to 23 °C over 30 min. After 1 h, an aliquot of the resulting

ylide stock solution (20.0 µl, 5 equiv) was added dropwise to a solution of aldehyde **2.33** (3 µmol) in THF (0.3 mL) at 0 °C. After 1 h, the reaction was warmed up to 23 °C and stirred for 12 h. The reaction was quenched with water (1 mL) and EtOAc (1 mL). The layers were separated, and then the aqueous layer was extracted with EtOAc (3 × 5 mL). The combined organic layers were dried over $MgSO_4$. Evaporation under reduced pressure afforded the crude product, which was further purified by flash chromatography (1:199 Acetone:Benzene) to provide olefin **2.34** (1.0 mg, 64% yield over two steps) as a viscous light yellow oil. Olefin **2.34**: $R_f$ 0.5 (5:1 Hexanes:EtOAc); $^1$H NMR (500 MHz, $CDCl_3$): δ 8.54–8.47 (m, 1H), 6.97 (d, $J$ = 8.1, 1H), 6.80 (br s, 1H), 6.48 (d, $J$ = 8.1, 1H), 6.17 (dd, $J$ = 17.6, 10.6, 1H), 6.15 (br s, 1H), 5.36–5.23 (m, 3H), 5.13–5.03 (m, 1H), 4.31 (d, $J$ = 10.0, 1H), 4.24 (dd, $J$ = 10.0, 3.6, 1H), 3.63 (dd, $J$ = 10.0, 3.6, 1H), 3.46 (t, $J$ = 10.0, 1H), 3.13 (d, $J$ = 17.6, 1H), 3.00–2.85 (s, 5H), 2.85–2.73 (m, 1H), 2.65–2.57 (m, 1H), 2.55–1.73 (m, 5H), 1.65 (app s, 2H), 1.49–1.44 (m, 6H), 0.88 (s, 9H), 0.64 (d, $J$ = 6.8, 3H), 0.05 (s, 3H), 0.02 (s, 3H); $^{13}$C NMR (125 MHz, $CDCl_3$): δ 173.3, 148.6, 146.7, 137.7, 131.6, 124.8, 121.6, 121.0 120.1, 118.9, 114.2, 112.6, 106.5, 71.3, 65.5, 55.1, 43.4, 39.8, 38.7, 34.1, 33.0, 32.1, 28.7, 26.0, 24.2, 23.2, 21.7, 19.7, 18.4, 17.7, 14.3, -5.2, -5.3; IR (film): 2927, 2856, 1662, 1508, 1105 $cm^{-1}$; HRMS-ESI (*m/z*) $[M - H]^-$ calculated for $C_{33}H_{52}N_3O_2Si$, 550.38233; found, 550.38368; $[\alpha]^{20}_D$ –98.00 (c = 0.100, $CH_2Cl_2$).

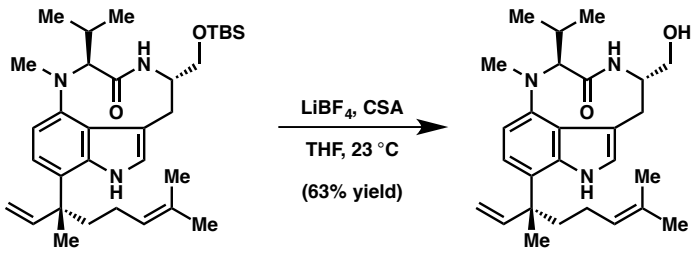


*2.34* *lyngbyatoxin A (2.3)*

**Lyngbyatoxin A (2.3).** Lyngbyatoxin A (**2.3**) was prepared following the general protocol for desilylation described by Kishi, with modifications.[36] A vial was charged with lithium tetrafluoroborate (85.0 mg, 0.91 mmol, 500 equiv) and $CH_3CN$ (0.91 mL). An aliquot of the resulting mixture (1.0 M, 9 μL, 9 μmol, 5 equiv) was added dropwise to a solution of **2.34** (1.0 mg, 1.8 μmol) in THF (0.25 mL) over 1 min. After the solution was stirred for 20 min, (±)-camphorsulfonic acid (2.1 mg, 9 μmol, 5 equiv) was added and the reaction was stirred for 24 h at 23 °C. The mixture was diluted with EtOAc (1 mL) and $H_2O$ (1 mL). The layers were separated, and then the aqueous layer was extracted with EtOAc (3 × 5 mL). The combined organic layers were dried over $MgSO_4$. Evaporation under reduced pressure afforded the crude product, which was further purified by flash chromatography (17:2:1 Hexanes:$CHCl_3$:*i*PrOH) to provide lyngbyatoxin A (**2.3**) (0.5 mg, 63% yield) as a viscous light yellow oil. Lyngbyatoxin A (**2.3**): $R_f$ 0.6 (100% EtOAc); $^1$H NMR (500 MHz, $CDCl_3$): δ (major conformer) 8.52 (br s, 1H), 6.97 (d, *J* = 8.2, 1H), 6.83–6.77 (m, 1H), 6.48 (d, *J* = 8.2, 1H), 6.34 (s, 1H), 6.18 (dd, *J* = 18.0, 10.5, 1H), 5.32 (d, *J* = 18.0, 1H), 5.28 (d, *J* = 10.5, 1H), 5.12–5.02 (m, 1H), 4.30 (d, *J* = 10.0, 1H), 4.29– 4.20 (m, 1H), 3.75 (dd, *J* = 10.7, 4.2 1H), 3.54–3.50 (m, 1H), 3.18 (br d, *J* = 17.0, 1H), 2.99 (dd, *J* = 15.0, 11.0, 1H), 2.91 (s, 3H), 2.58 (dqq, *J* = 10.7, 6.5, 6.5, 1H), 2.04–2.16 (m, 5H), 1.65 (s, 3H), 1.47 (s, 3H), 1.44 (s, 3H) 0.92 (d, *J* = 6.5, 3H), 0.64 (d, *J* = 6.5, 3H); δ (minor conformer) [27/39 protons were discernable] 8.76 (br s, 1H), 7.10 (d, *J* = 8.0, 1H), 7.01 (d, *J* = 8.0, 1H), 5.34 (d, *J* = 18.0, 1H), 4.46–4.40 (m, 1H), 3.46 (dd, *J* = 11.0, 6.7, 1H), 3.38 (dd, *J* =

11.0, 6.7, 1H), 2.80 (dd, *J* = 15.0, 1.5, 1H), 2.74 (s, 3H), 2.39 (dqq, *J* = 10.8, 6.5, 6.5, 1H), 1.63 (s, 3H), 1.50 (s, 3H), 1.49 (s, 3H), 1.25 (d, *J* = 6.5, 3H), 0.97 (d, *J* = 6.5, 3H).

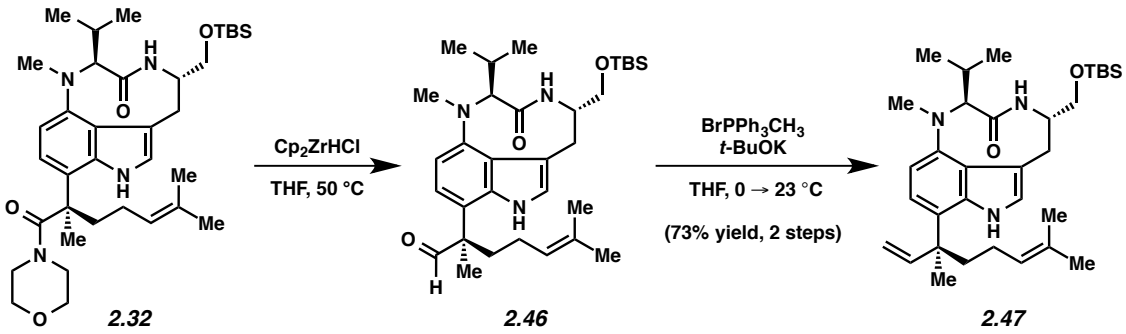


**Olefin 2.47.** Aldehyde **2.46** was prepared following the general protocol described by Georg for the reduction of tertiary amides, with modifications.[29] Inside a glove box, $Cp_2ZrHCl$ (7.7 mg, 0.03 mmol, 10 equiv) and THF (0.3 mL) were added to a vial containing **2.32** (1.9 mg, 3 μmol). The reaction vessel was placed into an aluminum block maintained at 50 °C. After stirring for 12 h, the vial was transferred out of the glove box. The reaction mixture was quenched with silica gel (10.0 mg) and EtOAc with 2% $Et_3N$ (1.0 mL), and then stirred for 1 h. The mixture was eluted through a plug of silica gel (EtOAc with 2% $Et_3N$ eluent). Evaporation under reduced pressure afforded crude **2.46**, which was used in the subsequent step without further purification. Aldehyde **2.46**: $R_f$ 0.9 (1:1 Hexanes:EtOAc); $^1$H NMR (500 MHz, $CDCl_3$): δ 9.33 (s, 1H), 8.5 (br s, 1H), 7.04 (d, *J* = 8.4, 1H), 6.84 (m, 1H), 6.55 (d, *J* = 8.4, 1H), 6.16 (s, 1H), 5.15–4.98 (m, 1H), 4.47–3.97 (m, 2H), 4.43 (d, *J* = 10.0, 1H), 3.78–3.68 (m, 1H), 3.61 (dd, *J* = 10.0, 4.3, 2H), 3.44 (t, *J* = 10.0, 1H), 3.17–3.10 (m, 2H), 2.91 (s, 3H), 2.79–2.54 (m, 3H), 2.23–1.81 (m, 5H), 1.41 (s, 3H), 0.87 (m, 9H), 0.77 (dd, *J* = 10.0, 6.7, 3H)  0.57 (d, *J* = 6.7, 3H), 0.05 (s, 3H), 0.02 (s, 3H).

A vial was charged with methyl triphenylphosphonium bromide (117.0 mg, 0.328 mmol, 110 equiv) and placed in a 0 °C bath. To this vial was added a solution of potassium *tert*-butoxide

(33.3 mg, 0.297 mmol, 100 equiv) in THF (1.0 mL) dropwise over 2 min and the resulting yellow mixture was allowed to warm to 23 °C over 30 min. After 1 h, an aliquot of the resulting ylide stock solution (50.0 μl, 5 equiv) was added dropwise to a solution of aldehyde **2.46** (3 μmol) in THF (0.3 mL) at 0 °C. After 1 h, the reaction was warmed up to 23 °C and stirred for 12 h. The reaction was quenched with water (1 mL) and EtOAc (1 mL). The layers were separated, and then the aqueous layer was extracted with EtOAc (3 × 5 mL). The combined organic layers were dried over $MgSO_4$. Evaporation under reduced pressure afforded the crude product, which was further purified by flash chromatography (1:199 Acetone:Benzene) to provide olefin **2.47** (1.2 mg, 73% yield over two steps) as a viscous light yellow oil. Olefin **2.47**: $R_f$ 0.5 (5:1 Hexanes:EtOAc); $^1$H NMR (500 MHz, $CDCl_3$): δ 8.54 (br m, 1H), 6.98 (d, *J* = 8.1, 1H), 6.82 (br s, 1H), 6.49 (d, *J* = 8.1, 1H), 6.21 (dd, *J* = 17.6, 10.6, 1H), 6.15 (br s, 1H), 5.32–5.22 (m, 2H), 5.13–5.01 (m, 1H), 4.31 (d, *J* = 10.1, 1H), 4.25 (m, 1H), 3.63 (dd, *J* = 10.1, 4.5, 1H), 3.45 (t, *J* = 10.1, 1H), 3.13 (d, *J* = 17.7, 1H), 2.91 (s, 3H), 2.88–2.74 (m, 2H), 2.66–2.54 (m, 1H), 2.10–1.70 (m, 3H), 1.65–1.61 (m, 2H), 1.45 (s, 2H), 1.43 (s, 1H), 1.38 (s, 2H), 0.88 (s, 9H), 0.85 (dd, *J* = 6.8, 4.5, 2H), 0.83–0.78 (m, 1H), 0.75 (dd, *J* = 4.5, 6.8, 2H), 0.60 (d, *J* = 6.8, 3H), 0.05 (s, 3H), 0.02 (s, 3H); $^{13}$C NMR (125 MHz, $CDCl_3$): δ 173.2, 149.3, 146.7, 137.6, 131.6, 124.7, 121.2, 120.4, 118.7, 114.1, 112.2, 106.0, 71.3, 65.5, 55.0, 43.5, 39.6, 38.1, 34.2, 32.9, 32.1, 28.7, 26.0, 24.9, 23.3, 22.7, 21.8, 19.6, 18.4, 17.5, 14.3, -5.2, -5.3; IR (film): 2927, 2854, 1662, 1466, 1105 $cm^{-1}$; HRMS-ESI (*m/z*) $[M - H]^-$ calculated for $C_{33}H_{52}N_3O_2Si$, 550.38233; found, 550.38371; $[\alpha]^{20}_D$ –136.00 (c = 0.100, $CH_2Cl_2$).

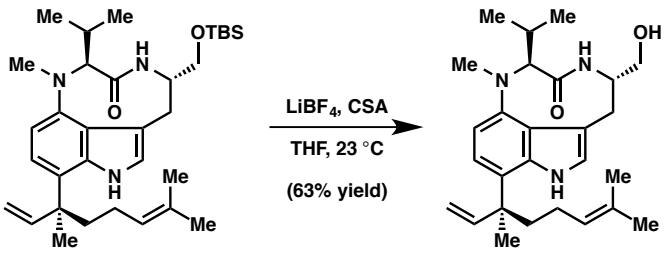


*2.47* *teleocidin A-2 (2.4)*

**Teleocidin A-2 (2.4).** Teleocidin A-2 (**2.4**) was prepared following the general protocol for desilylation described by Kishi, with modifications.[36] A vial was charged with lithium tetrafluoroborate (63.7 mg, 0.68 mmol, 250 equiv) and $CH_3CN$ (0.68 mL). An aliquot of the resulting mixture (1.0 M, 14 μL, 14 μmol, 5 equiv) was added dropwise to a solution of **2.47** (1.5 mg, 3 μmol) in THF (0.25 mL) over 1 min. After the solution was stirred for 20 min, (±)-camphorsulfonic acid (3.2 mg, 14 μmol, 5 equiv) was added and the reaction was stirred for 24 h at 23 °C. The mixture was diluted with EtOAc (1 mL) and $H_2O$ (1 mL). The layers were separated, and then the aqueous layer was extracted with EtOAc (3 × 5 mL). The combined organic layers were dried over $MgSO_4$. Evaporation under reduced pressure afforded the crude product, which was further purified by flash chromatography (17:2:1 Hexanes:$CHCl_3$:*i*PrOH) to provide teleocidin A-2 (**2.4**) (0.5 mg, 63% yield) as a viscous light yellow oil. Teleocidin A-2 (**2.4**): $R_f$ 0.6 (100% EtOAc); $^1$H NMR (500 MHz, $CDCl_3$): δ (major conformer) 8.53 (br s, 1H), 6.98 (d, *J* = 8.1, 1H), 6.83–6.80 (m, 1H), 6.49 (d, *J* = 8.1, 1H), 6.20 (dd, *J* = 18.0, 10.5, 1H), 5.30 (d, *J* = 18.0, 1H), 5.26 (d, *J* = 10.5, 1H), 5.10–5.05 (m, 1H), 4.34 (d, *J* = 10.5, 1H), 4.37– 4.30 (m, 1H), 3.72 (dd, *J* = 10.8, 4.0 1H), 3.54–3.44 (m, 1H), 3.18 (br d, *J* = 17.0, 1H), 2.96 (dd, *J* = 17.0, 4.0 1H), 2.92 (s, 3H) 2.60 (dqq, *J* = 10.8, 6.5, 6.5, 1H), 2.51–1.69 (m, 6H), 1.62 (s, 3H), 1.45 (s, 3H), 1.39 (s, 3H) 0.92 (d, *J* = 6.5, 3H), 0.60 (d, *J* = 6.5, 3H); δ (minor conformer) [31/39 protons were discernable] 8.75 (br s, 1H), 7.09 (d, *J* = 8.0, 1H), 7.01 (d, *J* = 8.0, 1H), 6.97 (s, 1H), 6.22 (dd, *J* = 17.9, 10.3, 1H), 5.35 (*J* = 17.9, 1H), 5.33 (d, *J* = 11.0, 1H), 5.12–5.02 (m, 1H)

4.48–4.39 (m, 1H), 3.46 (dd, $J$ = 11.0, 6.5, 1H), 3.39 (dd, $J$ = 11.0, 6.5, 1H), 2.80 (dd, $J$ = 15.0, 1.5, 1H), 2.73 (s, 3H), 2.39 (dqq, $J$ = 11.0, 6.5, 6.5, 1H), 1.65 (s, 3H), 1.47 (s, 3H), 1.42 (s, 3H), 1.25 (d, $J$ = 6.5, 3H), 0.94 (d, $J$ = 6.5, 3H).

## 2.6 Spectra Relevant to Chapter Two:

### Total Syntheses of Indolactam Alkaloids (–)-Indolactam V, (–)-Pendolmycin, (–)-Lyngbyatoxin A, and (–)-Teleocidin A-2

Noah F. Fine Nathel, Tejas K. Shah, Sarah M. Bronner, and Neil K. Garg.

*Chem. Sci.* **2014**, *5*, 2184–2190.

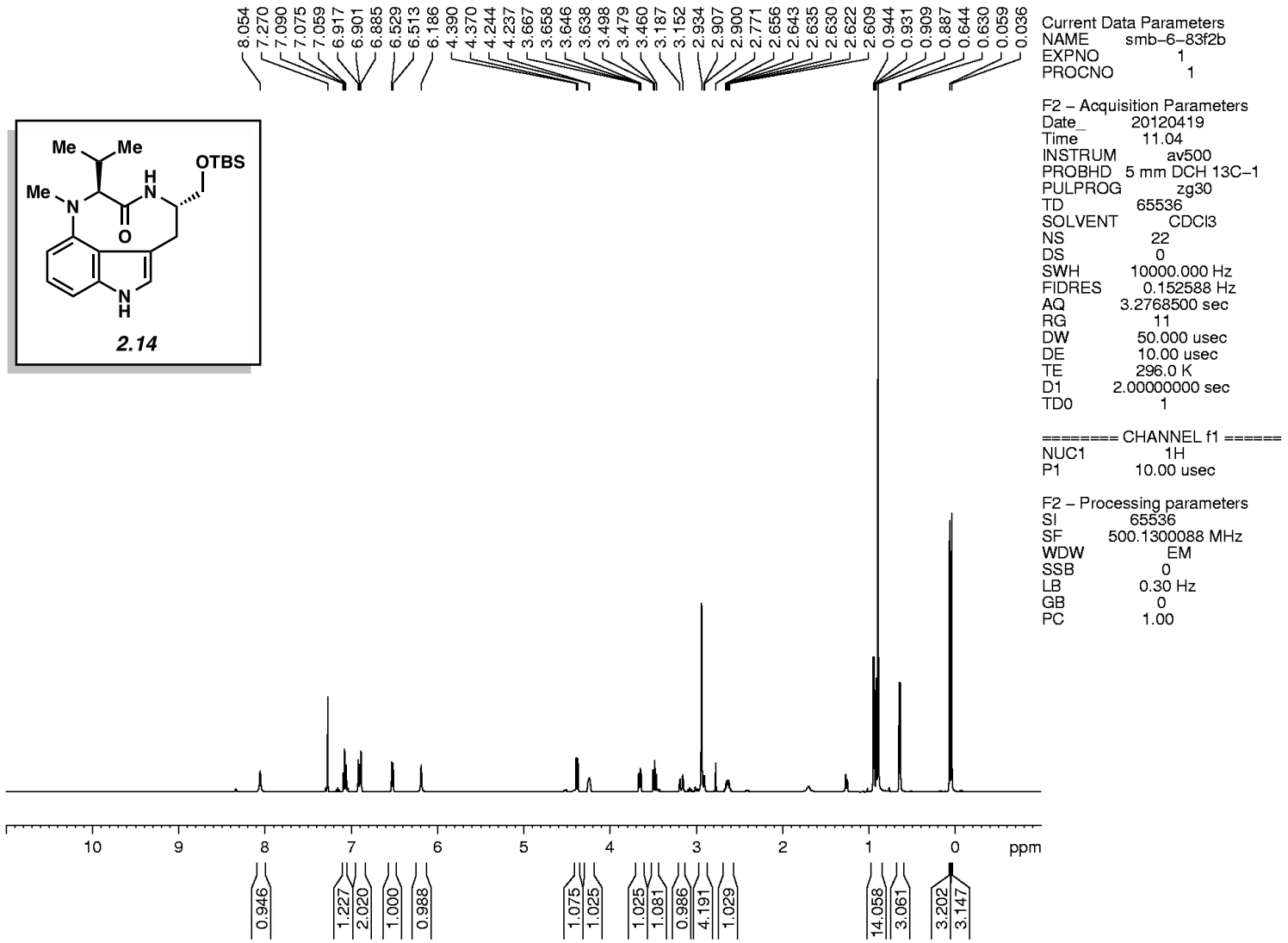


***Figure A2.2.*** $^{1}$H NMR (500 MHz, $CDCl_3$) of compound **2.14**.

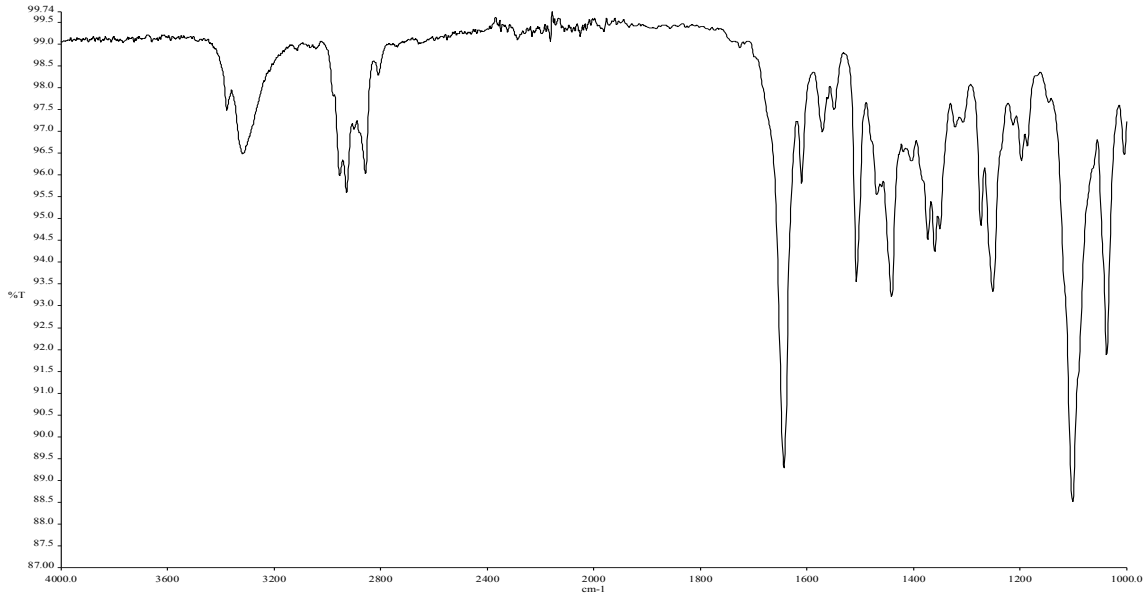


***Figure A2.3.*** Infrared spectrum of compound **2.14**.

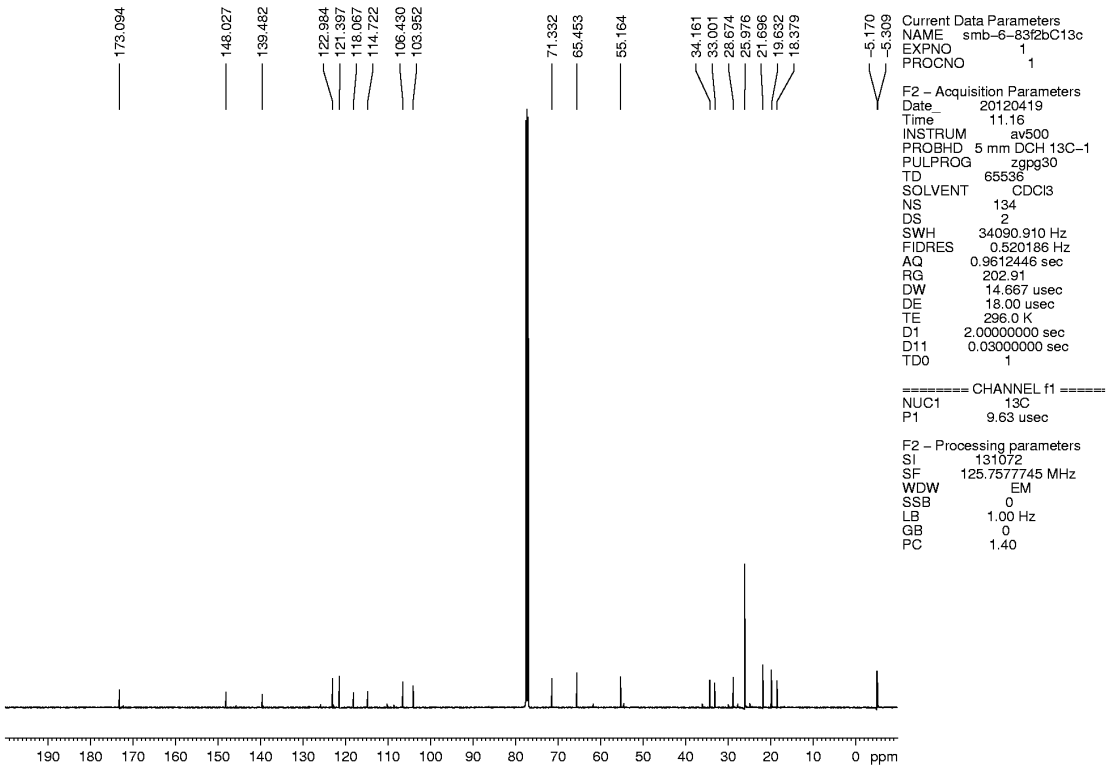


***Figure A2.4.*** $^{13}C$ NMR (125 MHz, $CDCl_3$) of compound **2.14**.

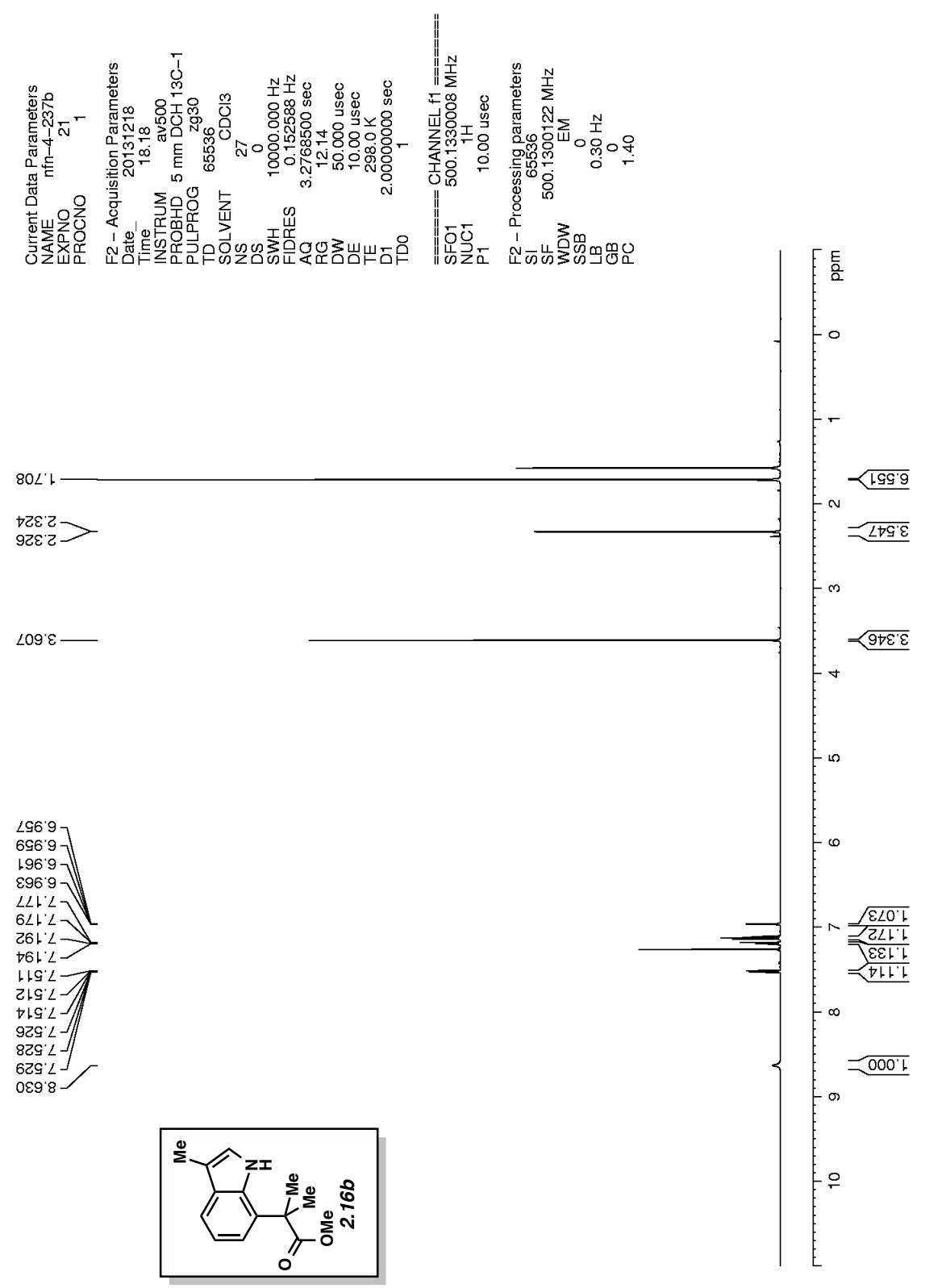


***Figure A2.5.*** $^{1}$H NMR (500 MHz, $CDCl_3$) of compound **2.16b**

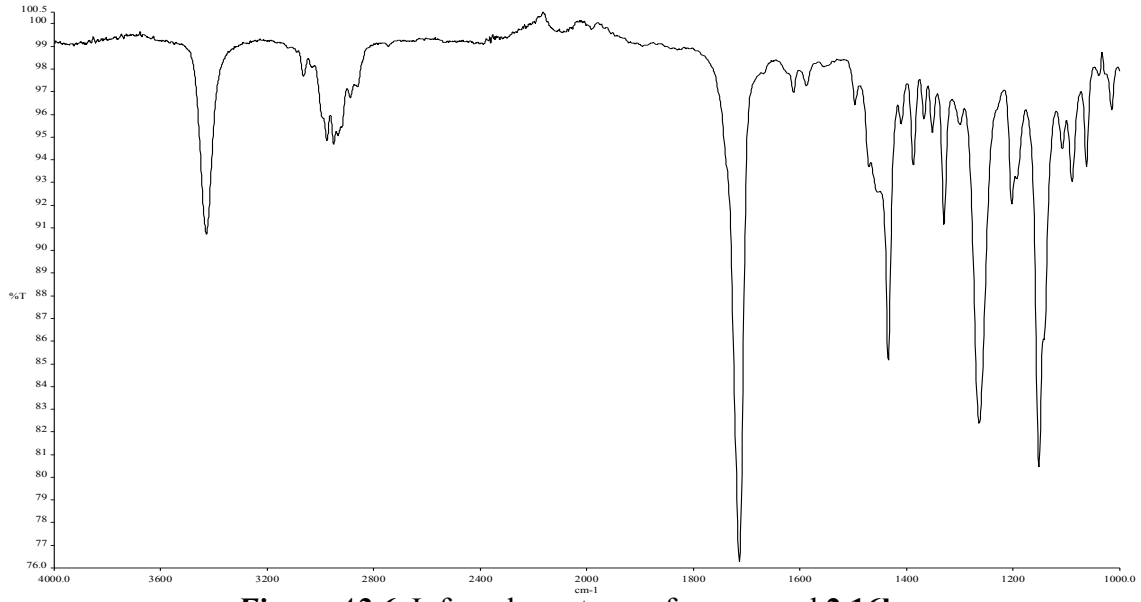


***Figure A2.6.*** Infrared spectrum of compound **2.16b**.

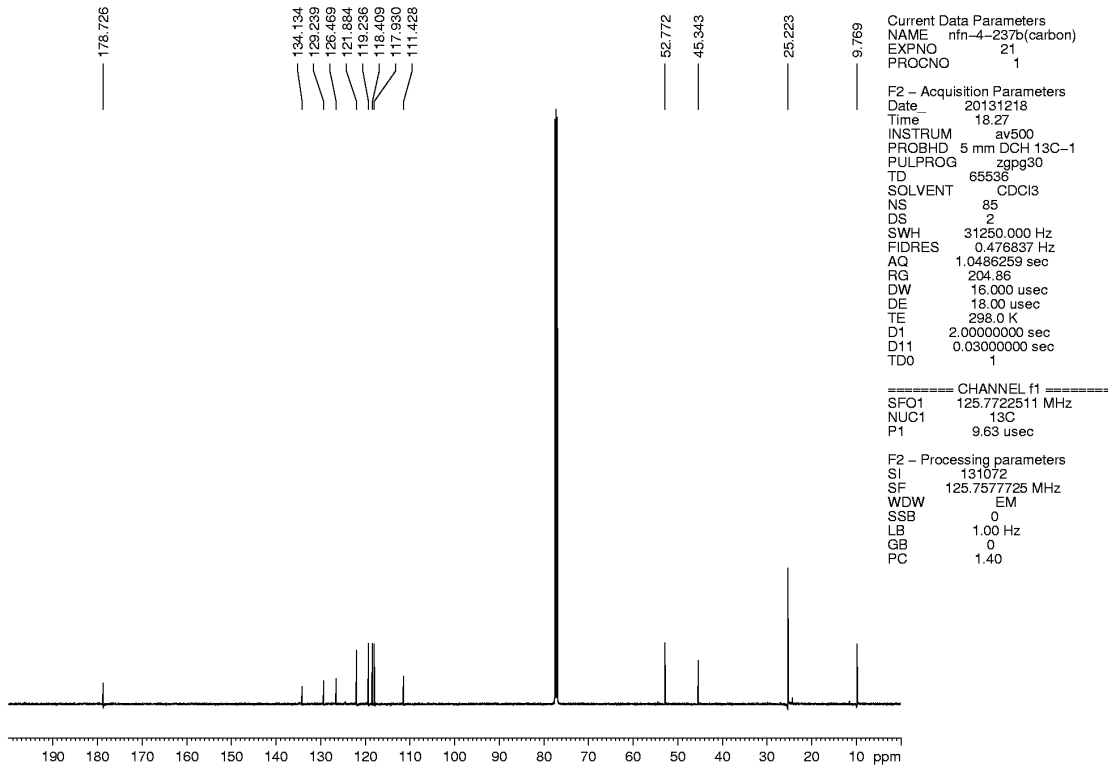


***Figure A2.7.*** $^{13}C$ NMR (125 MHz, $CDCl_3$) of compound **2.16b**.

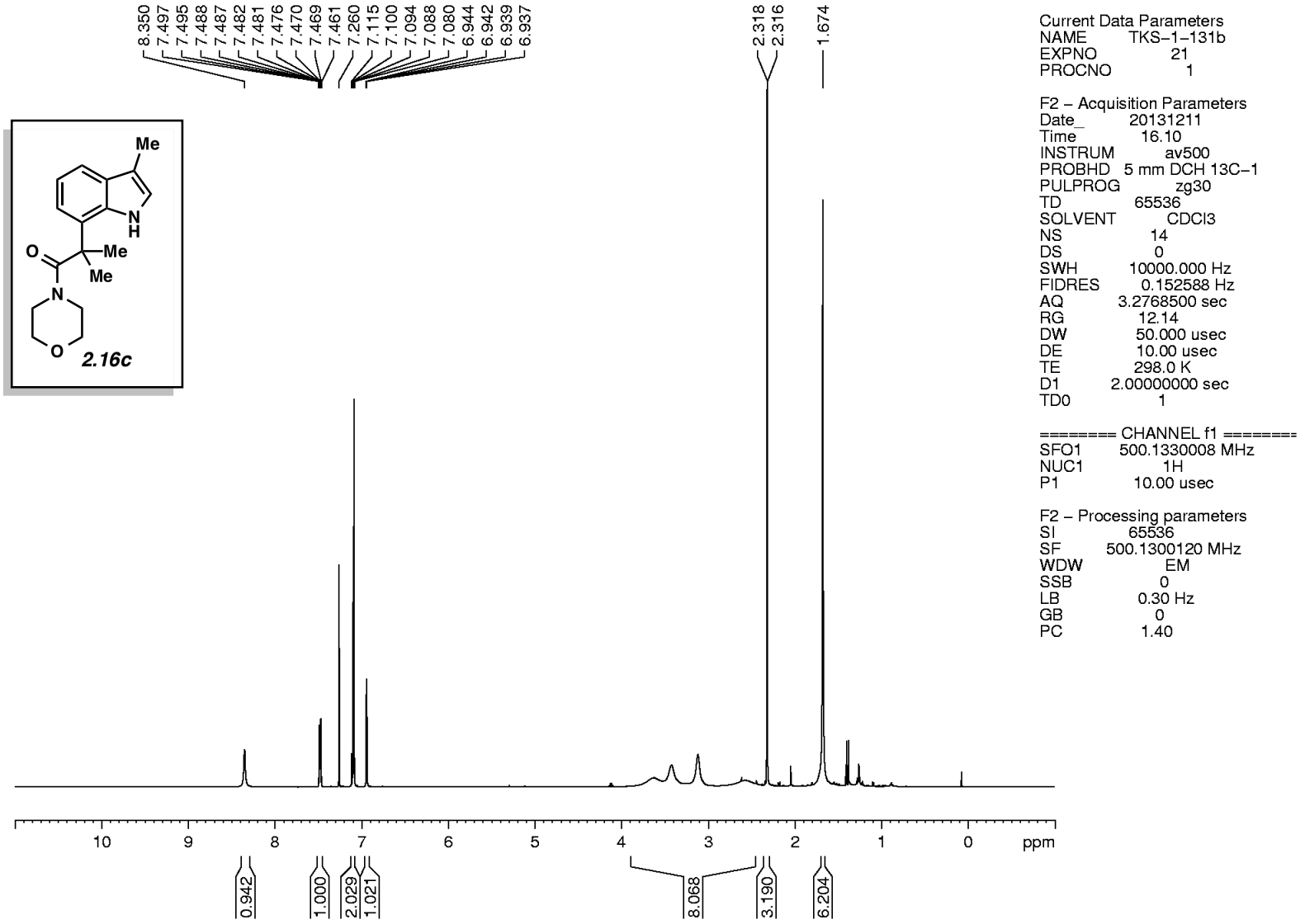


***Figure A2.8.*** $^{1}$H NMR (500 MHz, $CDCl_3$) of compound **2.16c**

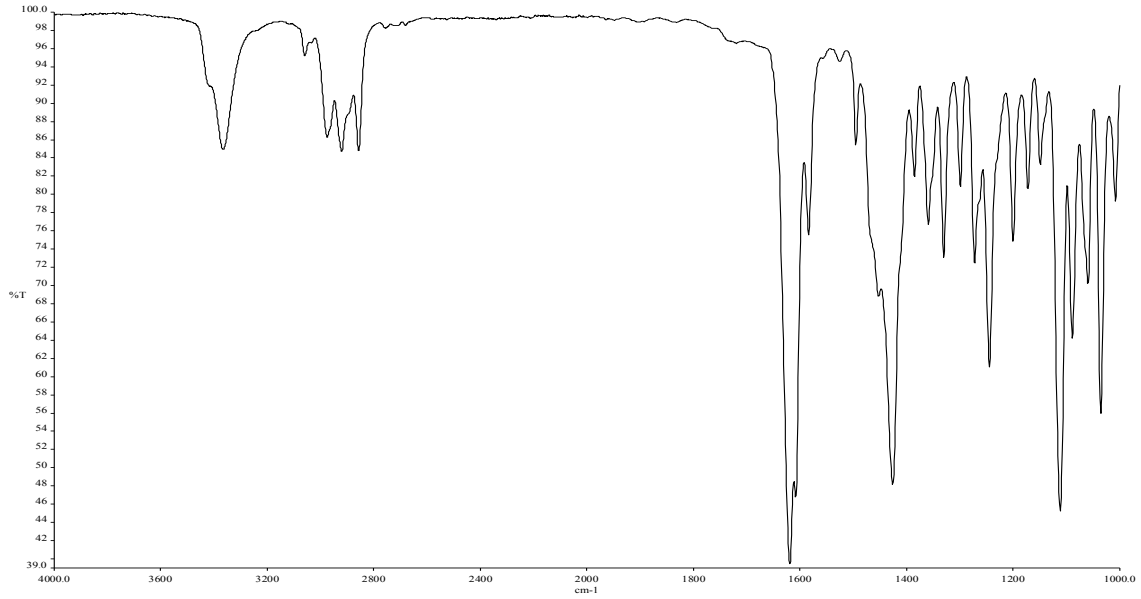


***Figure A2.9.*** Infrared spectrum of compound **2.16c**

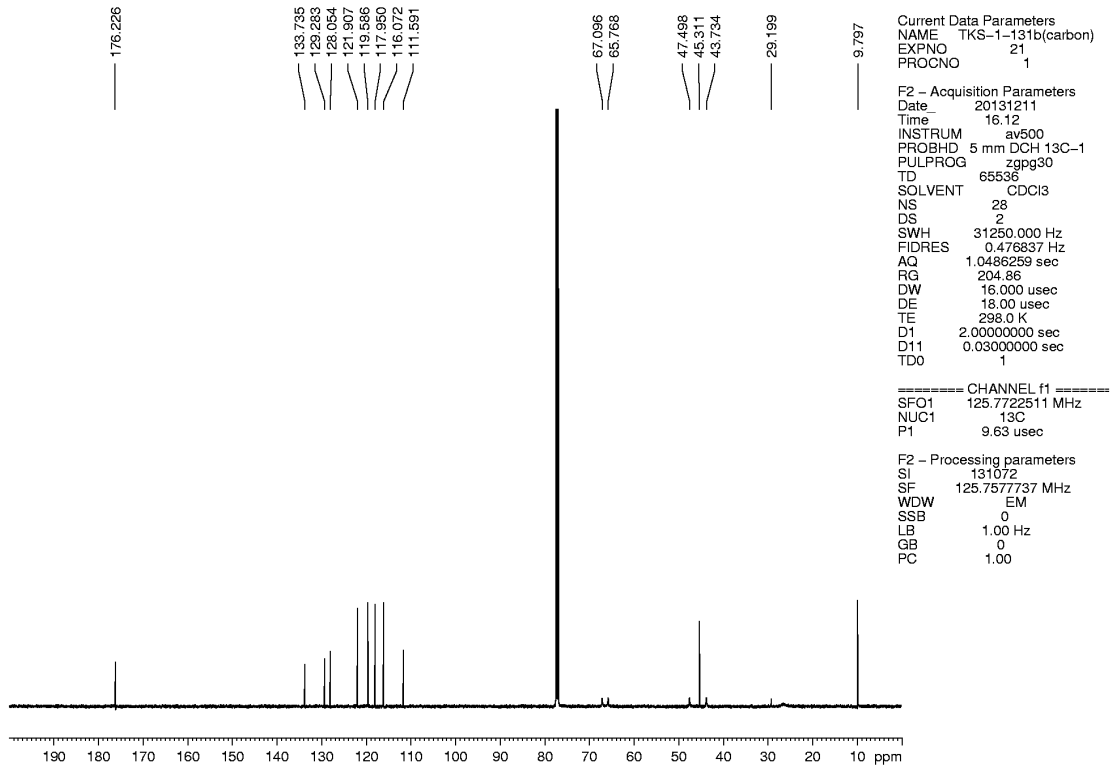


***Figure A2.10.*** $^{13}C$ NMR (125 MHz, $CDCl_3$) of compound **2.16c**.

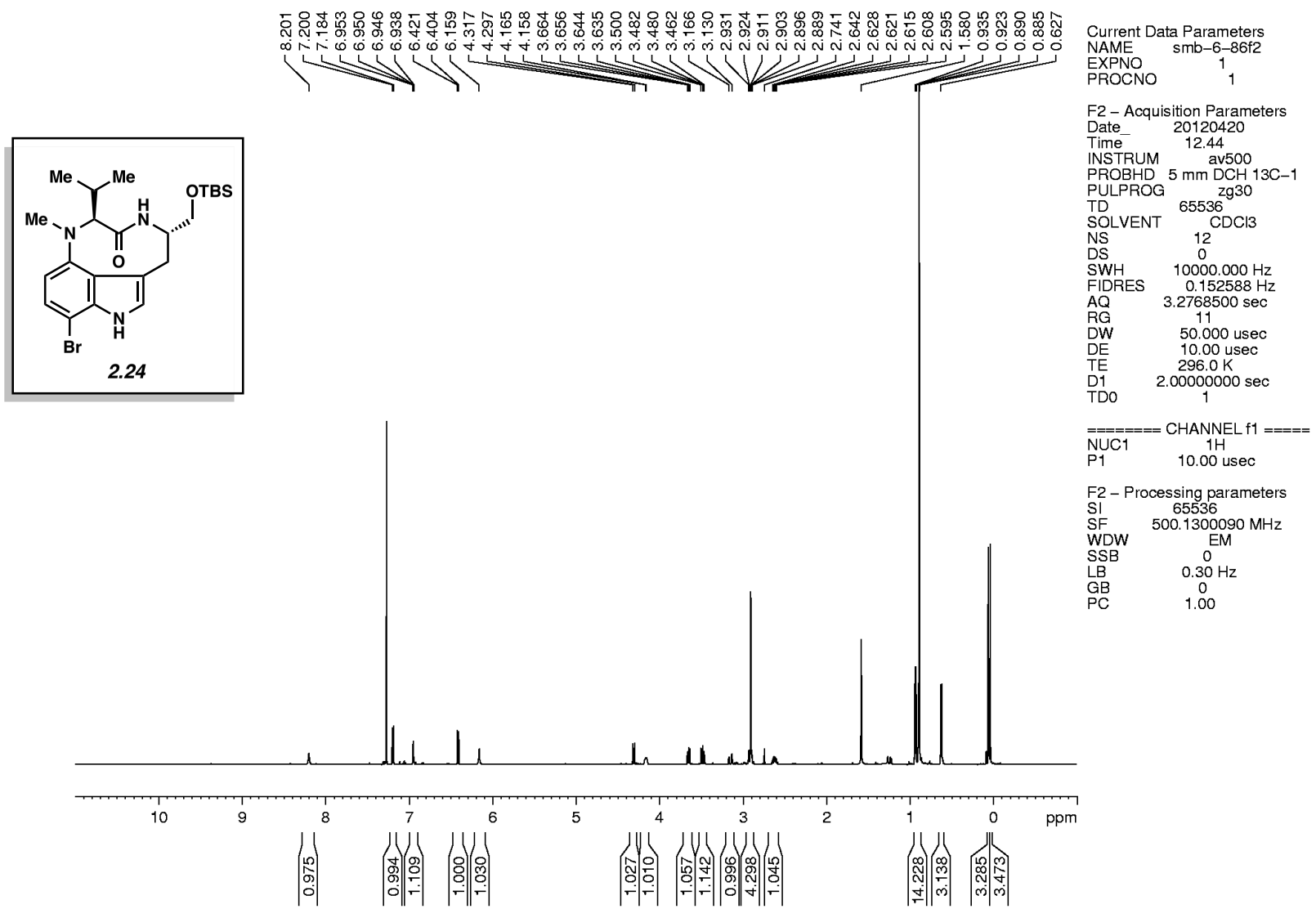


***Figure A2.11.*** $^{1}$H NMR (500 MHz, $CDCl_3$) of compound **2.24**

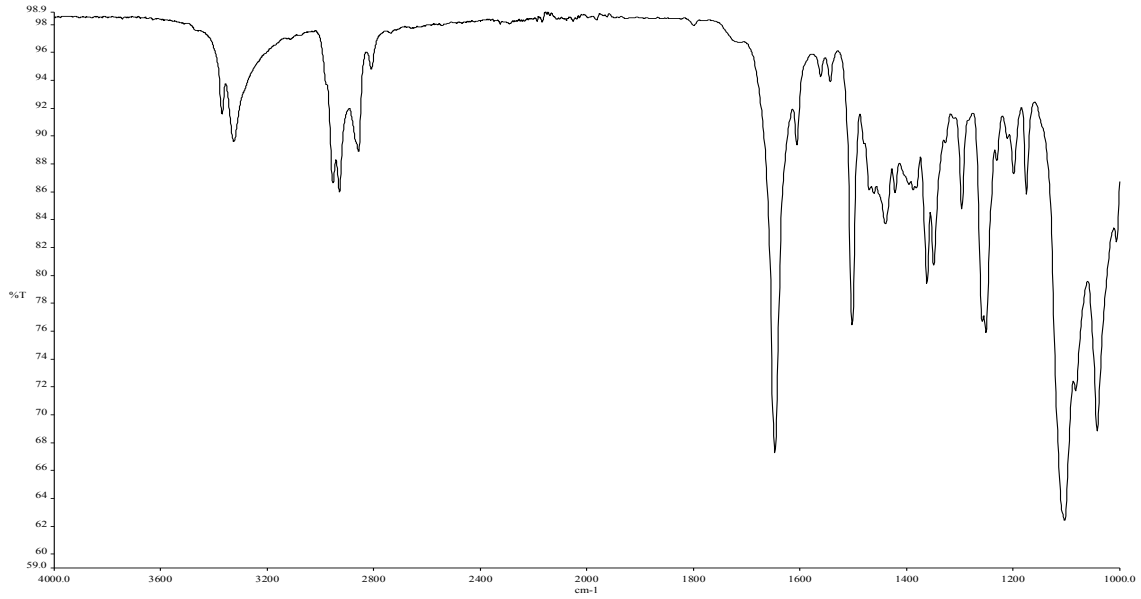


***Figure A2.12.*** Infrared spectrum of compound **2.24**.

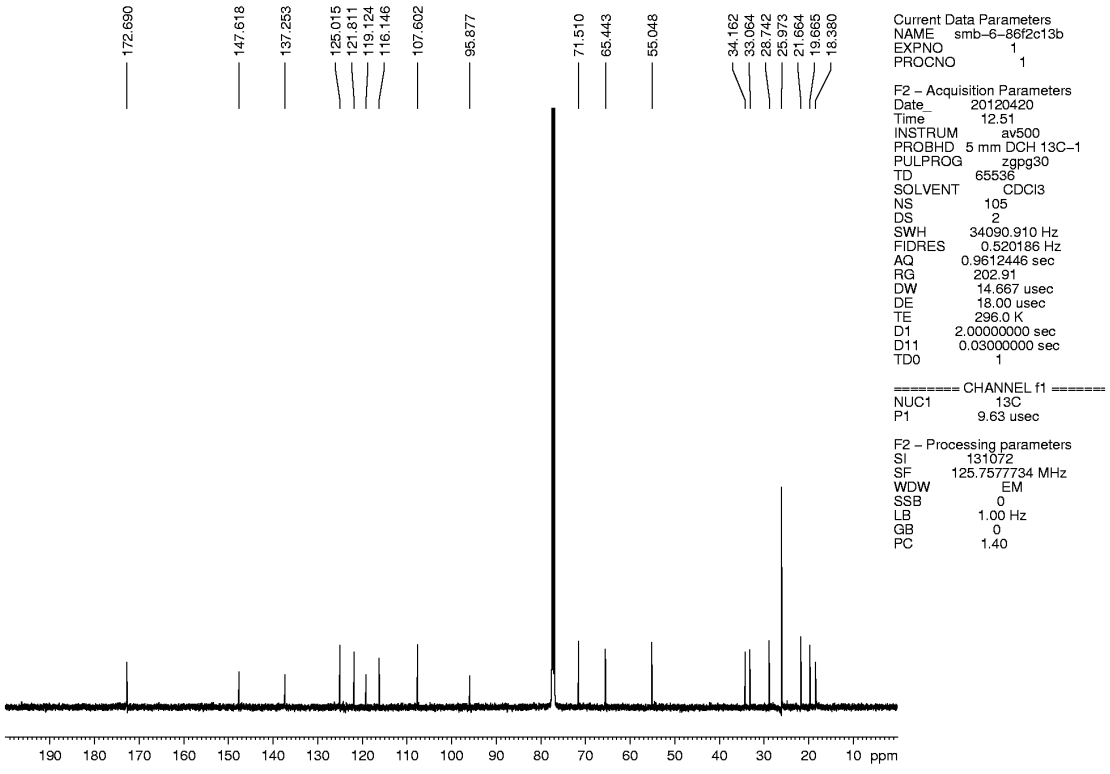


***Figure A2.13.*** $^{13}C$ NMR (125 MHz, $CDCl_3$) of compound **2.24**.

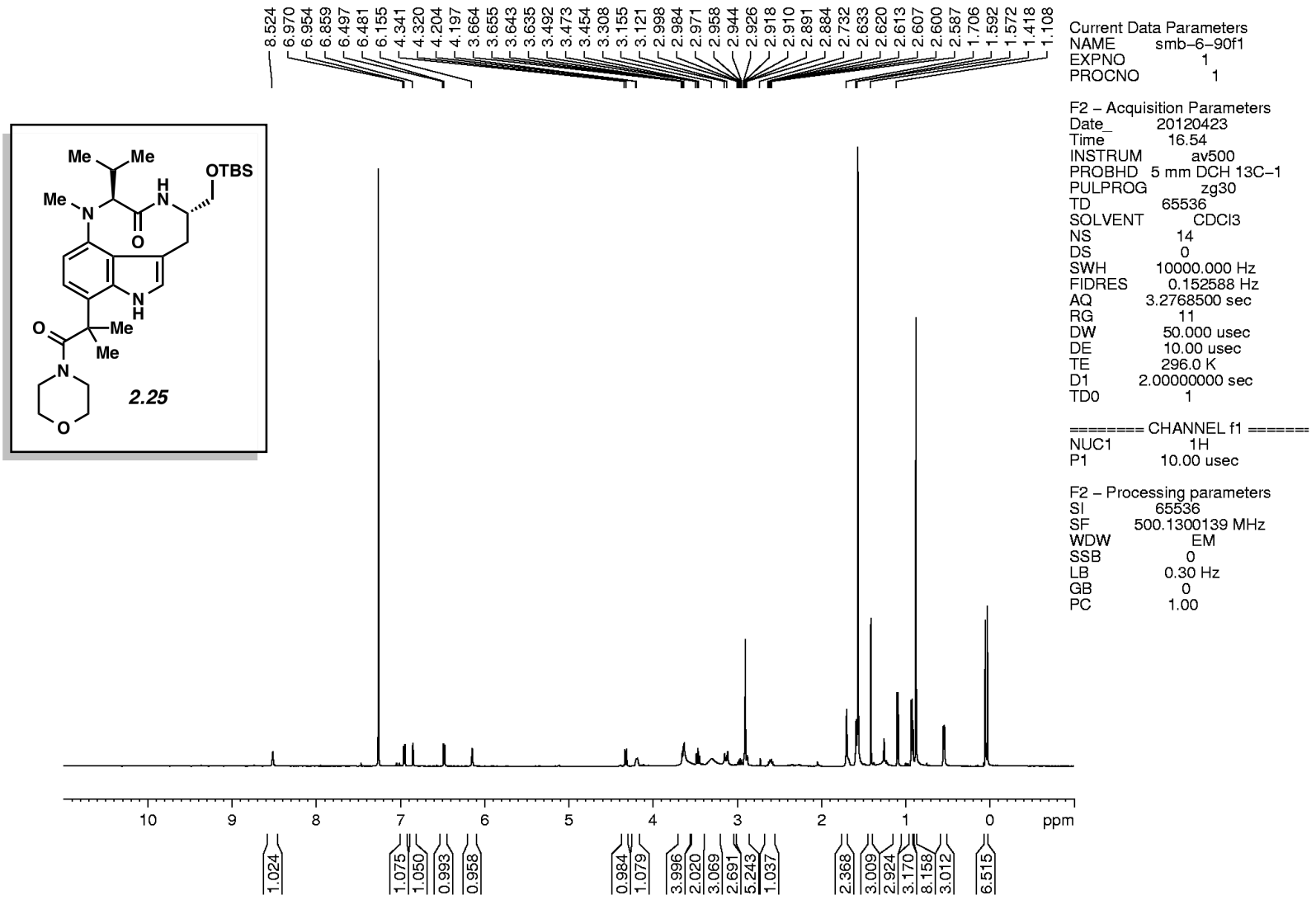


***Figure A2.14.*** $^{1}$H NMR (500 MHz, $CDCl_3$) of compound **2.25**

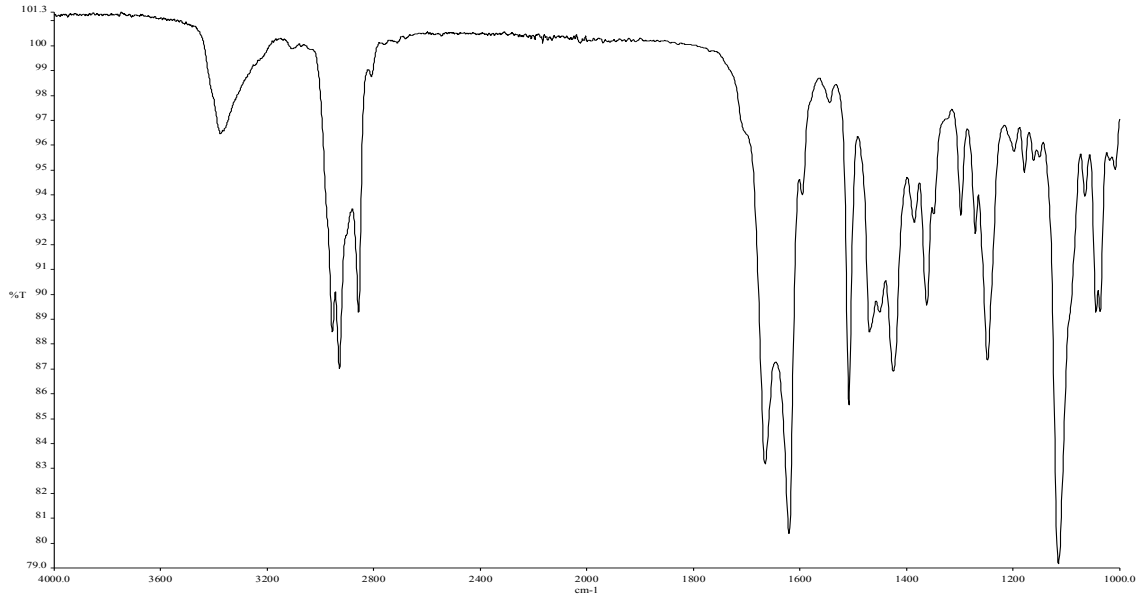


***Figure A2.15.*** Infrared spectrum of compound **2.25**.

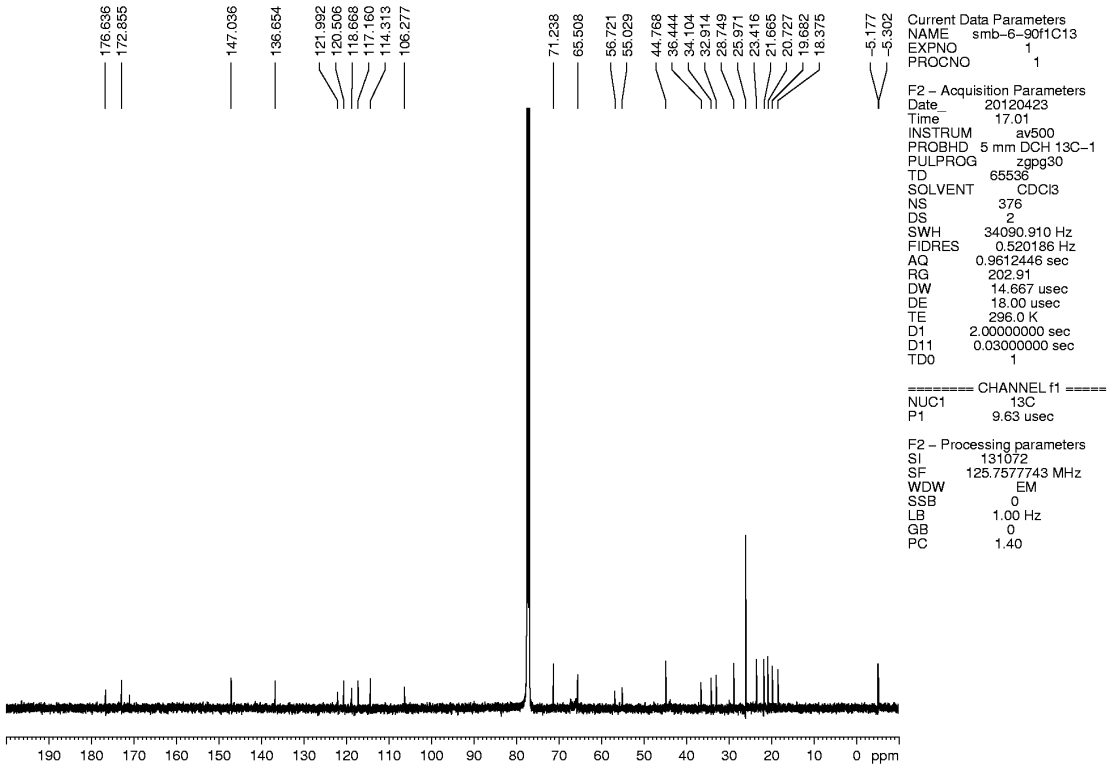


***Figure A2.16.*** $^{13}C$ NMR (125 MHz, $CDCl_3$) of compound **2.25**.

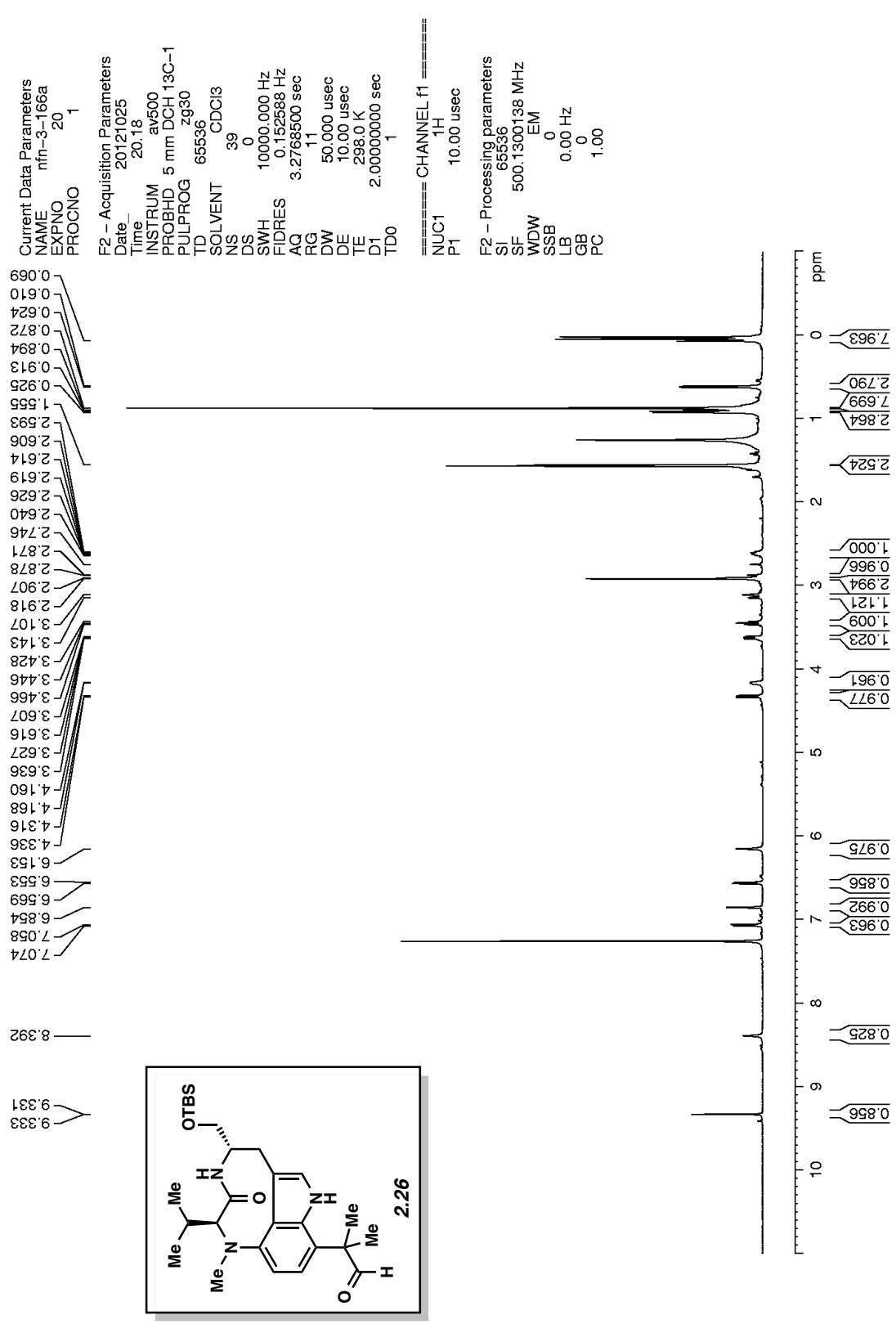


***Figure A2.17.*** $^1$H NMR (500 MHz, $CDCl_3$) of compound **2.26**

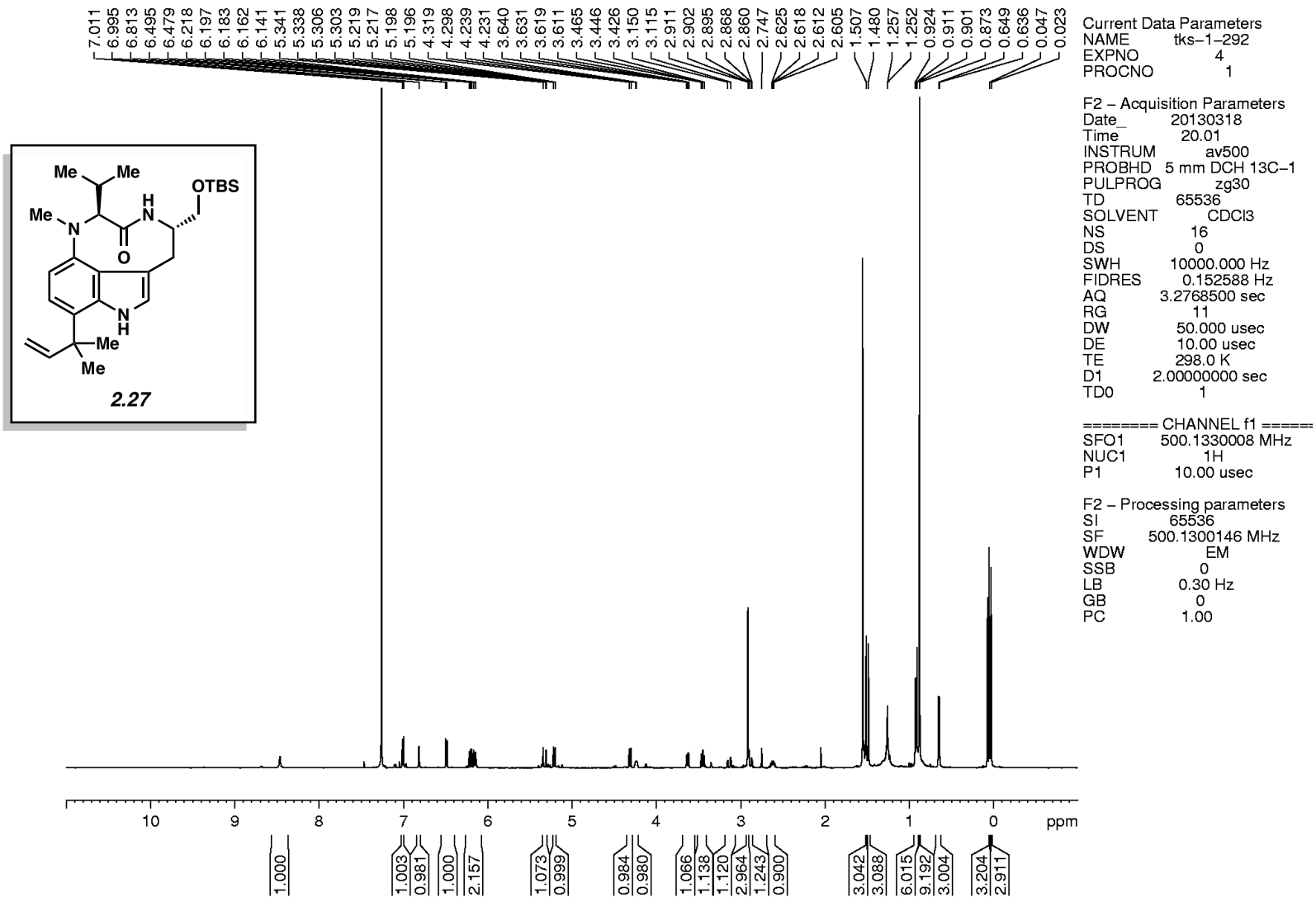


***Figure A2.18.*** $^{1}$H NMR (500 MHz, $CDCl_3$) of compound **2.27**

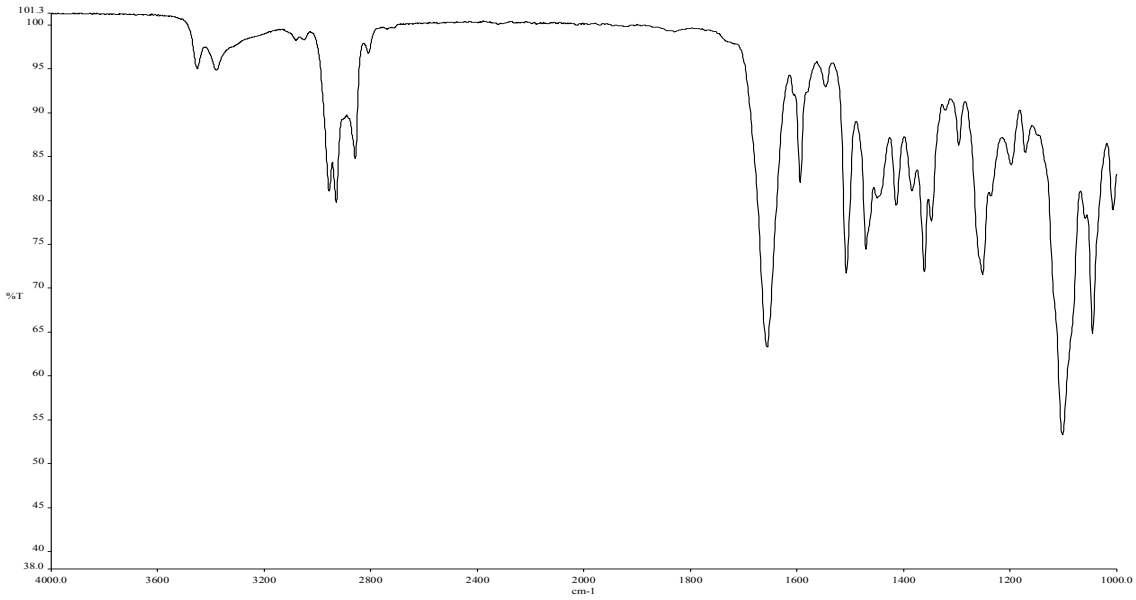


***Figure A2.19.*** Infrared spectrum of compound **2.27**.

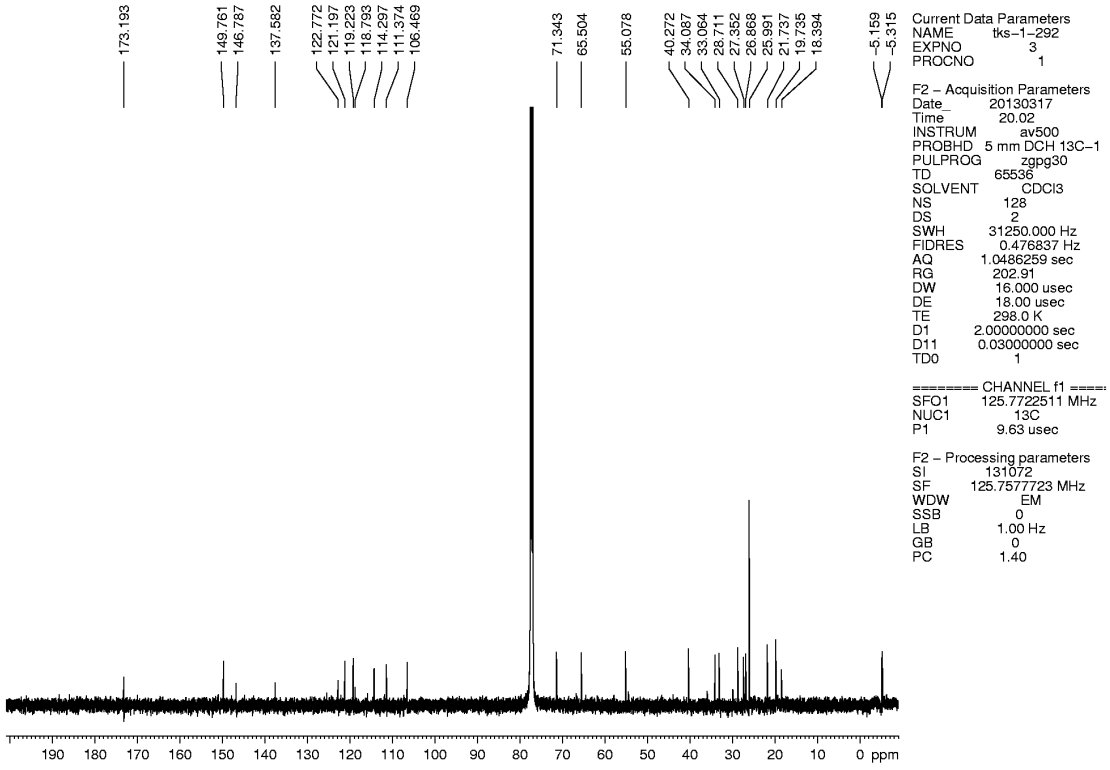


***Figure A2.20.*** $^{13}C$ NMR (125 MHz, $CDCl_3$) of compound **2.27**.

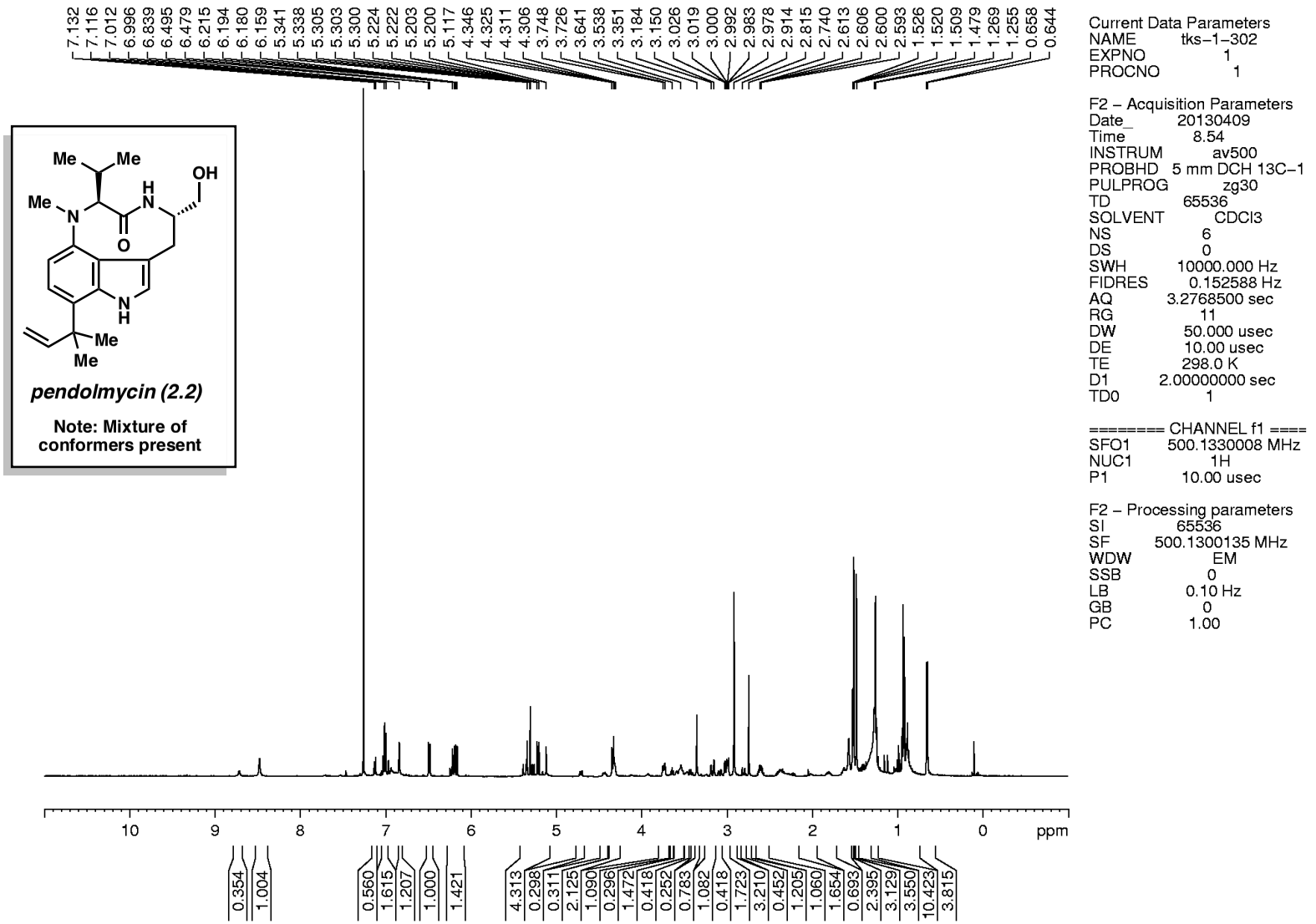


***Figure A2.21.*** $^{1}$H NMR (500 MHz, $CDCl_3$) of compound **2.2**

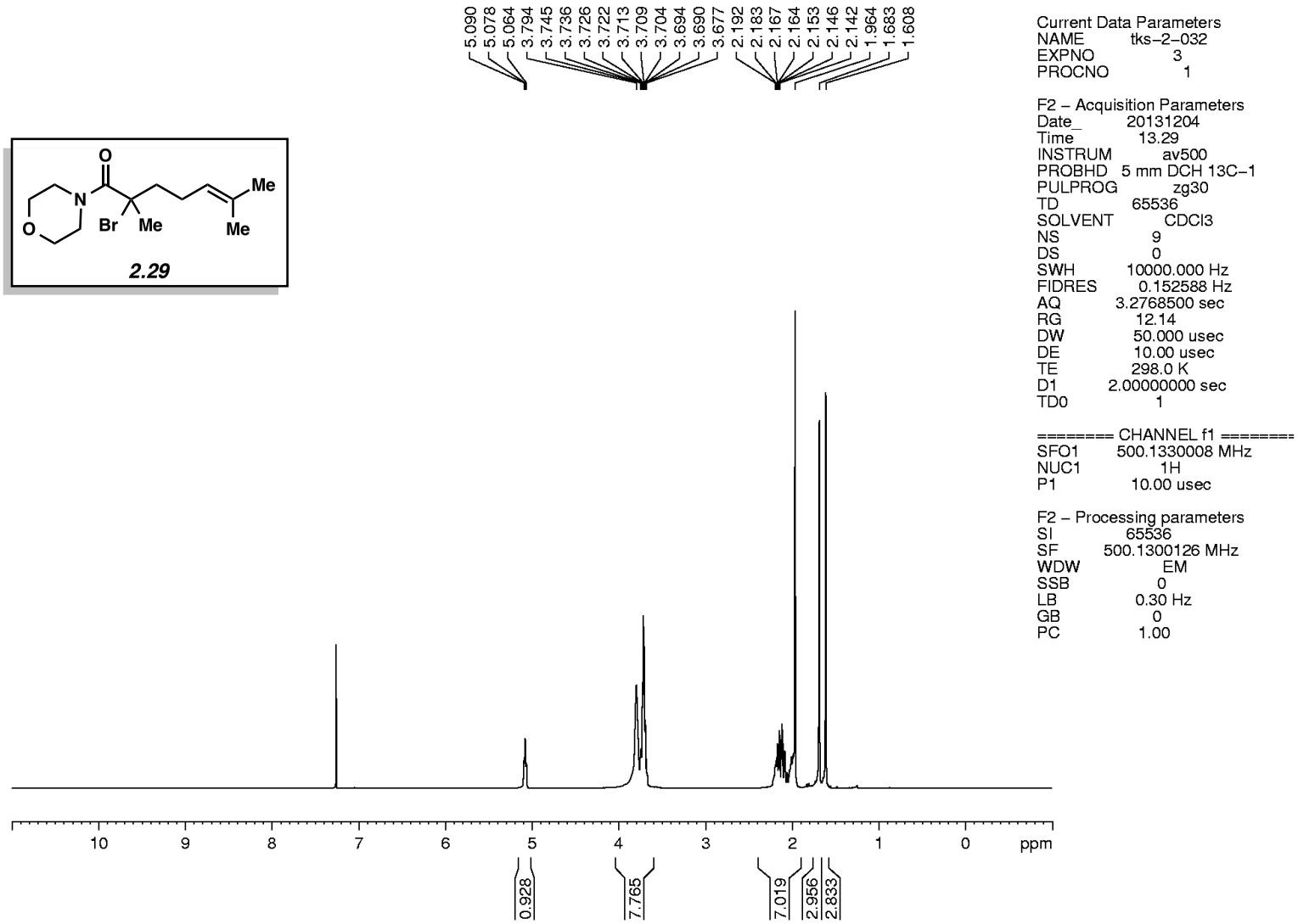


***Figure A2.22.*** $^{1}$H NMR (500 MHz, $CDCl_3$) of compound **2.29**

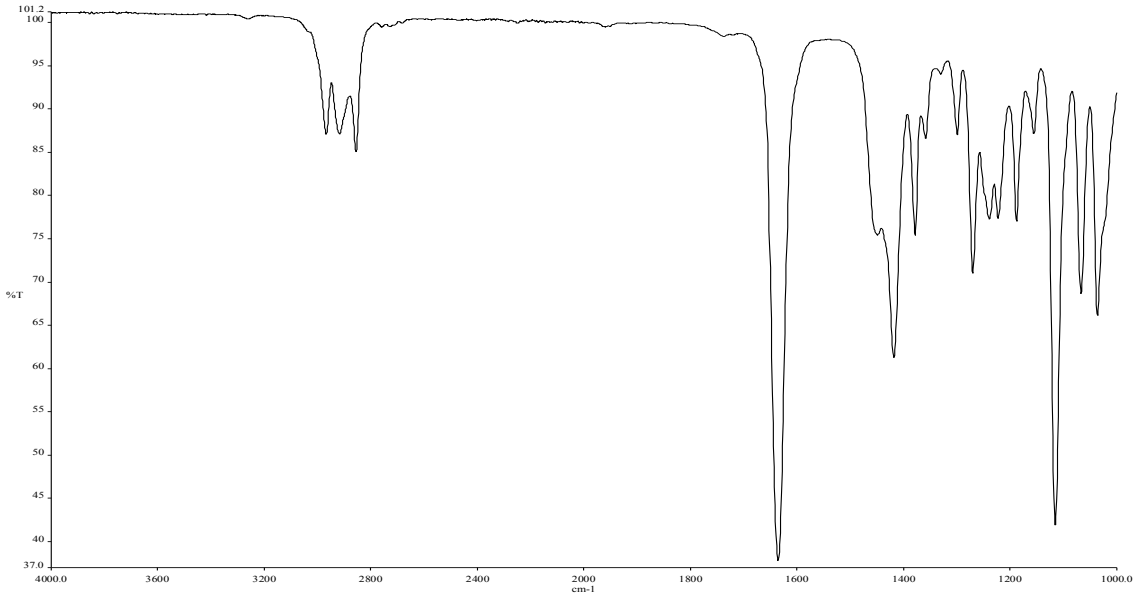


***Figure A2.23.*** Infrared spectrum of compound **2.29**.

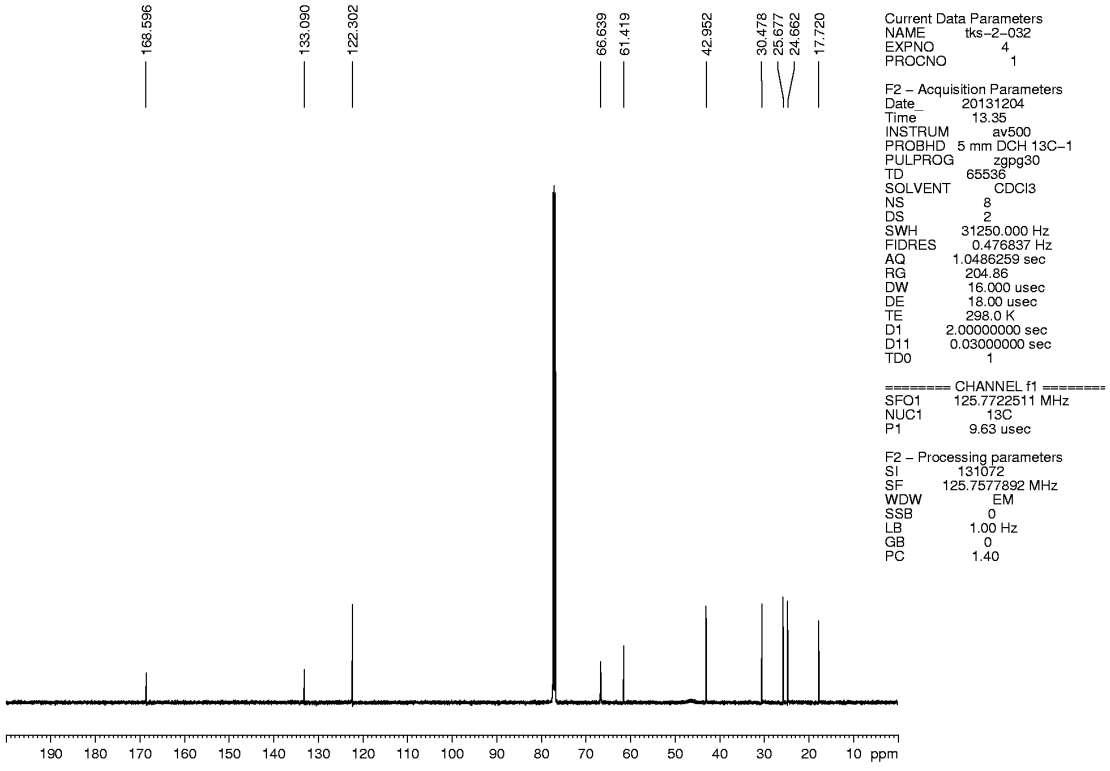


***Figure A2.24.*** $^{13}C$ NMR (125 MHz, $CDCl_3$) of compound **2.29**.

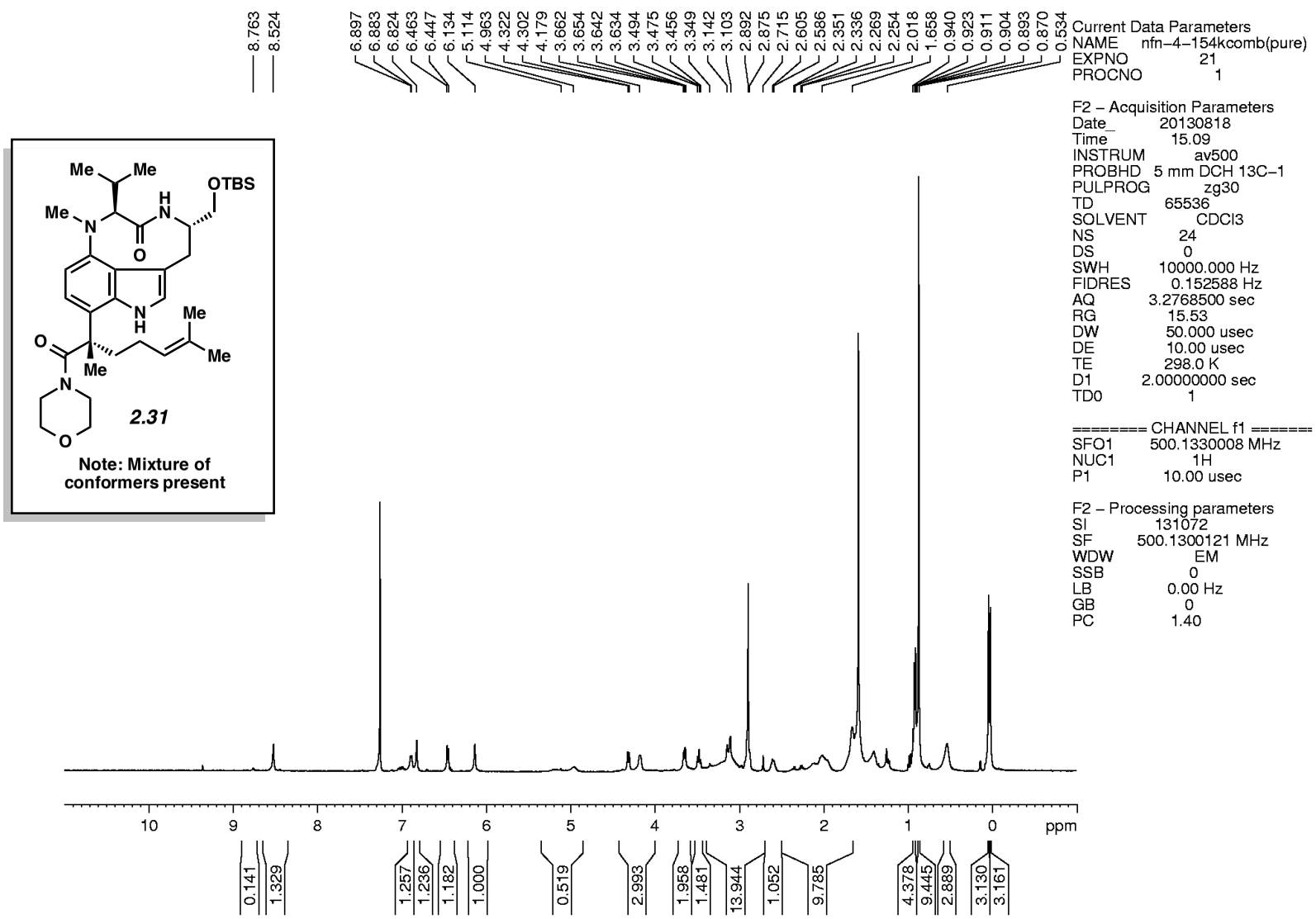


***Figure A2.25.*** $^{1}$H NMR (500 MHz, $CDCl_3$) of compound **2.31**

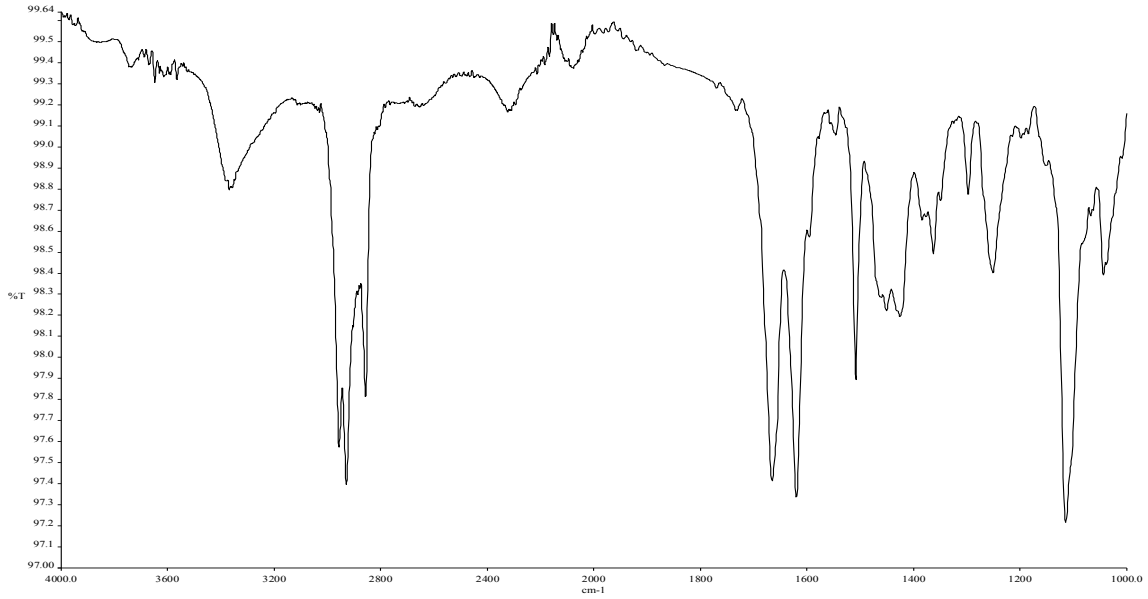


***Figure A2.26.*** Infrared spectrum of compound **2.31**.

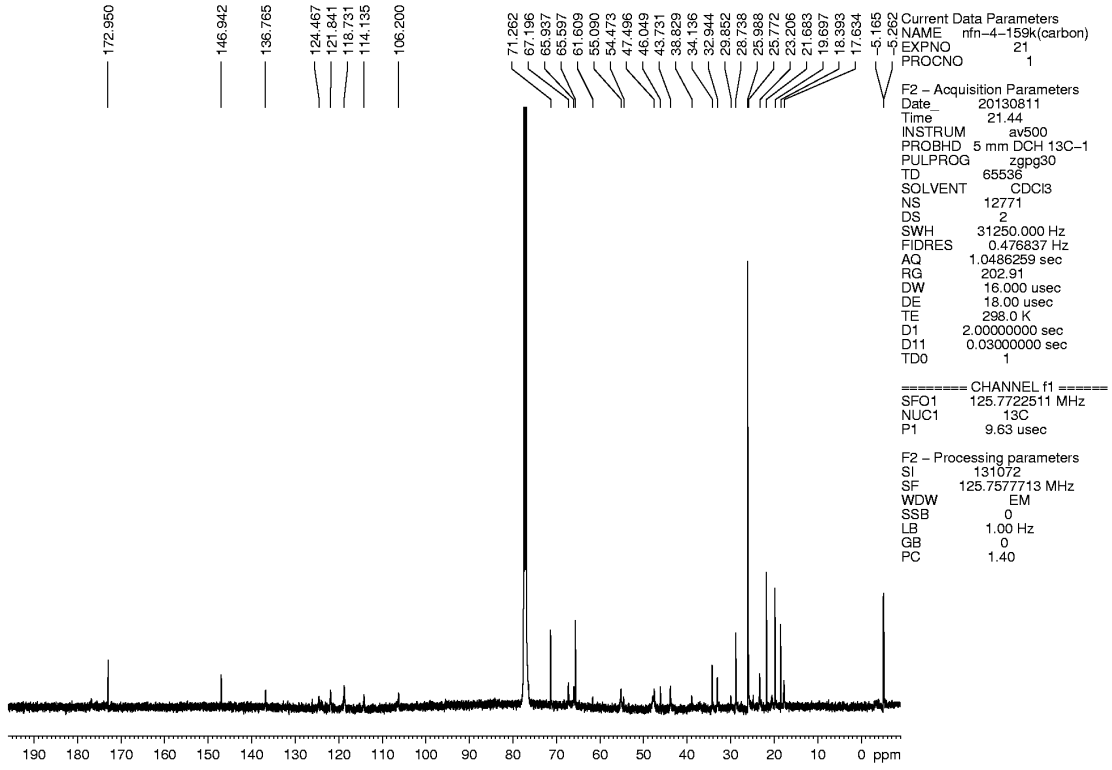


***Figure A2.27.*** $^{13}C$ NMR (125 MHz, $CDCl_3$) of compound **2.31**.

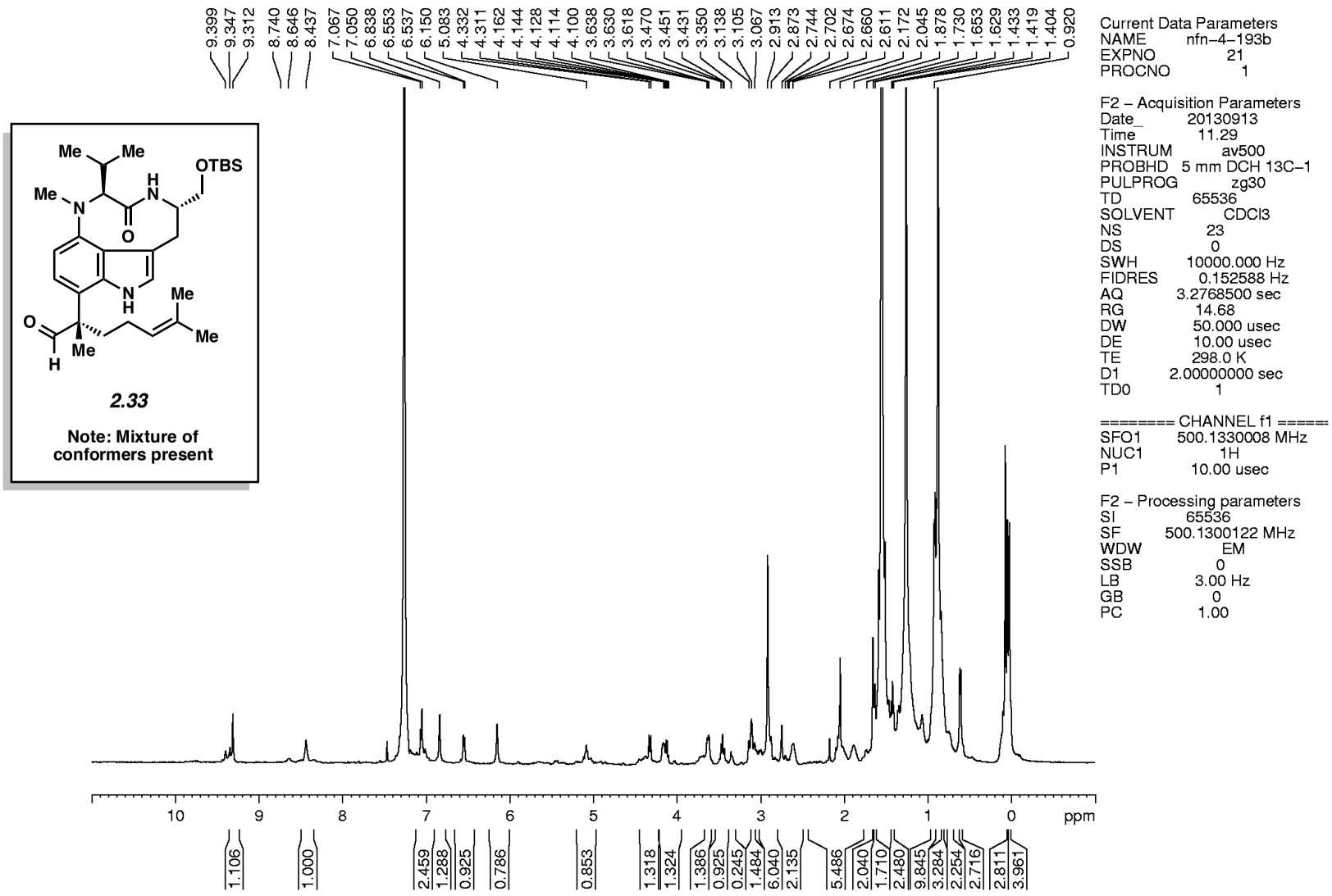


***Figure A2.28.*** $^{1}$H NMR (500 MHz, $CDCl_3$) of compound **2.33**

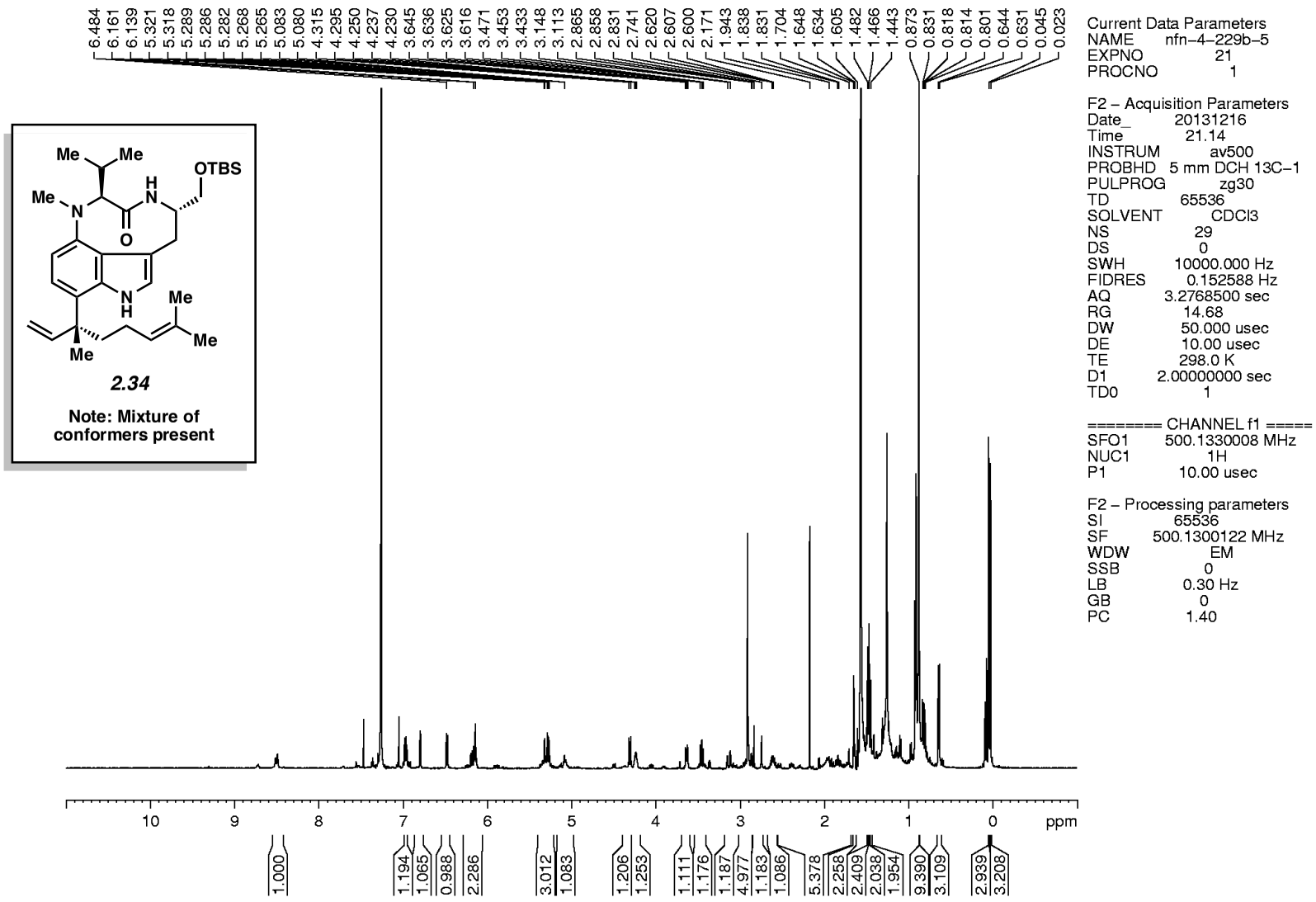


***Figure A2.29.*** $^{1}$H NMR (500 MHz, $CDCl_3$) of compound **2.34**

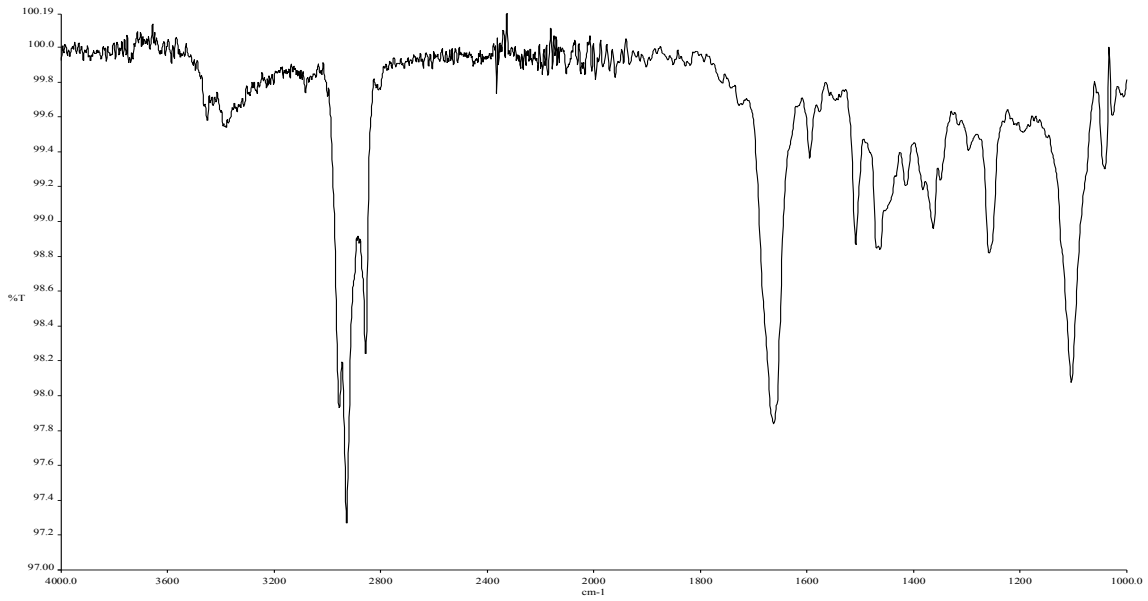


***Figure A2.30.*** Infrared spectrum of compound **2.34**.

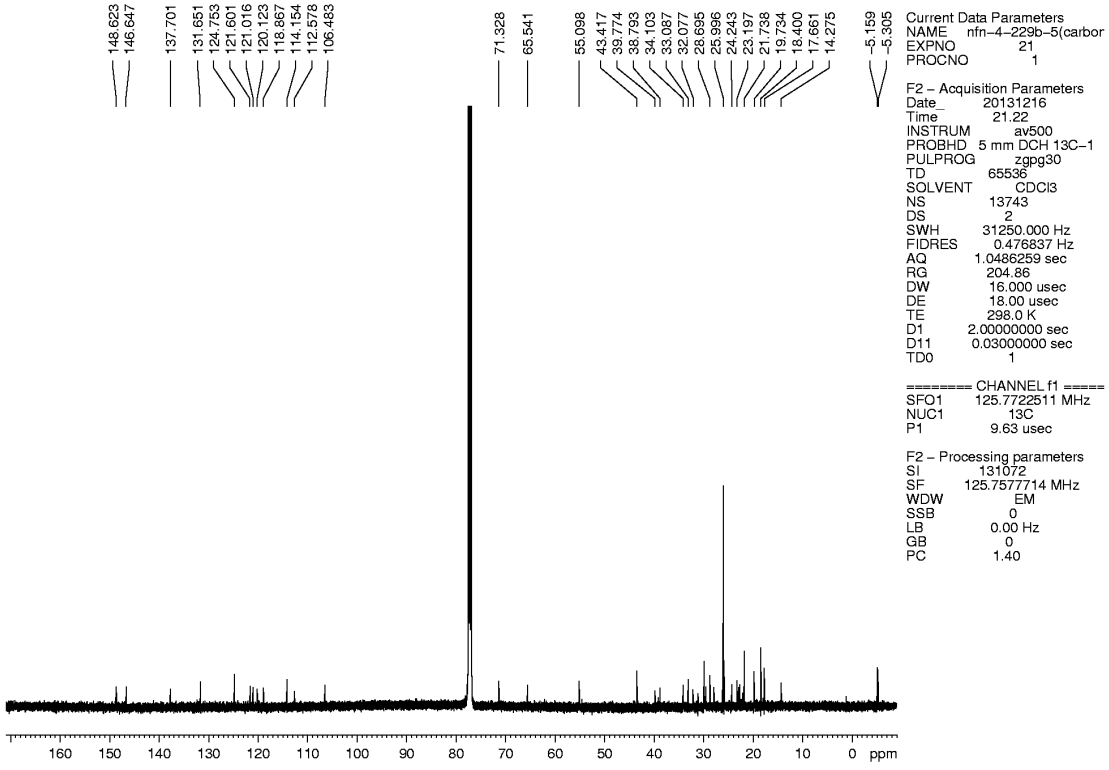


***Figure A2.31.*** $^{13}C$ NMR (125 MHz, $CDCl_3$) of compound **2.34**.

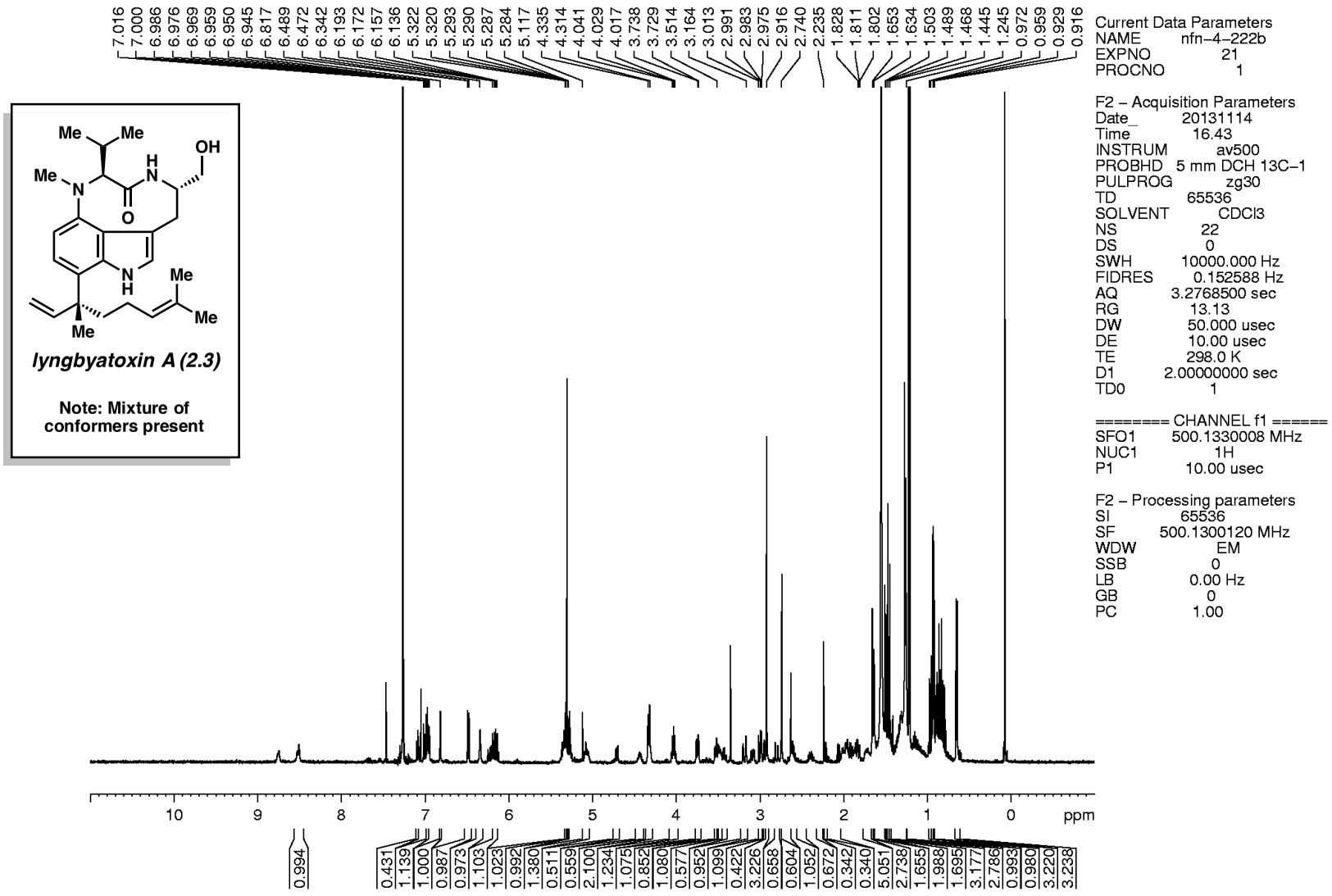


***Figure A2.32.*** $^{1}$H NMR (500 MHz, $CDCl_3$) of compound **2.3**

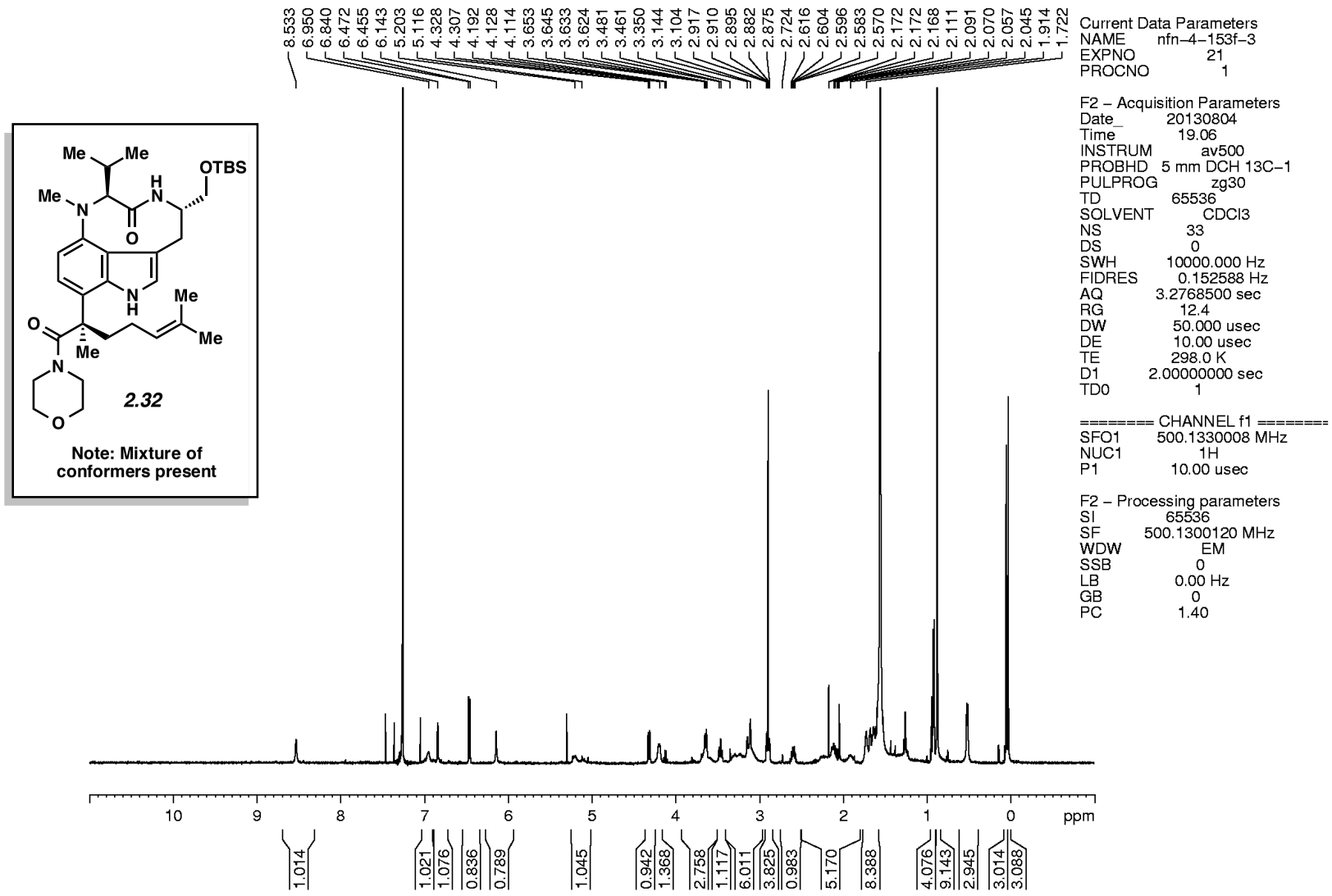


***Figure A2.33.*** $^{1}$H NMR (500 MHz, $CDCl_3$) of compound **2.32**

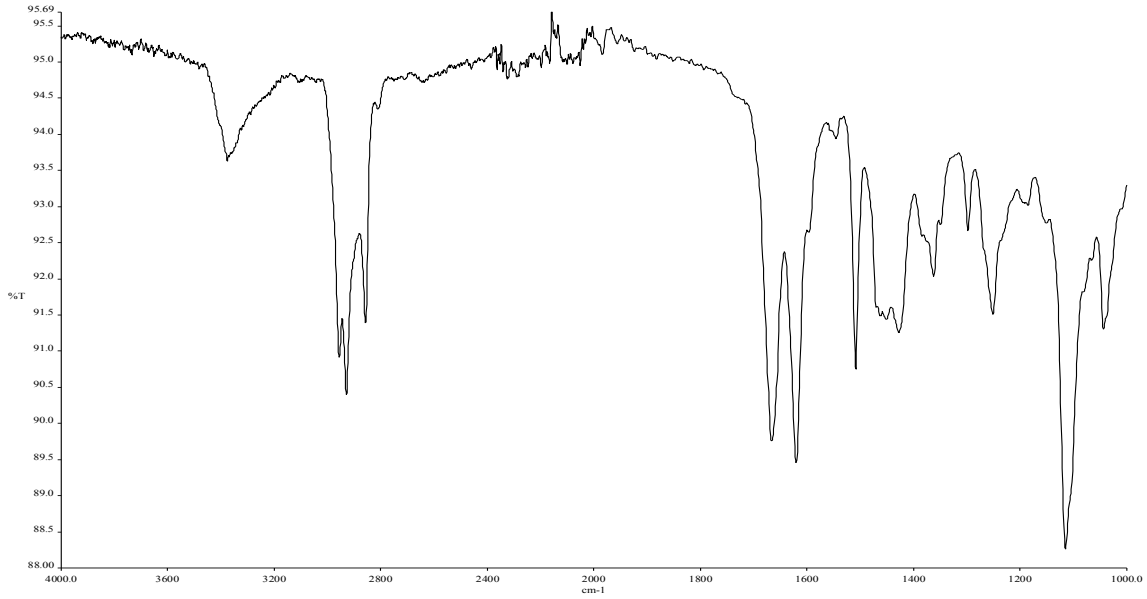


***Figure A2.34.*** Infrared spectrum of compound **2.32**.

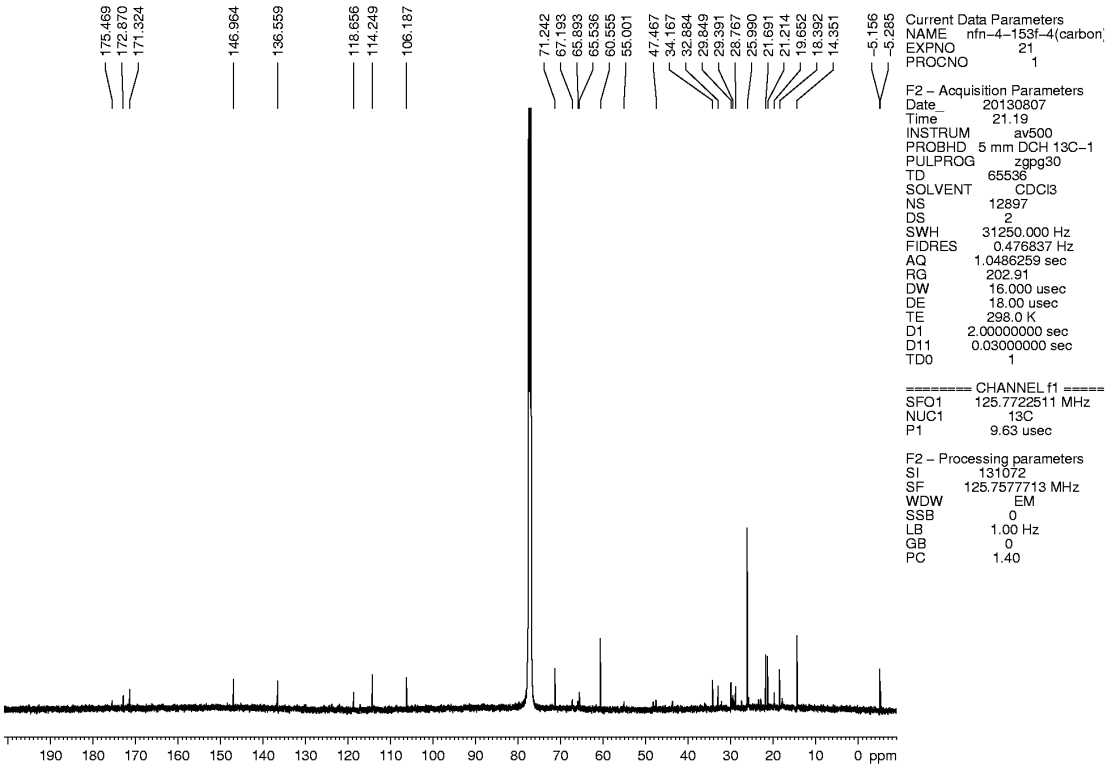


***Figure A2.35.*** $^{13}C$ NMR (125 MHz, $CDCl_3$) of compound **2.32**.

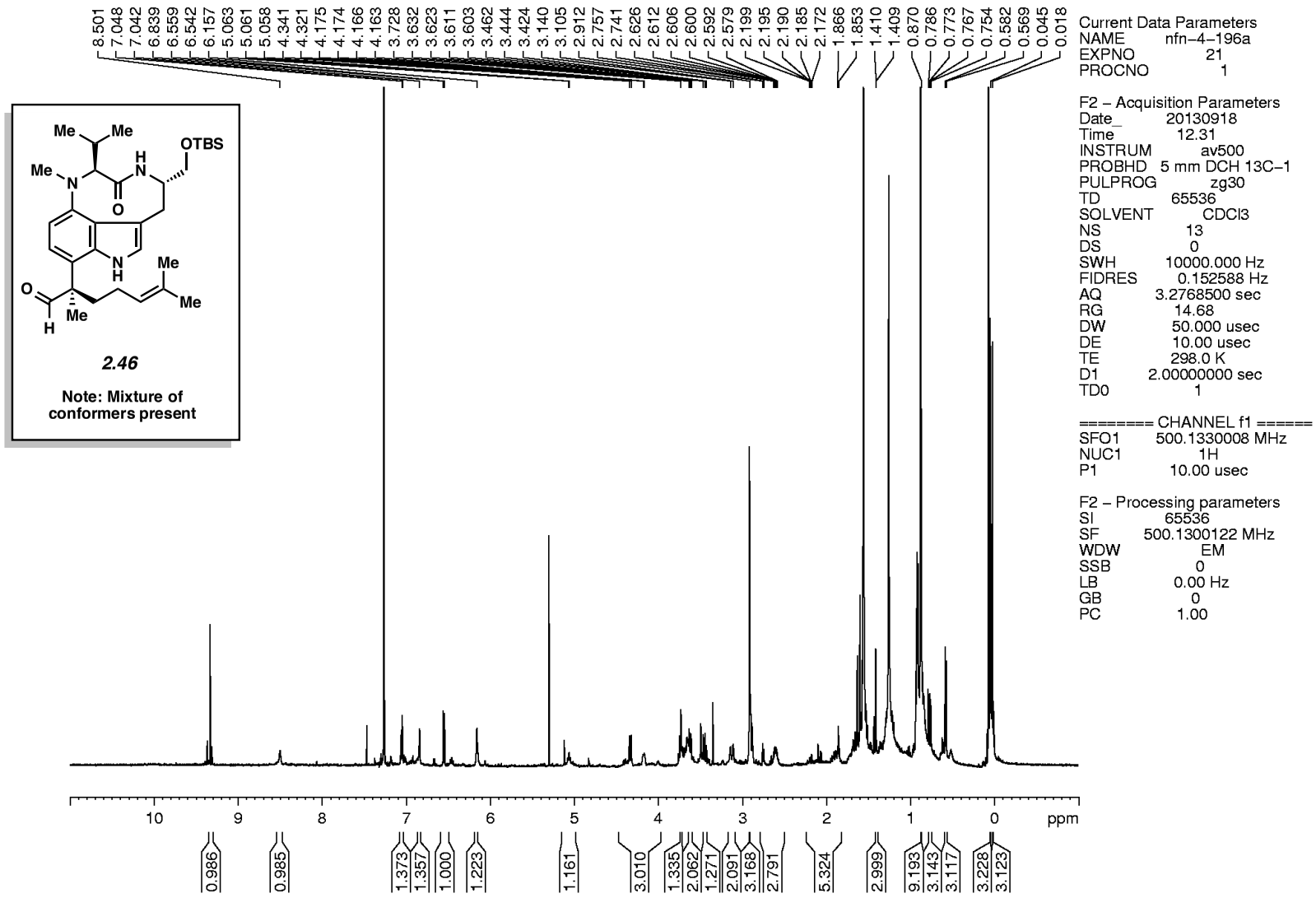


***Figure A2.36.*** $^{1}$H NMR (500 MHz, $CDCl_3$) of compound **2.46**

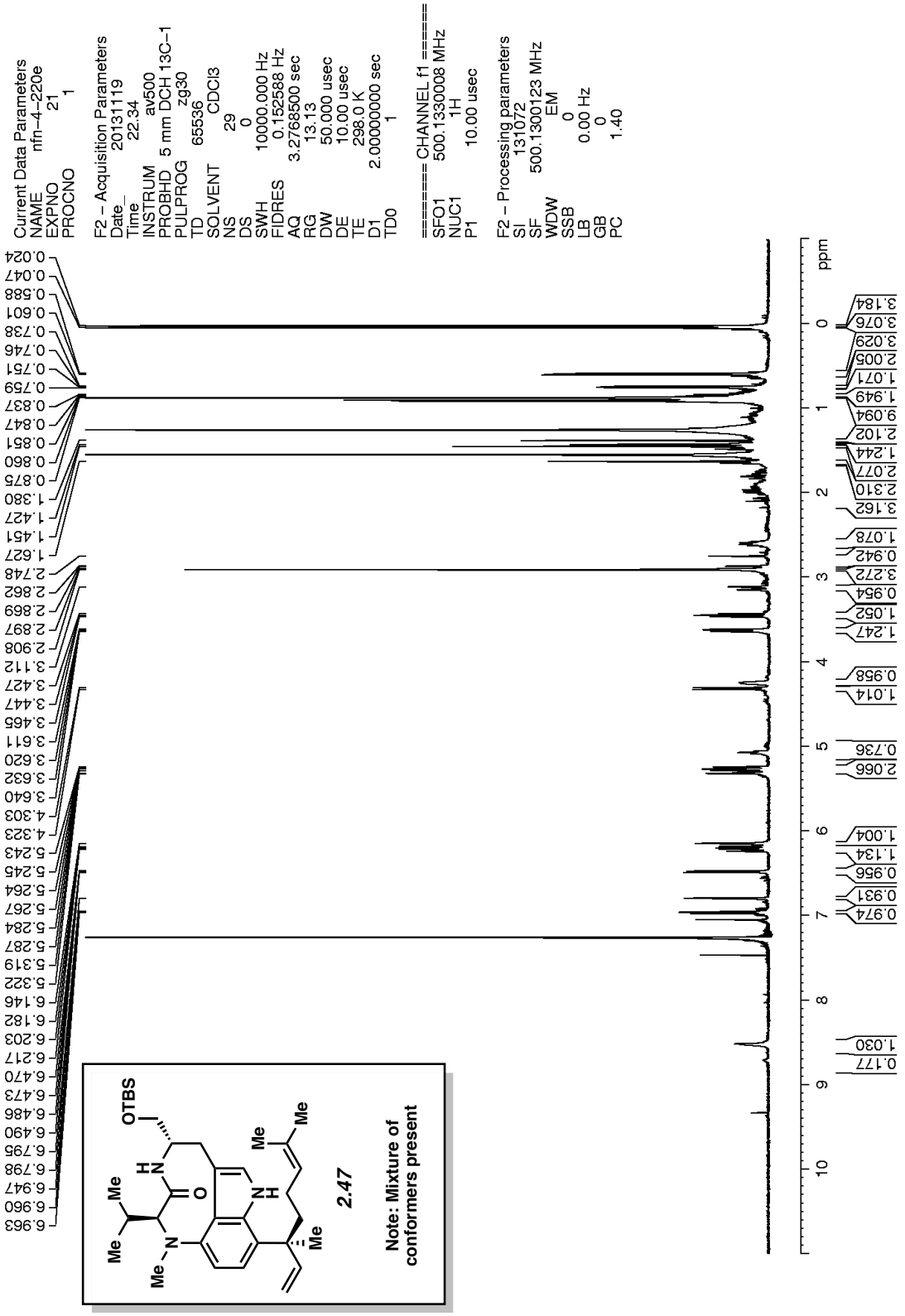


***Figure A2.37.*** $^1$H NMR (500 MHz, $CDCl_3$) of compound **2.47**

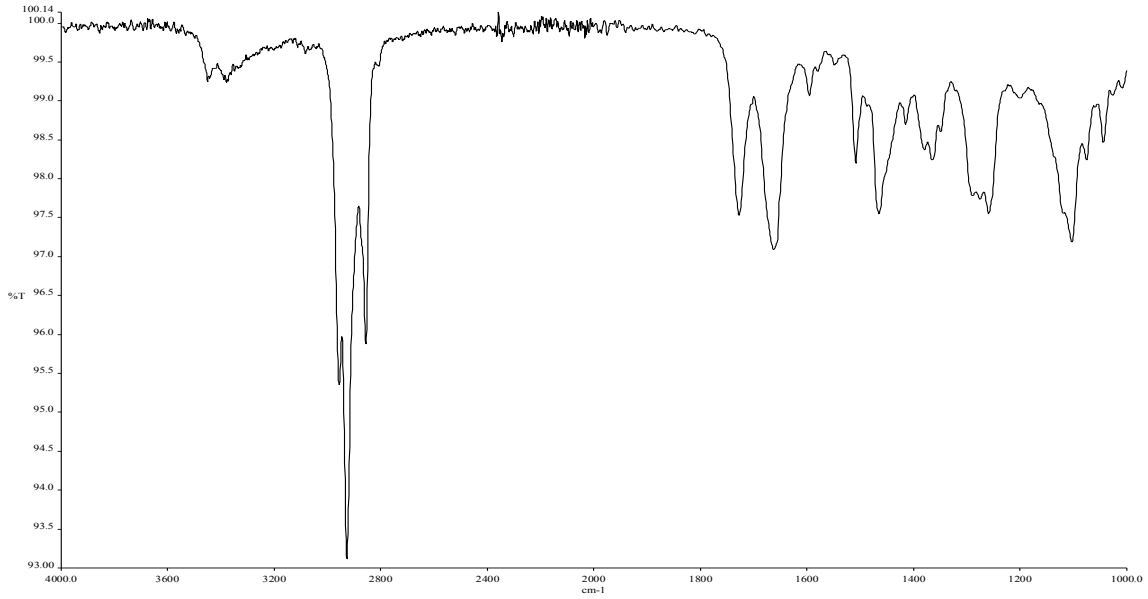


***Figure A2.38.*** Infrared spectrum of compound **2.47**.

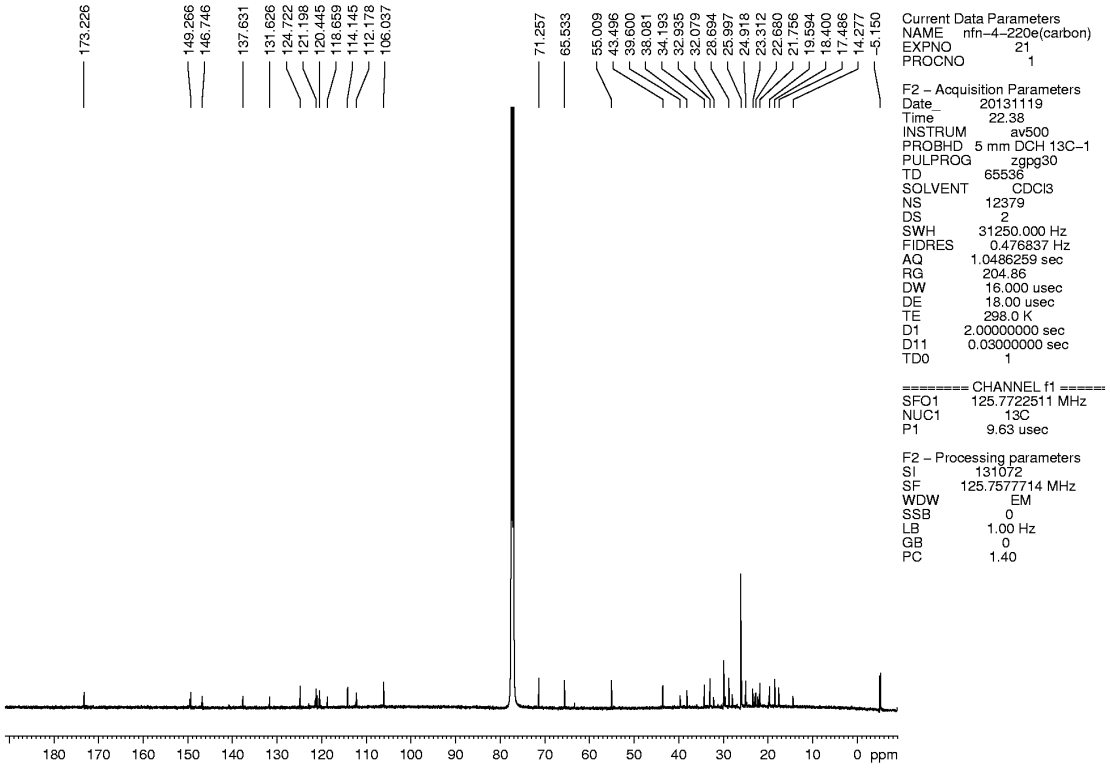


***Figure A2.39.*** $^{13}C$ NMR (125 MHz, $CDCl_3$) of compound **2.47**.

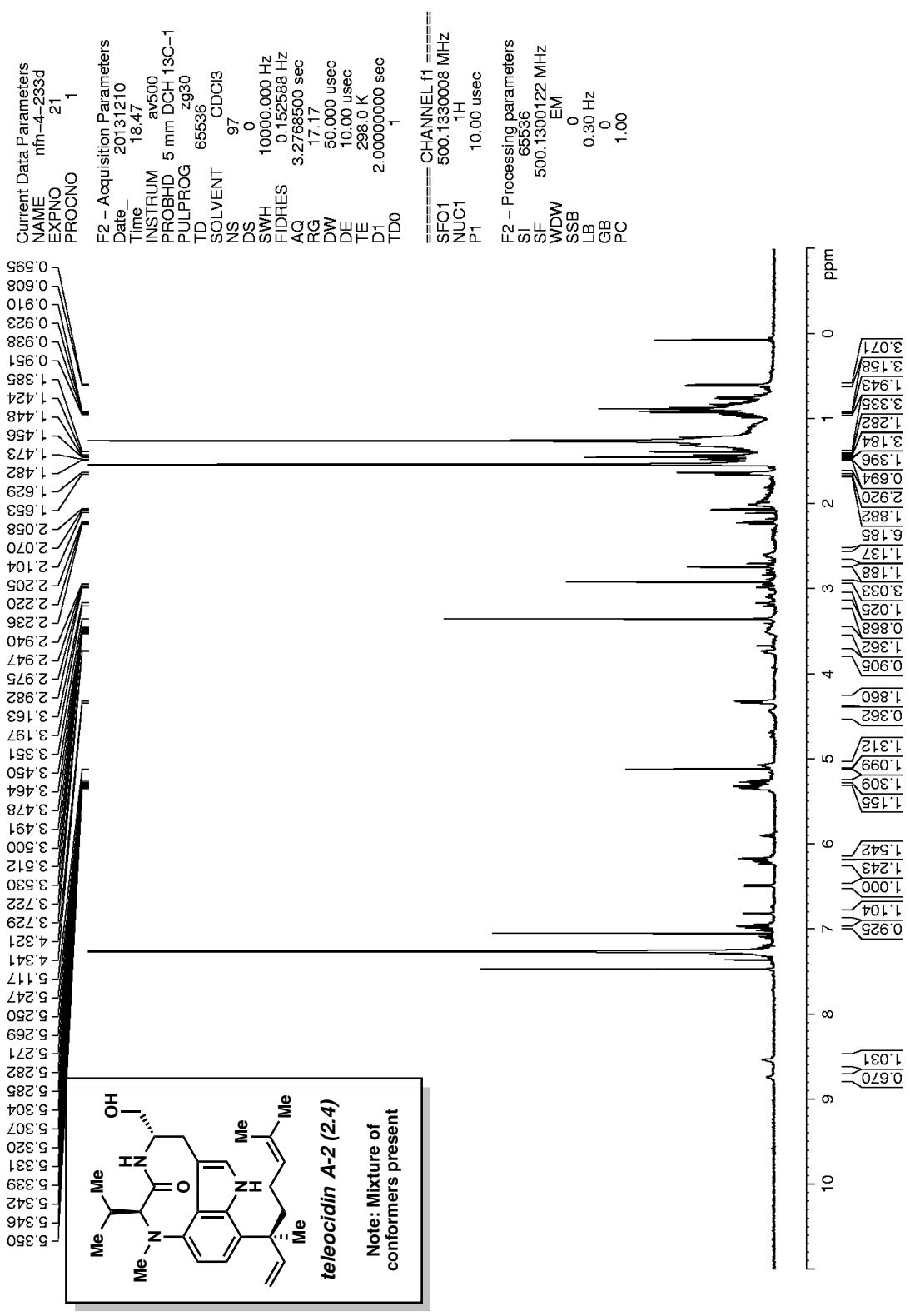


***Figure A2.40.*** $^{1}$H NMR (500 MHz, $CDCl_3$) of compound **2.4**

## 2.7 Notes and References

[1] For pertinent reviews on (–)-indolactam V isolation, tumor-promoting activity, and derivatives, see: (a) Irie, K.; Koshimizu, K. *Mem. Coll. Agric. Kyoto Univ.* **1988**, *132*, 1–59. (b) Irie, K.; Koshimizu, K. *Comments Agric. Food Chem.* **1993**, *3*, 1–25. (c) Irie, K. *Nippon Nogei Kagaku Kaishi* **1994**, *68*, 1289–1296. (d) Irie, K.; Nakagawa, Y.; Ohigashi, H. *Curr. Pharm. Des.* **2004**, *10*, 1371–1385. (e) Irie, K.; Nakagawa, Y.; Ohigashi, H. *Chem. Rec.* **2005**, *5*, 185–195.

[2] Irie, K.; Hirota, M.; Hagiwara, N.; Koshimizu, K.; Hayashi, H.; Murao, S.; Tokuda, H.; Ito, Y. *Agric. Biol. Chem.* **1984**, *48*, 1269–1274.

[3] For pioneering studies of (–)-indolactam V's ability to bind PKC see: (a) Fujiki, H.; Suginuma, M.; Nakayasu, M.; Tahira, T.; Endo, Y.; Shudo, K.; Sugimura, T. *Gann* **1984**, *75*, 866–870. (b) Irie, K.; Hagiwara, N.; Koshimizu, K.; Hayashi, H.; Murao, S.; Tokuda, H.; Ito, Y. *Agric. Biol. Chem.* **1985**, *49*, 221–223.

[4] For recent studies, see: (a) Meseguer, B.; Alonso-Díaz, D.; Griebenow, N.; Herget, T. and Waldmann, H. *Angew. Chem. Int. Ed.* **1999**, *38*, 2902–2906. (b) Meseguer, B.; Alonso-Díaz, D.; Griebenow, N.; Herget, T.; Waldmann, H. *Chem. Eur. J.* **2000**, *6*, 3943–3957. (c) Masuda, A.; Irie, K.; Nakagawa, Y.; Ohigashi, H. *Biosci. Biotechnol. Biochem.* **2002**, *66*, 1615–1617. (d) Nakagawa, Y.; Irie, K.; Yanagita, R. C.; Ohigashi, H.; Tsuda, K.-i. *J. Am. Chem. Soc.* **2005**, *127*, 5746–5747. (e) Nakagawa, Y.; Irie, K.; Yanagita, R. C.; Ohigashi, H.; Tsuda, K.-i.; Kashiwagi, K.; Saito, N. *J. Med. Chem.* **2006**, *49*, 2681–2688. (f) Yanagita, R. C.; Nakagawa, Y.; Yamanaka, N.; Kashiwagi, K.; Saito, N.; Irie, K. *J. Med. Chem.* **2008**, *51*, 46–56. (g) Sugimoto, T.; Itagaki, K.; Irie, K. *Bioorg. Med. Chem.* **2008**, *16*, 650–657.

[5] (a) Oka, S.; Owa, T.; Sugie, M.; Tanaka, H. *Agric. Biol. Chem.* **1989**, *53*, 2261–2262. (b) Chen, S.; Borowiak, M.; Fox, J. L.; Maehr, R.; Osafune, K.; Davidow, L.; Lam, K.; Peng, L. F.; Schreiber, S. L.; Rubin, L. L.; Melton, D. *Nat. Chem. Biol.* **2009**, 5, 258–265.

[6] Yamashita, T.; Imoto, M.; Isshiki, K.; Sawa, T.; Naganawa, H.; Kurasawa, S.; Zhu, B.-Q.; K. Umezawa, K. *J. Nat. Prod.* **1988**, *51*, 1184–1187.

[7] Huang, H.; Yao, Y.; He, Z.; Yang, T.; Ma, J.; Tian, X.; Li, Y.; Huang, C.; Chen, X.; Li, W.; Zhang, S.; Zhang, C.; Ju, J. *J. Nat. Prod.* **2011**, 74, 2122–2127.

[8] (a) Gallimore, W. A.; Galario, D. L.; Lacy, C.; Zhu, Y.; Scheuer, P. J. *J. Nat. Prod.* **2000**, *63*, 1022–1026. (b) Izumikawa, M.; Khan, S. T.; Komaki, H.; Takagi, M; Shin-ya, K. *J. Antibiot.* **2010**, *63*, 33–36.

[9] (a) Endo, Y.; Shudo, K.; Itai, A.; Hasegawa, M.;Sakai, S.-i. *Tetrahedron* **1986**, *42*, 5905–5924. (b) de Laszlo, S. E.; S. V. Ley, S. V.; Porter, R. A. *J. Chem. Soc., Chem. Commun.* **1986**, 344–346. (c) Nakatsuka, S.-I.; Masuda, T.; Sakai, K.; Goto, T. *Tetrahedron Lett.* **1986**, 27, 5735–5738. (d) Masuda, T.; Nakatsuka, S.-i.; Goto, T. *Agric. Biol. Chem.* **1989**, 53, 2257–2260. (e) Kogan, T. P.; Somers, T. C.; Venuti, M. C. *Tetrahedron* **1990**, *46*, 6623–6632. (f) Mascal, M.; Moody, C. J.; Slawin, A. M. Z.; Williams, D. J. *J. Chem. Soc. Perkin Trans. 1* **1992**, 823–830. (g) Semmelhack, M. F.; Rhee, H. *Tetrahedron Lett.* **1993**, *34*, 1395–1398. (h) Quick, J.; Saha, B.; Driedger, P. E. *Tetrahedron Lett.* **1994**, *35*, 8549–8552. (i) Suárez, A. I.; García; M. C.; Compagnone, R. S. *Synth. Commun.* **2004**, *34*, 523–531. (j) Xu, Z.; Zhang, F.; Zhang, L.; Jia, Y. *Org. Biomol. Chem.* **2011**, *9*, 2512–2517. (k) Mari, M.; Bartoccini, F.; Piersanti, G. *J. Org. Chem.* **2013**, *78*, 7727–7734.

[10] Bronner, S. M.; Goetz, A. E.; Garg, N. K. *J. Am. Chem. Soc.* **2011**, *133*, 3832–3835.

[11] For the total synthesis of (–)-**2.2**, see: (a) Okabe, K.; Muratake, H.; Natsume, M. *Tetrahedron* **1990**, *46*, 5113–5120. (b) Okabe, K.; Natsume, M. *Tetrahedron* **1991**, *47*, 7615–7624.

[12] For the total synthesis of (–)-**2.3** and (–)-**2.4**, see: (a) Muratake, H.; Natsume, M. *Tetrahedron Lett.* **1987**, *28*, 2265–2268. (b) Muratake, H.; Okabe, K.; Natsume, M. *Tetrahedron* **1991**, *47*, 8545–8558.

[13] For discussions on conformational analysis of indolactam alkaloids, see: (a) Endo, Y.; Hasegawa, M.; Itai, A.; Shudo, K.; Tori, M.; Asakawa, Y.; Sakai, S.-i. *Tetrahedron Lett.*, **1985**, *26*, 1069–1072. (b) Kawai, T.; Ichinose, T.; Endo, Y.; Shudo, K.; Itai, A.; *J. Med. Chem.* **1992**, *35*, 2248–2253.

[14] For seminal indolyne studies, see: (a) Julia, M.; Huang, Y.; Igolen, J. *C. R. Acad. Sci., Ser. C* **1967**, *265*, 110–112. (b) Igolen, J.; Kolb, A. *C. R. Acad. Sci., Ser. C* **1969**, *269*, 54–56. (c) Julia, M.; Le Goffic, F.; Igolen, J.; Baillarge, M. *Tetrahedron Lett.* **1969**, *10*, 1569–1571.

[15] For hetaryne studies from our laboratory, see reference 10 and the following: (a) Cheong, P. H.-Y.; Paton, R. S.; Bronner, S. M.; Im, G.-Y. J.; Garg, N. K.; Houk, K. N. *J. Am. Chem. Soc.* **2010**, *132*, 1267–1269. (b) Im, G-Y. J.; Bronner, S. M.; Goetz, A. E.; Paton, R. S.; Cheong, P. H-Y.; Houk, K. N.; Garg, N. K. *J. Am. Chem. Soc.* **2010**, *132*, 17933–17944. (c) Bronner, S. M.; Bahnck, K. B.; Garg, N. K. *Org. Lett.* **2009**, *11*, 1007–1010. (d) Bronner, S. M.; Goetz, A. E.; Garg, N. K. *Synlett* **2011**, 2599–2604. (e) Huters, A. D.; Quasdorf, K. W.; Styduhar, E. D.; Garg, N. K. *J. Am. Chem. Soc.* **2011**, *133*, 15797–15799. (f) Goetz, A. E.; Garg, N. K. *Nat. Chem.* **2013**, *3*, 54–60. (g) Goetz, A. E.; Garg, N. K. *J. Org. Chem*. **2014**, *79*, 846–851.

[16] For other indolyne studies, see: (a) Buszek, K. R.; Luo, D.; Kondrashov, M.; Brown, N.; VanderVelde, D. *Org. Lett*. **2007**, *9*, 4135–4137. (b) Brown, N.; Luo, D.; VanderVelde, D.; Yang, S.; Brassfield, A.; Buszek, K. R. *Tetrahedron Lett.* **2009**, *50*, 63–65. (c) Buszek, K. R.; Brown, N.; Luo, D. *Org. Lett.* **2009**, *11*, 201–204. (d) Brown, N.; Luo, D.; Decapo, J. A.; Buszek, K. R. *Tetrahedron Lett.* **2009**, *50*, 7113–7115. (e) Thornton, P. D.; Brown, N.; Hill, D.; Neuenswander, B.; Lushington, G. H.; Santini, C.; Buszek, K. R. *ACS Comb. Sci.* **2011**, *13*, 443–448. (f) Nguyen, T. D.; Webster, R.; Lautens, M. *Org. Lett.* **2011**, *13*, 1370–1373. (g) Candito, D. A.; Panteleev, J.; Lautens, M. *J. Am. Chem. Soc.* **2011**, *133*, 14200–14203. (h) Candito, D. A.; Dobrovolsky, D.; Lautens, M. *J. Am. Chem. Soc.* **2012**, *134*, 15572–15580. (i) Chandrasoma, N.; Brown, N.; Brassfield, A.; Nerurkar, A.; Suares, S.; Buszek, K. R. *Tetrahedron Lett.* **2013**, *54*, 913–917. (j) Nerurkar, A.; Chandrasoma, N.; Maina, L.;Brassfield, A.; Luo, D.; Brown, N.; Buszek, K. R. *Synthesis* **2013**, *45*, 1843–1852.

[17] (a) Endo, Y.; Sato, Y.; Shudo, K. **1987**, *43*, 2241–2247. (b) Nakagawa, Y.; Irie, K.; Nakamura, Y.; Ohigashi, H. *Biosci. Biotechnol. Biochem.* **1998**, *62*, 1568–1573. (c) Mckittrick, B.; Failli, A.; Steffan, R. J.; Soll, R. M.; Hughes, P.; Schmid, J.; Asselin, A. A.; Shaw, C. C.; Noureldin, R.; Gavin, G. *J. Heterocyclic Chem.* **1990**, *27*, 2151–2163. (d) Haenchen, A.; Suessmuth, R. D. *Synlett* **2009**, 2483–2486. (e) Wu, Y.-S.; Coumar, M. S.; Chang, J.-Y.; Sun, H.-Y.; Kuo, F.-M.; Kuo, C.-C.; Chen, Y.-J.; Chang, C.-Y.; Hsiao, C.-L.; Liou, J.-P.; Chen, C.-P.; Yao, H.-T.; Chiang, Y.-K.; Tan, U. K.; Chen, C.-T.; Chu, C.-Y.; Wu, S.-Y.; Yeh, T.-K.; Lin, C.-Y.; Hsieh, H.-P. *J. Med. Chem.* **2009**, *52*, 4941–4945. (f) Shi, L., Aza-ring Fused Indole and Indoline Derivatives. U.S. Patent 0152308A1, Jun 23, 2011. (g) Chakravarty, S., Hart, B. P., Jain, R. P., Pyrido[4,3-b]indole et derives de Pyrido[3,4-b]indole

et Procédés d'Utilisation. U.S. Patent 0217675A1, Aug 25, 2011. (h) Dahmann, G., Fiegen, D., Fleck, M., Hoffmann, M., Klicic, J., East, S. P., Napier, S. C. R., Scott, J., Substituted Pyridyl-Pyrimidines and their Use as Medicaments. U.S. Patent 023502A1, Jan 24, 2013.

[18] The transformations used to prepare **2.9** are identical to those previously developed in our laboratory, but with modified procedures to improve the yields. See the experimental procedures for details.

[19] Our previously reported yield for the formation of **2.11** from **2.9** and **2.10** was 62%; see reference 10.

[20] Less than 5% of the corresponding C5-substituted product was detected.

[21] Angelini, E.; Balsamini, C.; Bartoccini, F.;Lucarini, S.; Piersanti, G. *J. Org. Chem.* **2008**, *73*, 5654–5657.

[22] Our previously reported yield for the formation of **2.12** was 56%; see reference 10.

[23] Martín, R.; Buchwald, S. L. *Angew. Chem. Int. Ed*. **2007**, *46*, 7236–7239.

[24] The use of $K_3PO_4$ and NaO*t*Bu gave similar results.

[25] Jørgensen, M.; Lee, S.; Liu, X.; Wolkowski, J. P.; Hartwig, J. F. *J. Am. Chem. Soc.* **2002**, *124*, 12557–12565.

[26] (a) Hama, T.; Liu, X.; Culkin, D. A.; Hartwig, J. F. *J. Am. Chem. Soc.* **2003**, *125*, 11176–11177. (b) Liu, X.; Hartwig, J. F. *J. Am. Chem. Soc*. **2004**, *126*, 5182–5191.

[27] Hama, T.; Culkin, D. A.; Hartwig, J. F. *J. Am. Chem. Soc.* **2006**, *128*, 4976–4985.

[28] Moreno, O. A.; Kishi, Y. *J. Am. Chem. Soc.* **1996**, *118*, 8180–8181.

[29] For reactions involving the Schwartz Reagent, see: e-EROS Encyclopedia of Reagents for Organic Synthesis, Chlorobis(cyclopentadienyl)hydridozirconium.

http://onlinelibrary.wiley.com/doi/10.1002/047084289X.rc074.pub2/abstract, (accessed January 2014). For reduction of tertiary amides using the Schwartz reagent, see: White, J. M.; Tunoori, A. R.; Georg, G. I. *J. Am. Chem. Soc.*, **2000**, *122*, 11995–11996.

[30] For the reduction of secondary amides using the Schwartz reagent, see: (a) Schedler, D. J. A.; Godfrey, A. G.; Ganem, B. *Tetrahedron Lett.* **1993**, *34*, 5035–5038. (b) Schedler, D. J. A.; Li, J.; Ganem, B. *J. Org. Chem.* **1996**, *61*, 4115–4119.

[31] Webber, M. J.; Weston, M.; Grainger, D. M.; Lloyd, S.; Warren, S. A.; Powell, L.; Alanine, A.; Stonehouse, J. P.; Frampton, C. S.; White, A. J. P.; Spivey, A. C. *Synlett* **2011**, 2693–2696.

[32] Crowley, P., Salmon, R., Quinolin-Isoquinolin-and Quinazolin-Oxyalkylamides and their Use as Fungicides. U.S. Patent 0072884A1, Mar 29, 2007.

[33] Garg, N. K.; Caspi, D. D.; Stoltz, B. M. *J. Am. Chem. Soc.* **2005**, *127*, 5970–5978.

[34] The addition of LiBr helped to suppress the competitive formation of des-bromo compound **2.14**.

[35] The stereochemical configurations at the newly formed quaternary centers of **2.31** and **2.32** were assigned after conversion to the natural products **2.3** and **2.4**, respectively.

[36] Moreno, O. A.; Kishi, Y. *Bioorg. Med. Chem.* **1998**, *6*, 1243–1254.

[37] Igarashi, Y.; Yanagisawa, E.; Ohshima, T.; Takeda, S.; Aburada, M.; Miyamoto, K. *Chem. Pharm. Bull.* **2007**, *55*, 328–333.

[38] Kauch, M.; Hoppe, D. *Can. J. Chem.* **2001**, *79*, 1736–1746.

[39] Kauch, M.; Snieckus, V.; Hoppe, D. *J. Org. Chem.* **2005**, *70*, 7149–7158.

[40] Griffen, E. J.; Roe, D. G.; Snieckus, V. *J. Org. Chem.* **1995**, *60*, 1484–1485.

[41] Dobbs, A. *J. Org. Chem.* **2001**, *66*, 638–641.

[42] Jelf, C. P.; Salmon, R. (Syngenta LTD, USA). Quinolin-, isoquinolin-, and quinazolin-oxyalkylamides and their use as fungicides. US Patent 0072884, March 29, 2007.

# CHAPTER THREE

## Expanding the Strained Alkyne Toolbox: Generation and Utility of Oxygen-Containing Strained Alkynes

Tejas K. Shah, Jose M. Medina, and Neil K. Garg.

*J. Am. Chem. Soc.* **2016**, *138*, 4948–4954.

### 3.1 Abstract

We report synthetic methodology that permits access to two oxacyclic strained intermediates, the 4,5-benzofuranyne and the 3,4-oxacyclohexyne. In situ trapping of these intermediates affords an array of heterocyclic scaffolds by the formation of one or more new C–C or C–heteroatom bonds. Experimentally determined regioselectivities were consistent with predictions made using the distortion / interaction model and were also found to be greater compared to selectivities seen in the case of trapping experiments of the corresponding *N*-containing intermediates. These studies demonstrate the synthetic versatility of oxacyclic arynes and alkynes for the synthesis of functionalized heterocycles, while further expanding the scope of the distortion / interaction model. Moreover, these efforts underscore the value of harnessing strained heterocyclic intermediates as a unique approach to building polycyclic heteroatom-containing frameworks.

## 3.2 Introduction

New approaches for the synthesis of decorated heterocycles remain highly sought after because of the prevalence of heterocycles in drugs, agrochemicals, materials, and natural products.[1] One unique strategy for heterocycle construction involves the trapping of transient heterocyclic arynes or alkynes.[2] For example, pyridynes,[2m,3] indolynes,[4,5,6] and piperidynes[7] (e.g., **3.1**–**3.3**, Figure 3.1) can now be used as building blocks for the synthesis of functionalized heterocycles in a predictable manner using the distortion / interaction model.[8]

Whereas advances in heterocyclic aryne and alkyne chemistry have focused on nitrogen-containing reactive intermediates, the corresponding chemistry of oxacycles has remained underdeveloped. The first aryne ever proposed was the 2,3-benzofuranyne;[9] however, this structural assignment was later called into question.[2b] Subsequent contributions in the area of oxacyclic arynes are limited to scattered examples involving dehydrohalogenation of benzofuran derivatives[10] and access to the 6,7-benzofuranyne using butyllithium reagents.[11] With regard to oxacyclohexynes, even less is known, with only two studies involving metalated oxacyclohexynes in the literature.[12] Silyl triflate precursors to oxacyclic arynes or alkynes have not been synthesized previously; likewise, no general methodologies for oxacyclic aryne or alkyne trapping have been reported to date.

We reasoned that mild methodologies involving the trapping of oxacyclic arynes and alkynes through a multitude of cycloadditions would provide a new avenue for building *O*-containing compounds. Oxygenated heterocycles, such as benzofuran and pyran derivatives, are often seen in natural products and drugs.[13] Notable examples include Saprisartan (treatment of hypertension),[14] hopeafuran (antimicrobial agent),[15] artemisinin (antimalarial drug),[16] rhoeadine (sedative & antitussive),[17] and frenolicin B (kinase inhibitor).[18] Moreover, some oxygen-

containing heterocycles are known bioisosteres for their nitrogen and sulfur-containting counterparts in medicinal chemistry.[19]

In the present study, we describe synthetic methodology to access two oxacyclic strained intermediates: the 4,5-benzofuranyne (**3.4**) and the 3,4-oxacyclohexyne (**3.5**) (Figure 3.1). In addition to establishing synthetic routes to silyl triflate precursors to **3.4** and **3.5** and using these species to build an assortment of functionalized heterocycles, we show that reliable regioselectivity predictions can be made prior to experiment using the distortion / interaction model. Selectivities are compared to those seen in the case of trapping experiments of the corresponding *N*-containing intermediates. Overall, our studies demonstrate that oxacyclic arynes and alkynes can be harnessed to efficiently construct decorated oxygen-containing heterocycles. The methodology is expected to prove useful in the synthesis of new pharmaceuticals and natural products.

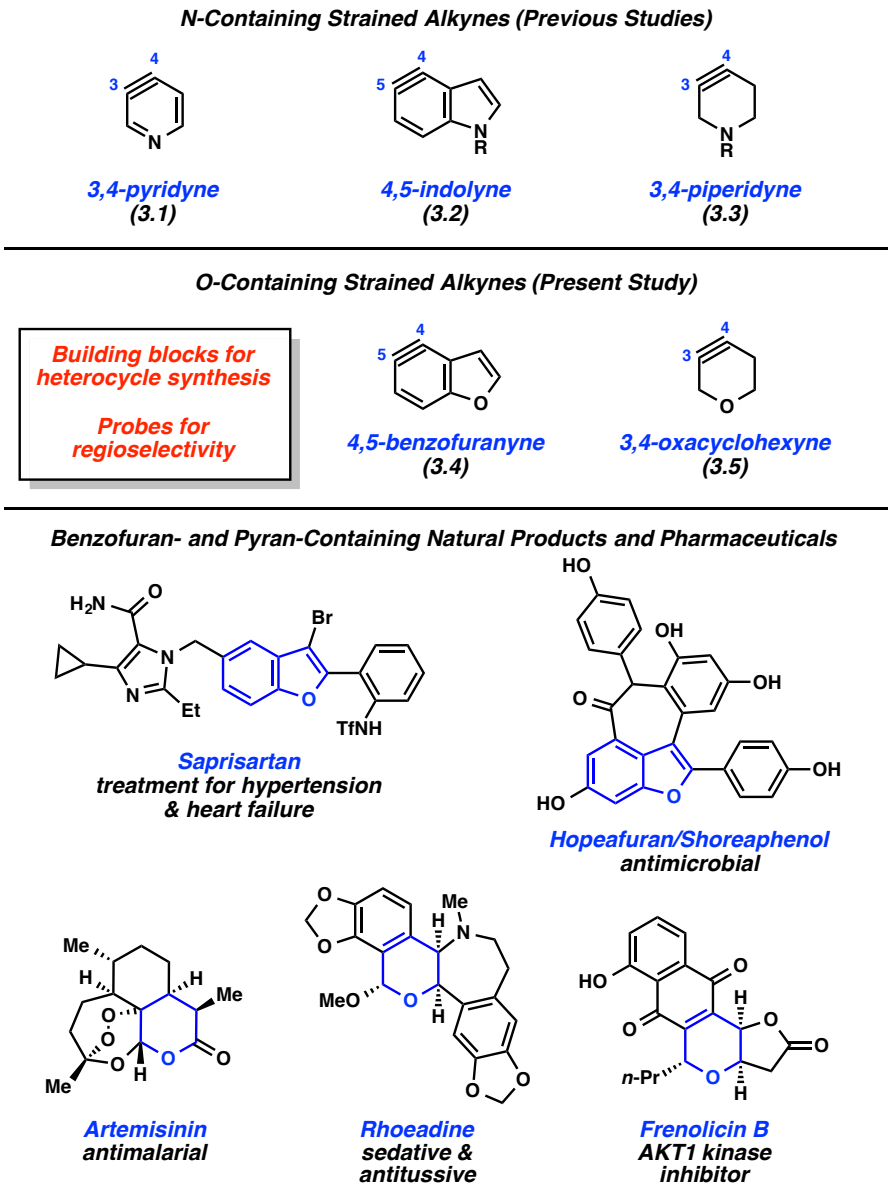


***Figure 3.1.*** Well studied *N*-containing cyclic alkynes **3.1**–**3.3**, *O*–containing strained alkynes **3.4** and **3.5** (present study), and representative drugs and natural products

## 3.3 Results and Discussion

### 3.3.1 Prediction of Regioselectivities Based on the Distortion / Interaction Model

An attractive aspect of using strained alkynes as synthetic building blocks is the ability to make reliable regioselectivity predictions prior to experiments using the distortion / interaction

model.[8] Briefly stated, substituted arynes or cyclic alkynes are unsymmetrically distorted in their ground state. Nucleophilic addition occurs at the terminus of the aryne (or alkyne) that is more distorted toward linearity (i.e., the site that possesses a larger internal angle). The geometry of the unsymmetrical aryne or alkyne can readily be determined by performing simple geometry optimization calculations using DFT methods. In addition to revealing the preferred site of attack by nucleophiles, these calculations can also be used to roughly assess the degree of regioselectivities. The greater the difference in internal angles between the two aryne (or alkyne) termini ($\Delta\theta$), the more pronounced regioselectivities are expected.

With the aim of predicting the site of nucleophilic attack on 4,5-benzofuranyne (**3.4**) and 3,4-oxacyclohexyne (**3.5**), while drawing comparisons to the corresponding *N*-containing heterocyclic alkynes **3.6** and **3.7**, we performed geometry optimizations using DFT calculations (B3LYP/6-31G(d)) (Figure 3.2).[20] First, we compared the optimized structures of 4,5-benzofuranyne (**3.4**) and 4,5-indolyne (**3.6**); each is distorted such that nucleophilic addition is expected to occur at C5, which is the more linear terminus. 4,5-Benzofuranyne (**3.4**) was found to be unsymmetrically distorted with the C5–C4 $\Delta q$ being 7°. In comparsion, 4,5-indolyne (**3.6**) is less distorted, with the C5–C4 $\Delta\theta$ being 4°.[5e,5f] As the $\Delta\theta$ is greater in the case of 4,5-benzofuranyne (**3.4**), we predicted this species would react with greater regioselectivity compared to 4,5-indolyne (**3.6**). To see if this trend extended to non-aromatic strained alkynes, we compared 3,4-oxacyclohexyne (**3.5**) and 3,4-piperidyne **3.7**. For both cyclic alkynes, nucleophilic attack is preferred to occur at C4, the site further distorted toward linearity. C4–C3 $\Delta\theta$ is 15° in the case of 3,4-oxacyclohexyne (**3.5**), but slightly less (i.e., 12°) for 3,4-piperidyne **3.7**.[7c] As such, we surmised that 3,4-oxacyclohexyne (**3.5**) would react with greater regioselectivities compared to 3,4-piperidyne **3.7**.

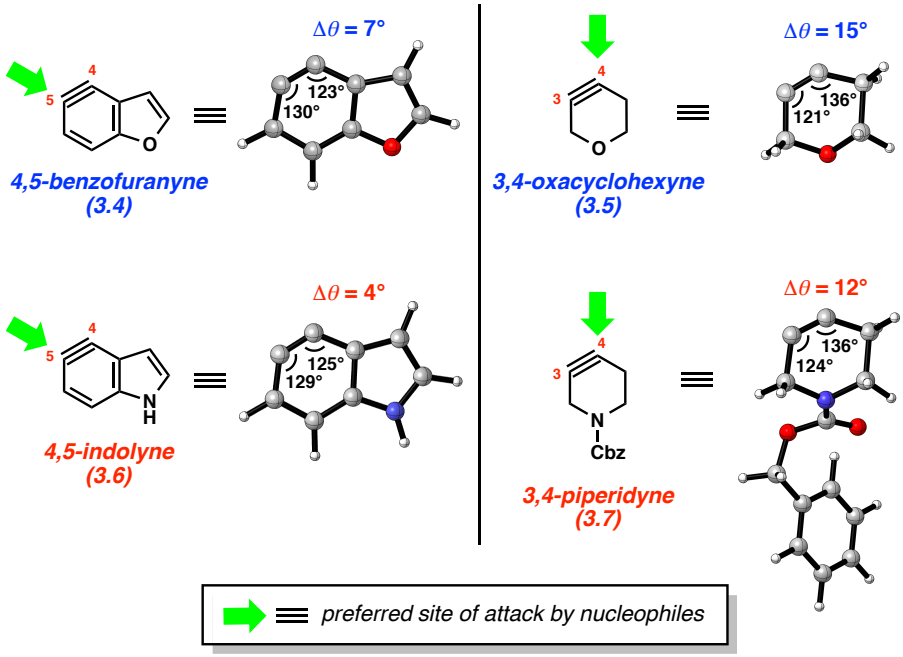


***Figure 3.2.*** Geometry optimized structures of **3.4**–**3.7** obtained at the B3LYP/6-31G(d) level and predicted site of nucleophilic attack. *Δθ* represents the net distortion of the alkyne

### 3.3.2 Synthesis of Silyl Triflate Precursors

Our study relied on developing efficient syntheses of suitable precursors to 4,5-benzofuranyne (**3.4**) and 3,4-oxacyclohexyne (**3.5**). Given the well-known versatility of silyl triflate precursors to arynes,[21] we targeted silyl triflates **3.10** and **3.14** (Scheme 3.1). The benzofuranyne precursor was derived from 5-hydroxybenzofuran (**3.8**), which is commercially available or readily accessible from hydroquinone.[22] Bromination of **3.8** proceeded smoothly to deliver the known bromoalcohol **3.9**.[23] Subsequent *O*-silylation, followed by retro-Brook rearrangement and triflation, furnished silyl triflate **3.10** in 81% yield. 3,4-Oxacyclohexyne precursor **3.14** could be synthesized in four steps beginning from commercially available 4-oxotetrahydropyran **3.11**. α-Bromination of **3.11** was performed using a known two-step sequence to provide bromoketone **3.12**.[24] Treatment of **3.12** with DABCO and TESCl afforded

silyl enol ether **3.13** in 91% yield. Finally, lithiation, retro-Brook rearrangement, and triflation delivered silyl triflate **3.14**.

***Scheme 3.1.*** Syntheses of Silyl Triflates **3.10** and **3.14**

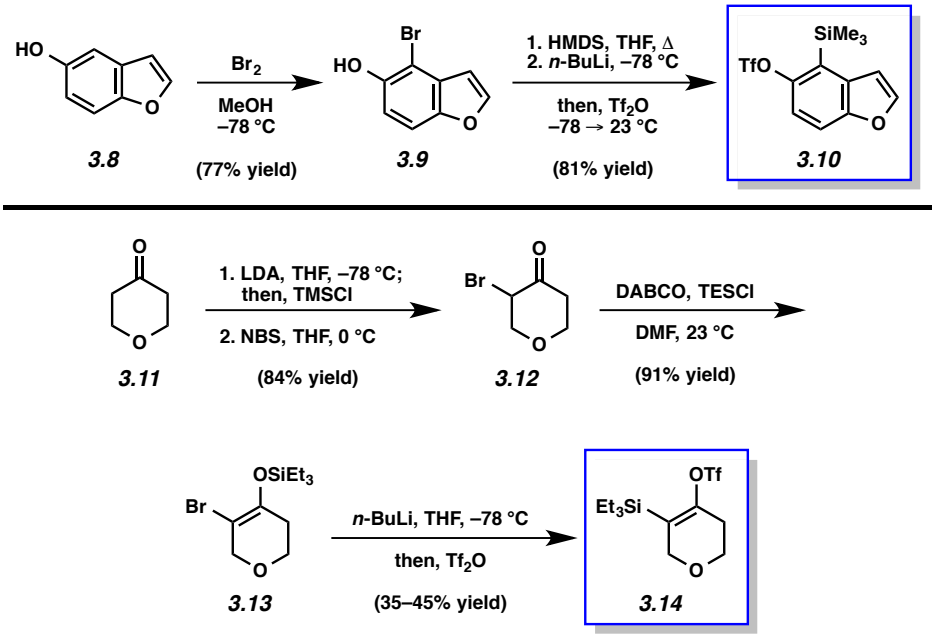


### 3.3.3 Generation & Trapping of 4,5-Benzofuranyne

With the silyl triflate precursors in hand, we first investigated the generation and trapping of the 4,5-benzofuranyne (**3.4**) with symmetrical cycloaddition partners (Table 3.1). Thus, silyl triflate **3.10** was exposed to 2-pyrone and CsF in MeCN at 50 °C; to our delight the desired benzannulated product was obtained via a Diels–Alder / retro-Diels–Alder sequence (entry 1). We also performed trapping experiments with furan and *N*-Boc pyrrole (entries 2 and 3). In each case, the corresponding [2.2.1]-bridged bicyclic adduct was formed in synthetically useful yields. These results not only validated that the 4,5-benzofuranyne (**3.4**) can be generated, but also demonstrated how this intermediate can be used to build two new C–C bonds on the benzofuran

motif in an efficient manner. In the latter case, the two linkages formed are $sp^2$–$sp^3$ C–C bonds, which would be difficult to introduce by known means.

***Table 3.1.*** Diels–Alder Cycloadditions of 4,5-Benzofuranyne (**3.4**)

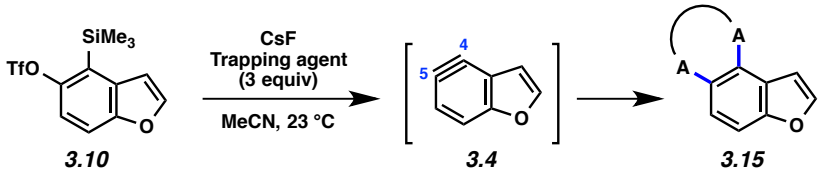


*3.10* *3.4* *3.15*

| *Entry* | *Trapping agent* | *Product* | *Yield*[a] |
|---|---|---|---|
| 1 | 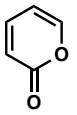 | 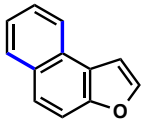 | *68%*[b] |
| 2 | | 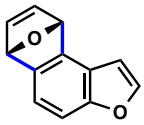 | *96%* |
| 3 | | 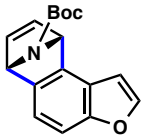 | *75%* |

[a] Reported yields are the average of two experiments and are based on the amount of isolated products. [b] Reaction performed at 50 °C.

With the aim of probing regioselectivity trends and accessing functionalized benzofurans, we shifted our attention to trapping benzofuranyne **3.4** with nucleophiles and unsymmetrical cycloaddition partners (Table 3.2). We found that *p*-cresol, morpholine, and *N*-Me-aniline could be employed as trapping agents,[25] to furnish benzofuranyne adducts in good yields (entries 1–3). In all cases, the major product was indicative of nucleophilic attack occurring at C5, consistent with the prediction made by the distortion / interaction model. To access more unique scaffolds and further examine regioselectivities, we surveyed trapping agents that would allow for the

appendage of seven-, six-, or five-membered heterocycles on the benzofuran motif. In situ trapping of **3.4** with 1,3-dimethyl-2-imidazolidinone[26] furnished the corresponding product of formal C–N bond insertion in 90% yield (entry 4). Only one constitutional isomer was observed in this case, although the subsequent trappings led to mixtures with a preference for initial bond formation also occurring at C5. The use of an amido acrylate trapping agent[27] allowed for the appendage of substituted pyridine rings to the benzofuran unit (entry 5). With regard to the formation of 5-membered rings, several trapping agents were deemed successful and could be used to forge C–C, C–O, and C–N bonds (entries 6–11).[28–33] In all cases, synthetically useful yields of substituted heterocycles were prepared with the expected regioselectivities. Thus, with access to a single new aryne precursor (i.e., **3.10**), one can build arrays of decorated benzofurans using this methodology.

***Table 3.2.*** Reactions of Silyl Triflate **3.10** with Nucleophiles and Cycloaddition Partners

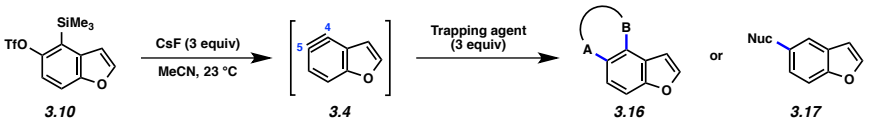


3.10 3.4 3.16 3.17

| Entry | Trapping agent | Product(s) | Yield[a] (ratio) |
|---|---|---|---|
| 1 | 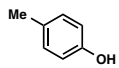 | 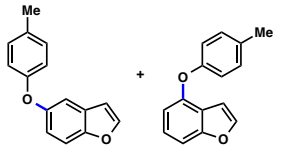 | 73% (8.5:1) |
| 2 | | 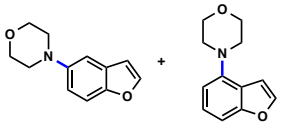 | 78% (4.2:1) |
| 3 | | 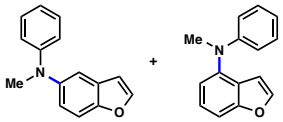 | 83% (10:1) |
| 4 | 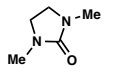 | 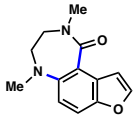 | 90%[b] |
| 5 | 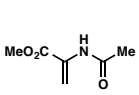 | 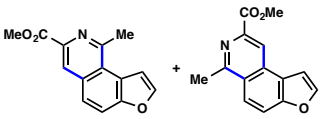 | 51% (2.9:1) |
| 6 | 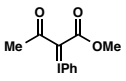 | 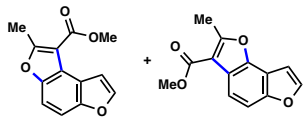 | 66% (12:1) |
| 7 | | 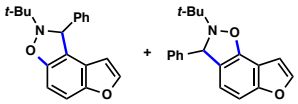 | 82% (5.4:1) |
| 8 | 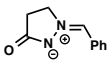 | 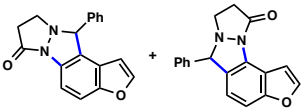 | 64% (4.5:1) |
| 9 | | 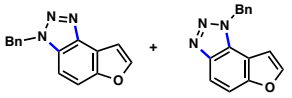 | 71% (6.2:1) |
| 10 | 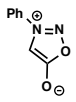 | 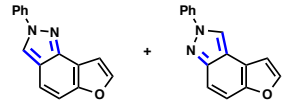 | 85% (1.3:1) |
| 11 | | 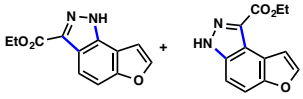 | 65% (2.5:1) |

[a] Reported yields are the average of two experiments and are based on the amount of isolated products. [b] Reaction performed neat with 1,3-dimethyl-2-imidazolidinone (10 equiv) at 50 °C with yield determined by $^1$H NMR analysis using 1,3,5-trimethoxybenzene as an external standard.

### 3.3.4 Generation & Trapping of 3,4-Oxacyclohexyne (3.5)

Efforts were also put forth to generate and trap 3,4-oxacyclohexyne (**3.5**). To confirm the in situ formation of the strained alkyne, we first examined trappings with dienes to give Diels–Alder adducts (Table 3.3). Thus, silyl triflate **3.14** was treated with CsF in the presence of 3 equivalents of tetracyclone in THF at 60 °C. This furnished the desired benzannulated product in quantitative yield (entry 1). Trapping with 2-pyrone, delivered the expected benzannulated product (entry 2). To arrive at more complex, heterocyclic adducts, Diels–Alder trappings were

performed with 2,5-dimethylfuran and *N*-Boc-pyrrole. In each case, the desired [2.2.1]-bicycles, which would arguably be difficult to make by other means, were formed (entries 3 and 4).

***Table 3.3.*** Diels–Alder Cycloadditions of 3,4-Oxacyclohexyne (**3.5**)

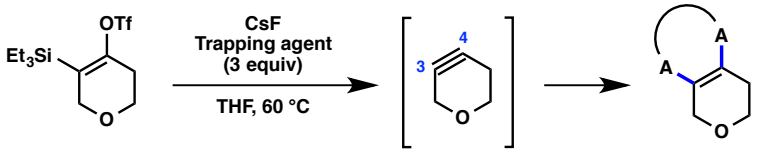


*3.14* *3.5* *3.18*

| *Entry* | *Trapping agent* | *Product* | *Yield*[a] |
|---|---|---|---|
| 1 | 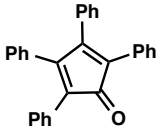 | 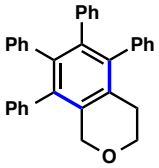 | *100%* |
| 2 | 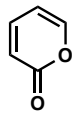 | 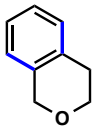 | *49%* |
| 3 | 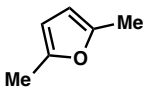 | 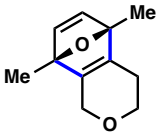 | *50%* |
| 4 | 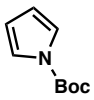 | | *48%* |

[a] Reported yields are the average of two experiments and are based on the amount of isolated products.

Analogous to our studies involving the 4,5-benzofuranyne (**3.4**), we tested the generation and trapping of 3,4-oxacyclohexyne (**3.5**) with nucleophiles and unsymmetrical cycloaddition partners (Table 3.4). Trapping with imidazole was examined primarily as a means to probe regioselectivity (entry 1). In this case, the 4-substituted adduct was obtained in >20:1

regiochemical preference. Addition at C4 was also seen in a variety of other trapping experiments, consistent with the predictions made by the distortion / interaction model. For example, interception of **3.5** with methyl salicylate[34] gave two products, both indicative of the same regioselectivity trend (entry 2). We also performed the trapping with an amido acrylate species,[27] which led to the appendage of pyridine motifs, albeit with modest selectivity (entry 3). Several efforts to annulate the oxacyclohexyne with 5-membered heterocycles were also put forth. Trapping with an iodoniun ylide[28] led to the introduction of a furan (entry 4), whereas nitrone trapping[29] gave the expected isoxazoline product (entry 5). Similarly, an azide cycloaddition[31] proceeded smoothly to give triazole-containing products (entry 6). In two additional examples, pyrazole derivatives could be obtained by trapping the oxacyclohexyne intermediate with either a sydnone[32] or diazoester[33] (entries 7 and 8). With this methodology, a variety of annulated oxacycles can be readily accessed from silyl triflate **3.14**, with good to excellent control of regioselectivity. It should be noted that the products obtained from these trapping studies possess significant $sp^3$ character. The generation of such $sp^3$-rich heterocyclic frameworks is an important direction in modern drug discovery.[35]

***Table 3.4.*** Reactions of Silyl Triflate **3.14** with Nucleophiles and Cycloaddition Partners

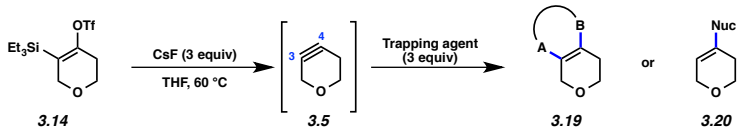


| Entry | Trapping agent | Product(s) | Yield[a] (ratio) | Entry | Trapping agent | Product(s) | Yield[a] (ratio) |
|---|---|---|---|---|---|---|---|
| 1 | | 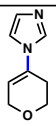 | 59% (>20:1) | 5 | | 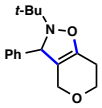 | 73% (>20:1) |
| 2 | | 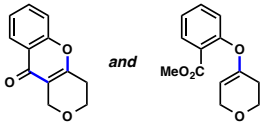 | 79% (>20:1) | 6 | | 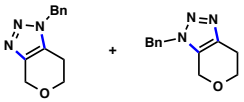 | 69% (7.2:1) |
| 3 | 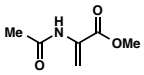 | 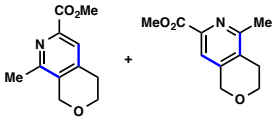 | 71% (2.6:1) | 7 | 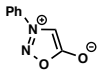 | 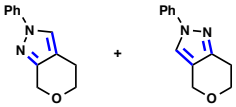 | 88% (1.5:1) |
| 4 | 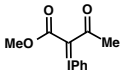 | 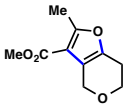 | 70%[b] (>20:1) | 8 | | 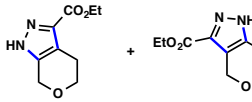 | 64% (6.1:1) |

[a] Reported yields are average of two experiments and are based on the amount of isolated products. [b] Reaction performed with MeCN as the solvent.

### 3.3.5 Comparison of Regioselectivities for *N*- and *O*-Containing Strained Alkynes

As noted earlier, we predicted that the 4,5-benzofuranyne (**3.4**) and the 3,4-oxacyclohexyne (**3.5**) would react with significant regioselectivities to give nucleophilic addition preferentially at C5 and C4, respectively. These predictions were verified, as described above. Additionally, we predicted that **3.4** and **3.5** would undergo trapping with more significant regioselectivities in comparison to their *N*-containing analogs, **3.22** and **3.7**.

Table 3.5 shows a comparison of regioselectivities for trapping experiments of 4,5-benzofuranyne (**3.4**) and *N*-Me-4,5-indolyne (**3.22**). When *p*-cresol was used as the nucleophile (entry 1), the indolyne reacted to furnish the C5- and C4-substituted adducts in a 3.0 : 1 ratio. In the case of benzofuranyne **3.4**, a higher degree of selectivity was observed (8.5 : 1). Similarly, in

the trapping of the arynes with benzylazide (entry 2), selectivity was greater in the case of the benzofuranyne (2.4 : 1 vs 6.2 : 1), consistent with predictions.

***Table 3.5.*** Comparison of 4,5-Indolyne and 4,5-Benzofuranyne Regioselectivities

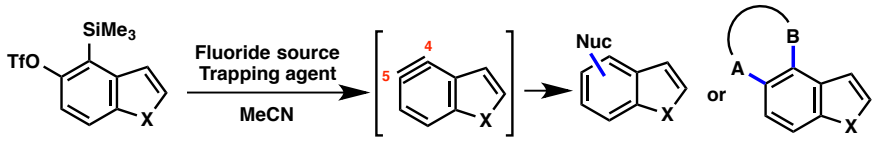


*3.21; X = NMe*
*3.10; X = O*

*3.22; X = NMe*
*3.4; X = O*

**X = NMe or O**

| *Entry* | *Trapping agent* | *Products* | *Ratio (Yield) X = NMe* | *Ratio (Yield) X = O* |
|---|---|---|---|---|
| 1 | 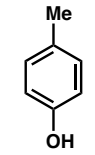 | 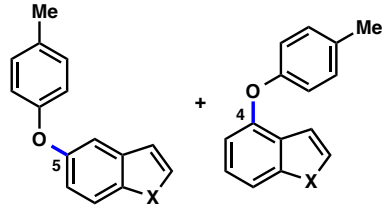 | *3.0 : 1*[a] *(80%)* | *8.5 : 1*[b] *(73%)* |
| 2 | 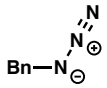 | 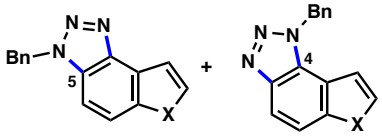 | *2.4 : 1*[c] *(86%)* | *6.2 : 1*[b] *(71%)* |

[a] Reaction performed with *p*-cresol (1.5 equiv) and CsF (3 equiv) at 50 °C.
[b] Reactions performed with trapping agent (3 equiv) and CsF (3 equiv) at 23 °C.
[c] Reaction performed with benzyl azide (5 equiv) and TBAF (2 equiv) at 23 °C.

Similar comparisons were made between the 3,4-oxacyclohexyne (**3.5**) and the corresponding *N*-Cbz-protected piperidyne **3.7** using cycloaddition reactions (Table 3.6). In the case of nitrone trapping (entry 1), the piperidyne undergoes cycloaddition to give a 12.7 : 1 ratio of products. However, use of the oxacyclic variant gave >20:1 selectivity. Likewise, slightly higher selectivities were seen in the trapping of oxacyclohexyne **3.5** with benzyl azide, compared to the trapping of piperidyne **7** (entry 2). The more pronounced selectivities seen in the case of the 4,5-benzofuranyne (**3.4**) and the 3,4-oxacyclohexyne (**3.5**), compared to their nitrogen-

containing counterparts, can be attributed to the greater electronegativity of oxygen. The oxygen atom has a stronger inductive effect that leads to increased distortion,[36] which in turn parlays into the more significant selectivities observed.

***Table 3.6.*** Comparison of Oxacyclohexyne and Piperidyne Regioselectivities

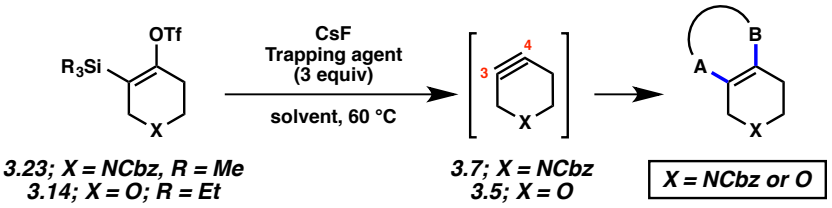


*3.23; X = NCbz, R = Me*
*3.14; X = O; R = Et*

*3.7; X = NCbz*
*3.5; X = O*

*X = NCbz or O*

| *Entry* | *Trapping agent* | *Products* | *Ratio (Yield)[a] X = NCbz* | *Ratio (Yield)[b] X = O* |
|---|---|---|---|---|
| 1 | 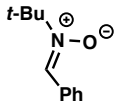 | 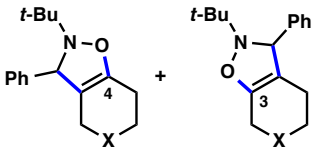 | *12.7:1 (84%)* | *>20:1 (73%)* |
| 2 | 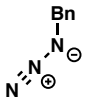 | 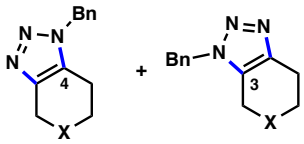 | *5.3:1 (81%)* | *7.2:1 (69%)* |

[a] Reaction performed with MeCN as the solvent. [b] Reactions performed with THF as the solvent.

## 3.4 Conclusion

In summary, we have developed methodology that allows for the generation and trapping of two oxacyclic strained intermediates, the 4,5-benzofuranyne and the 3,4-oxacyclohexyne. Interception of these species by nucleophiles and cycloaddition partners provides a new means to prepare arrays of heterocyclic scaffolds by the formation of one or more new C–C or C–heteroatom bonds. The distortion / interaction model was used to make regioselectivity predictions about the preferred sites of reactivity, which were validated by experiments.

Moreover, greater selectivities were seen in the trapping of the oxacyclic strained intermediates compared to the corresponding *N*-containing compounds, also consistent with computational predictions. Our studies demonstrate that oxacyclic arynes and alkynes can be generated from silyl triflate precursors and strategically harnessed to build decorated oxygen-containing heterocycles. Given the abundance of aryne trapping reactions available in the literature, this methodology is expected to find utility in the synthesis of medicinal substances and natural products.

## 3.5 Experimental Section

### 3.5.1 Materials and Methods

Unless stated otherwise, reactions were conducted in flame-dried glassware under an atmosphere of nitrogen using anhydrous solvents (freshly distilled or passed through activated alumina columns). All commercially obtained reagents were used as received unless otherwise specified. Cesium fluoride (CsF) was obtained from Strem Chemicals. Trifluoromethanesulfonic anhydride ($Tf_2O$) and Triethylsilyl chloride (TESCl) were obtained from Oakwood Products, Inc. and distilled before use. Furan, *N*-*tert*-butyl-α-phenylnitrone, methyl 2-acetamidoacrylate, and methyl salicylate were obtained from Alfa Aesar. Hexamethyldisilane, *N*-Boc-pyrrole, *N*-methylaniline, 1,3-dimethyl-2-imidazolidinone, ethyl diazoacetate, tetracyclone, and 2,5-dimethylfuran were obtained from Sigma Aldrich. 2-Pyrone, *p*-cresol was obtained from Acros Organics. Morpholine was obtained from Spectrum Chemical and distilled before use. Reaction temperatures were controlled using an IKAmag temperature modulator and, unless stated otherwise, reactions were performed at room temperature (rt, approximately 23 °C). Thin layer chromatography (TLC) was conducted with EMD gel 60 F254 pre-coated plates (0.25 mm) and

visualized using a combination of UV light and potassium permanganate staining. Preparative thin layer chromatography (TLC) was conducted with EMD gel 60 F254 pre-coated plates (0.5 mm) and visualized using UV light. Silicycle Siliaflash P60 (particle size 0.040–0.063 mm) was used for flash column chromatography. $^{1}$H NMR and 2D-NOESY spectra were recorded on Bruker spectrometers (500 MHz) and are reported relative to deuterated solvent signals. Data for $^{1}$H NMR spectra are reported as follows: chemical shift (δ ppm), multiplicity, coupling constant (Hz) and integration. $^{13}$C NMR spectra were recorded on Bruker spectrometers (125 MHz) and are reported relative to deuterated solvent signals. Data for $^{13}$C NMR spectra are reported in terms of chemical shift and, when necessary, multiplicity, and coupling constant (Hz). IR spectra were obtained using a Perkin-Elmer UATR Two FT-IR spectrometer and are reported in terms of frequency absorption ($cm^{-1}$). High-resolution mass spectra were obtained on Waters LCT Premier with ACQUITY LC and Thermo Scientific™ Exactive Mass Spectrometers with DART ID-CUBE. Images in Figure 3.2 were created using CYLview.[37]

### 3.5.2 Experimental Procedures.

#### 3.5.2.1 Synthesis of 3,4-Benzofuranyne Precursor

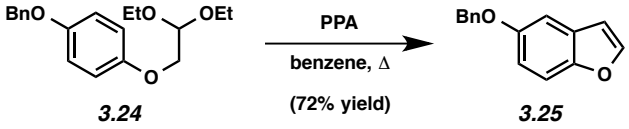


*3.24* *3.25*

**5-Benzyloxybenzofuran (3.25)**. To a solution of known diethylacetal[22] **3.24** (13.0 g, 41.1 mmol) in benzene (550 mL, 0.075 M) was added polyphosphoric acid (13.0 g, 1 equiv by weight). The flask was topped with a water condenser and the system placed under $N_2$. The reaction was heated to reflux and stirred for 2 h. After cooling, the reaction mixture was diluted with $H_2O$

(150 mL) and EtOAc (150 mL). The layers were separated, and the aqueous layer was extracted with EtOAc (3 x 150 mL). The organic layers were combined and dried over $MgSO_4$. Evaporation under reduced pressure and further purification by flash chromatography (20:1 Hexanes:EtOAc) afforded known 5-benzyloxybenzofuran **3.25**[22] (6.6 g, 72% yield) as an off white solid.

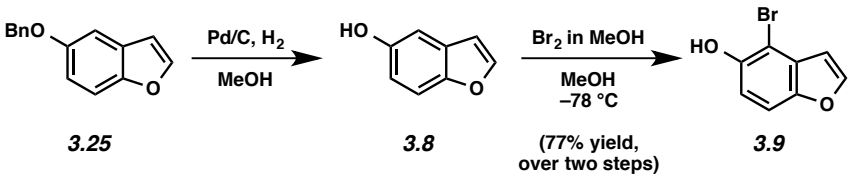


**4-Bromo-5-hydroxybenzofuran (3.9)**. To a solution of 5-benzyloxybenzofuran (**3.25**) (3.08 g, 13.73 mmol) in MeOH (137 mL, 0.1 M) was added 10% Pd/C (146 mg, 0.137 mmol, 1.0 mol% Pd). The mixture was placed under an atmosphere of hydrogen (double-balloon), stirred for 4 h at 23 °C, and then filtered over celite (EtOAc eluent). Evaporation of the solvent under reduced pressure afforded crude product **3.8**[38] as an off white solid, which was used in the subsequent step without further purification.

To a stirred solution of 5-hydroxybenzofuran (**3.8**) (1.8 g, 13.73 mmol) in MeOH (274 mL, 0.05 M) at –78 °C was added a solution of $Br_2$ in MeOH (14.4 mL, 1.0 M, 13.73 mmol, 1 equiv) dropwise over 30 min. The resulting mixture was stirred at –78 °C for 2 h, quenched with sat. $NaHCO_3$ (50 mL), and then diluted with EtOAc (100 mL). The layers were separated, and the aqueous layer was extracted with EtOAc (3 x 100 mL). The organic layers were combined and dried over $MgSO_4$. Evaporation under reduced pressure and further purification by flash chromatography (20:1 Hexanes:$Et_2O$) afforded known 4-bromo-5-hydroxybenzofuran[23] (**3.9**) as a yellow solid (2.3 g, 77% yield).

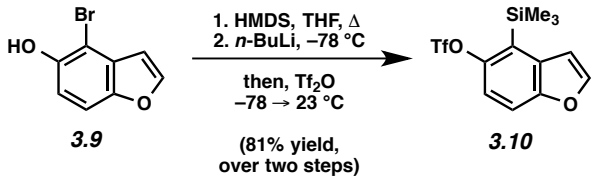


**Silyl Triflate 3.10**. To a solution of 4-bromo-5-hydroxybenzofuran (**3.9**) (900 mg, 4.22 mmol) in THF (7.7 mL, 0.55 M) was added hexamethyldisilane (1.9 mL, 9.3 mmol, 2.2 equiv). The flask was fitted with a reflux condenser, flushed with $N_2$, and then heated to reflux. After 12 h, the reaction mixture was cooled to room temperature. Evaporation of the volatiles under reduced pressure afforded the silyl ether, which was used in the subsequent step without further purification.

To the crude material was added THF (8.5 mL, 0.5 M) at –78 °C, followed by *n*-BuLi (2.9 mL, 1.75 M in hexanes, 5.07 mmol, 1.2 equiv) dropwise over 5 min. The resulting solution was stirred at –78 °C for an additional 20 min, and then neat $Tf_2O$ (0.85 mL, 5.07 mmol, 1.2 equiv) was added dropwise over 5 min. The resulting mixture was stirred at –78 °C for 2 h and allowed to warm to 23 °C over 12 h. The reaction was quenched with sat. $NaHCO_3$ (5 mL) and then diluted with EtOAc (10 mL). The layers were separated and the aqueous layer was extracted with EtOAc (3 x 30 mL). The organic layers were combined and dried over $MgSO_4$. Evaporation under reduced pressure and further purification by flash chromatography (50:1 Hexanes:$Et_2O$) afforded silyl triflate **3.10** as a colorless oil (1.2 g, 81% yield). Silyl triflate **3.10**: $R_f$ 0.6 (20:1 Hexanes:EtOAc); $^1$H NMR (500 MHz, $CDCl_3$): δ 7.74 (d, $J$ = 2.3, 1H), 7.53 (dd, $J$ = 9.0, 0.9, 1H), 7.26 (d, $J$ = 9.0, 1H), 6.96 (dd, $J$ = 2.3, 0.9, 1H), 0.50 (s, 9H); $^{13}$C NMR (125 MHz, $CDCl_3$): δ 152.7, 150.4, 147.0, 133.2, 125.9, 118.7 (q, $J$ = 320.0, $CF_3$), 116.8, 113.6, 108.5, 0.9; IR (film): 2960, 1398, 1205 cm$^{-1}$; HRMS-ESI (*m/z*) $[M - H]^-$ calcd for $C_{12}H_{12}F_3O_4SSi$, 337.01722; found, 337.01828.

### 3.5.2.2 Synthesis of 3,4-Oxacyclohexyne Precursor

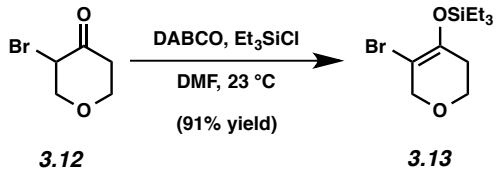


*3.12* *3.13*

**Silyl Enol Ether 3.13**. To a stirred solution of known bromoketone **3.12**[24] (2.31 g, 12.88 mmol) and DABCO (3.34 g, 29.62 mmol, 2.3 equiv) in DMF (12.0 mL, 1.1 M) was added $Et_3SiCl$ (3.55 mL, 20.61 mmol, 1.6 equiv). The reaction vessel was purged with $N_2$ gas and sealed. The solution was stirred for 24 h, and then quenched with saturated $NaHCO_3$ (20 mL). The layers were separated, and the aqueous layer was extracted with EtOAc (3 x 50 mL). The organic layers were combined and dried over $MgSO_4$. Evaporation under reduced pressure and further purification by flash chromatography (95:5 Hexanes:EtOAc) afforded silyl enol ether **3.13** as a faint yellow oil (3.4 g, 91% yield). Silyl enol ether **3.13**: $R_f$ 0.72 (9:1 Hexanes:EtOAc); $^1$H NMR (500 MHz, $C_6D_6$): δ 4.16 (t, *J* = 2.3, 2H), 3.43 (t, *J* = 5.5, 2H), 1.96–1.91 (m, 2H), 0.99 (t, *J* = 8.1, 9H), 0.63 (q, *J* = 8.1, 6H); $^{13}$C NMR (125 MHz, $C_6D_6$): δ 145.1, 98.1, 69.9, 64.8, 32.9, 7.0, 6.0; IR (film): 2954, 2907, 2874, 1673, 1457, 1246 cm$^{-1}$; HRMS-ESI (*m/z*) $[M + H]^+$ calcd for $C_{11}H_{22}BrO_2Si$, 293.05670; found, 293.05675

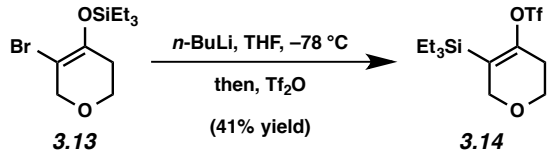


*3.13* *3.14*

**Silyl Triflate 3.14**. To a stirred solution of silyl enol ether **3.13** (250 mg, 0.85 mmol) in THF (8.5 mL, 0.1 M) at –78 °C was added *n*-BuLi (1.06 mL, 2.16 M in hexanes, 2.30 mmol, 2.7 equiv) dropwise over 5 min. The resulting solution was stirred at –78 °C for an additional 15 min, and then neat $Tf_2O$ (186 μL, 1.02 mmol, 1.2 equiv) was added dropwise over 2 min. The

resulting mixture was stirred at –78 °C for 1 h, quenched with saturated $NH_4Cl$ (10 mL), and allowed to warm to 23 °C over 30 min. The layers were separated, and the aqueous layer was extracted with EtOAc (3 x 20 mL). The organic layers were combined and dried over $MgSO_4$. Evaporation under reduced pressure and further purification by flash chromatography (95:5 Hexanes:$Et_2O$) afforded silyl triflate **3.14** as a colorless oil (120 mg, 41% yield). Silyl triflate **3.14**: $R_f$ 0.55 (9:1 Hexanes:$Et_2O$); $^1$H NMR (500 MHz, $C_6D_6$): δ 4.03 (t, $J$ = 2.7, 2H), 3.31 (t, $J$ = 5.5, 2H), 2.15 (sept, $J$ = 2.7, 2H), 0.87 (t, $J$ = 8.1, 9H), 0.63 (q, $J$ = 8.1, 6H); $^{13}$C NMR (125 MHz, $C_6D_6$): δ 151.5, 125.7, 118.8 (q, $J$ = 319.9, $CF_3$), 68.0, 64.0, 28.9, 7.3, 2.9; IR (film): 2958, 2879, 1654, 1415, 1213, 1138 cm$^{-1}$; HRMS-ESI (*m/z*) $[M + H]^+$ calcd for $C_{12}H_{22}F_3O_4SSi$, 347.09547; found, 347.09571.

### 3.5.2.3 4,5-Benzofuranyne Trapping Experiments

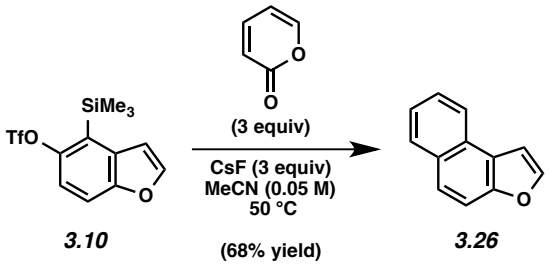


**Representative Procedure (Preparation of Benzofuran 3.26 is used as an example).**

**Benzofuran 3.26 (Table 3.1, entry 1).** To a stirred solution of silyl triflate **3.10** (50.0 mg, 0.148 mmol) and 2-pyrone (35 μL, 0.443 mmol, 3.0 equiv) in MeCN (2.9 mL, 0.05 M) was added CsF (67.3 mg, 0.443 mmol, 3.0 equiv). The reaction vessel was purged with $N_2$ gas, sealed, and placed in a preheated aluminum heating block maintained at 50 °C for 12 h. After cooling to 23 °C, the reaction mixture was filtered over silica gel (EtOAc eluent, 10 mL). Evaporation under reduced pressure and further purification by preparative thin layer chromatography (20:1

Hexanes:EtOAc) afforded known benzofuran **3.26**[39] as a white solid (68% yield, average of two experiments).

*Any modifications of the conditions shown in this representative procedure are specified in the following schemes, which depict all of the results shown in Tables 3.1 and 3.2.*

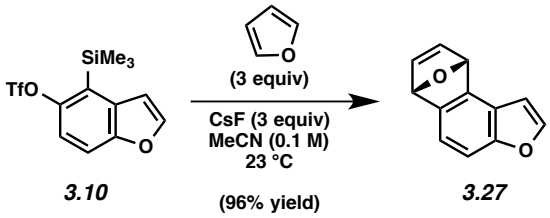


**Benzofuran 3.27 (Table 3.1, entry 2).** Purification by preparative thin layer chromatography (10:1 Hexanes:EtOAc) afforded benzofuran **3.27** as a white solid (96% yield, average of two experiments). Benzofuran **3.27**: $R_f$ 0.25 (10:1 Hexanes:EtOAc); $^1$H NMR (500 MHz, $CDCl_3$): δ 7.60 (d, *J* = 2.9, 1H), 7.24 (d, *J* = 7.9, 1H), 7.16–7.08 (m, 3H), 6.72 (dd, *J* = 2.3, 0.9, 1H), 5.96 (app t, *J* = 0.9, 1H), 5.83 (dd, *J* = 1.7, 0.7, 1H; $^{13}$C NMR (125 MHz, $CDCl_3$): δ 153.9, 146.5, 144.8, 144.1, 142.9, 142.7, 122.2, 116.5, 106.5, 104.0, 82.9, 81.7; IR (film): 3309, 3013, 1278, 864 cm$^{-1}$; HRMS-ESI (*m/z*) $[M + H]^+$ calcd for $C_{12}H_8O_2$, 185.06025; found, 185.05825.

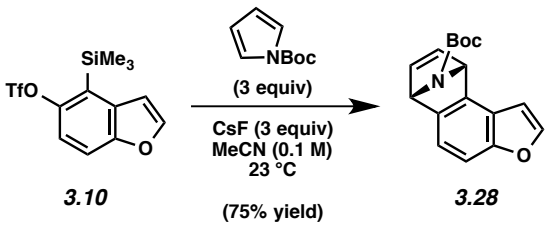


**Benzofuran 3.28 (Table 3.1, entry 3).** Purification by preparative thin layer chromatography (20:1 Hexanes:EtOAc) afforded benzofuran **3.28** as a tan solid (75% yield, average of two

experiments). Benzofuran **3.28**: $R_f$ 0.21 (20:1 Hexanes:EtOAc); $^1$H NMR (500 MHz, $CDCl_3$, 50 °C): δ 7.62–7.54 (br s, 3H), 7.23 (d, *J* = 7.8, 1H), 7.15–6.96 (m, 3H), 6.74 (br s, 1H), 5.73 (br s, 1H), 5.58 (br s, 1H), 1.38 (s, 9H); $^{13}$C NMR (125 MHz, $CDCl_3$, 52 °C): δ 155.2, 154.1, 146.4, 144.7, 143.7, 142.8, 142.1, 122.8, 117.1, 106.5, 104.1, 80.7, 67.2, 65.9, 28.4; IR (film): 2977, 1701, 1338, 1163 cm$^{-1}$; HRMS-ESI (*m/z*) $[M + H]^+$ calcd for $C_{17}H_{18}NO_3$, 284.12867; found, 284.12601.

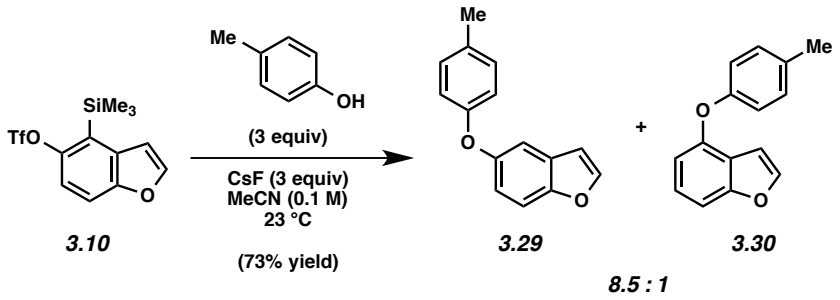


**Ethers 3.29 and 3.30 (Table 3.2, entry 1).** Purification by preparative thin layer chromatography (20:1 Hexanes:EtOAc) afforded ether **3.29** (65% yield, average of two experiments) as a colorless oil and ether **3.30** (8% yield, average of two experiments) as a colorless oil. Ether **3.29**: $R_f$ 0.42 (20:1 Hexanes:EtOAc); $^1$H NMR (500 MHz, $CDCl_3$): δ 7.63 (d, *J* = 1.9, 1H), 7.45 (d, *J* = 8.8, 1H), 7.19 (d, *J* = 2.4, 1H), 7.12 (d, *J* = 8.4, 2H), 7.01 (dd, *J* = 8.8, 2.4, 1H), 6.89 (d, *J* = 8.4, 2H), 6.70 (app t, *J* = 1.1, 1H), 2.33 (s, 3H); $^{13}$C NMR (125 MHz, $CDCl_3$): δ 156.1, 153.1, 151.3, 146.1, 132.2, 130.2, 128.3, 118.1, 116.6, 112.0, 110.8, 106.8, 20.7; IR (film): 3030, 2925, 1595, 1505, 1460, 1218 cm$^{-1}$; HRMS-ESI (*m/z*) $[M + H]^+$ calcd for $C_{15}H_{13}O_2$, 225.09101; found, 225.08969. Ether **3.30**: $R_f$ 0.48 (20:1 Hexanes:EtOAc); $^1$H NMR (500 MHz, $CD_3CN$): δ 7.67 (d, *J* = 2.2, 1H), 7.31 (dt, *J* = 8.3, 0.9, 1H), 7.26 (t, *J* = 8.0, 1H), 7.22–7.17 (m, 2H), 6.96–6.92 (m, 2H), 6.75 (dd, *J* = 7.8, 0.8, 1H), 6.64 (dd, *J* = 2.2, 0.9, 1H), 2.32 (s, 3H); $^{13}$C NMR (125 MHz, $CD_3CN$): δ 156.7, 154.9, 150.8, 145.0, 133.3, 130.3, 125.1,

119.3, 118.6, 111.2, 106.4, 103.8, 19.7; IR (film): 3030, 2855, 1596, 1506, 1481, 1242 $cm^{-1}$; HRMS-ESI (*m/z*) $[M - H]^-$ calcd for $C_{15}H_{11}O_2$, 223.07536; found, 223.07630.

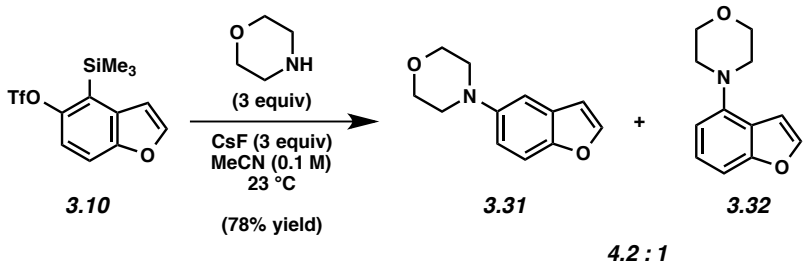


**Amines 3.31 and 3.32 (Table 3.2, entry 2).** Purification by preparative thin layer chromatography (10:1 Hexanes:$Et_2O$) afforded amine **3.31** (63% yield, average of two experiments) as a brown solid and amine **3.32** (15% yield, average of two experiments) as a white amorphous solid. Amine **3.31**: $R_f$ 0.27 (10:1 Hexanes:EtOAc); $^1H$ NMR (500 MHz, $CDCl_3$): δ 7.58 (d, *J* = 2.2, 1H), 7.41 (dt, *J* = 8.8, 0.7, 1H), 7.10 (d, *J* = 2.4, 1H), 6.99 (dd, *J* = 8.8, 2.4, 1H), 6.69 (dd, *J* = 2.2, 0.9, 1H), 3.93–3.87 (m, 4H), 3.17–3.10 (m, 4H); $^{13}C$ NMR (125 MHz, $CDCl_3$): δ 150.3, 148.1, 145.5, 128.0, 115.8, 111.6, 107.9, 106.7, 67.1, 51.5; IR (film): 3123, 2958, 2828, 1592, 1447, 1266, 1119, 736 $cm^{-1}$; HRMS-ESI (*m/z*) $[M + H]^+$ calcd for $C_{14}H_{14}NO_2$, 204.10245; found, 204.10179. Amine **3.32**: $R_f$ 0.36 (10:1 Hexanes:EtOAc); $^1H$ NMR (500 MHz, $CDCl_3$): δ 7.58 (d, *J* = 2.2, 1H), 7.24–7.16 (m, 2H), 6.78 (d, *J* = 1.6, 1H), 6.71 (d, *J* = 7.2, 1H), 3.98–3.89 (m, 4H), 3.26–3.16 (m, 4H); $^{13}C$ NMR (125 MHz, $CDCl_3$): δ 156.3, 146.4, 143.7, 125.1, 120.3, 109.7, 106.1, 105.3, 67.3, 51.8; IR (film): 2960, 2854, 1604, 1490, 1240, 1118, 749 $cm^{-1}$; HRMS-ESI (*m/z*) $[M + H]^+$ calcd for $C_{14}H_{14}NO_2$, 204.10245; found, 204.10192.

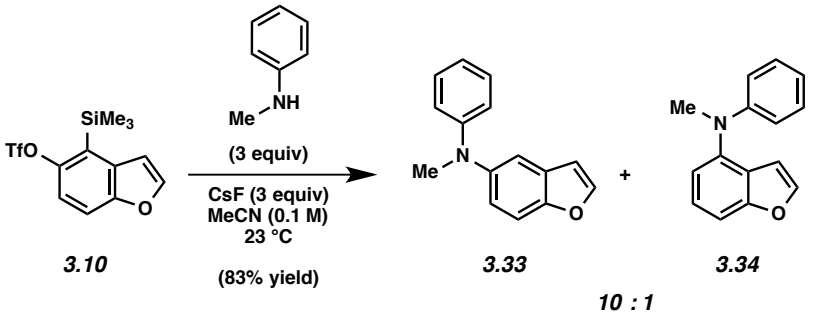


**Amines 3.33 and 3.34 (Table 3.2, entry 3).** Purification by preparative thin layer chromatography (10:1 Benzene:$Et_2O$) afforded amine **3.33** (75% yield, average of two experiments) as a white amorphous solid and amine **3.34** (8% yield, average of two experiments) as a colorless oil. Amine **3.33**: $R_f$ 0.46 (20:1 Hexanes:EtOAc); $^1$H NMR (500 MHz, $CDCl_3$): δ 7.63 (d, $J$ = 2.2, 1H), 7.47 (d, $J$ = 8.8, 1H), 7.38 (d, $J$ = 2.2, 1H), 7.24–7.19 (m, 2H), 7.11 (dd, $J$ = 8.8, 2.2, 1H), 6.86–6.79 (m, 3H), 6.73 (dd, $J$ = 2.1, 0.8, 1H), 3.33 (s, 3H); $^{13}$C NMR (125 MHz, $CDCl_3$): δ 152.2, 150.1, 145.8, 144.8, 129.1, 128.5, 122.5, 118.7, 117.3, 116.2, 112.3, 106.8, 41.0; IR (film): 3060, 2873, 2809, 1597, 1495, 1216 cm$^{-1}$; HRMS-ESI (*m/z*) [M + H]$^+$ calcd for $C_{15}H_{14}NO$, 224.10754; found, 224.10671. Amine **3.34**: $R_f$ 0.52 (20:1 Hexanes:EtOAc); $^1$H NMR (500 MHz, $CD_3CN$): δ 7.56 (d, $J$ = 2.2, 1H), 7.35–7.25 (m, 2H), 7.25–7.20 (m, 2H), 7.02 (dd, $J$ = 7.4, 1.1, 1H), 6.91–6.94 (m, 3H), 6.20 (dd, $J$ = 2.3, 0.9, 1H), 3.38 (s, 3H); $^{13}$C NMR (125 MHz, $CD_3CN$): δ 157.0, 150.3, 145.1, 143.4, 129.9, 126.2, 123.3, 121.0, 119.0, 117.4, 107.6, 106.5, 41.1; IR (film): 3025, 2872, 2808, 1597, 1495, 1216 cm$^{-1}$; HRMS-ESI (*m/z*) [M + H]$^+$ calcd for $C_{15}H_{14}NO$, 224.10754; found, 224.10675.

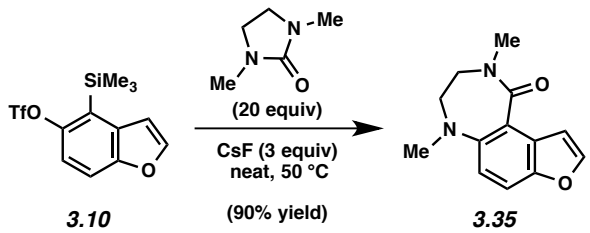


**Benzofuran 3.35 (Table 3.2, entry 4).** The yield was determined by $^{1}$H NMR analysis of the crude reaction mixture using 1,3,5-trimethoxybenzene as an external standard (90% yield of **3.35**, average of two experiments). The crude reaction mixture was placed under reduced pressure until most of the DMI was removed, and then purified by preparative thin layer chromatography (100% EtOAc) to give analytical sample of benzofuran **3.35**. Benzofuran **3.35**: $R_f$ 0.54 (100% EtOAc); $^{1}$H NMR (500 MHz, $CDCl_3$): δ 7.60 (d, $J$ = 2.1, 1H), 6.47 (dd, $J$ = 8.7, 0.9, 1H), 7.01 (dd, $J$ = 2.2, 0.9, 1H), 6.87 (d, $J$ = 8.8, 1H), 3.42 (t, $J$ = 5.8, 2H), 3.30 (t, $J$ = 5.8, 2H), 3.26 (s, 3H), 2.86 (s, 3H); $^{13}$C NMR (125 MHz, $CDCl_3$): δ 169.4, 151.1, 146.5, 142.9, 128.2, 121.3, 114.8, 113.9, 107.4, 55.9, 48.4, 40.9, 34.4; IR (film): 2939, 1628, 1485, 1438, 1253, 1033 $cm^{-1}$; HRMS-ESI (*m/z*) $[M + H]^+$ calcd for $C_{13}H_{15}N_2O_2$, 231.11280; found, 231.11300.

The structure of **3.35** was verified by 2D-NOESY, as the following interaction was observed:

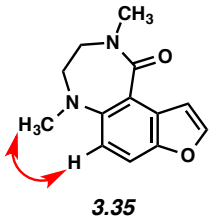

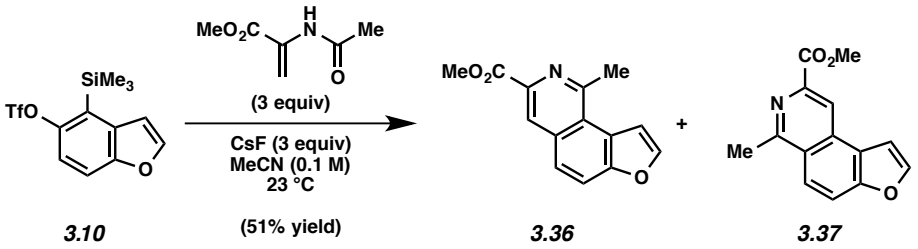


**Pyridines 3.36 and 3.37 (Table 3.2, entry 5).** Purification by preparative thin layer chromatography (2:1 Hexanes:EtOAc) afforded an inseparable mixture of pyridines **3.36** and **3.37** (51% yield, average of two experiments) as a white amorphous solid. **3.36** and **3.37**: $R_f$ 0.13 (2:1 Hexanes:EtOAc); $^1$H NMR (500 MHz, $CDCl_3$): **3.36** (major isomer): δ 8.59 (s, 1H), 7.97 (d, $J$ = 8.3, 1H), 7.93 (d, $J$ = 2.2, 1H), 7.86 (d, $J$ = 8.8, 1H), 7.48 (d, $J$ = 1.9, 1H), 4.07 (s, 3H), 3.25 (s, 3H); **3.37** (minor isomer): $^1$H NMR (500 MHz, $CDCl_3$): δ 8.76 (s, 1H), 8.09 (d, $J$ = 9.1, 1H), 7.91–7.88 (m, 2H), 7.37 (d, $J$ = 1.9, 1H), 4.08 (s, 3H), 3.11 (s, 3H); $^{13}$C NMR (125 MHz, $CDCl_3$): δ 166.8, 166.7, 157.7, 154.8, 154.7, 146.1, 145.6, 141.0, 139.9, 134.0, 131.2, 126.0, 125.7, 124.5, 123.7, 123.6, 122.7, 122.3, 119.3, 117.5, 115.6, 109.0, 106.1, 53.1, 53.0, 27.0, 23.6; IR (film): 3704, 2969, 2864, 1705, 1365, 1275, 1033, 1012 cm$^{-1}$; HRMS-ESI (*m/z*) [M + H]$^+$ calcd for $C_{14}H_{12}NO_3$, 242.08172; found, 242.07926.

The structure of **3.36** and **3.37** was verified by 2D-NOESY, as the following interactions were observed:

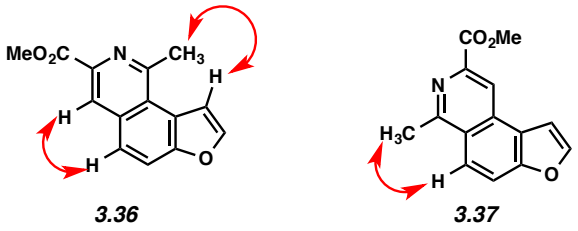

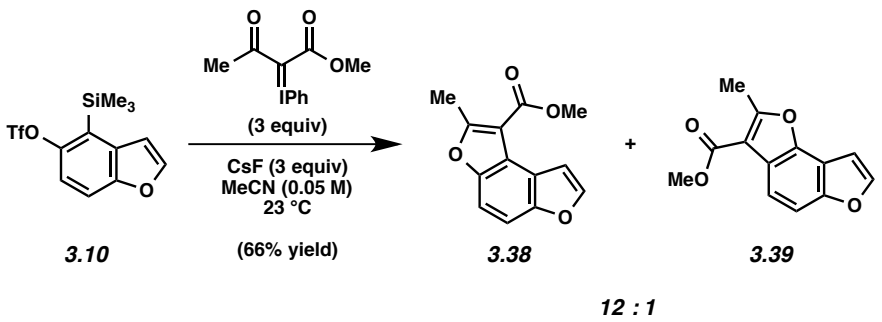


**Furans 3.38 and 3.39 (Table 3.2, entry 6).** Purification by preparative thin layer chromatography (20:1 Hexanes:EtOAc) afforded an inseparable mixture of furan adducts **3.38** and **3.39** (66% yield, average of two experiments) as a white solid. Furan **3.38**: $R_f$ 0.45 (20:1 Hexanes:EtOAc); $^1$H NMR (500 MHz, $CDCl_3$): δ 7.88 (d, $J$ = 8.7, 1H), 6.67 (d, $J$ = 2.2, 1H), 7.49 (dd, $J$ = 8.7, 0.9, 1H), 7.00 (dd, $J$ = 2.2, 0.9, 1H), 3.97 (s, 3H), 2.81 (s, 3H); $^{13}$C NMR (125 MHz, $CDCl_3$): δ 165.2, 162.5, 154.3, 146.2, 145.1, 120.8, 117.3, 112.7, 109.6, 108.2, 102.8, 51.6, 14.6; IR (film): 3145, 2953, 1714, 1597, 1444, 1261, 1099, 746 cm$^{-1}$; HRMS-ESI ($m/z$) [M + H]$^+$ calcd for $C_{13}H_{11}O_4$, 231.06519; found, 231.06430.

The structure of **3.38** was verified by 2D-NOESY, as the following interaction was observed:

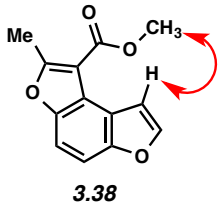

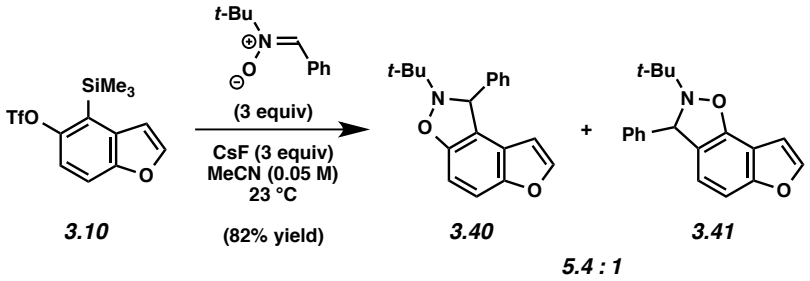


**Isoxazolines 3.40 and 3.41 (Table 3.2, entry 7).** Purification by preparative thin layer chromatography (50:1:1 Hexanes:Benzene:$Et_2O$) afforded isoxazoline **3.40** (69% yield, average of two experiments) as a yellow solid and isoxazoline **3.41** (13% yield, average of two experiments) as an off white solid. Isoxazoline **3.40**: $R_f$ 0.61 (50:1:1 Hexanes:Benzene:$Et_2O$); $^1$H NMR (500 MHz, $CDCl_3$): δ 7.48 (d, *J* = 2.1, 1H), 7.48–7.42 (m, 2H), 7.36–7.29 (m, 3H), 7.28–7.23 (m, 1H), 6.79 (d, *J* = 8.7, 1H), 6.27 (dd, *J* = 2.2, 0.9, 1H), 5.80 (s, 1H), 1.21 (s, 9H); $^{13}$C NMR (125 MHz, $CDCl_3$): δ 152.6, 151.3, 146.4, 143.3, 128.7, 127.8, 127.7, 123.1, 119.4, 111.1, 103.9, 103.8, 67.4, 61.2, 25.6; IR (film): 2973, 1607, 1478, 1432, 1223, 759, 697 $cm^{-1}$; HRMS-ESI (*m/z*) $[M + H]^+$ calcd for $C_{19}H_{20}NO_2$, 294.14886; found, 294.14917. Isoxazoline **3.41**: $R_f$ 0.66 (50:1:1 Hexanes:Benzene:$Et_2O$); $^1$H NMR (500 MHz, $CDCl_3$): δ 7.56 (d, *J* = 2.2, 1H), 7.45–7.37 (m, 2H), 7.36–7.29 (m, 2H), 7.26–7.22 (m, 1H), 6.98 (dd, *J* = 8.3, 0.7, 1H), 6.80 (dd, *J* = 2.2, 0.8, 1H), 6.78 (d, *J* = 8.3, 1H), 5.69 (s, 1H), 1.22 (s, 9H); $^{13}$C NMR (125 MHz, $CD_3CN$): δ 157.7, 149.9, 146.3, 145.8, 129.5, 128.2, 128.0, 123.7, 120.1, 110.6, 104.8, 103.8, 67.5, 62.0, 25.4; IR (film): 2974, 1601, 1473, 1210, 1050, 754, 699 $cm^{-1}$; HRMS-ESI (*m/z*) $[M + H]^+$ calcd for $C_{19}H_{20}NO_2$, 294.14886; found, 294.14895.

The structure of **3.41** was verified by 2D-NOESY, as the following interaction was observed:

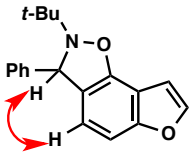


***3.41***

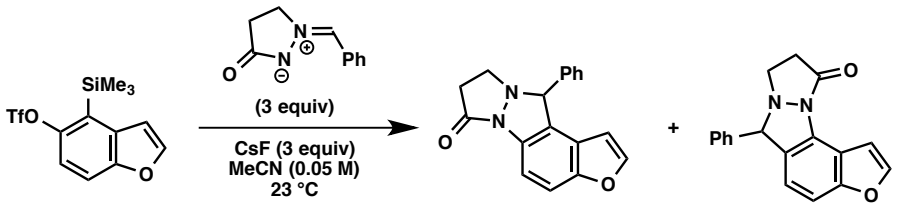


***3.10*** (66% yield) ***3.42*** ***3.43***

***4.5 : 1***

**Diazolidines 3.42 and 3.43 (Table 3.2, entry 8).** Purification by preparative thin layer chromatography (9:1 Benzene:Acetone) afforded diazolidine **3.42** (54% yield, average of two experiments) as a yellow solid and diazolidine **3.43** (12% yield, average of two experiments) as a orange solid. Diazolidine **3.42**: $R_f$ 0.40 (9:1 Benzene:Acetone); $^1$H NMR (500 MHz, $CD_3CN$): δ 7.64 (d, $J$ = 2.2, 1H), 7.56–7.47 (m, 4H), 7.46–7.40 (m, 3H), 6.08 (dd, $J$ = 2.2, 0.7, 1H), 5.48 (s, 1H), 3.55 (dt, $J$ = 8.7, 1.6, 1H), 3.27 (ddd, $J$ = 12.6, 8.8, 8.0, 1H), 3.04–2.94 (m, 1H), 2.76–2.68 (ddd, $J$ = 16.3, 7.8, 1.6, 1H); $^{13}$C NMR (125 MHz, $CD_3CN$): δ 164.2, 154.0, 148.4, 140.0, 131.4, 129.7, 129.7, 130.0, 127.0, 124.5, 112.0, 109.8, 104.7, 74.8, 52.8, 36.8, 36.8; IR (film): 3114, 3032, 2834, 1682, 1438, 1070, 702 cm$^{-1}$; HRMS-ESI (*m/z*) $[M + H]^+$ calcd for $C_{18}H_{15}N_2O_2$, 291.11280; found, 291.11424. Diazolidine **3.43**: $R_f$ 0.52 (9:1 Benzene:Acetone); $^1$H NMR (500 MHz, $CD_3CN$): δ 7.74 (d, $J$ = 2.2, 1H), 7.51–7.46 (m, 2H), 7.46–7.41 (m, 2H), 7.41–7.36 (m, 1H), 7.26 (dd, $J$ = 2.2, 0.9, 1H), 7.22 (dd, $J$ = 8.4, 0.8, 1H), 6.75 (dd, $J$ = 8.4, 0.8, 1H), 5.34 (s, 1H), 3.56 (dt, $J$ = 8.6, 1.5, 1H), 3.32–3.23 (m, 1H), 3.10–3.00 (m, 1H), 2.80–2.72 (ddd, $J$ = 16.2, 7.8, 1.6, 1H); $^{13}$C NMR (125 MHz, $CD_3CN$): δ 163.9, 157.2, 146.5, 140.5, 129.7, 129.6, 129.3,

129.3, 127.6, 120.4, 115.2, 108.3, 107.8, 74.9, 52.9, 36.8; IR (film): 3124, 3032, 2836, 1691, 1477, 1098, 704 $cm^{-1}$; HRMS-ESI (*m/z*) $[M + H]^+$ calcd for $C_{18}H_{15}N_2O_2$, 291.11280; found, 291.11346.

The structure of **3.43** was verified by 2D-NOESY, as the following interaction was observed:

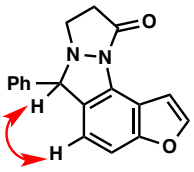


***3.43***

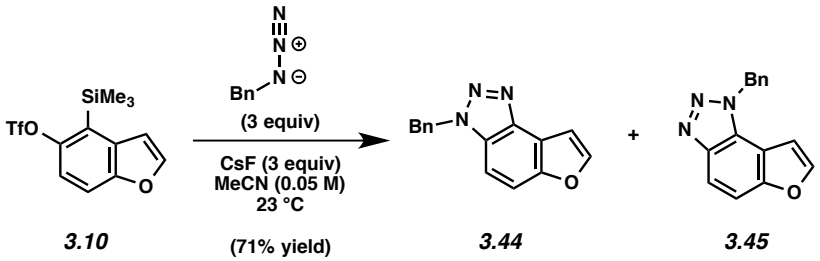


***3.10*** ***3.44*** ***3.45***

***6.2 : 1***

**Triazoles 3.44 and 3.45 (Table 3.2, entry 9).** Purification by preparative thin layer chromatography (10:1 Benzene:$Et_2O$) afforded triazole **3.44** (61% yield, average of two experiments) as an off white solid and triazole **3.45** (10% yield, average of two experiments) as an off white solid. Triazole **3.44**: $R_f$ 0.43 (10:1 Benzene:$Et_2O$); $^1H$ NMR (500 MHz, $CDCl_3$): δ 7.80 (d, *J* = 2.1, 1H), 7.59 (dd, *J* = 9.0, 0.9, 1H), 7.38 (dd, *J* = 2.1, 0.8, 1H), 7.35–7.26 (m, 5H), 7.21 (d, *J* = 9.0, 1H), 5.90 (s, 2H); $^{13}C$ NMR (125 MHz, $CDCl_3$): δ 152.5, 146.1, 140.4, 134.9, 130.3, 129.2, 128.6, 127.6, 117.9, 113.2, 105.5, 105.4, 52.7; IR (film): 3118, 3033, 1597, 1499, 1457, 1249, 1144, 1059, 721 $cm^{-1}$; HRMS-ESI (*m/z*) $[M + H]^+$ calcd for $C_{15}H_{12}N_3O$, 250.09804; found, 250.09552. Triazole **3.45**: $R_f$ 0.48 (10:1 Benzene:$Et_2O$); $^1H$ NMR (500 MHz, $CDCl_3$): δ

7.96 (d, $J$ = 9.1, 1H), 7.67 (d, $J$ = 2.2, 1H), 7.56 (dd, $J$ = 9.2, 0.8, 1H), 7.37–7.29 (m, 3H), 7.26–7.19 (m, 2H), 6.71 (dd, $J$ = 2.1, 0.9, 1H), 6.03 (s, 2H); $^{13}$C NMR (125 MHz, $CDCl_3$): δ 154.5, 145.3, 143.5, 135.1, 129.1, 128.5, 127.3, 126.9, 115.8, 110.3, 110.1, 104.4, 52.9; IR (film): 3116, 3033, 1637, 1499, 1455, 1242, 1147, 1052, 730 cm$^{-1}$; HRMS-ESI ($m/z$) $[M + H]^+$ calcd for $C_{15}H_{12}N_3O$, 250.09804; found, 250.09587.

The structure of **3.44** was verified by 2D-NOESY, as the following interaction was observed:

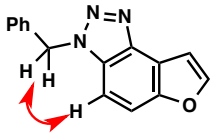


***3.44***

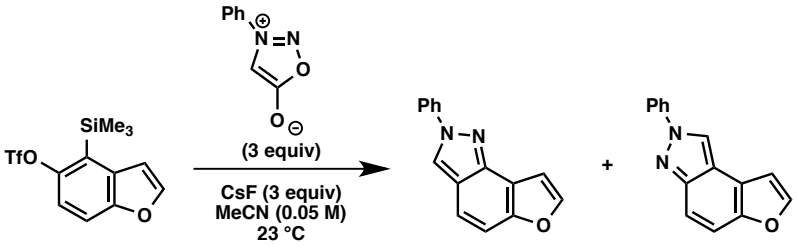


***3.10*** ***3.46*** ***3.47***

***1.3 : 1***

**Pyrazoles 3.46 and 3.47 (Table 3.2, entry 10).** Purification by preparative thin layer chromatography (20:1 Hexanes:$Et_2O$) afforded pyrazole **3.46** (48% yield, average of two experiments) as a black solid and pyrazole **3.47** (37% yield, average of two experiments) as a dark green solid. Pyrazole **3.46**: $R_f$ 0.21 (20:1 Hexanes:EtOAc); $^1$H NMR (500 MHz, $CDCl_3$): δ 8.46 (s, 1H), 7.94–7.90 (m, 2H), 7.71 (d, $J$ = 2.0, 1H), 7.58–7.51 (m, 3H), 7.43–7.36 (m, 2H), 7.30 (dd, $J$ = 2.0, 0.8, 1H); $^{13}$C NMR (125 MHz, $CDCl_3$): δ 154.5, 144.8, 143.7, 140.7, 129.7, 127.8, 121.7, 121.0, 120.2, 116.6, 115.1, 111.0, 105.8; IR (film): 3123, 2923, 1635, 1599, 1519,

1415, 1043, 735 $cm^{-1}$; HRMS-ESI (*m/z*) $[M + H]^+$ calcd for $C_{15}H_{11}N_2O$, 235.08714; found, 235.08663. Pyrazole **3.47**: $R_f$ 0.21 (20:1 Hexanes:EtOAc); $^1H$ NMR (500 MHz, $CDCl_3$): δ 8.54 (s, 1H), 7.96–7.60 (m, 2H), 7.71 (d, *J* = 2.0, 1H), 7.60 (d, *J* = 9.3, 1H), 7.59–7.50 (m, 3H), 7.40 (t, *J* = 7.4, 1H), 7.01 (dd, *J* = 2.0, 0.8, 1H); $^{13}C$ NMR (125 MHz, $CDCl_3$): δ 151.3, 148.5, 144.2, 140.8, 129.8, 127.8, 120.9, 118.9, 116.8, 116.7, 114.9, 114.8, 106.7; IR (film): 3120, 3070, 1600, 1517, 1504, 1387, 1062, 754 $cm^{-1}$; HRMS-ESI (*m/z*) $[M + H]^+$ calcd for $C_{15}H_{11}N_2O$, 235.08714; found, 235.08643.

The structure of **3.46** was verified by 2D-NOESY, as the following interaction was observed:

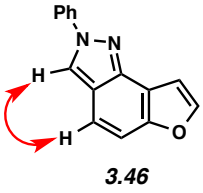


***3.46***

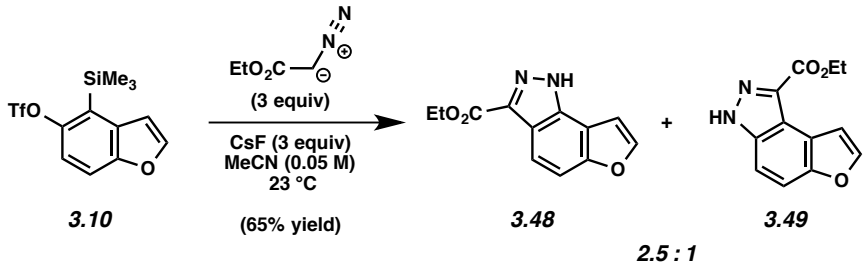


***3.10*** ***3.48*** ***3.49***

***2.5 : 1***

**Pyrazoles 3.48 and 3.49 (Table 3.2, entry 11).** Purification by preparative thin layer chromatography (3:1:1 Hexanes:$CH_2Cl_2$:$Et_2O$) afforded pyrazole **3.48** (46% yield, average of two experiments) as a white solid and pyrazole **3.49** (19% yield, average of two experiments) as a white solid. Pyrazole **3.48**: $R_f$ 0.48 (20:1 Hexanes:EtOAc); $^1H$ NMR (500 MHz, $CDCl_3$): δ 8.04 (d, *J* = 9.0, 1H), 7.71 (d, *J* = 2.1, 1H), 7.51 (dd, *J* = 9.0, 0.7, 1H), 7.17 (dd, *J* = 2.8, 0.8, 1H), 4.48 (q, *J* = 7.2, 2H) 1.39 (t, *J* = 7.2, 3H); $^{13}C$ NMR (125 MHz, $CDCl_3$): δ 163.3, 155.0 144.5,

136.9, 135.8, 118.8, 117.7, 111.2, 109.8, 104.7, 61.3, 14.4; IR (film): 3195, 3123, 2980, 1714, 1485, 1251, 1150, 740 $cm^{-1}$; HRMS-ESI (*m/z*) $[M + H]^+$ calcd for $C_{12}H_{11}N_2O_3$, 231.07697; found, 231.07500. Pyrazole **3.49**: $R_f$ 0.48 (20:1 Hexanes:EtOAc); $^1H$ NMR (500 MHz, $CDCl_3$): δ 7.79 (d, *J* = 2.0, 1H), 7.67 (d, *J* = 9.1, 1H), 7.64 (d, *J* = 1.9, 1H), 7.56 (d, *J* = 9.1, 1H), 4.59 (q, *J* = 7.1, 2H), 1.51 (t, *J* = 7.1, 3H); $^{13}C$ NMR (125 MHz, $CDCl_3$): δ 162.9, 152.0, 145.0, 139.4, 136.3, 119.1, 116.2, 113.4, 108.7, 107.3, 61.5, 14.7; IR (film): 3246, 3168, 2980, 1710, 1447, 1227, 1148, 768 $cm^{-1}$; HRMS-ESI (*m/z*) $[M - H]^-$ calcd for $C_{12}H_9N_2O_3$, 229.06132; found, 229.06117.

The structure of **3.48** was verified by 2D-NOESY, as the following interaction was observed:

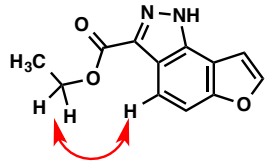


***3.48***

### 3.5.2.4 Oxacyclohexyne Trapping Experiments

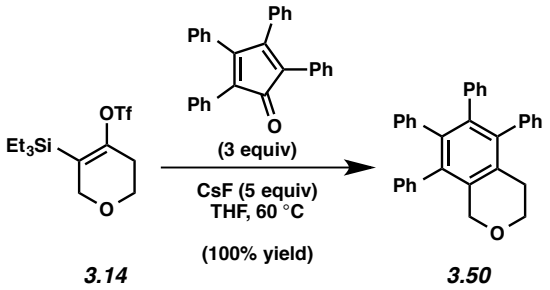


***3.14*** ***3.50***

**Representative Procedure (Preparation of Pyran 3.50 is used as an example).**

**Pyran 3.50 (Table 3.3, entry 1).** To a stirred solution of silyl triflate **3.14** (50.2 mg, 0.145 mmol) and tetracyclone (168 mg, 0.434 mmol, 3.0 equiv) in THF (5.0 mL, 0.03 M) was added

CsF (100 mg, 0.725 mmol, 5.0 equiv). The reaction vessel was purged with $N_2$ gas, sealed, and placed in a preheated aluminum heating block maintained at 60 °C for 24 h. After cooling to 23 °C, the reaction mixture was filtered over silica gel (EtOAc eluent, 12 mL). Evaporation under reduced pressure and further purification by preparative thin layer chromatography (1:1 Benzene:Hexanes) afforded pyran **3.50** as a faint yellow amorphous solid (100% yield, average of two experiments). Pyran **3.50**: $R_f$ 0.52 (9:1 Hexanes:EtOAc); $^1$H NMR (500 MHz, $CDCl_3$): δ 7.21–7.17 (m, 4H), 7.14–7.06 (m, 6H), 6.85–6.77 (m, 10H), 4.55 (s, 2H), 3.91 (t, $J$ = 5.8, 2H), 2.64 (t, $J$ = 5.8, 2H); $^{13}$C NMR (125 MHz, $CDCl_3$) [24/33 carbons were discernable]: δ 140.7, 140.2, 139.9, 139.8, 139.4, 139.0, 138.8, 137.8, 132.3, 131.4, 131.3, 131.1, 130.3, 130.0, 127.9, 127.8, 126.7, 126.6, 126.4, 125.4, 125.3, 68.2, 65.4, 28.6; IR (film): 3080, 3057, 2244, 1950, 1809, 1603 cm$^{-1}$; HRMS-ESI (*m/z*) $[M + H]^+$ calcd for $C_{33}H_{27}O$, 439.20564; found, 439.19306.

*Any modifications of the conditions shown in this representative procedure are specified in the following schemes, which depict all of the results shown in Tables 3.3 and 3.4.*

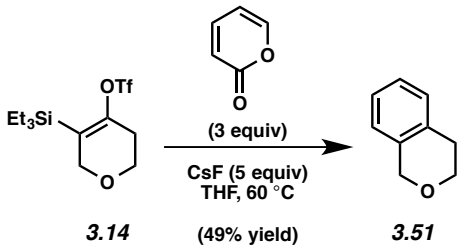


**Isochroman (3.51) (Table 3.3, entry 2).** Purification by preparative thin layer chromatography (2:1 Hexanes:EtOAc) afforded isochroman (**3.51**) as a colorless oil (49% yield, average of two experiments). Isochroman (**3.51**): $R_f$ 0.50 (9:1 Hexanes:$Et_2O$); $^1$H NMR (500 MHz, $CDCl_3$): δ 7.18–7.10 (m, 3H), 6.99–6.96 (m, 1H), 4.78 (s, 2H), 3.99 (t, $J$ = 5.7, 2H), 2.87 (t, $J$ = 5.7, 2H);

$^{13}$C NMR (125 MHz, $CDCl_3$): δ 135.1, 133.4, 129.1, 126.5, 126.1, 124.5, 68.1, 65.5, 28.5; IR (film): 3061, 2930, 2832, 1649, 1495, 1452 $cm^{-1}$; HRMS-ESI (*m/z*) $[M + H]^+$ calcd for $C_9H_{11}O$, 135.08044; found, 135.07911.

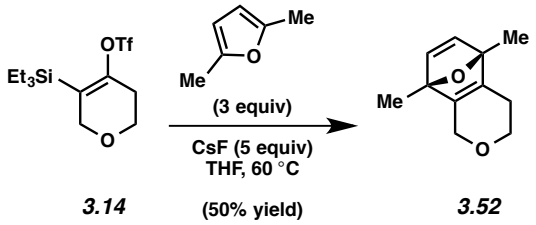


*3.14* (50% yield) *3.52*

**Pyran 3.52 (Table 3.3, entry 3).** Purification by preparative thin layer chromatography (1:1 Hexanes:EtOAc) afforded pyran **3.52** as a colorless oil (50% yield, average of two experiments). Pyran **3.52**: $R_f$ 0.25 (9:1 Hexanes:$Et_2O$); $^1$H NMR (500 MHz, $CDCl_3$): δ 6.86 (s, 2H), 4.46 (app. dt, *J* = 16.3, 3.7, 1H), 3.97 (app. ddd, *J* = 16.3, 3.7, 0.8, 1H), 3.68–3.65 (m, 2H), 2.39–2.31 (m, 1H), 2.00–1.92 (m, 1H), 1.64 (s, 3H), 1.61 (s, 3H); $^{13}$C NMR (125 MHz, $CDCl_3$): δ 150.0, 149.6, 148.1, 147.7, 91.0, 90.1, 64.7, 63.8, 24.1, 15.4, 15.1; IR (film): 2972, 2930, 2898, 1715, 1668, 1387 $cm^{-1}$; HRMS-ESI (*m/z*) $[M + H]^+$ calcd for $C_{11}H_{15}O_2$, 179.10666; found, 179.10518.

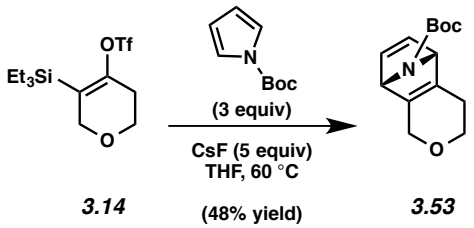


*3.14* (48% yield) *3.53*

**Pyran 3.53 (Table 3.3, entry 4).** Purification by preparative thin layer chromatography (1:1 Hexanes:EtOAc) afforded pyran **3.53** as a faint orange oil (48% yield, average of two experiments). Pyran **3.53**: $R_f$ 0.78 (1:1 Hexanes:EtOAc); $^1$H NMR (500 MHz, $CDCl_3$, 60 °C): δ 7.00 (br s, 2H), 4.97 (app. d, *J* = 9.6, 2H), 4.49 (app. d, *J* = 15.8, 1H), 4.02 (dt, *J* = 16.4, 3.2, 1H),

3.70–3.65 (m ,1H), 3.64–3.59 (m, 1H), 2.44 (app. d, $J$ = 16.4, 1H), 2.12–2.04 (m, 1H), 1.41 (s, 9H); $^{13}$C NMR (125 MHz, $CDCl_3$, 60 °C): δ 154.9, 147.3, 146.8, 143.3, 143.0, 80.5, 68.8, 66.8, 66.0, 64.1, 28.4, 26.4; IR (film): 2977, 2921, 1701, 1368, 1335, 1255 cm$^{-1}$; HRMS-ESI (*m/z*) [M + H]$^+$ calcd for $C_{14}H_{20}NO_3$, 250.14377; found, 250.14157.

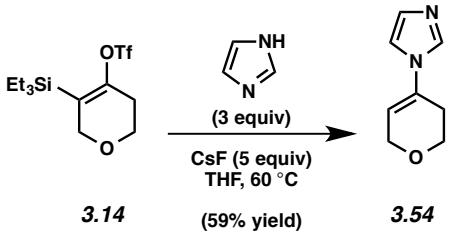


**Pyran 3.54 (Table 3.4, entry 1).** Purification by preparative thin layer chromatography (5:4:1 Benzene:EtOAc:$Et_3N$) afforded pyran **3.54** as a colorless oil (59% yield, average of two experiments). Pyran **3.54**: $R_f$ 0.35 (5:4:1 Benzene:EtOAc:$Et_3N$); $^1$H NMR (500 MHz, $C_6D_6$): δ 7.44 (s, 1H), 7.25 (s, 1H), 6.64 (s, 1H), 4.94 (sept, $J$ = 1.5, 1H), 3.79 (q, $J$ = 2.7, 2H), 3.35 (t, $J$ = 5.5, 2H), 1.73–1.68 (m, 2H); $^{13}$C NMR (125 MHz, $C_6D_6$): δ 134.3, 131.1, 130.5, 115.7, 112.2, 64.2, 63.5, 26.8; IR (film): 3381, 2930, 2841, 1678, 1495, 1382 cm$^{-1}$; HRMS-ESI (*m/z*) [M + H]$^+$ calcd for $C_8H_{11}N_2O$, 151.08659; found, 151.08530.

The structure of **3.54** was verified by 2D-NOESY, as the following interaction was observed:

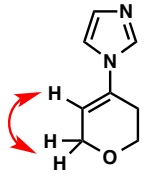


*3.54*

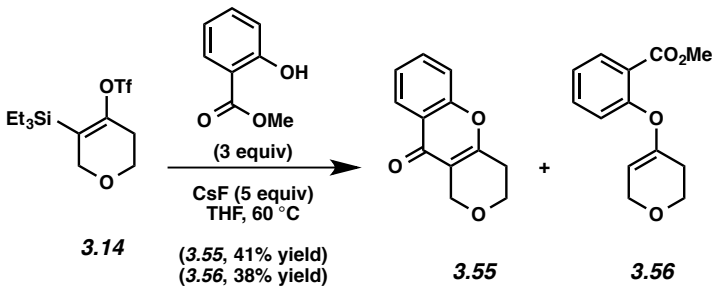


**Pyrone 3.55 and Enol Ether 3.56 (Table 3.4, entry 2).** Purification by preparative thin layer chromatography (9:1 Benzene:EtOAc) afforded adduct **3.55** (41% yield, average of two experiments) as a white amorphous solid and **3.56** (38% yield, average of two experiments) as a colorless oil. Pyrone **3.55**: $R_f$ 0.20 (9:1 Benzene:EtOAc); $^1$H NMR (500 MHz, $CDCl_3$): δ 8.17 (dd, *J* = 8.0, 1.5, 1H), 7.66–7.60 (m, 1H), 7.40 (app. dd, *J* = 8.4, 0.5, 1H), 7.38–7.33 (m, 1H), 4.65 (t, *J* = 1.8, 2H), 4.00 (t, *J* = 5.7, 2H), 2.77 (tt, *J* = 5.7, 1.8, 2H); $^{13}$C NMR (125 MHz, $CDCl_3$): δ 175.8, 160.9, 156.1, 133.5, 125.7, 125.0, 123.6, 117.9, 117.2, 63.9, 62.7, 27.7; IR (film): 3066, 2855, 1649, 1607, 1471, 1429 cm$^{-1}$; HRMS-ESI (*m/z*) $[M + H]^+$ calcd for $C_{12}H_{11}O_3$, 203.07027; found, 203.06829. Enol ether **3.56**: $R_f$ 0.40 (9:1 Benzene:EtOAc); $^1$H NMR (500 MHz, $CDCl_3$): δ 7.88 (dd, *J* = 7.7, 1.7, 1H), 7.49 (ddd, *J* = 8.1, 7.7, 1.7, 1H), 7.19 (dt, *J* = 7.7, 1.1, 1H), 7.12 (dd, *J* = 8.1, 1.1, 1H), 4.62 (sept, *J* = 1.1, 1H), 4.13 (q, *J* = 2.5, 2H), 3.90 (t, *J* = 5.6, 2H), 3.89 (s, 3H), 2.44–2.39 (m, 2H); $^{13}$C NMR (125 MHz, $C_6D_6$): δ 165.7, 154.9, 153.1, 133.3, 132.2, 124.6, 124.1, 122.7, 101.0, 64.5, 64.4, 51.7, 28.2; IR (film): 2949, 2836, 1729, 1678, 1603, 1485 cm$^{-1}$; HRMS-ESI (*m/z*) $[M + H]^+$ calcd for $C_{13}H_{15}O_4$, 235.09649; found, 235.09445.

The structure of **3.56** was verified by 2D-NOESY, as the following interaction was observed:

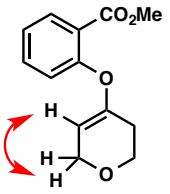

*3.56*

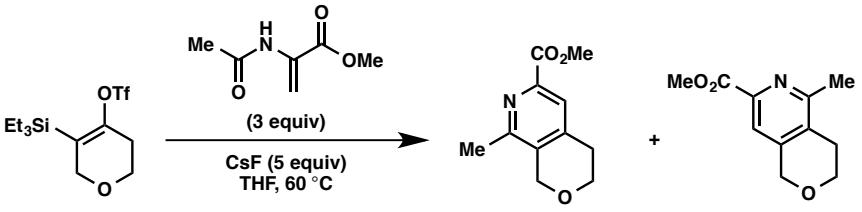


*3.14* *3.57* *3.58*

*2.6 : 1*

**Pyridines 3.57 and 3.58 (Table 3.4, entry 3).** Purification by preparative thin layer chromatography (9:1 Benzene:Acetone) afforded an inseparable mixture of pyridine adducts **3.57** and **3.58** (71% yield, average of two experiments) as a white amorphous solid. Pyridines **3.57** and **3.58**: $R_f$ 0.50 (9:1 Benzene:Acetone); $^1$H NMR (500 MHz, $CDCl_3$): **3.57** (major isomer): δ 7.75 (s, 1H), 4.72 (s, 2H), 3.96 (s, 3H), 3.93 (t, $J$ = 5.8, 2H), 2.87 (t, $J$ = 5.8, 2H), 2.42 (s, 3H); **3.58** (minor isomer): $^1$H NMR (500 MHz, $CDCl_3$): δ 7.63 (s, 1H), 4.73 (s, 2H), 4.00 (t, $J$ = 5.8, 2H), 3.95 (s, 3H), 2.76 (t, $J$ = 5.8, 2H), 2.53 (s, 3H); $^{13}$C NMR (125 MHz, $CDCl_3$): **3.57** (major isomer): δ 166.1, 154.5, 145.0, 143.6, 133.1, 123.7, 65.7, 64.1, 53.0, 28.2, 21.3; **3.58** (minor isomer): δ 166.1, 157.8, 144.6, 144.4, 131.7, 119.2, 67.2, 64.9, 53.0, 25.8, 22.0; IR (film): 3451, 2949, 2850, 1715, 1598, 1433 cm$^{-1}$; HRMS-ESI ($m/z$) $[M + H]^+$ calcd for $C_{11}H_{14}NO_3$, 208.09682; found, 208.09521.

The structure of **3.57** was verified by 2D-NOESY, as the following interaction was observed:

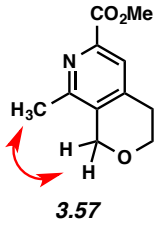


***3.57***

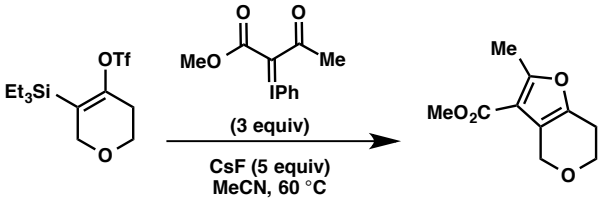


***3.14*** ***3.59***

*The solvent used in this reaction was acetonitrile. The solubility of the trapping agent prevented the use of tetrahydrofuran.*

**Furan 3.59 (Table 3.4, entry 4).** Purification by preparative thin layer chromatography (9:1 Hexanes:EtOAc) afforded furan **3.59** (70% yield, average of two experiments) as a colorless oil. Furan **3.59**: $R_f$ 0.52 (9:1 Benzene:EtOAc); $^1$H NMR (500 MHz, $CDCl_3$): δ 4.55 (s, 2H), 3.86 (t, *J* = 5.5, 2H), 3.81 (s, 3H), 2.75–2.71 (m, 2H), 2.55 (s, 3H); $^{13}$C NMR (125 MHz, $CDCl_3$): δ 165.1, 158.6, 146.2, 115.3, 112.7, 65.4, 63.2, 51.3, 23.9, 14.0; IR (film): 2954, 2846, 1715, 1584, 1443, 1293 cm$^{-1}$; HRMS-ESI (*m/z*) $[M + H]^+$ calcd for $C_{10}H_{13}O_4$, 197.08084; found, 197.07904.

The structure of **3.59** was verified by 2D-NOESY, as the following interaction was observed:

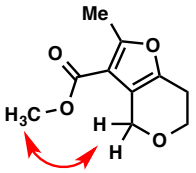


***3.59***

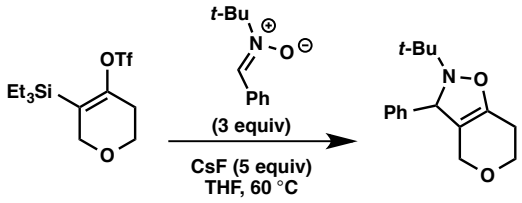


***3.14*** ***3.60***

**Isoxazoline 3.60 (Table 3.4, entry 5).** Purification by preparative thin layer chromatography (1:1 Hexanes:EtOAc) afforded isoxazoline **3.60** (73% yield, average of two experiments) as a colorless oil. Isoxazoline **3.60**: $R_f$ 0.95 (1:1 Hexanes:EtOAc); $^1$H NMR (500 MHz, $C_6D_6$): δ 7.37 (app. d, $J$ = 8.1, 2H), 7.18 (app. d, $J$ = 7.6, 2H), 7.07 (tt, $J$ = 7.0, 1.3, 1H), 4.90 (s, 1H), 4.01 (d, $J$ = 14.1, 1H), 3.84 (d, $J$ = 14.1, 1H), 3.51–3.46 (m, 1H), 3.34–3.28 (m, 1H), 2.05–1.89 (m, 2H), 1.11 (s, 9H); $^{13}$C NMR (125 MHz, $C_6D_6$): δ 146.0, 143.6, 128.4, 127.1, 127.0, 105.2, 68.3, 63.4, 62.9, 60.0, 24.9, 23.0; IR (film): 2972, 2902, 1729, 1457, 1363, 1232 cm$^{-1}$; HRMS-ESI (*m/z*) [M + H]$^+$ calcd for $C_{16}H_{22}NO_2$, 260.16451; found, 260.16226.

The structure of **3.60** was verified by 2D-NOESY, as the following interaction was observed:

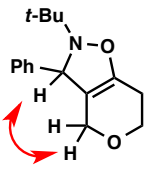


***3.60***

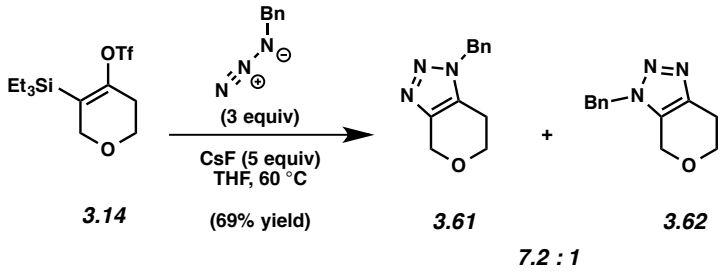


**Triazoles 3.61 and 3.62 (Table 3.4, entry 6).** Purification by preparative thin layer chromatography (4:1 EtOAc:Hexanes) afforded an inseparable mixture of triazoles **3.61** and **3.62** (69% yield, average of two experiments) as a white amorphous solid. Triazoles **3.61** and **3.62**: $R_f$ 0.30 (4:1 EtOAc:Hexanes); $^1$H NMR (500 MHz, $CDCl_3$): **3.61** (major isomer): δ 7.37–7.31 (m, 3H), 7.22–7.17 (m, 2H), 5.48 (s, 2H), 4.80 (t, $J$ = 1.2, 2H), 3.86 (t, $J$ = 5.5, 2H), 2.54 (tt, $J$ = 5.5, 1.2, 2H); **3.62** (minor isomer): δ 7.37–7.31 (m, 3H), 7.22–7.17 (m, 2H), 5.43 (s, 2H), 4.40 (t, $J$ = 1.2, 2H), 3.85 (t, $J$ = 5.5, 2H), 2.88 (tt, $J$ = 5.5, 1.2, 2H); $^{13}$C NMR (125 MHz, $CDCl_3$): **3.61** (major isomer): δ 142.3, 134.5, 129.7, 129.2, 128.7, 127.7, 64.2, 64.0, 52.3, 21.9; **3.62** (minor isomer): δ 141.3, 134.0, 130.4, 129.3, 128.9, 127.9, 65.2, 61.8, 52.9, 23.5; IR (film): 3446, 2925, 2855, 2353, 1499, 1189 cm$^{-1}$; HRMS-ESI (*m/z*) $[M + H]^+$ calcd for $C_{12}H_{14}N_3O$, 216.11314; found, 216.11143.

The structure of **3.61** was verified by 2D-NOESY, as the following interaction was observed:

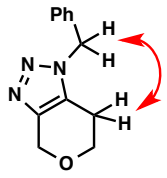


*3.61*

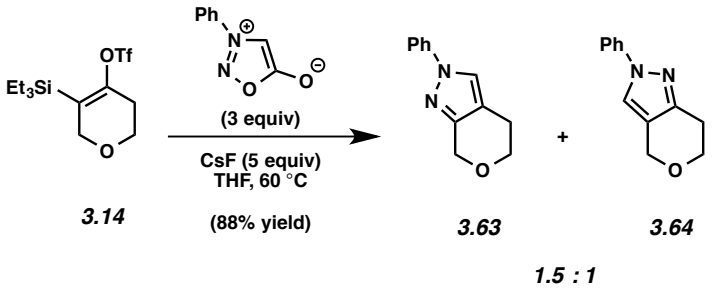


*3.14* *3.63* *3.64*

*1.5 : 1*

**Pyrazoles 3.63 and 3.64 (Table 3.4, entry 7).** Purification by preparative thin layer chromatography (4:1 Benzene:EtOAc) afforded pyrazole **3.63** (53% yield, average of two experiments) as a yellow oil and pyrazole **3.64** (35% yield, average of two experiments) as a yellow oil. Pyrazole **3.63**: $R_f$ 0.65 (4:1 Benzene:EtOAc); $^1$H NMR (500 MHz, $CDCl_3$): δ 7.69 (s, 1H), 7.62 (dd, *J* = 8.7, 1.9, 2H), 7.42 (tt, *J* = 7.5, 1.2, 2H), 7.24 (dd, *J* = 8.7, 7.5, 1H), 4.85 (s, 2H), 3.92 (t, *J* = 5.6, 2H), 2.76 (t, *J* = 5.6, 2H); $^{13}$C NMR (125 MHz, $CDCl_3$): δ 149.0, 140.4, 129.5, 126.2, 124.0, 118.9, 115.0, 65.6, 65.2, 21.8; IR (film): 3113, 3052, 2841, 1598, 1504, 1391 $cm^{-1}$; HRMS-ESI (*m/z*) $[M + H]^+$ calcd for $C_{12}H_{13}N_2O$, 201.10224; found, 201.10053. Pyrazole **3.64**: $R_f$ 0.55 (4:1 Benzene:EtOAc); $^1$H NMR (500 MHz, $CDCl_3$): δ 7.65–7.61 (m, 3H), 7.45–7.39 (m, 2H), 7.27–7.23 (m, 1H), 4.77 (s, 2H), 4.00 (t, *J* = 5.8, 2H), 2.91 (t, *J* = 5.8, 2H); $^{13}$C NMR (125 MHz, $CDCl_3$): δ 147.8, 140.4, 129.5, 126.2, 121.4, 119.0, 116.6, 65.6, 63.3, 24.5; IR (film): 2944, 2846, 1598, 1570, 1509, 1377 $cm^{-1}$; HRMS-ESI (*m/z*) $[M + H]^+$ calcd for $C_{12}H_{13}N_2O$, 201.10224; found, 201.10039.

The structure of **3.63** was verified by 2D-NOESY, as the following interaction was observed:

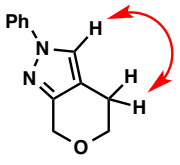


*3.63*

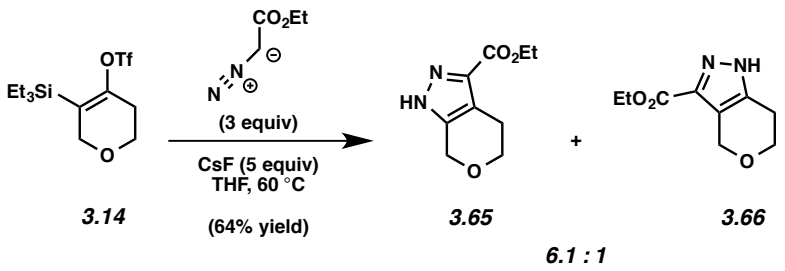


*3.14* *3.65* *3.66*

*6.1 : 1*

**Pyrazoles 3.65 and 3.66 (Table 3.4, entry 8).** Purification by preparative thin layer chromatography (9:1 Benzene:MeOH) afforded an inseparable mixture of pyrazoles **3.65** and **3.66** (64% yield, average of two experiments) as a yellow oil. Pyrazoles **3.65** and **3.66**: $R_f$ 0.45 (9:1 Benzene:MeOH); $^1$H NMR (500 MHz, $C_6D_6$): **3.65** (major isomer): δ 4.93 (s, 2H), 4.01 (q, $J$ = 7.2, 2H), 3.61 (t, $J$ = 5.7, 2H), 2.70 (t, $J$ = 5.7, 2H), 0.95 (t, $J$ = 7.2, 3H); **3.66** (minor isomer): δ 4.89 (s, 2H), 3.94 (q, $J$ = 7.2, 2H), 3.62 (t, $J$ = 5.7, 2H), 2.77 (t, $J$ = 5.7, 2H), 0.89 (t, $J$ = 7.2, 3H); $^{13}$C NMR (125 MHz, $C_6D_6$): **3.65** (major isomer): δ 161.5, 144.9, 134.9, 116.6, 64.9, 64.3, 60.6, 23.3, 14.2; **3.66** (minor isomer): δ 161.7, 142.3, 134.9, 117.9, 64.3, 64.2, 60.7, 23.8, 14.1; IR (film): 3212, 2958, 2850, 1720, 1448, 1255 cm$^{-1}$; HRMS-ESI (*m/z*) [M + H]$^+$ calcd for $C_9H_{13}N_2O_3$, 197.09207; found, 197.09016.

The structure of **3.65** was verified by 2D-NOESY, as the following interaction was observed:

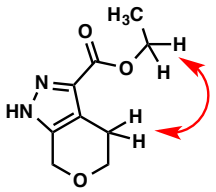


*3.65*

### 3.5.3 Computational Methods.

All computations were carried out using Spartan '10 Parallel Suite for Mac unless otherwise noted.[40] All structures were minimized using Molecular Mechanics, and then further minimized using Density Functional Theory B3LYP/6–31G*. Computational data for structures **5.6** and **5.7** have previously been reported.[5e, 5f, 7c, 8a]

#### 3.5.3.1 Cartesian Coordinates of Strained Alkynes

Structure **3.4**

| | | | |
|---|---|---|---|
| C | -0.915310 | -1.508769 | -0.000000 |
| C | -1.136055 | 1.214394 | 0.000000 |
| C | 0.309699 | -0.842830 | -0.000000 |
| C | -2.014499 | -0.917769 | 0.000000 |
| C | -2.312414 | 0.443151 | 0.000000 |
| C | 0.110164 | 0.568133 | 0.000000 |
| H | -3.298649 | 0.893331 | 0.000000 |
| H | -1.185215 | 2.298979 | 0.000000 |
| C | 1.732086 | -1.043564 | -0.000000 |
| H | 2.270565 | -1.980214 | -0.000000 |
| O | 1.328037 | 1.193936 | 0.000000 |
| C | 2.274967 | 0.201642 | -0.000000 |
| H | 3.297172 | 0.550090 | -0.000000 |

Structure **3.5**

| | | | |
|---|---|---|---|
| H | -2.395709 | -0.204146 | 0.568566 |
| C | -1.552912 | -0.184770 | -0.132100 |
| C | 0.647654 | -1.340220 | 0.041322 |
| C | 1.506487 | -0.118244 | 0.081443 |
| C | -0.574405 | -1.258131 | -0.000894 |
| C | -0.610478 | 1.052425 | 0.236791 |
| H | 1.897936 | 0.043069 | 1.096118 |
| H | -0.560416 | 1.106573 | 1.334921 |
| H | -1.951206 | -0.099172 | -1.149939 |
| H | 2.342505 | -0.121492 | -0.622200 |
| H | -1.059463 | 1.971018 | -0.152238 |
| O | 0.680025 | 0.996295 | -0.325870 |

### 3.5.3.2 Energies of Strained Alkynes

| Structure | Energy (hartrees) | Energy (kcal/mol) |
|---|---|---|
| 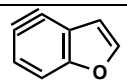 ***3.4*** | –382.332940 | –239917.743 |

| Structure | Energy (hartrees) | Energy (kcal/mol) |
|---|---|---|
| ***3.5*** | –269.218809 | –168937.494 |

## 3.6 Spectra Relevant to Chapter Three:

**Expanding the Strained Alkyne Toolbox: Generation and Utility of Oxygen-Containing Strained Alkynes**

Tejas K. Shah, Jose M. Medina, and Neil K. Garg.

*J. Am. Chem. Soc.* **2016**, *138*, 4948–4954.

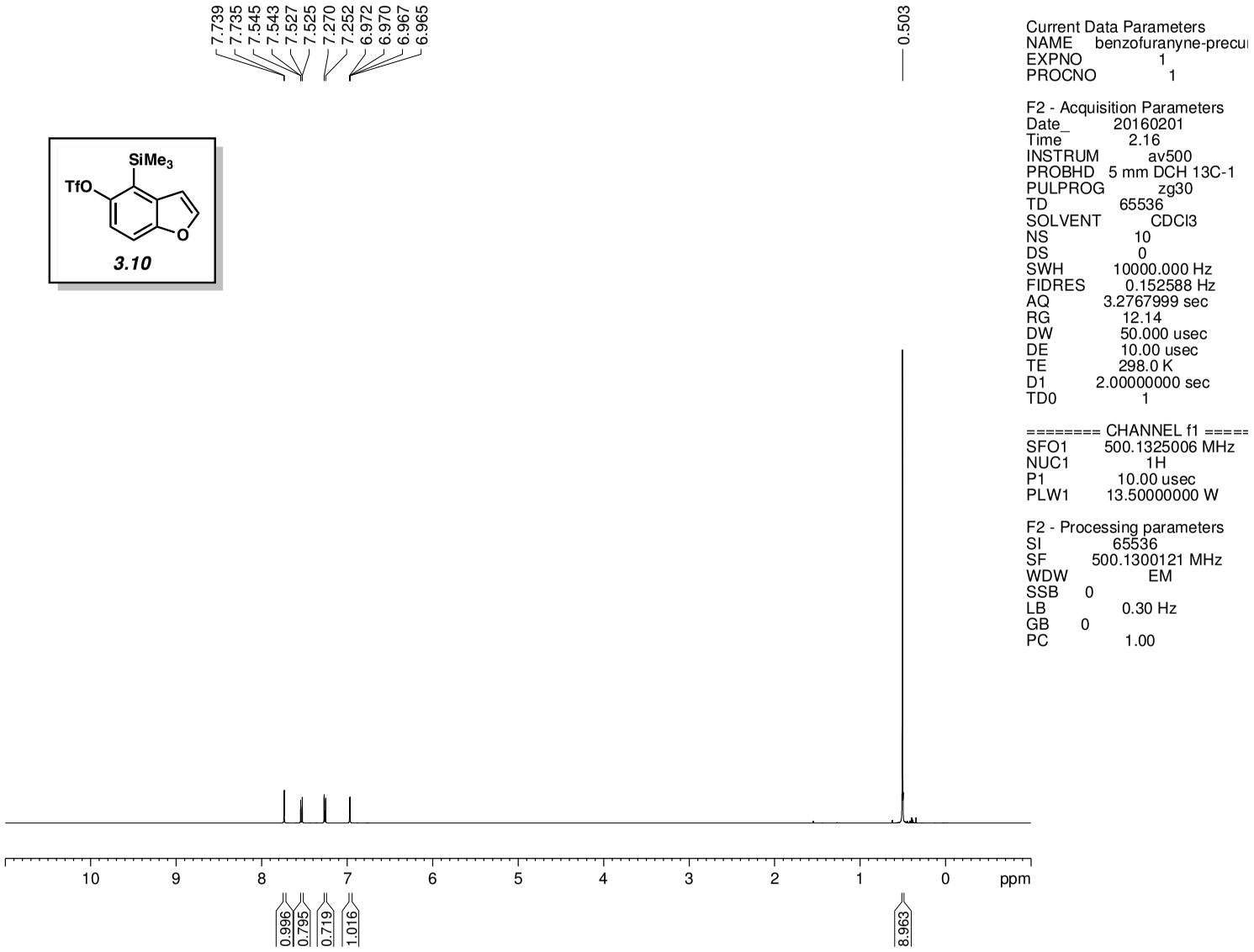


***Figure A3.3.*** $^{1}$H NMR (500 MHz, $CDCl_3$) compound **3.10**

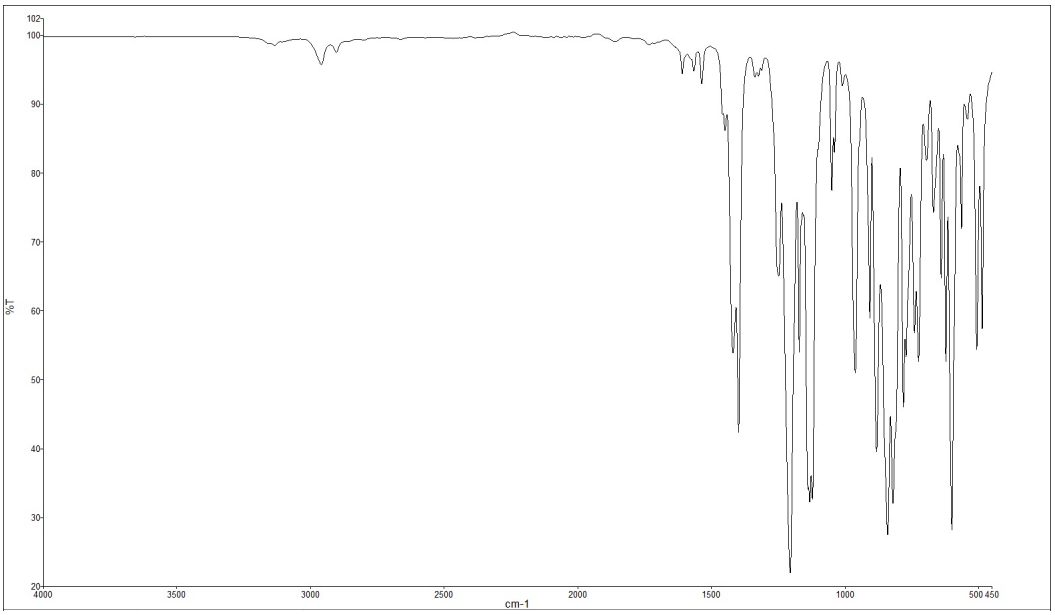


***Figure A3.4.*** Infrared spectrum of compound **3.10**

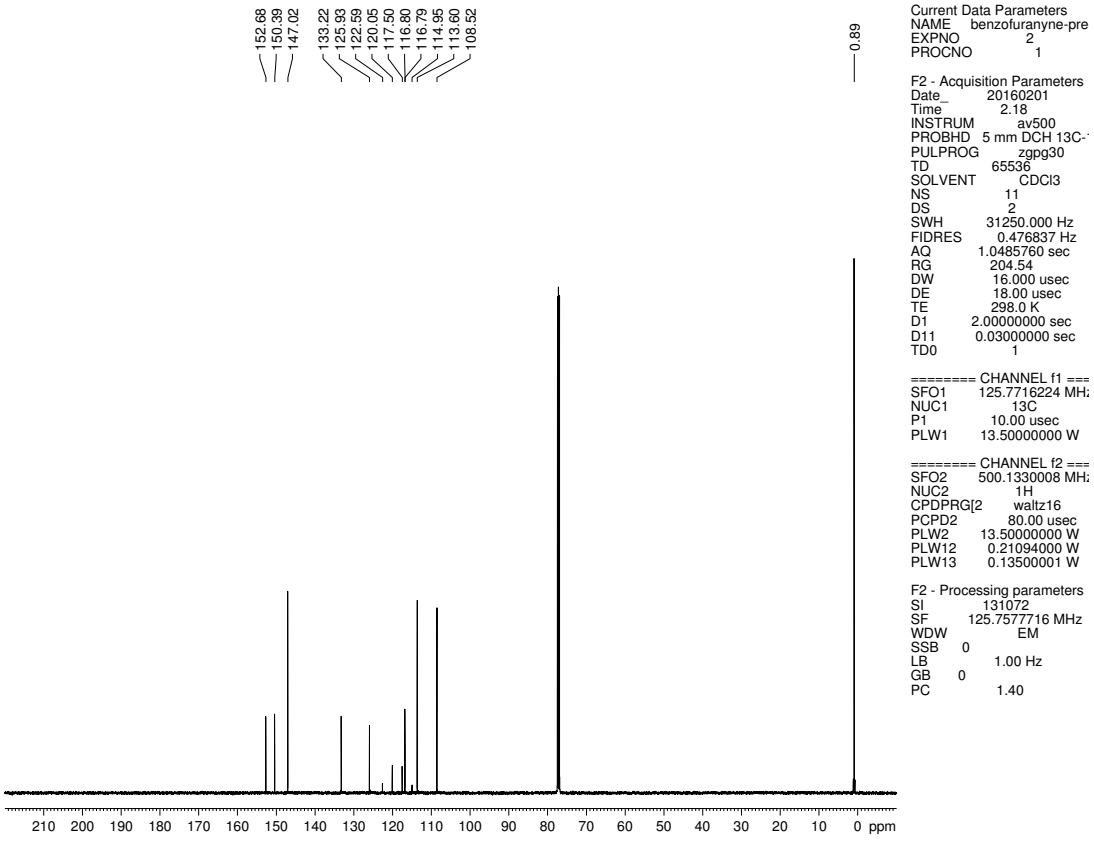


***Figure A3.5.*** $^{13}C$ NMR (125 MHz, $CDCl_3$) of compound **3.10**

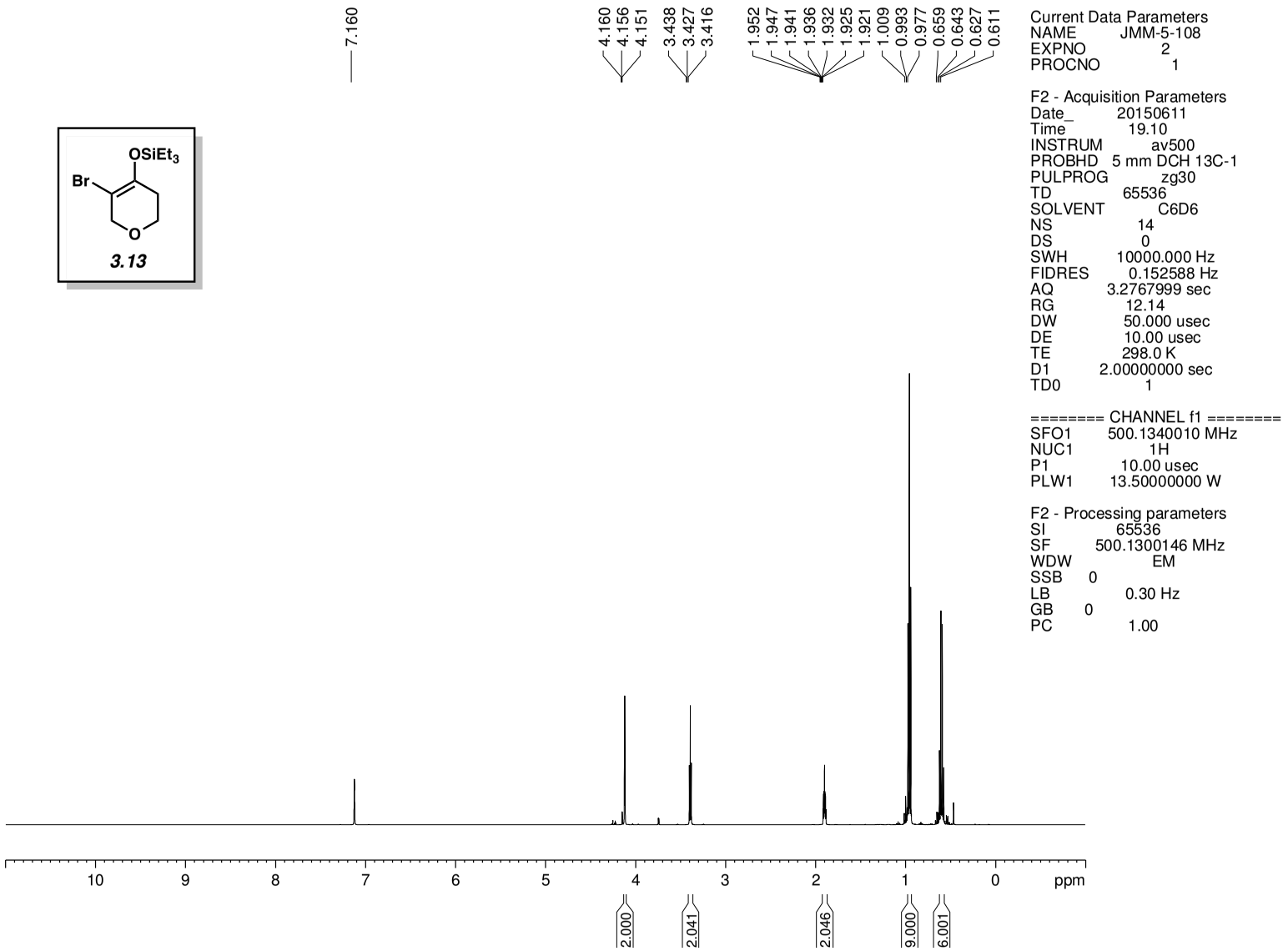


***Figure A3.6.*** $^{1}$H NMR (500 MHz, $C_6D_6$) compound **3.13**

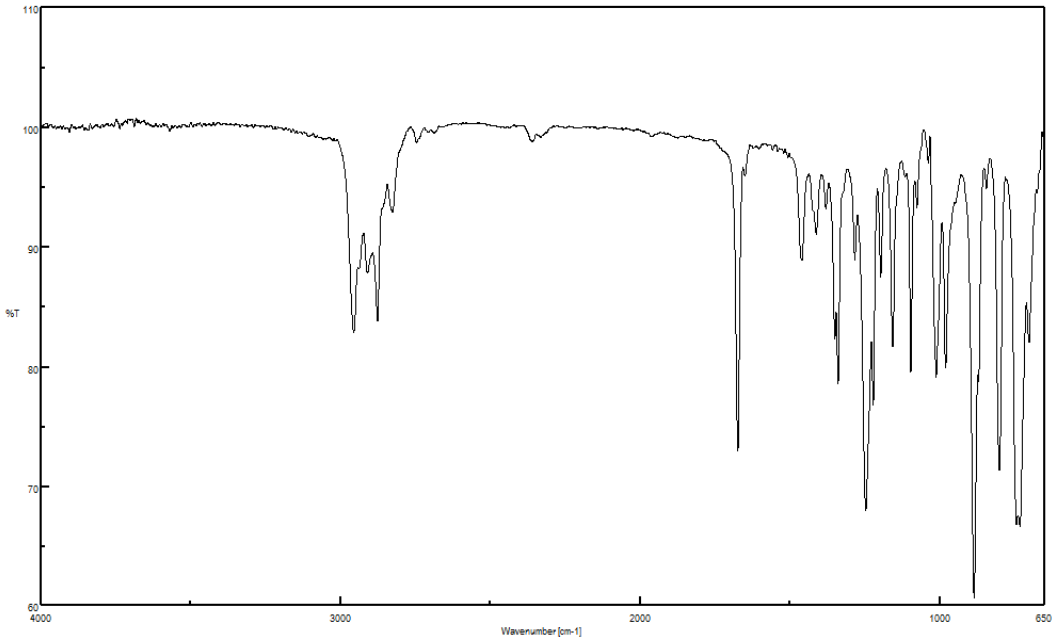


***Figure A3.7.*** Infrared spectrum of compound **3.13**

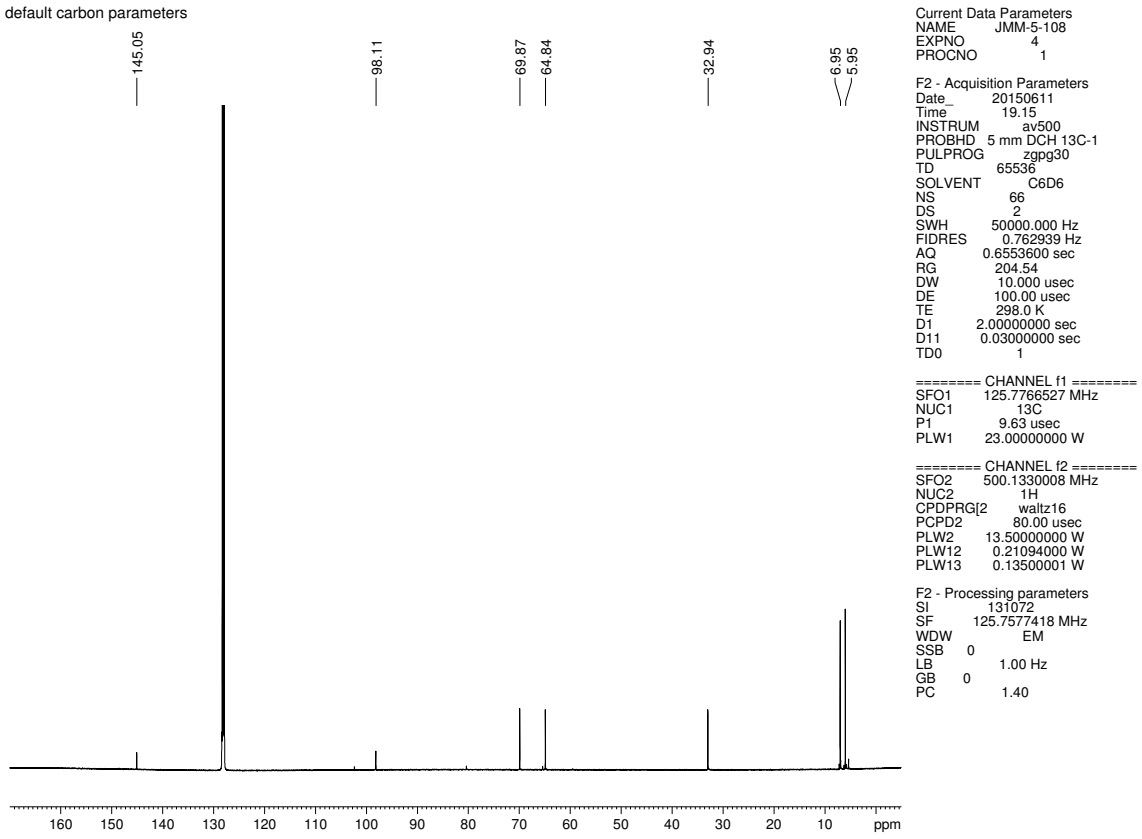


***Figure A3.8.*** $^{13}C$ NMR (125 MHz, $C_6D_6$) of compound **3.13**

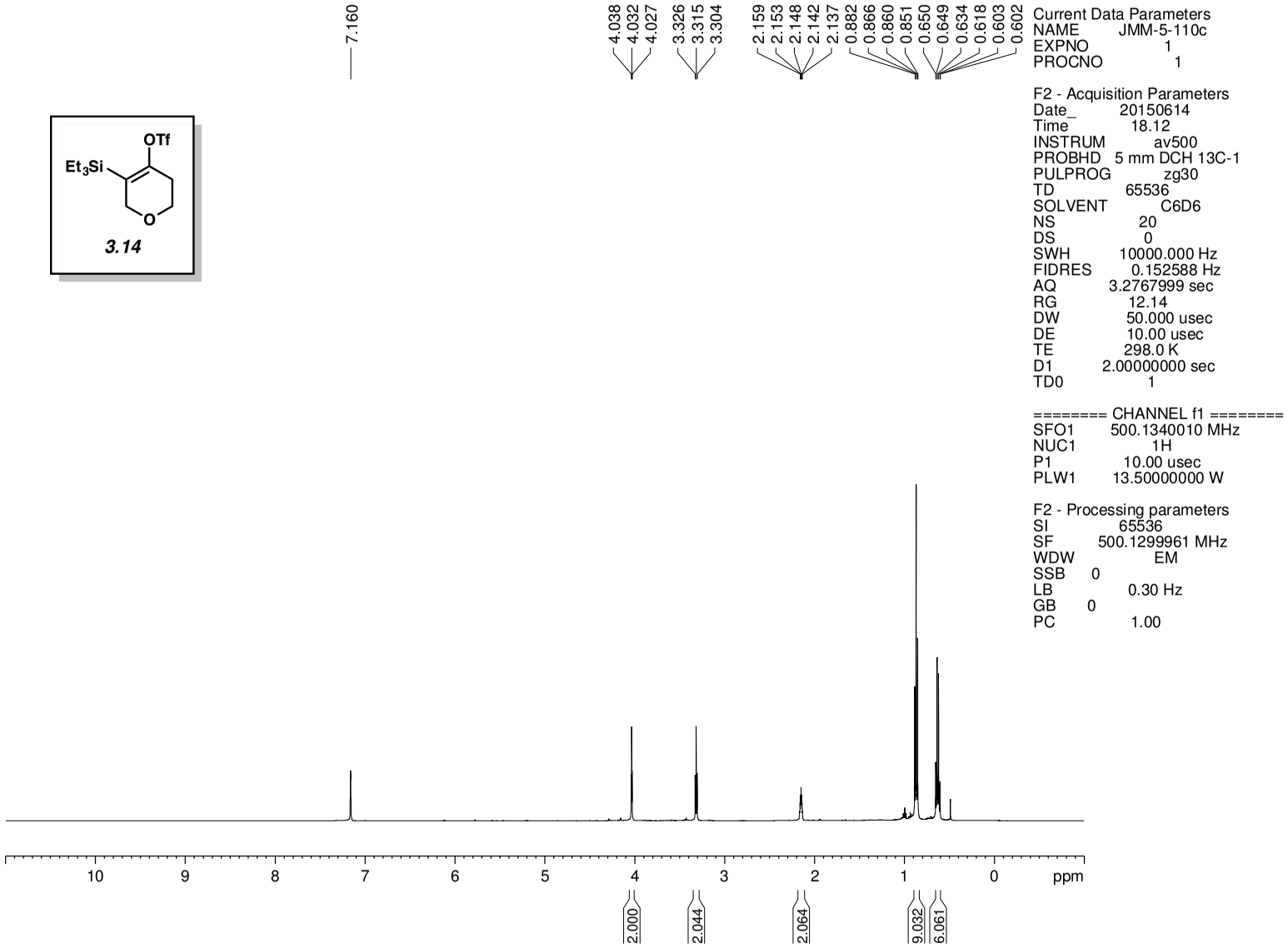


***Figure A3.9.*** $^{1}$H NMR (500 MHz, $C_6D_6$) compound **3.14**

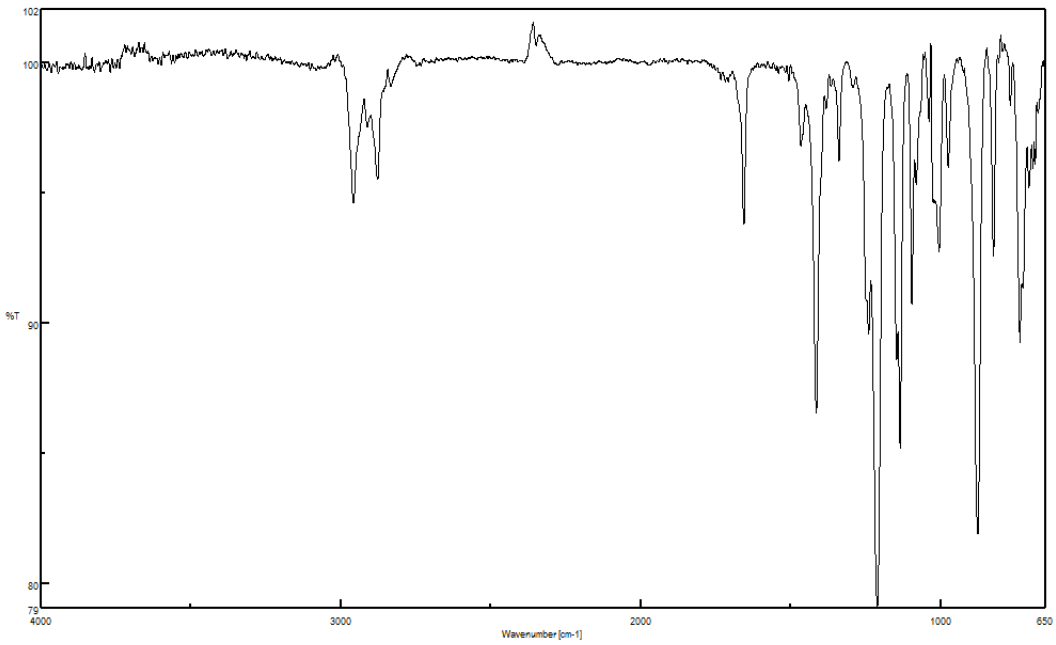


***Figure A3.10.*** Infrared spectrum of compound **3.14**

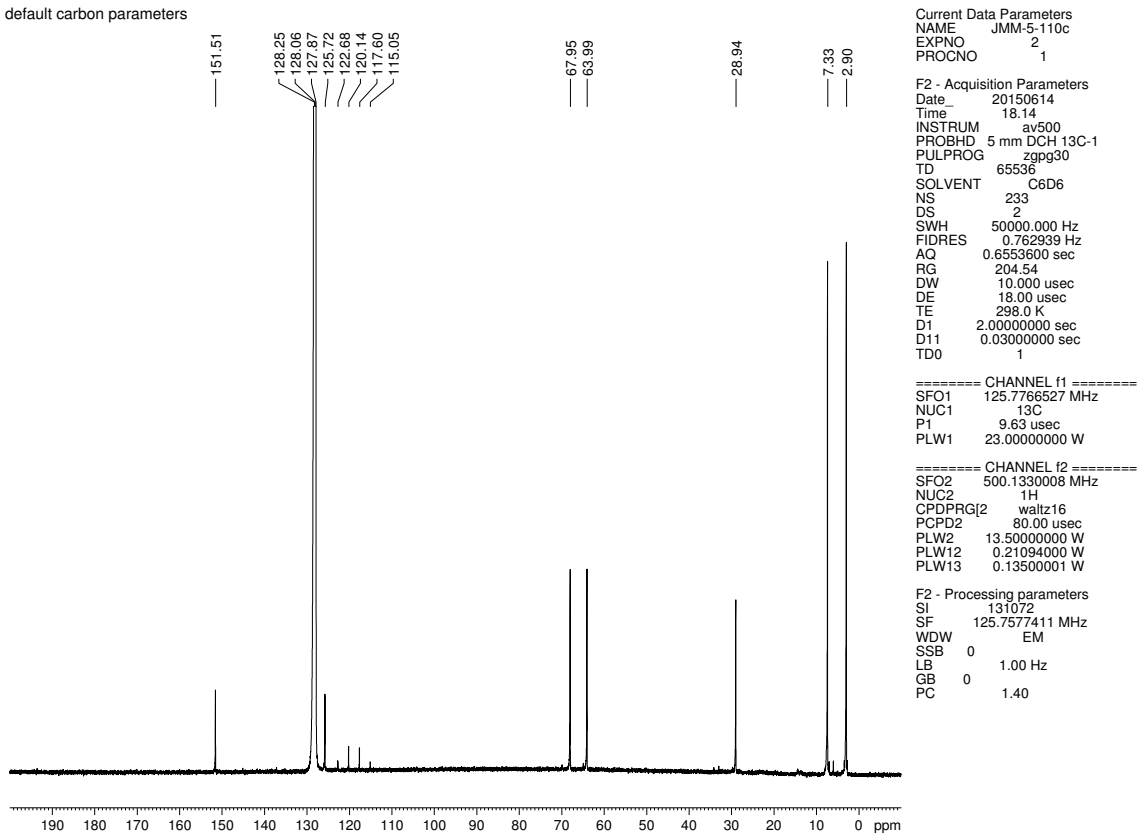


***Figure A3.11.*** $^{13}C$ NMR (125 MHz, $C_6D_6$) of compound **3.14**

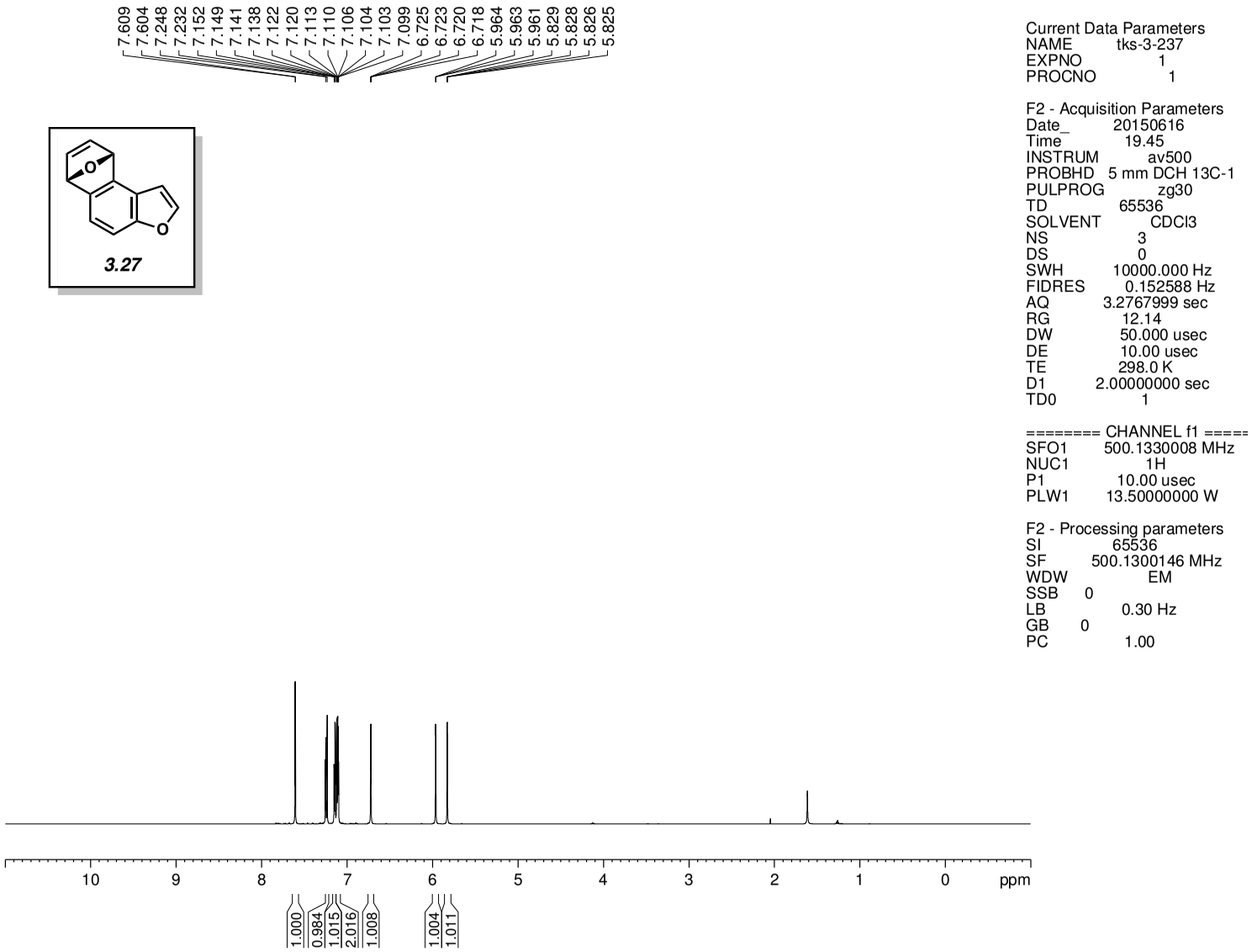


***Figure A3.12.*** $^{1}$H NMR (500 MHz, $CDCl_3$) compound **3.27**

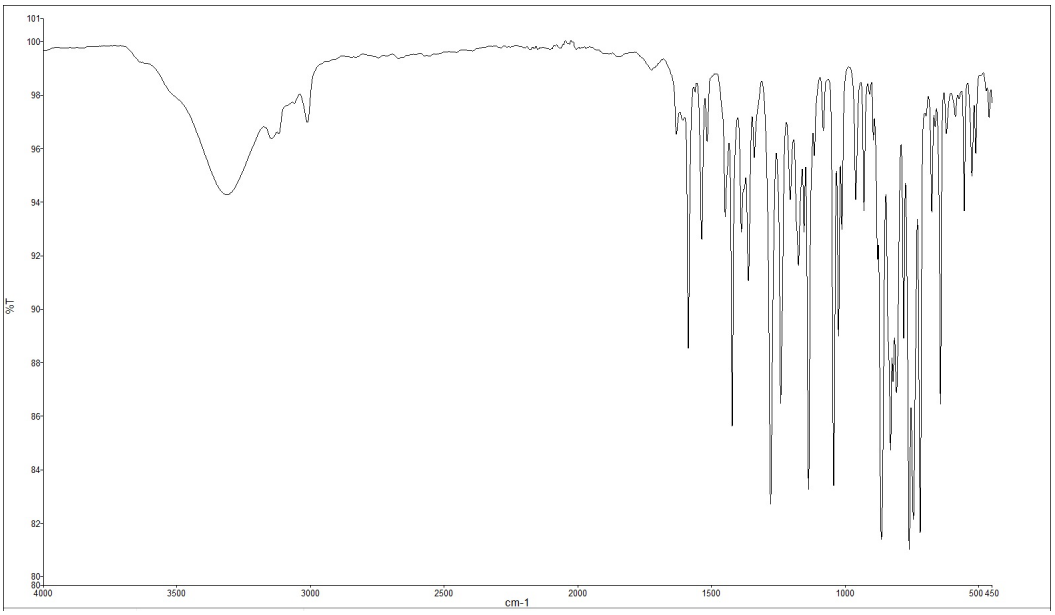


***Figure A3.13.*** Infrared spectrum of compound **3.27**

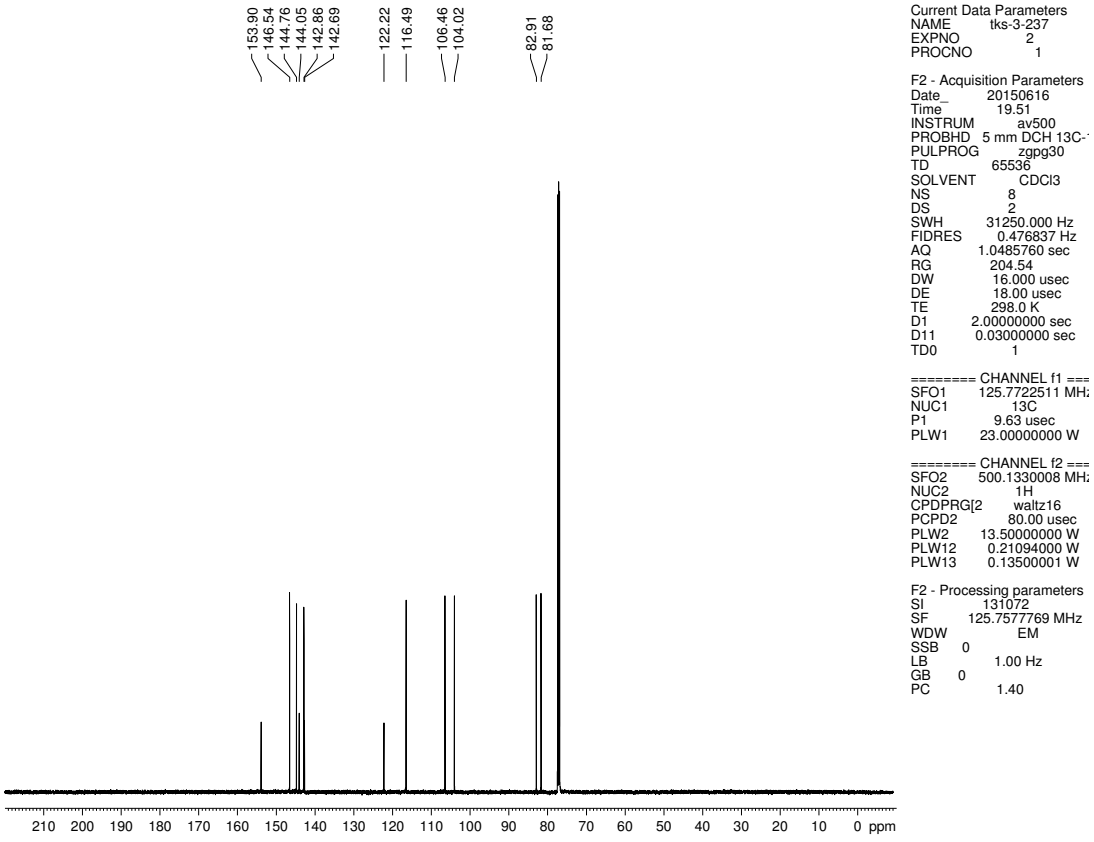


***Figure A3.14.*** $^{13}C$ NMR (125 MHz, $CDCl_3$) of compound **3.27**

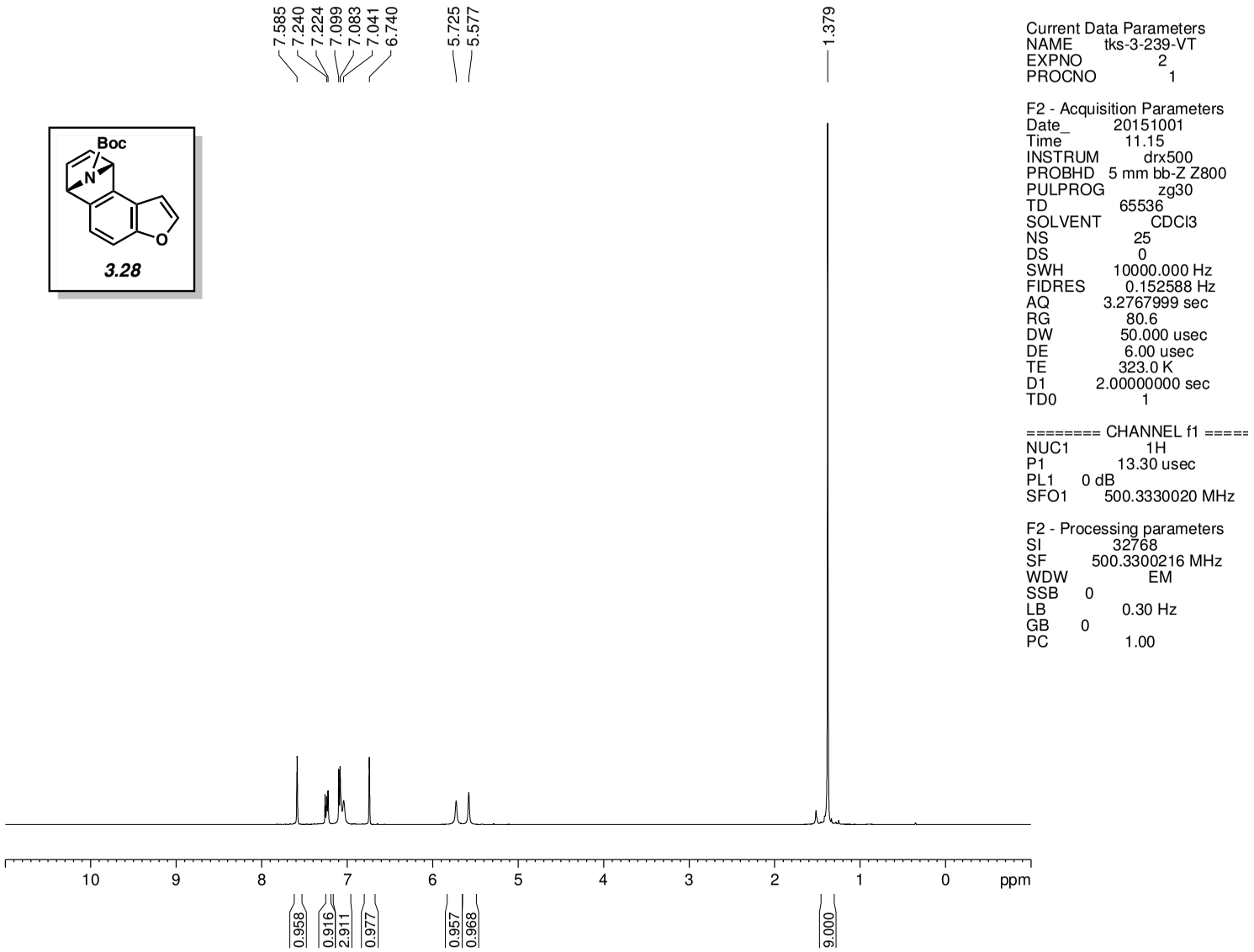


***Figure A3.15.*** $^{1}$H NMR (500 MHz, $CDCl_3$) compound **3.28**

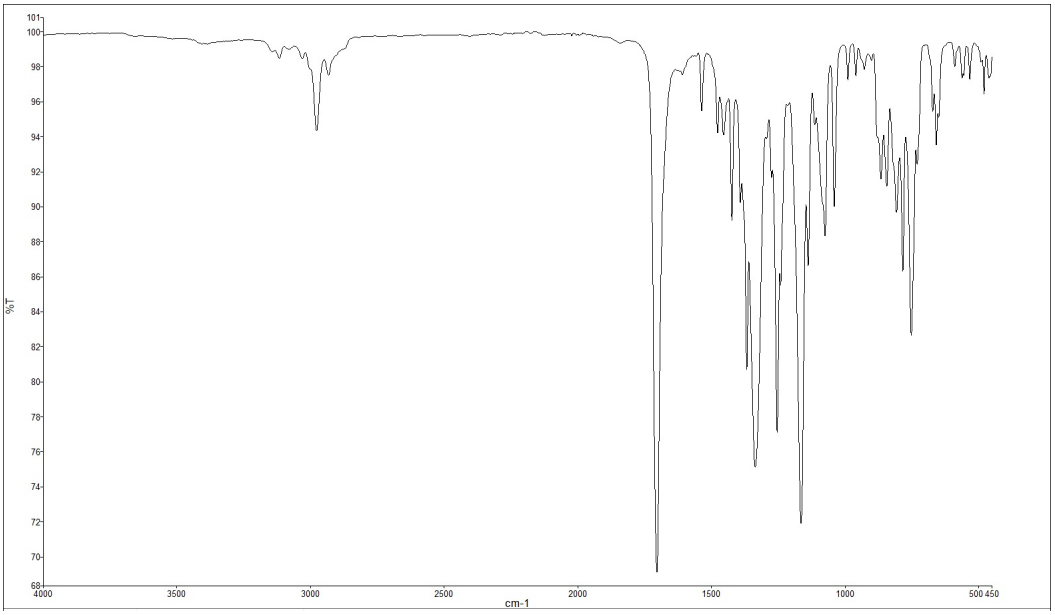


***Figure A3.16.*** Infrared spectrum of compound **3.28**

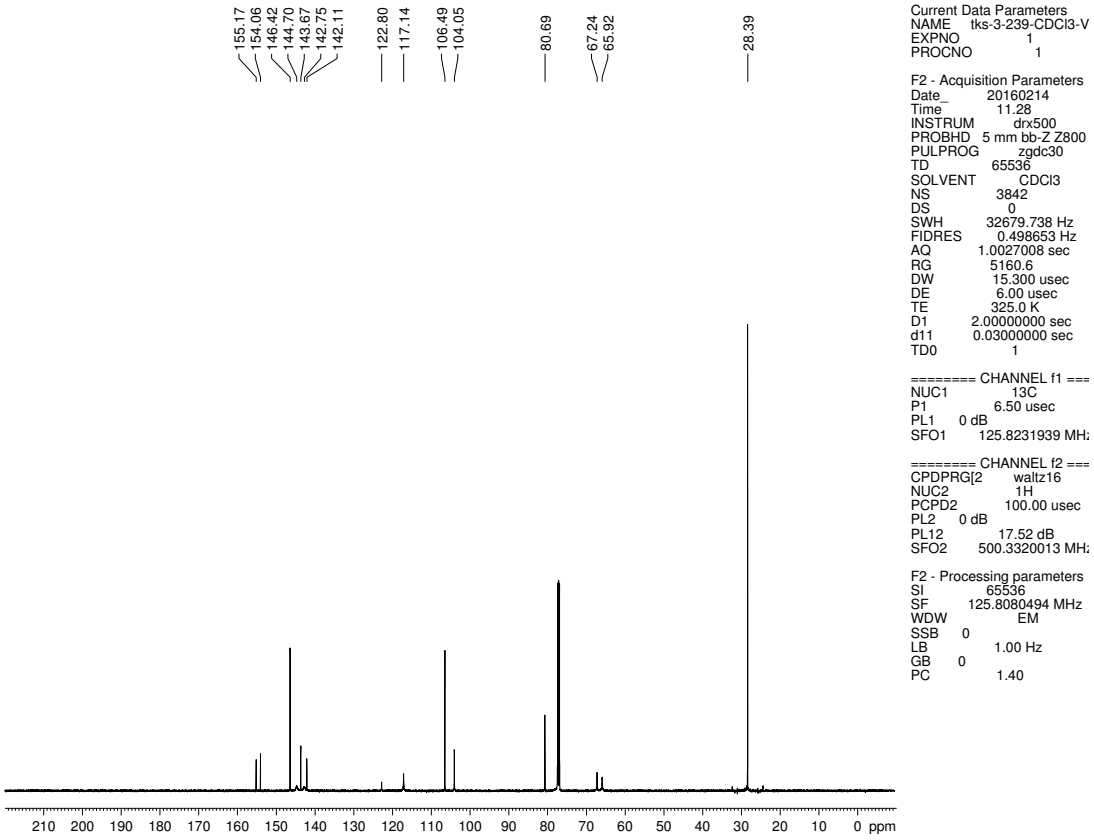


***Figure A3.17.*** $^{13}C$ NMR (125 MHz, $CDCl_3$) of compound **3.28**

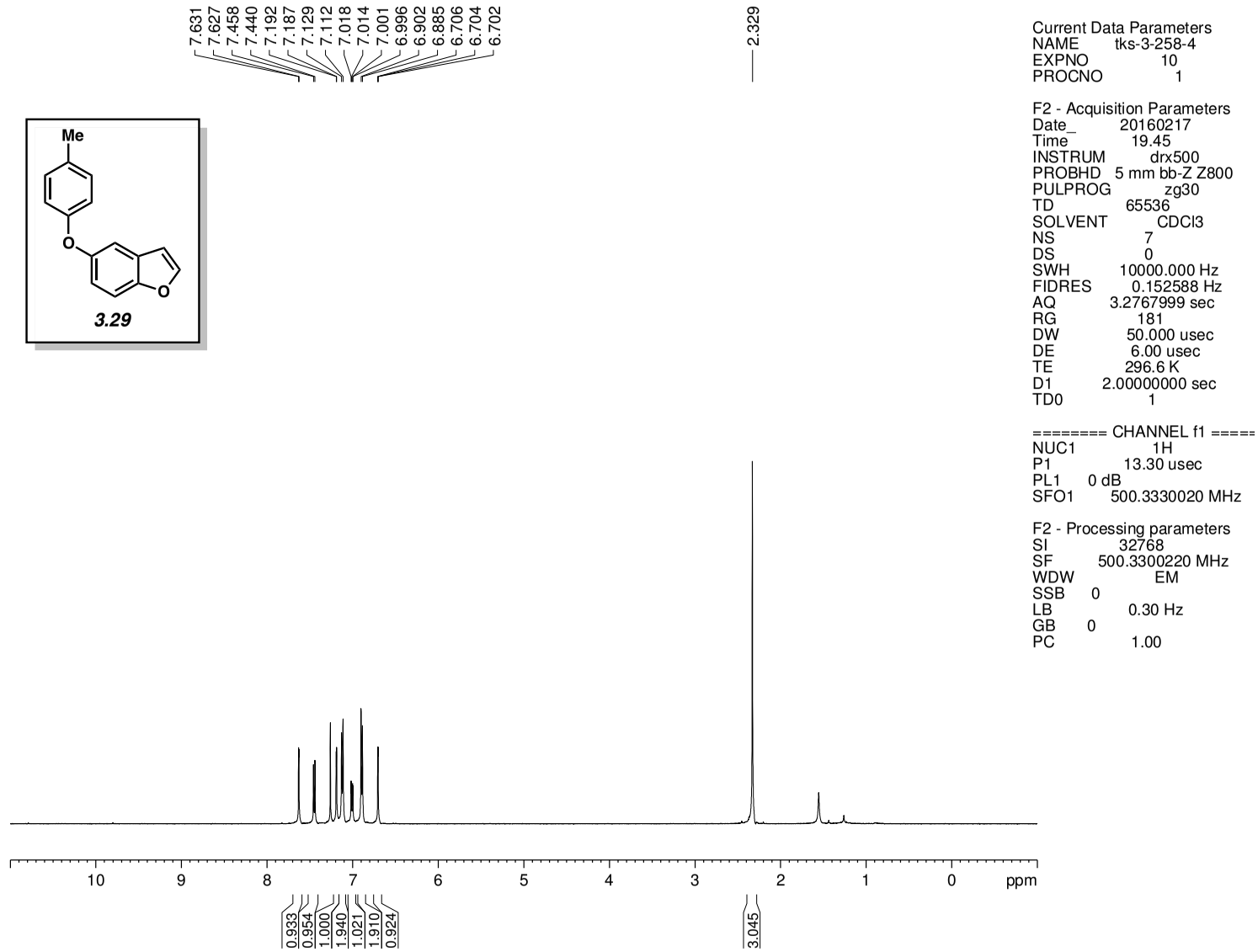


***Figure A3.18.*** $^{1}$H NMR (500 MHz, $CDCl_3$) compound **3.29**

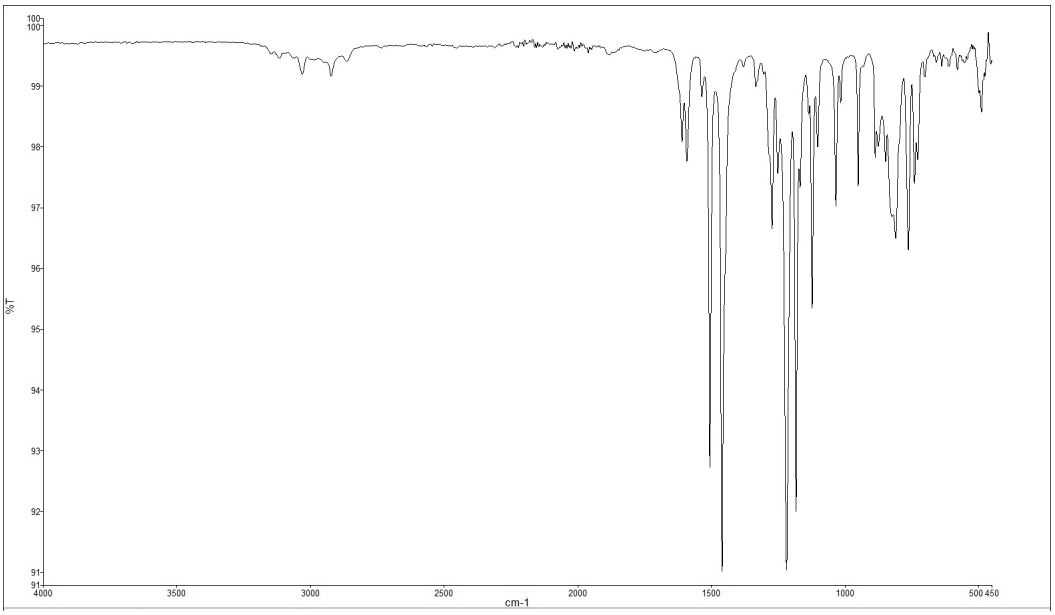


***Figure A3.19.*** Infrared spectrum of compound **3.29**

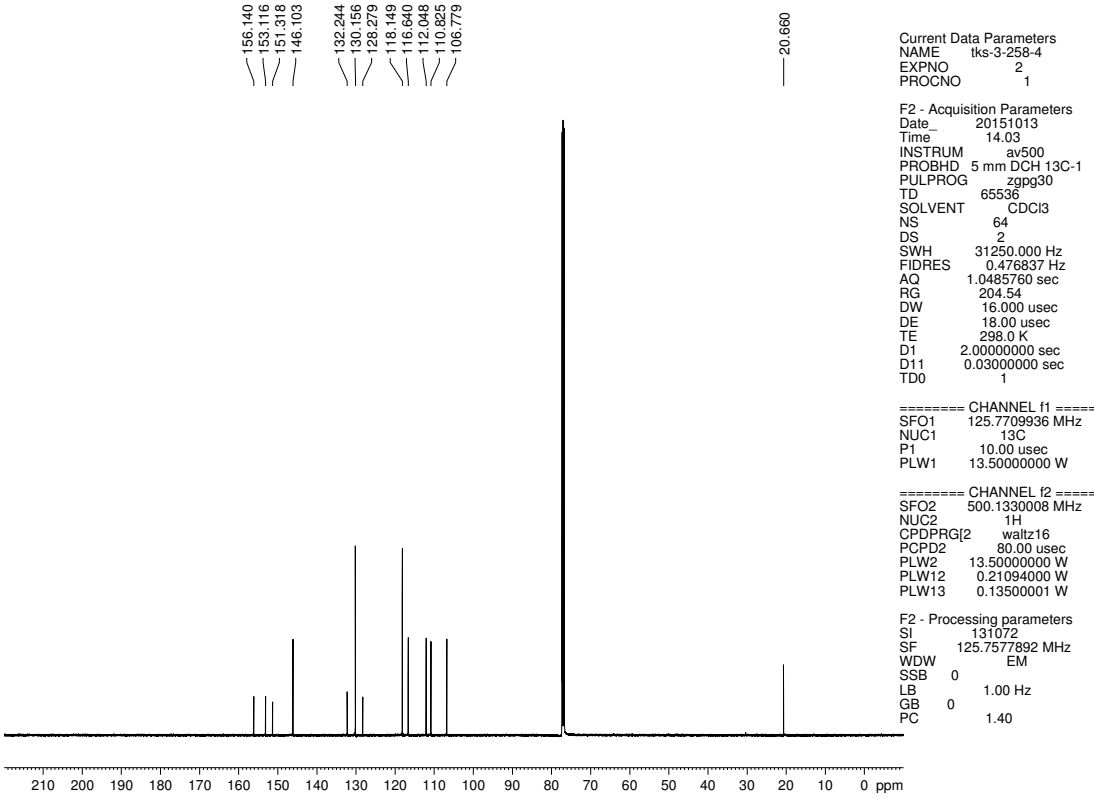


***Figure A3.20.*** $^{13}C$ NMR (125 MHz, $CDCl_3$) of compound **3.29**

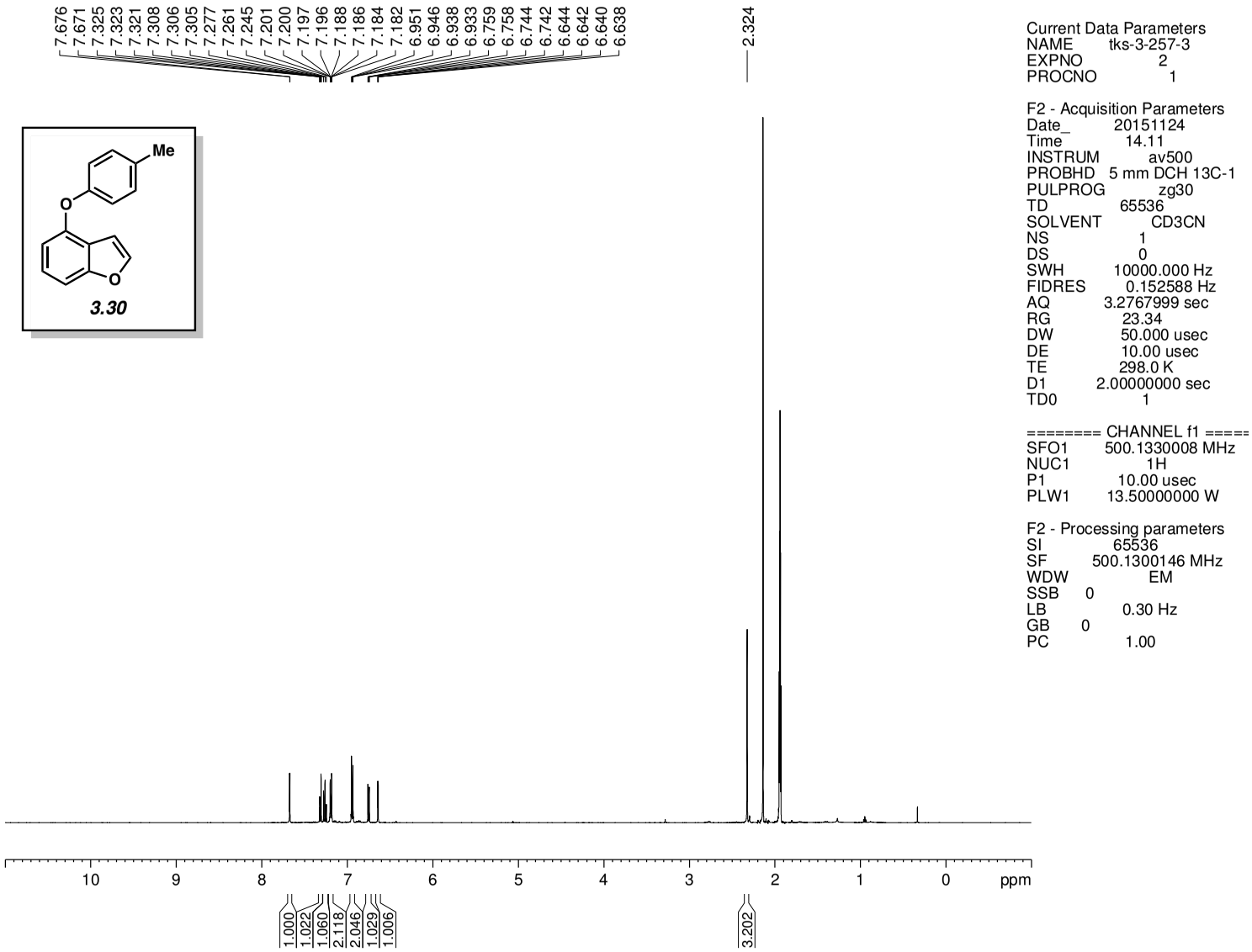


***Figure A3.21.*** $^{1}$H NMR (500 MHz, $CD_3CN$) compound **3.30**

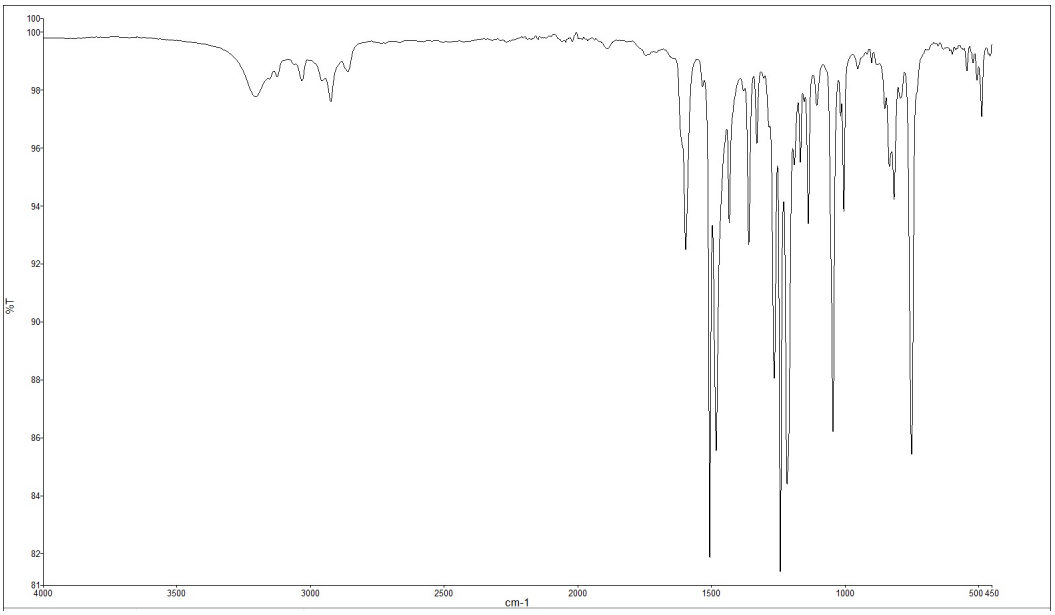


***Figure A3.22.*** Infrared spectrum of compound **3.30**

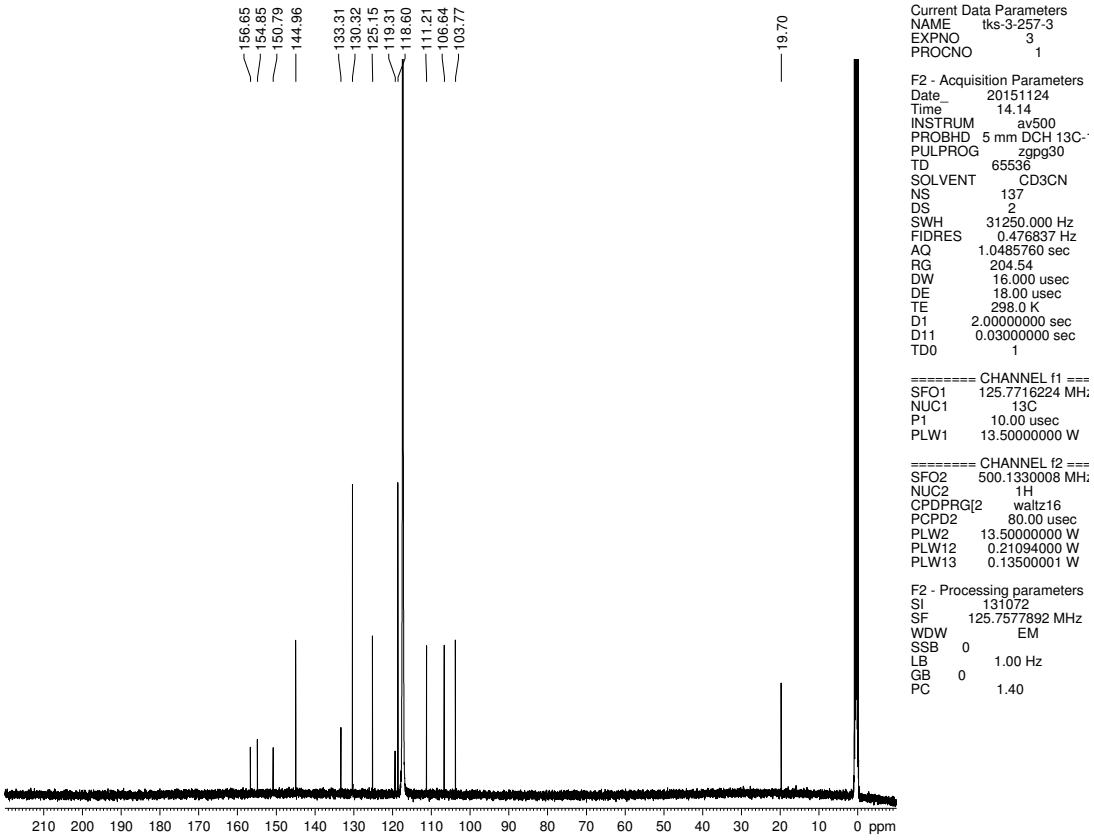


***Figure A3.23.*** $^{13}C$ NMR (125 MHz, $CD_3CN$) of compound **3.30**

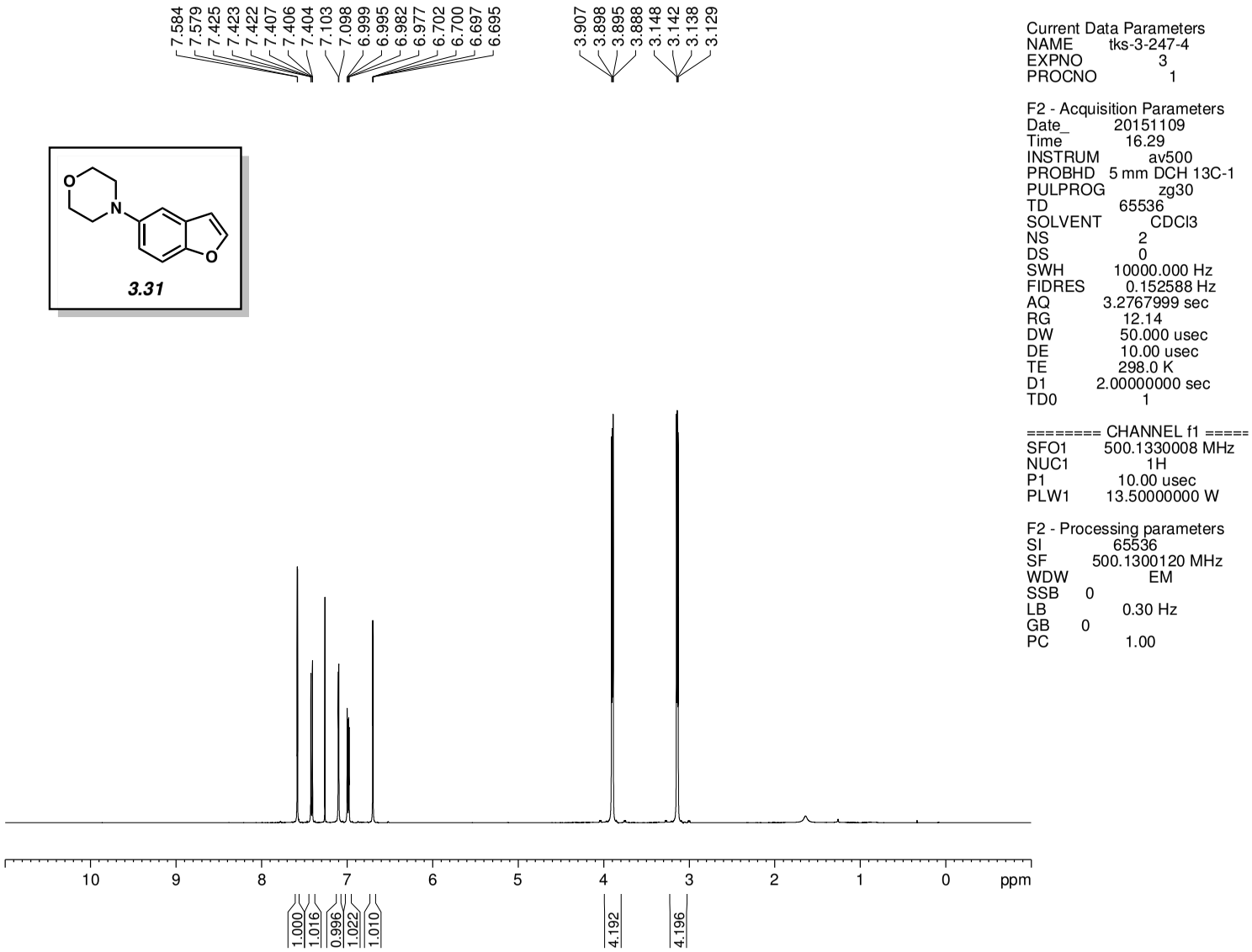


***Figure A3.24.*** $^{1}$H NMR (500 MHz, $CDCl_3$) compound **3.31**

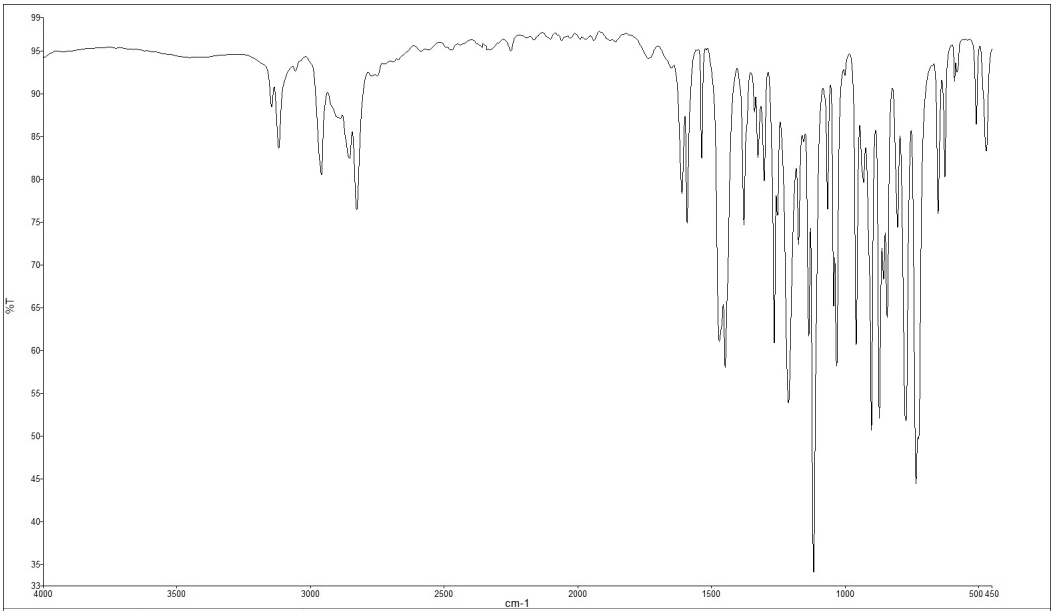


***Figure A3.25.*** Infrared spectrum of compound **3.31**

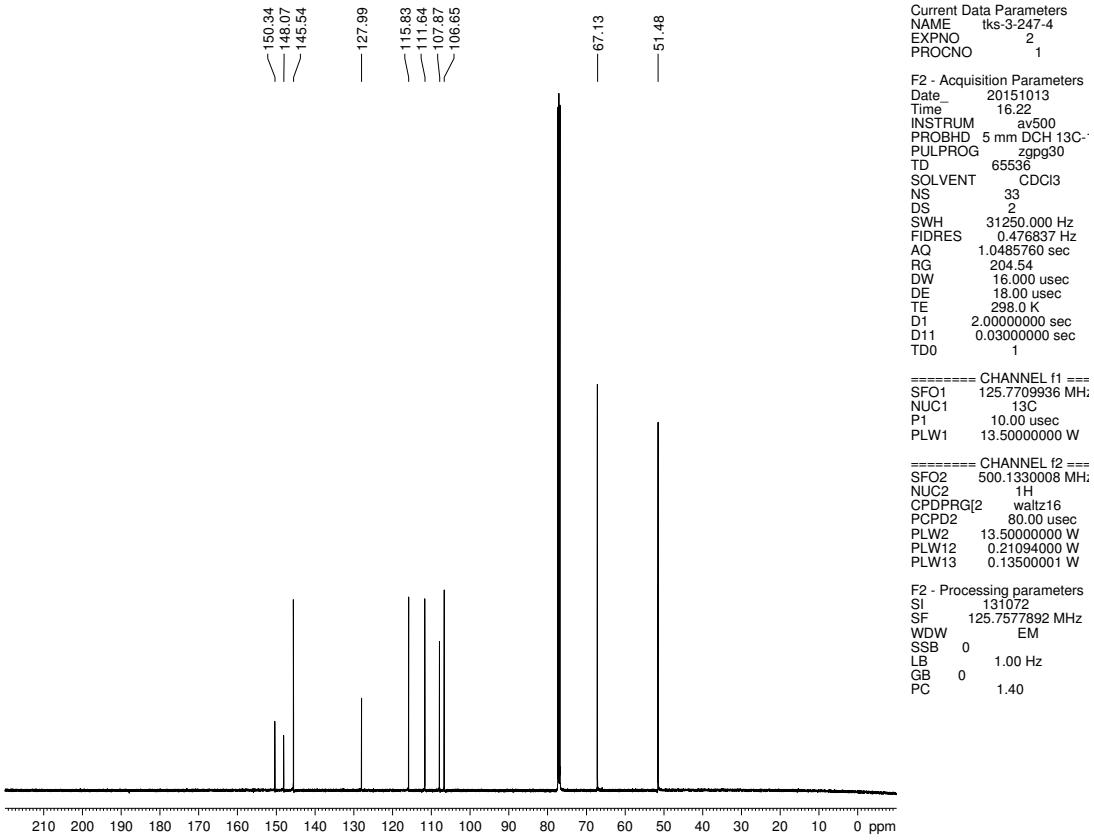


***Figure A3.26.*** $^{13}C$ NMR (125 MHz, $CDCl_3$) of compound **3.31**

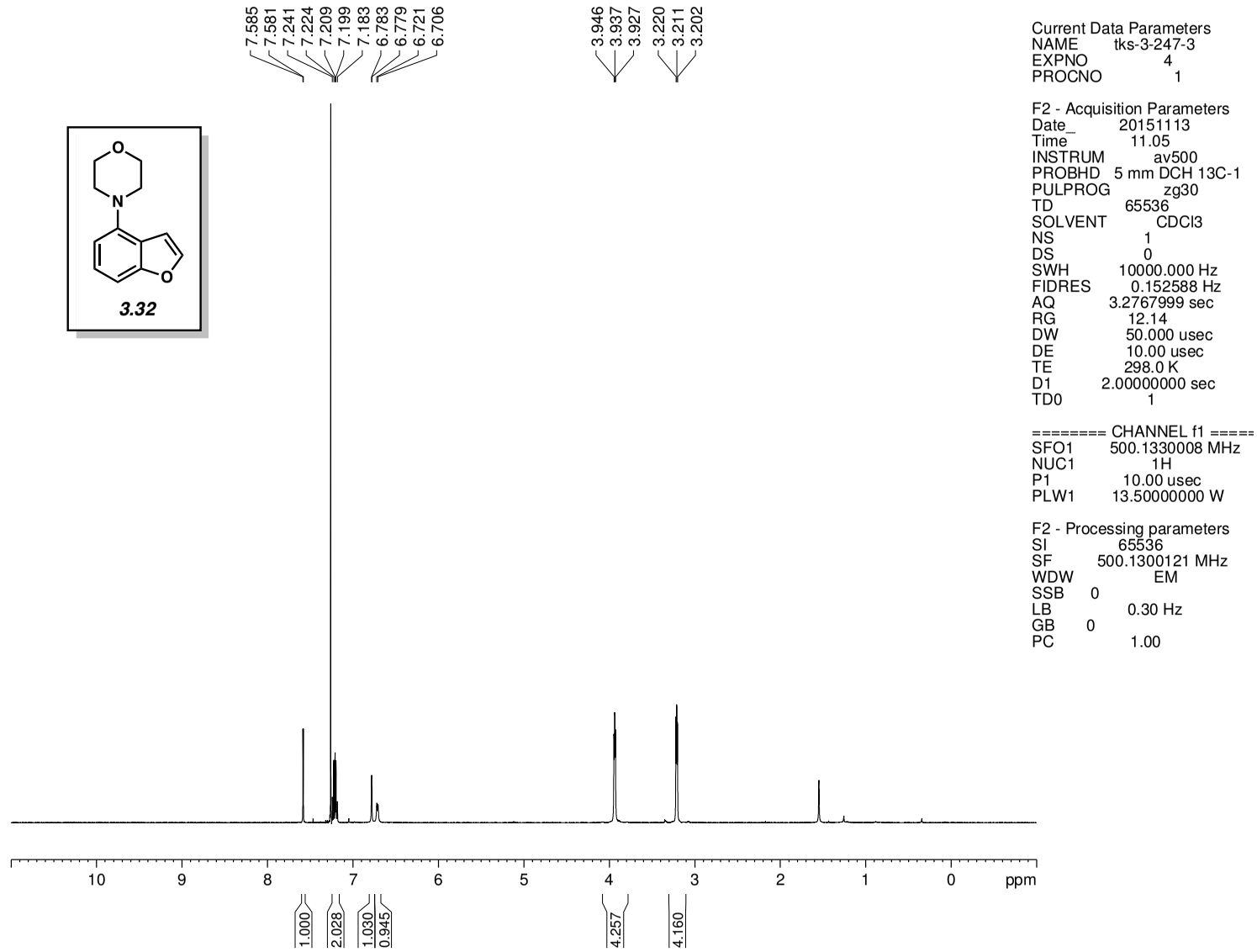


***Figure A3.27.*** $^{1}$H NMR (500 MHz, $CDCl_3$) compound **3.32**

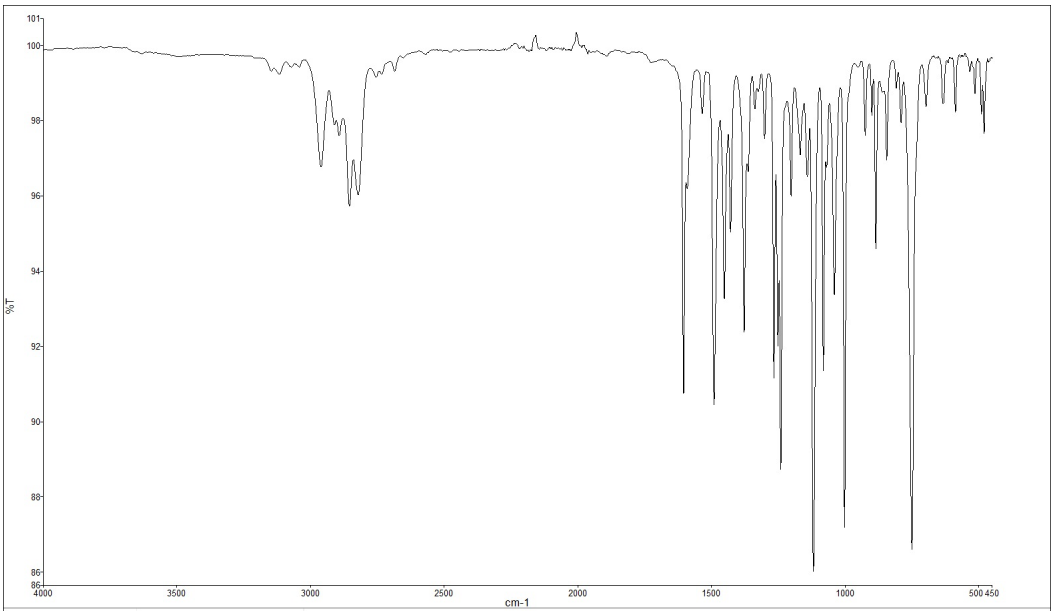


***Figure A3.28.*** Infrared spectrum of compound **3.32**

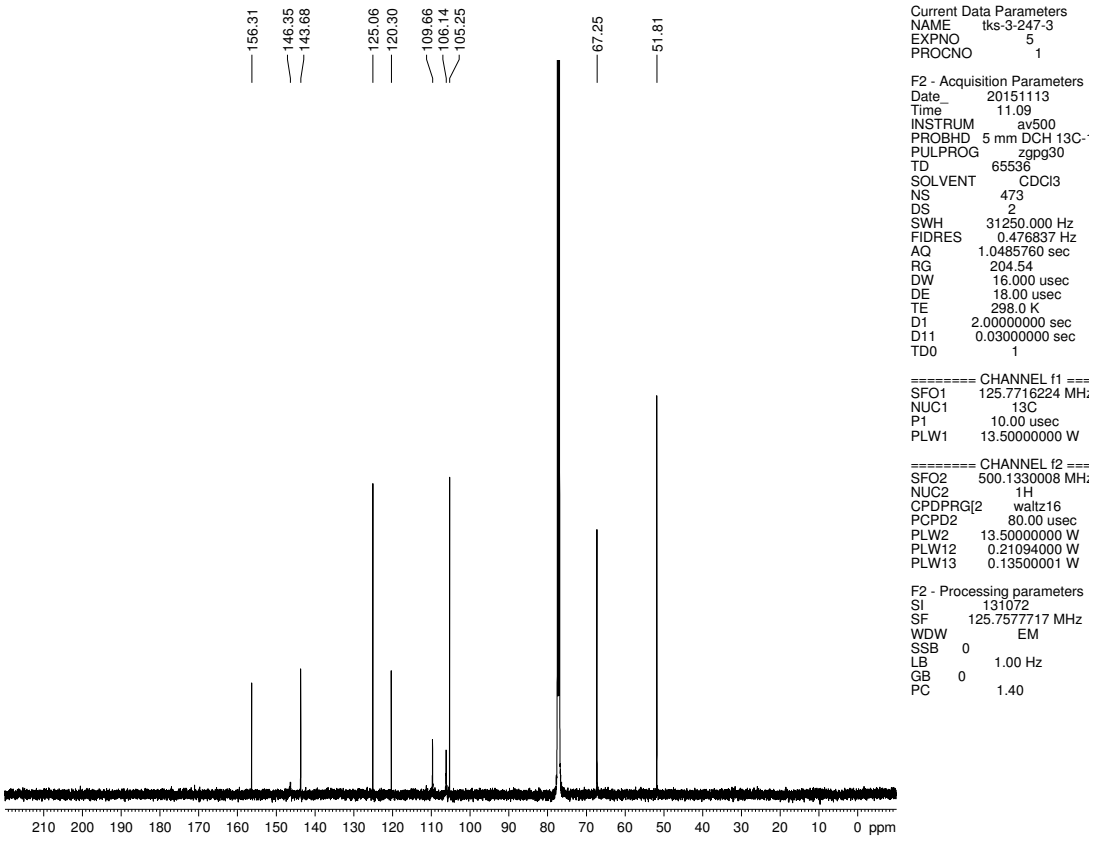


***Figure A3.29.*** $^{13}C$ NMR (125 MHz, $CDCl_3$) of compound **3.32**

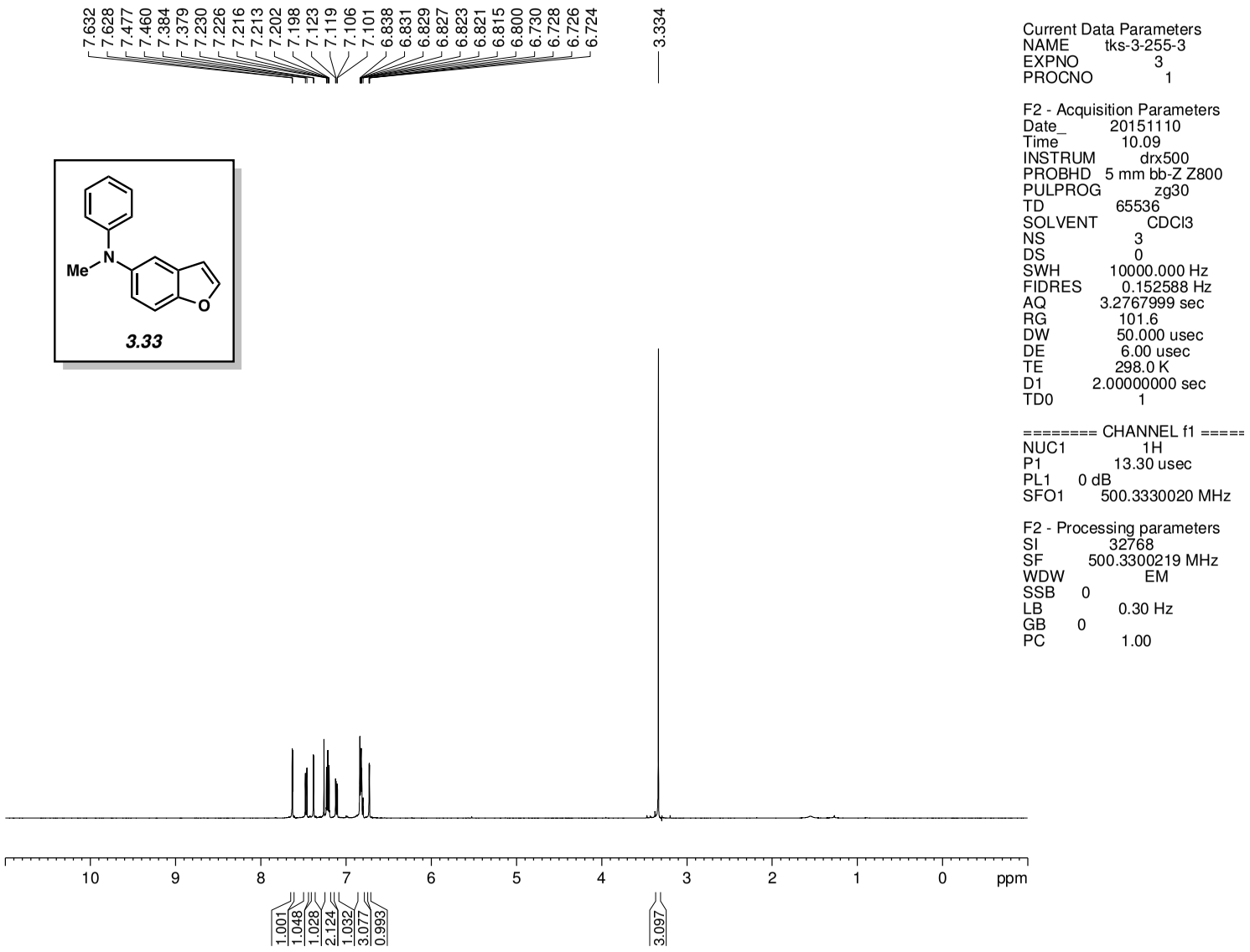


***Figure A3.30.*** $^{1}$H NMR (500 MHz, $CDCl_3$) compound **3.33**

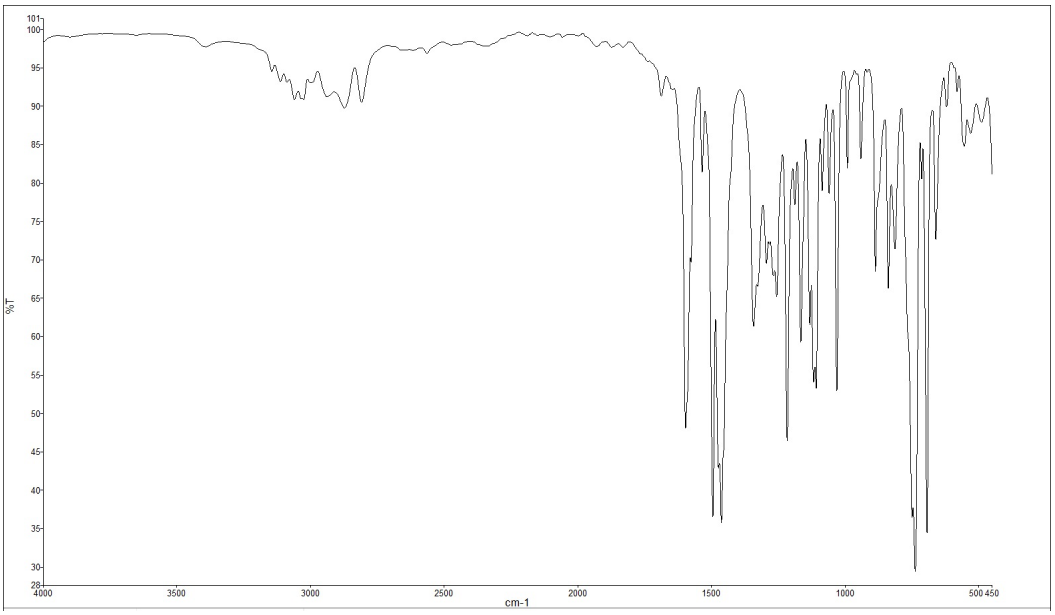


***Figure A3.31.*** Infrared spectrum of compound **3.33**

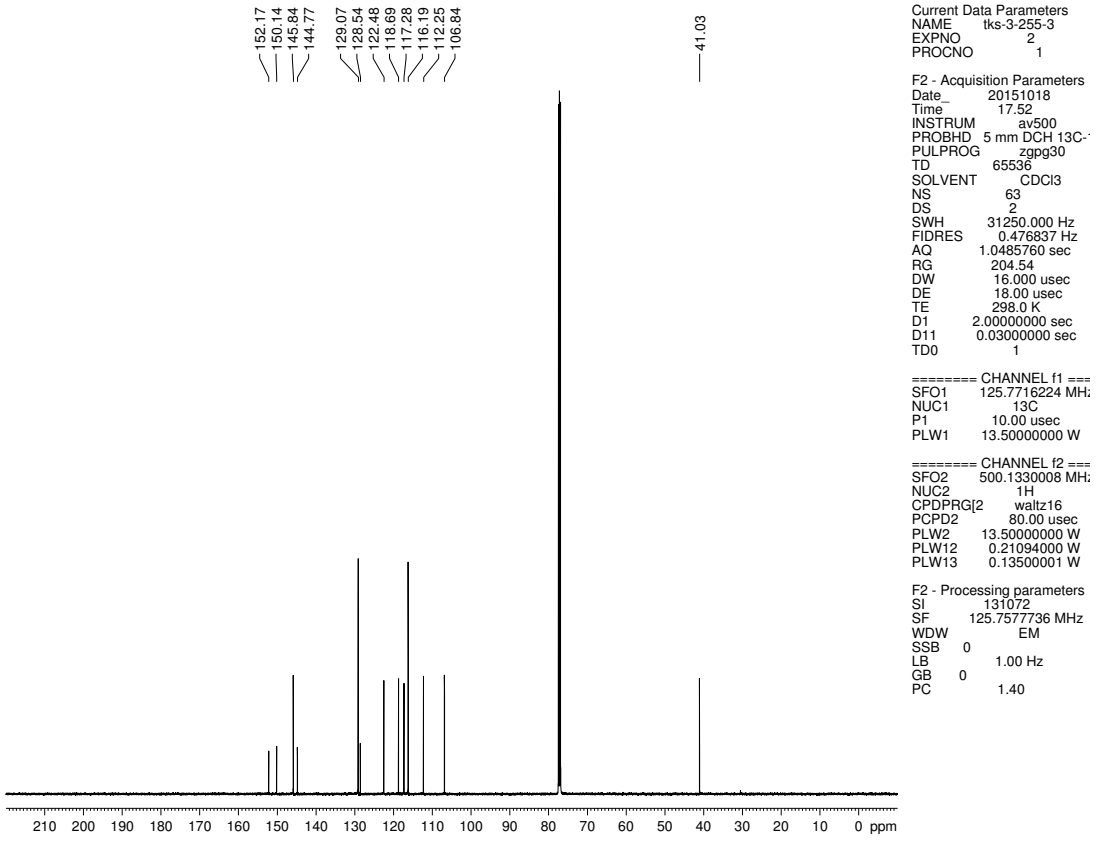


***Figure A3.32.*** $^{13}C$ NMR (125 MHz, $CDCl_3$) of compound **3.33**

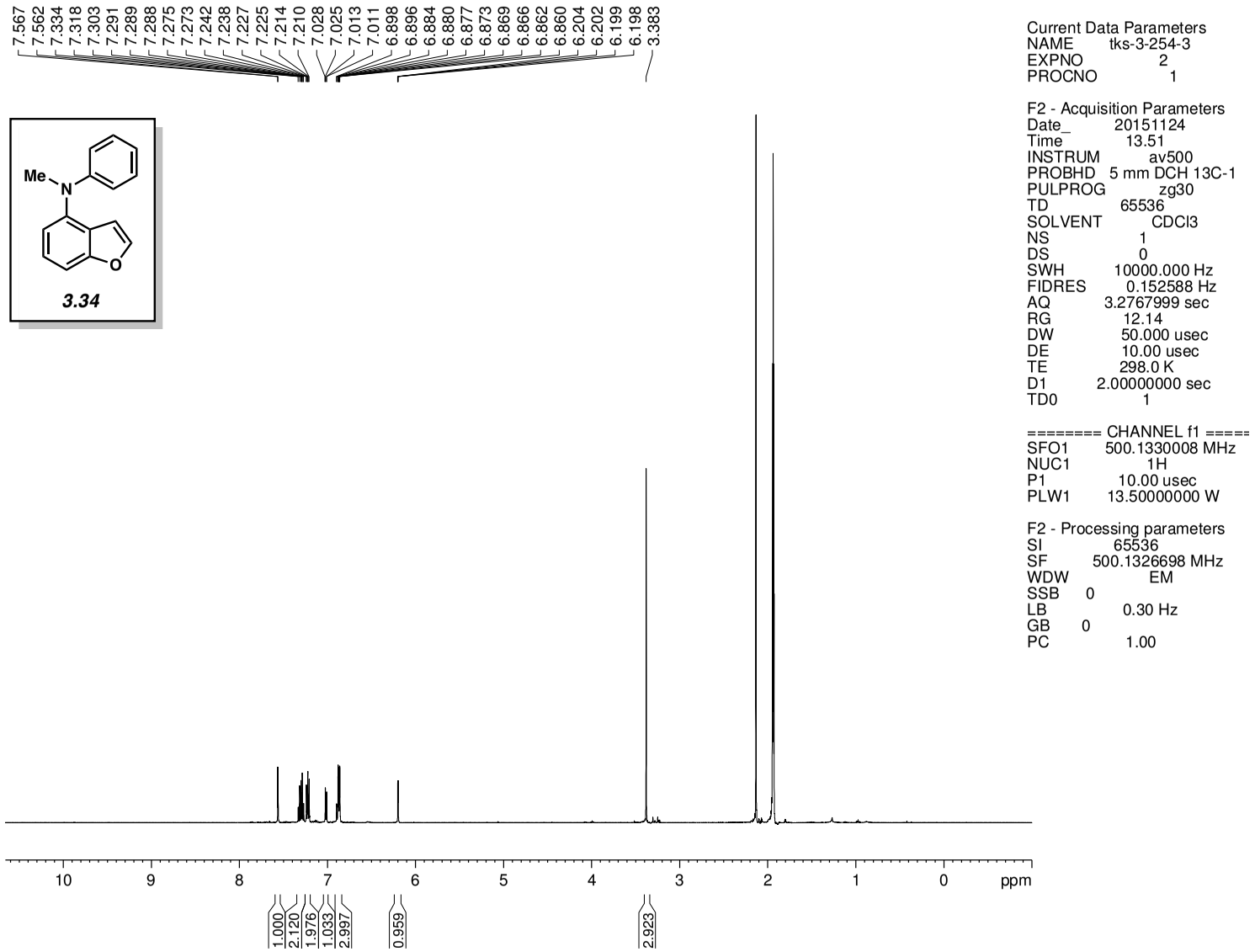


***Figure A3.33.*** $^{1}$H NMR (500 MHz, $CD_3CN$) compound **3.34**

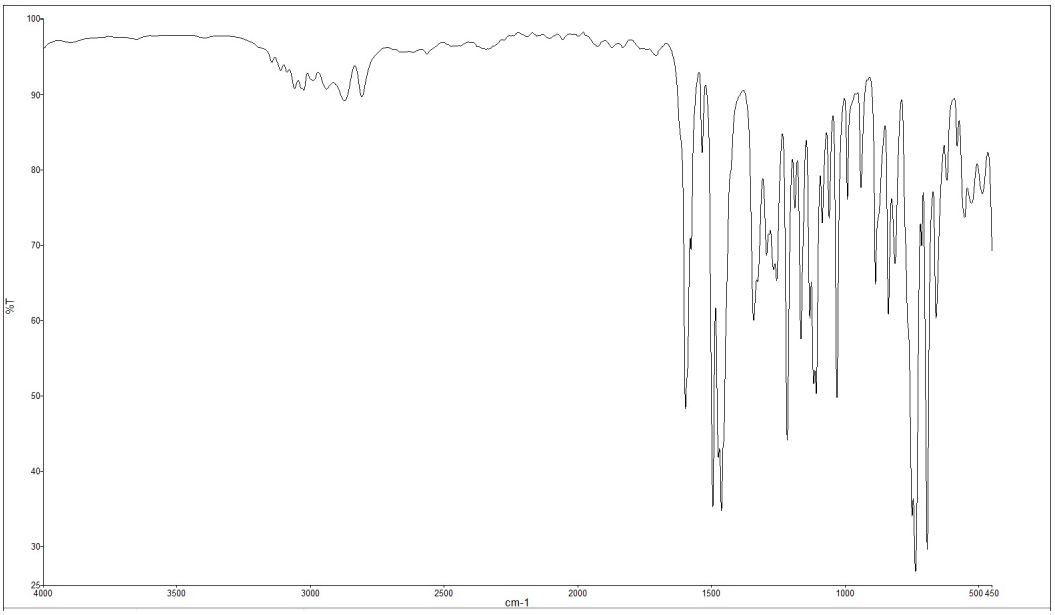


***Figure A3.34.*** Infrared spectrum of compound **3.34**

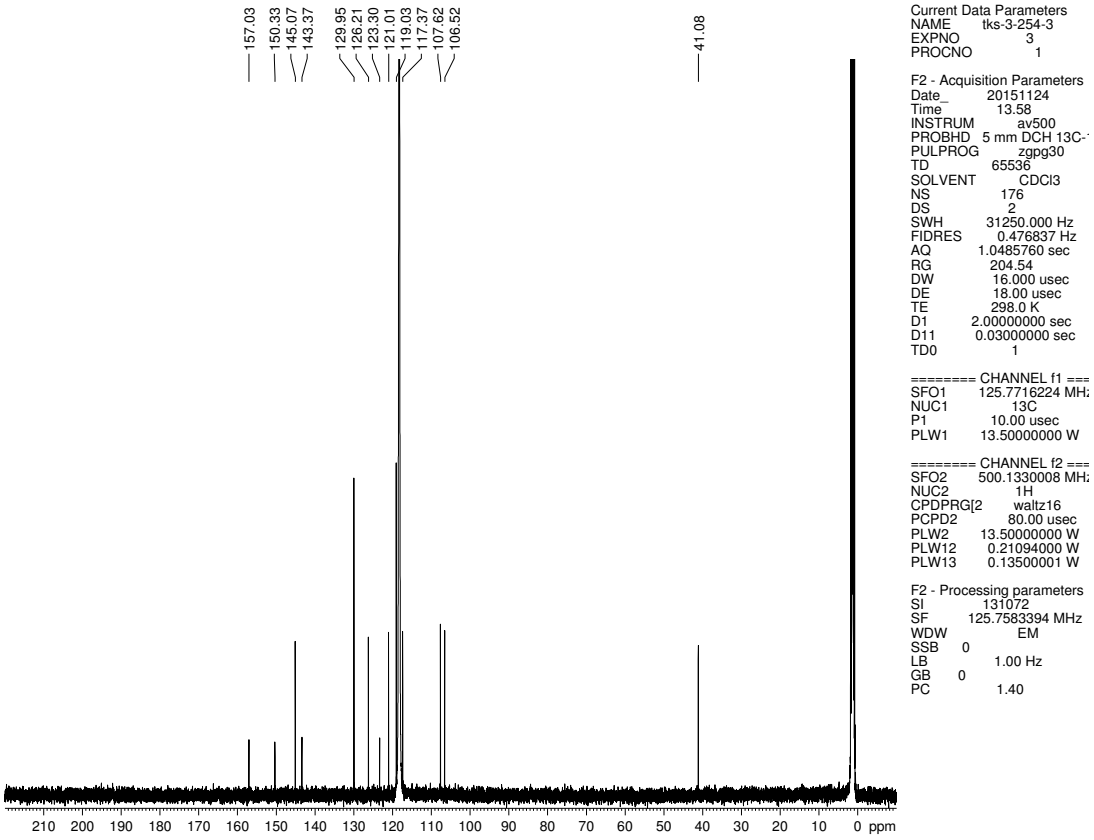


***Figure A3.35.*** $^{13}C$ NMR (125 MHz, $CDCl_3$) of compound **3.34**

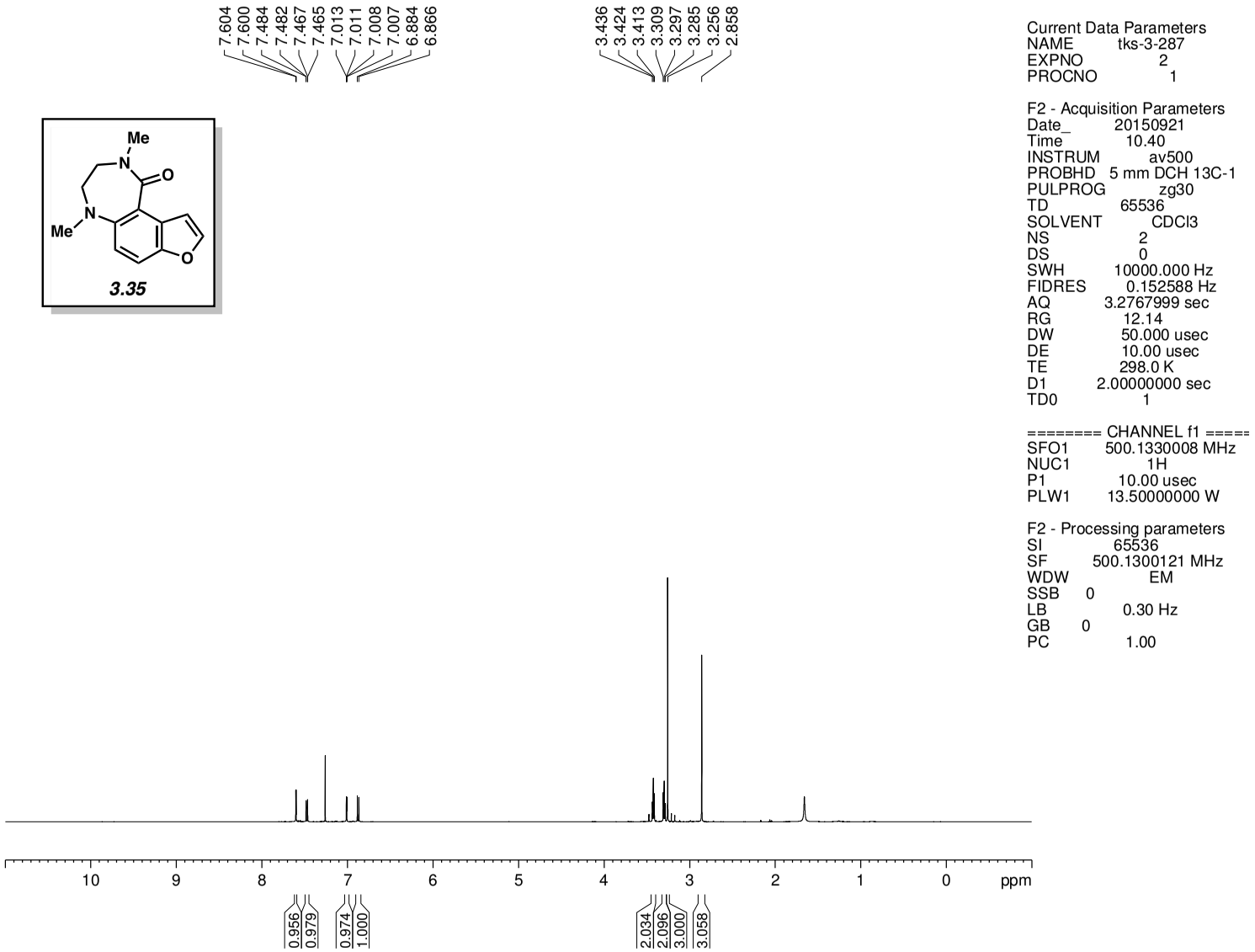


***Figure A3.36.*** $^{1}$H NMR (500 MHz, $CDCl_3$) compound **3.35**

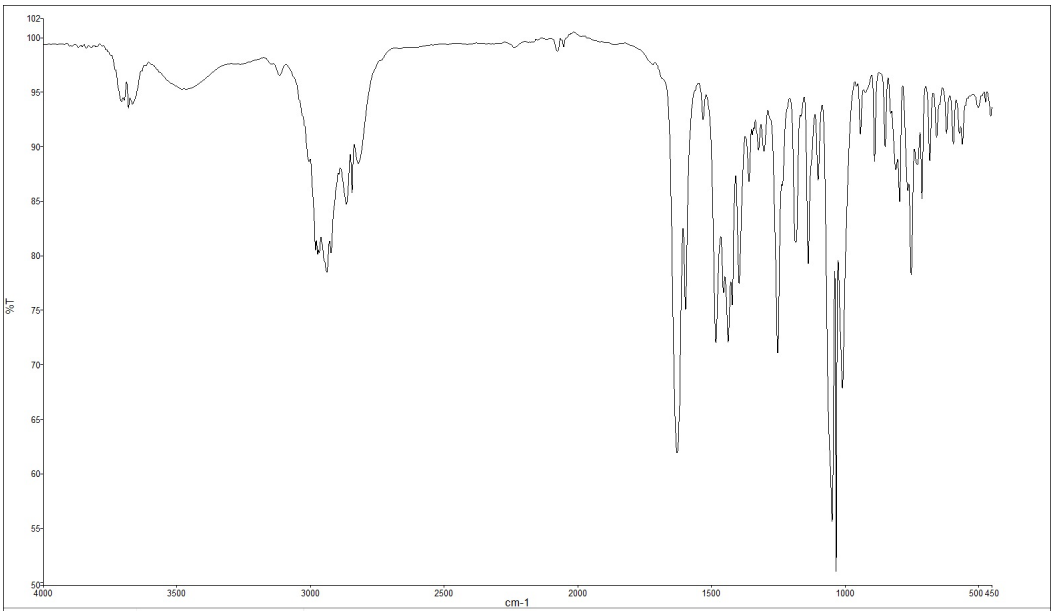


***Figure A3.37.*** Infrared spectrum of compound **3.35**

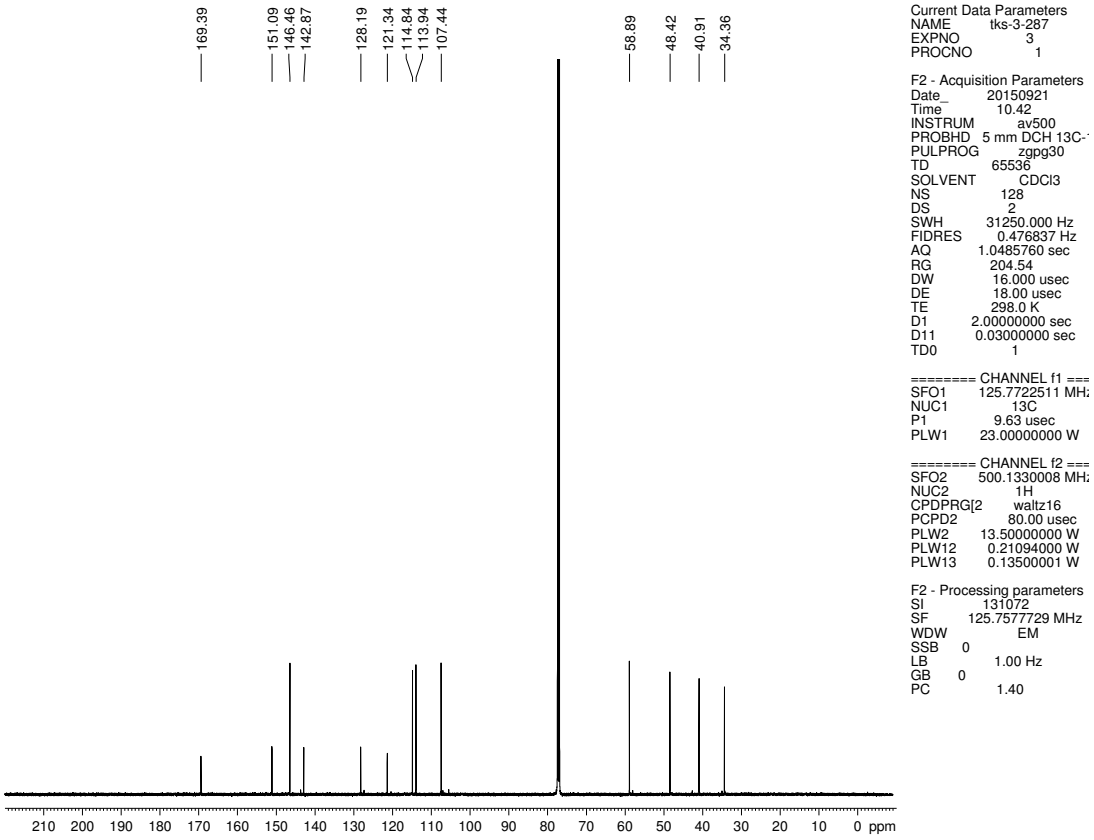


***Figure A3.38.*** $^{13}C$ NMR (125 MHz, $CDCl_3$) of compound **3.35**

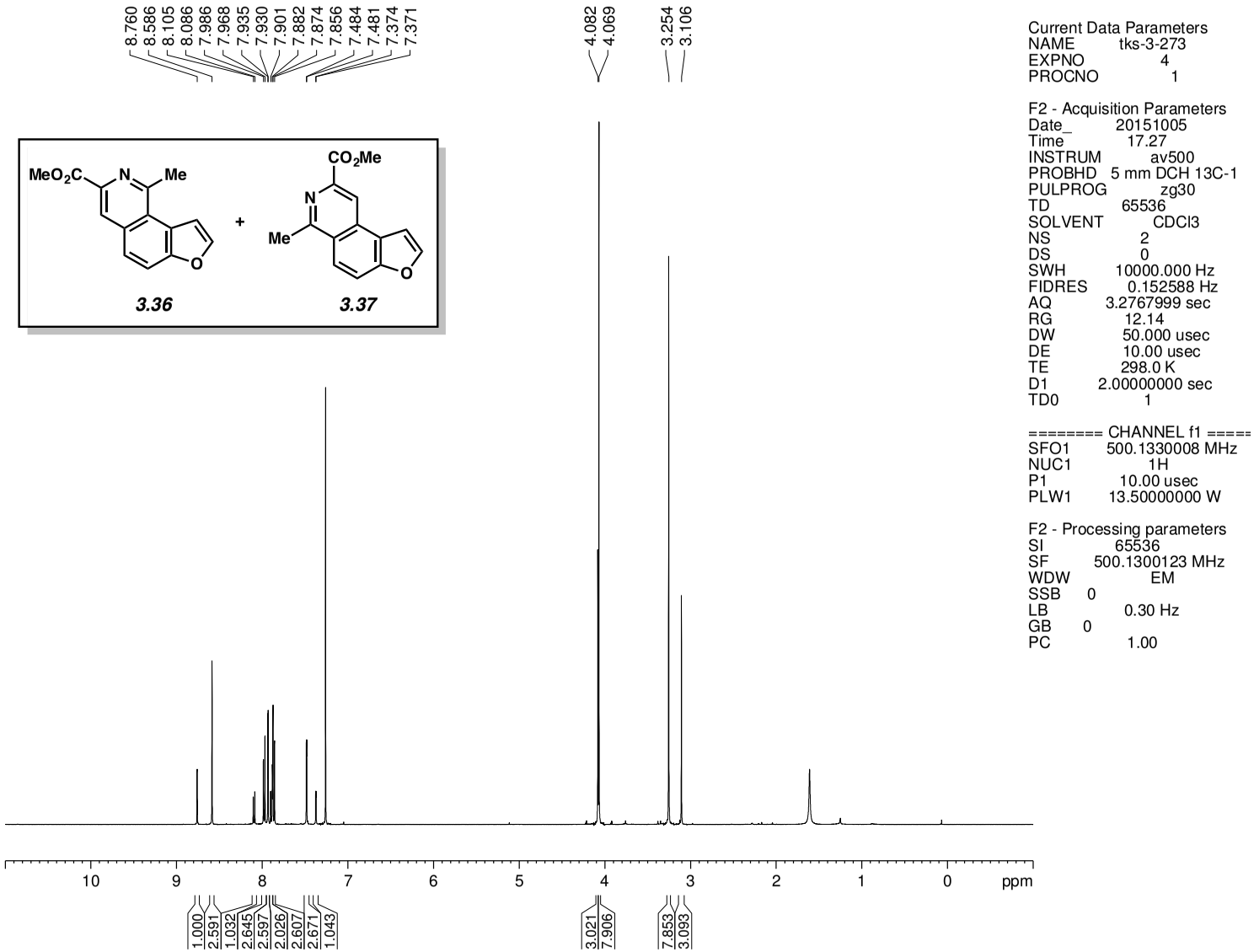


***Figure A3.39.*** $^{1}$H NMR (500 MHz, $CDCl_3$) compounds **3.36** & **3.37**

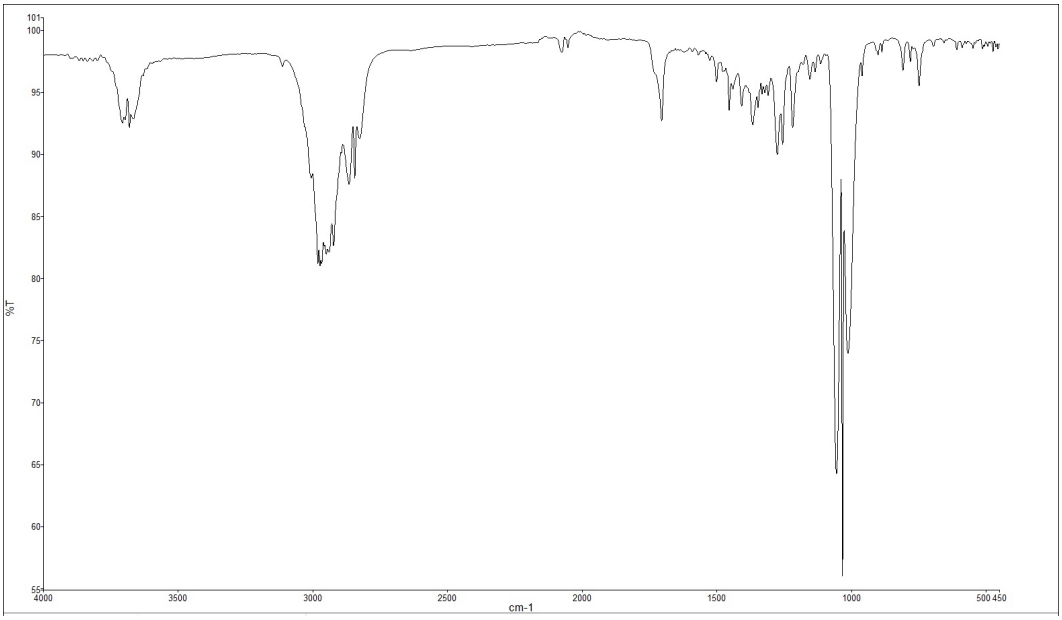


***Figure A3.40.*** Infrared spectrum of compounds **3.36** & **3.37**

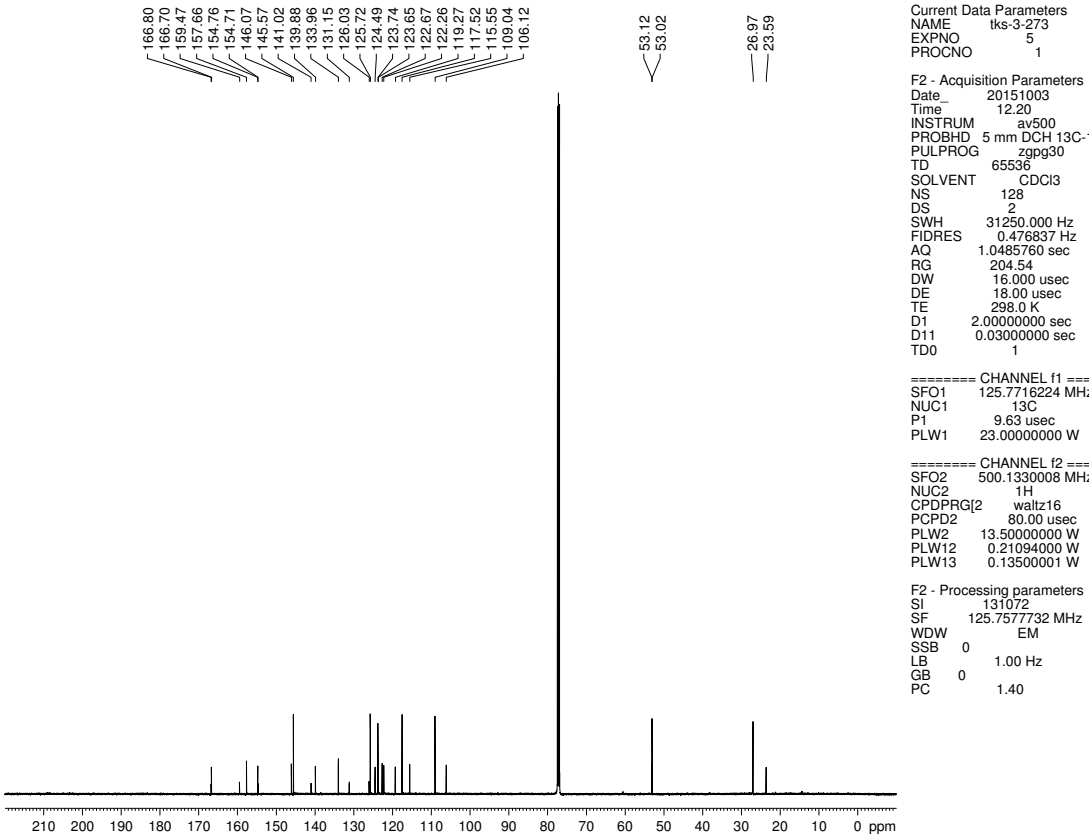


***Figure A3.41.*** $^{13}C$ NMR (125 MHz, $CDCl_3$) of compounds **3.36** & **3.37**

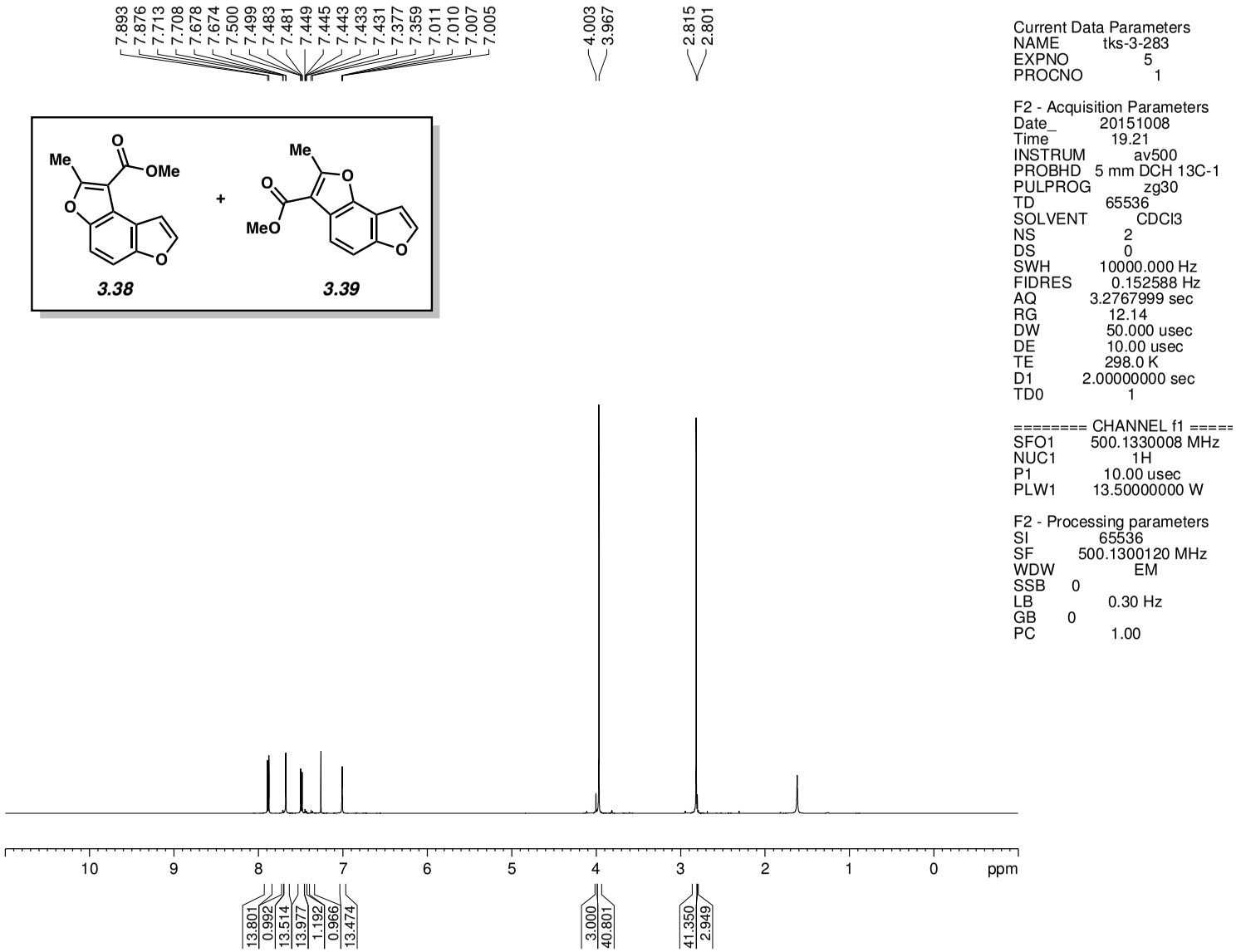


***Figure A3.42.*** $^{1}$H NMR (500 MHz, $CDCl_3$) compounds **3.38** & **3.39**

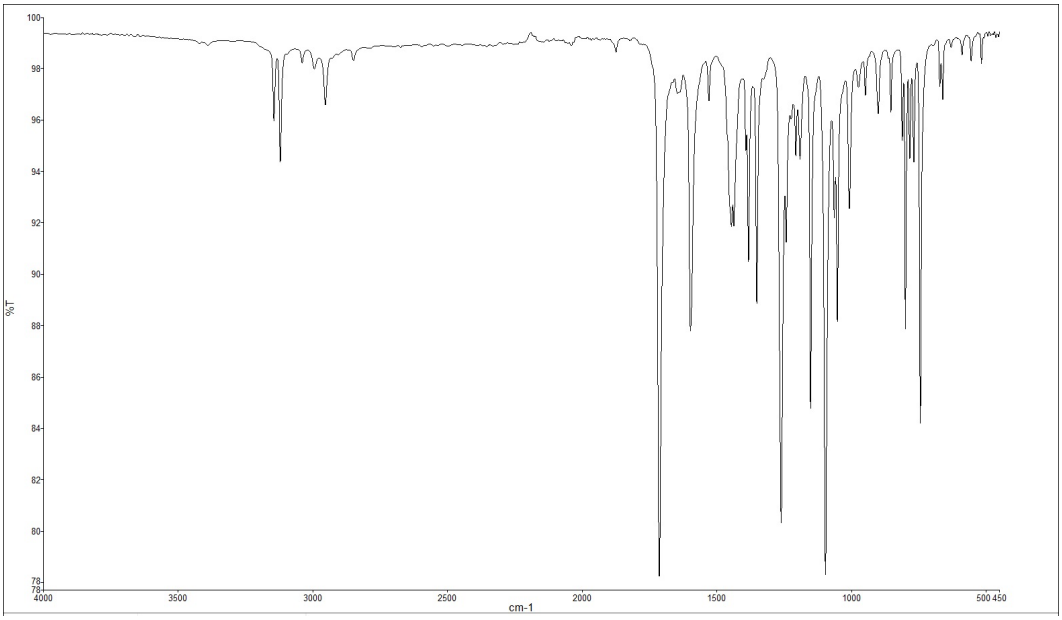


***Figure A3.43.*** Infrared spectrum of compound **3.38** & **3.39**

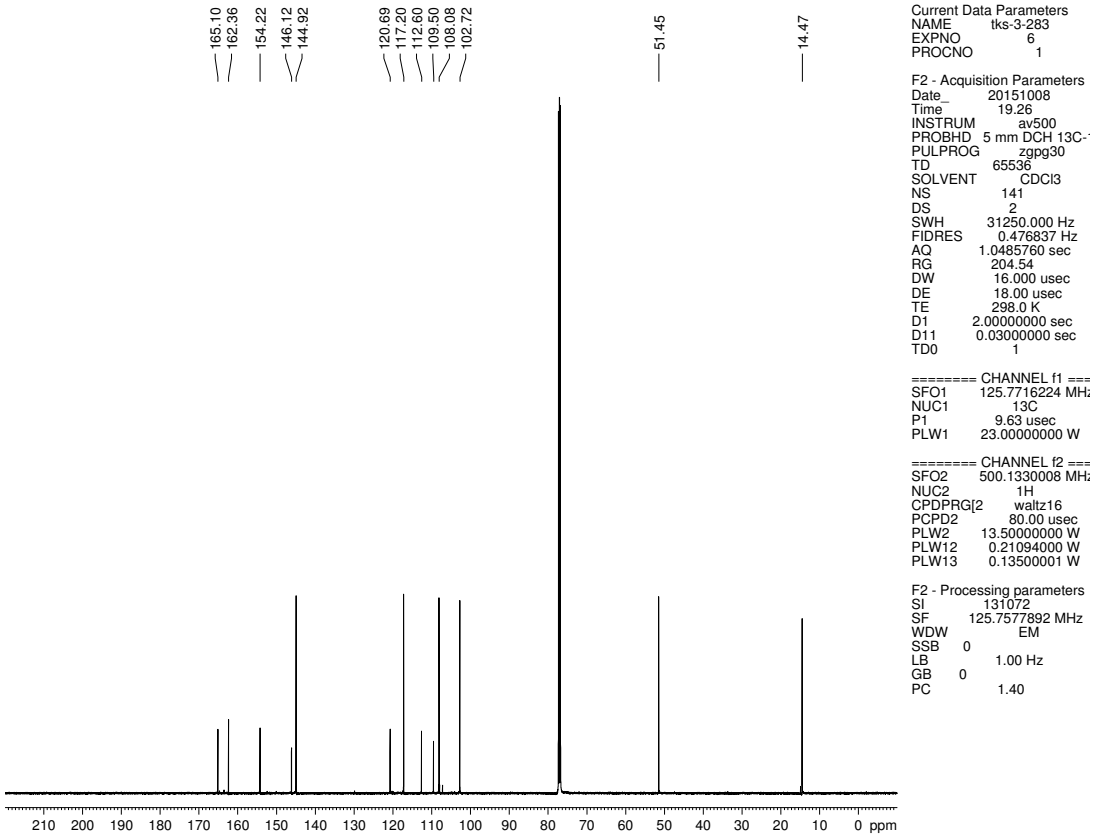


***Figure A3.44.*** $^{13}C$ NMR (125 MHz, $CDCl_3$) of compound **3.38**

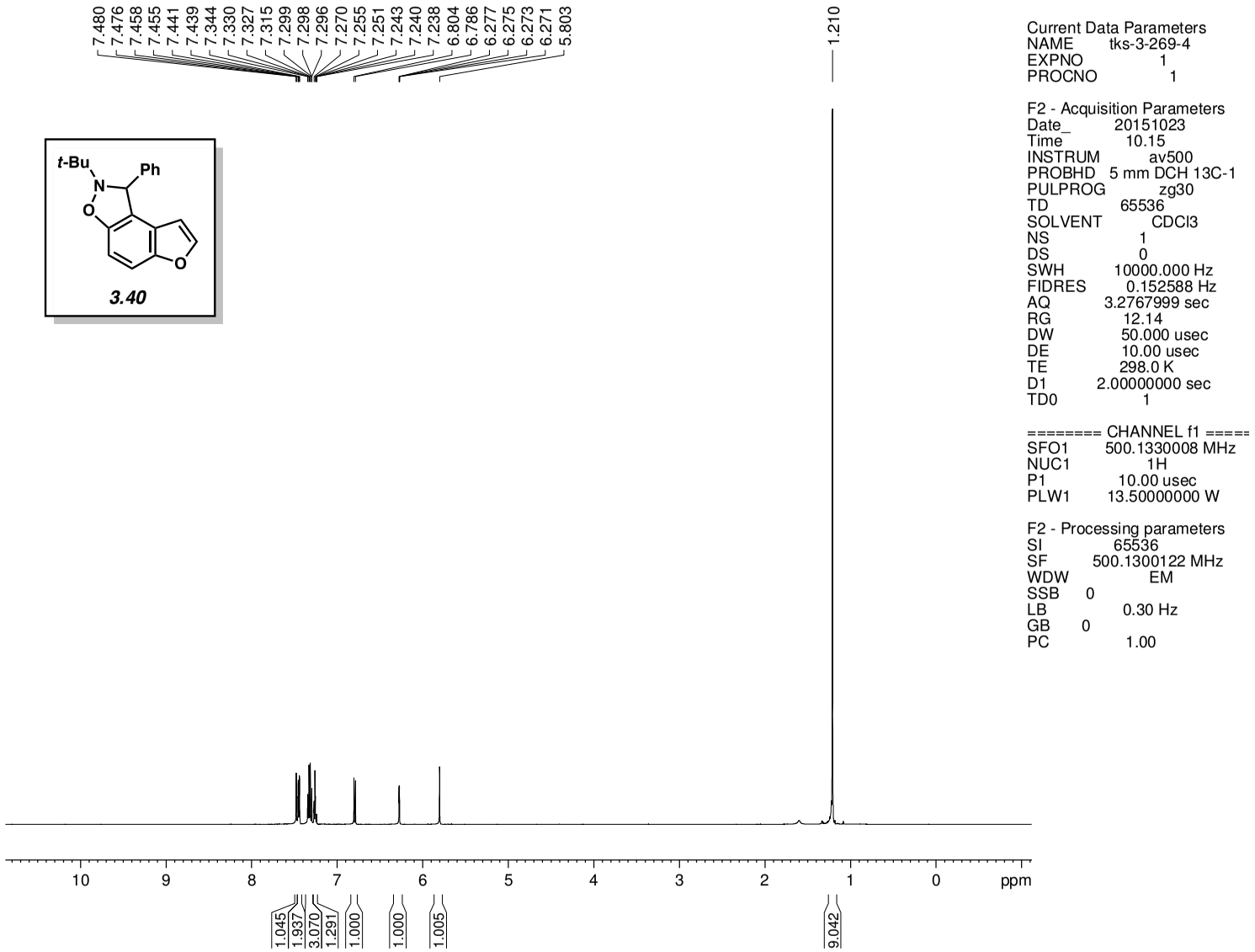


***Figure A3.45.*** $^{1}$H NMR (500 MHz, $CDCl_3$) compound **3.40**

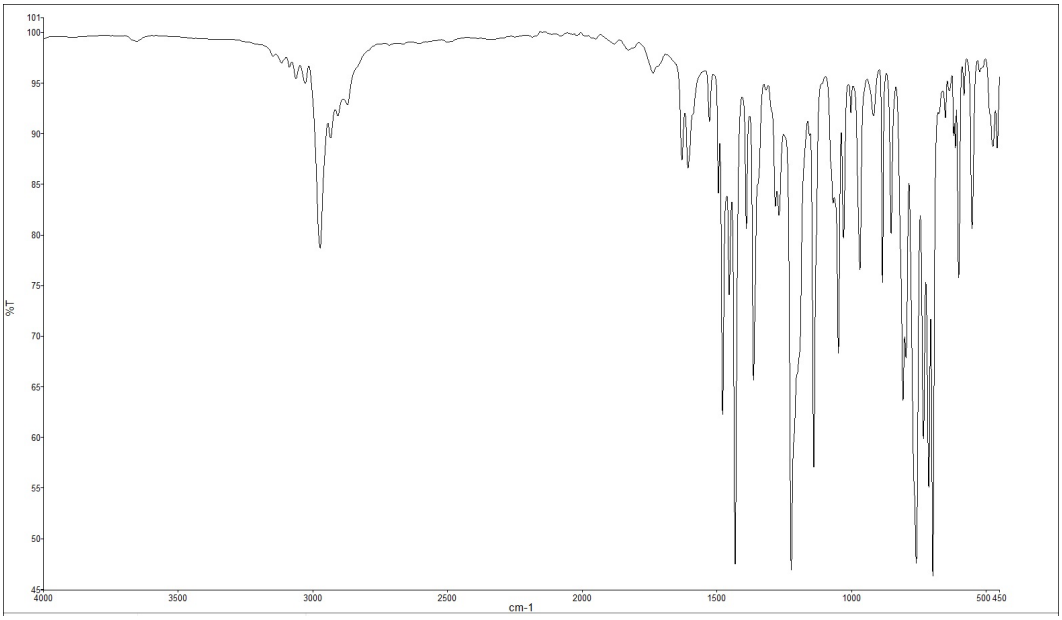


***Figure A3.46.*** Infrared spectrum of compound **3.40**

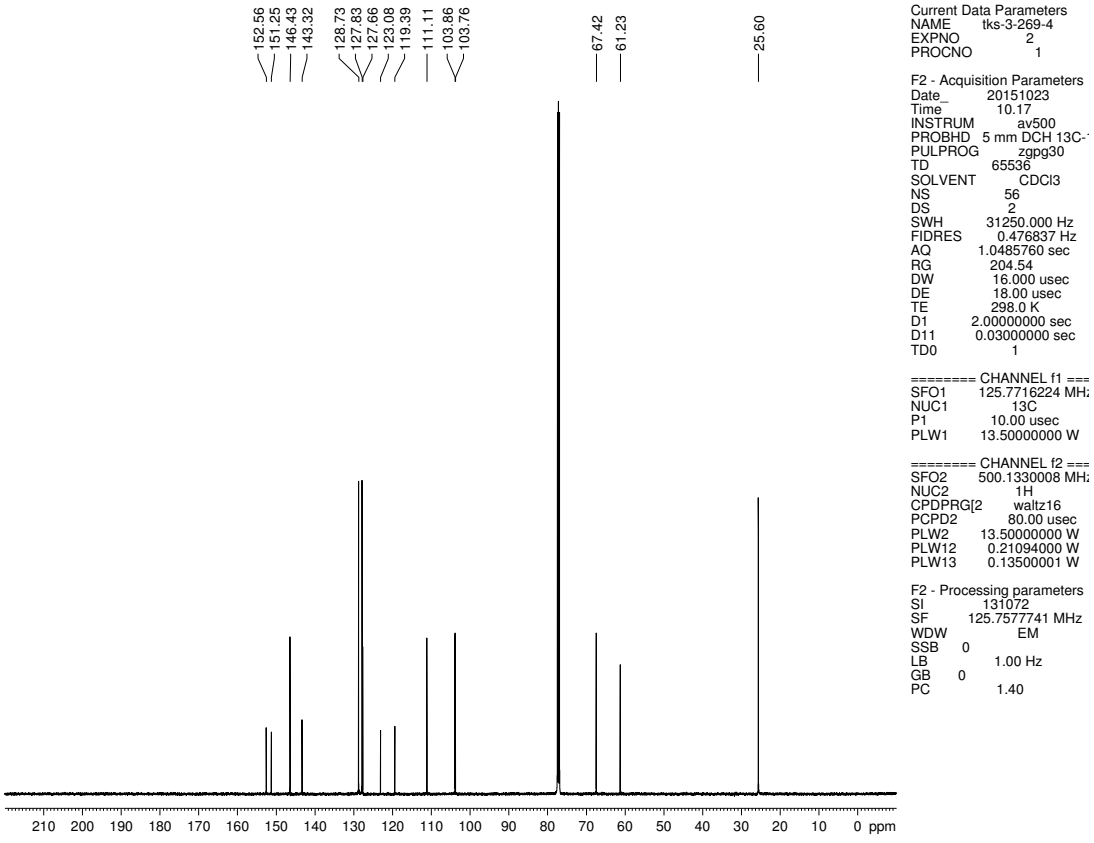


***Figure A3.47.*** $^{13}$C NMR (125 MHz, $CDCl_3$) of compound **3.40**

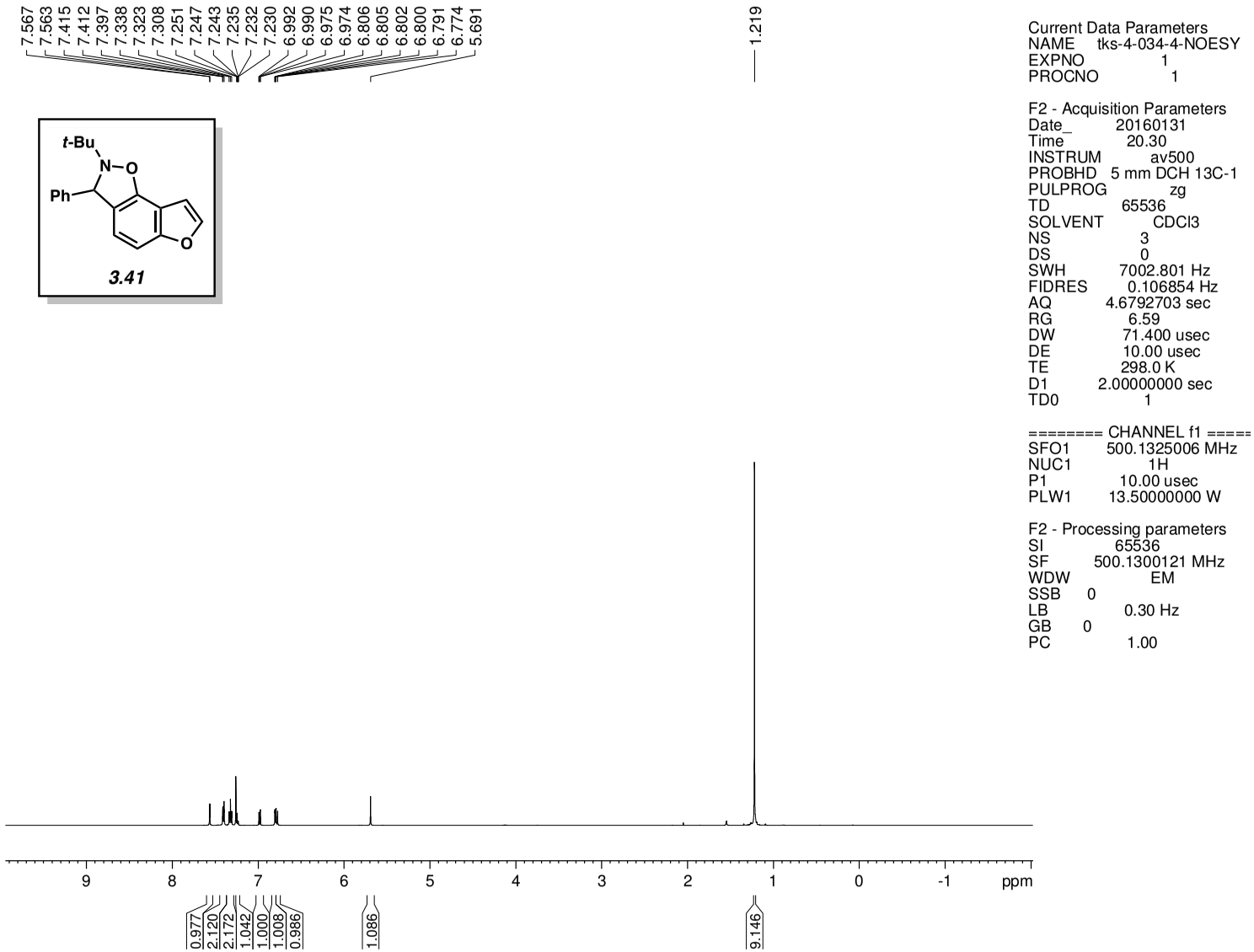


***Figure A3.48.*** $^{1}$H NMR (500 MHz, $CDCl_3$) compound **3.41**

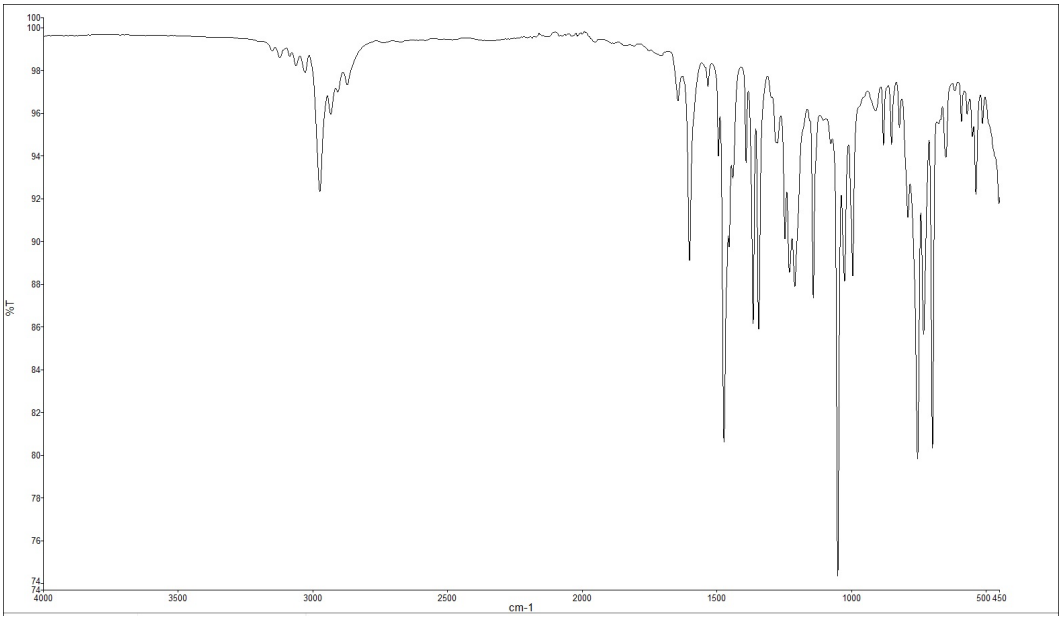


***Figure A3.49.*** Infrared spectrum of compound **3.41**

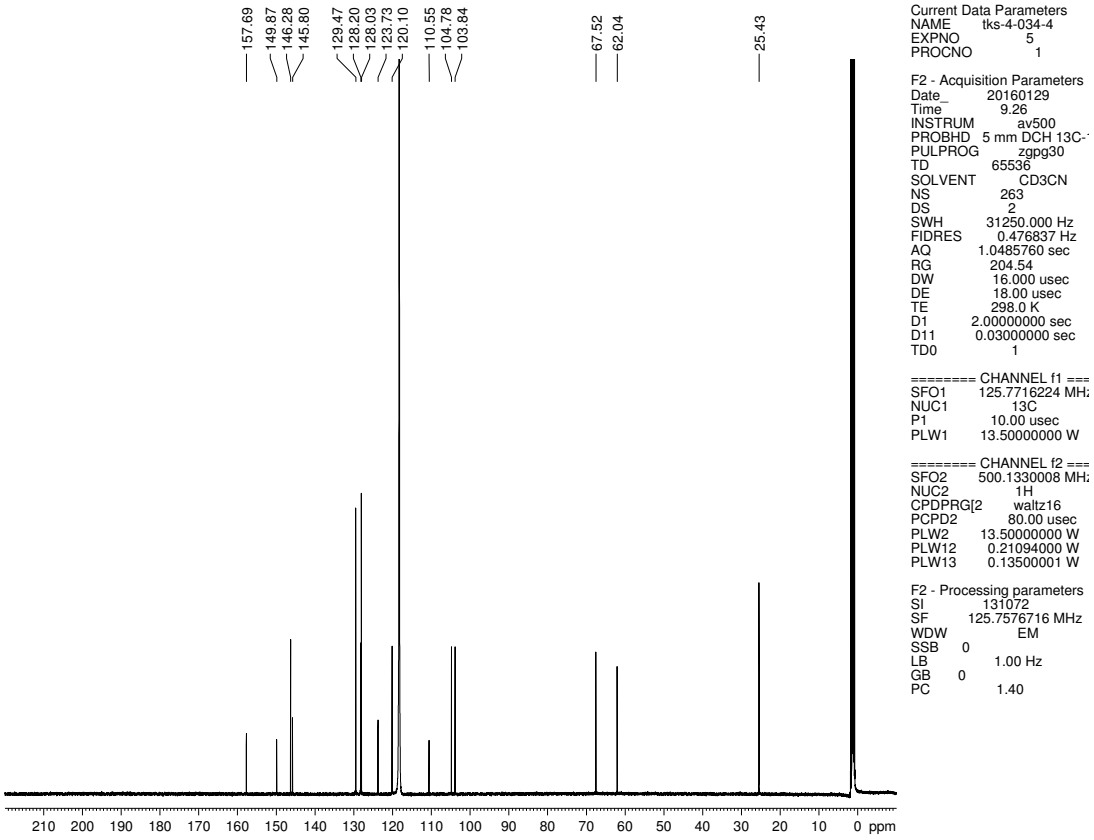


***Figure A3.50.*** $^{13}C$ NMR (125 MHz, $CDCl_3$) of compound **3.41**

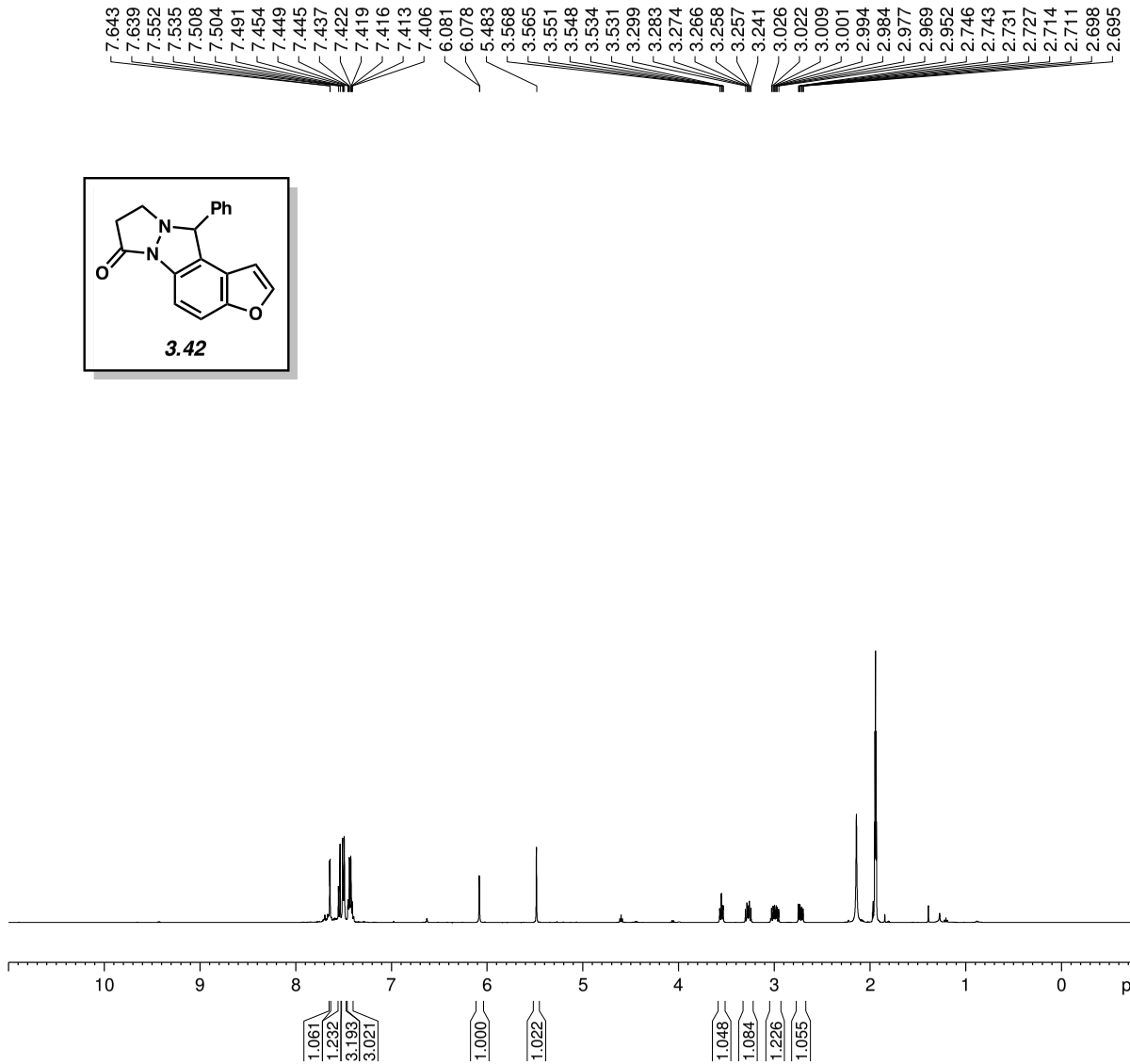


***Figure A3.51.*** $^{1}$H NMR (500 MHz, $CD_3CN$) compound **3.42**

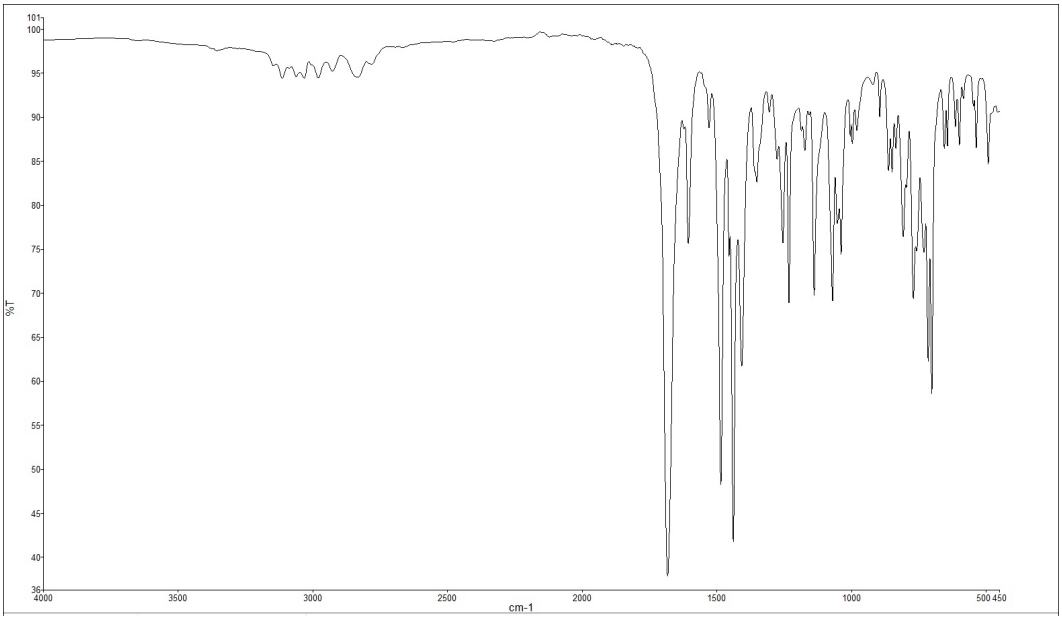


***Figure A3.52.*** Infrared spectrum of compound **3.42**

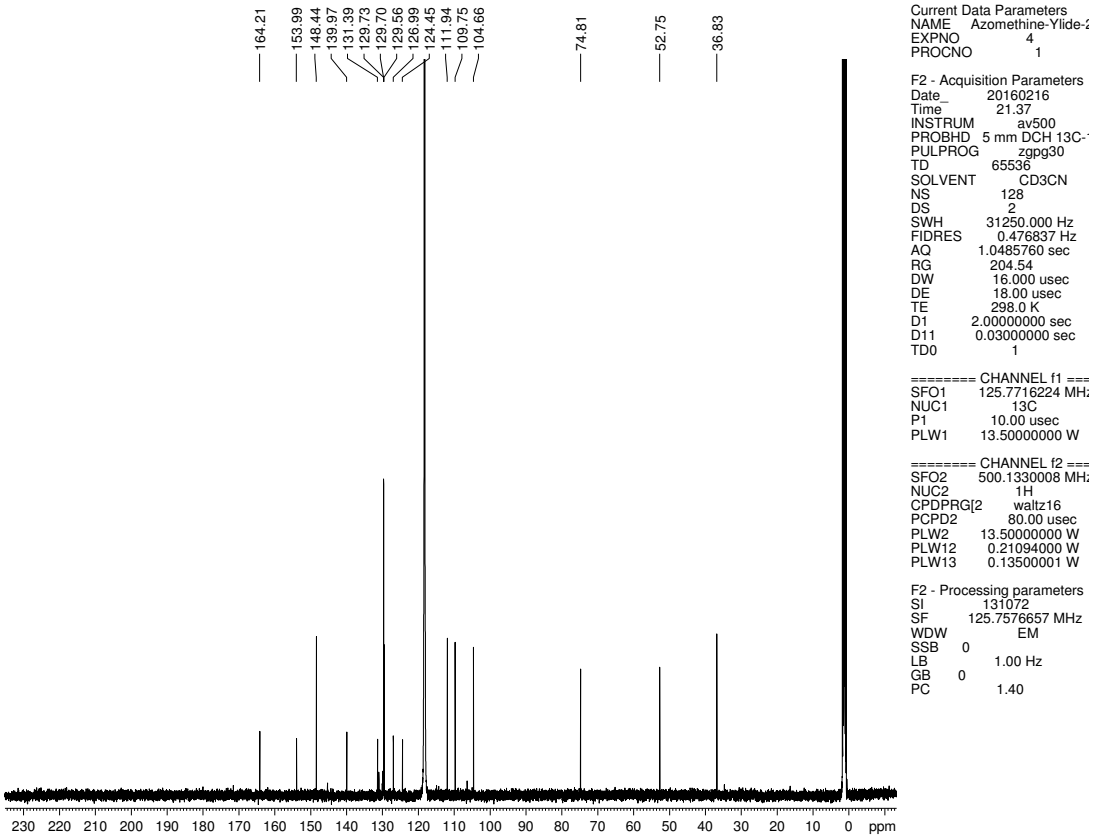


***Figure A3.53.*** $^{13}$C NMR (125 MHz, $CD_3CN$) of compound **3.42**

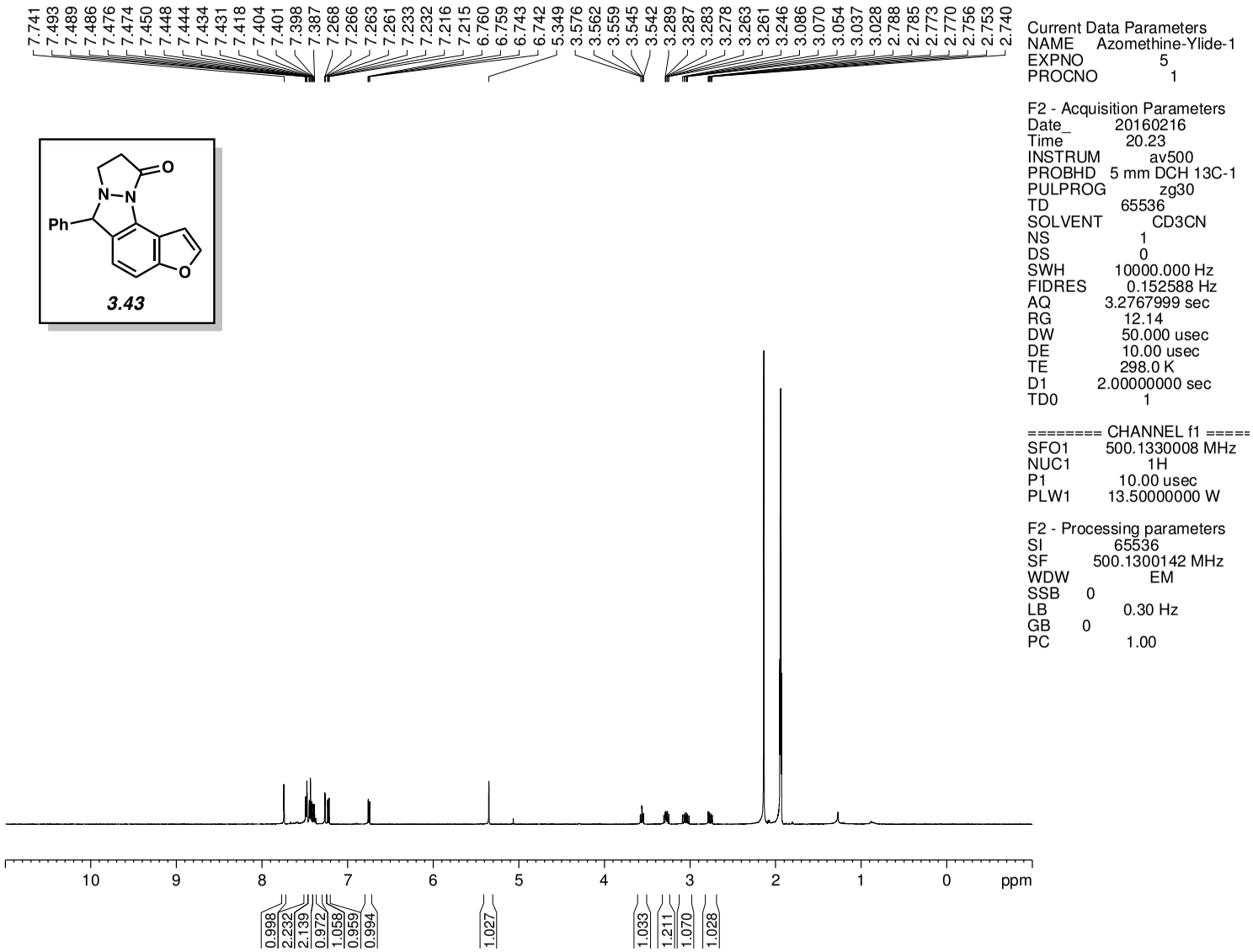


***Figure A3.54.*** $^{1}$H NMR (500 MHz, $CD_3CN$) compound **3.43**

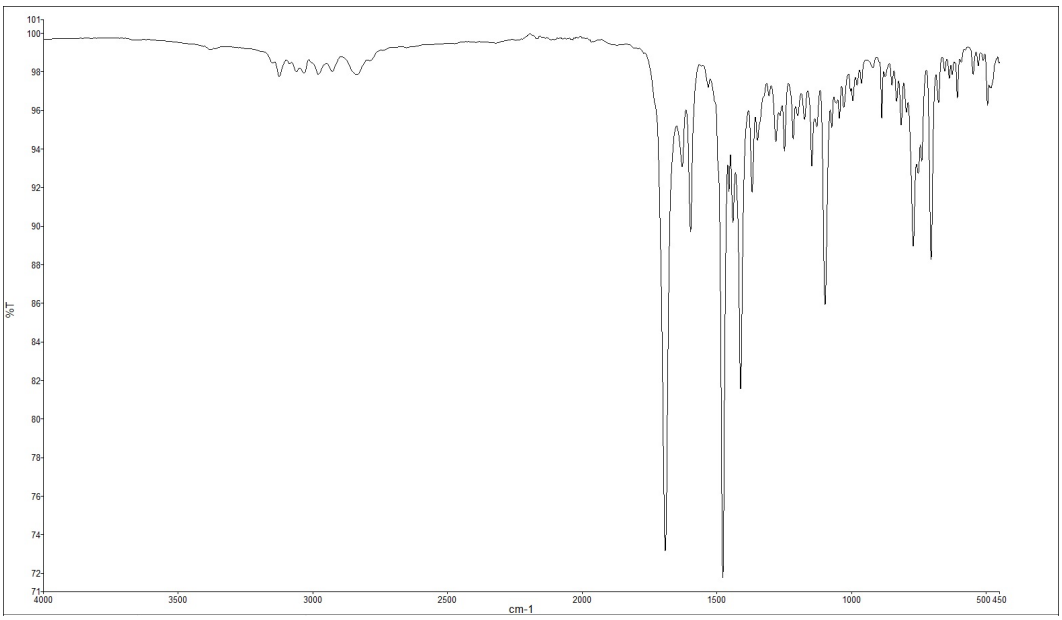


***Figure A3.55.*** Infrared spectrum of compound **3.43**

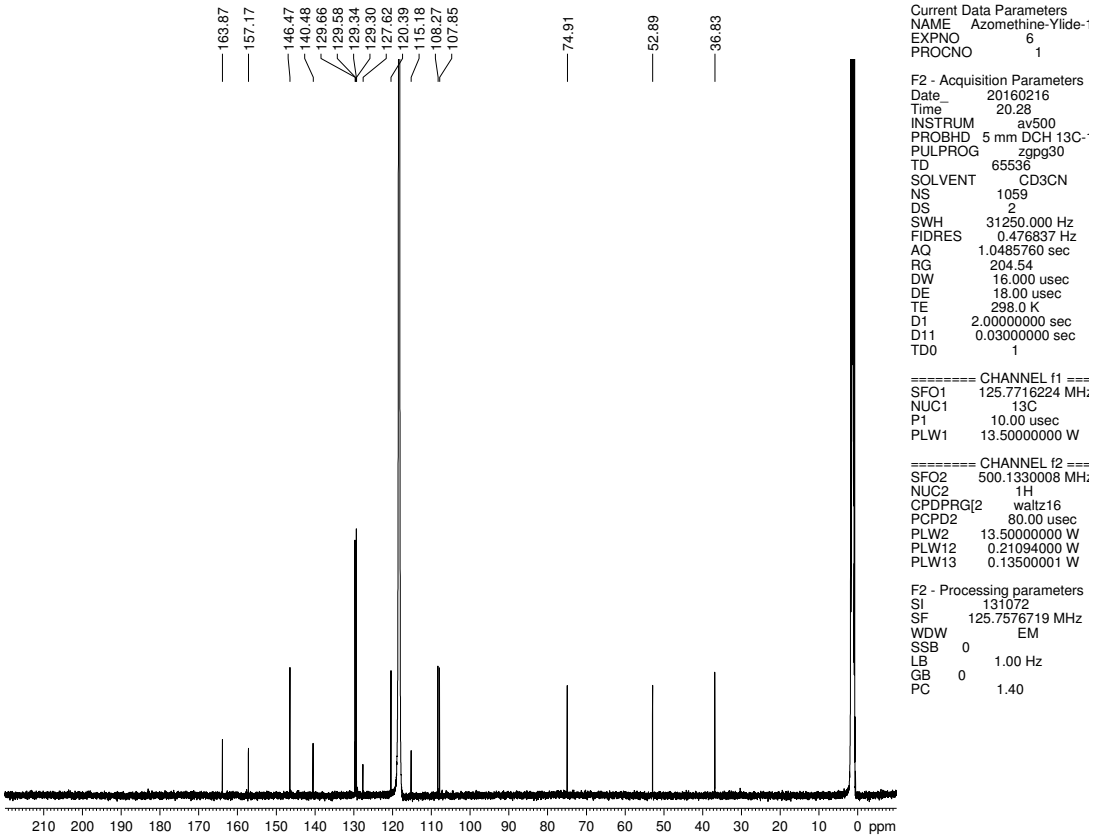


***Figure A3.56.*** $^{13}C$ NMR (125 MHz, $CD_3CN$) of compound **3.43**

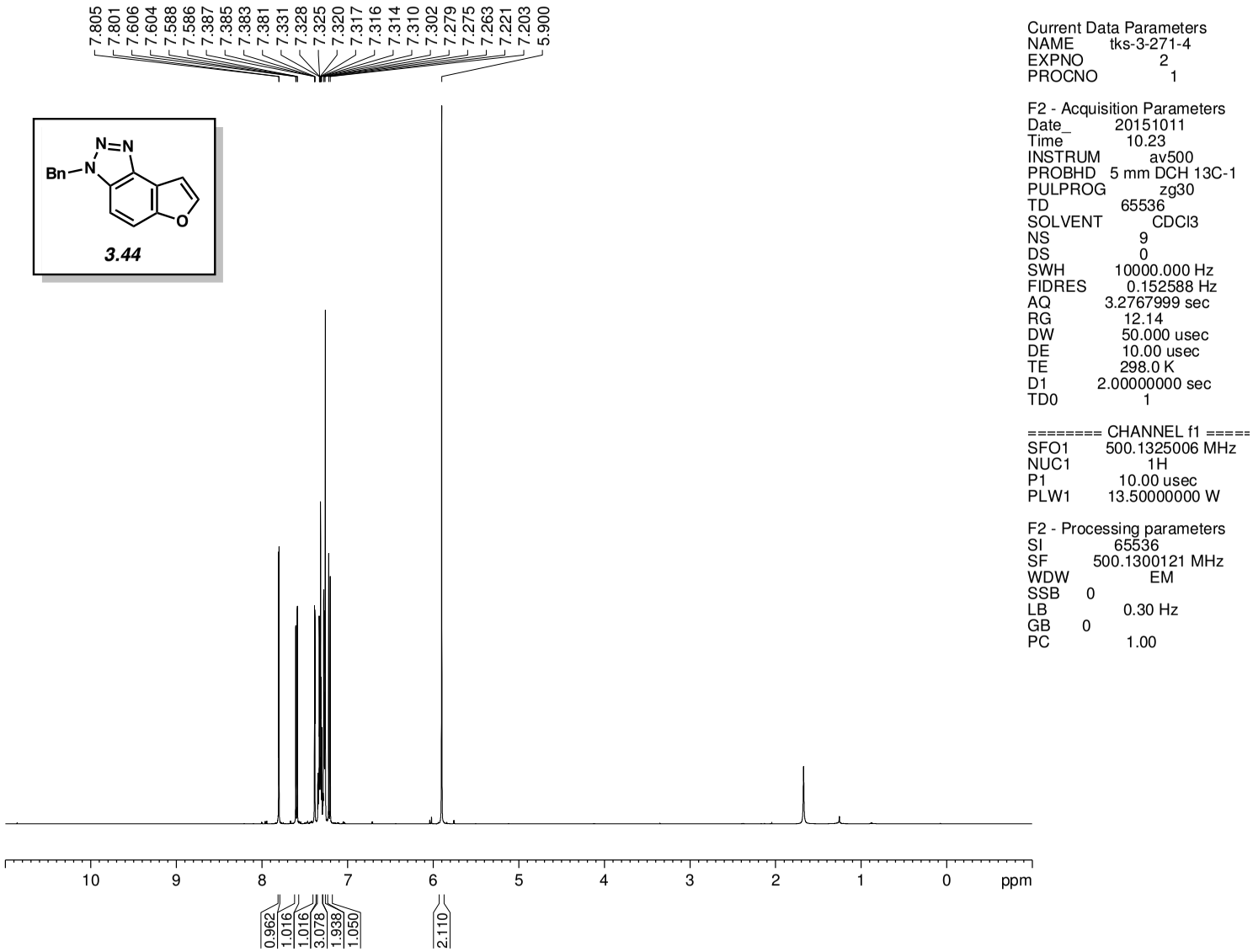


***Figure A3.57.*** $^{1}$H NMR (500 MHz, $CDCl_3$) compound **3.44**

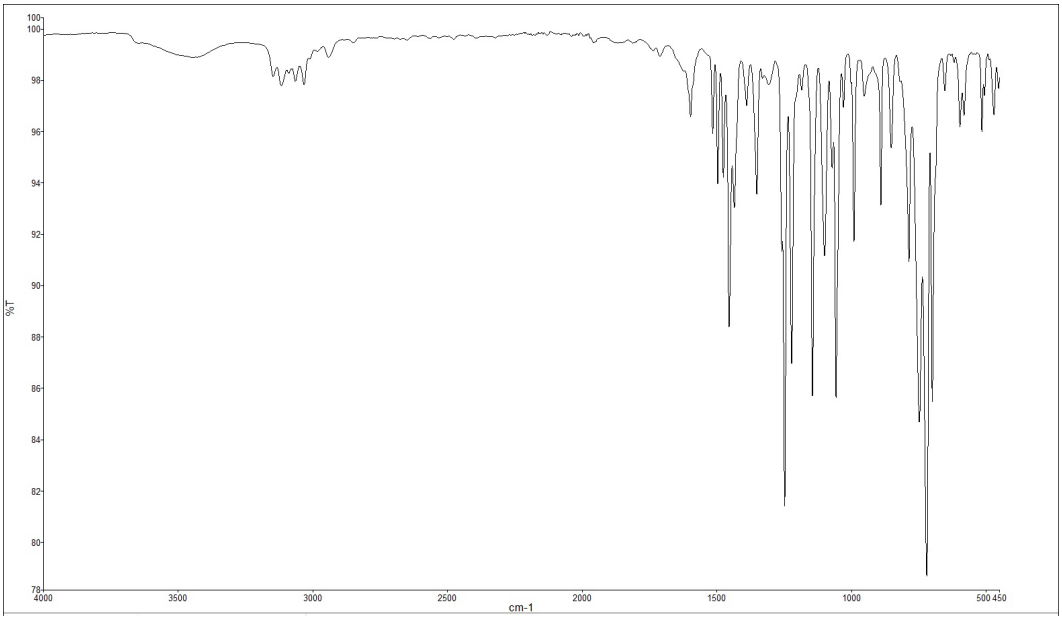


***Figure A3.58.*** Infrared spectrum of compound **3.44**

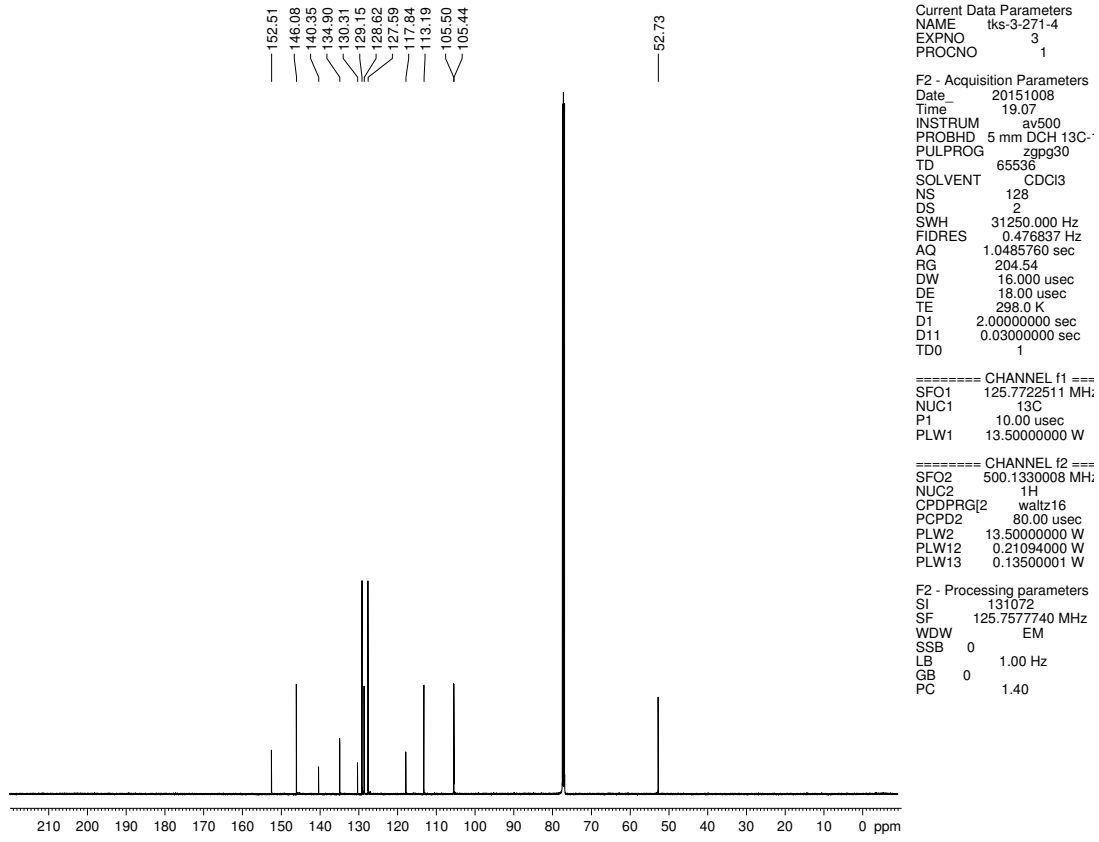


***Figure A3.59.*** $^{13}C$ NMR (125 MHz, $CDCl_3$) of compound **3.44**

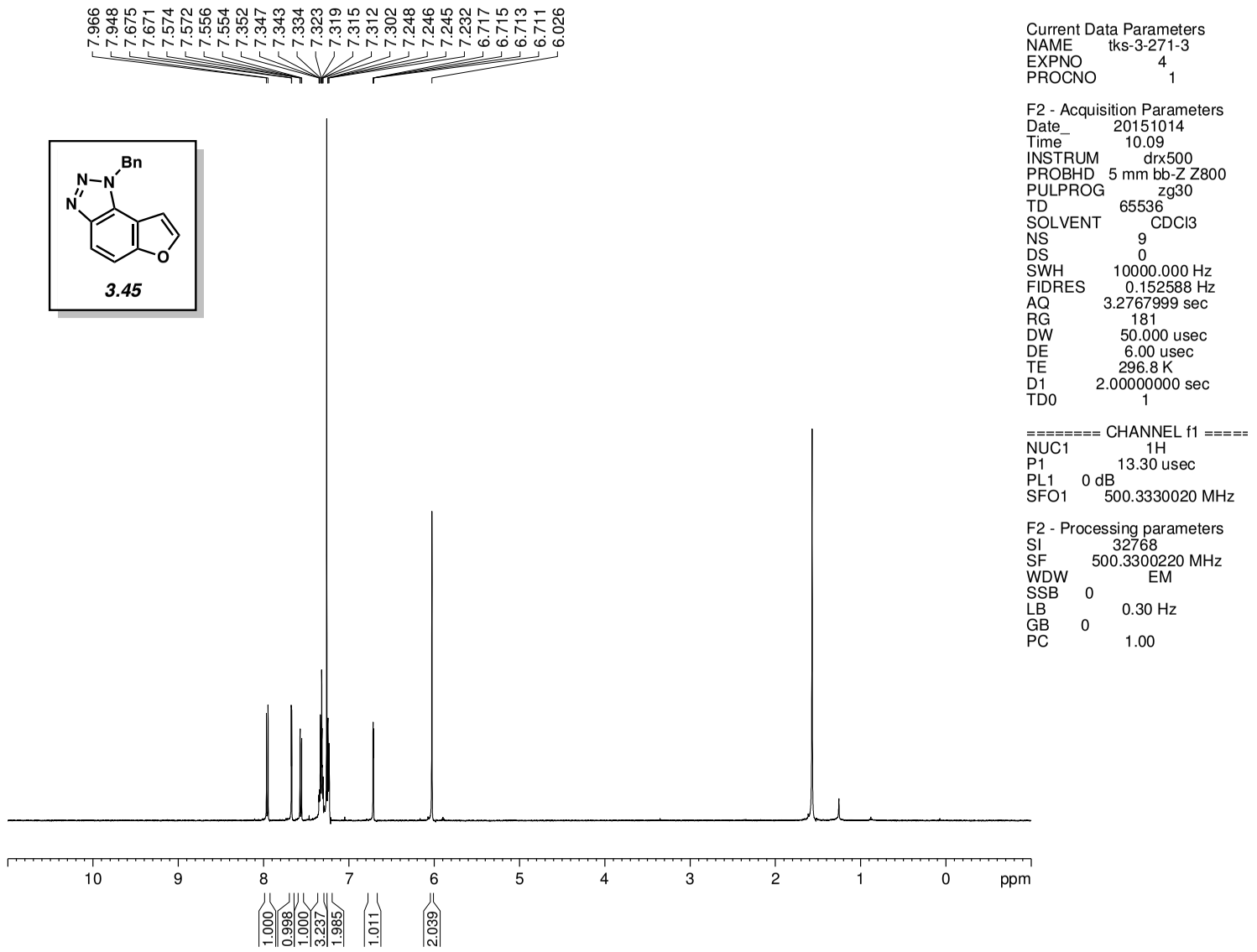


***Figure A3.60.*** $^{1}$H NMR (500 MHz, $CDCl_3$) compound **3.45**

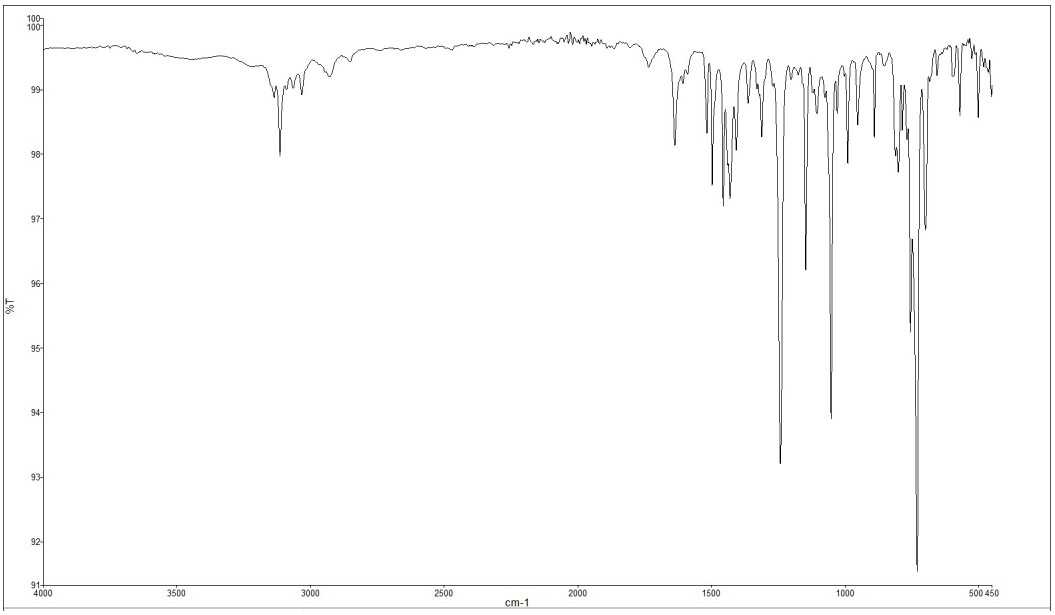


***Figure A3.61.*** Infrared spectrum of compound **3.45**

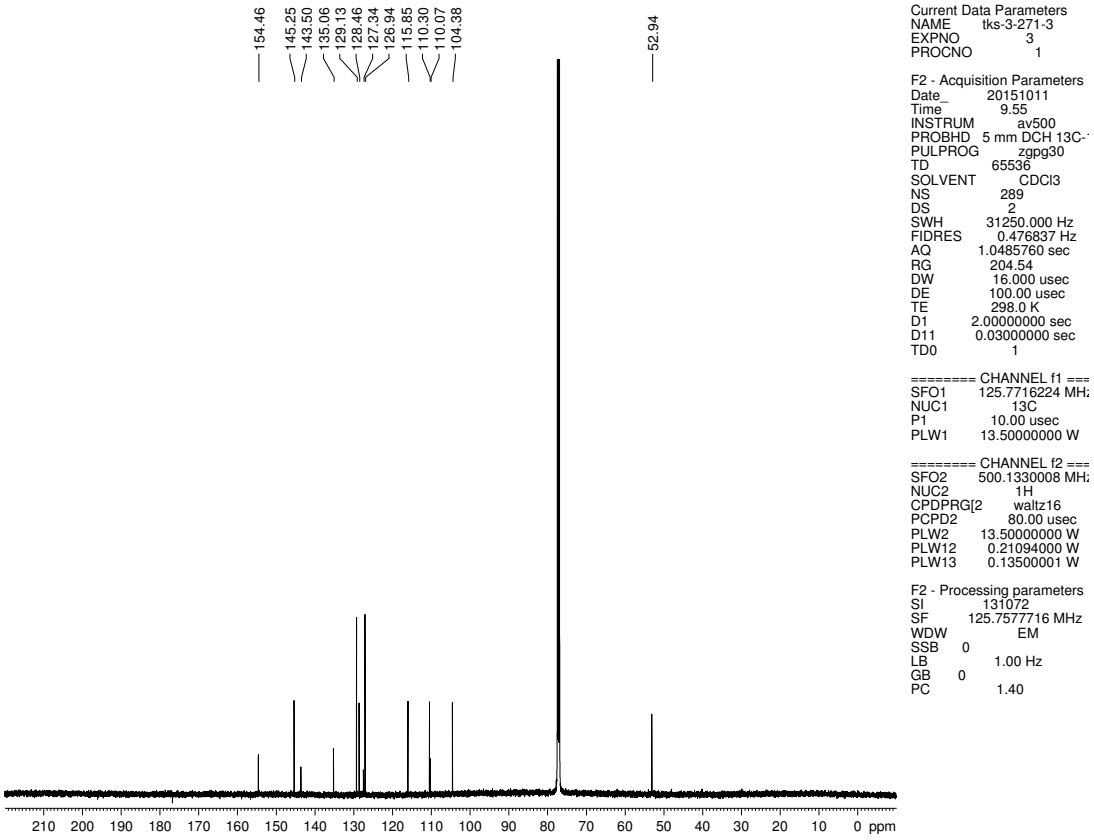


***Figure A3.62.*** $^{13}C$ NMR (125 MHz, $CDCl_3$) of compound **3.45**

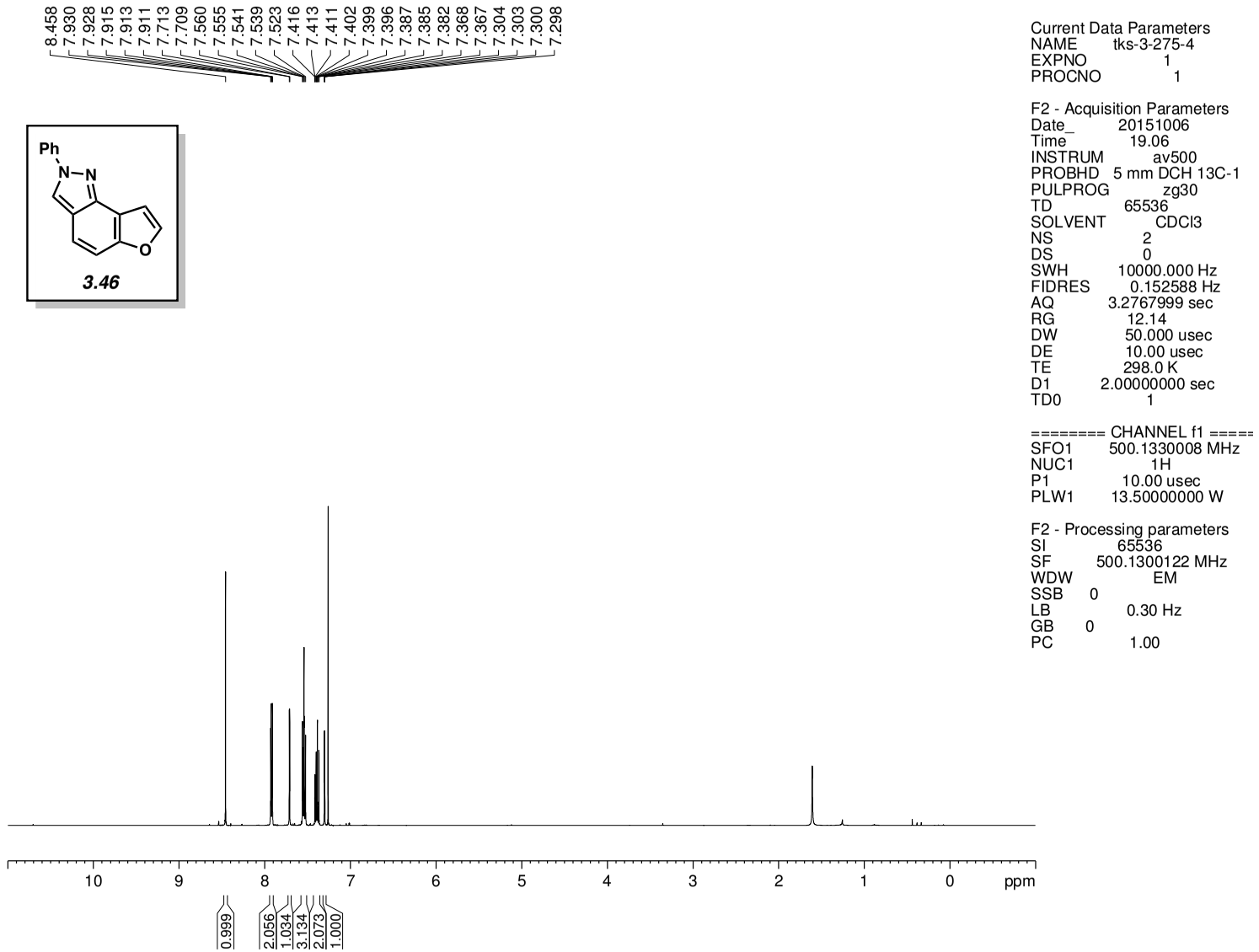


***Figure A3.63.*** $^{1}$H NMR (500 MHz, $CDCl_3$) compound **3.46**

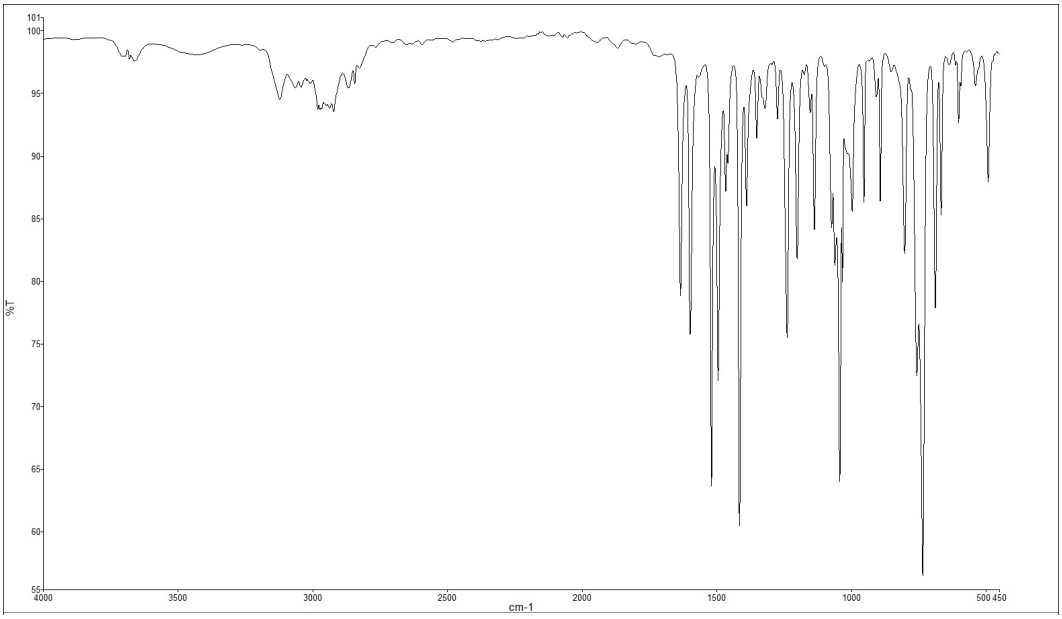


***Figure A3.64.*** Infrared spectrum of compound **3.46**

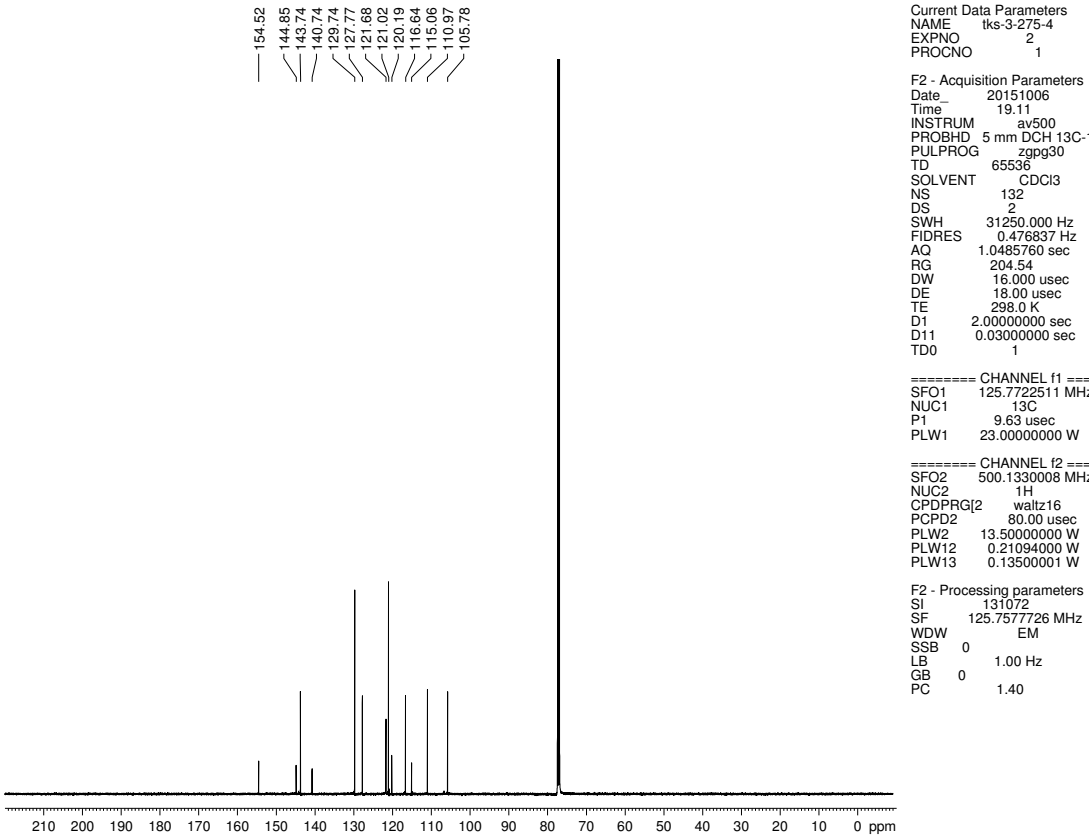


***Figure A3.65.*** $^{13}C$ NMR (125 MHz, $CDCl_3$) of compound **3.46**

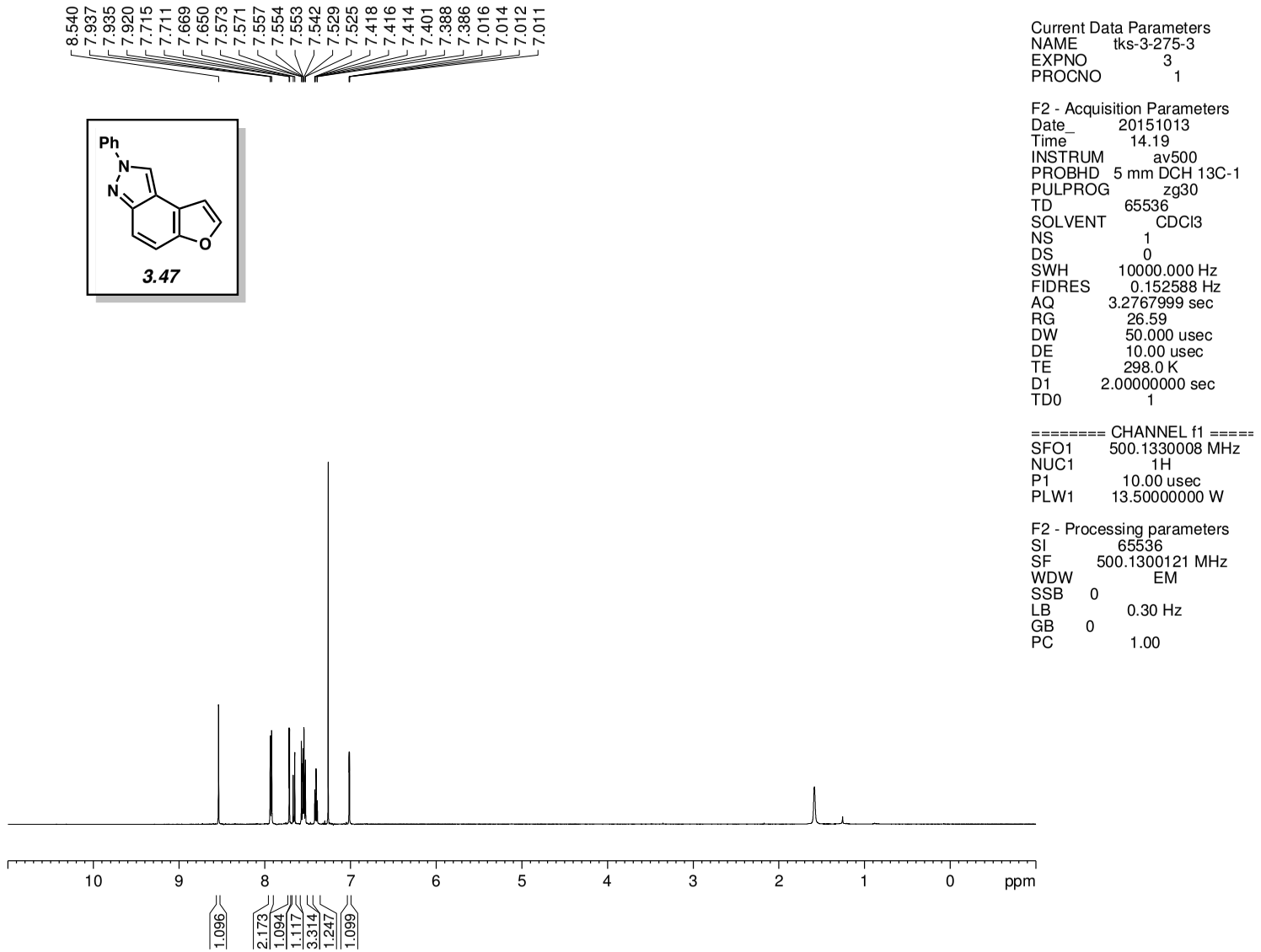


***Figure A3.66.*** $^{1}$H NMR (500 MHz, $CDCl_3$) compound **3.47**

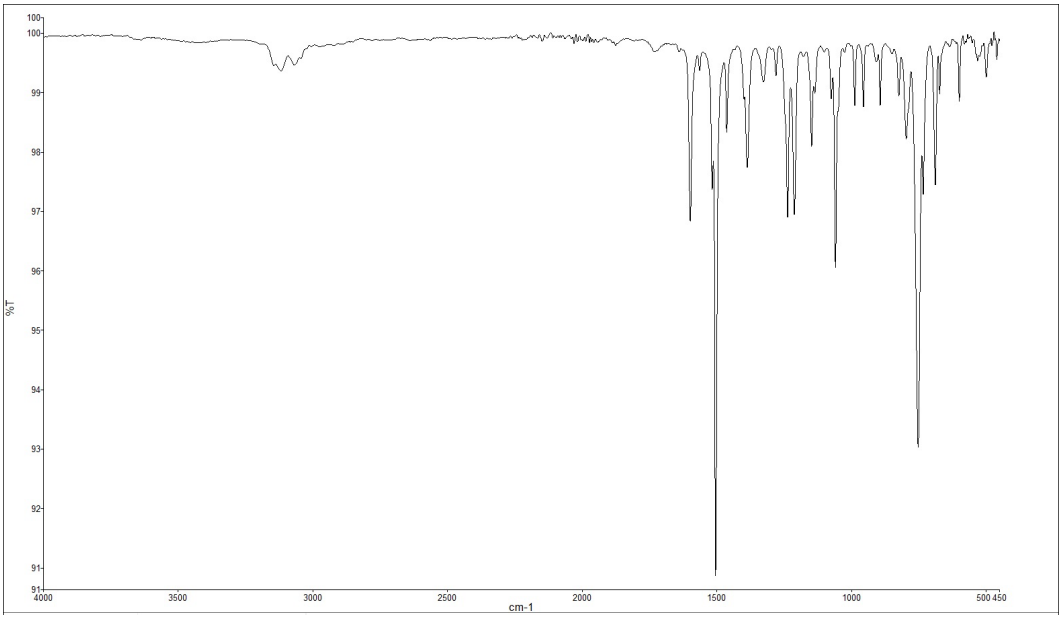


***Figure A3.67.*** Infrared spectrum of compound **3.47**

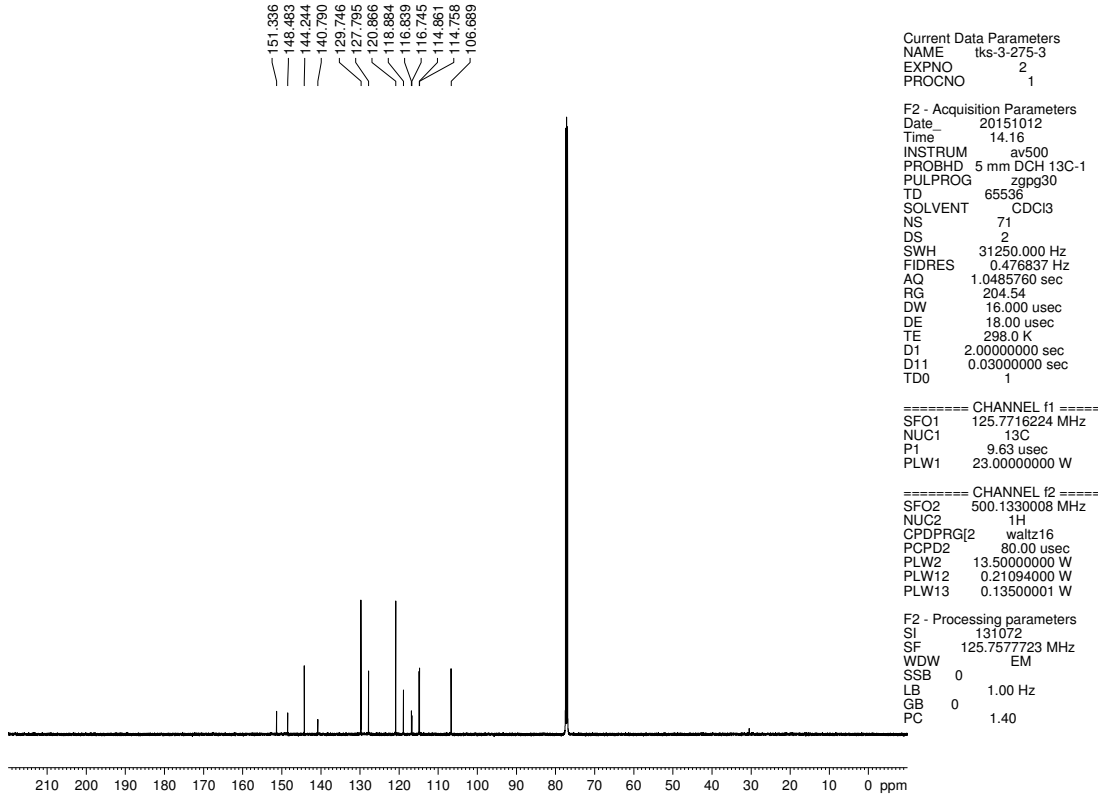


***Figure A3.68.*** $^{13}C$ NMR (125 MHz, $CDCl_3$) of compound **3.47**

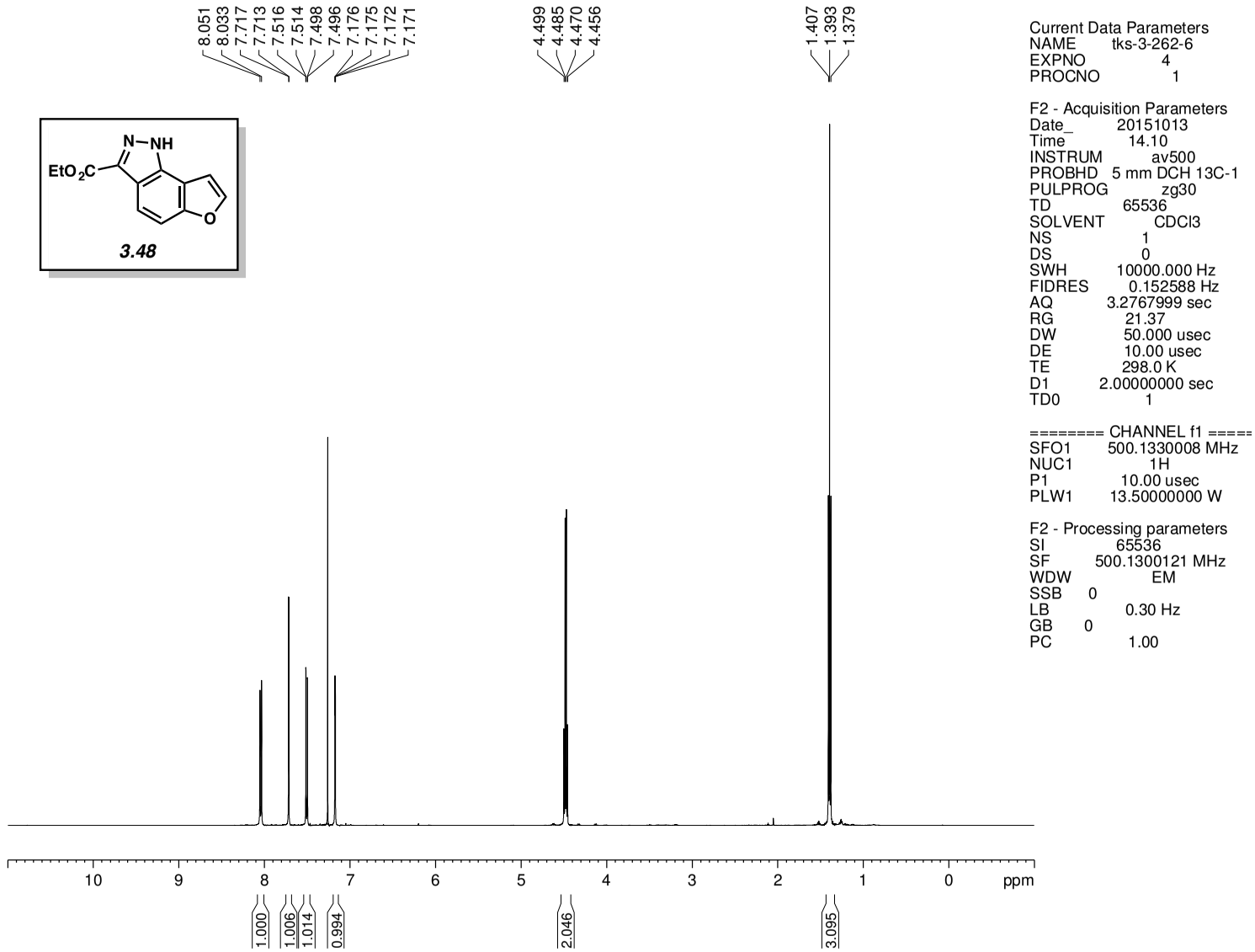


***Figure A3.69.*** $^{1}$H NMR (500 MHz, $CDCl_3$) compound **3.48**

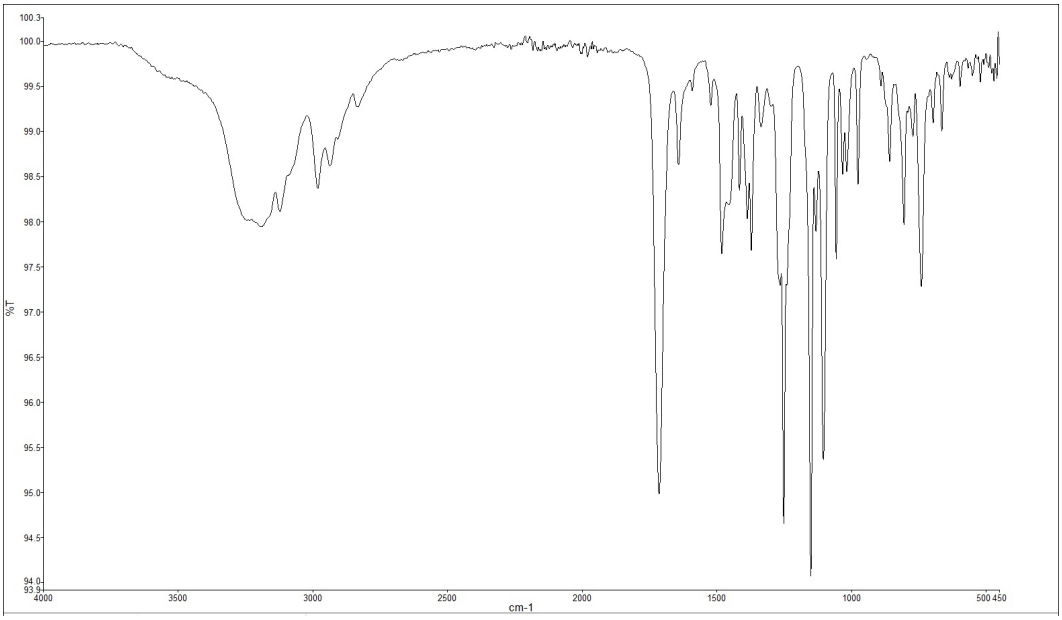


***Figure A3.70.*** Infrared spectrum of compound **3.48**

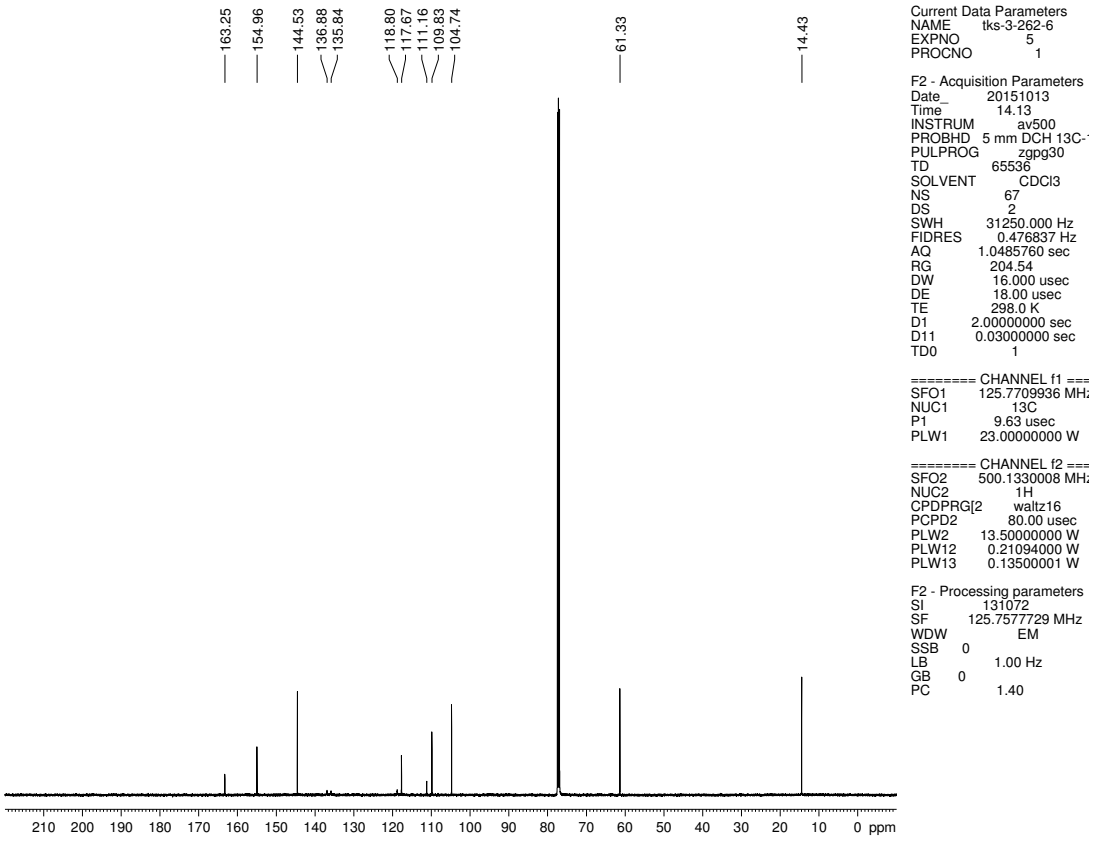


***Figure A3.71.*** $^{13}C$ NMR (125 MHz, $CDCl_3$) of compound **3.48**

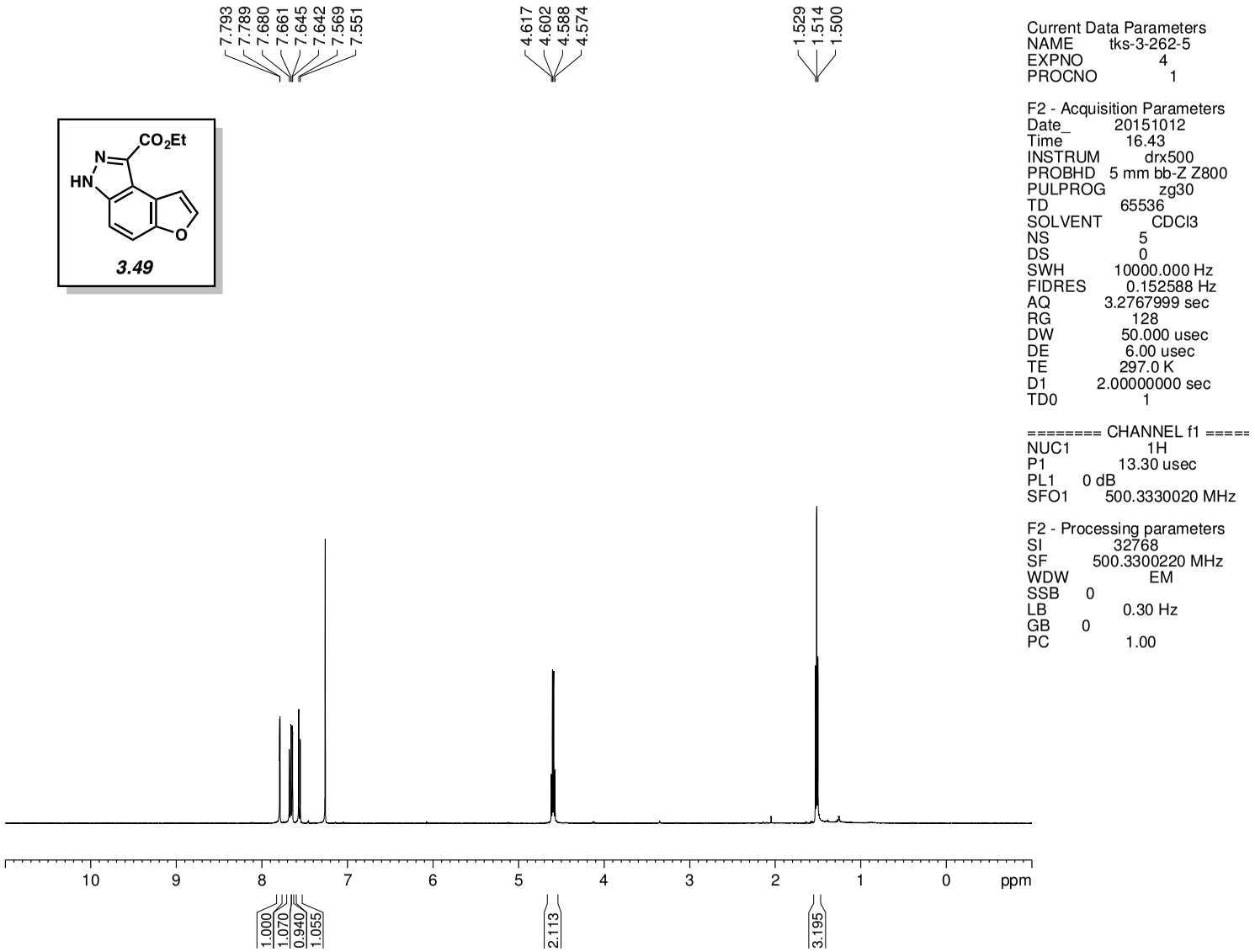


***Figure A3.72.*** $^{1}$H NMR (500 MHz, $CDCl_3$) compound **3.49**

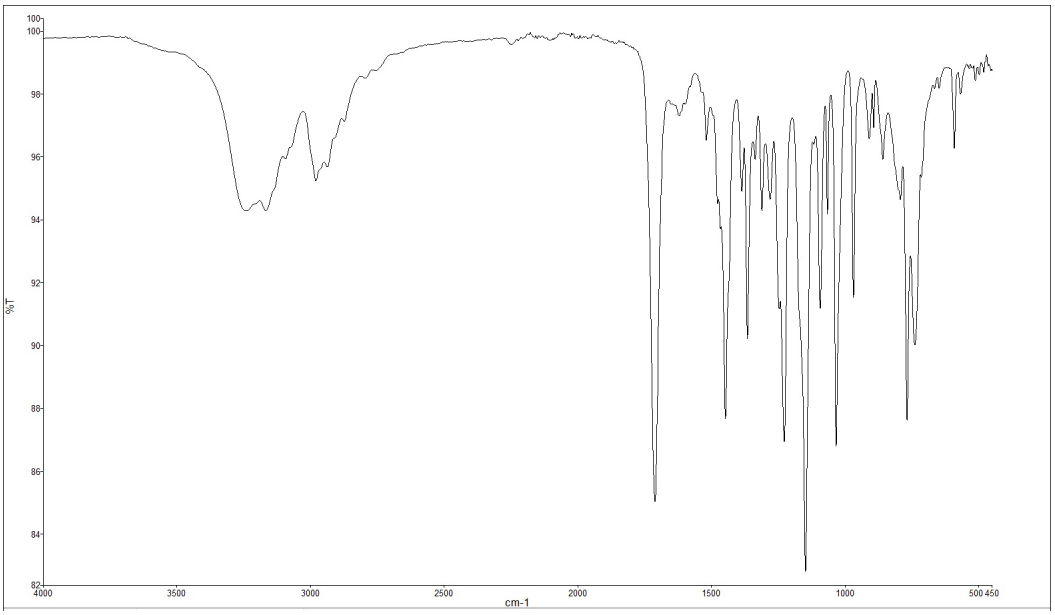


***Figure A3.73.*** Infrared spectrum of compound **3.49**

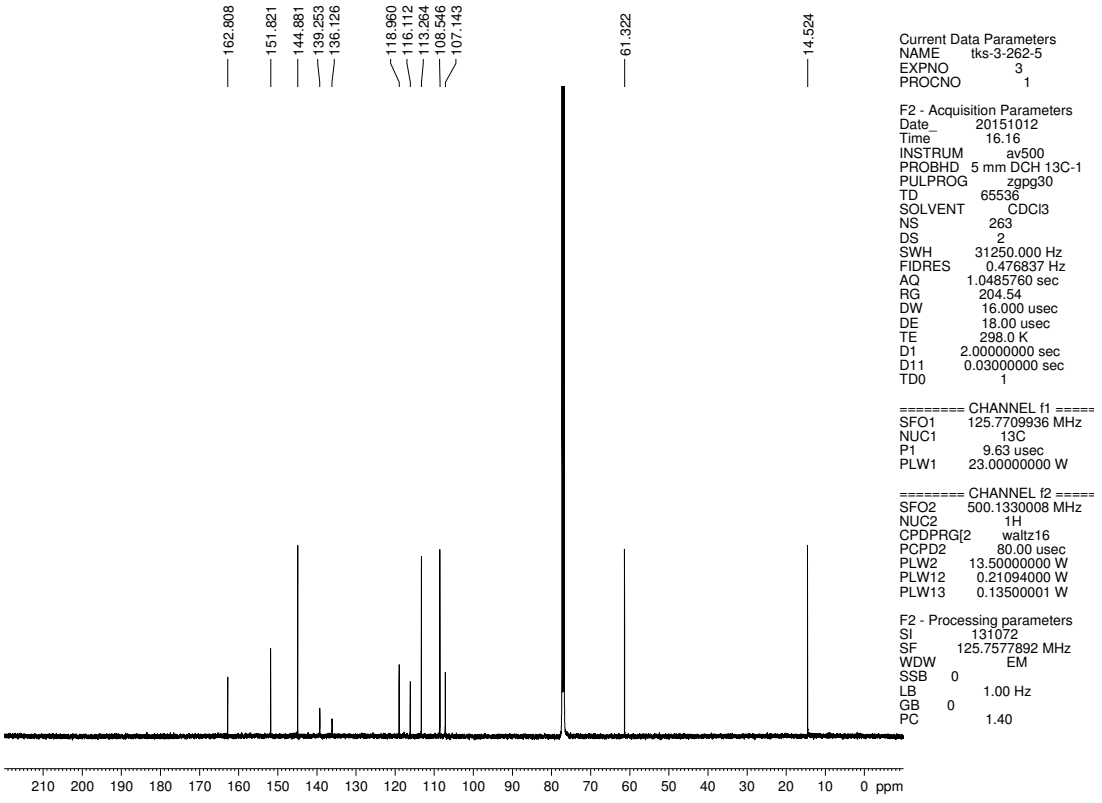


***Figure A3.74.*** $^{13}C$ NMR (125 MHz, $CDCl_3$) of compound **3.49**

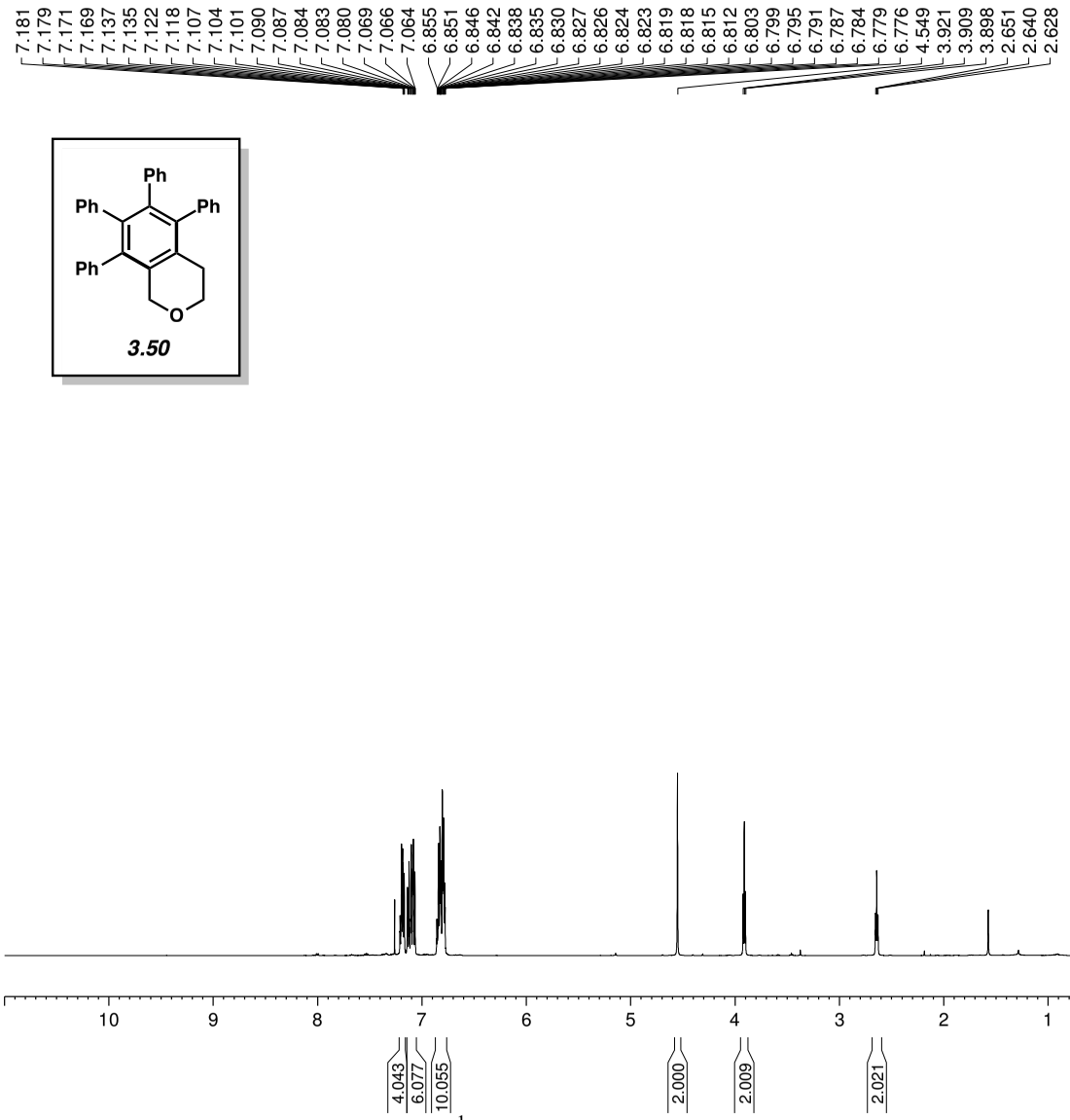


***Figure A3.75.*** $^{1}$H NMR (500 MHz, $CDCl_3$) compound **3.50**

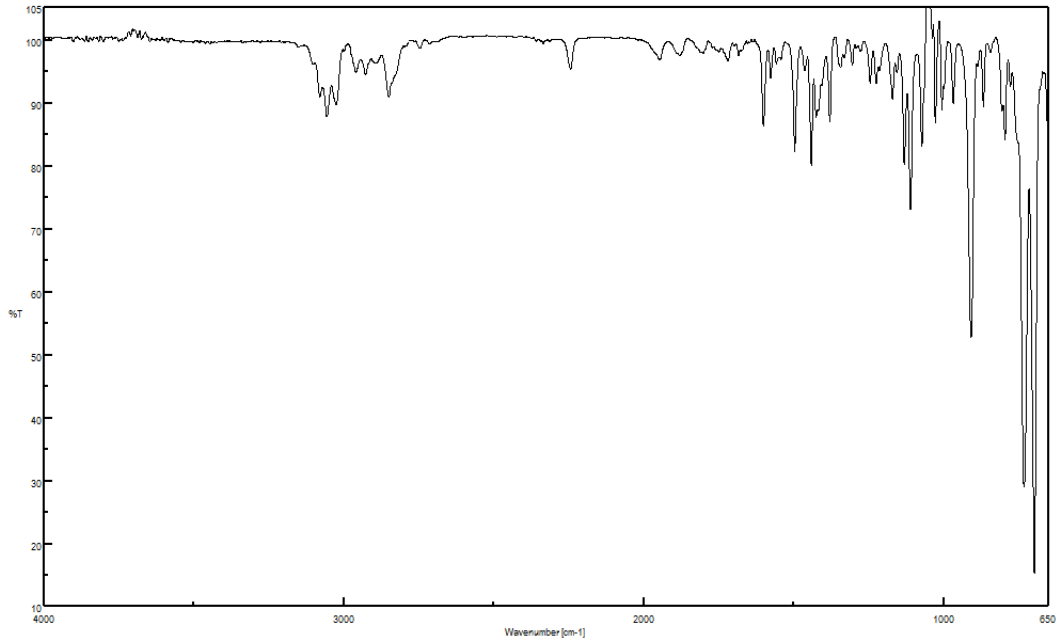


***Figure A3.76.*** Infrared spectrum of compound **3.50**

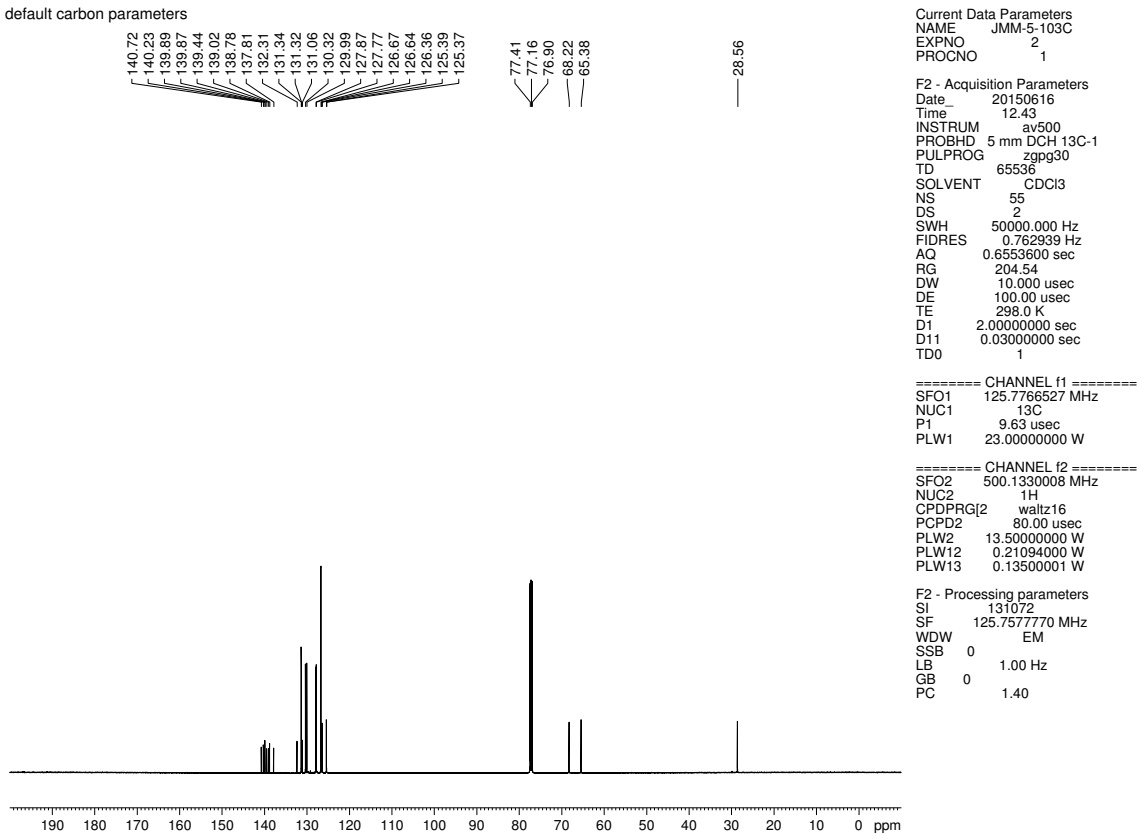


***Figure A3.77.*** $^{13}$C NMR (125 MHz, $CDCl_3$) of compound **3.50**

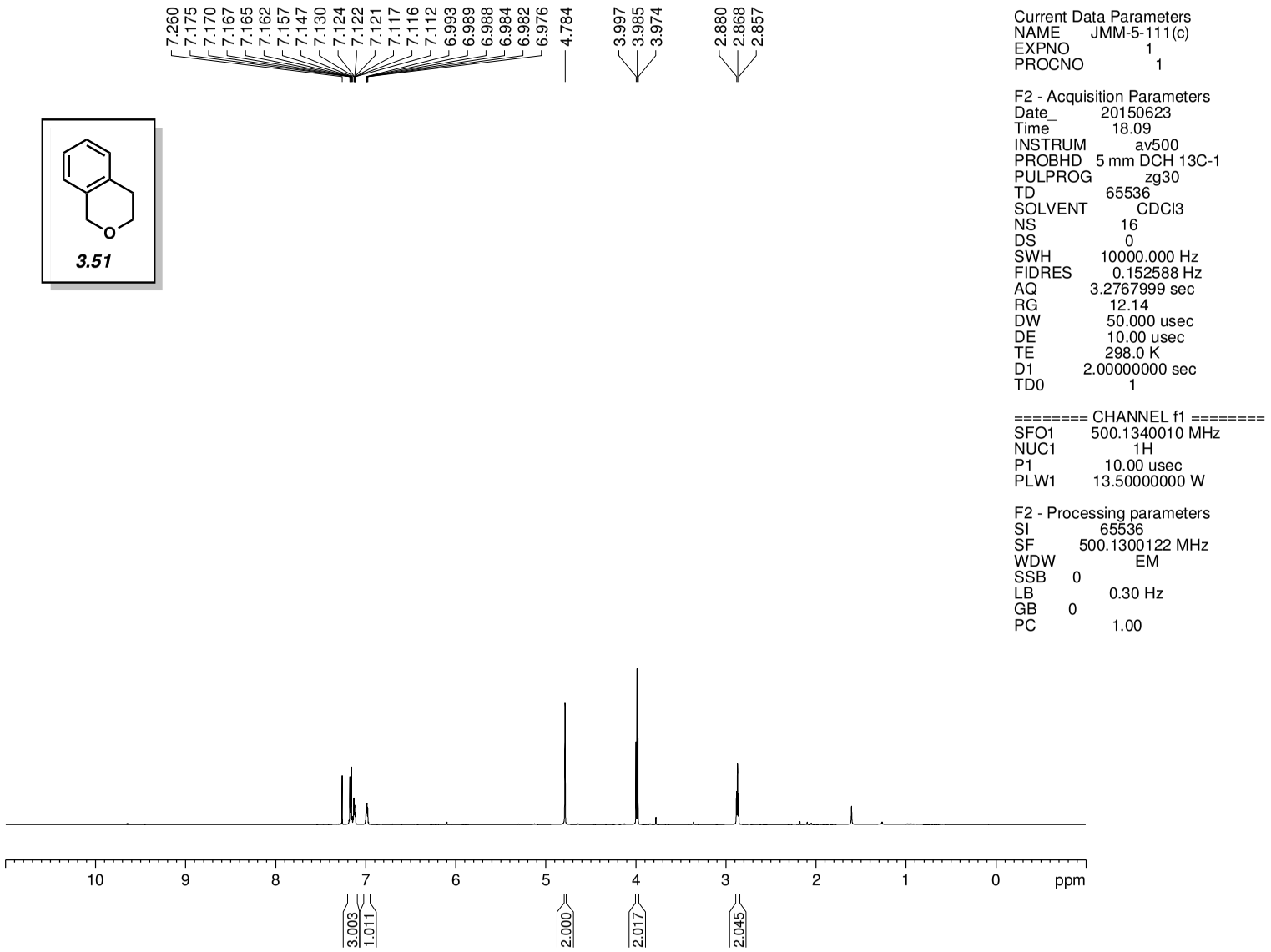


***Figure A3.78.*** $^{1}$H NMR (500 MHz, $CDCl_3$) compound **3.51**

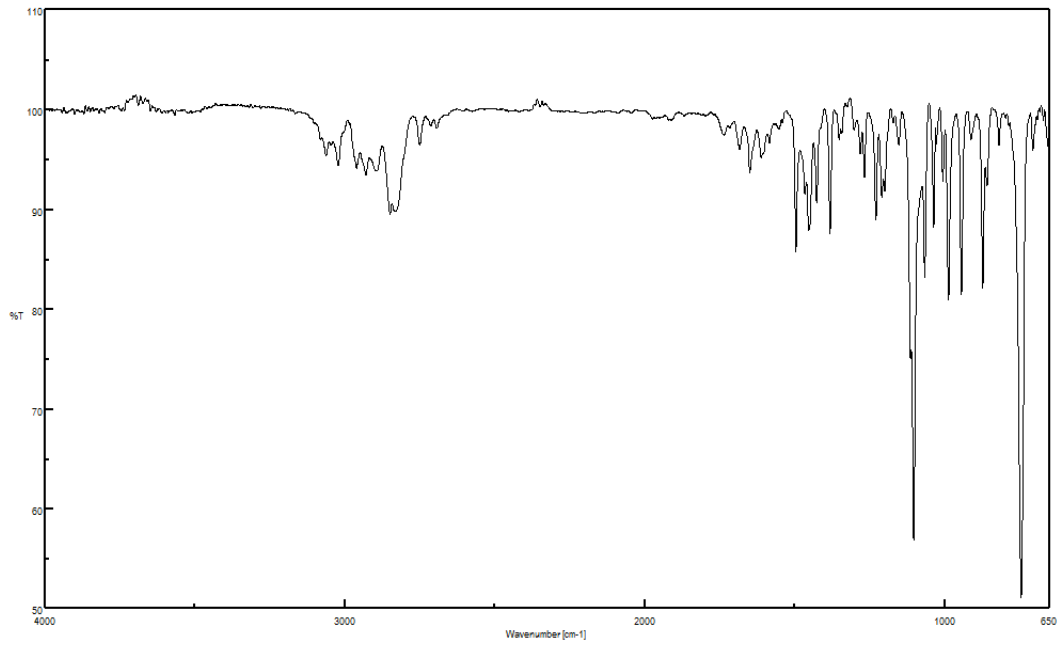


***Figure A3.79.*** Infrared spectrum of compound **3.51**

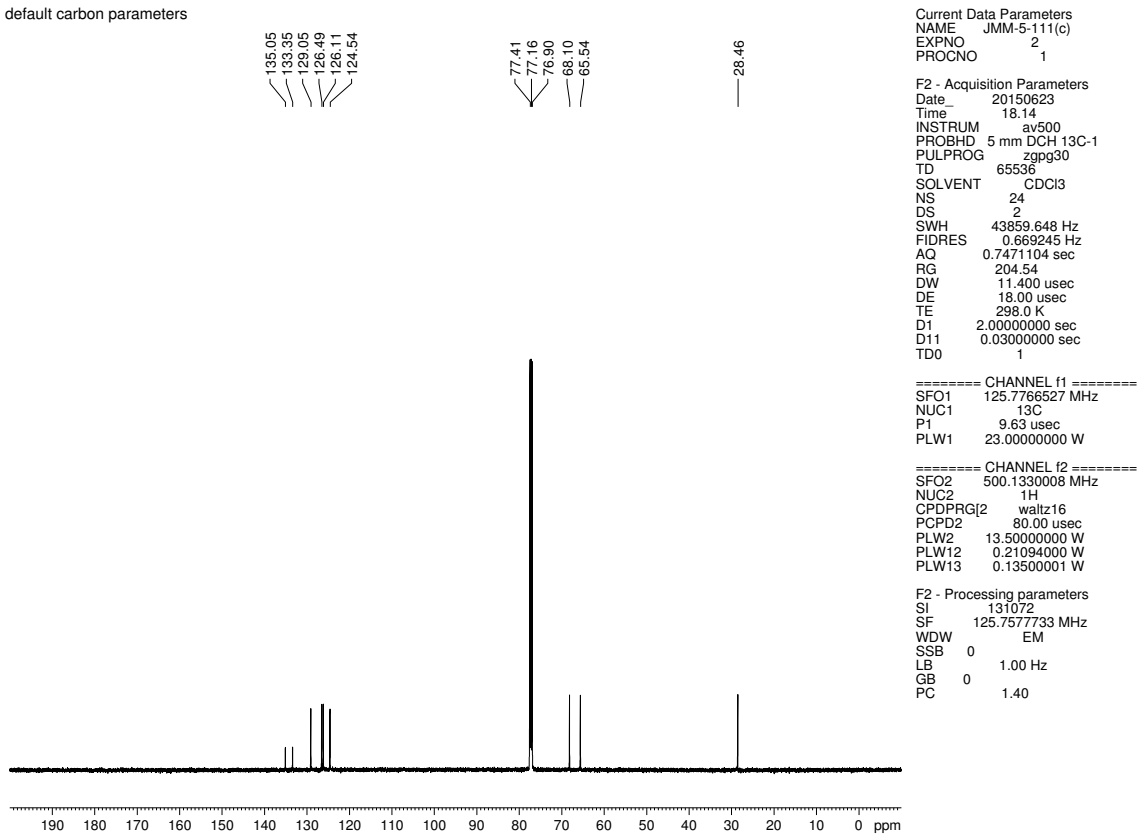


***Figure A3.80.*** $^{13}C$ NMR (125 MHz, $CDCl_3$) of compound **3.51**

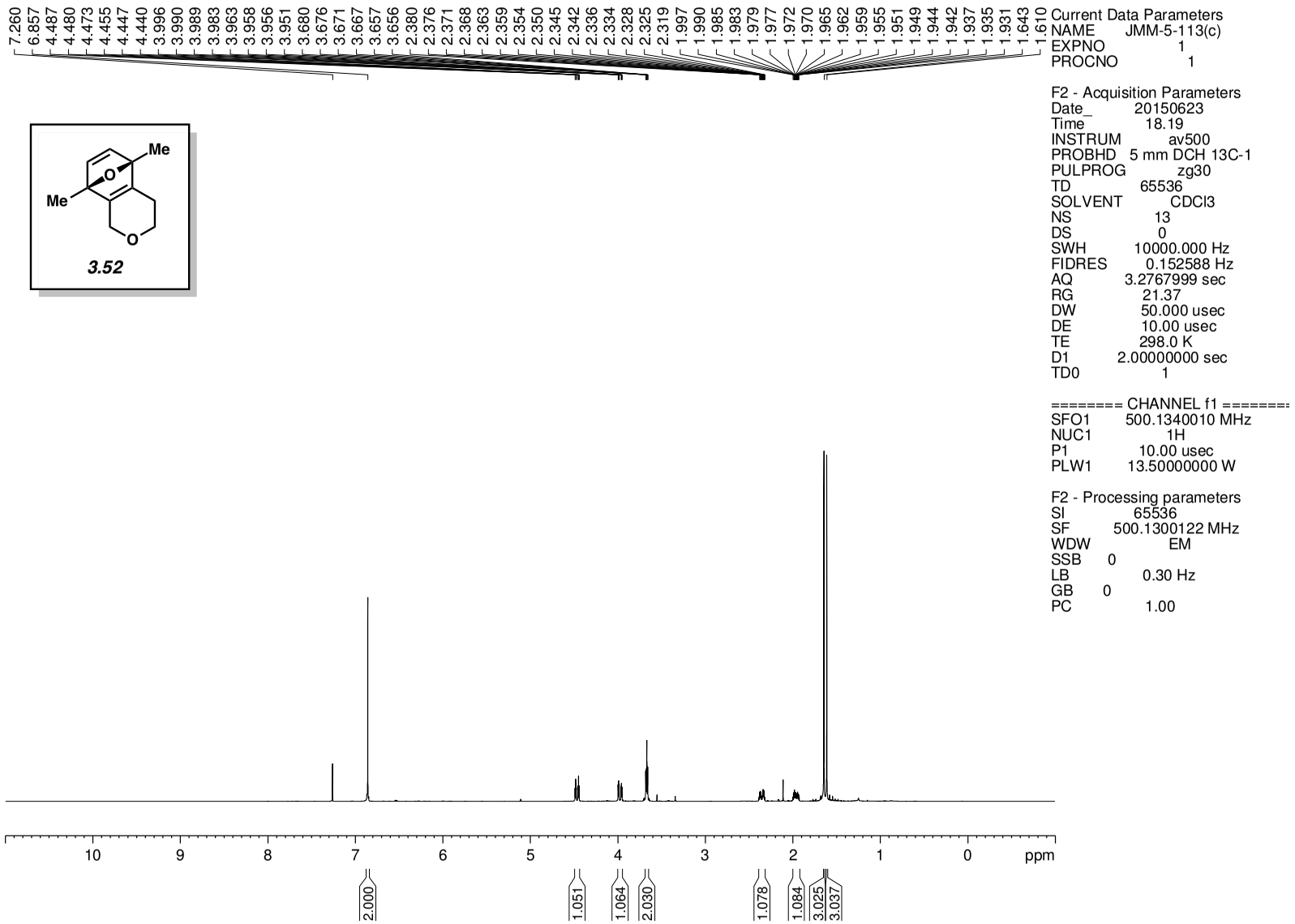


***Figure A3.81.*** $^{1}$H NMR (500 MHz, $CDCl_3$) compound **3.52**

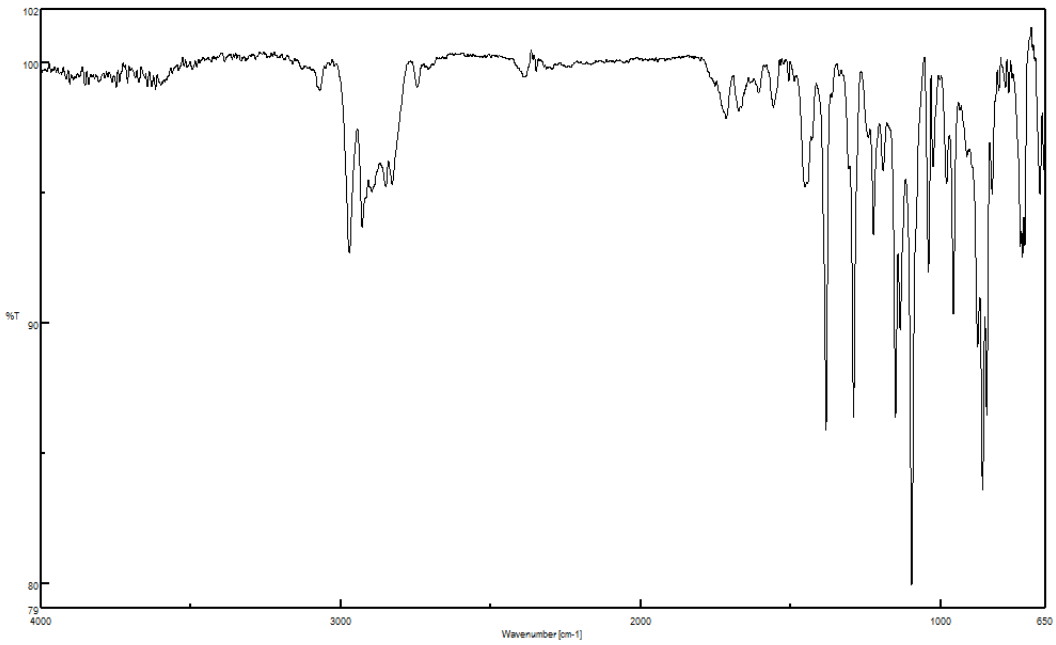


***Figure A3.82.*** Infrared spectrum of compound **3.52**

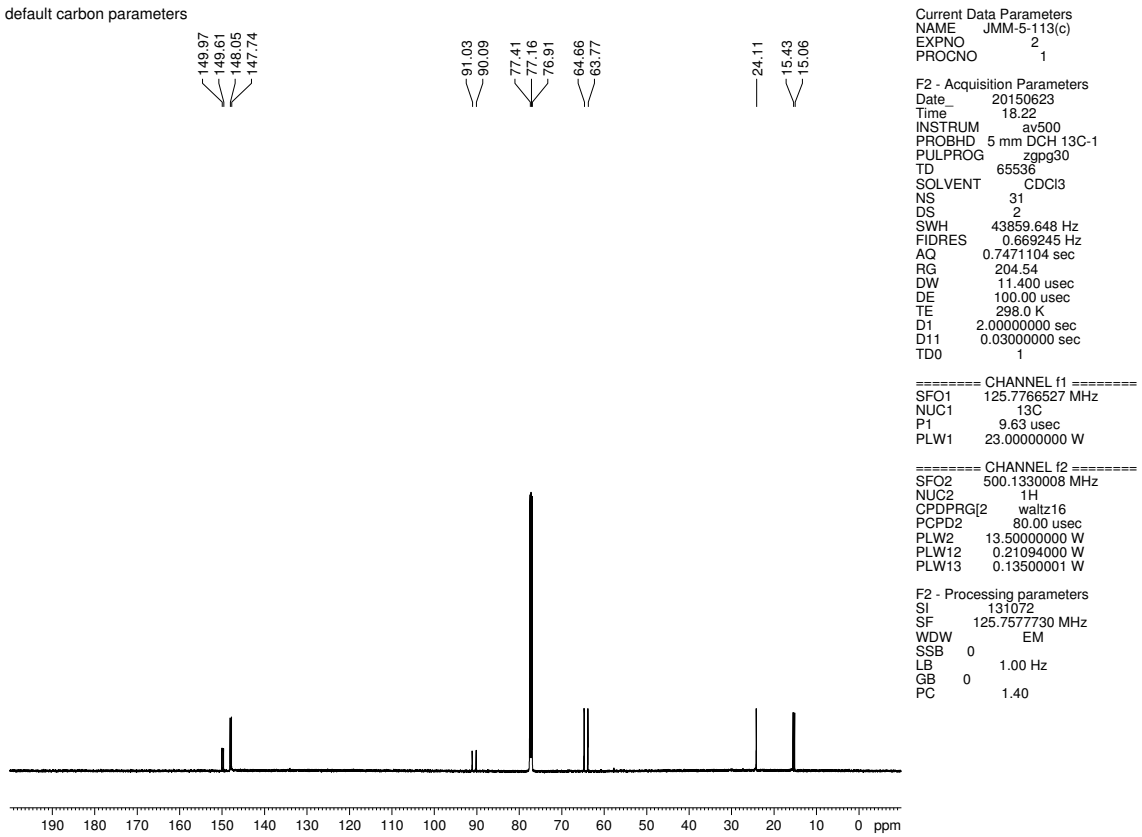


***Figure A3.83.*** $^{13}C$ NMR (125 MHz, $CDCl_3$) of compound **3.52**

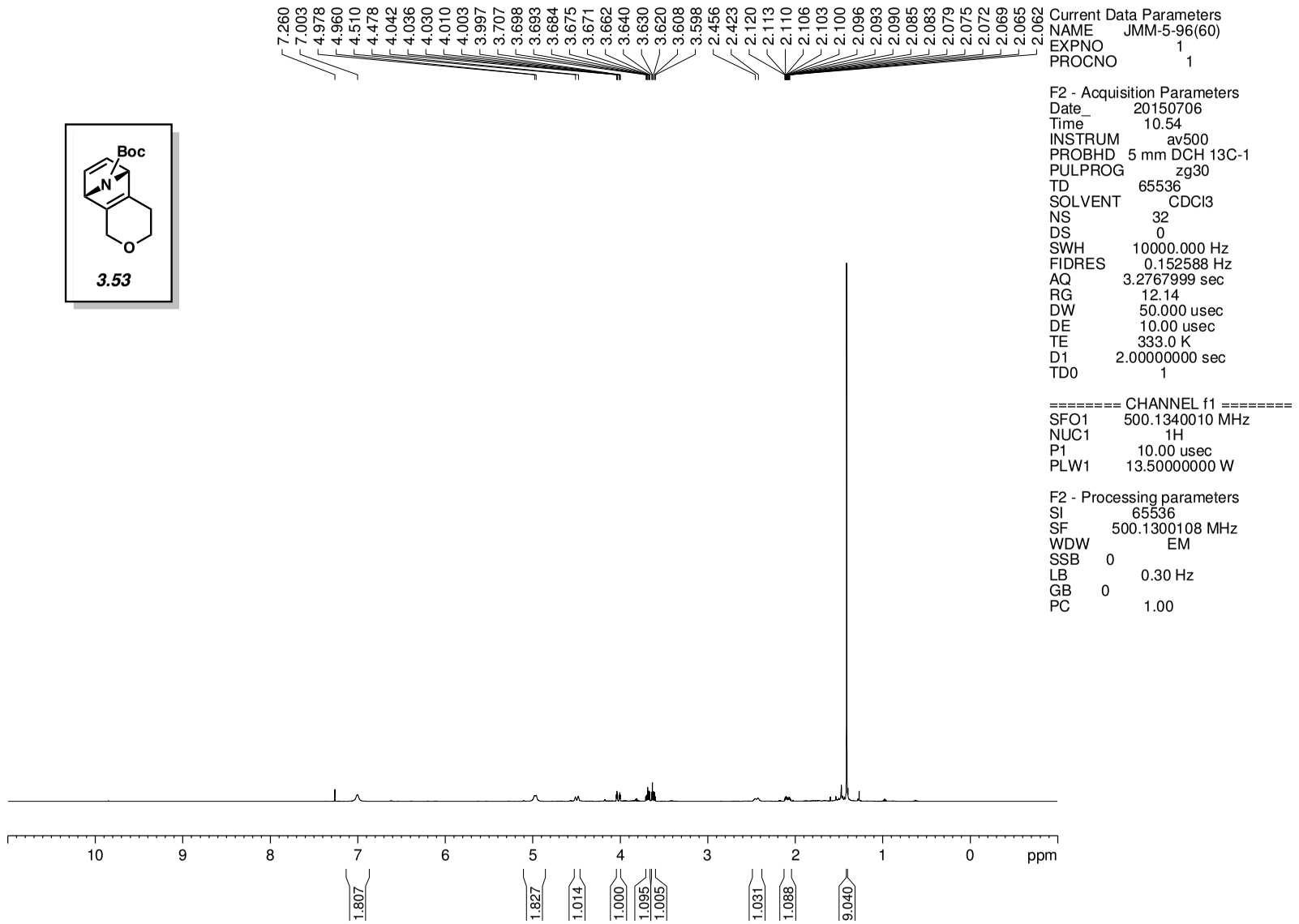


***Figure A3.84.*** $^{1}$H NMR (500 MHz, $CDCl_3$) compound **3.53**

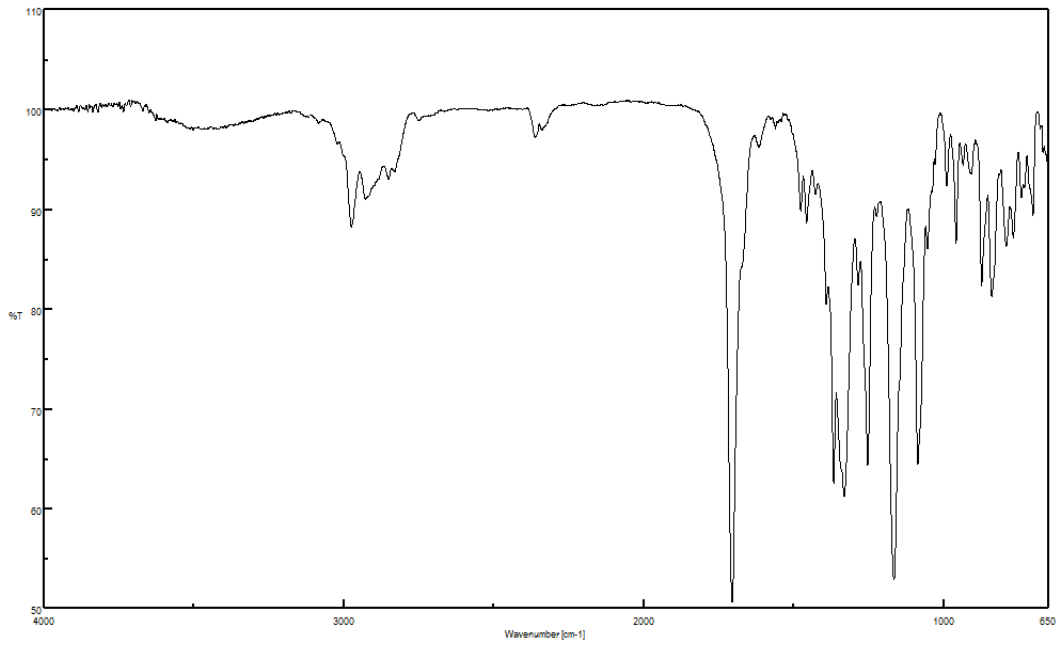


***Figure A3.85.*** Infrared spectrum of compound **3.53**

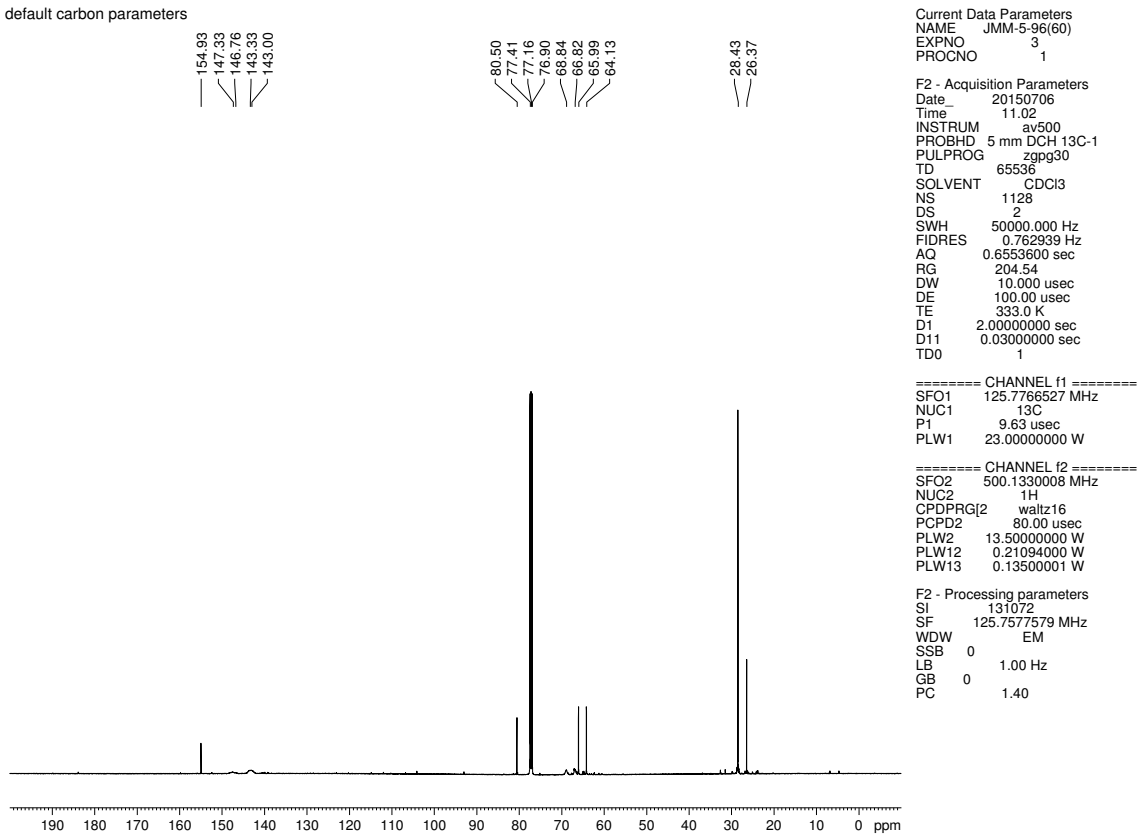


***Figure A3.86.*** $^{13}C$ NMR (125 MHz, $CDCl_3$) of compound **3.53**

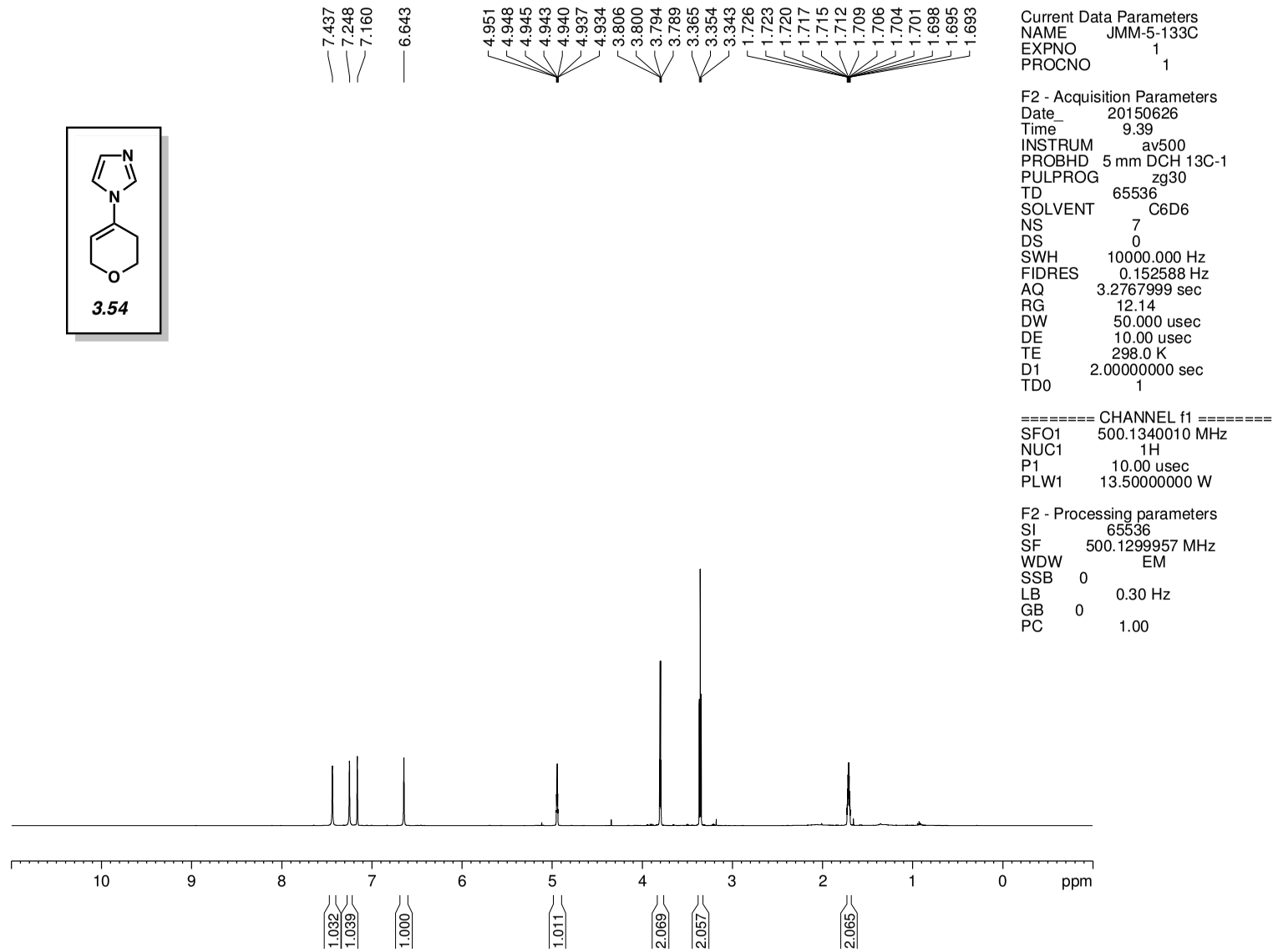


***Figure A3.87.*** $^{1}$H NMR (500 MHz, $C_6D_6$) compound **3.54**

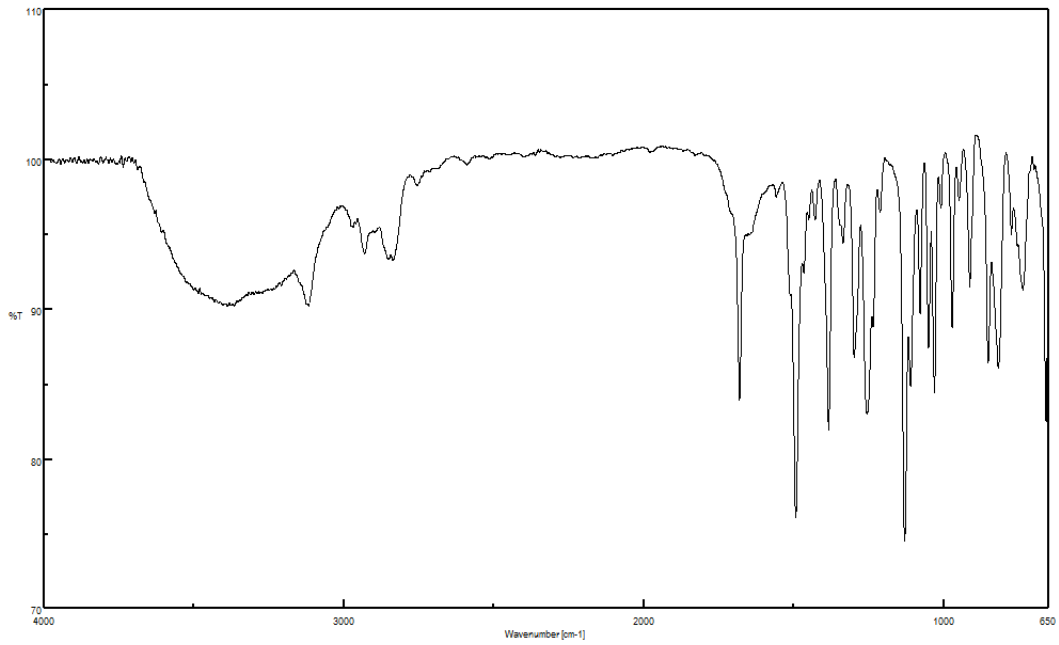


***Figure A3.88.*** Infrared spectrum of compound **3.54**

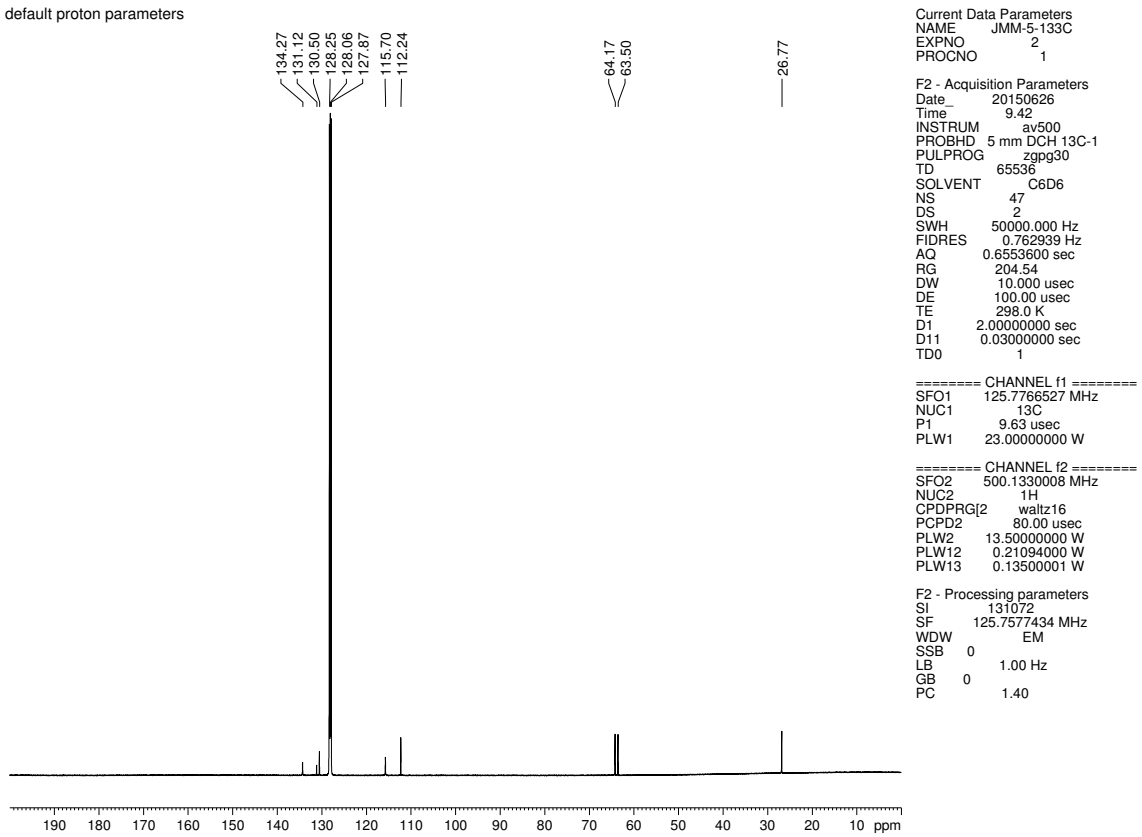


***Figure A3.89.*** $^{13}$C NMR (125 MHz, $C_6D_6$) of compound **3.54**

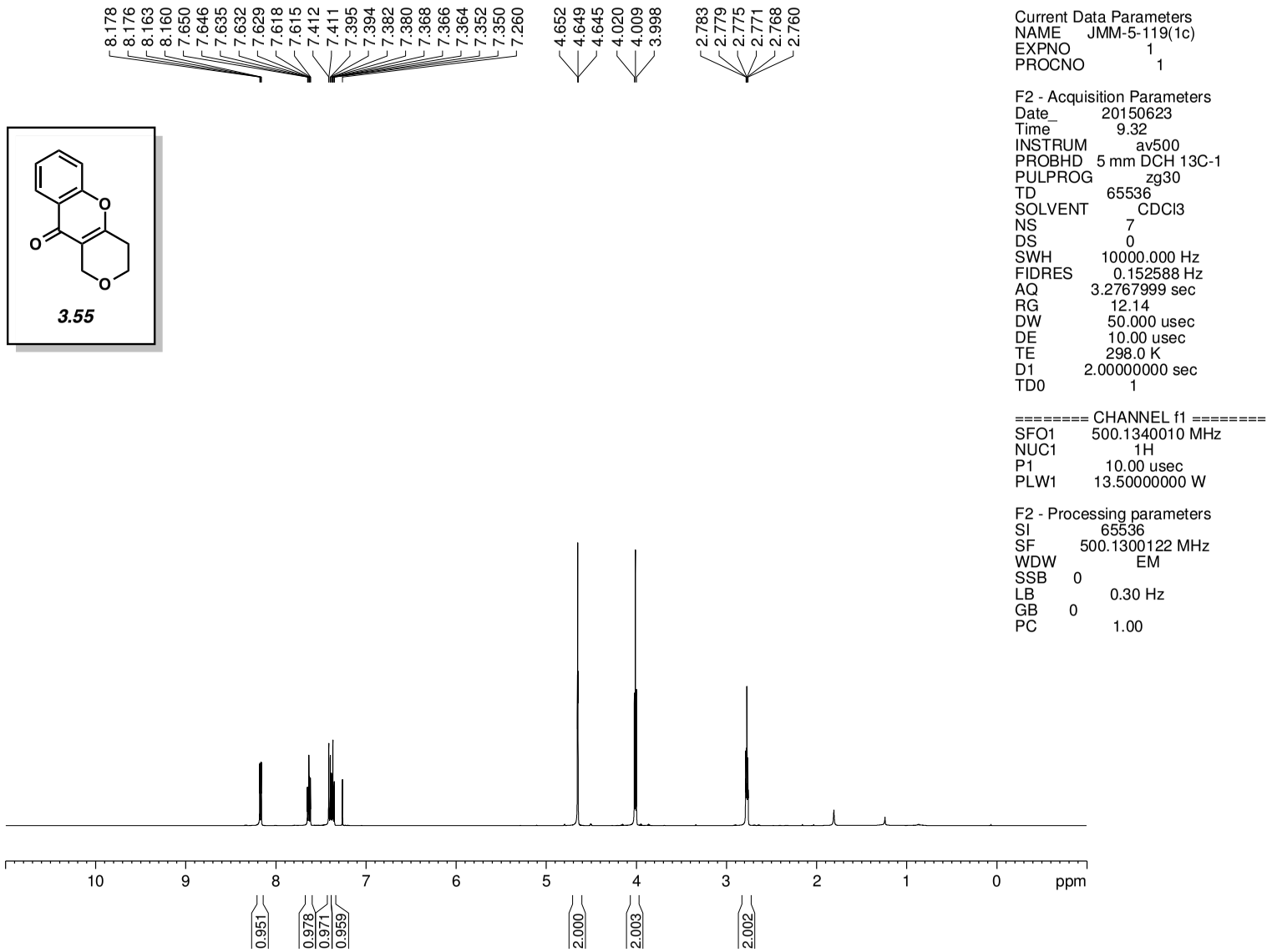


***Figure A3.90.*** $^{1}$H NMR (500 MHz, $CDCl_3$) compound **3.55**

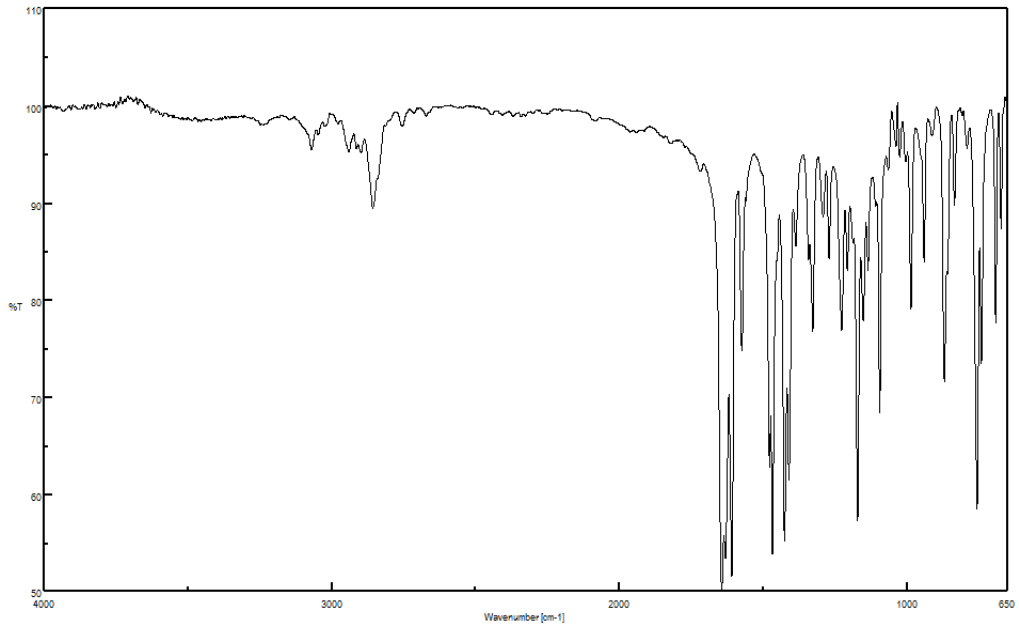


***Figure A3.91.*** Infrared spectrum of compound **3.55**

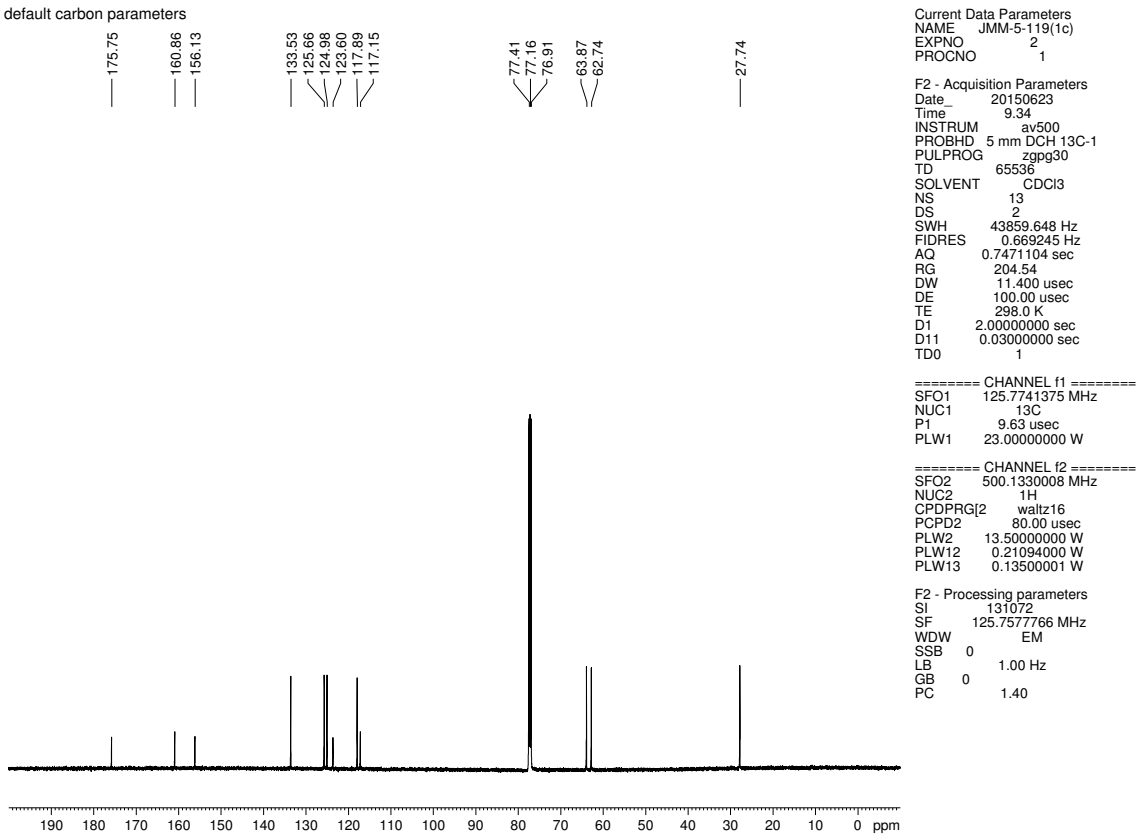


***Figure A3.92.*** $^{13}$C NMR (125 MHz, $CDCl_3$) of compound **3.55**

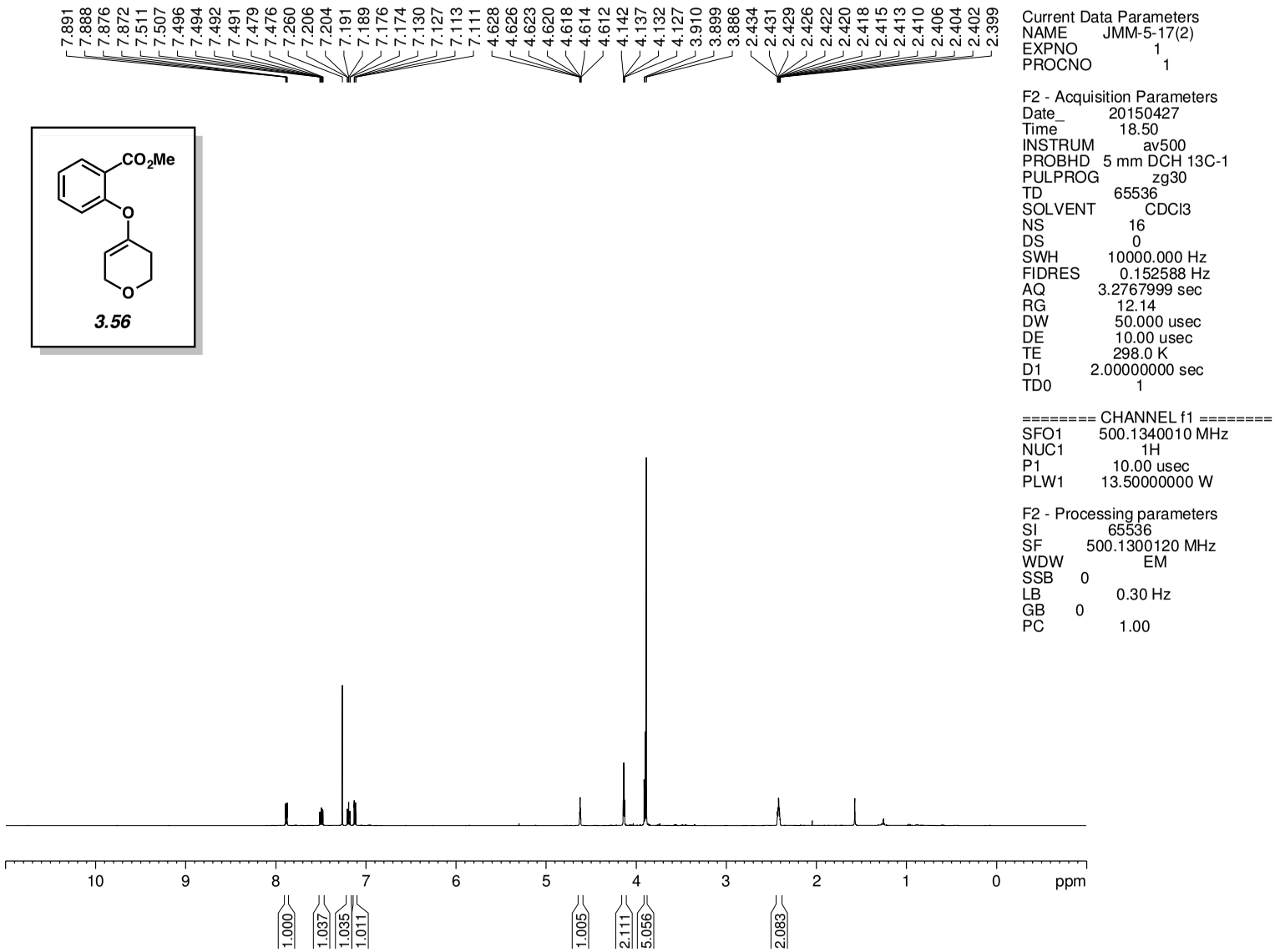


***Figure A3.93.*** $^{1}$H NMR (500 MHz, $CDCl_3$) compound **3.56**

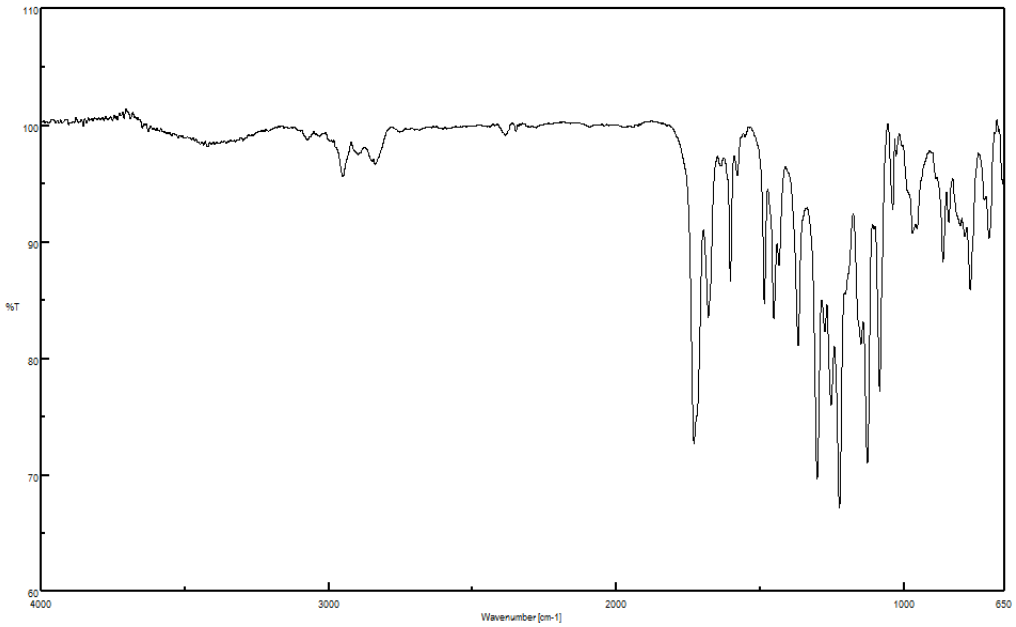


***Figure A3.94.*** Infrared spectrum of compound **3.56**

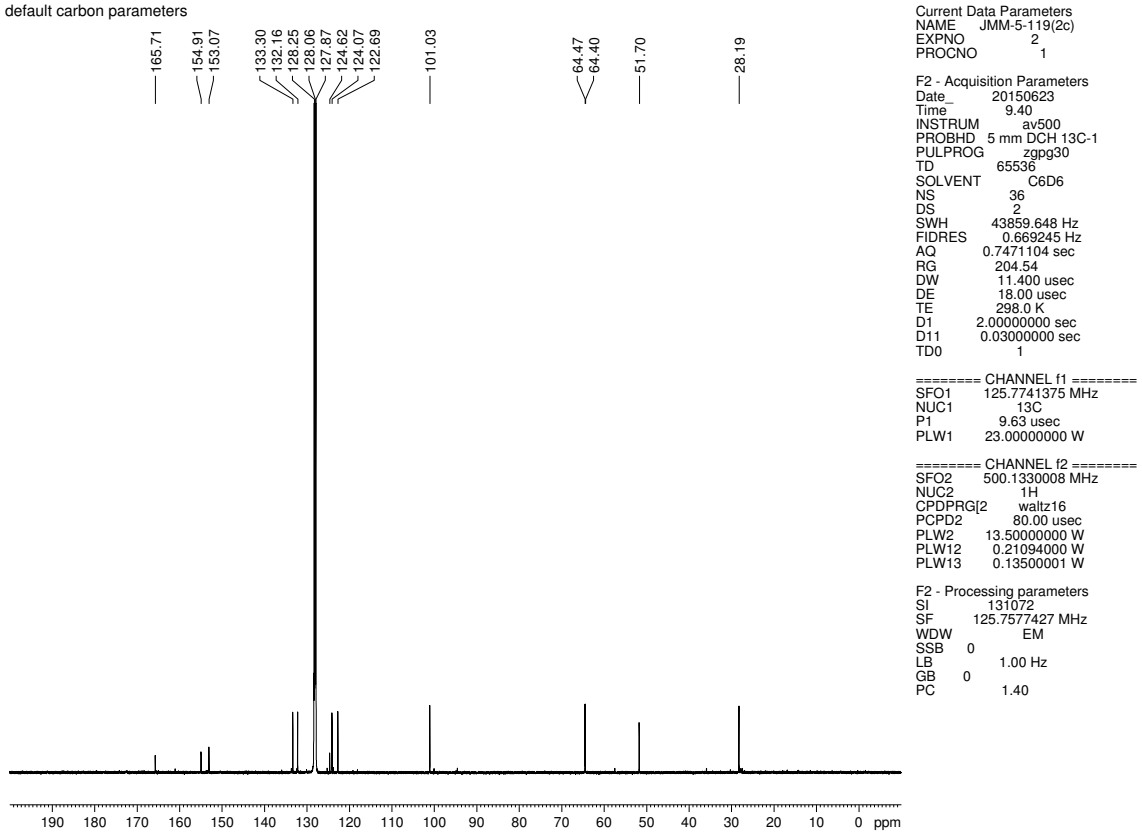


***Figure A3.95.*** $^{13}C$ NMR (125 MHz, $C_6D_6$) of compound **3.56**

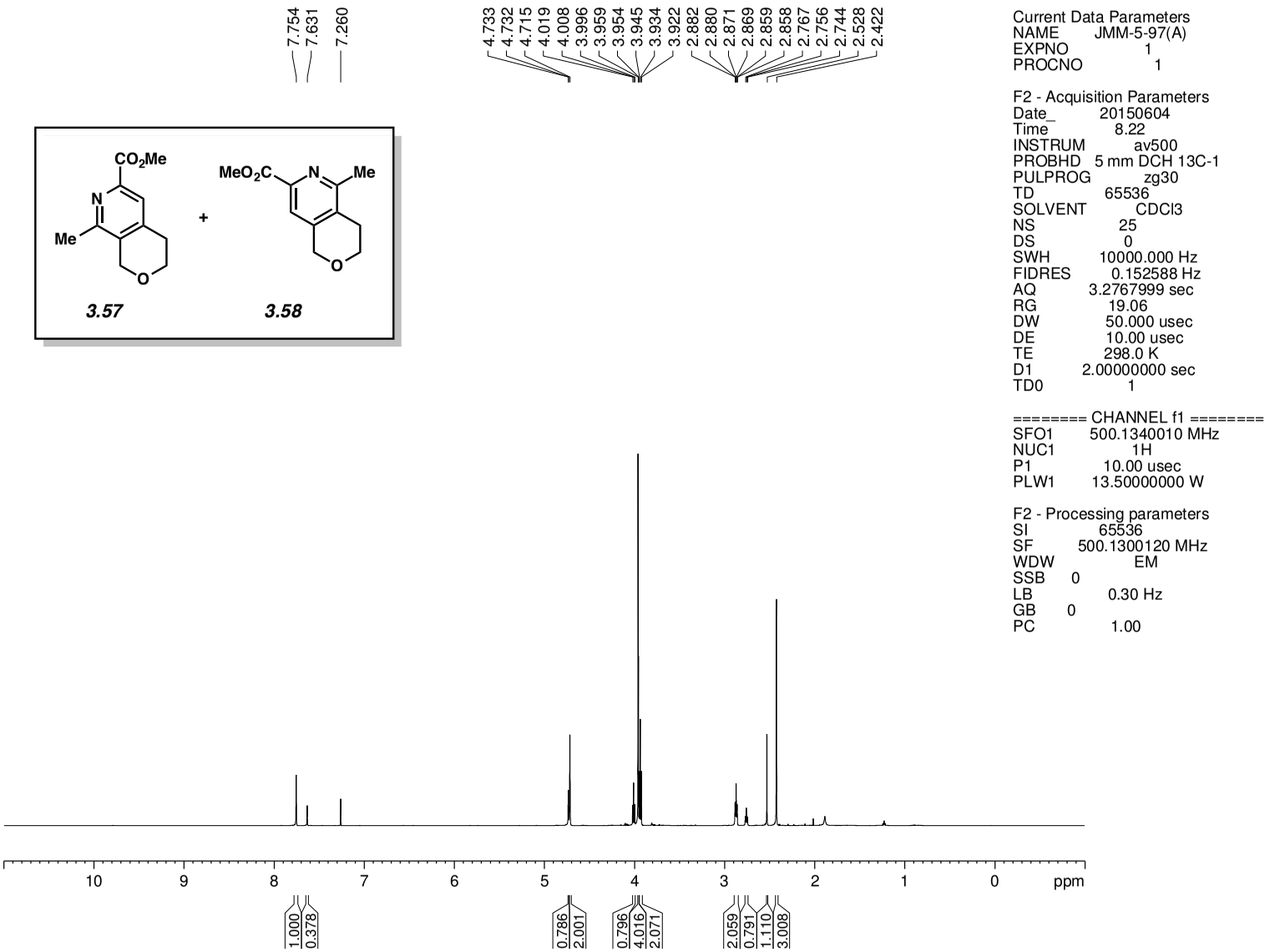


***Figure A3.96.*** $^{1}$H NMR (500 MHz, $CDCl_3$) compound **3.57** & **3.58**

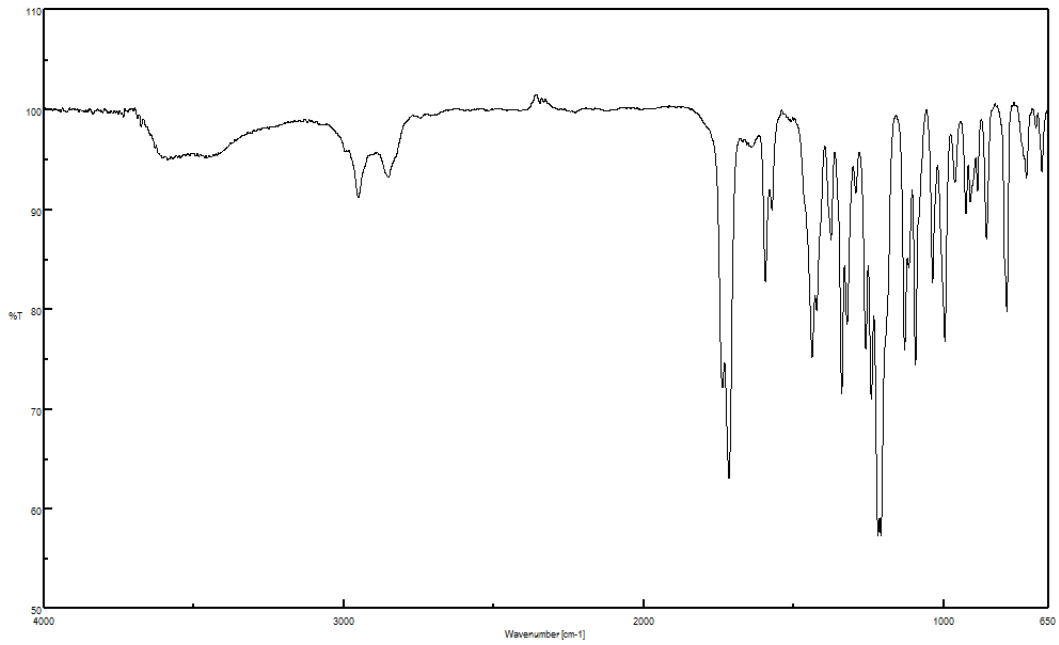


***Figure A3.97.*** Infrared spectrum of compound **3.57** & **3.58**

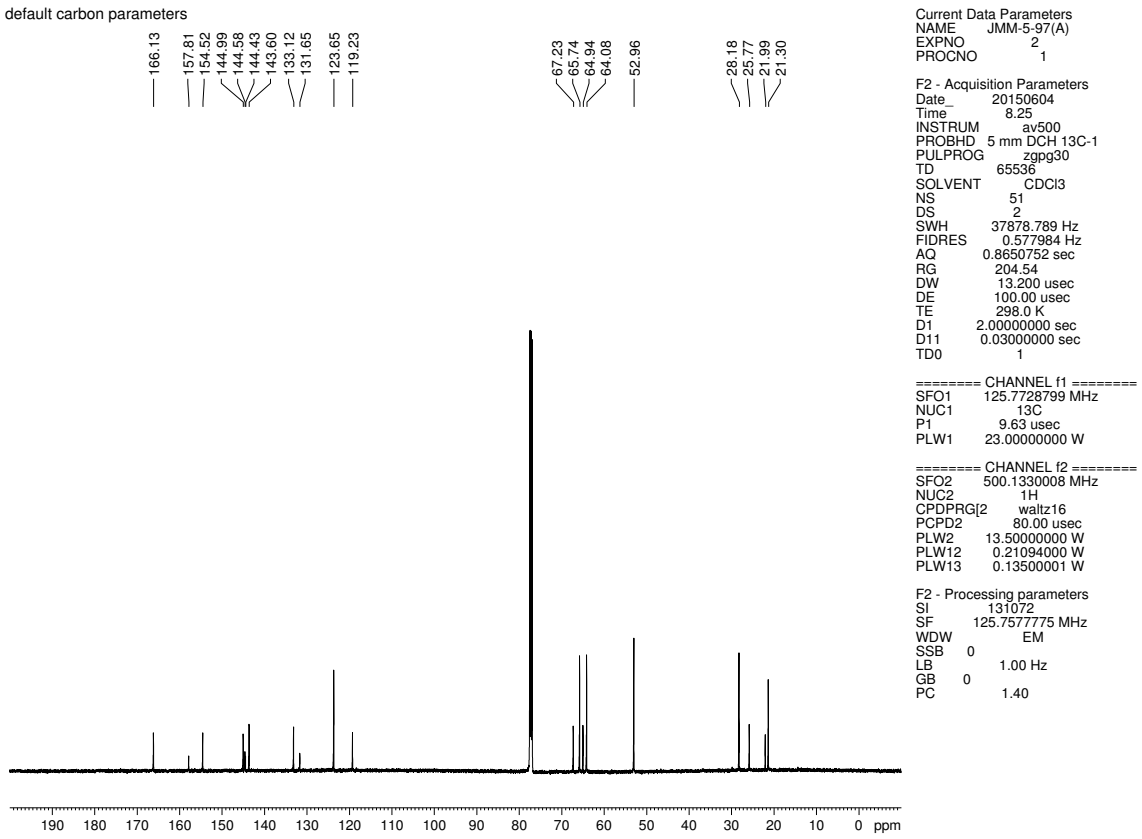


***Figure A3.98.*** $^{13}C$ NMR (125 MHz, $CDCl_3$) of compound **3.57** & **3.58**

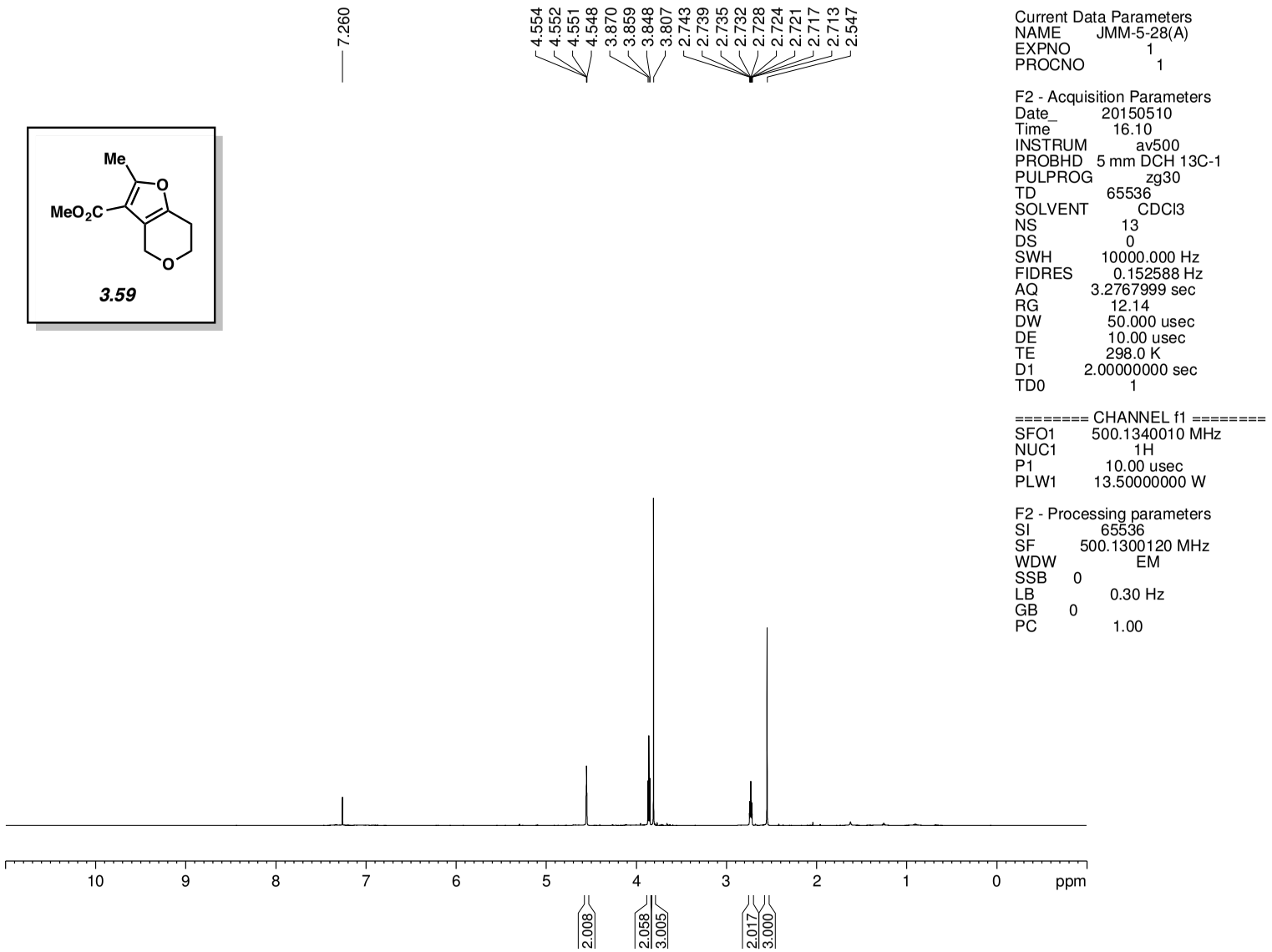


***Figure A3.99.*** $^{1}$H NMR (500 MHz, $CDCl_3$) compound **3.59**

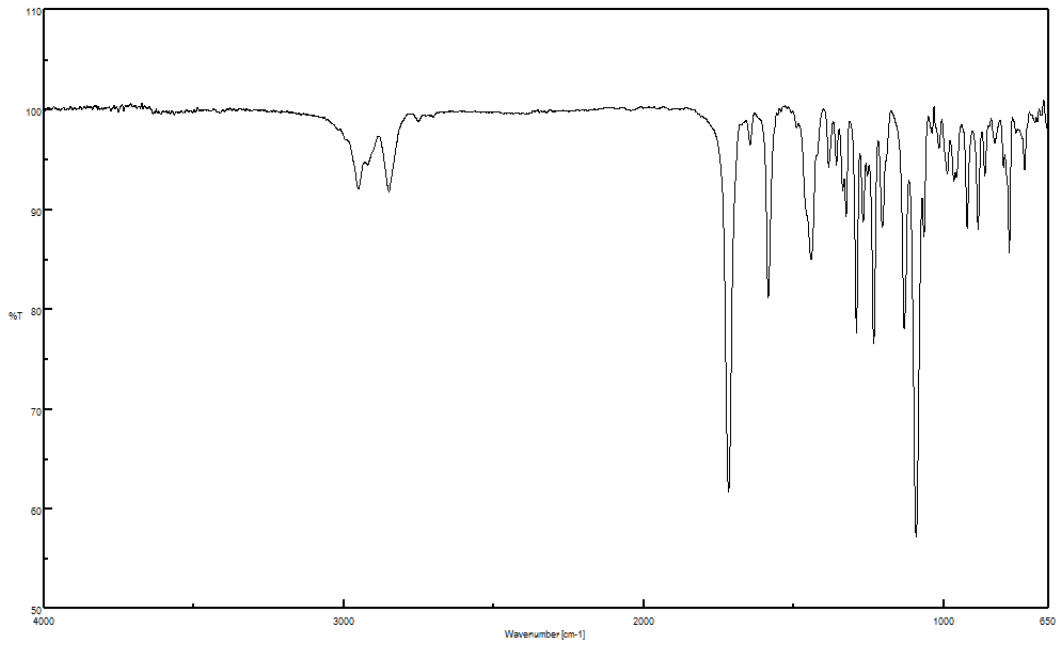


***Figure A3.100.*** Infrared spectrum of compound **3.59**

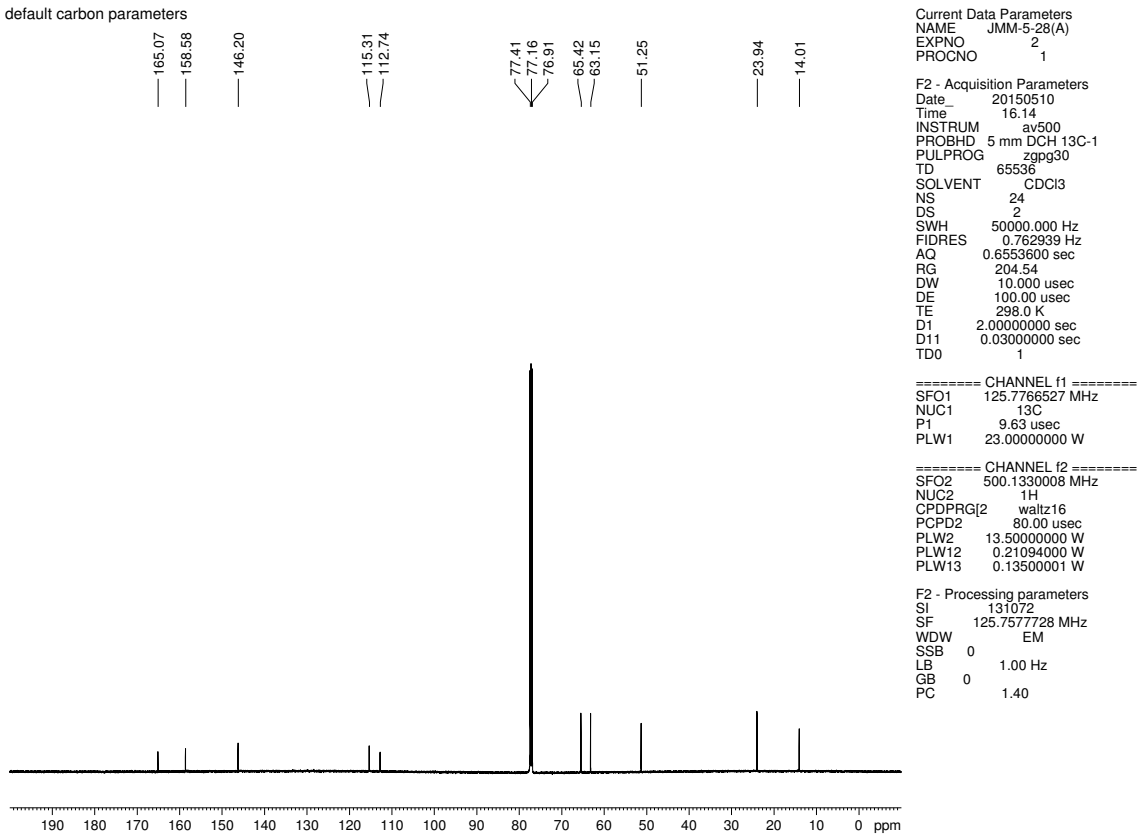


***Figure A3.101.*** $^{13}C$ NMR (125 MHz, $CDCl_3$) of compound **3.59**

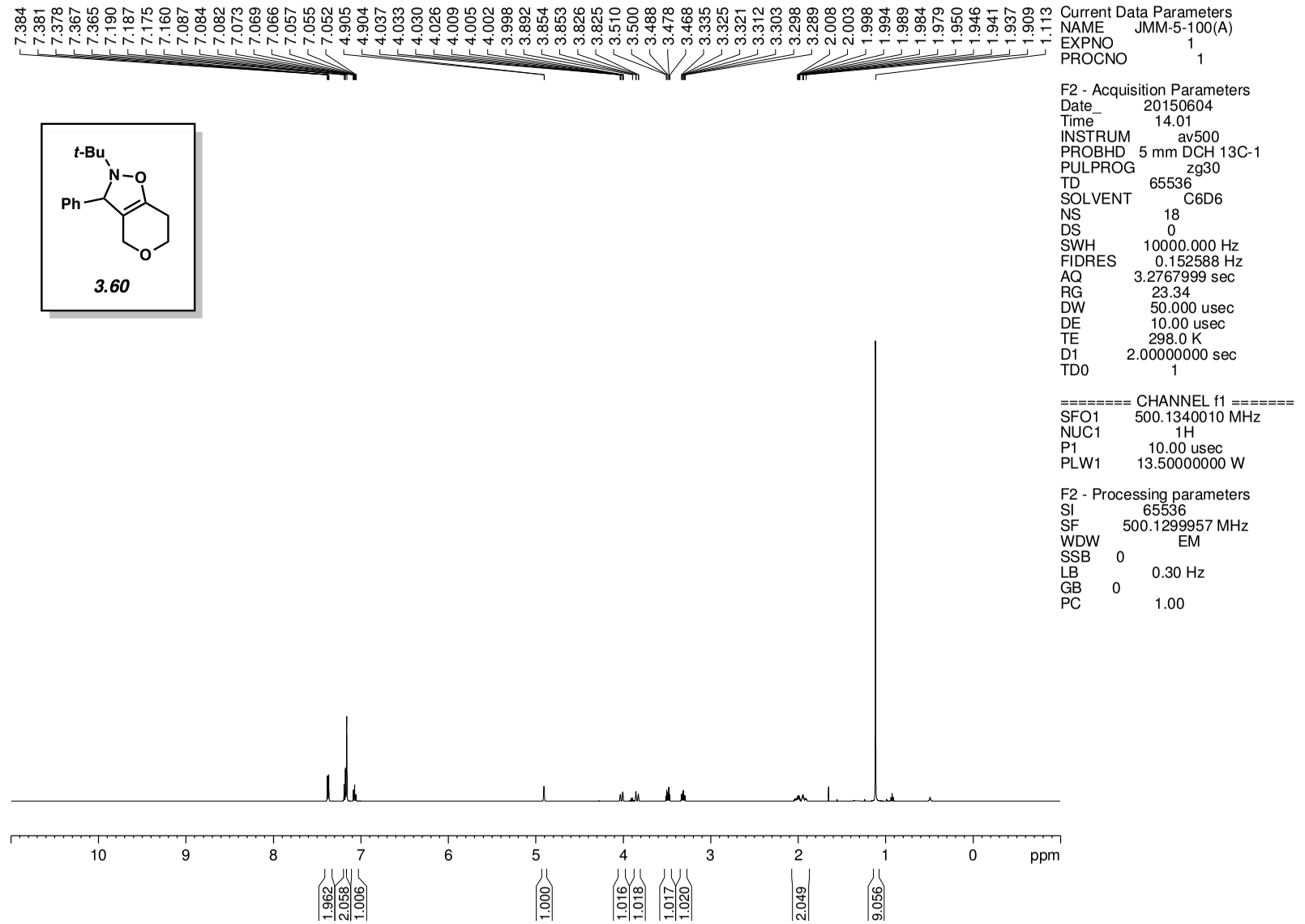


***Figure A3.102.*** $^{1}$H NMR (500 MHz, $C_6D_6$) compound **3.60**

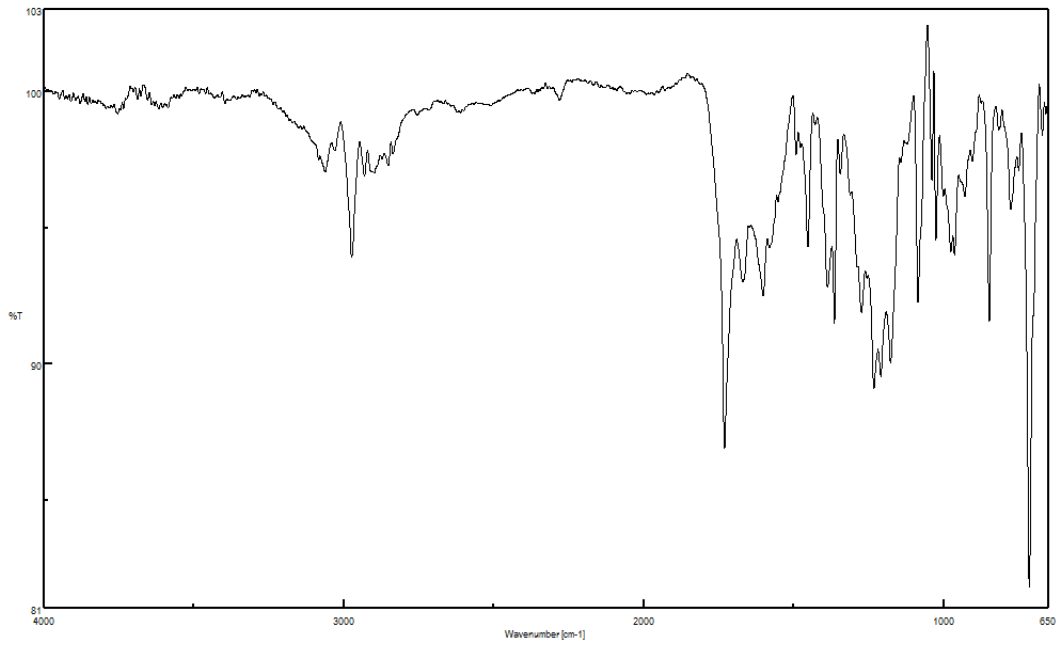


***Figure A3.103.*** Infrared spectrum of compound **3.60**

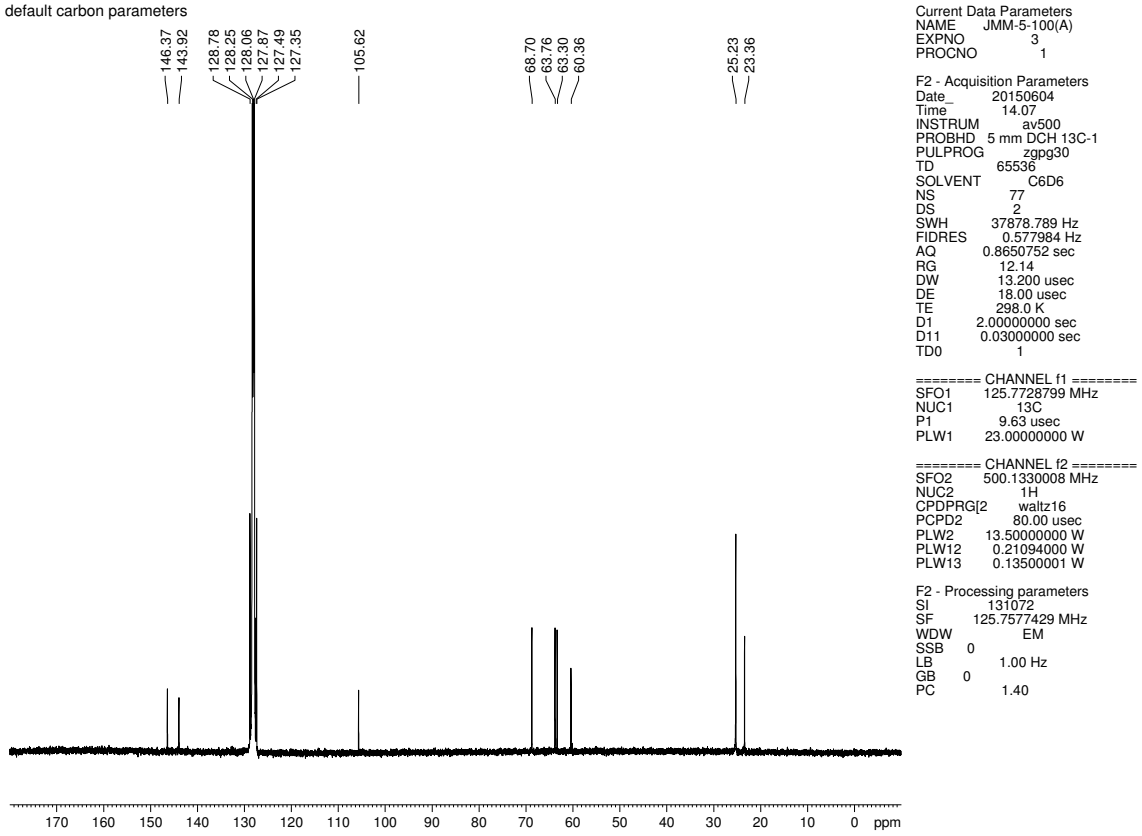


***Figure A3.104.*** $^{13}$C NMR (125 MHz, $C_6D_6$) of compound **3.60**

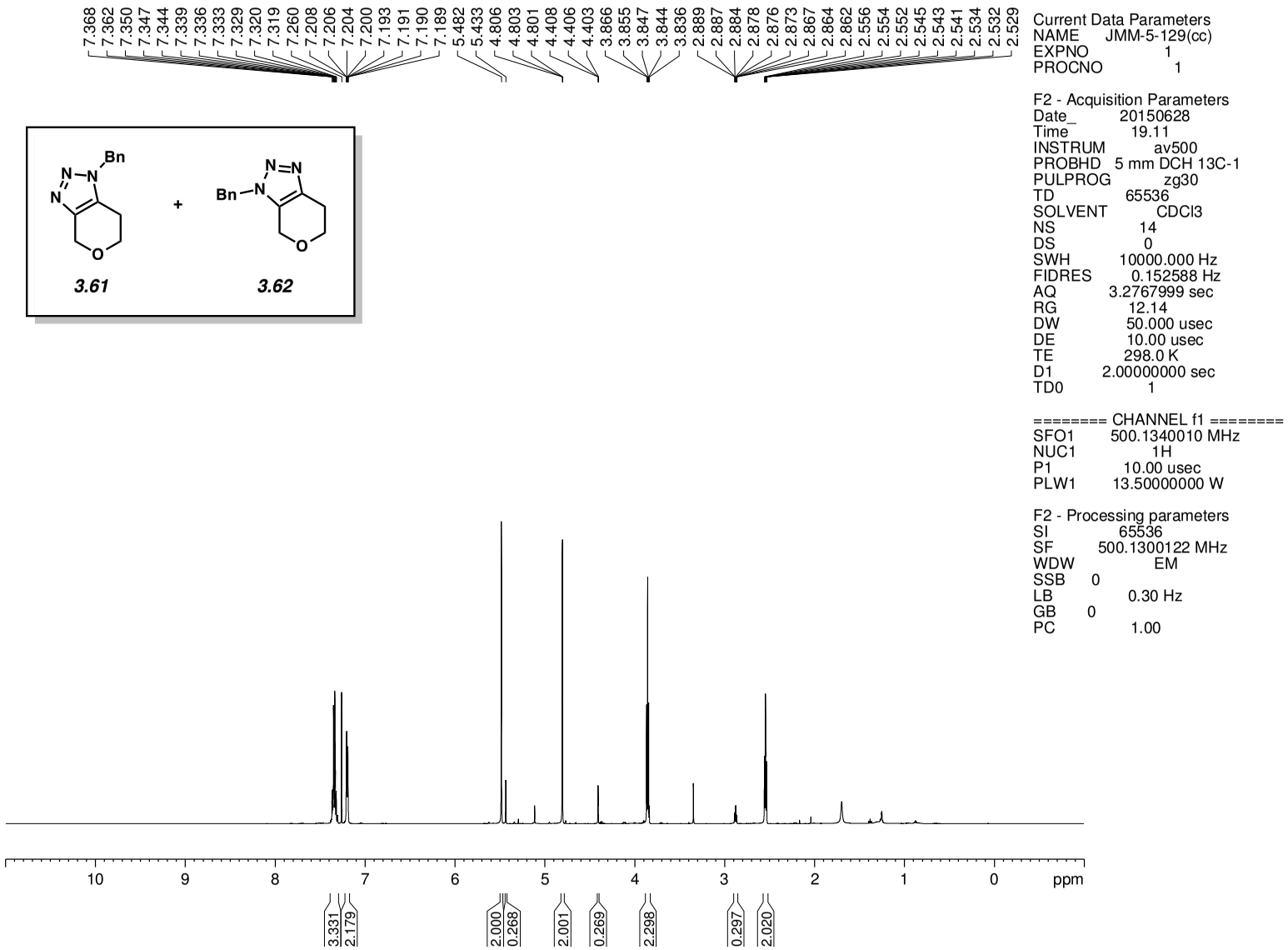


***Figure A3.105.*** $^{1}$H NMR (500 MHz, $CDCl_3$) compounds **3.61** & **3.62**

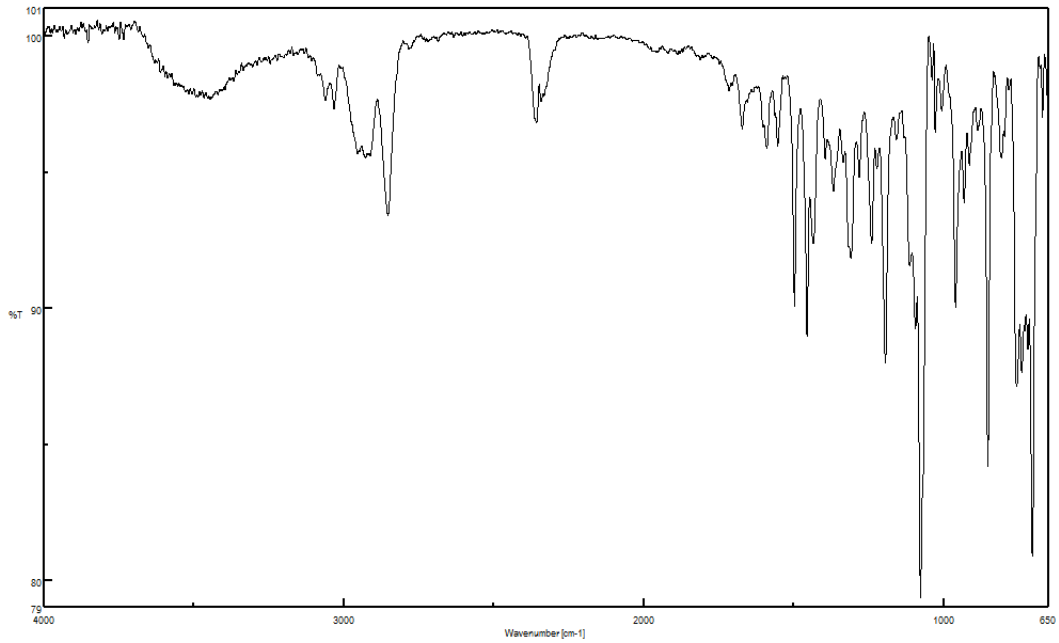


***Figure A3.106.*** Infrared spectrum of compounds **3.61** & **3.62**

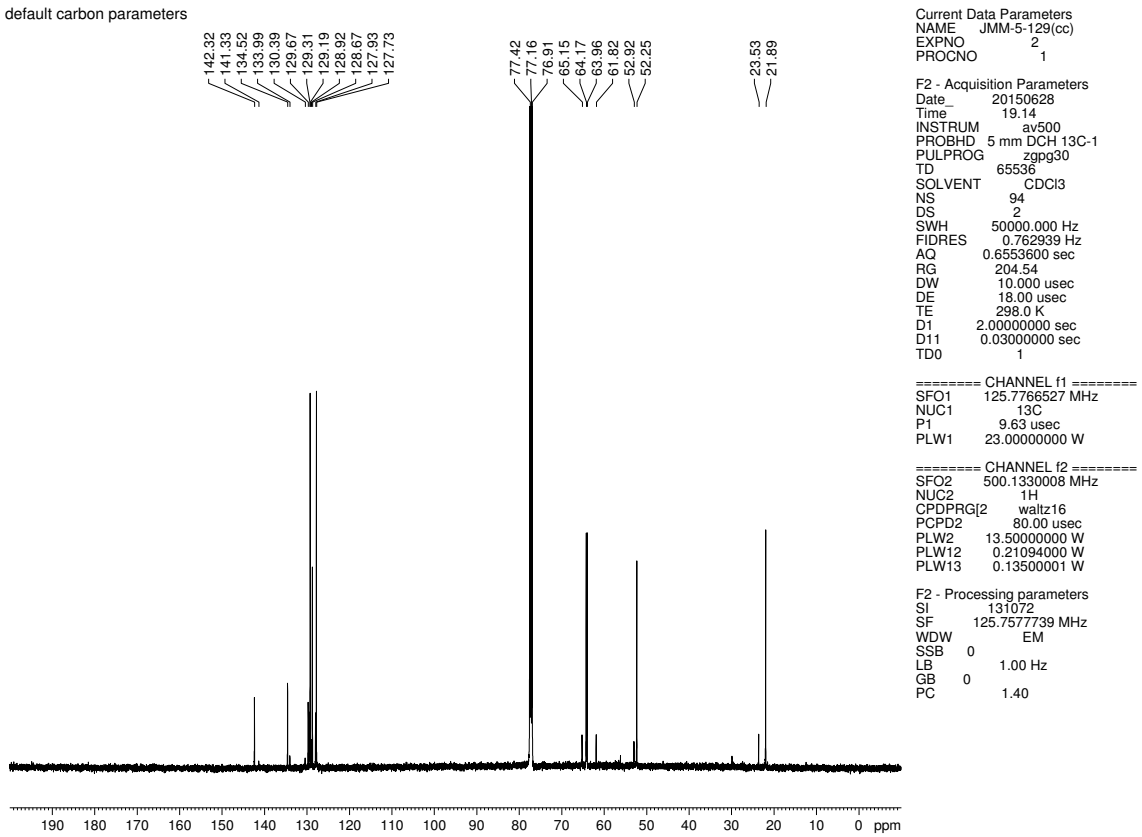


***Figure A3.107.*** $^{13}$C NMR (125 MHz, $CDCl_3$) of compounds **3.61** & **3.62**

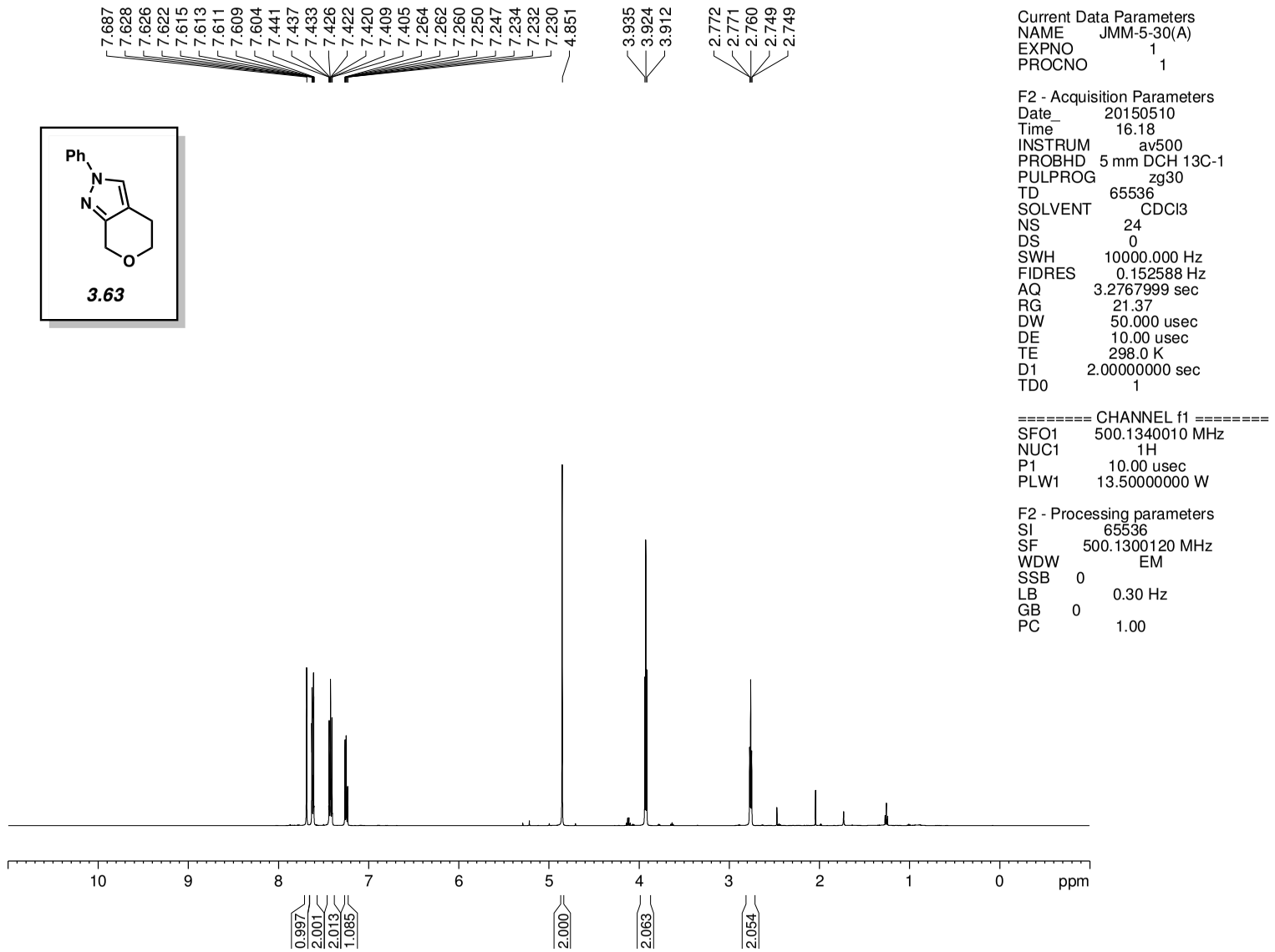


***Figure A3.108.*** $^{1}$H NMR (500 MHz, $CDCl_3$) compound **3.63**

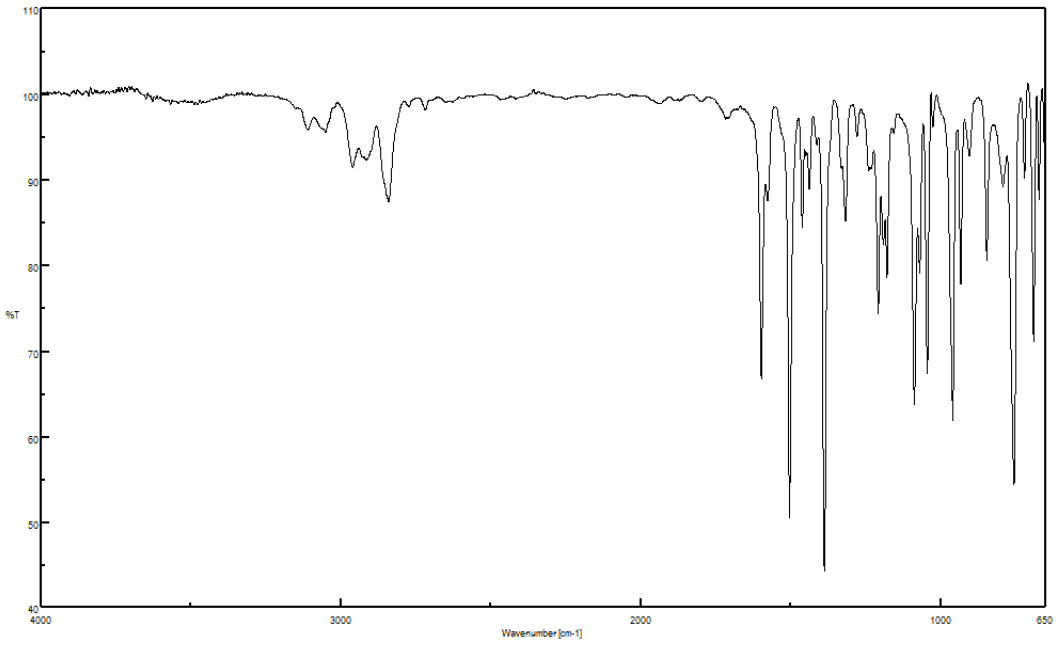


***Figure A3.109.*** Infrared spectrum of compound **3.63**

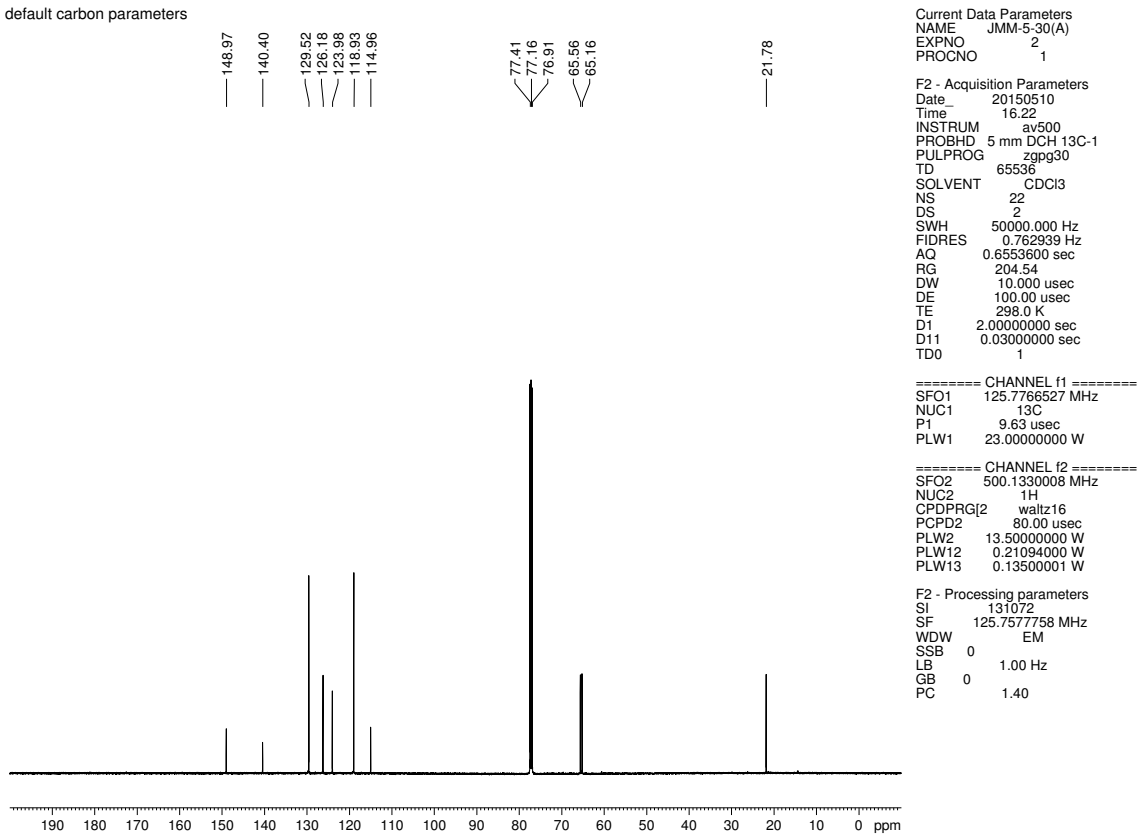


***Figure A3.110.*** $^{13}C$ NMR (125 MHz, $CDCl_3$) of compound **3.63**

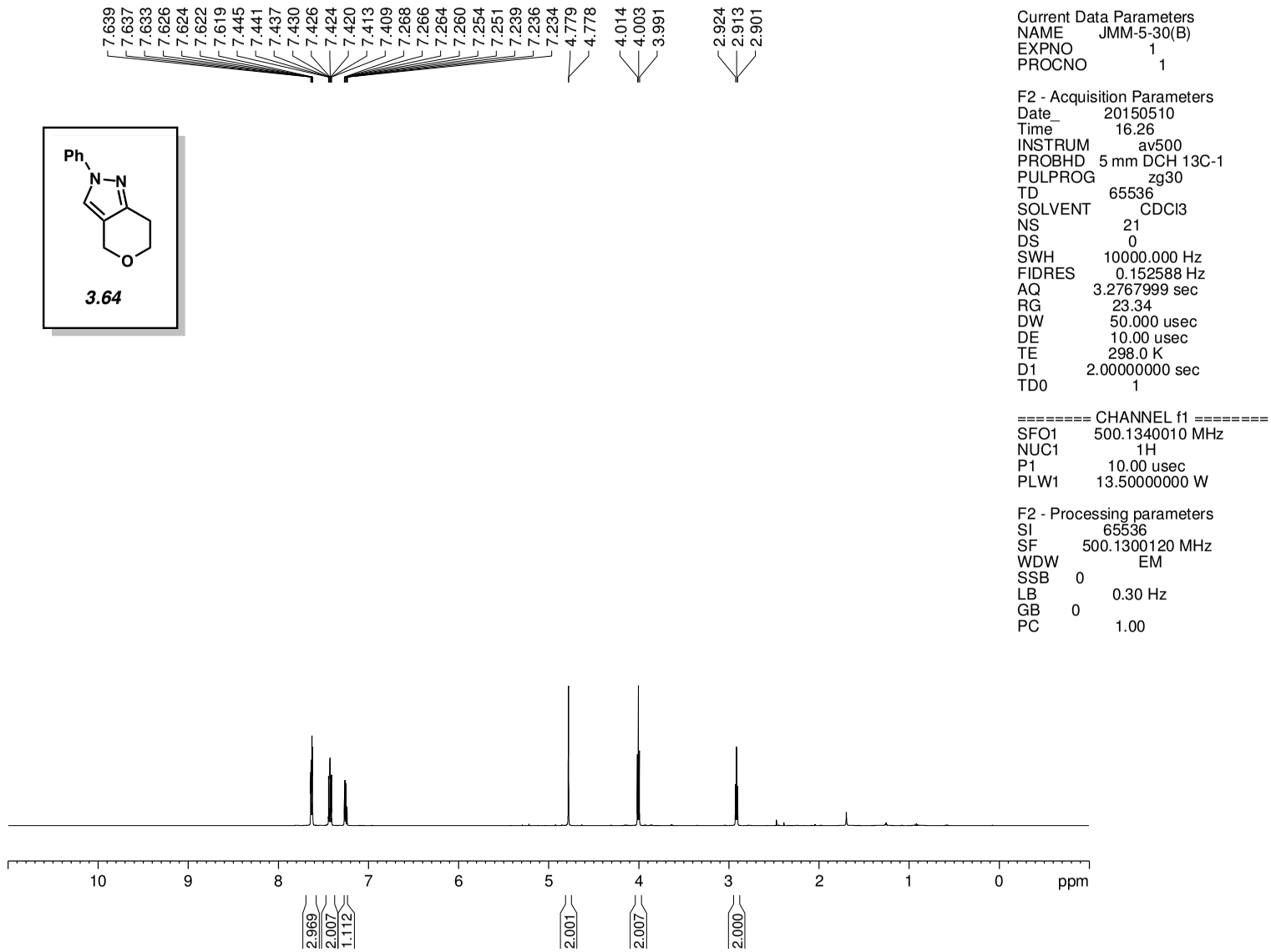


***Figure A3.111.*** $^{1}$H NMR (500 MHz, $CDCl_3$) compound **3.64**

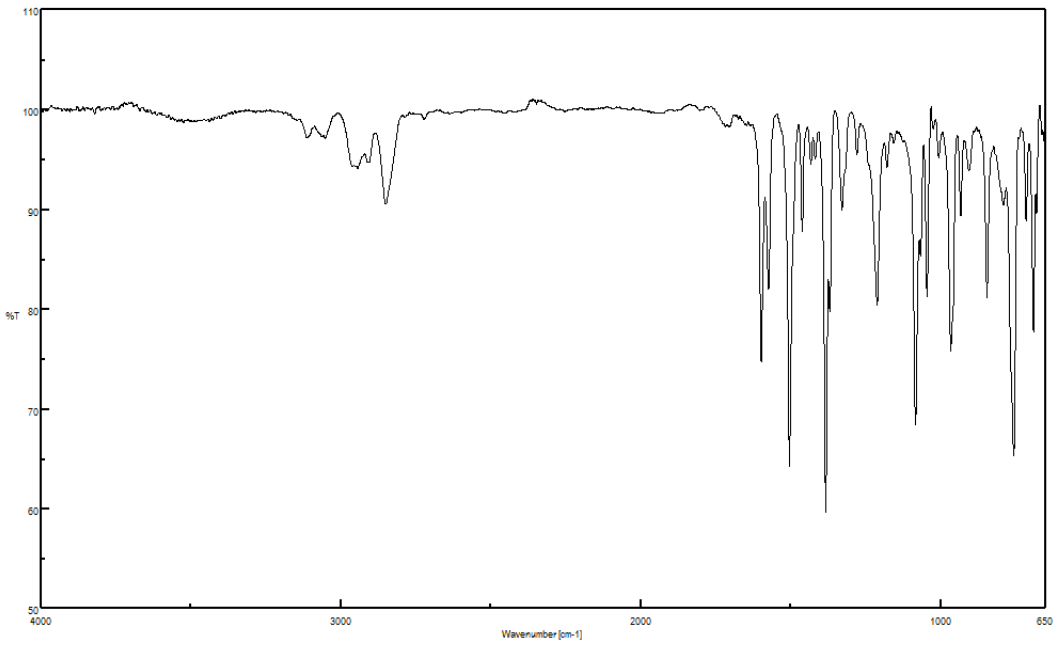


***Figure A3.112.*** Infrared spectrum of compound **3.64**

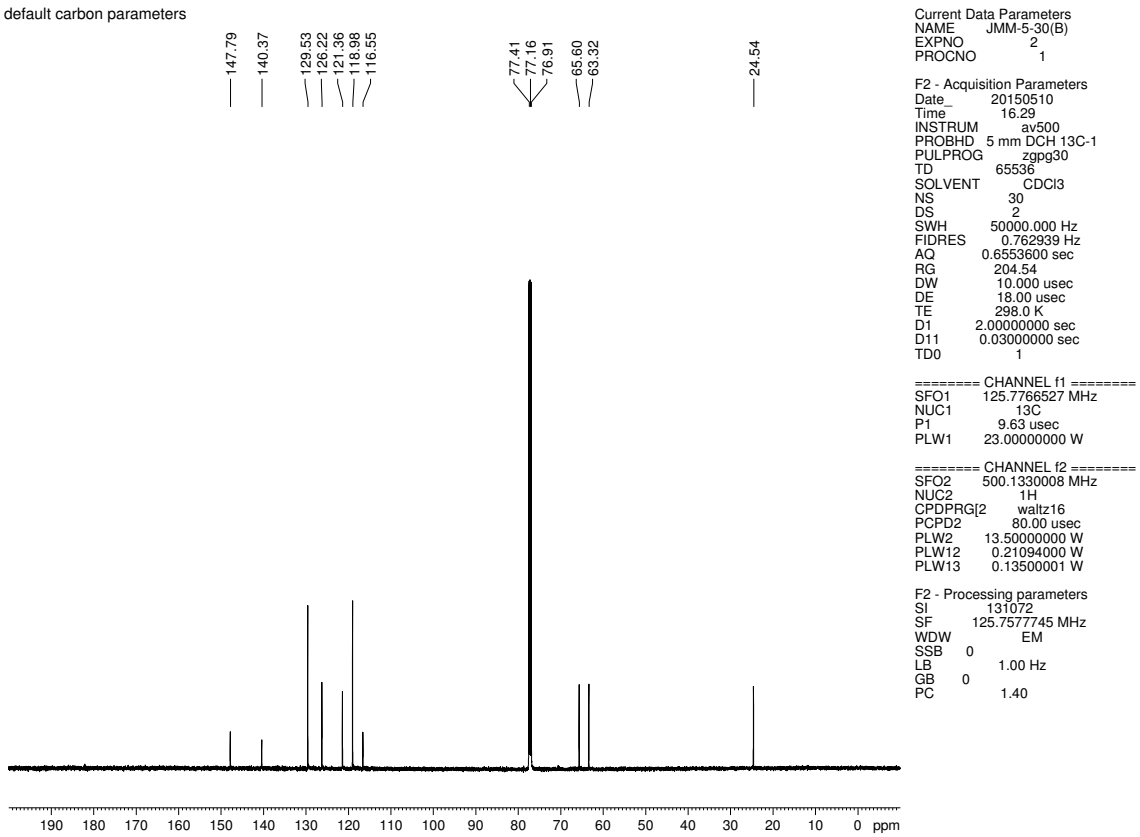


***Figure A3.113.*** $^{13}C$ NMR (125 MHz, $CDCl_3$) of compound **3.64**

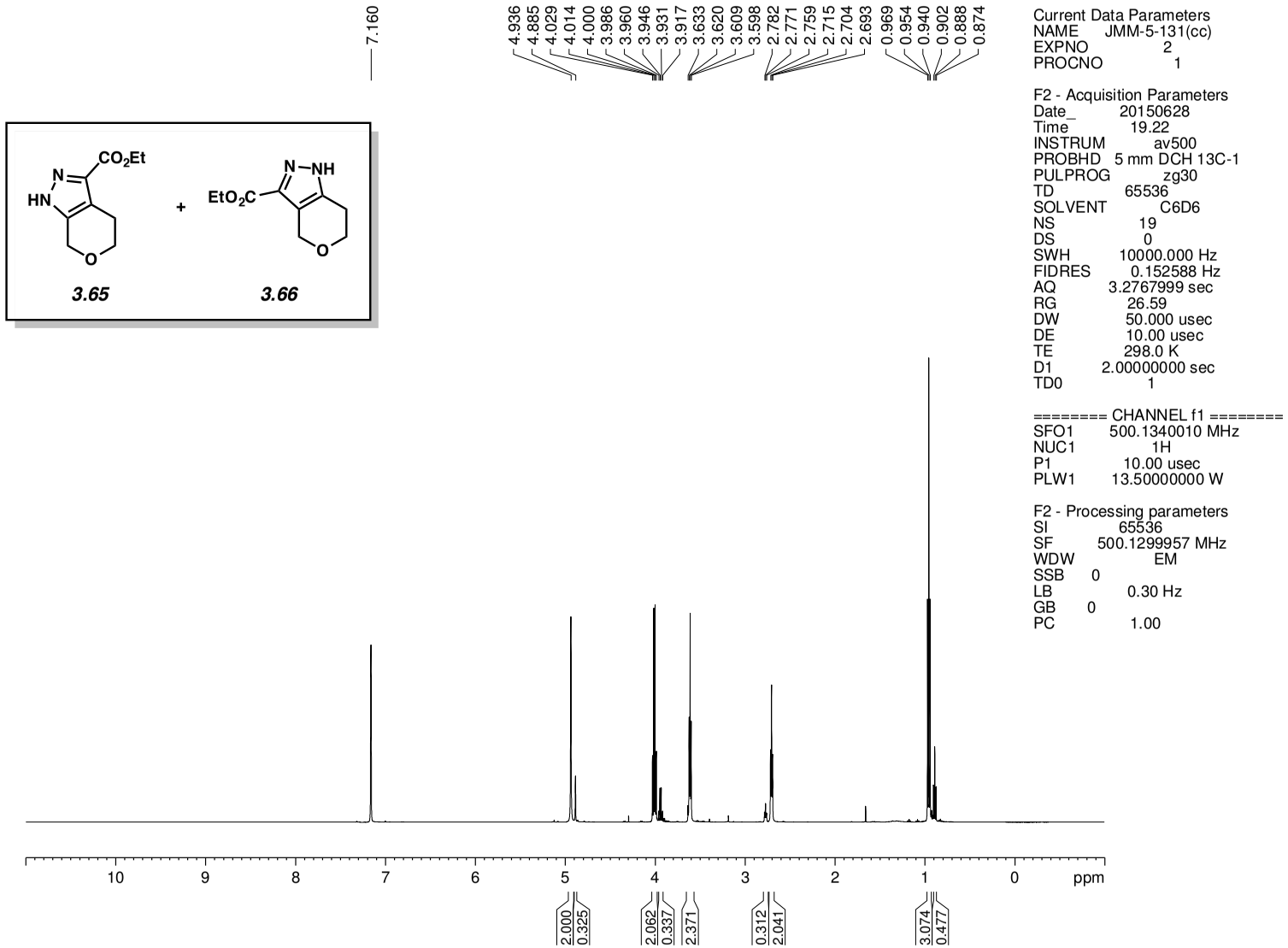


***Figure A3.114.*** $^{1}$H NMR (500 MHz, $CDCl_3$) compounds **3.65** & **3.66**

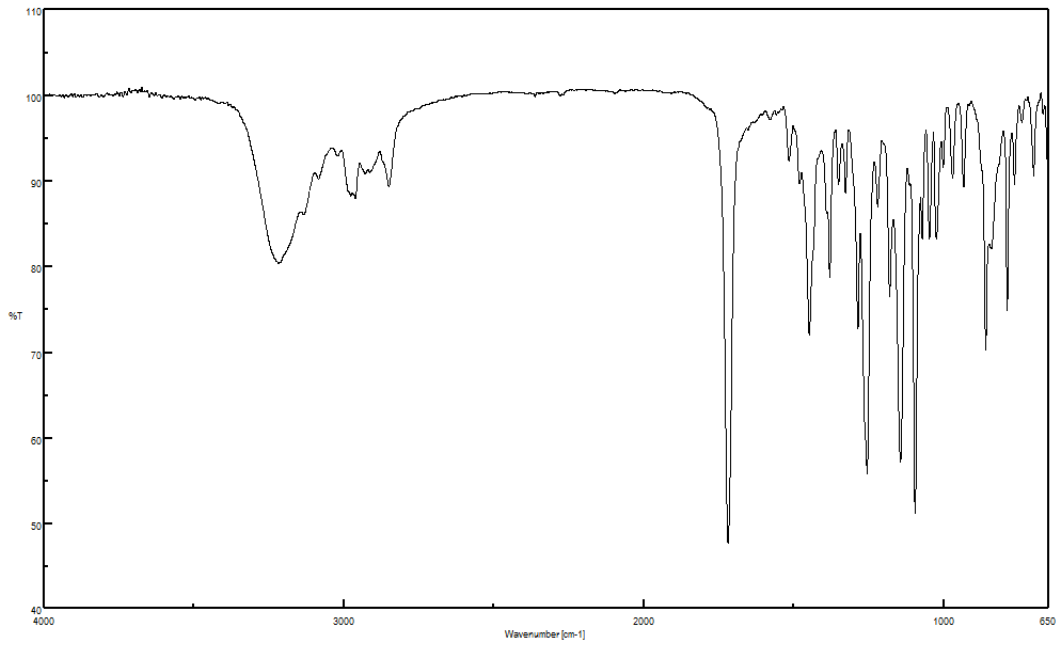


***Figure A3.115.*** Infrared spectrum of compounds **3.65** & **3.66**

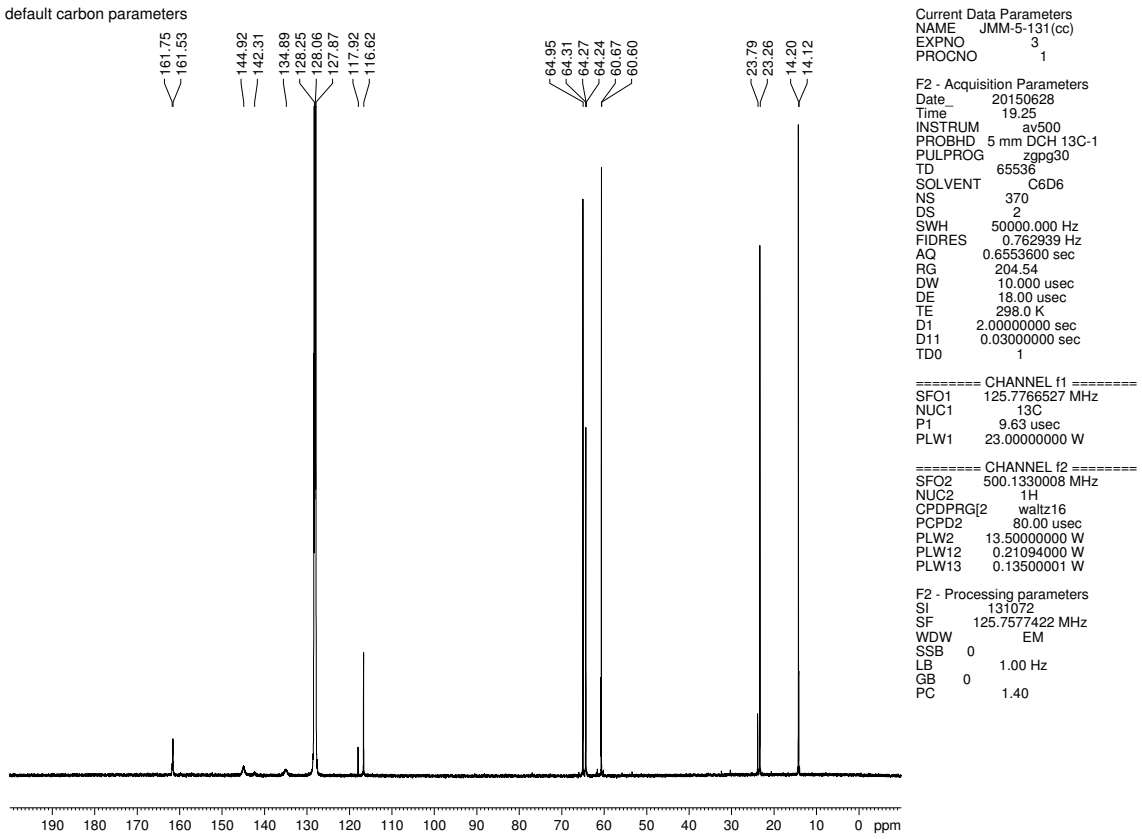


***Figure A3.116.*** $^{13}$C NMR (125 MHz, $C_6D_6$) of compounds **3.65** & **3.66**

## 3.7 Notes and References


[1] (a) Vitaku, E.; Smith, B. R.; Smith, D. T.; Njardarson, J. T. http://njardarson.lab.arizona.edu/sites/njardarson.lab.arizona.edu/files/Top%20US%20Pharmaceutical%20Products%20of%202013.pdf (accessed February 9, 2016). (b) McGrath, N. A.; Brichacek, M.; Njardarson, J. T. *J. Chem. Educ.* **2010**, *87*, 1348–1349. (c) Dinges, J., Lamberth, C., Eds. *Bioactive Heterocyclic Compounds Classes: Agrochemicals*; Wiley-VCH: Weinheim, Germany, 2012. (d) Gilchrist, T. L. *J. Chem. Soc., Perkin Trans. 1* **1999**, 2849–2866.

[2] For reviews of arynes and hetarynes, see: (a) Kauffmann, T. *Angew. Chem. Int. Ed. Engl.* **1965**, *4*, 543–618. (b) Reinecke, M. G. *Tetrahedron* **1982**, *38*, 427–498. (c) Pellissier, H.; Santelli, M. *Tetrahedron* **2003**, *59*, 701–730. (d) Wenk, H. H.; Winkler, M.; Sander, W. *Angew. Chem. Int. Ed.* **2003**, *42*, 502–528. (e) Sanz, R. *Org. Prep. Proced. Int.* **2008**, *40*, 215–291. (f) Bronner, S. M.; Goetz, A. E.; Garg, N. K. *Synlett* **2011**, 2599–2604. (g) Tadross, P. M.; Stoltz, B. M. *Chem. Rev.* **2012**, *112*, 3550–3557. (h) Gampe, C. M.; Carreira, E. M. *Angew. Chem. Int. Ed.* **2012**, *51*, 3766–3778. (i) Bhunia, A.; Yetra, S. R.; Biju, A. T. *Chem. Soc. Rev.* **2012**, *41*, 3140–3152. (j) Yoshida, H.; Takaki, K. *Synlett* **2012**, 1725–1732. (k) Dubrovskiy, A. V.; Markina, N. A.; Larock, R. C. *Org. Biomol. Chem.* **2013**, *11*, 191–218. (l) Wu, C.; Shi, F. *Asian J. Org. Chem.* **2013**, *2*, 116–125. (m) Goetz, A. E.; Garg, N. K. *J. Org. Chem.* **2014**, *79*, 846–851. (n) Goetz, A. E.; Shah, T. K.; Garg, N. K. *Chem. Commun*. **2015**, *51*, 34–45.

[3] For a recent example from our laboratory, see: Goetz, A. E.; Garg, N. K. *Nat. Chem*. **2013**, *5*, 54–60.

[4] (a) Julia, M.; Goffic, F. L.; Igolen, J.; Baillarge, M. *C. R. Acad. Sci., Ser. C* **1967**, *264*, 118–120. (b) Julia, M.; Huang, Y.; Igolen, J. *C. R. Acad. Sci., Ser. C* **1967**, *265*, 110–112. (c) Igolen, J.; Kolb, A. *C. R. Acad. Sci., Ser. C* **1969**, *269*, 54–56. (d) Julia, M.; Igolen, J.; Kolb, M. *C. R. Acad. Sci., Ser. C* **1971**, *273*, 1776–1777.

[5] (a) Buszek, K. R.; Luo, D.; Kondrashov, M.; Brown, N. VanderVelde, D. *Org. Lett.* **2007**, *9*, 4135–4137. (b) Brown, N.; Luo, D.; VanderVelde, D.; Yang, S.; Brassfield, A.; Buszek, K. R. *Tetrahedron Lett.* **2009**, *50*, 63–65. (c) Bronner, S. M.; Bahnck, K. B.; Garg, N. K. *Org. Lett.* **2009**, *11*, 1007–1010. (d) Garr, A. N.; Luo, D.; Brown, N.; Cramer, C. J.; Buszek K. R.; VanderVelde, D. *Org. Lett.* **2010**, *12*, 96–99. (e) Cheong, P. H.-Y.; Paton, R. S.; Bronner, S. M.; Im, G.-Y. J.; Garg, N. K.; Houk, K. N. *J. Am. Chem. Soc.* **2010**, *132*, 1267–1269. (f) Im, G.-Y. J.; Bronner, S. M.; Goetz, A. E.; Paton, R. S.; Cheong, P. H.-Y.; Houk, K. N.; Garg, N. K. *J. Am. Chem. Soc.* **2010**, *132*, 17933–17944. (g) Thornton, P. D.; Brown, N.; Hill, D.; Neuenswander, B.; Lushington, G. H.; Santini, C.; Buszek, K. R. *ACS Comb. Sci.* **2011**, *13*, 443–448. (h) Candito, D. A.; Dobrovolsky, D.; Lautens, M. *J. Am. Chem. Soc.* **2012**, *134*, 15572–15580. (i) Nerurkar, A.; Chandrasoma, N.; Maina, L.; Brassfield, A.; Luo, D.; Brown, N. Buszek, K. R. *Synthesis* **2013**, *45*, 1843–1852. (j) Picazo, E.; Houk, K. N.; Garg, N. K. *Tetrahedron Lett.* **2015**, *56*, 3511–3514.

[6] For the recent use of indolynes and related species in total synthesis, see: (a) Julia, M.; Le Goffic, F.; Igolen, J.; Baillarge, M. *Tetrahedron Lett.* **1969**, *10*, 1569–1572. (b) Iwao, M.; Motoi, O.; Fukuda, T.; Ishibashi, F. *Tetrahedron* **1998**, *54*, 8999–9010. (c) Moro-oka, Y.; Fukuda, T.; Iwao, M. *Tetrahedron Lett.* **1999**, *40*, 1713–1716. (d) Buszek, K. R.; Brown, N.; Luo, D. *Org. Lett.* **2009**, *11*, 201–204. (*e*) Tian, X.; Huters, A. D.; Douglas, C. J.; Garg, N. K.

*Org. Lett.* **2009**, *11*, 2349–2351. (f) Brown, N.; Luo, D.; Decapo, J. A.; Buszek, K. R. *Tetrahedron Lett.* **2009**, *50*, 7113–7115. (g) Bronner, S. M.; Goetz, A. E.; Garg, N. K. *J. Am. Chem. Soc.* **2011**, *133*, 3832–3835. (h) Huters, A. D.; Quasdorf, K. W.; Styduhar, E. D.; Garg, N. K. *J. Am. Chem. Soc.* **2011**, 133, 15797–15799. (i) Quasdorf, K. W.; Huters, A. D.; Lodewyk, M. W.; Tantillo, D. J.; Garg, N. K. *J. Am. Chem. Soc.* **2012**, *134*, 1396–1399. (j) Styduhar, E. D.; Huters, A. D.; Weires, N. A.; Garg, N. K. *Angew. Chem. Int. Ed.* **2013**, *52*, 12422–12425. (k) Chandrasome, N.; Brown, N.; Brassfield, A.; Nerukar, A.; Suarez, S.; Buszek, K. R. *Tetrahedron Lett.* **2013**, *54*, 913–917. (l) Fine Nathel, N. F.; Shah, T. K.; Bronner, S. M.; Garg, N. K. *Chem. Sci.* **2014**, *5*, 2184–2190. (m) Goetz, A. E.; Silberstein, A. L.; Corsello, M. A.; Garg, N. K. *J. Am. Chem. Soc.* **2014**, *136*, 3036–3039. (n) Weires, N. A.; Styduhar, E. D.; Baker, E. L.: Garg, N. K. *J. Am. Chem. Soc.* **2014**, *136*, 14710–14713. (o) Chandrasome, N.; Pathmanathan, S.; Buszek, K. R. *Tetrahedron Lett.* **2015**, *56*, 3507–3510.

[7] (a) Wentrup, C.; Blanch, R.; Briehl, H.; Gross, G. *J. Am. Chem. Soc.* **1988**, *110*, 1874–1880. (b) Tlais, S. F.; Danheiser, R. L. *J. Am. Chem. Soc*. **2014**, *136*, 15489–15492. (c) McMahon, T. C.; Medina, J. M.; Yang, Y.–F.; Simmons, B. J.; Houk, K. N.; Garg, N. K. *J. Am. Chem. Soc*. **2015**, *137*, 4082–4085.

[8] For our collaborative studies with Houk et al. on the distortion-interaction model, see references 2m, 3, 5e, 5f, 5j, 6g, 6l, 7c, and the following: (a) Goetz, A. E.; Bronner, S. M.; Cisneros, J. D.; Melamed, J. M.; Paton, R. S.; Houk, K. N.; Garg, N. K. *Angew. Chem. Int. Ed.* **2012**, *51*, 2758–2762. (b) Bronner, S. M.; Mackey, J. L.; Houk, K. N.; Garg, N. K. *J. Am. Chem. Soc.* **2012**, *134*, 13966–13969. (c) Medina, J. M.; Mackey, J. L.; Garg, N. K.; Houk, K.

N. *J. Am. Chem. Soc*. **2014**, *136*, 15798–15805. (d) Medina, J. M.; McMahon, T. C.; Jimenez-Osés, G.; Houk, K. N. Garg, N. K. *J. Am. Chem. Soc.* **2014**, *136*, 14706–14709.

[9] Stoermer, R.; Kahlert, B. *Ber.* **1902**, *35*, 1633–1640.

[10] (a) Townsend, C. A.; Whittamore, P. R. O.; Brobst, S. W. *J. Chem. Soc. Chem. Commun.* **1988**, 726–728. (b) Graybill, T. L.; Casillas, E. G.; Pal, K.; Townsend, C. A. *J. Am. Chem. Soc.* **1999**, *121*, 7729–7746. (c) Gilman, H.; Willis, H. B.; Swislowsky, J. *J. Am. Chem. Soc.* **1939**, *61*, 1371–1373.

[11] For studies on 6,7-benzofuranyne, see: Brown, N.; Buszek, K. R. *Tetrahedron Lett.* **2012**, *53*, 4022–4025.

[12] (a) Harris, M. C. J.; Whitby, R. J.; Blagg, J. *Synlett* **1993**, 705–707. (b) Closser, K. D.; Quintal, M. M.; Shea, K. M. *J. Org. Chem*. **2009**, *74*, 3680–3688.

[13] (a) Miyabe, H.; Miyata, O.; Naito, T. Pyran and its derivatives. In Heterocycles in Natural Product Synthesis; Majumdar, K. C., Chattopadhyay, S. K., Eds.; Wiley-VCH: Weinheim, Germany, 2011; pp. 153–186. (b) Kaur, P.; Arora, R.; Gill, N.S. *Indo Am. J. Pharm. Res.* **2013**, *3*, 9067–9084. (c) Atul, G.; Amit, K.; Ashutosh, R. *Chem. Rev.* **2013**, *113*, 1614–1640. (d) Radadiya, A.; Shah, A. *Eur. J. Med. Chem.* **2015**, *97*, 356–376.

[14] (a) Aukakh, G. K.; Sodhi, R. K.; Singh, M. *Life Sci.* **2007**, *81*, 615–639. (b) Hilditch, A.; Hunt, A. A.; Travers, A.; Polley, J.; Drew, G. M.; Middlemiss, D.; Judd, D. B.; Ross, B. C.; Robertson, M. J. *J. Pharmacol. Exp. Ther.* **1995**, *272*, 750–757.

[15] (a) Tanaka, T.; Ito, T.; Ido, Y.; Nakaya, K.-i.; Iinuma, M.; Chelladurai, V. *Chem. Pharm. Bull.* **2001**, *49*, 785–787. (b) Ge, H. M.; Huang, B.; Tan, S. H.; Shi, D. H.; Song, Y. C.; Tan, R. X.

*J. Nat. Prod.* **2006**, *69*, 1800–1802. (c) Kim, I.; Choi, J. *Org. Biomol. Chem.* **2009**, *7*, 2788–2795.

[16] (a) Klayman, D. L. *Science* **1985**, *228*, 1049–1055. (b) Dondorp, A. M.; Nosten, F.; Yi, P.; Das, D.; Phyo, A. P.; Tarning, J.; Lwin, K. M.; Ariey, F.; Hanpithakpong, W.; Lee, S. J.; Ringwald, P.; Silamut, K.; Imwong, M.; Chotivanich, K.; Lim, P.; Herdman, T.; An, S. S.; Yeung, S.; Singhasivanon, P.; Day, N. P. J.; Lindegardh, N.; Socheat, D.; White, N. J. *N. Engl. J. Med*. **2009**, *361*, 455–467.

[17] Montgomery, C. T.; Cassels, B. K.; Shamma, M. *J. Nat. Prod*. **1983**, *46*, 441–453.

[18] Salaski, E. J.; Krishnamurthy, G.; Ding, W.-D.; Yu, K.; Insaf, S. S.; Eid, C.; Shim, J.; Levin, J. I.; Tabei, K.; Toral-Barza, L.; Zhang, W.-G.; McDonald, L. A.; Honores, E.; Hanna, C.; Yamashita, A.; Johnson, B.; Li, Z.; Laakso, L.; Powell, D.; Mansour, T. S. *J. Med. Chem*. **2009**, *52*, 2181–2184.

[19] (a) Tomaszewski, Z.; Johnson, M. P.; Huang, X.; Nichols, D. E. *J. Med. Chem*. **1992**, *35*, 2061–2064. (b) Marugán, J. J.; Manthey, C.; Anaclerio, B.; Lafrance, L.; Lu, T.; Markotan, T.; Leonard, K. A.; Crysler, C.; Eisennagel, S.; Dasgupta, M.; Tomczuk, B. *J. Med. Chem*. **2005**, *48*, 926–934. (c) Nevagi, R. J.; Dighe, S. N.; Dighe, S. N. *Eur. J. Med. Chem*. **2015**, *97*, 561–581. (d) Zhang, S.; Zhen, J.; Reith, M. E. A.; Dutta, A. K. *Bioorg. Med. Chem*. **2004**, *12*, 6301–6315. (e) Zhang, S.; Reith, M. E. A.; Dutta, A. K. *Bioorg. Med. Chem. Lett*. **2003**, *13*, 1591–1595.

[20] We have previously demonstrated that DFT calculations (B3LYP/6-31G(d)) are well suited for the aryne distortion model, although ab initio methods (MP2/6-311+G**) can also be used; see reference 8a.

[21] Arynes and cyclic alkynes can be generated from silyl triflates using mild fluoride-based conditions. In turn, an array of trapping experiments can be carried out in synthetically useful yields (see references 2c–2n). For the initial use of silyl triflates as aryne precursors, see: Himeshima, Y.; Sonoda, T.; Kobayashi, H. *Chem. Lett.* **1983**, *12*, 1211–1214.

[22] (a) For benzylation of hydroquinone, see: Frlan, R.; Gobec, S.; Kikelj, D. *Tetrahedron* **2007**, *63*, 10698–10708. (b) For formation of diethyl acetal and subsequent benzofuran, see: Hisashi, S.; Takao, I.; Hideki, Y. US Patent 6410561 B1, 2002.

[23] Fliri, A. J.; O'Donnell, C. J.; Claffey, M.; Gallaschun; R. J. US Patent 0058361 A1, 2006

[24] Smith III, A. B.; Empfield, J. R.; Vaccaro, H. A. *Tetrahedron Lett*. **1989**, *30*, 7325–7328.

[25] Liu, Z.; Larock, R. C. *J. Org. Chem.* **2006**, *71*, 3198–3209.

[26] Yoshida, H.; Shirakawa, E.; Honda, Y.; Hiyama, T. *Angew. Chem. Int. Ed.* **2002**, *41*, 3247–3249.

[27] Gilmore, C. D.; Allan, K. M.; Stoltz, B. M. *J. Am. Chem. Soc.* **2008**, *130*, 1558–1559.

[28] For the trapping of arynes with iodonium ylides, see: Huang, X.-C.; Liu, Y.-L.; Liang, Y.; Pi, S.-F.; Wang, F.; Li, J.-H. *Org. Lett.* **2008**, *10*, 1525–1528.

[29] For the trapping of arynes with nitrones, see: Lu, C.; Dubrovskiy, A. V.; Larock, R. C. *J. Org. Chem*. **2012**, *77*, 2279–2284.

[30] For the trapping of arynes with azomethine imines, see: Shi, F.; Mancuso, R.; Larock, R. C. *Tetrahedron Lett*. **2009**, *50*, 4067–4070.

[31] For the trapping of arynes with azides, see: Shi, F.; Waldo, J. P.; Chen, Y.; Larock, R. C. *Org. Lett*. **2008**, *10*, 2409–2412.

[32] For the trapping of arynes with sydnones, see: Wu, C.; Fang, Y.; Larock, R. C.; Shi, F. *Org. Lett*. **2010**, *12*, 2234–2237.

[33] For the trapping of arynes with diazoesters, see: Jin, T.; Yamamoto, Y. *Angew. Chem. Int. Ed*. **2007**, *46*, 3323–3325.

[34] Zhao, J.; Larock, R. C. *Org. Lett*. **2005**, *7*, 4273–4275.

[35] The ability to access heterocyclic scaffolds with significant aliphatic character is an important direction in modern drug discovery; see: (a) Lovering, F.; Bikker, J.; Humblet, C. *J. Med. Chem.* **2009**, *52*, 6752–6756. (b) Ritchie, T. J.; Macdonald, S. J. F. *Drug Discovery Today* **2009**, *14*, 1011–1020.

[36] Bent, H. *Chem. Rev.* **1961**, *61*, 275-311.

[37] Legault, C. Y. CYLview, 1.0b; Université de Sherbrooke: Québec, Montreal, Canada, 2009; http://www.cylview.org.

[38] Also commercially available from Combi Blocks, Inc.

[39] Liu, Y.; Park, S. K.; Xiao, Y.; Chae, J. *Org. Biomol. Chem.* **2014**, *12*, 4747–4753.

[40] Spartan ’10; Wavefunction, Inc: Irvine, CA, 2010.

# CHAPTER FOUR

## A New Class of Conjugated Trimeric Scaffolds Accessible Using Indolyne Cyclotrimerizations

Tejas K. Shah, Janice Lin, Adam E. Goetz, K. N. Houk, and Neil K. Garg

*Manuscript in preparation*.

### 4.1 Abstract

We report the design and synthesis of a new class of indole-based conjugated trimers. The targeted compounds are accessed from in situ generated, highly reactive indolyne intermediates using Pd-catalyzed cyclotrimerization reactions. By harnessing three indolyne isomers, six isomeric indole trimers are accessible, none of which have been previously synthesized. We describe the photophysical properties of these unique compounds, in addition to structural analyses based on computational studies. Our efforts mark the first reported use of indolynes in transition metal-catalyzed reactions, while providing access to a new class of conjugated trimers, including several non-planar heteroaromatic compounds.

## 4.2 Introduction

Novel conjugated small molecules are highly sought after due to potential applications in organic electronics: light-emitting diodes,[1] field-effect transistors,[2] and photovoltaic devices.[3] Most conjugated materials used in such applications rely on two-directional electron-rich fragments, (e.g., 2,5-disubstituted thiophenes). In contrast, tri-directional conjugated compounds are much less well studied, in part due to limitations in chemical synthesis. Perhaps the most well studied conjugated trimer is triphenylene (**4.1**) first prepared in 1880[4] (Figure 4.1). More recently, indole-based variants **4.2** and **4.3** have also been reported.[5] Collectively, **4.1**–**4.3** have been used in two-photon absorption spectroscopy,[6] discotic liquid crystals,[7,8] photovoltaics,[9,10] and organic light emitting diodes,[11] thus highlighting the importance of these types of trimeric scaffolds.

With the ultimate goal of accessing novel trimeric scaffolds using unusual synthetic transformations, we targeted the class of indole-based trimers, as suggested by structure **4.4**. This structure and isomers that vary by positioning of the pyrrole unit have never been accessed previously. We hypothesized that such motifs could be directly synthesized using an unconventional approach, namely, using the transition metal-catalyzed trimerization of highly reactive hetarynes[12] (e.g., 4,5-indolyne **4.5**).[13,14] Transition metal-catalyzed reactions of indolynes have not been described previously and, to our knowledge, no examples of hetaryne trimerizations have been reported. In this manuscript, we report the successful trimerization of three isomeric indolynes, which, in turn, permits access to six new bent aromatic indole trimers that display varying photophysical properties.

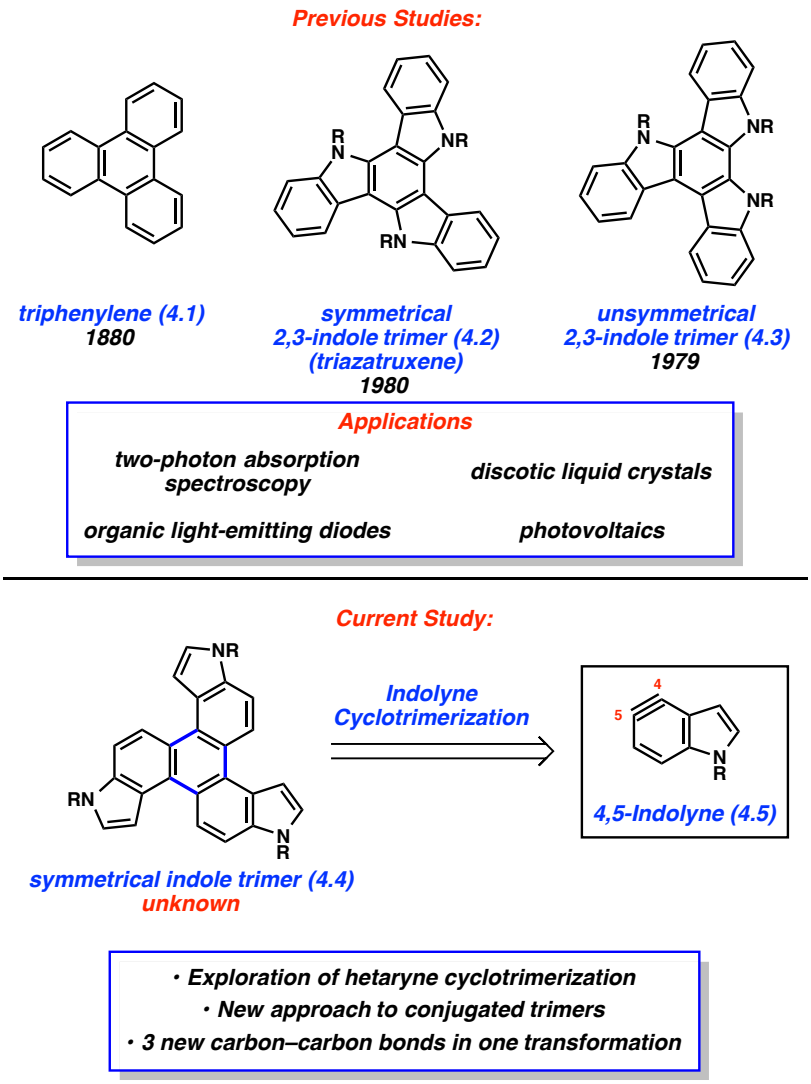


***Figure 4.1.*** Previously studied conjugated trimers **4.1–4.3** and indole trimer (present study)

## 4.3 Results and Discussion

### 4.3.1 Optimization of 4,5-Indolyne Cyclotrimerization

Although prior studies have established the feasibility of benzyne trimerization,[15] the corresponding metal-catalyzed union of hetarynes was unknown, as noted above. Thus, our first objective was to elucidate reaction conditions that allow for the trimerization of indolynes to take place. We elected to initially perform trimerization studies using an in situ-generated 4,5-

indolyne. As shown in Table 4.1, 4,5-indolyne precursor **4.6**[13] was subjected to Pd-based conditions to effect trimerization. Initial studies involved the use of $Pd(PPh_3)_4$ as the catalyst, in the presence of CsF in acetonitrile. At 35 °C, we were delighted to find that symmetrical trimer **4.7** and unsymmetrical trimer **4.8** were obtained in 34% yield, in a 1 : 2.1 ratio, respectively (entry 1). Increasing the temperature to 50 °C led to an improvement in yield (entry 2), whereas heating to 65 °C led to only modest change (entry 3). By performing the trimerization at 50 °C and at a concentration of 0.5 M, the yield increased to 85% (entry 4). The use of higher concentrations was less productive (entry 5), as was the use of $Pd(P\textit{t}\text{-}Bu_3)_2$ (entry 6). Finally, by maintaining the optimal temperature and concentration (i.e., 50 °C and 0.5 M), but switching to the use of $Pd_2dba_3$ and BINAP, isomers **4.7** and **4.8** were obtained in 93% yield (entry 7, 1:2 ratio, respectively). It should be noted that the trimerization allows for the formation three new C–C bonds with excellent efficiency.

***Table 4.1.*** Optimization of Cyclotrimerization

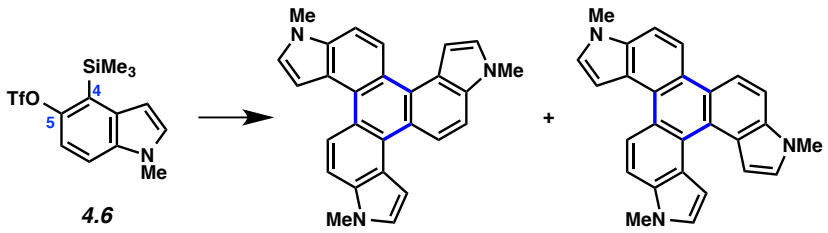


***4.6*** ***4.7*** ***4.8***

| *Entry* | *Conditions* | *Yield*[a] | *Ratio of 4.7 to 4.8* |
|---|---|---|---|
| 1 | CsF (3 equiv)<br>$Pd(PPh_3)_4$ (20 mol%)<br>MeCN (0.2 M), 35 °C | *34%* | *1 : 2.1* |
| 2 | CsF (3 equiv)<br>$Pd(PPh_3)_4$ (20 mol%)<br>MeCN (0.2 M), 50 °C | *46%* | *1 : 2.2* |
| 3 | CsF (3 equiv)<br>$Pd(PPh_3)_4$ (20 mol%)<br>MeCN (0.2 M), 65 °C | *39%* | *1 : 2.2* |
| 4 | CsF (3 equiv)<br>$Pd(PPh_3)_4$ (20 mol%)<br>MeCN (0.5 M), 50 °C | *85%*[b] | *1 : 2.1* |
| 5 | CsF (3 equiv)<br>$Pd(PPh_3)_4$ (20 mol%)<br>MeCN (1.0 M), 50 °C | *48%* | *1 : 2.0* |
| 6 | CsF (3 equiv)<br>$Pd(Pt\text{-}Bu_3)_2$ (20 mol%)<br>MeCN (0.5 M), 50 °C | *< 5%* | *N/A* |
| 7 | CsF (3 equiv)<br>$Pd(dba)_2$ (10 mol%)<br>BINAP (20 mol%)<br>MeCN (0.5 M), 50 °C | *93%*[b] | *1 : 2.0* |

[a] Yield determined by $^1$H NMR analysis using 1,3,5-trimethoxybenzene as an external standard. [b.] Isolated yields.

### 4.3.2 Cyclotrimerization of 5,6- and 6,7-Indolynes

Having achieved the trimerization of a 4,5-indolyne, we attempted the corresponding transformation using 5,6- and 6,7-indolyne precursors **4.9** and **4.12**, respectively (Figure 4.2).[13] In both cases, the use of $Pd(PPh_3)_4$ gave the most promising results. 5,6-indolyne precursor **4.9** underwent trimerization to give a 1 : 3 ratio of isomers **4.10** and **4.11**, respectively, in 80% yield. The corresponding trimerization of 6,7-indolyne precursor **4.12** proved much more difficult.

Nonetheless, the two desired trimers, **4.13** and **4.14**, could be accessed in a 1 : 1 ratio, albeit in modest yield. The fact that products **4.13** and **4.14** are formed to any extent, despite severe steric crowding, as discussed in Section 4.3.4 Structural Analysis, page 252, highlights the power of indolyne and aryne methodology for the synthesis of highly congested scaffolds.

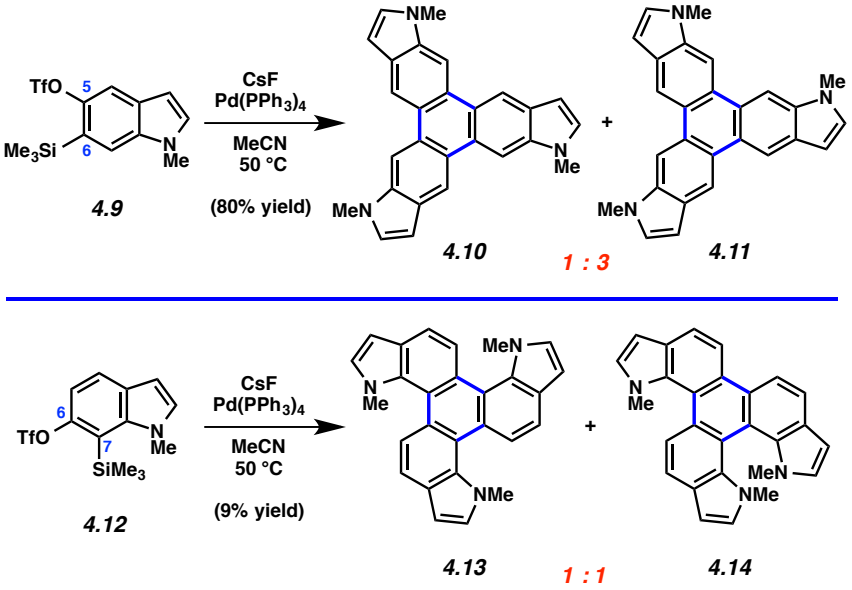


***Figure 4.2.*** Trimerization of indolyne precursors **4.9** and **4.12**.

### 4.3.3 Photophysical Properties of Trimers

With the six new indole trimers in hand, we performed measurements of various photophysical properties. Figure 4.3 highlights UV-Vis absorption and fluorescence emission data. In the case of 4,5-indolyne trimers **4.7** and **4.8**, the UV-Vis data display variable characteristic peaks. Whereas the symmetrical isomer **4.7** exhibits a strong absorption band at 309 nm, the unsymmetrical isomer absorbs across a broader range, with a major band at 225 nm. Fluorescence emissions are similar, with both **4.7** and **4.8** displaying an emission band at roughly

410 nm. Similar variations are seen when comparing the symmetrical and unsymmetrical trimers of the 5,6-indolyne. The $\lambda_{max}$ for the symmetrical isomer **4.10** is 291 nm, whereas the $\lambda_{max}$ for unsymmetrical isomer **4.11** is 235 nm. Fluorescence emission bands are roughly 400 nm for each trimer derived from the 5,6-indolyne. Finally, the UV-Vis and fluorescence data are very similar for the two trimers derived from the 6,7-indolyne. Both isomers, **4.13** and **4.14**, display a $\lambda_{max}$ of roughly 320 nm, along with fluorescence emissions bands around 433 nm. It is notable that the six isomers display varying photophysical properties. The change of photophysical properties based on structural variation is the subject of ongoing investigation.

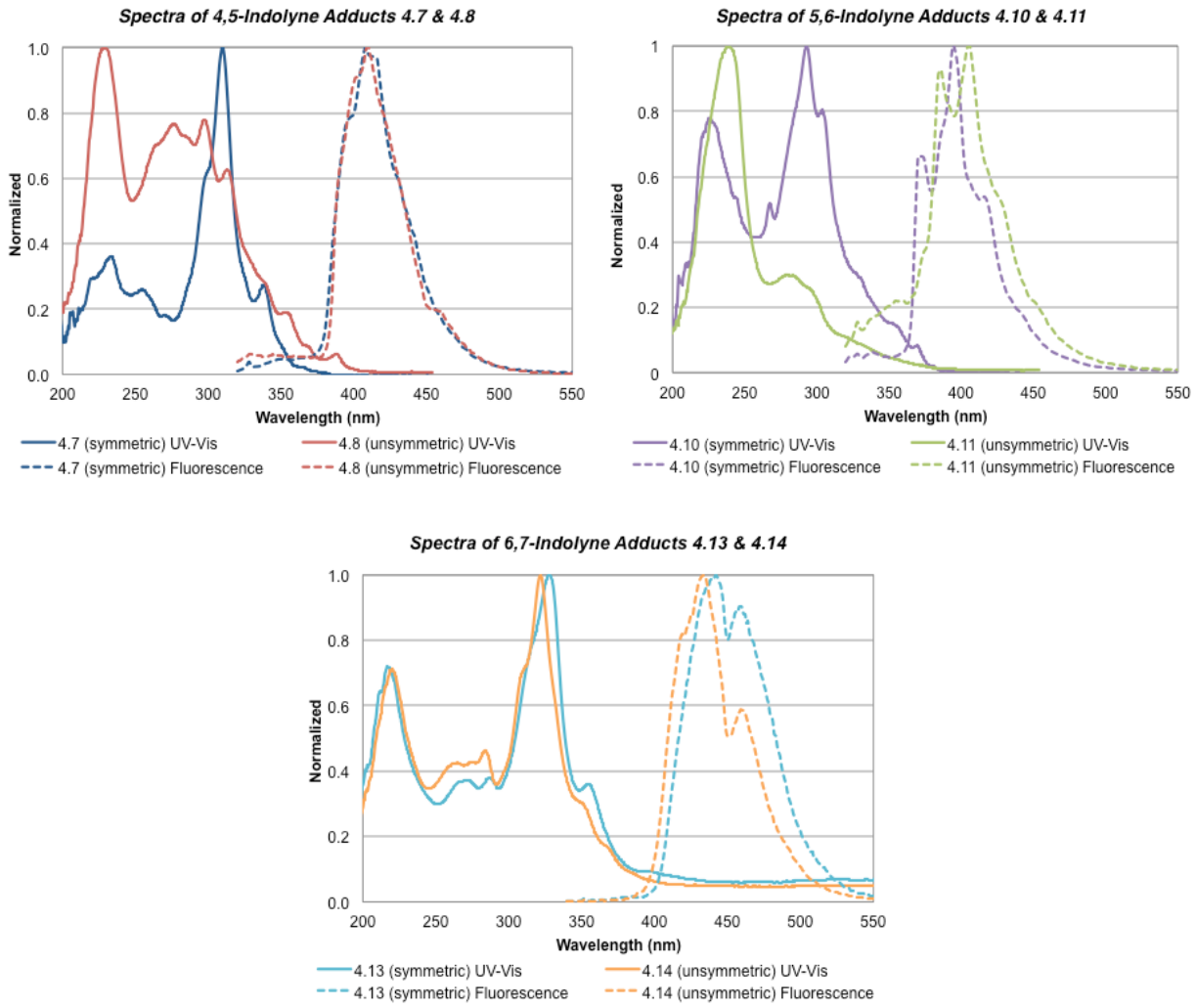


***Figure 4.3.*** UV-Vis absorbance and fluorescence emission spectra for trimers **4.7**, **4.8**, **4.10**, **4.11**, **4.13**, and **4.14** in methylcyclohexane.

### 4.3.4 Structural Analysis

The novel trimers were also inspected by computational analysis. The geometry of each compound, **4.7**, **4.8**, **4.10**, **4.11**, **4.13**, and **4.14**, was minimized using DFT wB97X-D/6-31+G(d,p) (Figure 4.4). Interestingly, both trimers **4.7** and **4.8** arising from the 4,5-indolyne are non-planar. In the case of the symmetrical trimer **4.7**, all three branches are twisted out of

planarity by 11, 21, and 21 degrees. For the unsymmetrical trimer **4.8**, the two symmetrical branches lie largely in the plan of the central arene; however, the unsymmetrical branch is twisted 18 and 30 degrees out of planarity. In both cases, the twisting occurs to relieve steric repulsion between neighboring C–H bonds. On the other hand, trimers **4.10** and **4.11** derived from the 5,6-indolyne are completely flat. The most unusual of the trimers are **4.13** and **4.14**, derived from the 6,7-indolyne. Both isomers are plagued by severe steric repulsion, due to the trajectory of the *N*-Me substituents. For symmetrical isomer **4.13**, out of plane twisting helps to alleviate interactions between the *N*-Me substituents and aryl C–H bonds. In the case of unsymmetrical isomer **4.14**, twisting relieves two types of steric interactions: those between two *N*-Me substituents (of neighboring indoles) and interactions between one *N*-Me substituent and proximal aryl C–H bonds. The maximum out-of-plane twisting is 18° in **4.13** and 38° in **4.14**. To our knowledge, **4.14** is the most bent heteroaromatic compound known to date.[16]

The distorted nature of the trimers correlates to the relative free energies of the molecules. Due to the steric repulsion, trimers **4.7** and **4.8** are 5.2 and 5.5 kcal $mol^{-1}$ higher in energy compared to planar trimer **4.10**. The unsymmetrical counterpart to **4.10**, **4.11**, is only slightly higher in energy (0.8 kcal $mol^{-1}$). Lastly, the extremely distorted 6,7 indolyne trimers **4.13** and **4.14** are significantly higher in energy compared to **4.10**, with free energies of 20.0 and 15.8 kcal $mol^{-1}$, respectively.

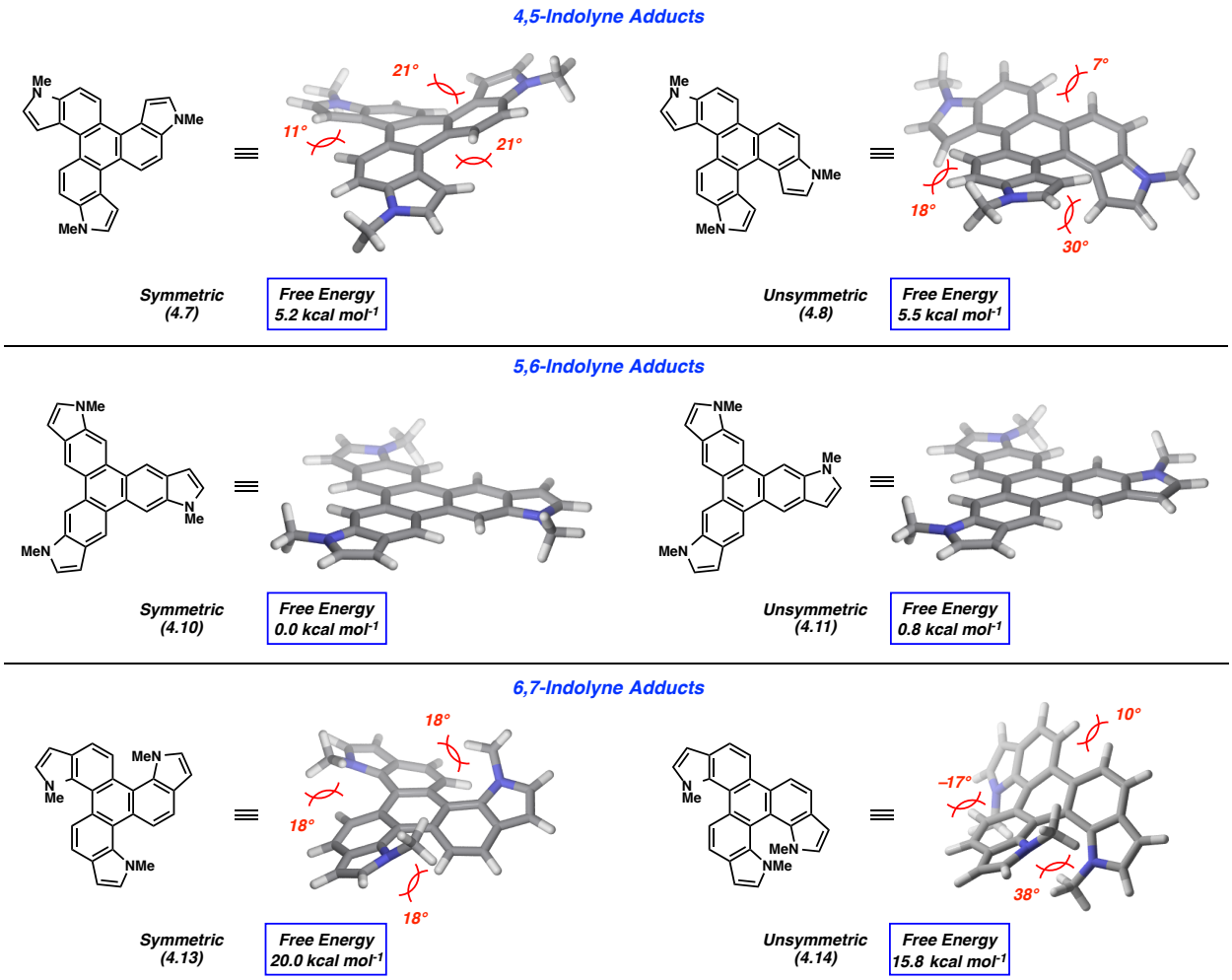


***Figure 4.4.*** Geometry-optimized structures and computed energies of trimers.

## 4.4 Conclusion

In summary, we have designed and synthesized a new class of indole-based conjugated trimers. Our approach to these unique scaffolds relies on the in situ generation of highly reactive indolyne intermediates, which undergo Pd-catalyzed cyclotrimerization. The process results in the formation of three new C–C bonds and has proven useful to prepare six previously unknown trimers. The photophysical properties of these species are heavily influenced by structure. In fact, several of the trimers are severly bent out of planarity to alleviate steric interactions, as shown by

computational studies. Our efforts not only provide access to a new class of conjugated trimers, including several highly bent heteroaromatic compounds, but also mark the first reported use of indolynes in transition metal-catalyzed reactions.

## 4.5 Experimental Section

### 4.5.1 Materials and Methods

Unless stated otherwise, reactions were conducted in flame-dried glassware under an atmosphere of nitrogen using anhydrous solvents (freshly distilled or passed through activated alumina columns). All commercially obtained reagents were used as received unless otherwise specified. Cesium fluoride (CsF)**,** Bis(dibenzylideneacetone)palladium(0) ($Pd(dba)_2$), and tetrakis(triphenylphosphine)palladium(0) ($Pd(PPh_3)_4$) were obtained from Strem Chemicals. BINAP was obtained from Sigma Aldrich. Reaction temperatures were controlled using an IKAmag temperature modulator and, unless stated otherwise, reactions were performed at room temperature (rt, approximately 23 °C). Thin layer chromatography (TLC) was conducted with EMD gel 60 F254 pre-coated plates (0.25 mm) and visualized using a UV light. Preparative thin layer chromatography (TLC) was conducted with EMD gel 60 F254 pre-coated plates (0.5 mm) and visualized using UV light. Silicycle Siliaflash P60 (particle size 0.040–0.063 mm) was used for flash column chromatography. $^1$H NMR spectra were recorded on Bruker spectrometers (500 MHz) and are reported relative to deuterated solvent signals. Data for $^1$H NMR spectra are reported as follows: chemical shift (δ ppm), multiplicity, coupling constant (Hz) and integration. $^{13}$C NMR spectra were recorded on Bruker spectrometers (125 MHz) and are reported relative to deuterated solvent signals. Data for $^{13}$C NMR spectra are reported in terms of chemical shift and, when necessary, multiplicity, and coupling constant (Hz). IR spectra were obtained using a

Perkin-Elmer UATR Two FT-IR spectrometer and are reported in terms of frequency absorption ($cm^{-1}$). UV-Vis spectra were recorded using an Ocean Optics USB2000 spectrophotometer equipped with DT-MINI-2-GS light source. Fluorescence spectra were recorded using an Edinburgh Instruments FLSP920 spectrometer equipped with a Xe900 xenon bulb. The UV-Vis and fluorescence spectra were recorded using a 1-mm quartz cuvette, with spectra-grade methylcyclohexane as the solvent. High-resolution mass spectra were obtained on Thermo Scientific™ Exactive Mass Spectrometers with DART ID-CUBE.

### 4.5.2 Experimental Procedures

#### 4.5.2.1 Cyclotrimerization of Indolyne Precursors

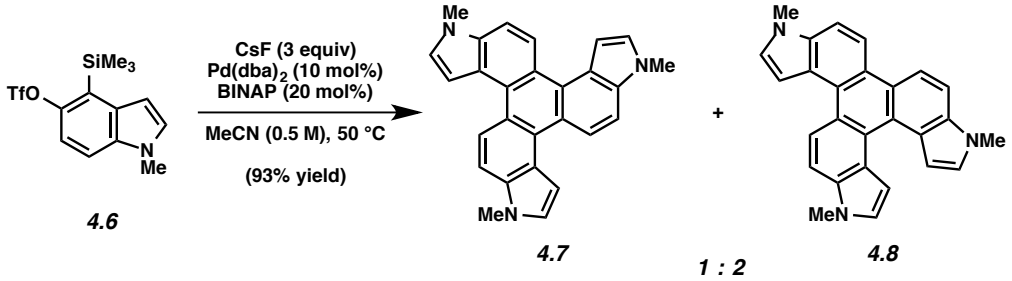


**Symmetric & Unsymmetric 4,5-Indole Trimers (4.7 & 4.8)**. A 1-dram vial containing silyl triflate **4.6** (20 mg, 0.0569 mmol) and a magnetic stir bar was charged with $Pd(dba)_2$ (3 mg, 0.0.00569 mmol, 10 mol%) and BINAP (7 mg, 0.01138 mmol, 20 mol%) in a glove box. Subsequently, MeCN (0.114 mL, 0.5 M) and then CsF (26 mg, 0.170 mmol, 3 equiv) were added. The vial was sealed with a Teflon-lined screw cap, removed from the glove box, and stirred at 50 °C for 12 h. After cooling to 23 °C, the mixture was filtered over a plug of silica gel (4:1 Benzene:Acetonitrile eluent, 10 mL). The volatiles were removed under reduced pressure, and the crude residue was purified by reiterative preparative thin layer chromatography (4x) (20:1 Benzene:Acetonitrile) to afford symmetric trimer **4.7** (2.3 mg, 31% yield) as a brown solid

and unsymmetric trimer **4.8** (4.6 mg, 62% yield) as a brown solid. Symmetric Trimer **4.7**: $R_f$ 0.2 (20:1 Hexanes : EtOAc); $^1$H NMR (500 MHz, $CD_3CN$): δ 9.11 (d, $J$ = 9.1, 3H), 7.79 (dd, $J$ = 9.1, 0.8, 3H), 7.59 (d, $J$ = 3.1, 3H), 7.43 (d, $J$ = 3.1, 3H), 3.99 (s, 9H); $^{13}$C NMR (125 MHz, $CD_3CN$): δ 136.7, 129.6, 126.9, 124.4, 124.0, 122.0, 110.1, 104.7, 33.7; IR (film): 3103, 2911, 1510, 1343, 729 cm$^{-1}$; HRMS-ESI (*m/z*) [M + H]$^+$ calcd for $C_{27}H_{22}N_3$, 388.18082; found, 388.17728. Unsymmetric Trimer **4.8**: $R_f$ 0.3 (20:1 Hexanes : EtOAc); $^1$H NMR (500 MHz, $CD_3CN$): δ 9.10 (d, $J$ = 9.1, 1H), 8.55 (dd, $J$ = 9.1, 2.7, 2H), 7.81 (dd, $J$ = 9.0, 0.7, 1H), 7.76 (dd, $J$ = 9.0, 0.8, 1H), 7.68 (dd, $J$ = 9.0, 0.7, 1H), 7.50 (d, $J$ = 3.1, 1H), 7.39 (d, $J$ = 3.1, 1H), 7.25–7.20 (m, 3H), 7.13 (dd, $J$ = 3.1, 0.8, 1H), 3.96–3.92 (m, 9H); $^{13}$C NMR (125 MHz, $CD_2Cl_2$): δ 136.1, 135.8, 135.6, 128.4, 126.6, 126.4, 126.0, 125.6, 125.0, 124.9, 124.8, 124.7, 124.3, 123.4, 123.2, 121.1, 117.8, 117.7, 110.4, 110.1, 109.5, 106.1, 106.0, 104.2, 33.5, 33.4, 33.4; IR (film): 3103, 2926, 1508, 1412, 720 cm$^{-1}$; HRMS-ESI (*m/z*) [M + H]$^+$ calcd for $C_{27}H_{22}N_3$, 388.18082; found, 388.17737.

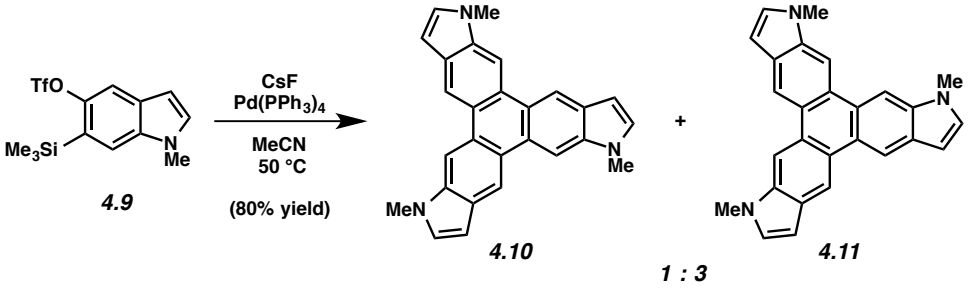


**Symmetric & Unsymmetric 5,6-Indole Trimers (4.10 & 4.11)**. A 1-dram vial containing silyl triflate **4.9** (151 mg, 0.429 mmol) and a magnetic stir bar was charged with $Pd(PPh_3)_4$ (99 mg, 0.0858 mmol, 10 mol%) in a glove box. Subsequently, MeCN (0.85 mL, 0.5 M) and then CsF (196 mg, 1.29 mmol, 3 equiv) were added. The vial was sealed with a Teflon-lined screw cap, removed from the glove box, and stirred at 50 °C for 12 h. After cooling to 23 °C, the mixture

was filtered over a plug of silica gel (9:1 $CH_2Cl_2$:MeOH eluent, 10 mL). The volatiles were removed under reduced pressure, and the crude residue was purified by preparative thin layer chromatography (3:1 Hexane:EtOAc) to afford symmetric trimer **4.10** (11 mg, 20% yield) as a brown solid and unsymmetric trimer **4.11** (33 mg, 60% yield) as a brown solid. Symmetric Trimer **4.10**: $R_f$ 0.4 (20:1 Hexanes : EtOAc); $^1$H NMR (500 MHz, $CD_3CN$): δ 8.98 (s, 3H), 8.62 (s, 3H), 7.33 (d, *J* = 3.1, 3H), 6.64 (dd, *J* = 3.1, 0.7, 1H), 3.99 (s, 9H); $^{13}$C NMR (125 MHz, $CD_3CN$): δ 138.3, 132.6, 129.5, 127.5, 124.7, 115.5, 103.4, 101.2, 33.4; IR (film): 3098, 2926, 1492, 1453, 704 cm$^{-1}$; HRMS-ESI (*m/z*) $[M + H]^+$ calcd for $C_{27}H_{22}N_3$, 388.18082; found, 388.17826. Unsymmetric Trimer **4.11**: $R_f$ 0.3 (20:1 hexanes : EtOAc); $^1$H NMR (500 MHz, $CD_3CN$): δ 8.99 (s, 1H), 8.88 (s, 1H), 8.87 (s, 1H), 8.70 (s, 1H), 8.69 (s, 1H), 8.61 (s, 1H), 7.35 (d, *J* = 3.1, 1H), 7.33 (d, *J* = 3.1, 1H), 7.31 (d, *J* = 3.1, 1H), 6.65 (dd, *J* = 3.1, 0.8, 1H), 6.63 (dd, *J* = 3.1, 0.8, 1H), 6.61 (dd, *J* = 3.1, 0.8, 1H), 4.03 (s, 3H), 4.02 (s, 3H), 3.98 (s, 3H); $^{13}$C NMR (125 MHz, $CD_2Cl_2$): δ 137.6, 137.4, 137.3, 131.8, 131.7, 131.4, 129.2, 129.1, 128.8, 126.8, 126.5, 126.3, 124.8, 124.7, 124.3, 114.8, 114.8, 114.6, 102.5, 102.4, 102.4, 100.9, 100.9, 100.8, 33.5, 33.4, 33.3; IR (film): 3103, 2981, 1513, 1471, 723 cm$^{-1}$; HRMS-ESI (*m/z*) $[M + H]^+$ calcd for $C_{27}H_{22}N_3$, 388.18082; found, 388.17919.

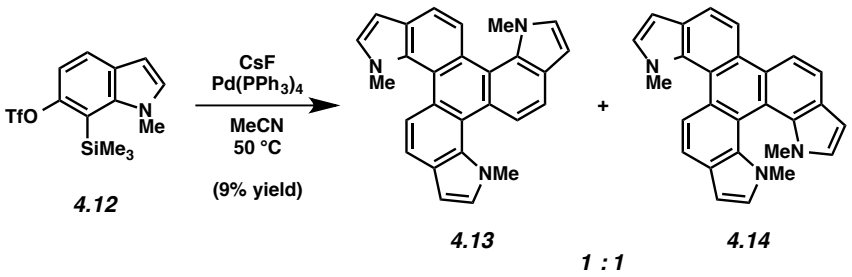


**Symmetric & Unsymmetric 6,7-Indole Trimers (4.13 & 4.14)**. A 1-dram vial containing silyl triflate **4.12** (40 mg, 0.114 mmol) and a magnetic stir bar was charged with $Pd(PPh_3)_4$ (7 mg,

0.0114 mmol, 10 mol%) in a glove box. Subsequently, MeCN (0.228 mL, 0.5 M) and then CsF (52 mg, 0.340 mmol, 3 equiv) were added. The vial was sealed with a Teflon-lined screw cap, removed from the glove box, and stirred at 50 °C for 12 h. After cooling to 23 °C, the mixture was filtered over a plug of silica gel (9:1 $CH_2Cl_2$:MeOH eluent, 10 mL). The volatiles were removed under reduced pressure, and the crude residue was purified by reiterative preparative thin layer chromatography (3x) (10:10:1 Benzene:Hexanes:$CH_2Cl_2$) to afford symmetric trimer **4.13** (0.6 mg, 4.4% yield) as a brown solid and unsymmetric trimer **4.14** (0.6 mg, 4.6% yield) as a light brown solid. Symmetric Trimer **4.13**: $R_f$ 0.2 (20:1 Hexanes : EtOAc); $^1$H NMR (500 MHz, $CD_2Cl_2$): δ 8.17 (d, *J* = 8.5, 3H), 7.77 (d, *J* = 8.5, 3H), 7.32 (d, *J* = 3.1, 3H), 6.81 (d, *J* = 3.1, 3H), 3.79 (s, 9H); $^{13}$C NMR (125 MHz, $CD_2Cl_2$): δ 137.3, 135.3, 130.6, 126.7, 124.2, 122.1, 120.1, 105.9, 40.7; IR (film): 3361, 2923, 1661, 1321, 799 cm$^{-1}$; HRMS-ESI (*m/z*) $[M + H]^+$ calcd for $C_{27}H_{22}N_3$, 388.18082; found, 337.01828. Unsymmetric Trimer **4.14**: $R_f$ 0.2 (20:1 Hexanes : EtOAc); $^1$H NMR (500 MHz, $CD_3CN$): δ 8.31 (dd, *J* = 8.5, 0.4, 1H), 8.27 (dd, *J* = 8.5, 0.4, 1H), 8.08 (d, *J* = 8.5, 1H), 7.89 (d, *J* = 4.0, 1H), 7.88 (d, *J* = 4.0, 1H), 7.79 (d, *J* = 8.5, 1H), 7.79 (d, *J* = 8.5, 1H), 7.36 (d, *J* = 3.1, 1H), 7.18 (d, *J* = 3.1, 1H), 7.14 (d, *J* = 3.1, 1H), 6.77 (d, *J* = 3.1, 1H), 6.71 (d, *J* = 3.1, 1H), 6.70 (d, *J* = 3.1, 1H), 3.89 (s, 3H), 3.21 (s, 3H), 2.85 (s, 3H); $^{13}$C NMR (125 MHz, $CD_3CN$): δ 136.2, 136.2, 135.6, 134.2, 133.3, 131.8, 130.2, 129.3, 128.9, 128.3, 128.2, 125.3, 121.5, 121.1, 120.9, 120.0, 119.1, 116.1, 115.5, 114.1, 113.3, 104.7, 103.7, 103.5, 38.5, 35.1, 34.9; IR (film): 3101, 2924, 1676, 1317, 821 cm$^{-1}$; HRMS-ESI (*m/z*) $[M + H]^+$ calcd for $C_{27}H_{22}N_3$, 388.18082; found, 388.17688.

### 4.5.3 Photophysical Properties

#### 4.5.3.1 UV-Vis and Fluorescence Spectra

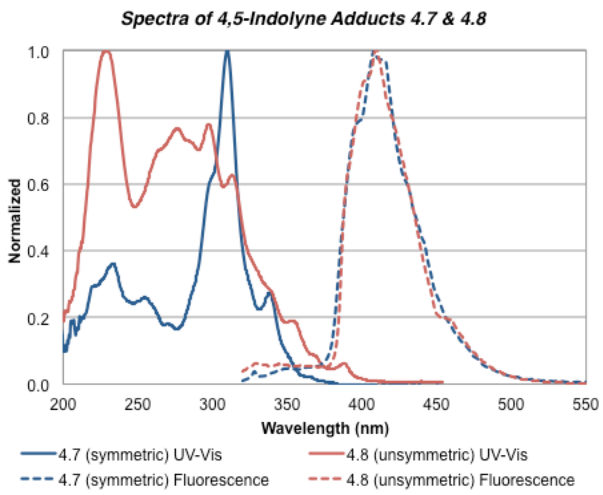


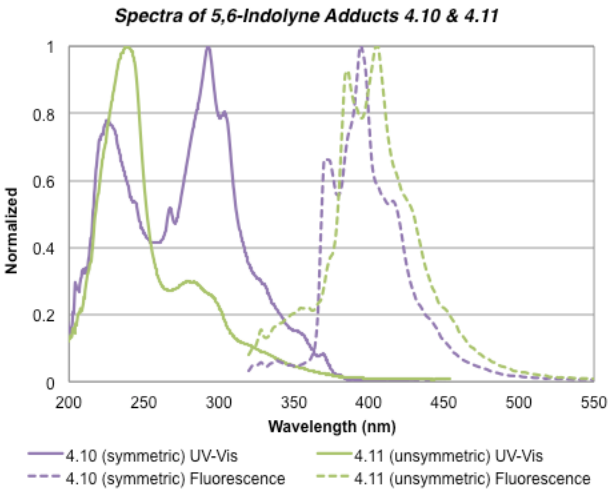


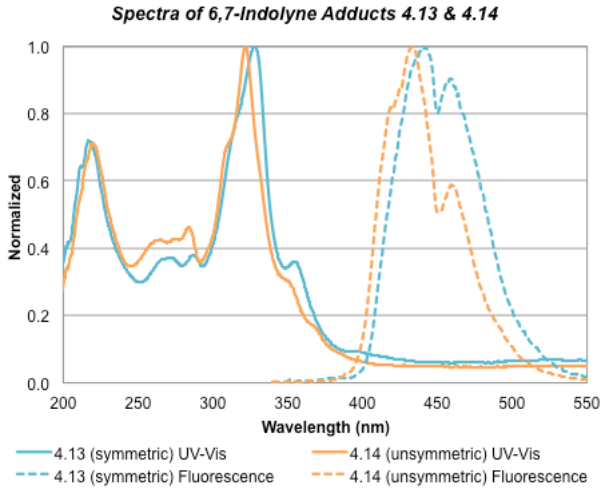


*Note: The UV-Vis and fluorescence spectra were recorded using a 0.0001 M solution with spectra-grade methylcyclohexane in a 1-mm quartz cuvette*

### 4.5.3.2 Cyclic Voltammetry Spectra

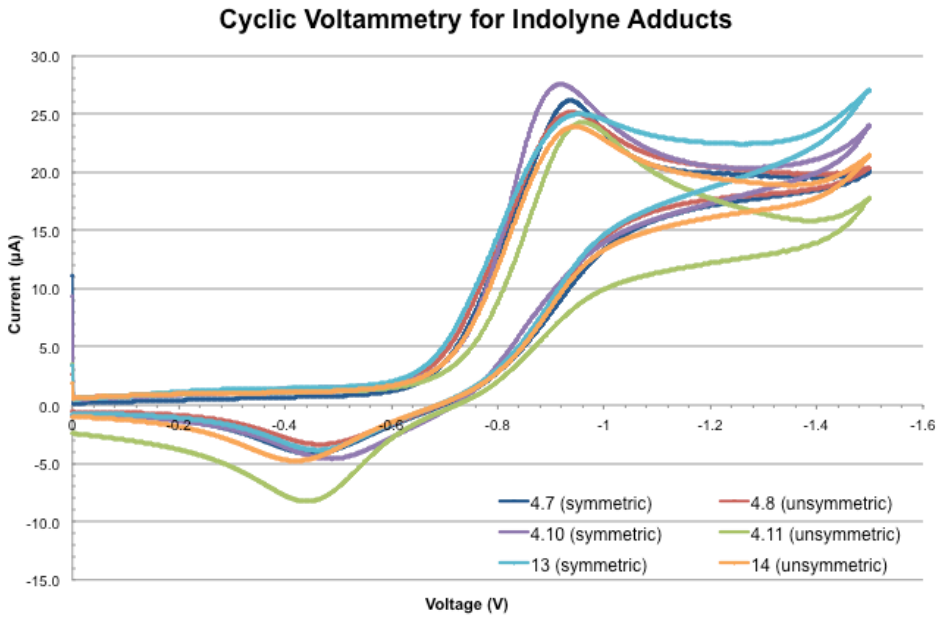


*Note: The electrochemical cyclic voltammetry (CV) were carried out at room temperature conducted with Pt disk, Pt wire, and Silver wire as working electrode, counter electrode, and reference electrode, respectively, in a 0.1 mol L-1 tetrabutylammonium hexafluorophosphate ($Bu_4NPF_6$) dichloromethane solution, and the scan rate was 100 mV $s^{-1}$.*

## 4.6 Spectra Relevant to Chapter Four:

## A New Class of Conjugated Trimeric Scaffolds Accessible Using Indolyne Cyclotrimerizations

Tejas K. Shah, Janice Lin, Adam E. Goetz, K. N. Houk, and Neil K. Garg

*Manuscript in preparation.*

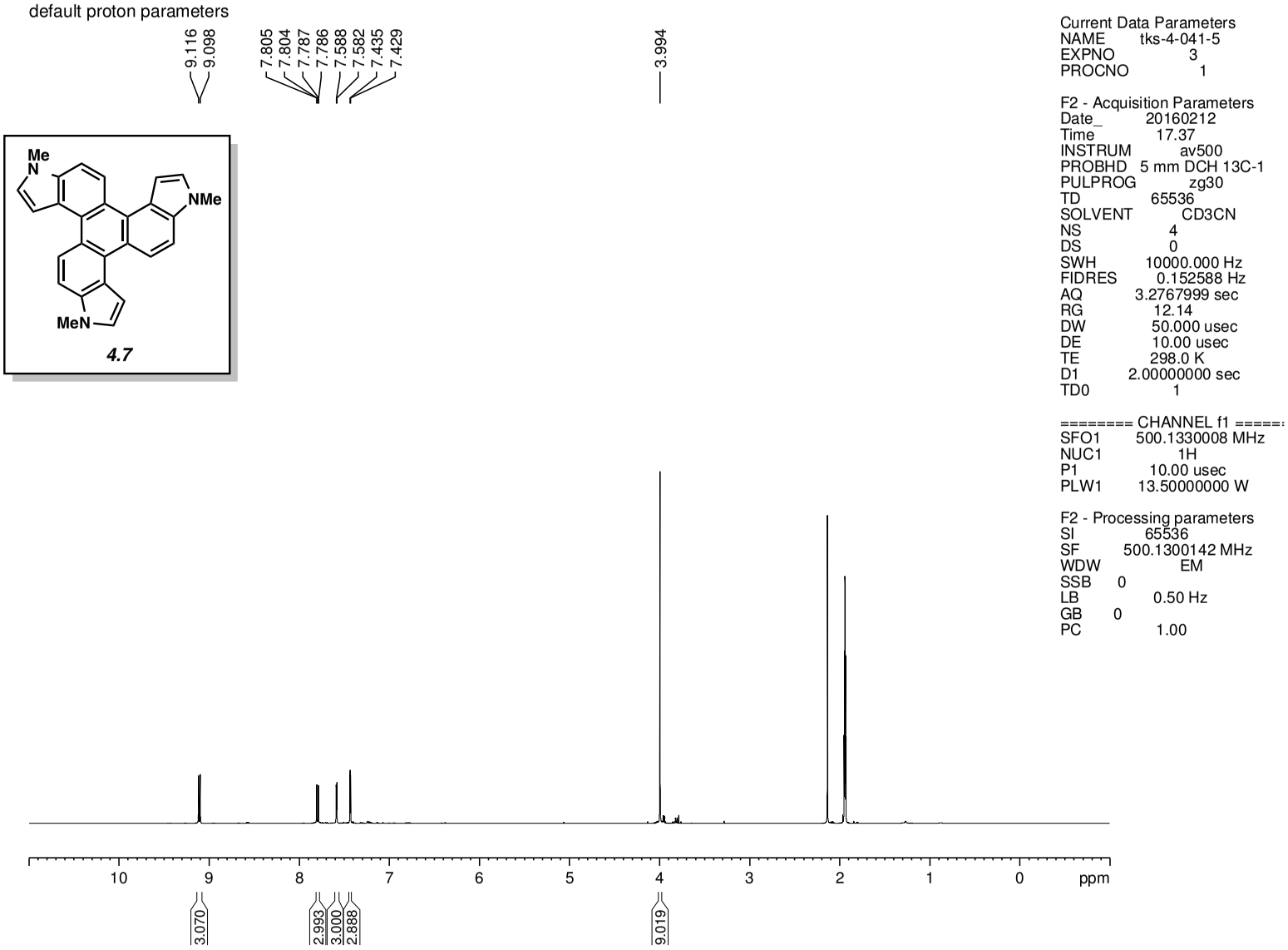


***Figure A4.5.*** $^{1}$H NMR (500 MHz, $CD_3CN$) compound **4.7**

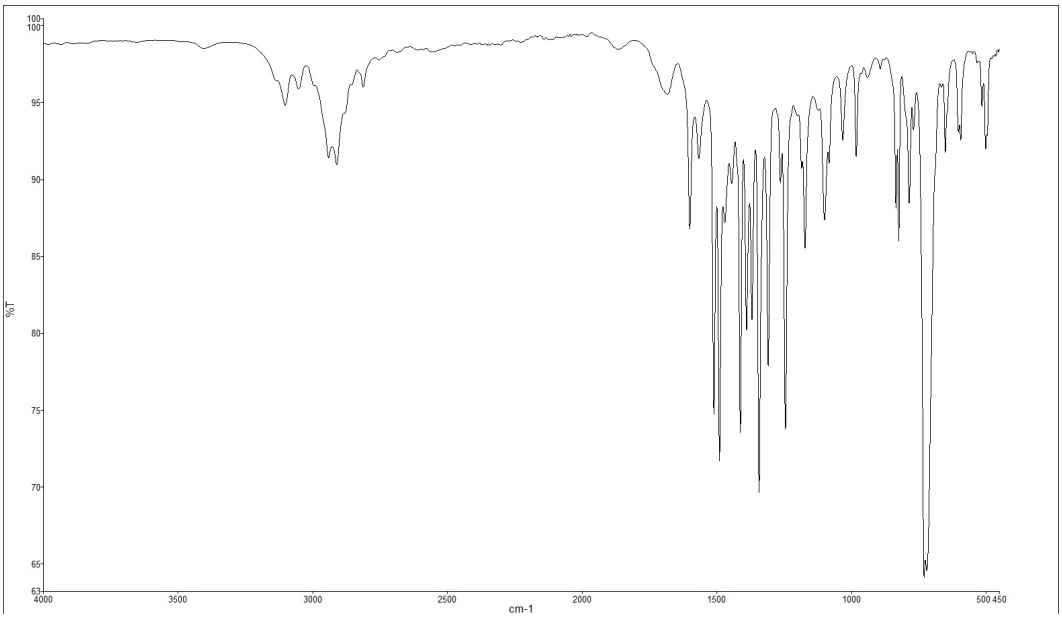


***Figure A4.6.*** Infrared spectrum of compound **4.7**

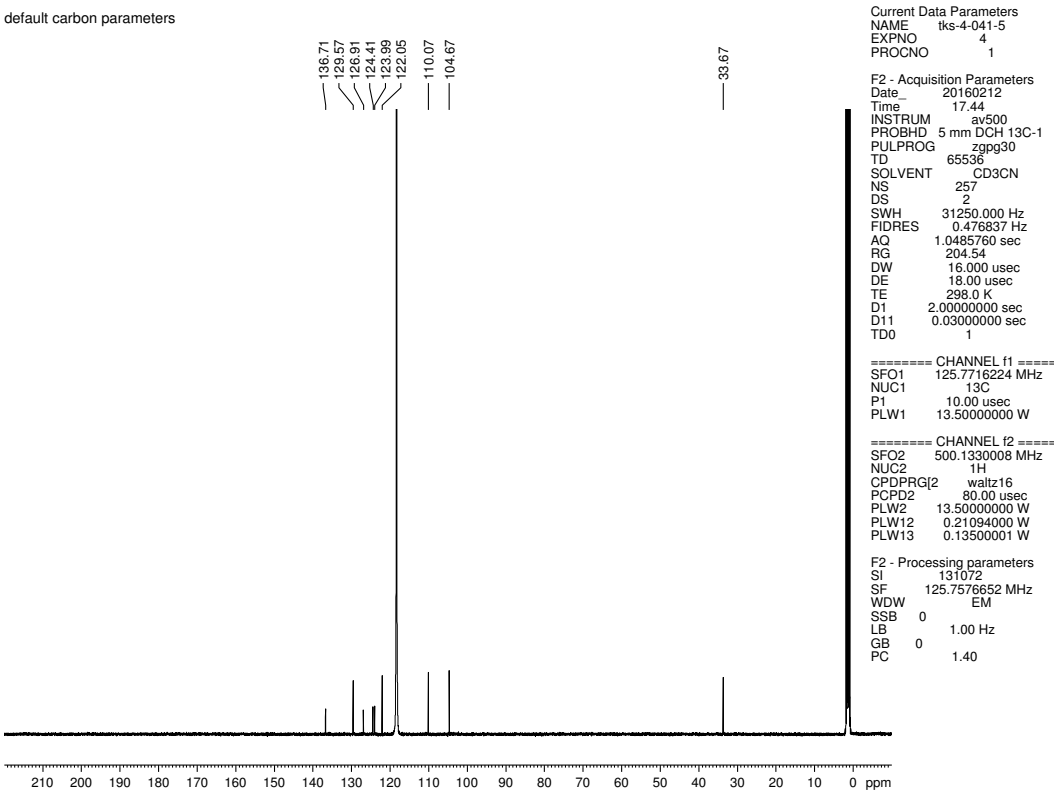


***Figure A4.7.*** $^{13}C$ NMR (125 MHz, $CD_3CN$) of compound **4.7**

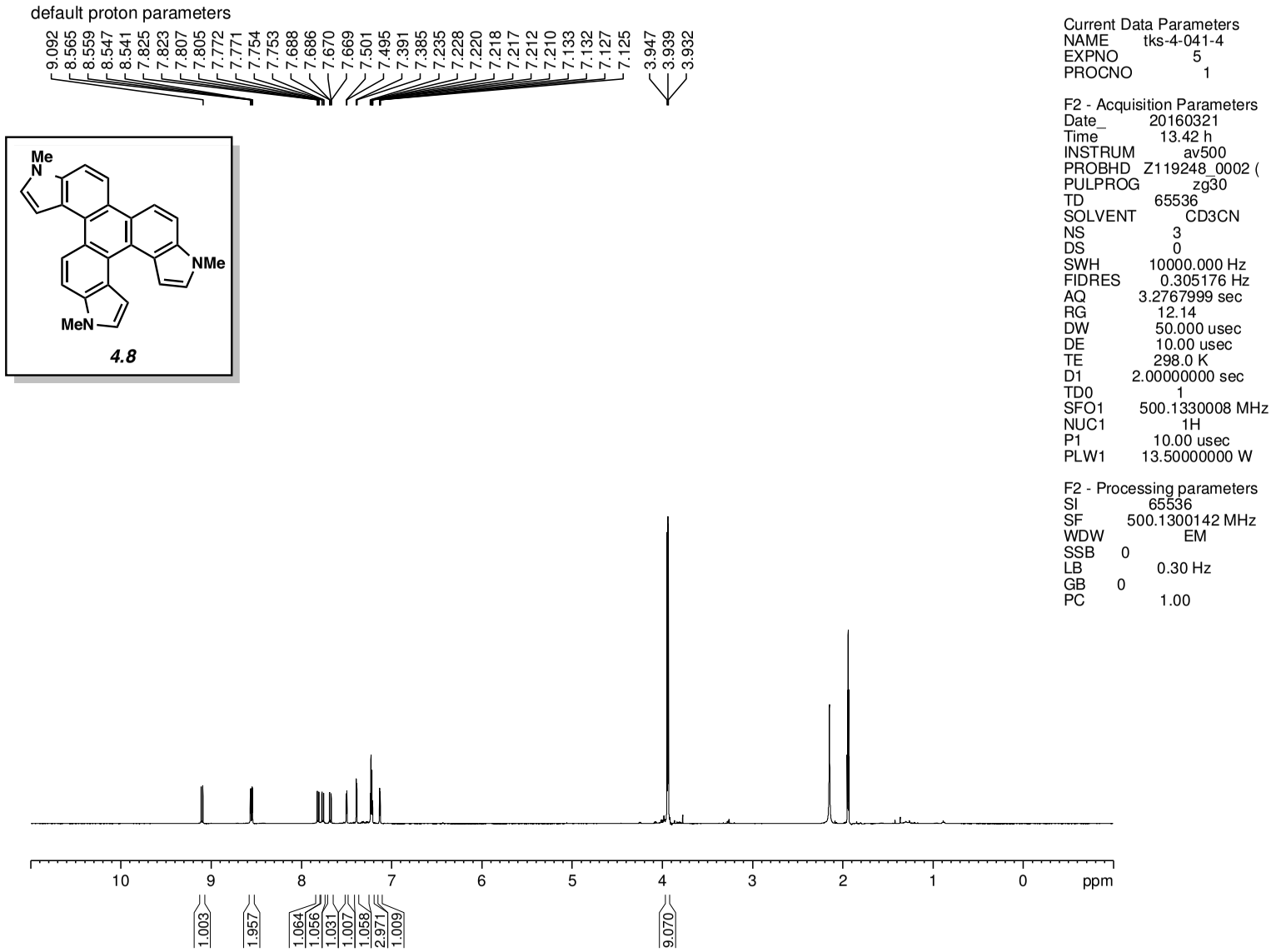


***Figure A4.8.*** $^{1}$H NMR (500 MHz, $CD_3CN$) compound **4.8**

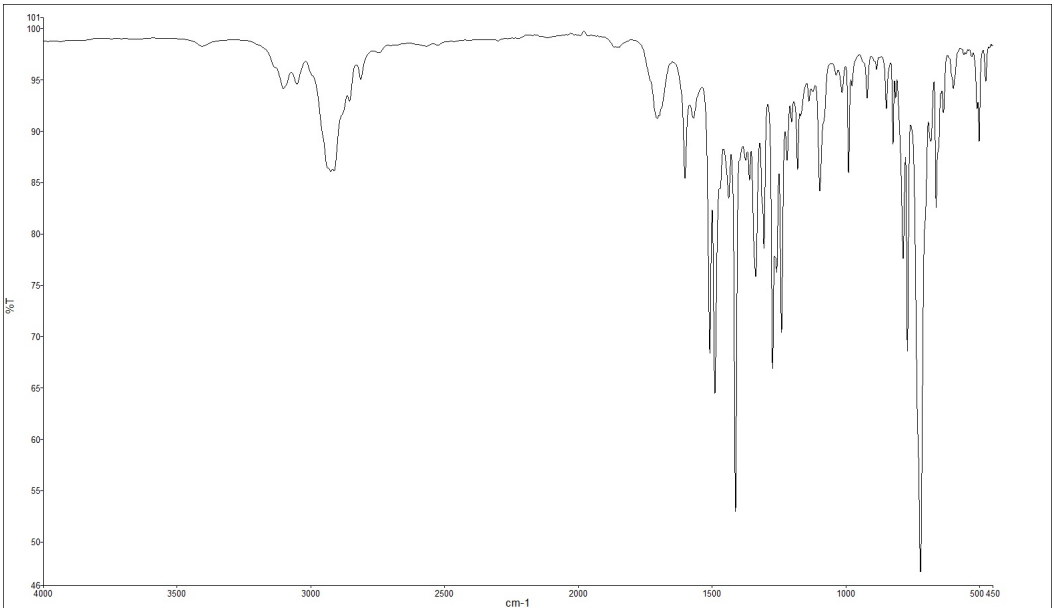


***Figure A4.9.*** Infrared spectrum of compound **4.8**

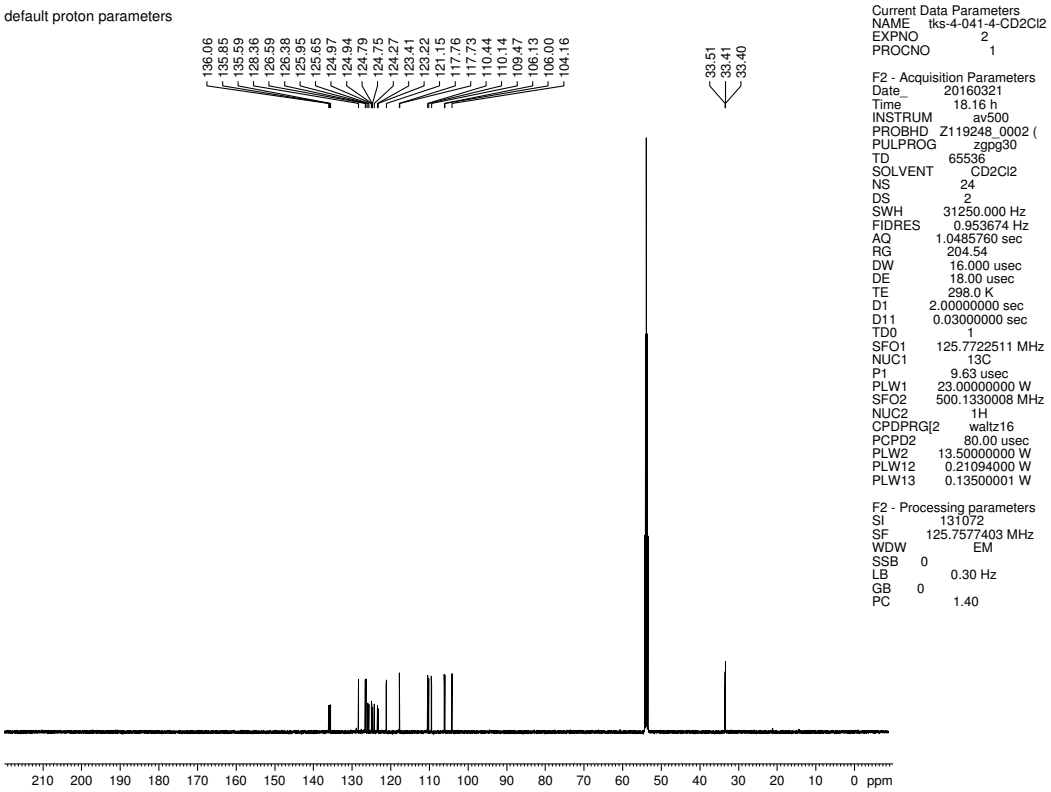


***Figure A4.10.*** $^{13}C$ NMR (125 MHz, $CD_2Cl_2$) of compound **4.8**

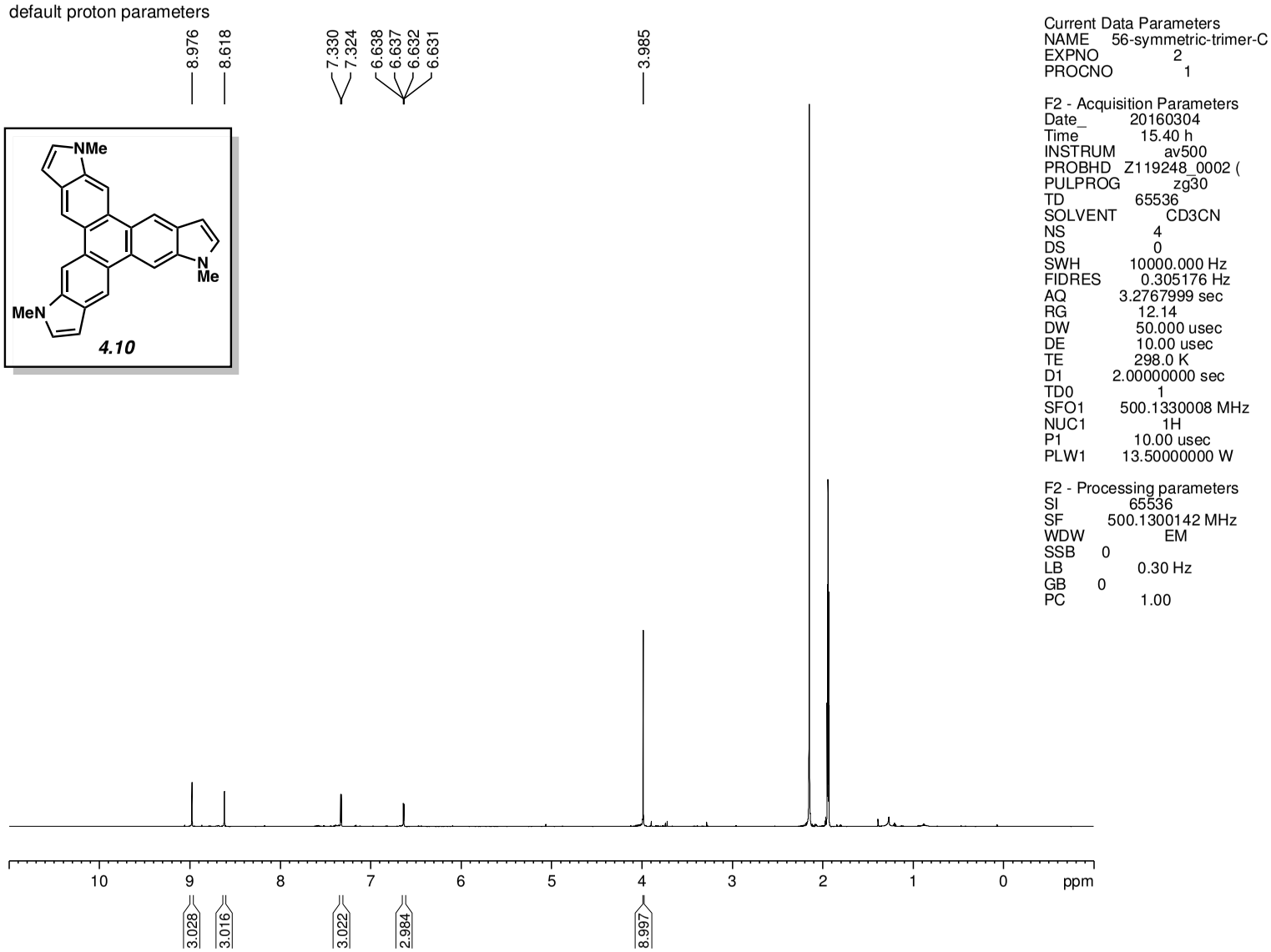


***Figure A4.11.*** $^{1}$H NMR (500 MHz, $CD_3CN$) compound **4.10**

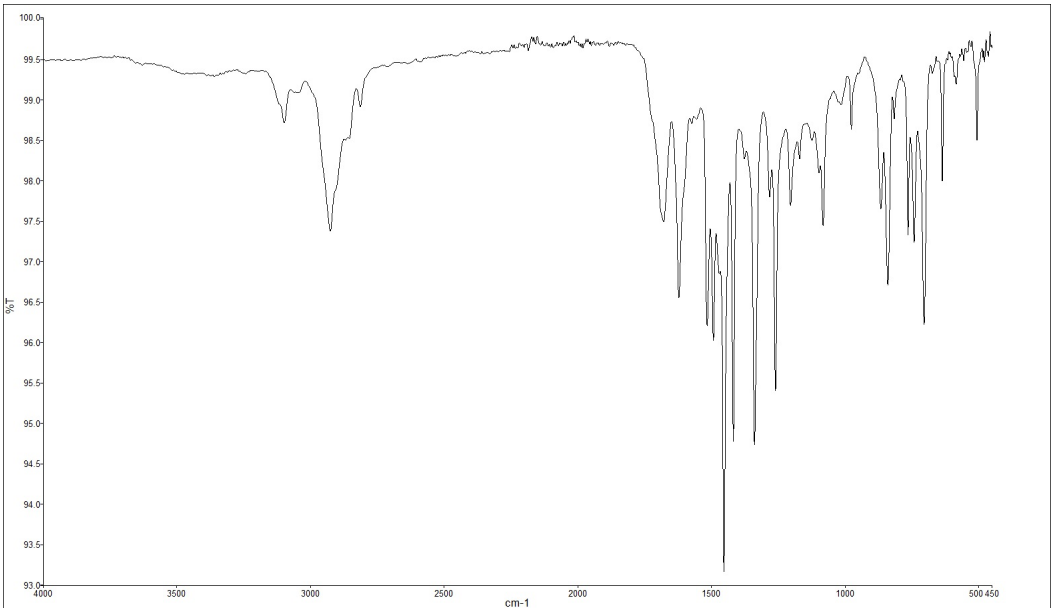


***Figure A4.12.*** Infrared spectrum of compound **4.10**

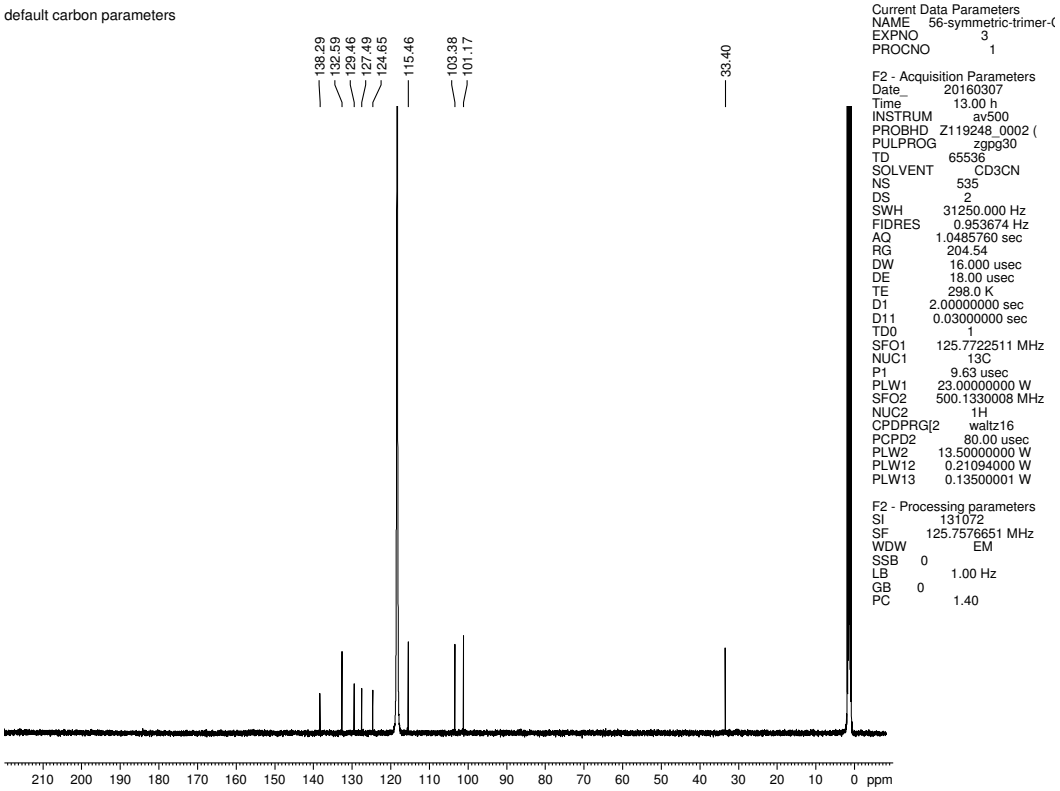


***Figure A4.13.*** $^{13}C$ NMR (125 MHz, $CD_3CN$) of compound **4.10**

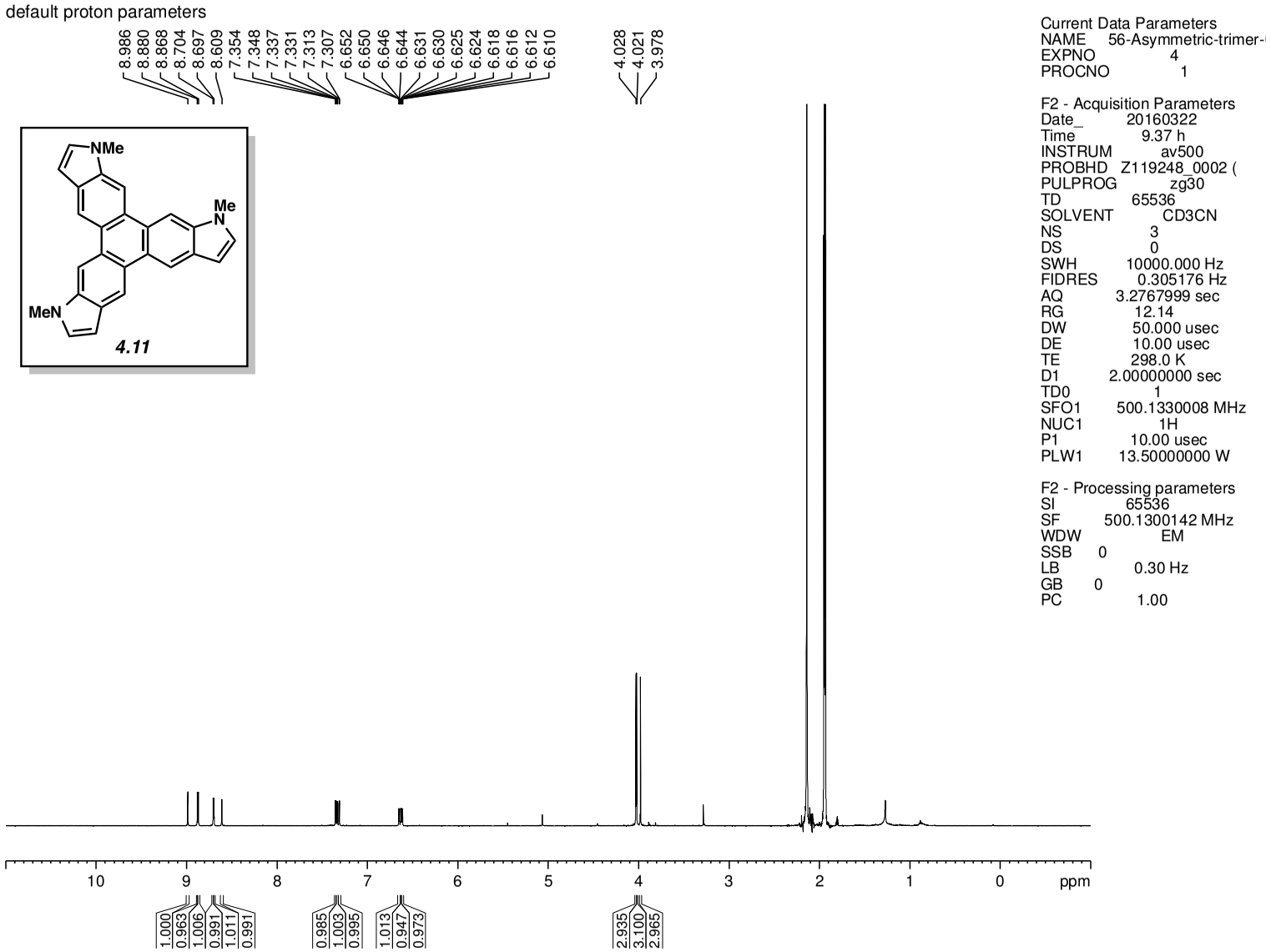


***Figure A4.14.*** $^{1}$H NMR (500 MHz, $CD_3CN$) compound **4.11**

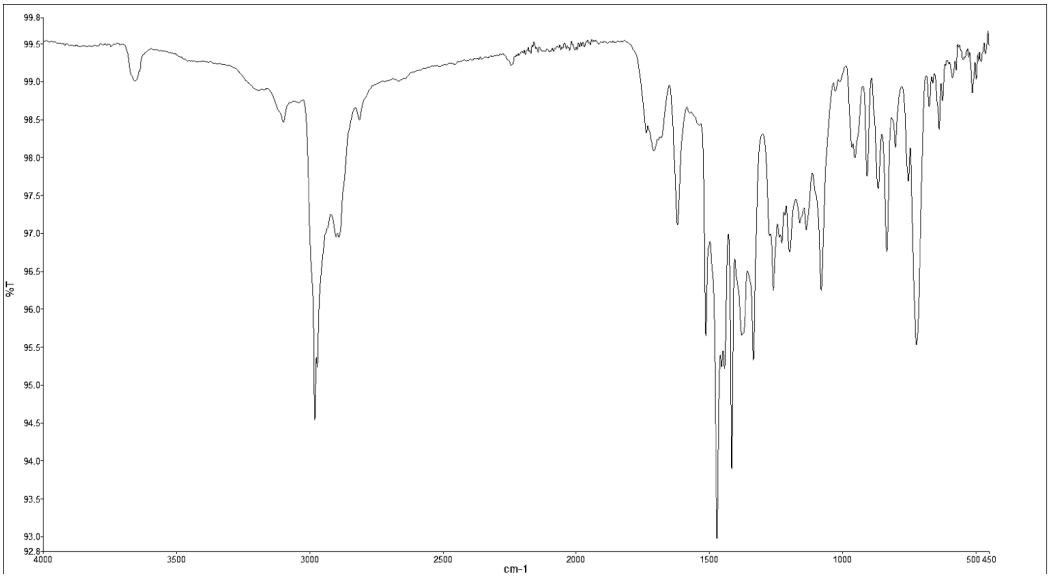


***Figure A4.15.*** Infrared spectrum of compound **4.11**

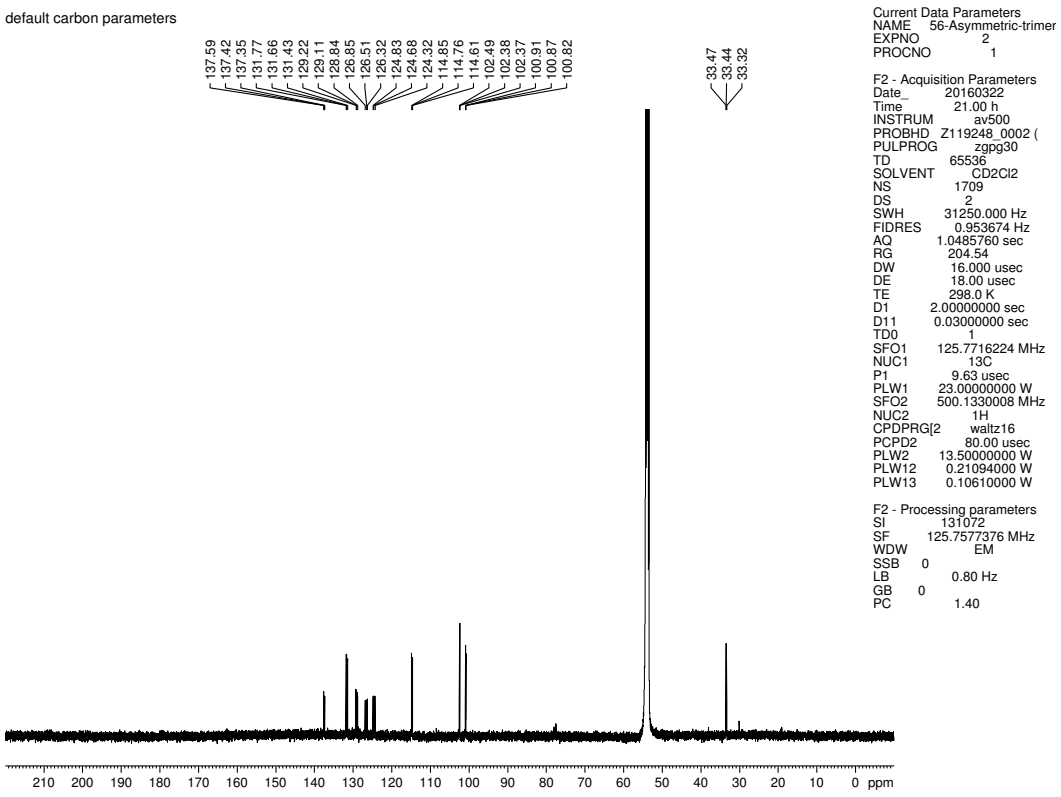


***Figure A4.16.*** $^{13}C$ NMR (125 MHz, $CD_2Cl_2$) of compound **4.11**

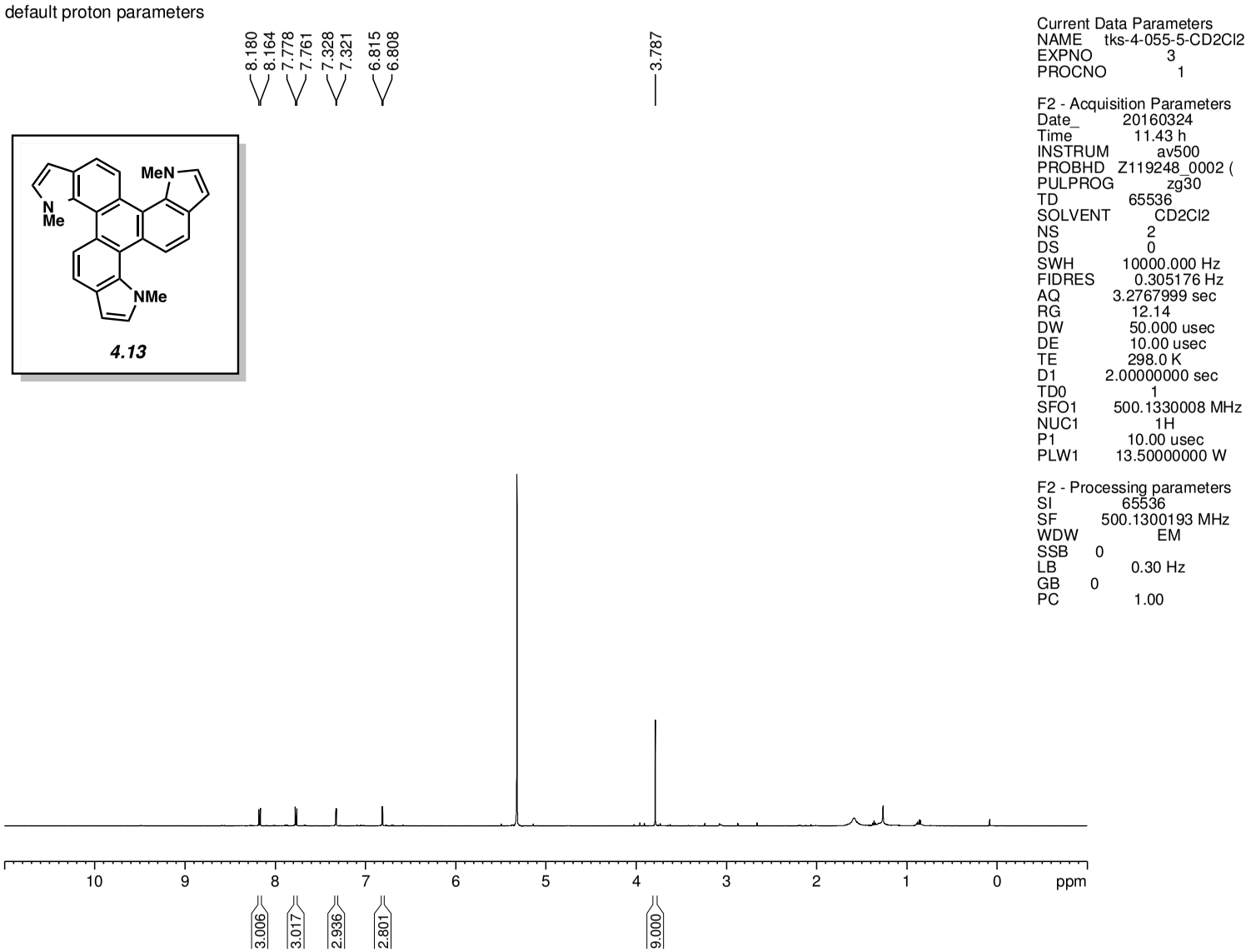


***Figure A4.17.*** $^{1}$H NMR (500 MHz, $CD_2Cl_2$) compound **4.12**

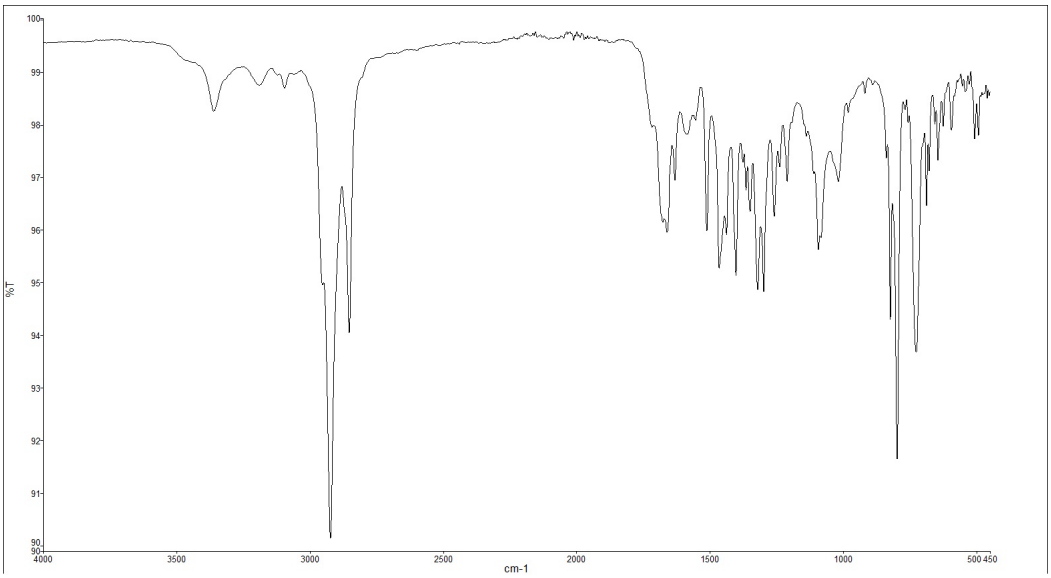


***Figure A4.18.*** Infrared spectrum of compound **4.13**

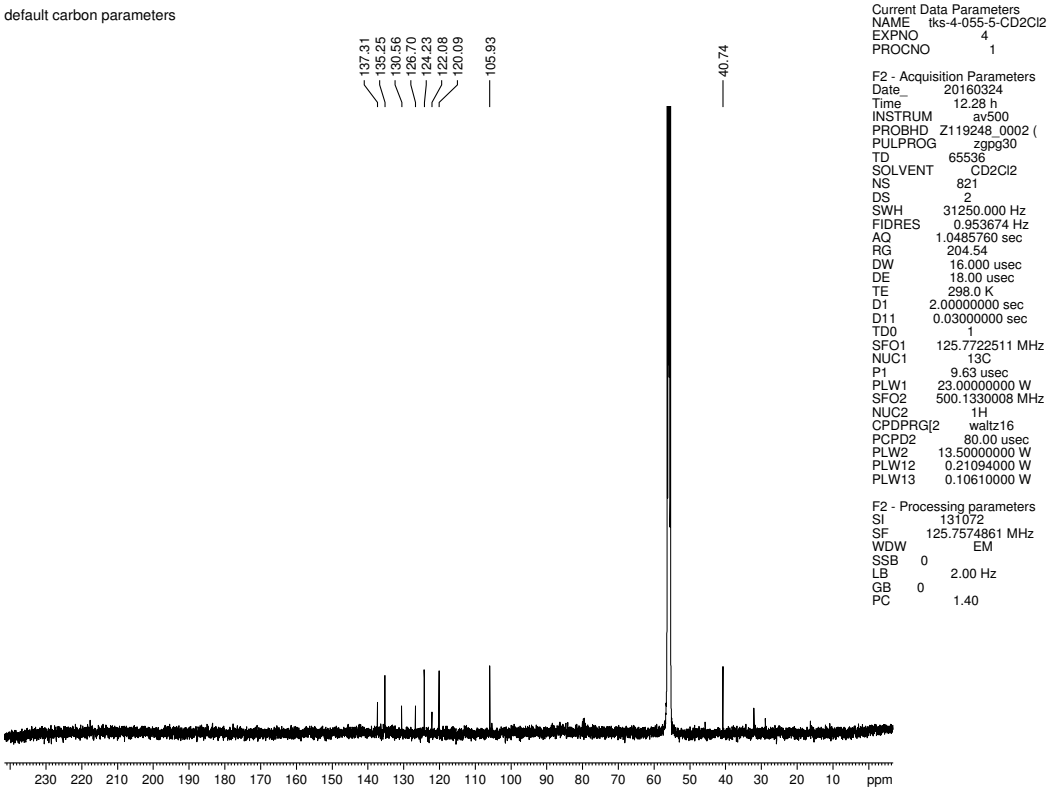


***Figure A4.19.*** $^{13}C$ NMR (125 MHz, $CD_2Cl_2$) of compound **4.13**

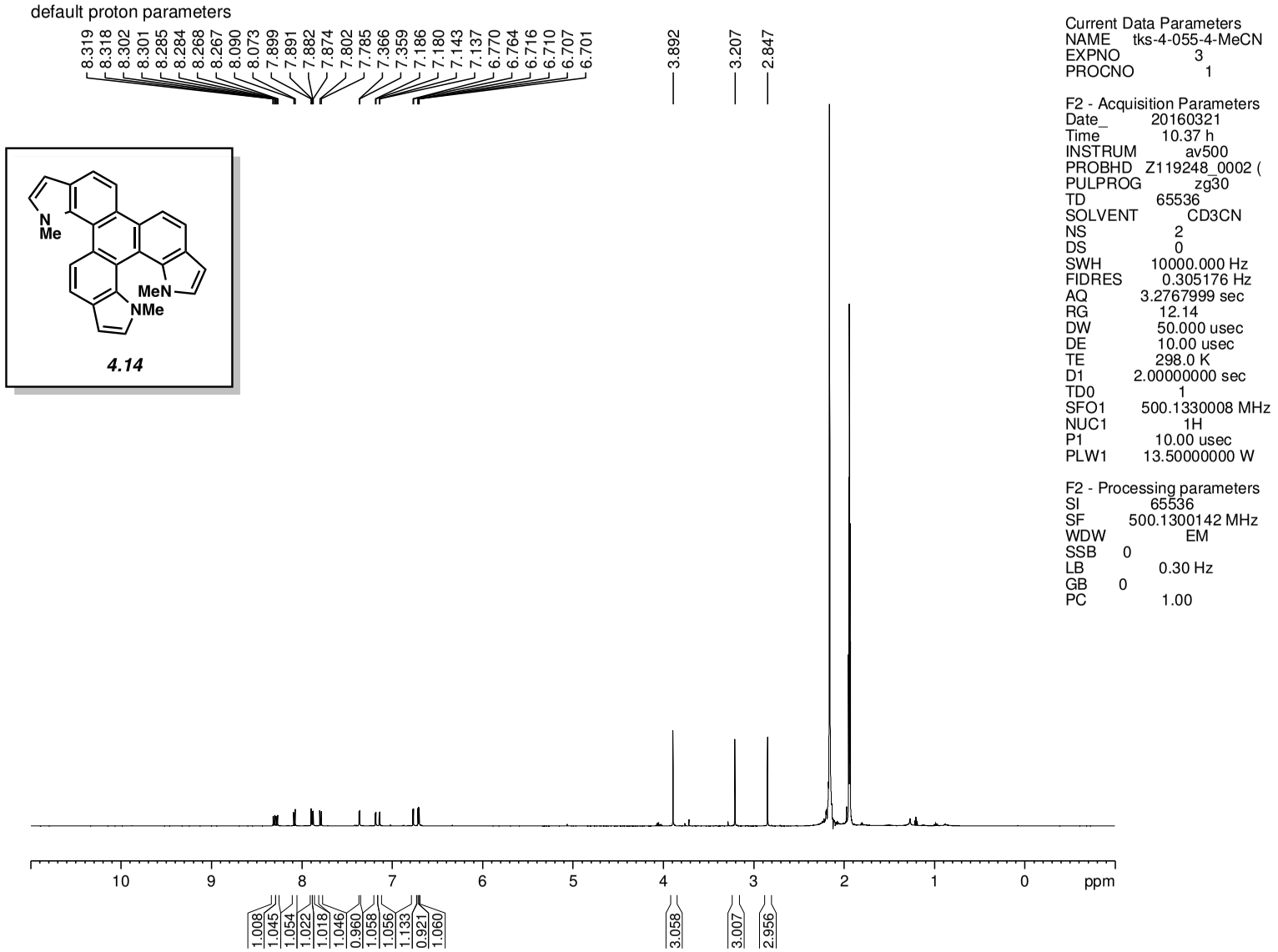


***Figure A4.20.*** $^{1}$H NMR (500 MHz, $CD_3CN$) compound **4.14**

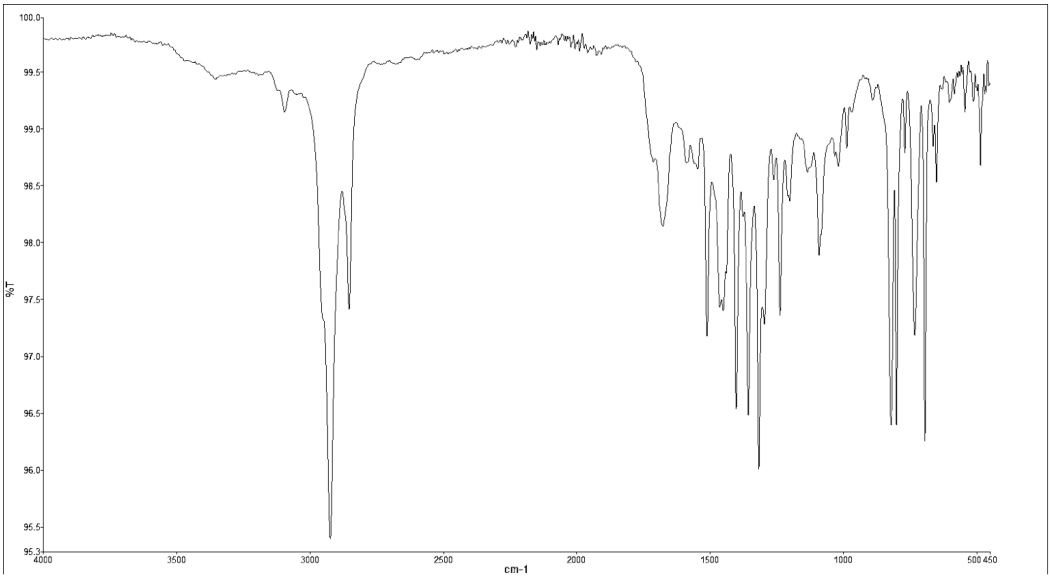


***Figure A4.21.*** Infrared spectrum of compound **4.14**

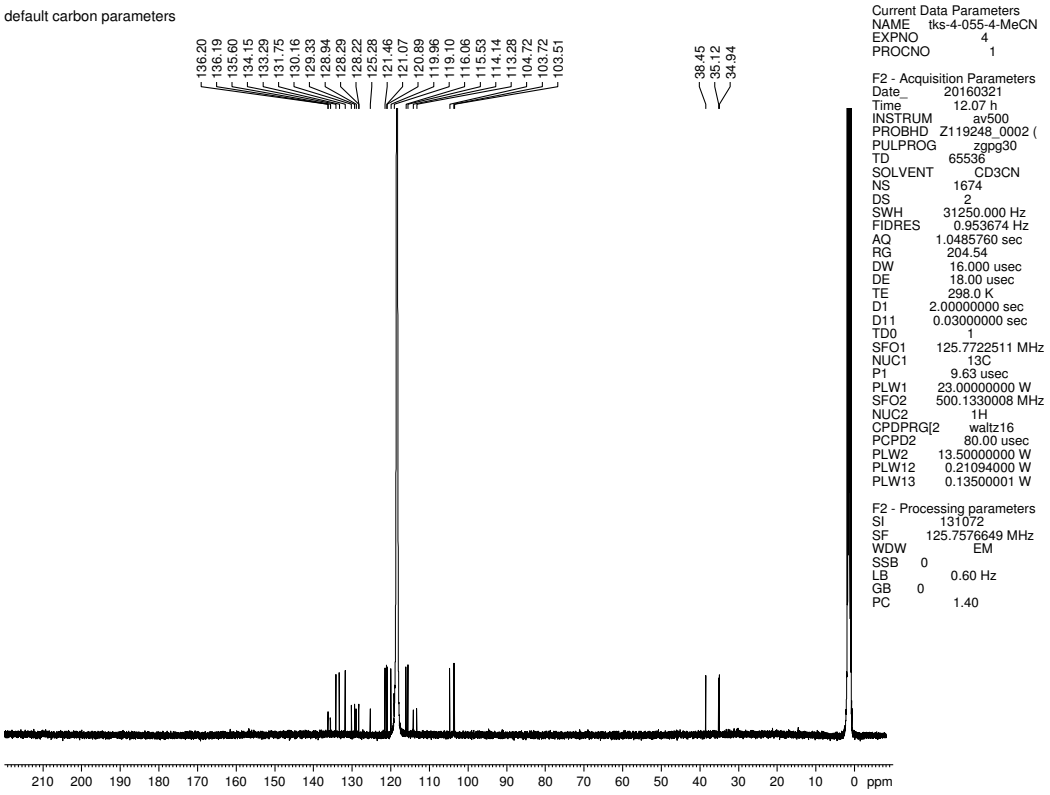


***Figure A4.22.*** $^{13}$C NMR (125 MHz, $CD_3CN$) of compound **4.14**

## 4.7 Notes and References


[1] (a) Kulkarni, A. P.; Tonzola, C. J.; Babel A.; Jenekhe, S. A. *Chem. Mater.* **2004**, *16*, 4556–4573. (b) Duan, L.; Hou, L.; Lee, T.-W.; Qiao, J.; Zhang, D.; Dong, G.; Wang, L.; Qiu, Y. *J. Mater. Chem.* **2010**, *20*, 6392–6407. (c) Tao, Y.; Yang, C.; Qin, J. *Chem. Soc. Rev.* **2011**, *40*, 2943–2970. (d) Yu, T.; Liu, L; Xie, Z; Ma, Y. *Sci. China Chem.* **2015**, *58*, 907–915.

[2] (a) Mas-Torrent, M.; Rovira, C. *Chem. Soc. Rev.* **2008**, *37*, 827–838. (b) Allard, S.; Forster, M.; Souharce, B.; Thiem, H.; Scherf, U. *Angew. Chem. Int. Ed.* **2008**, *47*, 4070–4098. (c) Sirringhaus, H. *Adv. Mater.* **2014**, *26*, 1319–1335. (d) Back, J. Y.; Kim, Y.; An, T. K.; Kang, M. S.; Kwon, S.-K.; Park, C. E.; Kim, Y.-H. *Dyes Pigments* **2015**, *112*, 220–226.

[3] (a) Mishra, A.; Bäuerle, P. *Angew. Chem. Int. Ed.* **2012**, *51*, 2020–2067. (b) Lin, Y.; Li, Y.; Zhan, X. *Chem. Soc. Rev.* **2012**, *41*, 4245–4272. (c) Roncali, J.; Leriche, P.; Blanchard, P. *Adv. Mater.* **2014**, *26*, 3821–3838.

[4] Schmidt, H.; Schultz, G. *Justus Liebigs Ann. Chem.* **1880**, *203*, 118–137.

[5] (a) H. Muller, PhD thesis, University of Heidelberg, 1964. (b) Kaneko, T.; Matsuo, M. *Heterocycles* **1979**, *12*, 471–474. (c) Bergman, J.; Eklund, N. *Tetrahedron* **1980**, *36*, 1439–1443. (d) Bergman, J.; Eklund, N. *Tetrahedron* **1980**, *36*, 1445–1450.

[6] For studies on triazatruxene as two-photon absorption chromophores, see: (a) Ji, L.; Fang, Q.; Yuan, M.-s.; Liu, Z.-q.; Shen, Y.-x.; Chen, H.-f. *Org. Lett.* **2010**, *12*, 5192–5195. (b) Shao, J.; Guan, Z.; Yan, Y.; Jiao, C.; Xu, Q.-H.; Chi, C. *J. Org. Chem.* **2010**, *76*, 780–790.

[7] For a review on triphenylene-based discotic liquid crystals, see: Pal, S. K.; Setia, S.; Avinash, B. S.; Kumar, S. *Liq. Cryst.* **2013**, *40*, 1769–1816.

[8] For studies on triazatruxene-based discotic liquid crystals, see: (a) Gómez-Lor, B.; Alonso, B.; Omenat, A.; Serrano, J. L. *Chem. Commun.* **2006**, 5012–5014. (b) Talarico, M.; Termine, R.; García–Frutos, E. M.; Omenat, A.; Serrano, J. L.; Gómez-Lor, B.; Golemme, A. *Chem. Mater.* **2008**, *20*, 6589–6591. (c) García–Frutos, E. M.; Gutierrez-Puebla, E.; Monge, M. A.; Ramírez, R.; de Andrés, P.; de Andrés, A.; Ramírez, R.; Gómez-Lor, B. *Org. Electron.* **2009**, *10*, 643–652. (d) Zhao, B.; Liu, B.; Png, R. Q.; Zhang, K.; Lim, K. A.; Luo, J.; Shao, J.; Ho, P. K. H.; Chi, C.; Wu, J. *Chem. Mater.* **2010**, *22*, 435–449.

[9] For recent studies on triphenylene based solar cells, see: (a) KR Pat., KR20110098302, 2011. (b) WO Pat., WO2012048781, 2012. (c) Bajpai, M.; Yadav, N.; Kumar, S.; Srivastava, R. Dhar, R. *Liq. Cryst.* **2016**, DOI: 10.1080/02678292.2016.1149239.

[10] For studies on triazatruxene based solar cells, see: (a) Bura, T.; Leclerc, N.; Fall, S.; Lévêque, P. Heiser, T.; Ziessel, R. *Org. Lett.* **2011**, *13*, 6030–6033. (b) Shelton, S. W.; Chen, T. L.; Barclay, D. E.; Ma, B. *ACS Appl. Mater. Interfaces* **2012**, *4*, 2534–2540. (c) Rakstys, K.; Abate, A.; Dar, M. I.; Gao, P.; Jankauskas, V.; Jacopin, G.; Kamarauskas, E.; Kazim, S.; Ahmad, S.; Grätzel, S.; Nazeeruddin, M. K. *J. Am. Chem. Soc.* **2015**, *137*, 16172–16178.

[11] For a study on triazatruxene based organic light-emitting diodes, see: Lai, W.-Y.; He, Q.-Y.; Zhu, R.; Chen, Q.-Q.; Huang, W. *Adv. Funct. Mater.* **2008**, *18*, 265–276.

[12] For reviews of arynes and hetarynes, see: (a) Kauffmann, T. *Angew. Chem. Int. Ed. Engl.* **1965**, *4*, 543–618. (b) Reinecke, M. G. *Tetrahedron* **1982**, *38*, 427–498. (c) Pellissier, H.; Santelli, M. *Tetrahedron* **2003**, *59*, 701–730. (d) Wenk, H. H.; Winkler, M.; Sander, W. *Angew. Chem. Int. Ed.* **2003**, *42*, 502–528. (e) Sanz, R. *Org. Prep. Proced. Int.* **2008**, *40*, 215–291. (f) Bronner, S. M.; Goetz, A. E.; Garg, N. K. *Synlett* **2011**, 2599–2604. (g) Tadross,

P. M.; Stoltz, B. M. *Chem. Rev.* **2012**, *112*, 3550–3557. (h) Gampe, C. M.; Carreira, E. M. *Angew. Chem. Int. Ed.* **2012**, *51*, 3766–3778. (i) Bhunia, A.; Yetra, S. R.; Biju, A. T. *Chem. Soc. Rev.* **2012**, *41*, 3140–3152. (j) Yoshida, H.; Takaki, K. *Synlett* **2012**, 1725–1732. (k) Dubrovskiy, A. V.; Markina, N. A.; Larock, R. C. *Org. Biomol. Chem.* **2013**, *11*, 191–218. (l) Wu, C.; Shi, F. *Asian J. Org. Chem.* **2013**, *2*, 116–125. (m) Goetz, A. E.; Garg, N. K. *J. Org. Chem.* **2014**, *79*, 846–851. (n) Goetz, A. E.; Shah, T. K.; Garg, N. K. *Chem. Commun*. **2015**, *51*, 34–45.

[13] For seminal studies on indolynes, see: (a) Julia, M.; Goffic, F. L.; Igolen, J.; Baillarge, M. *C. R. Acad. Sci., Ser. C* **1967**, *264*, 118–120. (b) Julia, M.; Huang, Y.; Igolen, J. *C. R. Acad. Sci., Ser. C* **1967**, *265*, 110–112. (c) Igolen, J.; Kolb, A. *C. R. Acad. Sci., Ser. C* **1969**, *269*, 54–56. (d) Julia, M.; Igolen, J.; Kolb, M. *C. R. Acad. Sci., Ser. C* **1971**, *273*, 1776–1777.

[14] For select studies involving indolynes, see: (a) Buszek, K. R.; Luo, D.; Kondrashov, M.; Brown, N. VanderVelde, D. *Org. Lett.* **2007**, *9*, 4135–4137. (b) Brown, N.; Luo, D.; VanderVelde, D.; Yang, S.; Brassfield, A.; Buszek, K. R. *Tetrahedron Lett.* **2009**, *50*, 63–65. (c) Bronner, S. M.; Bahnck, K. B.; Garg, N. K. *Org. Lett.* **2009**, *11*, 1007–1010. (d) Garr, A. N.; Luo, D.; Brown, N.; Cramer, C. J.; Buszek K. R.; VanderVelde, D. *Org. Lett.* **2010**, *12*, 96–99. (e) Cheong, P. H.-Y.; Paton, R. S.; Bronner, S. M.; Im, G.-Y. J.; Garg, N. K.; Houk, K. N. *J. Am. Chem. Soc.* **2010**, *132*, 1267–1269. (f) Im, G.-Y. J.; Bronner, S. M.; Goetz, A. E.; Paton, R. S.; Cheong, P. H.-Y.; Houk, K. N.; Garg, N. K. *J. Am. Chem. Soc.* **2010**, *132*, 17933–17944. (g) Thornton, P. D.; Brown, N.; Hill, D.; Neuenswander, B.; Lushington, G. H.; Santini, C.; Buszek, K. R. *ACS Comb. Sci.* **2011**, *13*, 443–448. (h) Candito, D. A.; Dobrovolsky, D.; Lautens, M. *J. Am. Chem. Soc.* **2012**, *134*, 15572–15580. (i) Nerurkar, A.;

Chandrasoma, N.; Maina, L.; Brassfield, A.; Luo, D.; Brown, N. Buszek, K. R. *Synthesis* **2013**, *45*, 1843–1852. (j) Picazo, E.; Houk, K. N.; Garg, N. K. *Tetrahedron Lett.* **2015**, *56*, 3511–3514.

[15] (a) Peña, D.; Escudero, S.; Pérez, D.; Guitián, E.; Castedo, L. *Angew. Chem. Int. Ed.* **1998**, *37*, 2659–2661. (b) Peña, D.; Pérez, D.; Guitián, E.; Castedo, L. *J. Am. Chem. Soc.* **1999**, *121*, 5827–5828. (c) Peña, D.; Pérez, D.; Guitián, E.; Castedo, L. *Org. Lett.* **1999**, *1*, 1555–1557. (d) Peña, D.; Cobas, A.; Pérez, D.; Guitián, E. Castedo, L. *Org. Lett.* **2000**, *2*, 1629–1632. (e) Peña, D.; Cobas, A.; Pérez, D.; Guitián, E.; Castedo, L. *Org. Lett.* **2003**, *5*, 1863–1866. (f) Iglesias, B.; Cobas, A.; Pérez, D.; Guitián, E.; *Org. Lett.* **2004**, *6*, 3557–3560. (g) Romero, C.; Peña, D.; Pérez, D.; Guitián, E. *Chem. Eur. J.* **2006**, *12*, 5677–5684. (h) Wang, Y.; Stretton, A. D.; McConnell, M. C.; Wood, P. A.; Parsons, S.; Henry, J. B.; Mount, A. R.; Galow, T. H. *J. Am. Chem. Soc.* **2007**, *129*, 13193–13200. (i) Peña, D.; Pérez, D.; Guitián, E. *Chem. Rec.* **2007**, *7*, 326–333. (j) Romero, C.; Peña, D.; Pérez, D.; Guitián, E. *J. Org. Chem.* **2008**, *73*, 7996–8000. (k) Yin, J.; Qu, H.; Zhang, K.; Luo, J.; Zhang, X.; Chi, C.; Wu, J. *Org. Lett.* **2009**, *11*, 3028–3031. (l) Lynett, P. T.; Maly, K. E.; *Org. Lett.* **2009**, *11*, 3726–3729. (m) Peña, D.; Pérez, D.; Guitián, E. *Org. Biomol. Chem.* **2010**, *8*, 3386–3388. (n) Alonso, J. M.; Díaz-Álvarez, A. E.; Criado, A.; Pérez, D.; Peña, D. Guitián, E. *Angew. Chem. Int. Ed.* **2012**, *51*, 173–177. (o) García-López, J.-A.; Greaney, M. F. *Org. Lett.* **2014**, *16*, 2338–2341. (p) Chen, L.; Zhang, C.; Wen, C.; Zhang, K.; Liu, W.; Chen, Q. *Catal. Commun.* **2015**, *65*, 81–84.

[16] Non-planar aromatic compounds are currently being sought after for new opportunities in materials chemistry. For recent examples, see: (a) Fujikawa, T.; Segawa, Y.; Itami, K. *J. Am.*

*Chem. Soc.* **2015**, *137*, 7763–7768. (b) Fujikawa, T.; Segawa, Y.; Itami, K. *J. Am. Chem. Soc.* **2016**, *138*, 3587–3595.

# CHAPTER FIVE

## Conversion of Amides to Esters by the Nickel-Catalyzed Activation of Amide C–N Bonds

Liana Hie, Noah F. Fine Nathel, Tejas K. Shah, Emma L. Baker, Xin Hong,

Yun-Fang Yang, Peng Liu, K. N. Houk & Neil K. Garg

*Nature* **2015**, *524*, 79–83.

### 5.1 Abstract

Amides are common functional groups that have been studied for more than a century.[1] They are the key building blocks of proteins and are present in a broad range of other natural and synthetic compounds. Amides are known to be poor electrophiles, which is typically attributed to the resonance stability of the amide bond.[1,2] Although amides can readily be cleaved by enzymes such as proteases,[3] it is difficult to selectively break the carbon–nitrogen bond of an amide using synthetic chemistry. Here we demonstrate that amide carbon–nitrogen bonds can be activated and cleaved using nickel catalysts. We use this methodology to convert amides to esters, which is a challenging and underdeveloped transformation. The reaction methodology proceeds under exceptionally mild reaction conditions, and avoids the use of a large excess of an alcohol nucleophile. Density functional theory calculations provide insight into the thermodynamics and catalytic cycle of the amide-to-ester transformation. Our results provide a way to harness amide functional groups as synthons and are expected to lead to the further use of amides in the construction of carbon–heteroatom or carbon–carbon bonds using non-precious-metal catalysis.

## 5.2 Introduction

The ability to interconvert functional groups is important in synthetic chemistry and many biological processes. Methodologies[4,5] have been developed that enable chemists to strategically harness the reactivity of most functional groups. Likewise, breakthroughs in biochemistry have led to an understanding of how changes in functional groups regulate physiological processes.[6]

One particularly interesting dichotomy exists in considering the amide functional group,[1] which is the key component of all proteins (Figure 5.1a). Since Schwann's initial discovery of pepsin—the first enzyme to be discovered—in 1836, scientists have been intrigued by the ability of enzymes to break down amide linkages.[3,6] Such amide cleavage processes govern many cellular regulatory functions and are responsible for the degradation of proteins to amino acids.[1,3] In contrast, the synthetic chemistry of amide-bond cleavage has remained underdeveloped, even though amides are well suited for use in multistep synthesis because of their stability under a variety of reaction conditions. Commonly used methods to break amide carbon–nitrogen (C–N) bonds include the reductive conversion of amides to aldehydes using Schwartz's reagent[7] and the displacement of Weinreb's *N*-OMe-*N*-Me amides with organometallic reagents en route to ketones.[8] Following Pauling's seminal postulate regarding amide planarity,[2] the poor reactivity of amides is now well understood as being a result of the strength of the resonance-stabilized amide C–N bond.[1]

To circumvent the long-standing problem involving the low reactivity of amides and their modest synthetic use in C–N bond cleavage processes, we designed the general approach shown in Figure 5.1b. The C–N bond of amide **5.1** undergoes activation by a transition-metal catalyst. Following oxidative addition, the resultant acyl metal species **5.2** is trapped by an appropriate

nucleophile to furnish product **5.3**, with the release of amine **5.4**. This approach allows for the breakdown of amides, and renders amides useful synthetic building blocks. Although examples exist for the metal-catalyzed C–heteroatom bond activation of acid chlorides,[9] anhydrides,[9] and 2-pyridyl esters,[10] to our knowledge, the direct metal-catalyzed activation of C–N bonds of amides is unknown. This is notable given the widespread use of transition-metal catalysis in organic synthesis, where there exist many examples of catalytic transformations occurring smoothly in the presence of amide linkages.

We validate the strategy outlined in Figure 5.1b through the conversion of amides to esters (Figure 5.1c). Amide to ester conversion, much like transamidation,[11,12] remains a challenging and underdeveloped synthetic transformation. Amides are often stable enough that esterification is difficult and requires the use of harsh acidic or basic conditions, while employing a large excess of nucleophile (for example, using the alcohol nucleophile as a solvent).[1] Perhaps the most promising protocol to achieve amide-to-ester conversions is Keck's methylation/hydrolysis sequence,[13] although this methodology is limited to the synthesis of methyl esters. Esterifications using acyl aziridines[14] and *N*-methylamides (albeit with activation by nitrosation)[15] have also been reported. Here we demonstrate the nickel-catalyzed conversion of amides to esters, which proceeds under exceptionally mild reaction conditions. In addition to establishing the scope of this methodology, we use density functional theory (DFT) calculations to predict whether the amide-to-ester conversion, or the reverse, is thermodynamically favored. DFT calculations are also used to predict a plausible catalytic cycle. These experimental and computational studies not only substantiate the notion of using non-precious-metal catalysis for the activation of amide C–N bonds, but also lay the foundation for further studies aimed at the strategic manipulation of amides as synthetic building blocks using catalysis.

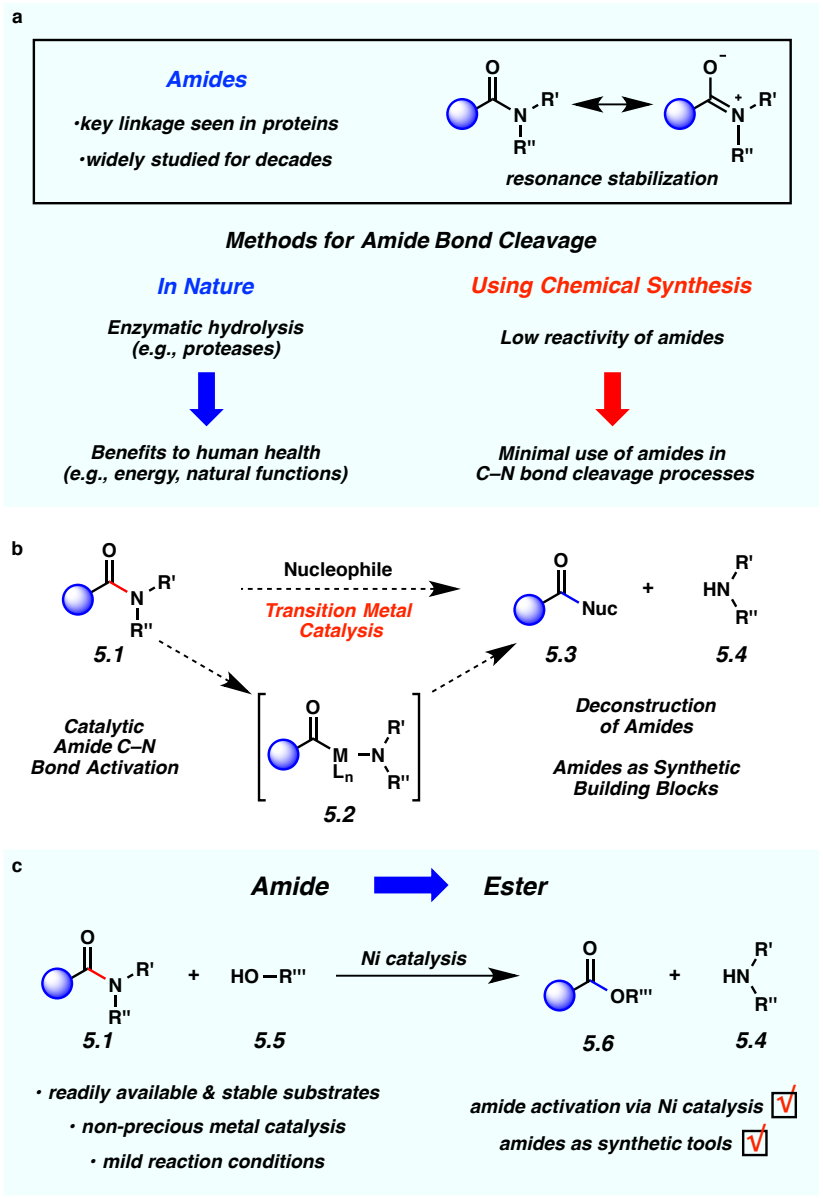


***Figure 5.1.*** Amide-bond cleavage using transition-metal catalysis. **a**. An illustration of the stability of amides and the contrast between how amides are used in nature and in chemical synthesis. **b**. Design of amide C–N bond activation to deconstruct amides and exploit them as synthetic building blocks (nuc, nucleophile; $L_n$, ligands coordinated to transition metal; blue spheres, R', R", and R"', any carbon-based functional groups). **c**. Strategy for the conversion of amides to esters

## 5.3 Optimization and Substrate Scope

We examined the conversion of benzamides **5.7** to methyl benzoate **5.8a** both computationally (using the Gaussian '09 software; see section 5.7.4.1 Complete Reference of Gaussian 09, page 333) and experimentally (Table 5.1). Because amides are known for their stability, we assessed whether the amide-to-ester conversion could be rendered thermodynamically favorable by the judicious choice of amide *N*-substituents. Using DFT methods, we calculated the change in Gibbs free energy $\Delta G$ for the reaction of amides **5.7** with methanol to give esters **5.8a** and amines **5.4**. Whether this transformation is favorable or not depends on the nature of the *N*-substituents (entries 1–8). Methanolysis of Weinreb amide **5.7d** (entry 4) and *N*-arylated substrates **5.7f** and **5.7g** (entries 6–8) were found to be the most energetically favorable. In contrast, esterifications of *N*-alkyl amides **5.7a**, **5.7b**, and **5.7e** were deemed thermodynamically unfavorable. This is in line with the experimentally measured equilibrium constant for the reaction of *N*,*N*-dimethylbenzamide **5.7b** and methanol (entry 2), in which the reverse reaction is thermodynamically favored (see section 5.7.4.6 Free Energy and Enthalpy of Amide and Ester Formation, page 338 for further discussion).[16]

Encouraged by the unique ability of nickel to catalyze the activation of strong aryl–heteroatom bonds,[17–19] particularly those in phenol,[19] aniline,[20–22] and phthalimide[23] derivatives, we also calculated the activation free energies for acyl C–N bond oxidative addition of each amide substrate using nickel catalysis. The barriers calculated for commercially available *N*-heterocyclic carbene ligand SIPr (entries 1–8) reveal that the oxidative addition barriers are reasonable in some cases. We studied these reactions experimentally using 10 mol% $Ni(cod)_2$, 10 mol% SIPr, 2.0 equivalents of methanol, and toluene as solvent at 110 °C for 12 h. There was good agreement between our observations and computational predictions. No reaction or low

yields were seen for substrates **5.7a**–**5.7e** (entries 1–5). However, when the calculated Δ*G* and the oxidative addition barrier were favorable, substantial formation of product **5.8a** was observed (entries 6 and 7). Coupling of substrate **5.7g** gave a quantitative yield of product (entry 7), and further optimization showed that even with only 1.2 equivalents of methanol and a temperature of 80 °C, product formation occurred smoothly (entry 8) to give complete conversion to **5.8a**. Importantly, no reaction takes place if either the precatalyst or the ligand are omitted, whereas the use of alternative *N*-heterocyclic carbene or phosphine ligands typically leads to lower yields or no reaction. We conclude that nickel catalysis is indeed operative in the amide activation/esterification process.

***Table 5.1.*** Experimental and computational study of amide-bond activation during the conversion of benzamides **5.7** to methyl benzoate **5.8a**

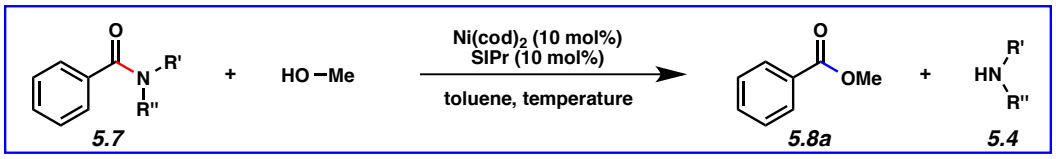


| Entry | | | Calculated $\Delta G^a$ (kcal/mol) | Calculated oxidative addition barrier with Ni /SIPr (kcal/mol)[b] | Temp | Equivalents of MeOH | Yield of ester[c] |
|---|---|---|---|---|---|---|---|
| 1 | | *5.7a* | +2.4 | 36.8 | 110 °C | 2.0 | 0% |
| 2 | | *5.7b* | 0.0 | 36.2 | 110 °C | 2.0 | 0% |
| 3 | | *5.7c* | –1.1 | 34.0 | 110 °C | 2.0 | 23% |
| 4 | | *5.7d* | –6.1 | 31.9 | 110 °C | 2.0 | 22% |
| 5 | | *5.7e* | +3.1 | 39.0 | 110 °C | 2.0 | 0% |
| 6 | | *5.7f* | –4.3 | 30.6 | 110 °C | 2.0 | 55% |
| 7 | | *5.7g* | –6.8 | 26.0 | 110 °C | 2.0 | >99% |
| 8 | | | | | 80 °C | 1.2 | >99% |

[a] The ΔG values for the overall reactions were obtained using DFT calculations (assuming a temperature of 298 K). [b] DFT methods were used to calculate oxidative addition barriers using Ni/SIPr as the metal/ligand combination. [c] Reactions were carried out with bis(1,5-cyclooctadiene)nickel(0) ($Ni(cod)_2$, 10 mol%), SIPr (10 mol%), substrate (50.0 mg, 1.0 equiv), methanol (1.2 or 2.0 equiv), and toluene (1.0 M), for 12 h at the specified temperatures. Yields were determined by $^1H$ nuclear magnetic resonance (NMR) analysis using hexamethylbenzene as an internal standard. (Me, methyl; OMe, methoxy; Ph, phenyl).

Having determined the optimal reaction conditions, we examined the scope of the transformation with regard to the amide substrate (Table 5.2a). In addition to the parent benzamide (entry 1), substrates containing the electron-withdrawing trifluoromethyl or fluoride substituents (entries 2 and 3) or the electron-donating methoxy or methyl substituents (entries 4 and 5) were well tolerated. The transformation also proceeded smoothly using *meta*- and *ortho*-methyl-substituted

substrates to give the desired esters in excellent yields (entries 6 and 7). Beyond the use of phenyl derivatives, we examined naphthyl and heterocyclic substrates. Naphthyl compounds readily coupled (entries 8 and 9), as did furan, quinoline, and isoquinoline substrates (entries 10–12, respectively). However, amides derived from alkyl carboxylic acids did not undergo the nickel-catalyzed esterification under our reaction conditions. This attribute provides opportunities to realize selective amide C–N bond cleavages in more complex substrates (see section 5.5 Selective Amide Bond Activation, page 292).

A variety of *N*-substituents were also surveyed, as shown in Table 5.2a. In addition to the longer *N*-butyl (Bu) and the branched *N*-*iso*-propyl alkyl chains (entries 13 and 14, respectively), we found that a cyclic amide derived from indoline was tolerated by the methodology (entry 15). Lastly, protected *N*-alkyl benzamides were tested. Although use of the *N*-*p*-toluenesulfonyl (Ts) derivative gave the corresponding ester in modest yield (entry 16), the corresponding *N*-*tert*-butyloxycarbonyl (Boc) substrate more efficiently underwent conversion to ester **5.8a** (entry 17). The analogous *N*-benzyl, *N*-*tert*-butyloxycarbonyl (*N*-Bn,Boc) substrate was also evaluated and gave the desired ester in 89% yield (entry 18). These results show that the methodology is not restricted to anilide substrates, as long as the overall reaction energetics are thermodynamically favorable (see section 5.7.4.5 Analysis of *N*-Me,Boc Amide Esterification, page 336 for energetics involving the *N*-Boc,Me substrate). Moreover, secondary benzamides can be used strategically as substrates for esterification, following a straightforward activation step (Boc-protection).

Using amide **5.7g** as the substrate, we evaluated the scope of the methodology with respect to the alcohol nucleophile (Table 5.2b). As shown, synthetically useful yields of product were obtained using only 1.2 equivalents of the alcohol, even when complex and hindered

alcohols were used. Cyclohexanol, *tert*-butanol, and 1-adamantol coupled smoothly to give the corresponding esters (entries 19–21, respectively); *tert*-butyl esters can readily be hydrolyzed to carboxylic acids under acidic conditions. Similarly, we found that cyclopropyl carbinol and an oxetane-derived alcohol could be used in the esterification reaction (entries 22 and 23, respectively). The use of the hindered secondary alcohol (–)-menthol was also tested and the desired ester was obtained in 88% yield (entry 24). Furthermore, we found that *N*-Boc-L-prolinol was tolerated in the methodology (entry 25), in addition to an indole-containing alcohol (entry 26), which further demonstrates the promise our methodology holds for reactions of heterocyclic substrates. As shown in entries 27 and 28, a complex sugar-containing alcohol bearing two acetals and an estrone-derived steroidal alcohol, respectively, also underwent the desired esterification reaction.

***Table 5.2.*** Scope of our methodology. **a**. **b**. The scope of the amide-to-ester transformation was evaluated with respect to the amide substrate (**a**), and with respect to the alcohol nucleophile, using **5.7g** as the amide substrate (**b**).

a

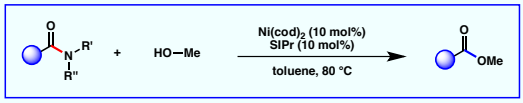


| Entry | Amide Substrate | Yield of Methyl Ester[a] |
|---|---|---|
| 1 | 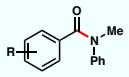 | 88% (R = H) |
| 2 | | 80% (R = *p*-$CF_3$) |
| 3 | | 92% (R = *p*-F) |
| 4 | | 90% (R = *p*-OMe) |
| 5 | | 90% (R = *p*-Me) |
| 6 | | 83% (R = *m*-Me) |
| 7 | | 89% (R = *o*-Me) |
| 8 | 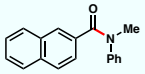 | 94% |
| 9 | 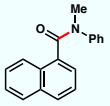 | 94% |
| 10 | 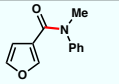 | 91%[b] |
| 11 | 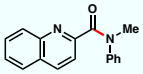 | 84% |
| 12 | 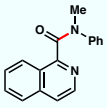 | 56% |
| 13 | 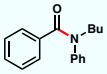 | 92% |
| 14 | 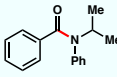 | 78% |
| 15 | 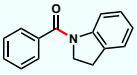 | 58% |
| 16 | 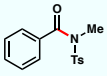 | 49% |
| 17 | 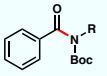 | 84% (R = Me) |
| 18 | | 89% (R = Bn) |

b

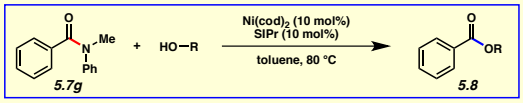


| Entry | Ester Product | Yield of Ester[a] |
|---|---|---|
| 19 | 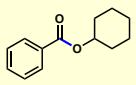 | 82% |
| 20 | 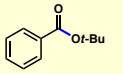 | 64% |
| 21 | 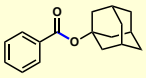 | 67% |
| 22 | 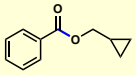 | 90% |
| 23 | 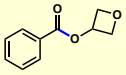 | 49% |
| 24 | 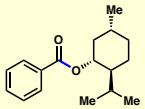 | 88% |
| 25 | 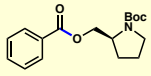 | 67% |
| 26 | 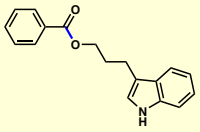 | 65% |
| 27 | 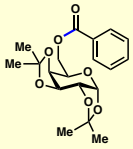 | 91% |
| 28 | 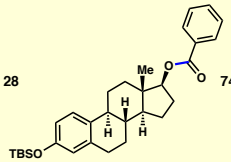 | 74% |

[a] Reactions were carried out with $Ni(cod)_2$ (10 mol%), SIPr (10 mol%), substrate (100.0 mg, 1.00 equiv), alcohol (1.2 equiv), and toluene (1.0 M) at 80 °C for 12 h. Yields shown reflect the average of two isolated experiments. [b] The yield for entry 10 was determined by $^1$H NMR analysis using hexamethylbenzene as an internal standard, owing to the volatility of the ester product. (*t*-Bu, *tert*-butyl; *p*, para; *m*, meta; *o*, ortho).

## 5.4 Computational Studies

Although nickel-catalyzed aryl and acyl C–O bond activation processes have been previously studied computationally,[24–28] no analogous studies involving C–N bond activation have been reported. Thus, to shed light on the mechanism of the facile amide-to-ester conversion, the catalytic cycle was computed using DFT calculations. Figure 5.2 provides the free energy profile using amide substrate **5.7g**. The [Ni(SIPr)$_2$] complex, **5.9**, is believed to be

the resting state of the catalytic cycle. Dissociation of one carbene ligand from complex **5.9** provides a coordination site for amide **5.7g**. Following coordination to give intermediate **5.10,** oxidative addition occurs via transition state **5.11**. This key event cleaves the amide C–N bond and produces acyl nickel species **5.12**. The next step of the catalytic cycle is ligand exchange, which proceeds by coordination of methanol to give intermediate **5.13**. Subsequent ligand exchange via transition state **5.14** facilitates the deprotonation of methanol, giving nickel complex **5.15**. Dissociation of *N*-Me-aniline produces acyl nickel species **5.16**, which in turn, undergoes reductive elimination via transition state **5.17** to deliver the ester-coordinated complex **5.18**. Finally, the ester product **5.8a** is released to regenerate catalyst **5.9**. The rate-determining step in the catalytic cycle is the oxidative addition (transition state **5.11**) with an overall barrier of 26.0 kcal $mol^{-1}$ relative to the resting state **5.9**. The overall reaction is thermodynamically favored by −6.8 kcal $mol^{-1}$. Because decarbonylation of acyl nickel species have been observed,[29,30] we also calculated the kinetic barrier for decarbonylation events (see section 5.7.4.2 Transition State Structures for Decarbonylation Pathway, page 334). Consistent with experiments, decarbonylation pathways from acyl nickel species **5.12** or **5.16** were found to be less favorable than the product formation pathways.

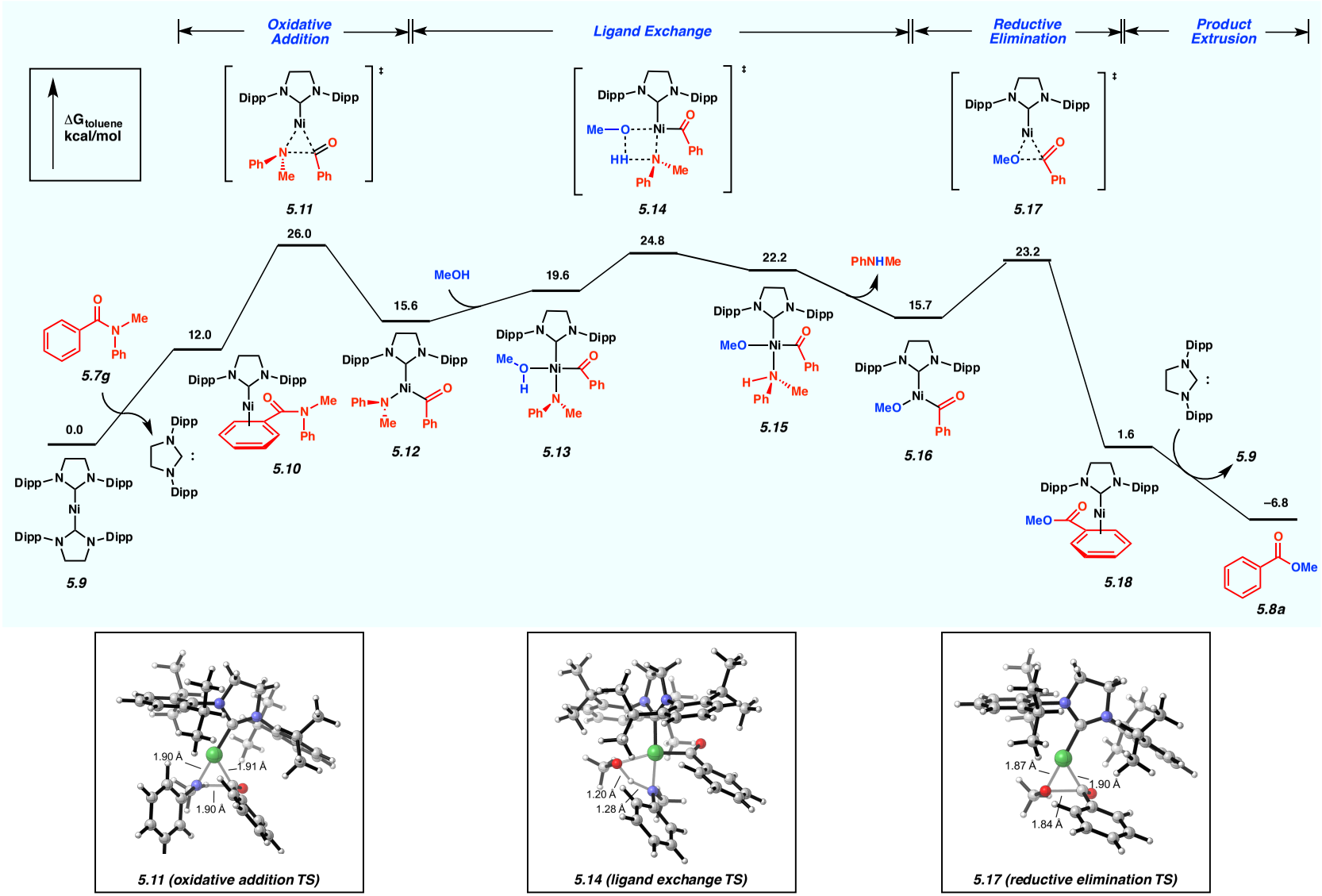


***Figure 5.2.*** Computational study of catalytic cycle. DFT methods were used to calculate the full catalytic cycle for the amide-to-ester conversion (assuming a temperature of 298 K). We propose that the reaction occurs by oxidative addition, ligand exchange, and reductive elimination. Key transition state structures (**5.11**, **5.14**, and **5.17**) are shown at the bottom. (Dipp, 2,6-diisopropylphenyl)

## 5.5 Selective Amide Bond Activation

As highlighted by the experiments shown in Figure 5.3, the nickel-catalyzed conversion of amides to esters can be used to achieve selective and mild amide-bond cleavages. First, we performed the esterification of bis(amide) substrate **5.19** using (–)-menthol (Figure 5.3a). Although both amides are *N*-arylated benzamides, only the tertiary amide was cleaved to give ester **21**, while also releasing aminoamide **5.22**. Second, bis(amide) **5.23**, which possesses two tertiary amides, was studied in the nickel-catalyzed esterification reaction (Figure 5.3b). In this case, the tertiary L-proline-derived alkyl amide was not disturbed, while the tertiary benzamide underwent cleavage to give ester **5.21** and aminoamide **5.24** in good yields. Lastly, we prepared L-valine derivative **5.25**, which also bears an ester (Figure 5.3c). Upon exposure of **5.25** to 1.2 equivalents of (–)-menthol and the nickel-catalyzed conditions, ester **5.21** and aminoester **5.26** were obtained in 70% and 79% yields, respectively. We believe that the ester functionality withstands the reaction conditions because it is not attached to an arene, analogous to the lack of reactivity seen in our attempts to esterify amides derived from alkyl carboxylic acids (for example, **5.23**). Compounds **5.24** and **5.26** were obtained in high enantiomeric excess, highlighting the mild nature of the reaction conditions, which avoid any substantial epimerization of the α stereocenters.

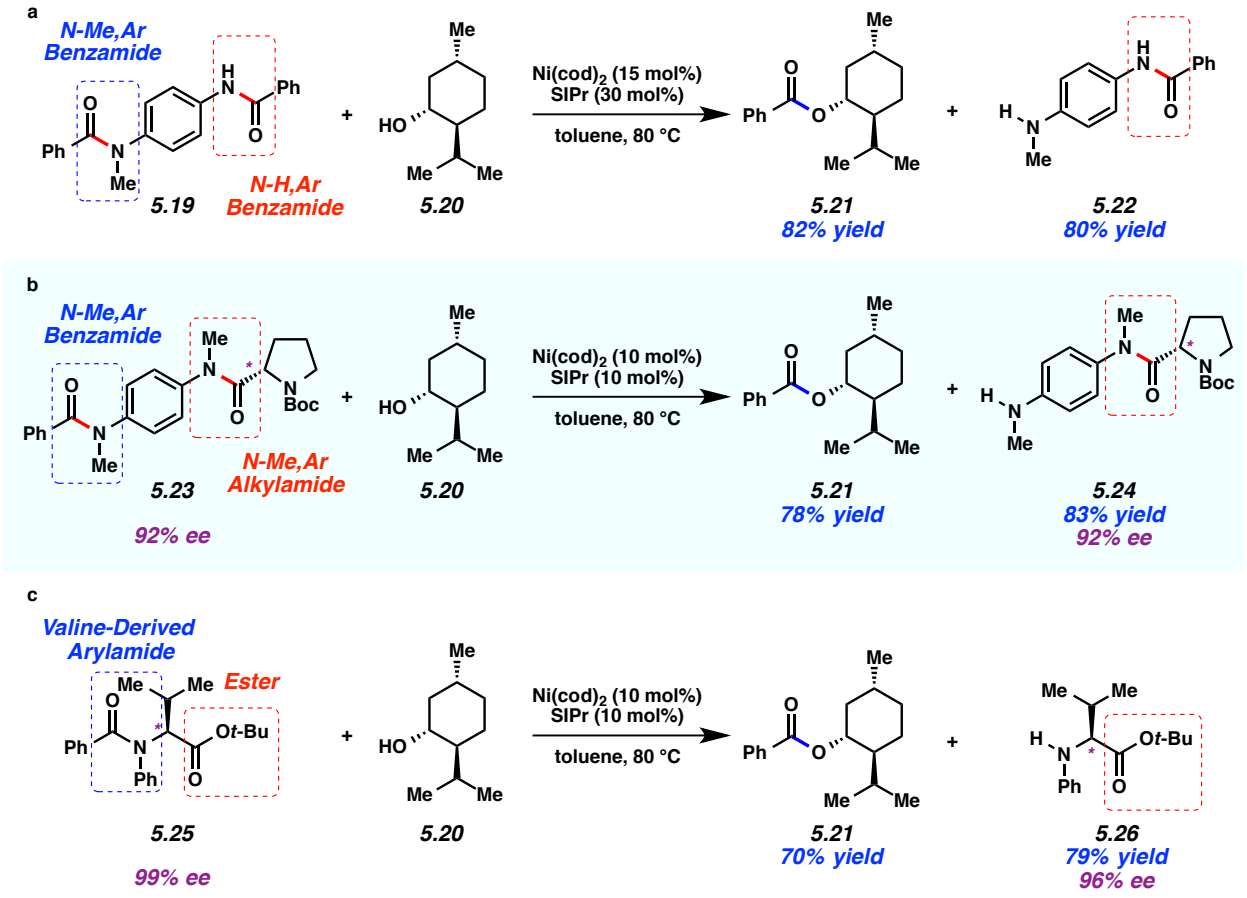


***Figure 5.3.*** Selective amide-bond cleavage processes. **a**. Cleavage of tertiary over secondary amide using menthol (1.2 equiv). **b**. Cleavage of benzamide over an alkyl prolinederived amide using menthol (1.2 equiv). **c**. Cleavage of valinederived amide in the presence of an ester using menthol (1.2 equiv). (ee, enantiomeric excess).

## 5.6 Conclusion

We have presented an efficient way to convert amides to esters. The methodology circumvents the classic problem of amides being poorly reactive functional groups by using nickel catalysis to achieve the previously unknown catalytic activation of amide C–N bonds. DFT calculations support a catalytic cycle that involves a rate-determining oxidative addition step, followed by ligand exchange and reductive elimination. The methodology is broad in scope, particularly with respect to the alcohol nucleophiles, and proceeds under exceptionally mild

reaction conditions using just 1.2 equivalents of the alcohol nucleophile. Moreover, selective amide-bond cleavage is achieved in the presence of other functional groups, including less reactive amides and esters, without the epimerization of α stereocenters. We envision that this methodology will lead to advances such as the catalytic esterification of primary amides, additional *N,N*-disubstituted amides, amides derived from alkyl or vinyl carboxylic acids, and perhaps even polyamide substrates bearing multiple stereocenters. This study may also lead to further harnessing of amides as valuable building blocks for the construction of C–heteroatom or C–C bonds using non-precious-metal catalysis.

## 5.7 Experimental Section

### 5.7.1 Materials and Methods

Unless stated otherwise, reactions were conducted in flame-dried glassware under an atmosphere of nitrogen and commercially obtained reagents were used as received. Non-commercially available substrates were synthesized following protocols specified in section 5.7.2.1 Syntheses of Amide Substrates, page 296. Alcohols and toluene were purified by distillation and taken through five freeze-pump-thaw cycles or recrystallized prior to use. Carboxylic acid **5.38**, amine **5.81**, and ester **5.87** were obtained from Combi-Blocks. Acid chlorides **5.27**, **5.29**, **5.32**, **5.34**, **5.36**, alcohols **5.63**, **5.65**, **5.67**, **5.69**, **5.71**, **5.73**, **5.75**, **5.77**, **5.79**, **5.20**, amines **5.28**, **5.30**, **5.82**, **5.84**, amide **5.7b**, benzamide and ligand SIMes were obtained from Sigma-Aldrich. Boronic acid **5.86** was obtained from Oakwood Products, Inc. $Ni(cod)_2$, SIPr, IMes, IPr, $PCy_3$, dppe, and dppf were obtained from Strem Chemicals. Amide **5.7e**, ligands $PPh_3$, $PPh_2Cy$, and $PCy_2Ph$ were obtained from Alfa Aesar. Reaction temperatures were controlled using an IKAmag temperature modulator, and unless stated otherwise, reactions were performed at room temperature

(approximately 23 °C). Thin-layer chromatography (TLC) was conducted with EMD gel 60 F254 pre-coated plates (0.25 mm for analytical chromatography and 0.50 mm for preparative chromatography) and visualized using a combination of UV, anisaldehyde, ceric ammonium molybdate, iodine, vanillin, and potassium permanganate staining techniques. Silicycle Siliaflash P60 (particle size 0.040–0.063 mm) was used for flash column chromatography. $^{1}$H NMR spectra were recorded on Bruker spectrometers (at 300, 400, 500, and 600 MHz) and are reported relative to residual solvent signals. Data for $^{1}$H NMR spectra are reported as follows: chemical shift (δ ppm), multiplicity, coupling constant (Hz), integration. Data for $^{13}$C NMR are reported in terms of chemical shift (at 75, 125, and 150 MHz). IR spectra were recorded on a Perkin-Elmer 100 spectrometer and are reported in terms of frequency absorption ($cm^{-1}$). High-resolution mass spectra were obtained on Thermo Scientific™ Exactive Mass Spectrometer with DART ID-CUBE. Determination of enantiopurity was carried out on a Mettler Toledo SFC (supercritical fluid chromatography) using a Daicel ChiralPak OJ-H column.

### 5.7.2 Experimental Procedures

#### 5.7.2.1 Syntheses of Amide Substrates

**Representative procedure for the synthesis of amide substrates from Table 5.1 and Table 5.2 (synthesis of amide 5.7a is used as an example).**

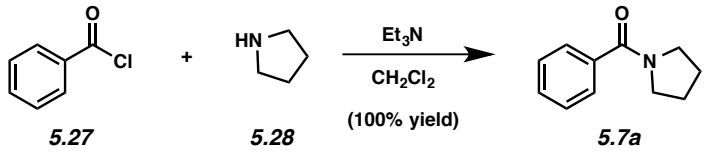


**Amide 5.7a (Table 5.1, entry 1)**. To a solution of pyrrolidine **5.28** (1.3 mL, 15.7 mmol, 1.1 equiv), triethylamine (2.5 mL, 17.8 mmol, 1.25 equiv), and dichloromethane (28.5 mL, 0.5 M) at 0 °C, was added acid chloride **5.27** (2.0 g, 14.2 mmol, 1.0 equiv). The reaction mixture was gradually warmed to 23 °C over 30 min and then stirred for 1 h. The reaction mixture was diluted with EtOAc (50 mL), and then washed successively with 1.0 M HCl (50 mL) and brine (50 mL). The organic layer was dried over $Na_2SO_4$ and concentrated under reduced pressure. The crude solid material was purified by flash chromatography (1:1 Hexanes:EtOAc) to yield amide product **5.7a** (2.5 g, 100% yield) as a white solid. Spectral data matched those previously reported.[31a]

Note: Experimental procedures for the syntheses of amides shown in Table 5.1 and Table 5.2 have previously been reported: **5.7a**,[31a] **5.7c**,[31b] **5.7d**,[31c] **5.7f**,[31d] **5.7g**,[31e] **5.41**,[31f] **5.43**,[31f] **5.45**,[31f] **5.47**,[31g] **5.50**,[31g] **5.52**,[31h] **5.57**,[31f] **5.58**,[31e] **5.59**,[31i] **5.60**,[31j] **5.61**,[31k] and **5.62**,[31l] with the exception of *p*-trifluoromethyl amide **5.31**, *o*-methyl amide **5.33**, furan **5.35,** quinoline **5.37**, and isoquinoline **5.39**. Syntheses for these latter compounds are as follows:

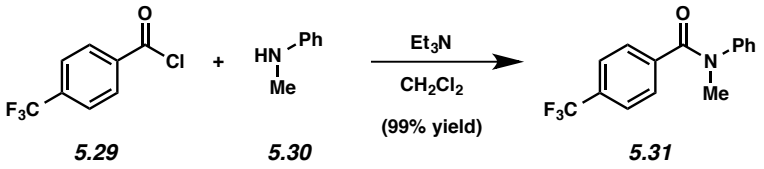


*5.29* *5.30* *5.31*

**Amide 5.31 (Table 5.2, entry 2)**. To a solution of triethylamine (2.1 mL, 15 mmol, 1.25 equiv) and *N*-Me aniline (**5.30**) (1.43 mL, 13.2 mmol, 1.1 equiv) in dichloromethane (24.0 mL, 0.5 M) at 0 °C, was added acid chloride **5.29** (2.5 g, 12.0 mmol, 1.0 equiv). The resulting heterogeneous mixture was allowed to stir at 23 °C for 12 h. The mixture was then diluted with EtOAc (30 mL) and 1.0 M HCl (40 mL). The organic layer was washed with brine (2 x 40 mL) and then dried over $Na_2SO_4$. The volatiles were removed under reduced pressure, and the crude oil was purified by flash chromatography (5:1 Hexanes:EtOAc) to yield amide product **5.31** (3.3 g, 99% yield) as a white solid. Amide **5.31**: $R_f$ 0.27 (5:1 Hexanes:EtOAc); $^1$H NMR (500 MHz, $CDCl_3$): δ 7.44 (q, $J$ = 8.4, 4H), 7.24–7.23 (m, 2H), 7.19 (t, $J$ = 7.4, 1H), 7.03 (d, $J$ = 7.55, 2H), 3.51 (s, 3H); $^{13}$C NMR (125 MHz, $CDCl_3$): δ 169.3, 144.3, 139.6, 131.4 (q, $J_{C-F}$ = 32.6 Hz), 129.5, 129.1, 127.2, 127.0, 124.9 (q, $J_{C-F}$ = 3.8 Hz), 122.7, 120.5, 38.5; IR (film): 2971, 1738, 1639, 1596, 1496, 1371, 1322, 1165, 1122, 1108, 1065, 1019 cm$^{-1}$; HRMS-ESI (*m/z*) $[M+H]^+$ calcd for $C_{15}H_{13}F_3NO$, 280.09492; found 280.09339.

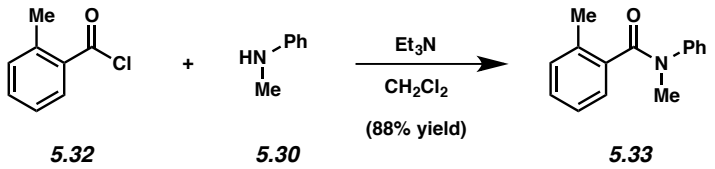


*5.32* *5.30* *5.33*

**Amide 5.33 (Table 5.2, entry 7)**. To a solution of acid chloride **5.32** (2.5 g, 16.0 mmol, 1.0 equiv) and dichloromethane (10 mL) at 0 °C, was added a solution of triethylamine (2.1 mL, 15 mmol, 1.25 equiv) and *N*-Me aniline (**5.30**) (1.43 mL, 13.2 mmol, 1.1 equiv) in dichloromethane

(22 mL). The resulting heterogeneous mixture was warmed to 23 °C and allowed to stir for 12 h. The mixture was then diluted with EtOAc (30 mL) and 1.0 M HCl (50 mL). The organic layer was washed with brine (50 mL) and then dried over $Na_2SO_4$. The volatiles were removed under reduced pressure, and the crude oil was purified by flash chromatography (5:1 Hexanes:EtOAc) to yield amide product **5.33** (3.2 g, 88% yield) as a white solid. Amide **5.33**: $R_f$ 0.30 (5:1 Hexanes:EtOAc); $^1$H NMR (400 MHz, $CDCl_3$): δ 7.18–7.03 (m, 9H), 3.49 (s, 3H), 2.33 (s, 3H); $^{13}$C NMR (125 MHz, $CDCl_3$): δ 171.3, 143.9, 136.7, 134.8, 130.3, 129.0, 128.7, 127.6, 126.7, 126.6, 125.2, 37.4, 19.6; IR (film): 3062, 2924, 1643, 1594, 1494, 1456, 1417, 1364, 1303, 1280, 1180, 1121, 1097, 1028 cm$^{-1}$; HRMS-ESI (*m/z*) $[M+H]^+$ calcd for $C_{15}H_{16}NO$, 226.12319; found 226.12159.

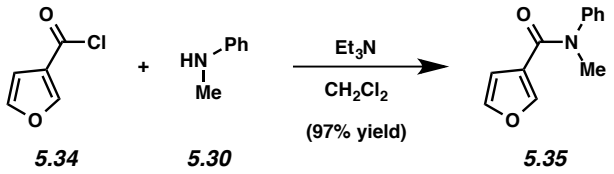


**Amide 5.35 (Table 5.2, entry 10)**. To a flask containing a solution of *N*-Me aniline (**5.30**) (1.3 mL, 12.3 mmol, 1.6 equiv) and triethylamine (1.1 mL, 7.7mmol, 1.0 equiv) in dichloromethane (11.5 mL, 0.67 M) at 0 °C, was added acid chloride **5.34** (1.0 g, 7.7 mmol, 1.0 equiv). The resulting heterogeneous mixture was warmed to 23 °C over 30 min and then heated to reflux for 1 h. After cooling to 23 °C, the reaction mixture was stirred for 12 h and then quenched with 1.0 M HCl (10 mL). The organic layer was washed with brine (30 mL) and then dried over $Na_2SO_4$. The volatiles were removed under reduced pressure, and the crude solid was purified by flash chromatography (5:1 Hexanes:EtOAc) to yield amide product **5.35** (1.5 g, 97% yield) as a white solid. Amide **5.35**: $R_f$ 0.24 (5:1 Hexanes:EtOAc); $^1$H NMR (300 MHz, $CDCl_3$): δ 7.44–7.36 (m,

3H), 7.23–7.19 (m, 2H), 7.14 (t, $J$ = 1.78, 1H), 6.89–6.87 (m, 1H), 6.11–6.10 (m, 1H), 3.41 (s, 3H); $^{13}$C NMR (75 MHz, $CDCl_3$): δ 163.2, 145.7, 144.1, 141.9, 129.7, 128.1, 127.8, 121.9, 111.0, 38.2; IR (film): 3481, 3129, 2970, 1739, 1630, 1593, 1561, 1497, 1379, 1354, 1157, 1074, 1040 cm$^{-1}$; HRMS-ESI (*m/z*) $[M+H]^+$ calcd for $C_{12}H_{12}NO_2$, 202.08680; found 202.08580.

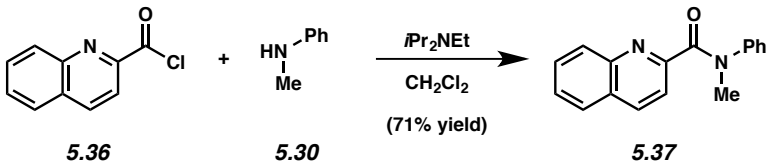


*5.36* *5.30* *5.37*

**Amide 5.37 (Table 5.2, entry 11)**. To a solution of *N*-Me aniline (**5.30**) (1.2 mL, 11.5 mmol, 1.1 equiv) and *N*,*N*-diisopropylethylamine (9.1 mL, 52.2 mmol, 5.0 equiv) in dichloromethane (100 mL, 0.1 M) at 0 °C, was added acid chloride **5.36** (2.0 g, 10.4 mmol, 1.0 equiv). The resulting heterogeneous mixture was allowed to stir at 23 °C. After 17 h, additional *N*-Me aniline (1.2 mL, 11.5 mmol, 1.1 equiv) and *N*,*N*-diisopropylethylamine (6.0 mL, 34.4 mmol, 3.3 equiv) were added sequentially. After stirring at 23 °C for 6 h, the reaction mixture was quenched with 1.0 M HCl (50 mL). The organic layer was washed with brine (50 mL) and then dried over $Na_2SO_4$. The volatiles were removed under reduced pressure, and the crude oil was purified by flash chromatography (5:1 Hexanes:EtOAc) to yield amide product **5.37** (2.0 g, 71% yield) as a white solid. Amide **5.37**: $R_f$ 0.40 (5:1 Hexanes:EtOAc); $^1$H NMR (500 MHz, $CDCl_3$): δ 8.03 (br s, 1H), 7.85 (br s, 1H), 7.77–7.58 (m, 2H), 7.57–7.43 (m, 2H), 7.24–6.99 (m, 5H), 3.59 (s, 3H); $^{13}$C NMR (125 MHz, $CDCl_3$): δ 168.9, 154.2, 146.9, 144.4, 136.4, 129.9, 129.8, 129.1, 127.7, 127.5, 127.5, 127.0, 126.7, 120.6, 38.2; IR (film): 3457, 2971, 1739, 1642, 1594, 1495, 1375.55, 1229, 1217, 1121, 1104 cm$^{-1}$; HRMS-ESI (*m/z*) $[M+H]^+$ calcd for $C_{17}H_{15}N_2O$, 263.11844; found 263.11718.

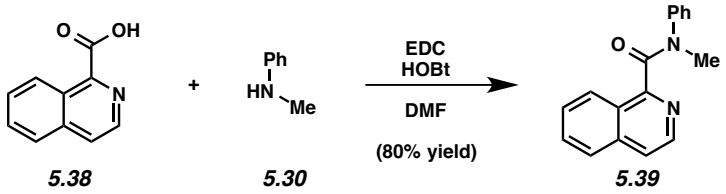


*5.38* *5.30* *5.39*

**Amide 5.39 (Table 5.2, entry 12)**. To a mixture of carboxylic acid **5.38** (1.0 g, 4.0 mmol, 1.0 equiv), EDC (0.7 g, 4.4 mmol, 1.1 equiv), HOBt (0.6 g, 4.4 mmol, 1.1 equiv), and DMF (60.0 mL, 0.067 M) was added *N*-Me aniline (**5.30**) (0.5 mL, 4.4 mmol, 1.1 equiv). The resulting mixture was stirred at 23 °C for 12 h, and then diluted with deionized water (100 mL) and EtOAc (100 mL). The aqueous layer was separated and the organic layer was extracted with EtOAc (3 X 100 mL). The combined organic layer was washed with brine (150 mL), dried over $Na_2SO_4$, and concentrated under reduced pressure. The crude oil was purified by flash chromatography with (1:1 Hexanes:EtOAc) to yield amide product **5.39** (0.9 g, 80% yield) as a white solid. Amide **5.39**: $R_f$ 0.50 (1:1 Hexanes:EtOAc); $^1$H NMR (500 MHz, $CDCl_3$): (major rotamer) δ 8.25 (d, $J$ = 5.8, 1H), 8.18–8.17 (m, 1H), 7.74–7.72 (m, 1H), 7.66–7.60 (m, 2H), 7.46 (d, $J$ = 5.8, 1H), 7.04–6.97 (m, 5H), 3.65 (s, 3H); (minor rotamer) [10/14 protons were discernable] δ 8.60–8.58 (m, 1H), 7.96–7.84 (m, 1H), 7.59–7.49 (m, 5H), 3.23 (s, 3H); $^{13}$C NMR (125 MHz, $CDCl_3$): δ 168.4, 155.8, 143.4, 141.4, 136.2, 130.5, 128.9, 128.0, 127.1, 126.9, 126.7, 126.0, 125.9, 121.1, 37.3; IR (film): 3060, 2939, 1651, 1595, 1561, 1496, 1460, 1431, 1399 1372, 1119, 1054, 1033 cm$^{-1}$; HRMS-ESI (*m/z*) $[M+H]^+$ calcd for $C_{17}H_{15}N_2O$, 263.11844; found 263.11768.

*Note: **5.39** was obtained as a 7.5:1 mixture of rotamers. These data represent empirically observed chemical shifts and coupling constants from the $^1$H NMR spectrum*

### 5.7.2.2 Methanolysis Control Experiments

***Table 5.3.*** Attempted Conversion of Amide **5.7g** to Methyl Benzoate **5.8a** Under Various Reaction Conditions[a]

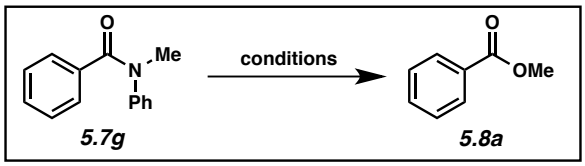


***5.7g*** ***5.8a***

| ***Reaction Conditions*** | ***Experimental Results*** | |
|---|---|---|
| | ***Recovered 5.7g*** | ***5.8a*** |
| **Conc. HCl (5.13 equiv), MeOH (0.12 M) 23 °C (2 h) → 75 °C (2 h) → 100 °C (17 h)** | **100%** | **0%** |
| **NaOMe (2.0 equiv), MeOH (0.12 M) 23 °C (4 h) → 80 °C (4 h) → 110 °C (13.5 h)** | **93%** | **7%** |
| **NaOMe (10.0 equiv), MeOH (0.12 M) 23 °C (1.5 h) → 80 °C (4 h) → 110 °C (14 h)** | **94%** | **6%** |
| **$K_2CO_3$ (1.0 equiv), MeOH (0.12 M) 23 °C (7 h) → 110 °C (12 h)** | **95%** | **5%** |

[a] Yields were determined by $^1$H NMR analysis using hexamethylbenzene as an internal standard.

### 5.7.2.3 Screening of Amide Substrates

***Table 5.4.*** Survey of Amide Substrates[a]

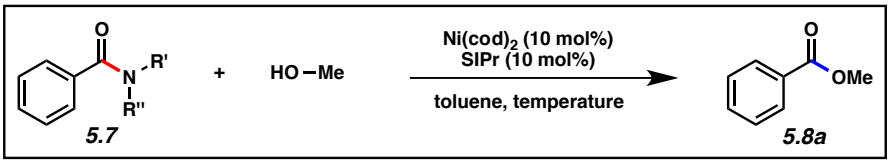


| Entry | | Temp | Equivalents of MeOH | Yield of ester | Remainder of the mass |
|---|---|---|---|---|---|
| 1 | *5.7a* | 110 °C | 2.0 | 0% | *5.7a* (100%) |
| 2 | *5.7b* | 110 °C | 2.0 | 0% | *5.7b* (100%) |
| 3 | *5.7c* | 110 °C | 2.0 | 23% | *5.7c* (77%) |
| 4 | *5.7d* | 110 °C | 2.0 | 22% | *5.7d* (72%) + 5.7*e* (6%) |
| 5 | *5.7e* | 110 °C | 2.0 | 0% | *5.7e* (100%) |
| 6 | *5.7f* | 110 °C | 2.0 | 55% | *5.7f* (45%) |
| 7 | *5.7g* | 110 °C | 2.0 | quant. | - |
| 8 | | 80 °C | 1.2 | quant. | - |

[a] Yields were determined by $^1$H NMR analysis using hexamethylbenzene as an internal standard.

*Note: The attempted esterification of benzamide using MeOH (2.0 equiv), Ni(cod)$_2$ (10 mol%), SIPr (10 mol%), and toluene (1.0 M) at 110 °C led to no reaction.*

### 5.7.2.4 Comparison of Ligands and Relevant Control Experiments

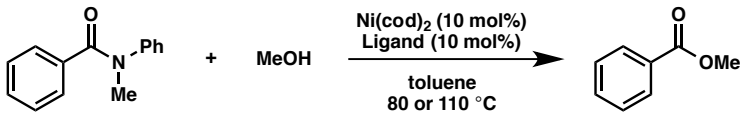


*5.7g* *5.8a*

**Representative Procedure for Esterifications of Benzamides from Table 5.4 and Table 5.5 (coupling of amide 5.7g is used as an example).** A 1-dram vial containing amide **5.7g** (50.0 mg, 0.24 mmol, 1.0 equiv), hexamethylbenzene (7.8 mg, 0.48 mmol, 0.2 equiv), and a magnetic stir bar was charged with $Ni(cod)_2$ (6.6 mg, 0.024 mmol, 10 mol%) and ligand (0.024 mmol, 10 mol%) in a glove box. Subsequently, toluene (0.24 mL, 1.0 M) and then methanol (19.4 μL, 0.48 mmol, 2.0 equiv) were added. The vial was sealed with a Teflon-lined screw cap, removed from the glove box, and stirred at 80 or 110 °C for 12 h. After cooling to 23 °C, the mixture was diluted with hexanes (0.5 mL) and filtered over a plug of silica gel (10 mL of EtOAc eluent). The volatiles were removed under reduced pressure, and the yield was determined by $^1H$ NMR analysis with hexamethylbenzene as an internal standard.

*Any modifications of the conditions shown in the representative procedure above are specified in the following Table 5.4 and Table 5.5.*

***Table 5.5.*** Ligand Screening for Nickel-Catalyzed Esterification[a]

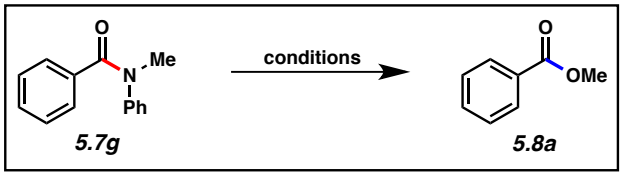


***5.7g*** ***5.8a***

| ***Reaction Conditions*** | ***Experimental Results*** | |
|---|---|---|
| | ***Recovered 5.7g*** | ***5.8a*** |
| MeOH (2.0 equiv), $Ni(cod)_2$ (10 mol%), SIPr (10 mol%) toluene (1.0 M), 110 °C, 12 h | 0% | 100% |
| MeOH (2.0 equiv), $Ni(cod)_2$ (10 mol%), IPr (10 mol%) toluene (1.0 M), 110 °C, 12 h | 0% | 100% |
| MeOH (2.0 equiv), $Ni(cod)_2$ (10 mol%), SIMes (10 mol%) toluene (1.0 M), 110 °C, 12 h | 0% | 0% |
| MeOH (2.0 equiv), $Ni(cod)_2$ (10 mol%), IMes (10 mol%) toluene (1.0 M), 110 °C, 12 h | 63% | 37% |
| MeOH (2.0 equiv), $Ni(cod)_2$ (10 mol%), $PPh_3$ (10 mol%) toluene (1.0 M), 110 °C, 12 h | 100% | 0% |
| MeOH (2.0 equiv), $Ni(cod)_2$ (10 mol%), $PPh_2Cy$ (10 mol%) toluene (1.0 M), 110°C, 12 h | 100% | 0% |
| MeOH (2.0 equiv), $Ni(cod)_2$ (10 mol%), $PCy_3$ (10 mol%) toluene (1.0 M), 110 °C, 12 h | 85% | 15% |
| MeOH (2.0 equiv), $Ni(cod)_2$ (10 mol%), $PhPCy_2$ (10 mol%) toluene (1.0 M), 110 °C, 12 h | 97% | 3% |
| MeOH (2.0 equiv), $Ni(cod)_2$ (10 mol%), dppe 10 mol%) toluene (1.0 M), 110 °C, 12 h | 100% | 0% |
| MeOH (2.0 equiv), $Ni(cod)_2$ (10 mol%), dppf (10 mol%) toluene (1.0 M), 110 °C, 12 h | 100% | 0% |
| ***Control Experiments:*** | | |
| MeOH (1.2 equiv), $Ni(cod)_2$ (10 mol%), SIPr (10 mol%) toluene (1.0 M), 80 °C, 12 h | 0% | 100% |
| MeOH (1.2 equiv), toluene (1.0 M), 80 °C, 12 h | 100% | 0% |
| MeOH (1.2 equiv), SIPr (10 mol%) toluene (1.0 M), 80 °C, 12 h | 100% | 0% |
| MeOH (1.2 equiv), $Ni(cod)_2$ (10 mol%) toluene (1.0 M), 80 °C, 12 h | 100% | 0% |

[a] Yields were determined by $^1H$ NMR analysis using hexamethylbenzene as an internal standard.

### 5.7.2.5 Scope of Methodology

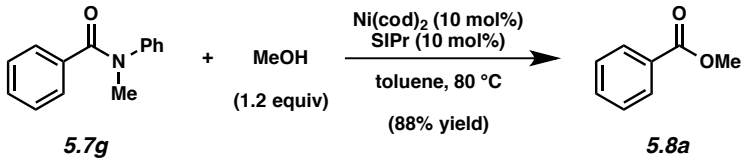


*5.7g* *5.8a*

**Representative Procedure (coupling of amide 5.7g and methanol is used as an example). Ester 5.8a (Table 5.2a, entry 1).** A 1-dram vial containing amide **5.7g** (100.0 mg, 0.47 mmol, 1.0 equiv) and a magnetic stir bar was charged with $Ni(cod)_2$ (13.0 mg, 0.047 mmol, 10 mol%) and SIPr (18.4 mg, 0.047 mmol, 10 mol%) in a glove box. Subsequently, toluene (0.47 mL, 1.0 M) and then methanol (23.0 μL, 0.56 mmol, 1.2 equiv) were added. The vial was sealed with a Teflon-lined screw cap, removed from the glove box, and stirred at 80 °C for 12 h. After cooling to 23 °C, the mixture was diluted with hexanes (0.5 mL) and filtered over a plug of silica gel (10 mL of EtOAc eluent). The volatiles were removed under reduced pressure, and the crude residue was purified by flash chromatography (20:1 Hexanes:EtOAc) to yield ester product **5.8a** (88% yield, average of two experiments) as a clear oil. Ester **5.8a**: $R_f$ 0.41 (20:1 Hexanes:EtOAc). Spectral data match those previously reported.[32]

*Any modifications of the conditions shown in the representative procedure above are specified in the following schemes, which depict all of the results shown in Table 5.2.*

*For each of the nickel-catalyzed reactions described herein, control experiments were performed concurrently where $Ni(cod)_2$ and both $Ni(cod)_2$ and SIPr were omitted from the reactions. In all cases, these control experiments led to the recovery of the amide substrates with no detectable conversion to the corresponding esters.*

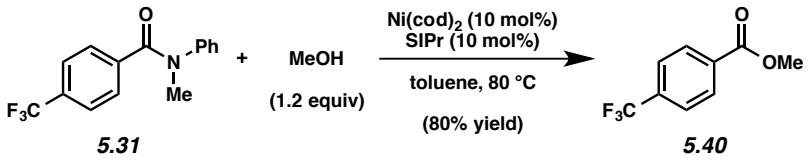


**Ester 5.40 (Table 5.2a, entry 2)**. Purification by flash chromatography (10:1 Hexanes:EtOAc) generated ester **5.40** (80% yield, average of two experiments) as a clear oil. Ester **5.40**: $R_f$ 0.59 (10:1 Hexanes:EtOAc). Spectral data match those previously reported.[33]

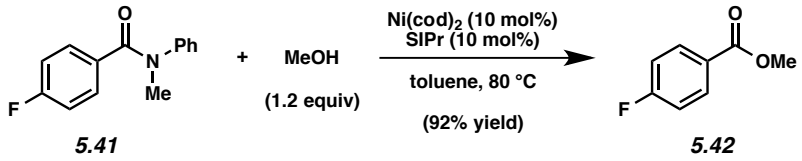


**Ester 5.42 (Table 5.2a, entry 3)**. Purification by flash chromatography (20:1 Hexanes:EtOAc) generated ester **5.42** (92% yield, average of two experiments) as a clear oil. Ester **5.42**: $R_f$ 0.37 (20:1 Hexanes:EtOAc). Spectral data match those previously reported.[34]

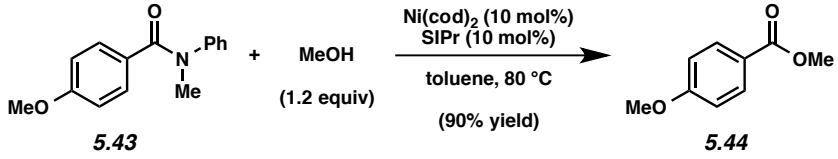


**Ester 5.44 (Table 5.2a, entry 4)**. Purification by flash chromatography (5:1 Hexanes:EtOAc) generated ester **5.44** (90% yield, average of two experiments) as a white solid. Ester **5.44**: $R_f$ 0.59 (10:1 Hexanes:EtOAc). Spectral data match those previously reported.[35]

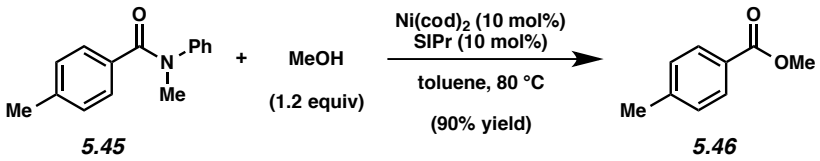


**Ester 5.46 (Table 5.2a, entry 5)**. Purification by flash chromatography (15:1 Hexanes:EtOAc) generated ester **5.46** (90% yield, average of two experiments) as a clear oil. Ester **5.46**: $R_f$ 0.60 (20:1 Hexanes:EtOAc). Spectral data match those previously reported.[35]

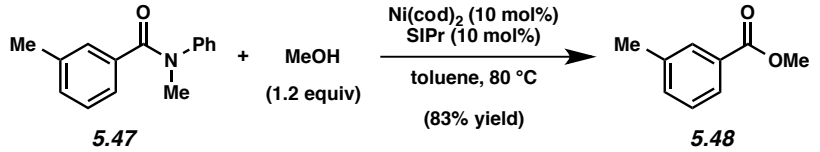


**Ester 5.48 (Table 5.2a, entry 6)**. Purification by flash chromatography (20:1 Hexanes:$Et_2O$) generated ester **5.48** (83% yield, average of two experiments) as a clear oil. Ester **5.48**: $R_f$ 0.52 (15:1 Hexanes:EtOAc). Spectral data match those previously reported.[36]

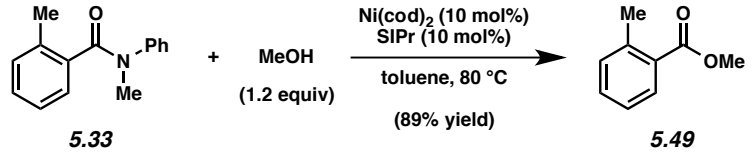


**Ester 5.49 (Table 5.2a, entry 7)**. Purification by flash chromatography (15:1 Hexanes:EtOAc) generated ester **5.49** (89% yield, average of two experiments) as a clear oil. Ester **5.49**: $R_f$ 0.69 (15:1 Hexanes:EtOAc). Spectral data match those previously reported.[34]

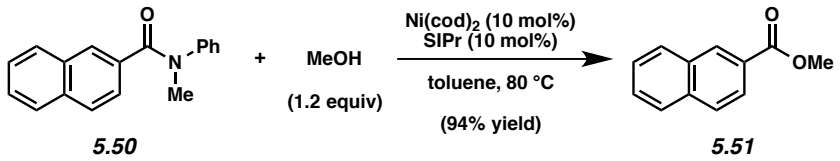


**Ester 5.51 (Table 5.2a, entry 8)**. Purification by flash chromatography (20:1 Hexanes:EtOAc) generated ester **5.51** (94% yield, average of two experiments) as a white solid. Ester **5.51**: $R_f$ 0.69 (10:1 Hexanes:EtOAc). Spectral data match those previously reported.[37]

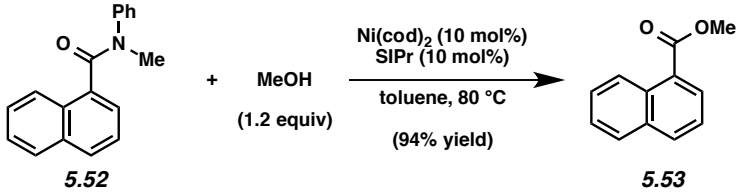


**Ester 5.53 (Table 5.2a, entry 9)**. Purification by flash chromatography (15:1 Hexanes:EtOAc) generated ester **5.53** (94% yield, average of two experiments) as a clear oil. Ester **5.53**: $R_f$ 0.57 (15:1 Hexanes:EtOAc). Spectral data match those previously reported.[38]

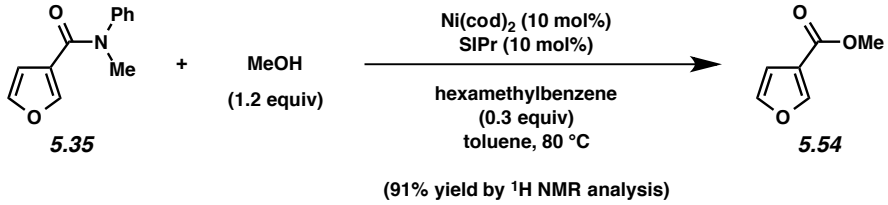


**Ester 5.54 (Table 5.2a, entry 10)**. The yield was determined by $^1$H NMR analysis of the crude reaction mixture using hexamethylbenzene (0.3 equiv based on **5.35**) as an external standard (91% yield, average of two experiments). Ester **5.54**: $^1$H NMR (300 MHz, $CDCl_3$): δ 8.02–8.01 (m, 1H), 7.43–7.42 (m, 1H), 6.76–6.74 (m, 1H), 3.85 (s, 3H). Spectral data of the crude mixture of ester **5.54** match those previously reported.[39]

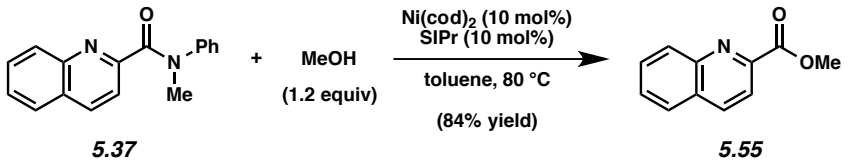


*5.37* *5.55*

**Ester 5.55 (Table 5.2a, entry 11)**. Purification by flash chromatography (1:1 Hexanes:EtOAc) generated ester **5.55** (84% yield, average of two experiments) as a white solid. Ester **5.55**: $R_f$ 0.39 (1:1 Hexanes:EtOAc). Spectral data match those previously reported.[40]

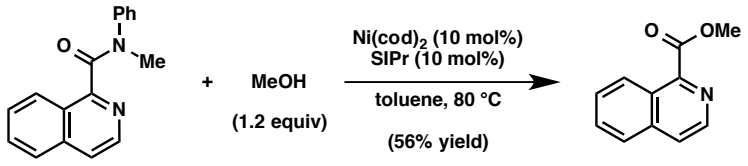


*5.39* *5.56*

**Ester 5.56 (Table 5.2a, entry 12)**. Purification by flash chromatography (1:1 Hexanes:EtOAc) generated ester **5.56** (56% yield, average of two experiments) as a clear oil. Ester **5.56**: $R_f$ 0.43 (1:1 Hexanes:EtOAc). Spectral data match those previously reported.[41]

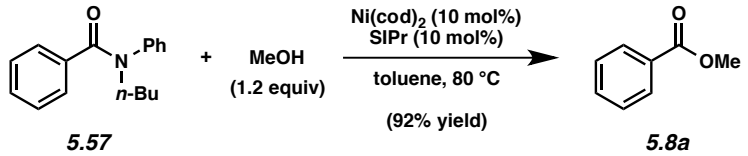


*5.57* *5.8a*

**Ester 5.8a (Table 5.2a, entry 13)**. Purification by flash chromatography (10:1 Hexanes:$Et_2O$) generated ester **5.8a** (92% yield, average of two experiments) as a clear oil. Ester **5.8a**: $R_f$ 0.44 (5:1 Hexanes:EtOAc). Spectral data match those previously reported.[32]

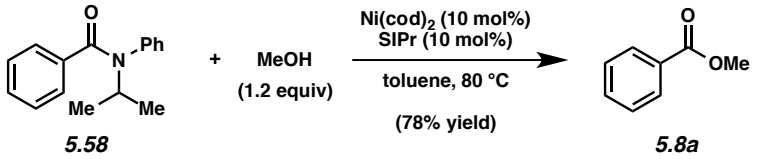


**Ester 5.8a (Table 5.2a, entry 14)**. Purification by flash chromatography (10:1 Hexanes:$Et_2O$) generated ester **5.8a** (78% yield, average of two experiments) as a clear oil. Ester **5.8a**: $R_f$ 0.44 (5:1 Hexanes:EtOAc). Spectral data match those previously reported.[32]

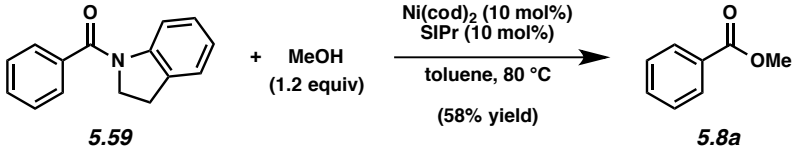


**Ester 5.8a (Table 5.2a, entry 15)**. Purification by flash chromatography (10:1 Hexanes:$Et_2O$) generated ester **5.8a** (58% yield, average of two experiments) as a clear oil. Ester **5.8a**: $R_f$ 0.44 (5:1 Hexanes:EtOAc). Spectral data match those previously reported.[32]

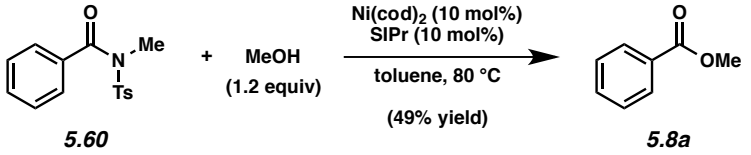


**Ester 5.8a (Table 5.2a, entry 16)**. Purification by flash chromatography (10:1 Hexanes:$Et_2O$) generated ester **5.8a** (49% yield, average of two experiments) as a clear oil. Ester **5.8a**: $R_f$ 0.44 (5:1 Hexanes:EtOAc). Spectral data match those previously reported.[32]

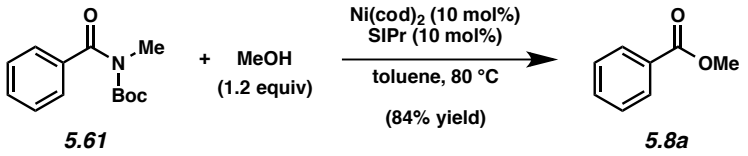


*5.61* *5.8a*

**Ester 5.8a (Table 5.2a, entry 17)**. Purification by flash chromatography (10:1 Hexanes:$Et_2O$) generated ester **5.8a** (84% yield, average of two experiments) as a clear oil. Ester **5.8a**: $R_f$ 0.44 (5:1 Hexanes:EtOAc). Spectral data match those previously reported.[32]

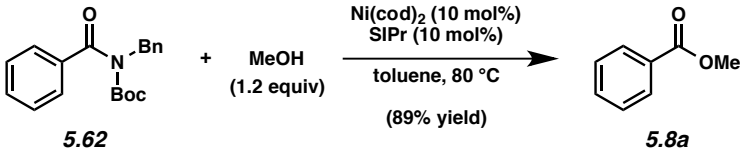


*5.62* *5.8a*

**Ester 5.8a (Table 5.2a, entry 18)**. Purification by flash chromatography (10:1 Hexanes:$Et_2O$) generated ester **5.8a** (89% yield, average of two experiments) as a clear oil. Ester **5.8a**: $R_f$ 0.44 (5:1 Hexanes:EtOAc). Spectral data match those previously reported.[32]

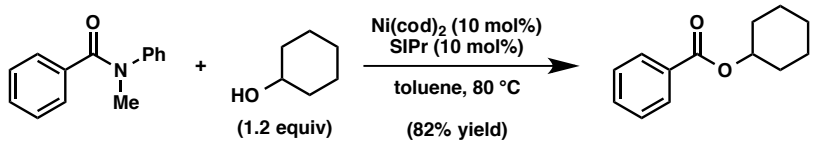


*5.7g* *5.63* *5.64*

**Ester 5.64 (Table 5.2b, entry 19)**. Purification by flash chromatography (100:1 Hexanes:EtOAc) generated ester **5.64** (82% yield, average of two experiments) as a clear oil. Ester **5.64**: $R_f$ 0.59 (5:1 Hexanes:EtOAc). Spectral data match those previously reported.[42]

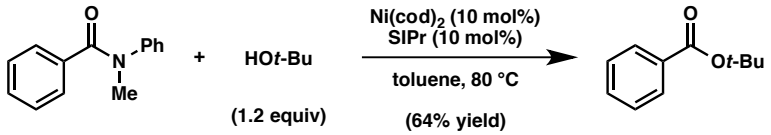


**Ester 5.66 (Table 5.2b, entry 20)**. Purification by flash chromatography (100:1 Hexanes:EtOAc) generated ester **5.66** (64% yield, average of two experiments) as a clear oil. Ester **5.66**: $R_f$ 0.71 (5:1 Hexanes:EtOAc). Spectral data match those previously reported.[43]

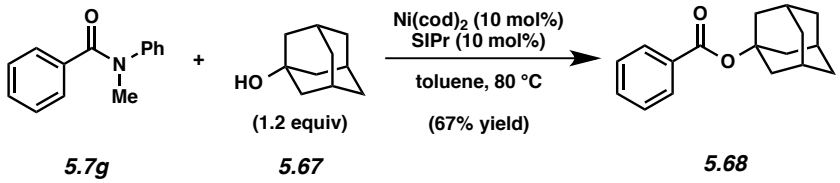


**Ester 5.68 (Table 5.2b, entry 21)**. Purification by flash chromatography (100:1 Hexanes:EtOAc) generated ester **5.68** (67% yield, average of two experiments) as a clear oil. Ester **5.68**: $R_f$ 0.76 (5:1 Hexanes:EtOAc). Spectral data match those previously reported.[44]

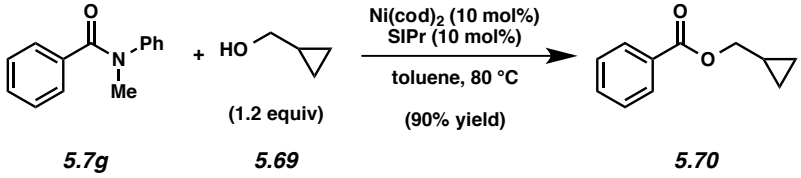


**Ester 5.70 (Table 5.2b, entry 22)**. Purification by flash chromatography (20:1 Hexanes:$Et_2O$) generated ester **5.70** (90% yield, average of two experiments) as a clear oil. Ester **5.70**: $R_f$ 0.88 (5:1 Hexanes:EtOAc); $^1$H NMR (600 MHz, $CDCl_3$): δ 8.09–8.05 (m, 2H), 7.57–7.54 (m, 1H), 7.46–7.42 (m, 2H), 4.16 (d, $J$ = 7.2, 2H), 1.30–1.23 (m, 1H), 0.64–0.57 (m, 2H), 0.41–0.32 (m, 2H), $^{13}$C NMR (125 MHz, $CDCl_3$): δ 166.9, 132.9, 130.7, 129.7, 128.4, 69.8, 10.0, 3.4; IR (film):

3079, 1451, 1712, 1272, 1114 $cm^{-1}$; HRMS-ESI (*m/z*) $[M+H]^+$ calcd for $C_{11}H_{13}O2$, 177.09101; found 177.09057.

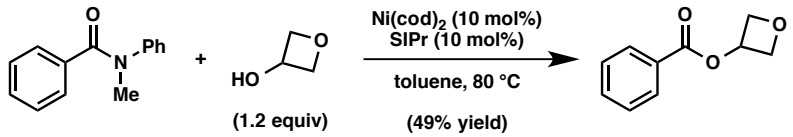


*5.7g* *5.71* *5.72*

**Ester 5.72 (Table 5.2b, entry 23)**. Purification by flash chromatography (10:1 Hexanes:$Et_2O$) generated ester **5.72** (49% yield, average of two experiments) as a clear oil. Ester **5.72**: $R_f$ 0.41 (5:1 Hexanes:EtOAc). Spectral data match those previously reported.[45]

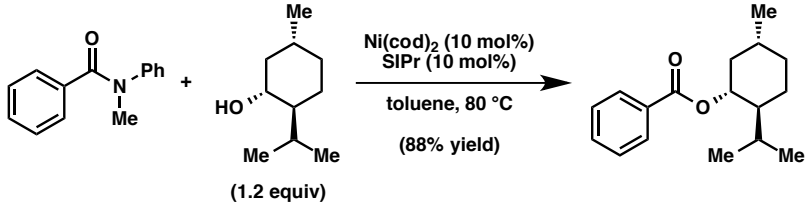


*5.7g* *5.20* *5.21*

**Ester 5.21 (Table 5.2b, entry 24)**. Purification by flash chromatography (100:1 Hexanes:EtOAc) generated ester **5.21** (88% yield, average of two experiments) as a white solid. Ester **5.21**: $R_f$ 0.59 (5:1 Hexanes:EtOAc). Spectral data match those previously reported.[46]

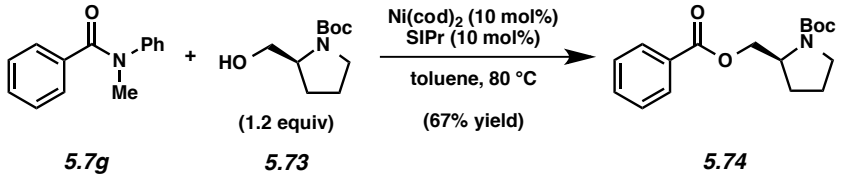


**Ester 5.74 (Table 5.2b, entry 25)**. Purification by flash chromatography (5:1 Hexanes:EtOAc) generated ester **5.74** (67% yield, average of two experiments) as a clear oil. Ester **5.74**: $R_f$ 0.81 (5:1 Hexanes:EtOAc). Spectral data match those previously reported.[47]

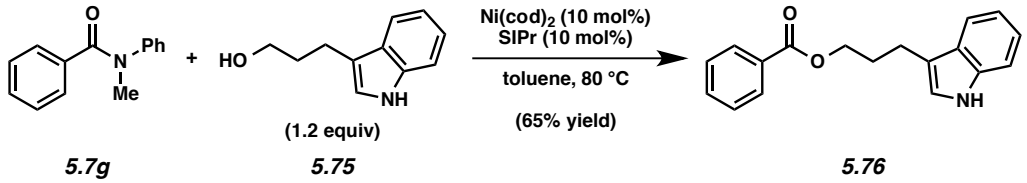


**Ester 5.76 (Table 5.2b, entry 26)**. Purification by flash chromatography (100:1 Benzene:Acetone) generated ester **5.76** (65% yield, average of two experiments) as a clear oil. Ester **5.76**: $R_f$ 0.26 (5:1 Hexanes:EtOAc); $^1$H NMR (500 MHz, $CDCl_3$): δ 8.06–8.03 (m, 2H), 8.00–7.90 (br s, 1H), 7.64–7.60 (m, 1H), 7.56 (tt, *J* = 7.3, 1.4, 1H), 7.48–7.42 (m, 2H), 7.37 (dt, *J* = 8.1, 0.9, 1H), 7.20 (ddd, *J* = 11.6, 7.5, 1.2, 1H), 7.12 (ddd, *J* = 11.6, 7.5, 1.2, 1H), 7.04–7.02 (m, 1H), 4.40 (t, *J* = 6.40, 2H), 2.98–2.92 (m, 2H) 2.24–2.17 (m, 2H); $^{13}$C NMR (125 MHz, $CDCl_3$): δ 166.9, 136.5, 133.0, 130.6, 129.7, 128.5, 127.5, 122.2, 121.6, 119.4, 118.9. 115.5, 111.3, 64.7, 29.2, 21.8; IR (film): 3411, 2360, 1702, 1273, 1117 cm$^{-1}$; HRMS-ESI (*m/z*) $[M+H]^+$ calcd for $C_{18}H_{18}NO_2$, 280.13321; found 280.13205.

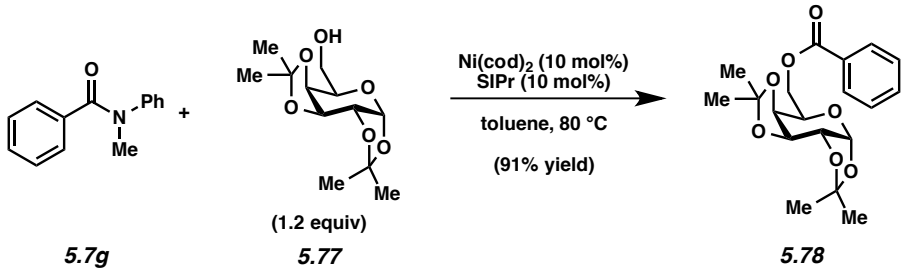


*5.7g* *5.77* *5.78*

**Ester 5.78 (Table 5.2b, entry 27)**. Purification by flash chromatography (10:1 Hexanes:$Et_2O$) generated ester **5.78** (91% yield, average of two experiments) as a clear oil. Ester **5.78**: $R_f$ 0.25 (5:1 Hexanes:$Et_2O$); $^1$H NMR (500 MHz, $CDCl_3$): δ 8.07–8.03 (m, 2H), 7.58–7.53 (m, 1H), 7.46–7.41 (m, 2H), 5.57 (d, *J* = 4.9, 1H), 4.65 (dd, *J* = 7.9, 2.5, 1H), 4.53 (dd, *J* = 11.5, 4.9, 1H), 4.43 (dd, *J* = 11.5, 7.5, 1H), 4.35 (dd, *J* = 5.0, 2.5, 1H), 4.33 (dd, *J* = 7.9, 2.0, 1H), 4.19 (ddd, *J* = 7.5, 5.0, 2.0, 1H), 1.52 (s, 3H), 1.48 (s, 3H), 1.36 (s, 3H), 1.34 (s, 3H); $^{13}$C NMR (125 MHz, $CDCl_3$): δ 166.6, 133.1, 130.2, 129.9, 128.5, 109.9, 109.0, 96.5, 71.3, 70.9, 70.7, 66.3, 64.0, 26.2, 26.1, 25.1, 24.7; IR (film): 2989, 1720, 1276 1108, 1070 cm$^{-1}$; HRMS-ESI (*m/z*) $[M+H]^+$ calcd for $C_{19}H_{25}O_7$, 365.15948; found 365.15835; $[\alpha]^{22.0}_D$ –70.4° (*c* = 1.000, $CH_2Cl_2$).

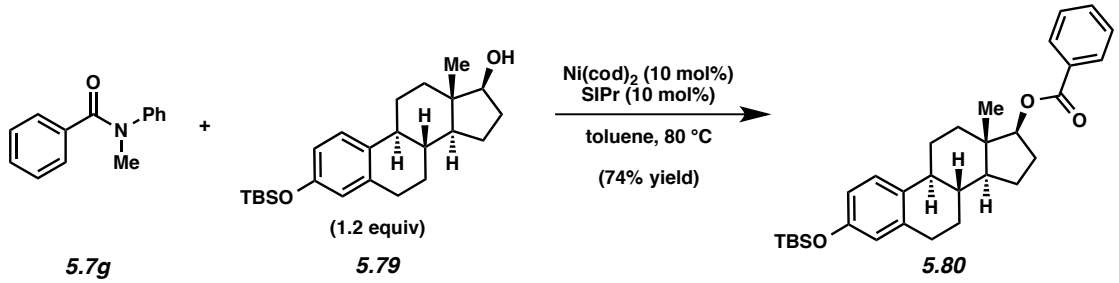


*5.7g* *5.79* *5.80*

**Ester 5.80 (Table 5.2b, entry 28)**. Purification by flash chromatography (100:1 Hexanes:EtOAc) generated ester **5.80** (74% yield, average of two experiments) as a clear oil. Ester **5.80**: $R_f$ 0.67 (5:1 Hexanes:EtOAc); $^1$H NMR (500 MHz, $CDCl_3$): δ 8.09–8.03 (m, 2H), 7.59–7.53 (m, 1H), 7.49–7.41 (m, 2H), 7.15–7.10 (m, 1H), 6.64–6.59 (m, 1H), 6.58–6.54 (m,

1H), 5.13–4.90 (m, 1H), 2.90–2.76 (m, 2H), 2.48–2.17 (m, 3H), 2.02–1.63 (m, 5H), 1.60–1.28 (m, 6H), 0.99–0.86 (m, 11H), 0.19 (s, 6H); $^{13}$C NMR (125 MHz, $CDCl_3$): δ 166.7, 166.3, 153.5, 153.5, 138.0, 137.9, 133.1, 133.1, 132.9, 131.0, 130.9, 129.7, 129.7, 128.5, 128.5, 126.3, 126.3, 120.1, 120.1, 117.3, 83.4, 82.8, 50.0, 49.7, 45.5, 44.0, 43.9, 43.5, 39.2, 38.7, 37.2, 32.3, 30.4, 29.9, 29.8, 28.2, 27.9, 27.4, 25.9, 24.6, 23.6, 18.3, 17.0, 12.5, -4.2; IR (film): 2928, 1717, 1496, 1274, 1256, 1116 cm$^{-1}$; HRMS-ESI (*m/z*) $[M+H]^+$ calcd for $C_{31}H_{43}O_3Si$, 491.28866; found 491.29615; $[\alpha]^{22.0}_D$ +56.2° (*c* = 1.000, $CH_2Cl_2$).

*Note: **5.80** was obtained as mixture of rotamers. These data represent empirically observed chemical shifts from the $^{13}$C NMR spectrum.*

### 5.7.2.6 Selective Cleavage of Tertiary over Secondary Amide

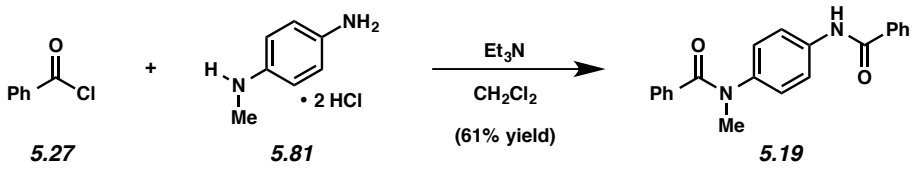


*5.27* *5.81* *5.19*

**Amide 5.19 (Figure 5.3a).** A mixture of amine salt **5.81** (3.1 g, 16.0 mmol, 1.0 equiv), dichloromethane (96.0 mL, 0.5 M), and triethylamine (8.9 mL, 64.0 mmol, 8.9 mL) was stirred at 23 °C for 30 min. The reaction vessel was cooled to 0 °C and benzoyl chloride (**5.27**) (5.6 mL, 48.0 mmol, 3.0 equiv) was added dropwise over 15 min with stirring. The resulting heterogeneous mixture was warmed to 23 °C over 30 min and stirred for 18 h. The reaction mixture was then diluted with EtOAc (50 mL) and then washed sequentially with 1.0 M HCl (50 mL) and brine (50 mL). The organic layer was dried over $Na_2SO_4$ and concentrated under reduced pressure. The crude mixture was purified via flash chromatography (1:1

Hexanes:EtOAc) to give amide **5.19** (3.2 g, 61% yield) as a white solid. Amide **5.19**: $R_f$ 0.34 (1:1 Hexanes:EtOAc); $^1$H NMR (400 MHz, $CDCl_3$): δ 7.85–7.80 (m, 2H), 7.76 (br s, 1H), 7.58–7.44 (m, 5H), 7.34–7.30 (m, 2H), 7.25–7.22 (m, 1H), 7.21–7.15 (m, 2H), 7.05 (d, $J$ = 8.9 Hz, 2H), 3.49 (s, 3H); $^{13}$C NMR (125 MHz, $CDCl_3$): δ 170.9, 166.0, 141.0, 140.9, 136.7, 136.6, 136.0, 134.8, 132.1, 132.1, 129.8, 128.9, 128.8, 128.8, 128.0, 127.6, 127.5, 127.2, 127.2, 120.9, 120.8, 38.6; IR (film): 3299, 2971, 2245, 1737, 1625, 1602, 1578, 1509, 1372, 1316, 1292, 1244, 1101 cm$^{-1}$; HRMS-ESI (*m/z*) $[M+H]^+$ calcd for $C_{21}H_{19}N_2O_2$, 331.14465; found 331.14229.

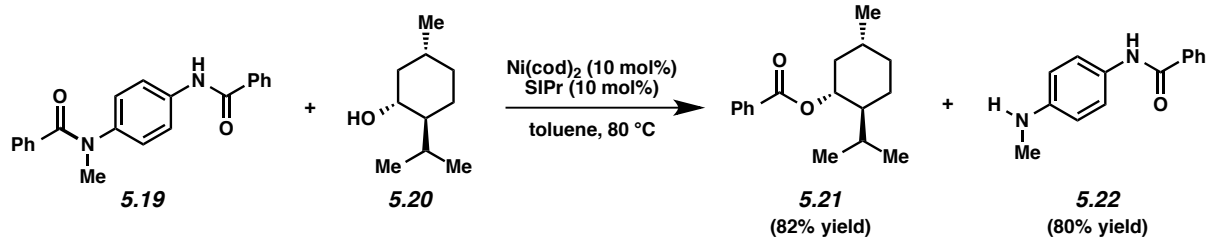


**Ester 5.21 and Aminoamide 5.22 (Figure 5.3a).** A 1-dram vial containing amide **5.19** (100.0 mg, 0.30 mmol, 1.0 equiv) and a magnetic stir bar was charged with $Ni(cod)_2$ (12.4 mg, 0.045 mmol, 15 mol%) and SIPr (35.2 mg, 0.045 mmol, 30 mol%) in a glove box. Subsequently, toluene (0.45 mL, 1.0 M) and then (–)-menthol (**5.20**) (56.0 mg, 0.36 mmol, 1.2 equiv) were added. The vial was sealed with a Teflon-lined screw cap, removed from the glove box, and stirred at 80 °C for 12 h. After cooling to 23 ºC, the mixture was diluted with hexanes (0.5 mL) and filtered over a plug of silica gel (10 mL of EtOAc eluent). The volatiles were removed under reduced pressure, and the crude residue was purified by flash chromatography (10:1 → 1:1 Hexanes:EtOAc) generated ester **5.21** (82% yield, average of two experiments) as a white solid and aminoamide **5.22** (80% yield, average of two experiments) as a white solid. Ester **5.21**: $R_f$ 0.90 (1:1 Hexanes:EtOAc). Spectral data matched those previously reported.[46] Aminoamide

**5.22**: $R_f$ 0.30 (1:1 Hexanes:EtOAc); $^1$H NMR (500 MHz, DMSO): δ 9.89 (s, 1H), 7.93 (d, *J* = 7.6, 2H), 7.58–7.40 (m, 5H), 6.52 (d, *J* = 8.4, 2H), 5.50 (br s, 1H), 2.66 (d, *J* = 4.9, 3H); $^{13}$C NMR (125 MHz, DMSO): δ 164.6, 146.7. 135.3, 131.1, 128.3, 128.0, 127.4, 122.2, 111.3, 30.0; IR (film): 3268, 1639, 1535, 1517, 1468, 1402, 1310, 1246, 1177, 1026 cm$^{-1}$; HRMS-ESI (*m/z*) $[M+H]^+$ calcd for $C_{14}H_{15}N_2O$, 227.11844; found 227.11649.

### 5.7.2.7 Selective Cleavage of Aryl Amide Over Alkyl Amide

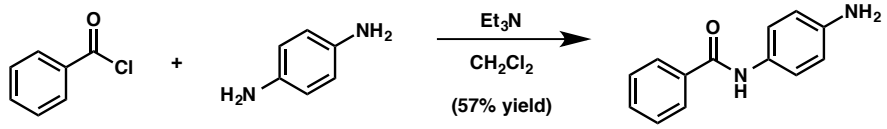


*5.27* *5.82* *5.83*

**Amide 5.83 (Figure 5.3b).** To a solution of amine **5.82** (7.7g, 71.1 mmol, 2.0 equiv) and triethylamine (6.2 mL, 44.5 mmol, 1.25 equiv) in dichloromethane (356.0 mL, 0.1 M) was added benzoyl chloride **5.27** (5.0 g, 35.6 mL, 1.0 equiv) dropwise over 15 min. After stirring at 23 °C for 12 h, the reaction mixture was then diluted with deionized water (200 mL) and dichloromethane (200 mL). The organic layer was separated and the aqueous layer was extracted with EtOAc (3 x 500 mL). The combined organic layers were dried over $MgSO_4$ and concentrated under reduced pressure. The resulting red solid was purified by flash chromatography (1:1 Hexanes:EtOAc → 100% EtOAc) to give a white solid (4.3 g, 57% yield). Amide **5.83**: $R_f$ 0.31 (1:1 Hexanes:EtOAc). Spectral data matched those previously reported.[48]

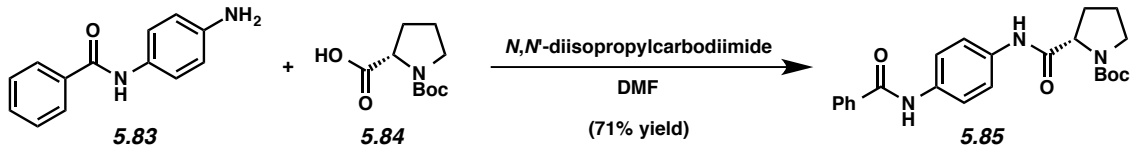


**Amide 5.85 (Figure 5.3b)**. To a mixture of amide **5.83** (1.5 g, 7.1 mmol, 1.0 equiv) and carboxylic acid **5.84** (1.52 g, 7.1 mmol, 1.0 equiv) in dry DMF (2.7 mL, 2.6 M) at 0 °C was added *N*,*N*'-diisopropylcarbodiimide (1.3 mL, 8.5 mmol, 1.2 equiv) dropwise over 5 min. The reaction was then stirred at 0 °C for 10 min and 23 °C for 12 h. The crude reaction mixture was poured into 1:1 $H_2O$:MeOH solution (1 L). The resulting solid was collected to afford amide **5.85** (2.1 g, 71% yield) as a white solid. Amide **5.85**: $R_f$ 0.69 (3:1 Acetone:Benzene); $^1$H NMR (500 MHz, $CDCl_3$): δ 9.53 (m, 1H), 7.90–7.84 (m, 2H), 7.76 (br s, 1H), 7.65–7.52 (m, 5H), 7.52–7.46 (m, 2H), 4.59–3.18 (m, 3H), 2.68–1.74 (m, 4H), 1.50 (s, 9H), $^{13}$C NMR (125 MHz, $CDCl_3$): δ 170.1, 165.7, 156.7, 135.4, 135.1, 133.8, 131.9, 128.9, 127.2, 121.2, 120.3, 81.1, 60.6, 47.4, 28.6, 27.4, 24.8; IR (film): 3295, 1668, 1515, 1405, 1308, 1162 cm$^{-1}$; HRMS-ESI (*m/z*) [M-H] calcd for $C_{23}H_{26}O_4N_3$, 408.19178; found 408.19340; $[\alpha]^{22.0}_D$ –50.0° (*c* = 0.100, $CHCl_3$).

*Note: **5.85** was obtained as mixture of rotamers. These data represent empirically observed chemical shifts and coupling constants from the $^1$H NMR and $^{13}$C NMR spectra.*

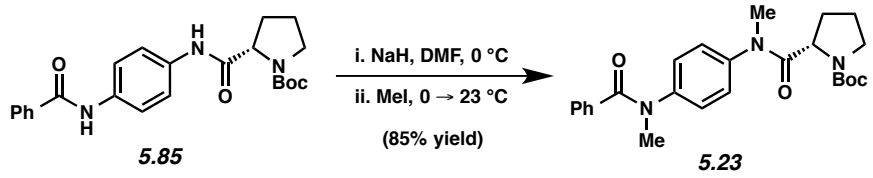


**Amide 5.23 (Figure 5.3b)**. To a solution of amide **5.85** (300.0 mg, 0.73 mmol) in dry DMF (12.0 mL, 0.06 M) at 0 °C, was added NaH (60% in oil dispersion, 62.0 mg, 1.5 mmol, 2.1

equiv). The mixture was stirred at 0 °C for 1 h and then methyl iodide (91.0 mL, 1.5 mmol, 2.0 equiv) was added. The solution was stirred at 0 °C for an additional hour and then warmed to 23 °C over 30 min. After 14 h, the reaction was quenched with a solution of saturated aqueous $NH_4Cl$ (5 mL) and diluted with deionized water (50 mL). The mixture was extracted with EtOAc (4 x 50 mL) and the combined organic layers were washed succesively with water (4 x 50 mL) and brine (50 mL), and then dried over $MgSO_4$. After concentration under reduced pressure, the crude residue was purified by flash chromatography (2:1 → 1:1 Hexanes:EtOAc) to provide amide **5.23** (272.0 mg, 85% yield) as a clear oil. Amide **5.23**: $R_f$ 0.33 (1:1 Hexanes:EtOAc); $^1$H NMR (500 MHz, $CDCl_3$): δ 7.91–7.37 (m, 1H), 7.33–7.24 (m, 2H), 7.24–7.14 (m, 6H), 4.25–3.98 (m, 1H), 3.59–3.48 (m, 3H), 3.52 (app d, $J$ = 8.6, 1H), 3.48–3.33 (m, 1H), 3.29–3.17 (m, 3H), 2.02–1.59 (m, 4H), 1.45 (app d, $J$ = 3.2, 9H) $^{13}$C NMR (125 MHz, $CDCl_3$): δ 172.6, 172.5, 170.8, 154.5, 153.9, 144.6, 144.4, 141.7, 141.4, 135.9, 135.8, 130.1, 129.9, 128.8, 128.8, 128.5, 128.2, 127.9, 127.9, 127.2, 79.9, 79.5, 57.2, 56.9, 47.3, 47.2, 38.3, 37.8, 37.7, 31.6, 30.3, 28.8, 28.7, 24.4, 23.6, 1.2; IR (film): 2974, 2876, 1643, 1509, 1364, 1119 cm$^{-1}$; HRMS-ESI (*m/z*) $[M+H]^+$ calcd for $C_{25}H_{32}O_4N_3$, 438.23873; found 438.23824; $[\alpha]^{22.0}_D$ +76.0° (*c* = 0.100, $CHCl_3$).

*Note: **5.23** was obtained as mixture of rotamers. These data represent empirically observed chemical shifts and coupling constants from the $^1$H NMR and $^{13}$C NMR spectra.*

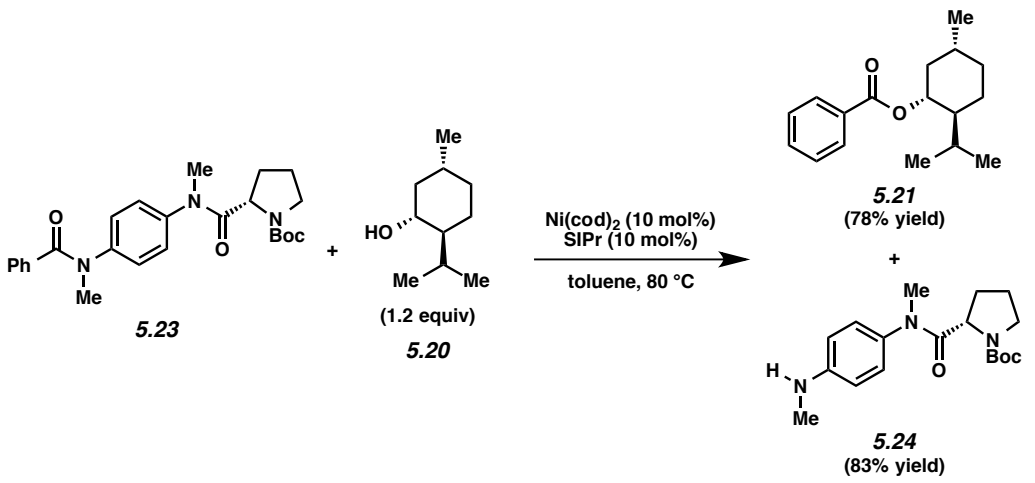


**Ester 5.21 and Amine 5.24 (Figure 5.3b)**. A 1-dram vial containing amide **5.23** (100.0 mg, 0.23 mmol, 1.0 equiv) and a magnetic stir bar was charged with $Ni(cod)_2$ (6.3 mg, 0.023 mmol, 10 mol%) and SIPr (8.9 mg, 0.023 mmol, 10 mol%) in a glove box. Subsequently, toluene (0.23 mL, 1.0 M) and then (–)-menthol (**5.20**) (42.9 mg, 0.27 mmol, 1.2 equiv) were added. The vial was sealed with a Teflon-lined screw cap, removed from the glove box, and stirred at 80 °C for 12 h. After cooling to 23 °C, the mixture was diluted with hexanes (0.5 mL) and filtered over a plug of silica gel (10 mL of EtOAc eluent). The volatiles were removed under reduced pressure, and the crude residue was purified by flash chromatography (100:1 → 1:1 Hexanes:EtOAc) provided ester **5.21** (78% yield, average of two experiments) as a white solid and amine **5.24** (83% yield, average of two experiments) as a clear oil. Ester **5.21**: $R_f$ 0.90 (1:1 Hexanes:EtOAc). Spectral data matched those previously reported.[46] Amine **5.24**: $R_f$ 0.18 (1:1 Hexanes:EtOAc); $^1$H NMR (500 MHz, $CDCl_3$): δ 7.16 (d, $J$ = 7.5, 1H), 7.03 (d, $J$ = 8.5, 1H), 6.63 (t, $J$ = 8.5, 2H), 4.60–3.25 (m, 4H), 3.22 (s, 3H), 2.86 (app d, $J$ = 7.3, 3H), 2.03–1.59 (m, 4H), 1.47 (app d, $J$ = 14.4, 9H); $^{13}$C NMR (125 MHz, $CDCl_3$): δ 128.9, 128.7, 79.6, 79.2, 57.3, 57.0, 47.4, 47.2, 38.0, 31.8, 30.9, 30.6, 28.8, 28.7, 24.4, 23.7; IR (film): 3368, 2976, 1649, 1524, 1390, 1160, 1119 cm$^{-}$

[1]; HRMS-ESI (*m/z*) $[M+H]^+$ calcd for $C_{18}H_{28}N_3O_3$, 334.21252; found 334.21195; $[\alpha]^{22.0}_D$ +66.00° (*c* = 0.100, $CHCl_3$).

*Note:* ***5.24*** *was obtained as mixture of rotamers. These data represent empirically observed chemical shifts and coupling constants from the* $^1$*H NMR and* $^{13}$*C NMR spectra.*

### 5.7.2.8 Selective Cleavage of Aryl Amide in the Presence of an Ester

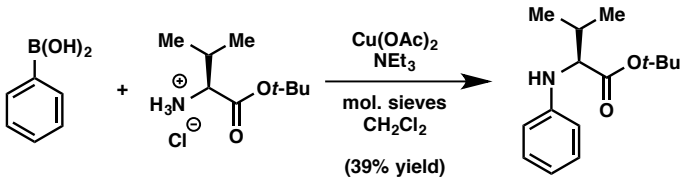


***5.86*** ***5.87*** ***5.26***

**Amine 5.26 (Figure 5.3c).** A round bottom flask was charged with 4Å molecular sieves (14.0 g, 2.0 equiv), ester **5.87** (7.0 g, 33.4 mmol, 1.0 equiv), boronic acid **5.86** (8.1 g, 66.8 mmol, 2.0 equiv), and $Cu(OAc)_2$ (6.7 g, 36.7 mmol, 1.1 equiv). The flask was evacuated by vacuum, backfilled with $O_2$, and then held under an $O_2$ atmosphere by balloon. Dichloromethane (333.0 mL, 0.1 M) and triethylamine (9.3 mL, 66.8 mmol, 2.0 equiv) were added sequentially, and the reaction mixture was stirred at 23 °C for 14 h. The reaction mixture was then quenched with a solution of ammonia in methanol (6N, 15 mL). After removing the volatiles under reduced pressure, the crude mixture was purified via flash chromatography (10:1 Hexanes:EtOAc) to give amine **5.26** as a white solid (3.2 g, 39% yield). Amide **5.26**: $R_f$ 0.65 (5:1 Hexanes:EtOAc); $^1$H NMR (500 MHz, $CDCl_3$): δ 7.18–7.13 (m, 2H), 6.71 (tt, *J* = 7.3, 1.0, 1H), 6.66–6.61 (m, 2H), 4.15 (br s, 1H), 3.75 (d, *J* = 5.6, 1H), 2.15–2.05 (m, 1H), 1.42 (s, 9H), 1.03 (dd, *J* = 11.3, 7.0, 6H); $^{13}$C NMR (125 MHz, $CDCl_3$): δ 172.9, 147.7, 129.4, 118.1, 113.8, 81.6, 63.0, 31.6, 28.2,

19.1, 18.8; IR (film): 3383, 2970, 1708, 1605, 1368, 1156 $cm^{-1}$; HRMS-ESI (*m/z*) $[M+H]^+$ calcd for $C_{15}H_{24}N_1O_2$, 250.18016; found 250.17955; $[\alpha]^{22.0}_D$ –26.00° (*c* = 0.100, $CHCl_3$)

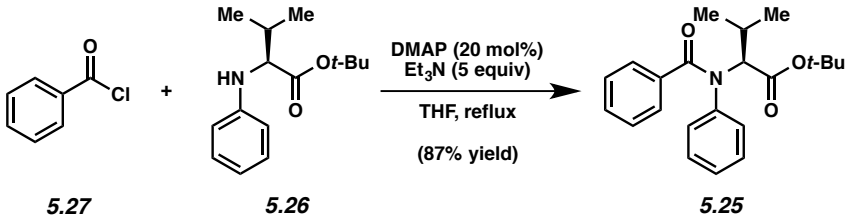


*5.27* *5.26* *5.25*

**Amide 5.25 (Figure 5.3c).** To a solution of amine **5.26** (887 mg, 3.55 mmol) in THF (35.5 mL, 0.1 M) was added DMAP (86.7 mg, 0.71 mmol, 0.2 equiv) and triethylamine (2.46 mL, 17.75 mmol, 5 equiv). Then, benzoyl chloride (**5.27**) (2.05 mL, 17.75 mmol, 5 equiv) was added dropwise into the flask over 5 min and then refluxed. After 18 h, the reaction mixture was cooled to 23 °C, quenched with 1.0 M HCl (20 mL), extracted with EtOAc (3 X 50 mL), and dried over $Na_2SO_4$. The volatiles were removed under reduced pressure and the crude residue was purified via flash chromatography (30:1 Hexanes:EtOAc) to give amide **5.25** as a yellow solid (1.09 g, 87% yield). Amide **5.25**: $R_f$ 0.43 (5:1 Hexanes:EtOAc); $^1$H NMR (500 MHz, $CDCl_3$): δ 7.26–7.25 (m, 2H), 7.21–7.10 (m, 8H), 4.56 (d, *J* = 9.7, 1H), 2.59–2.56 (m, 1H), 1.43 (s, 9H), 1.09 (d, *J* = 6.9, 6H); $^{13}$C NMR (125 MHz, $CDCl_3$): δ 170.8, 169.7, 143.2, 136.4, 129.6, 128.8, 128.7, 128.6, 127.8, 126.9, 81.6, 68.9, 28.8, 28.2, 21.4, 20.3; IR (film): 2973, 1734, 1649, 1493, 1368, 1153 $cm^{-1}$; HRMS-ESI (*m/z*) $[M+H]^+$ calcd for $C_{15}H_{24}NO_2$, 354.20692; found 354.20591; $[\alpha]^{22.0}_D$ –76.00° (*c* = 0.100, $CHCl_3$).

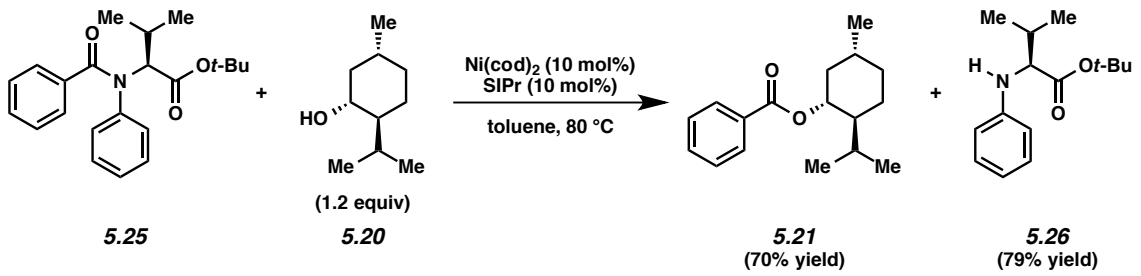


***5.25*** ***5.20*** ***5.21*** (70% yield) ***5.26*** (79% yield)

**Ester 5.21 and Amide 5.26 (Figure 5.3c)**. A 1-dram vial containing amide **5.25** (100.0 mg, 0.28 mmol, 1.0 equiv) and a magnetic stir bar was charged with $Ni(cod)_2$ (7.8 mg, 0.028 mmol, 10 mol%) and SIPr (11.1 mg, 0.028 mmol, 10 mol%) in a glove box. Subsequently, toluene (0.28 mL, 1.0 M) and then (–)-menthol (**5.20**) (53.1 mg, 0.34 mmol, 1.2 equiv) were added. The vial was sealed with a Teflon-lined screw cap, removed from the glove box, and stirred at 80 °C for 12 h. After cooling to 23 °C, the mixture was diluted with hexanes (0.5 mL) and filtered over a plug of silica gel (10 mL of EtOAc eluent). The volatiles were removed under reduced pressure, and the crude residue was purified by flash chromatography (100:1 Hexanes:EtOAc) generated ester **5.21** (70% yield) as a white solid and amine **5.26** (79% yield) as a clear oil. Ester **5.21**: $R_f$ 0.90 (1:1 Hexanes:EtOAc). Spectral data matched those previously reported.[46] Amide **5.26**: Spectral data of amide **5.26** matched the characterization data shown in page 322.

### 5.7.3 Verification of Enantiopurity

#### 5.7.3.1 Racemic Compound Syntheses

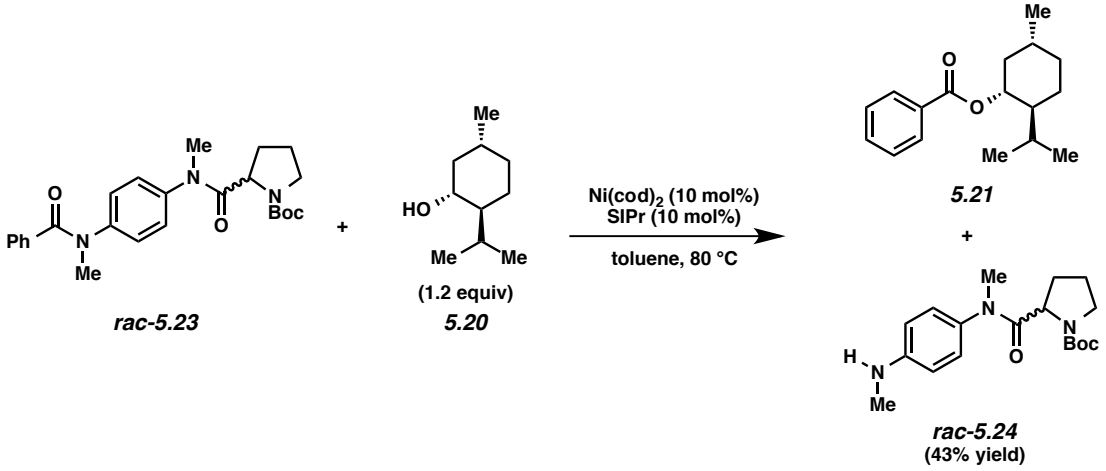


**Amine rac-5.24 (Figure 5.3b). Rac-5.23** was prepared using the procedure described earlier to synthesize (+)-**5.23** (see section 5.7.2.7 Selective Cleavage of Aryl Amide Over Alkyl Amide, page 318), except using the racemic Boc-proline **5.84**. A 1-dram vial containing **rac-5.23** (40.0 mg, 0.09 mmol, 1.0 equiv) and a magnetic stir bar was charged with $Ni(cod)_2$ (3.1 mg, 0.011 mmol, 12.5 mol%) and SIPr (4.5 mg, 0.011 mmol, 12.5 mol%) in a glove box. Subsequently, toluene (0.11 mL, 0.8 M) and then (–)-menthol **5.20** (21.4 mg, 0.24 mmol, 1.5 equiv) were added. The vial was sealed with a Teflon-lined screw cap, removed from the glove box, and stirred at 80 °C for 12 h. After cooling to 23 °C, the mixture was diluted with hexanes (0.5 mL) and filtered over a plug of silica gel (10 mL of EtOAc eluent). The volatiles were removed under reduced pressure. The crude residue was purified by preparative thin-layer chromatography (1:1 Hexanes:EtOAc) to give amine **rac-5.24** (13.2 mg, 43% yield) as a clear oil. Spectral data matched those reported in the section 5.7.2.7 Selective Cleavage of Aryl Amide Over Alkyl Amide, page 318.

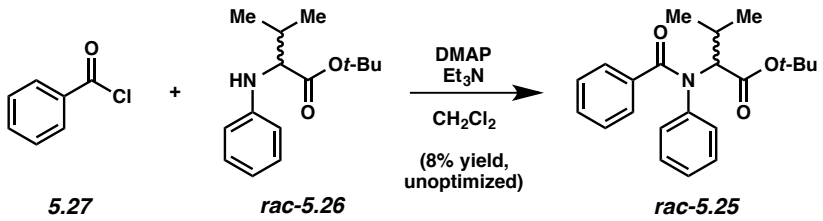


*5.27* *rac-5.26* *rac-5.25*

**Amide rac-5.25 (Figure 5.3c). Rac-5.26** was prepared using the procedure described earlier to synthesize (+)-**5.26** (see page 322), but using racemic ester **5.87**. A 1-dram vial containing a magnetic stir bar, aniline **rac-5.26** (20.0 mg, 0.080 mmol, 1.05 equiv), and $CH_2Cl_2$ (0.8 mL) was added $Et_3N$ (14 μL, 0.10 mmol, 1.3 equiv) and benzoyl chloride (8.9 μL, 0.076 mmol). The mixture was stirred at 23 °C for 2 d and then diluted in water (25 mL). After extraction with EtOAc (4 x 25 mL), the combined organic layers were washed with brine (25 mL) and dried over $MgSO_4$. The solution was filtered and concentrated under reduced pressure. The crude residue was purified by preparative thin-layer chromatography (5:1 EtOAc:Hexanes) to give **rac-5.25** (2.2 mg, 8% yield, unoptimized) as a clear oil.

### 5.7.3.2 Chiral SFC Assays

| Compound | Method Column /Temp | Polar Cosolvent | Method Flow Rate | Retention Times | Enantiomeric Ratio (er) |
|---|---|---|---|---|---|
| 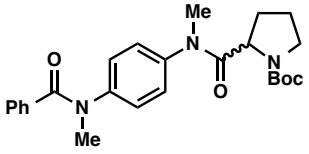 ***rac-5.23*** | Daicel ChiralPak OJ-H / 35°C | 7% MeOH | 2.00 mL/min | 4.00/4.67 min | 52:48 |
| 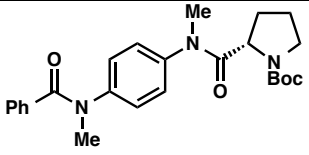 ***5.23*** | Daicel ChiralPak OJ-H / 35°C | 7% MeOH | 2.00 mL/min | 4.53/5.27 min | **96:4** |
| 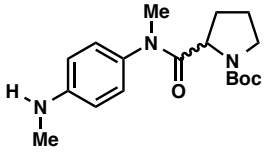 ***rac-5.25*** | Daicel ChiralPak OJ-H / 35°C | 15 % *i*-PrOH | 1.00 mL/min | 7.96/9.09 min | 52:48 |
| 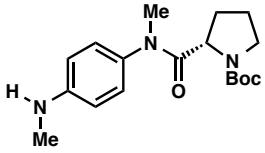 ***5.25*** | Daicel ChiralPak OJ-H / 35°C | 15 % *i*-PrOH | 1.00 mL/min | 7.60/8.78 min | **96:4** |

**No stereochemical erosion occurs during the nickel-catalyzed esterification.**

Date:12/16/2014
Sample:nfn-6-199b-bbb1
Method Name:NOT DEFINED
Run Info:N.A.

CCPFB2.tmp.DAT - Maximum absorbance

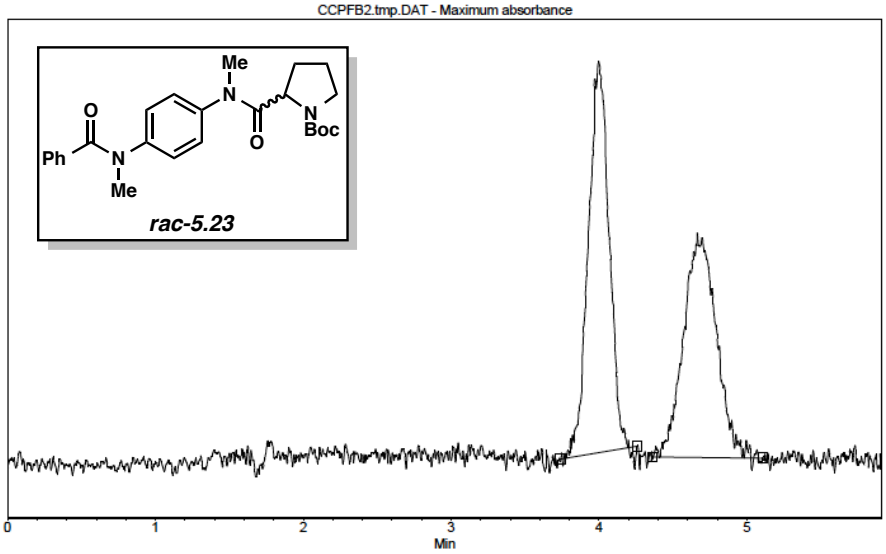


| Index | Name | Start | Time | End | RT Offset | Quantity | Height | Area | Area |
|---|---|---|---|---|---|---|---|---|---|
| | | [Min] | [Min] | [Min] | [Min] | [% Area] | [µV] | [µV.Min] | [%] |
| 1 | UNKNOWN | 3.74 | 4.00 | 4.26 | 0.00 | 52.37 | 119.3 | 19.2 | 52.367 |
| 2 | UNKNOWN | 4.36 | 4.67 | 5.11 | 0.00 | 47.63 | 68.6 | 17.5 | 47.633 |
| | | | | | | | | | |
| Total | | | | | | 100.00 | 187.9 | 36.7 | 100.000 |

Date:12/16/2014
Sample:nfn-6-107b1
Method Name:OJiso7%MeOH
Run Info:N.A.

CCPFC5.tmp.DAT - HP1100 DAD Signal B

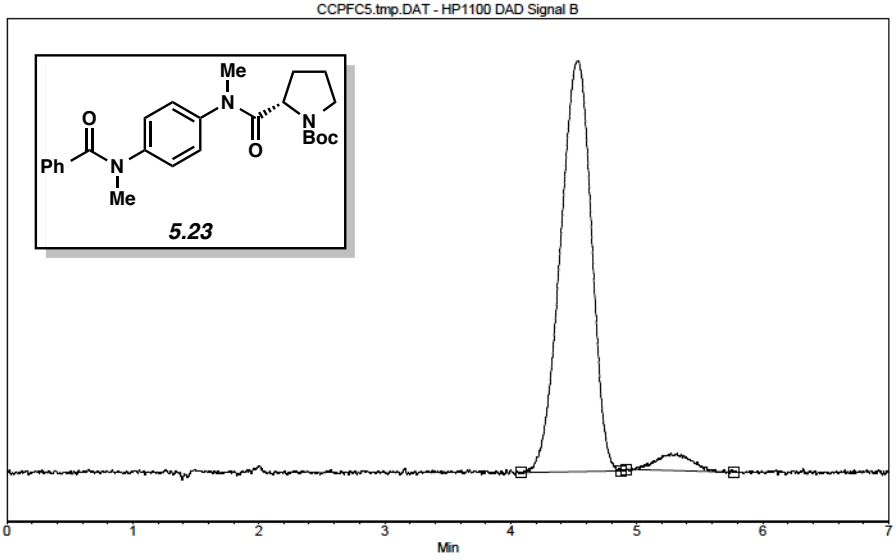


| Index | Name | Start | Time | End | RT Offset | Quantity | Height | Area | Area |
|---|---|---|---|---|---|---|---|---|---|
| | | [Min] | [Min] | [Min] | [Min] | [% Area] | [µV] | [µV.Min] | [%] |
| 1 | UNKNOWN | 4.08 | 4.53 | 4.87 | 0.00 | 95.57 | 311.2 | 89.1 | 95.569 |
| 2 | UNKNOWN | 4.92 | 5.27 | 5.77 | 0.00 | 4.43 | 13.3 | 4.1 | 4.431 |
| | | | | | | | | | |
| Total | | | | | | 100.00 | 324.5 | 93.2 | 100.000 |

Date:12/16/2014
Sample:nfn-6-197b-71
Method Name:OJiso15%iPrOH-A
Run Info:N.A.

CCPFBC.tmp.DAT - HP1100 DAD Signal B

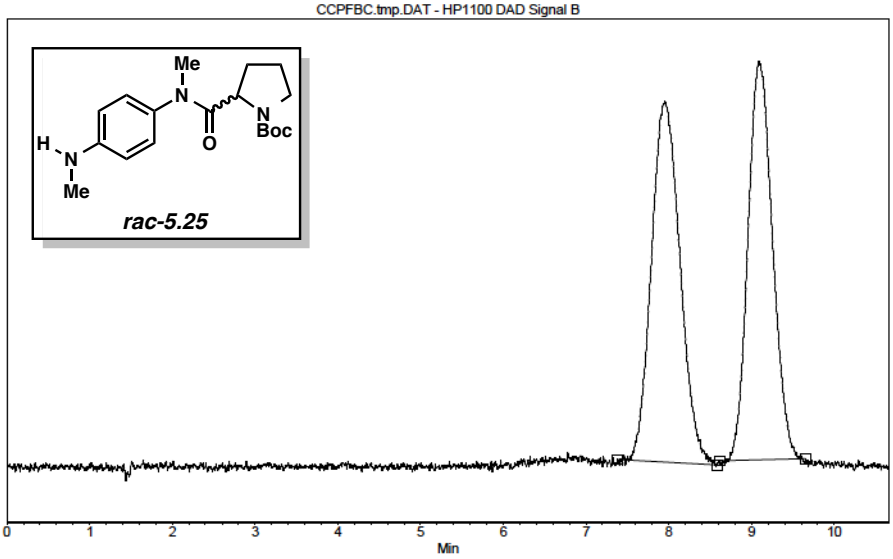


| Index | Name | Start | Time | End | RT Offset | Quantity | Height | Area | Area |
|---|---|---|---|---|---|---|---|---|---|
| | | [Min] | [Min] | [Min] | [Min] | [% Area] | [µV] | [µV.Min] | [%] |
| 1 | UNKNOWN | 7.38 | 7.96 | 8.59 | 0.00 | 51.46 | 112.9 | 45.2 | 51.463 |
| 2 | UNKNOWN | 8.61 | 9.09 | 9.65 | 0.00 | 48.54 | 124.9 | 42.7 | 48.537 |
| | | | | | | | | | |
| Total | | | | | | 100.00 | 237.8 | 87.9 | 100.000 |

Date:12/16/2014
Sample:nfn-6-197b-61
Method Name:OJiso15%iPrOH-A
Run Info:N.A.

CCPFBF.tmp.DAT - HP1100 DAD Signal B

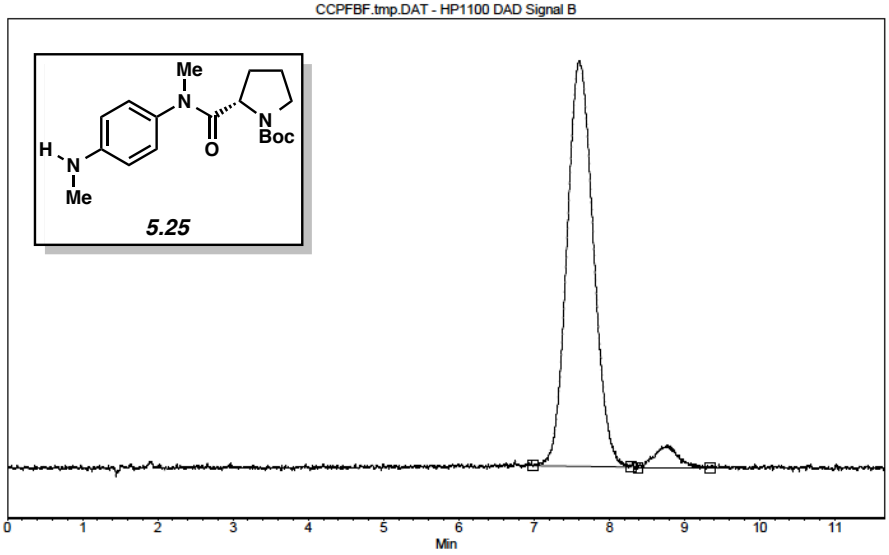


| Index | Name | Start | Time | End | RT Offset | Quantity | Height | Area | Area |
|---|---|---|---|---|---|---|---|---|---|
| | | [Min] | [Min] | [Min] | [Min] | [% Area] | [µV] | [µV.Min] | [%] |
| 1 | UNKNOWN | 6.99 | 7.60 | 8.29 | 0.00 | 95.51 | 208.2 | 84.5 | 95.512 |
| 2 | UNKNOWN | 8.39 | 8.78 | 9.35 | 0.00 | 4.49 | 11.3 | 4.0 | 4.488 |
| | | | | | | | | | |
| Total | | | | | | 100.00 | 219.5 | 88.5 | 100.000 |

| Compound | Method Column /Temp | Polar Cosolvent | Method Flow Rate | Retention Times | Enantiomeric Ratio (er) |
|---|---|---|---|---|---|
| 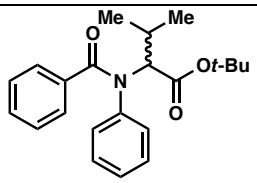 ***rac-5.26*** | Daicel ChiralPak OJ-H / 35°C | 0.5 % MeOH | 0.5 mL/min | 12.24/13.55 min | 50:50 |
| 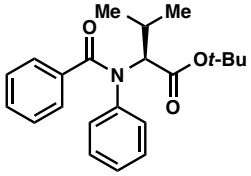 ***5.26*** | Daicel ChiralPak OJ-H / 35°C | 0.5 % MeOH | 0.5 mL/min | 12.23 min | **100:0** |
| 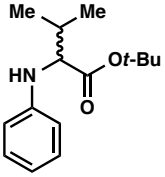 ***rac-5.27*** | Daicel ChiralPak OJ-H / 35°C | 5 % *i*-PrOH | 2.00 mL/min | 4.73/4.95 min | 50:50 |
| 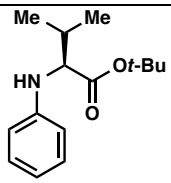 ***5.27*** | Daicel ChiralPak OJ-H / 35°C | 5 % *i*-PrOH | 2.00 mL/min | 4.77/4.99 min | **98:2** |

**Minimal stereochemical erosion during the nickel-catalyzed esterification was observed.**

Date:12/16/2014
Sample:nfn-6-201f-bb1
Method Name:OJiso.5iPrOH
Run Info:N.A.

CCPFAB.tmp.DAT - HP1100 DAD Signal B

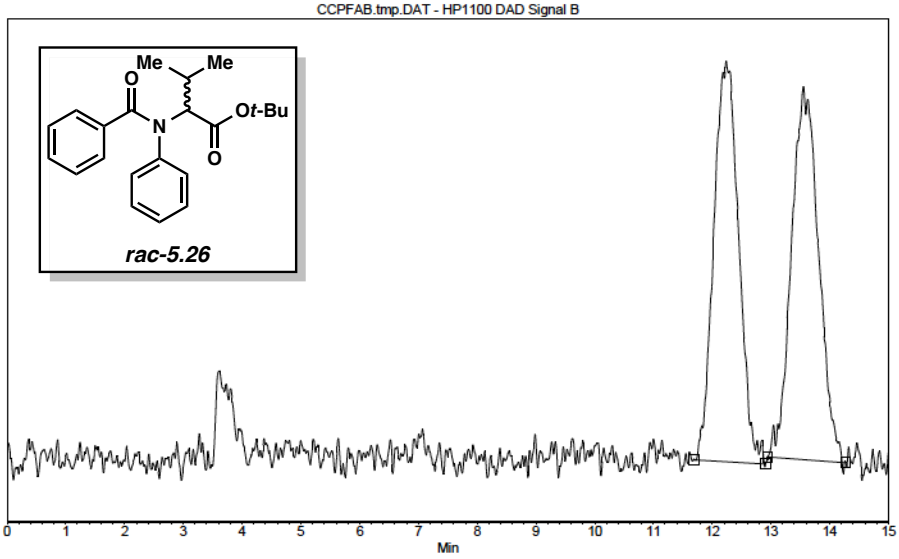


| Index | Name | Start | Time | End | RT Offset | Quantity | Height | Area | Area |
|---|---|---|---|---|---|---|---|---|---|
| | | [Min] | [Min] | [Min] | [Min] | [% Area] | [µV] | [µV.Min] | [%] |
| 1 | UNKNOWN | 11.70 | 12.24 | 12.91 | 0.00 | 49.67 | 91.0 | 44.6 | 49.672 |
| 2 | UNKNOWN | 12.94 | 13.55 | 14.28 | 0.00 | 50.33 | 84.6 | 45.2 | 50.328 |
| | | | | | | | | | |
| Total | | | | | | 100.00 | 175.6 | 89.8 | 100.000 |

Date:12/16/2014
Sample:nfn-6-171a-k0
Method Name:OJisopoint5flow1-3
Run Info:N.A.

CCPFAF.tmp.DAT - HP1100 DAD Signal B

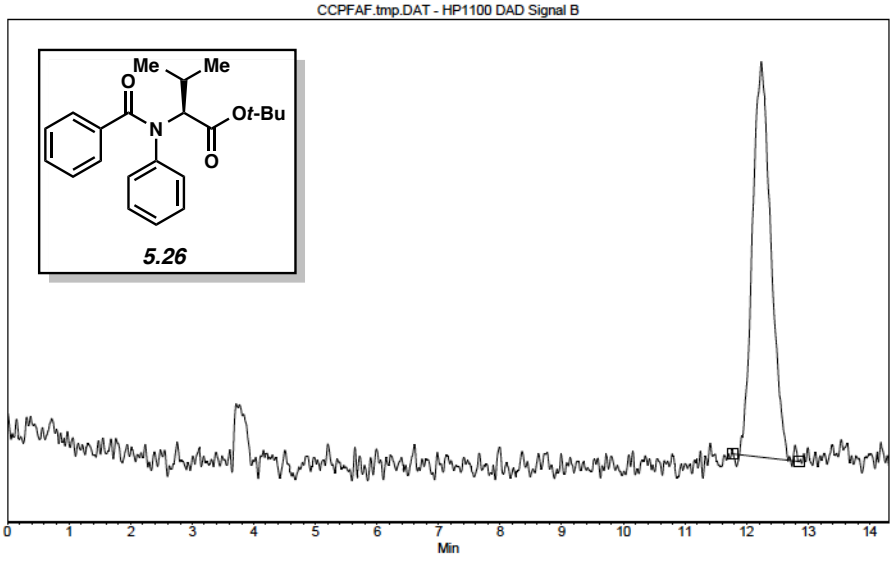


| Index | Name | Start | Time | End | RT Offset | Quantity | Height | Area | Area |
|---|---|---|---|---|---|---|---|---|---|
| | | [Min] | [Min] | [Min] | [Min] | [% Area] | [µV] | [µV.Min] | [%] |
| 1 | UNKNOWN | 11.78 | 12.23 | 12.85 | 0.00 | 100.00 | 100.4 | 34.7 | 100.000 |
| | | | | | | | | | |
| Total | | | | | | 100.00 | 100.4 | 34.7 | 100.000 |

Date:12/16/2014
Sample:NFN-6-195bb1
Method Name:NOT DEFINED
Run Info:N.A.

CCPFB9.tmp.DAT - Maximum absorbance

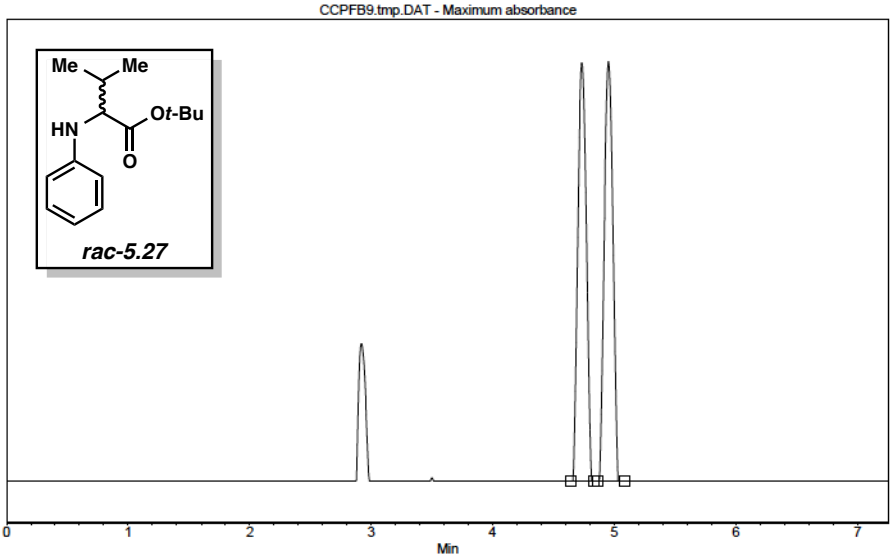


| Index | Name | Start | Time | End | RT Offset | Quantity | Height | Area | Area |
|---|---|---|---|---|---|---|---|---|---|
| | | [Min] | [Min] | [Min] | [Min] | [% Area] | [µV] | [µV.Min] | [%] |
| 1 | UNKNOWN | 4.64 | 4.73 | 4.83 | 0.00 | 49.64 | 137.3 | 11.2 | 49.644 |
| 2 | UNKNOWN | 4.87 | 4.95 | 5.09 | 0.00 | 50.36 | 137.6 | 11.3 | 50.356 |
| | | | | | | | | | |
| Total | | | | | | 100.00 | 274.9 | 22.5 | 100.000 |

Date:12/16/2014
Sample:nfn-6-195rrr1
Method Name:NOT DEFINED
Run Info:N.A.

CCPFB6.tmp.DAT - 240.00 nm

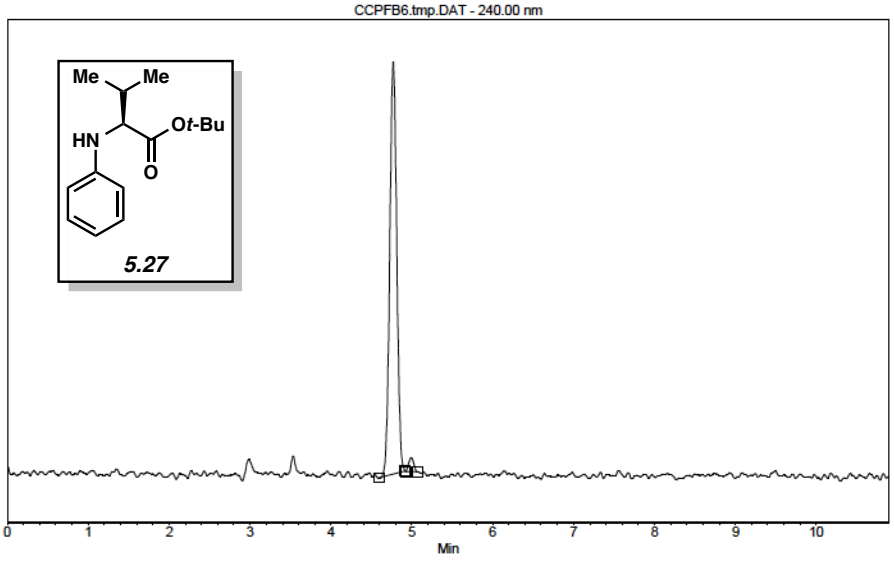


| Index | Name | Start | Time | End | RT Offset | Quantity | Height | Area | Area |
|---|---|---|---|---|---|---|---|---|---|
| | | [Min] | [Min] | [Min] | [Min] | [% Area] | [µV] | [µV.Min] | [%] |
| 1 | UNKNOWN | 4.59 | 4.77 | 4.92 | 0.00 | 97.64 | 509.0 | 50.9 | 97.643 |
| 2 | UNKNOWN | 4.93 | 4.99 | 5.07 | 0.00 | 2.36 | 17.4 | 1.2 | 2.357 |
| | | | | | | | | | |
| Total | | | | | | 100.00 | 526.4 | 52.2 | 100.000 |

### 5.7.4 Computational Methods

All the calculations were carried out with the Gaussian 09 package. Geometry optimizations were performed with B3LYP.[49] The LANL2DZ basis set[50] with ECP was used for Ni, and the 6-31G(d) basis set[51] was used for other atoms. Frequency analysis was conducted at the same level of theory to verify the stationary points to be minima or saddle points. The single-point energies and solvent effects in toluene were computed with M06[52]/SDD[53]-6-311+G(d,p) basis sets by using SMD solvation model.[54] Computed structures are illustrated using CYLView.[55]

#### 5.7.4.1 Complete Reference of Gaussian 09

Frisch, M. J.; Trucks, G. W.; Schlegel, H. B.; Scuseria, G. E.; Robb, M. A.; Cheeseman, J. R.; Scalmani, G.; Barone, V.; Mennucci, B.; Petersson, G. A.; Nakatsuji, H.; Caricato, M.; Li, X.; Hratchian, H. P.; Izmaylov, A. F.; Bloino, J.; Zheng, G.; Sonnenberg, J. L.; Hada, M.; Ehara, M.; Toyota, K.; Fukuda, R.; Hasegawa, J.; Ishida, M.; Nakajima, T.; Honda, Y.; Kitao, O.; Nakai, H.; Vreven, T.; Montgomery, Jr., J. A.; Peralta, J. E.; Ogliaro, F.; Bearpark, M.; Heyd, J. J.; Brothers, E.; Kudin, K. N.; Staroverov, V. N.; Keith, T.; Kobayashi, R.; Normand, J.; Raghavachari, K.; Rendell, A.; Burant, J. C.; Iyengar, S. S.; Tomasi, J.; Cossi, M.; Rega, N.; Millam, J. M.; Klene, M.; Knox, J. E.; Cross, J. B.; Bakken, V.; Adamo, C.; Jaramillo, J.; Gomperts, R.; Stratmann, R. E.; Yazyev, O.; Austin, A. J.; Cammi, R.; Pomelli, C.; Ochterski, J. W.; Martin, R. L.; Morokuma, K.; Zakrzewski, V. G.; Voth, G. A.; Salvador, P.; Dannenberg, J. J.; Dapprich, S.; Daniels, A. D.; Farkas, O.; Foresman, J. B.; Ortiz, J. V.; Cioslowski, J.; Fox, D. J. *Gaussian 09, Rev. D.01*; Gaussian, Inc., Wallingford, CT, **2010**.

### 5.7.4.2 Transition State Structures for Decarbonylation Pathway

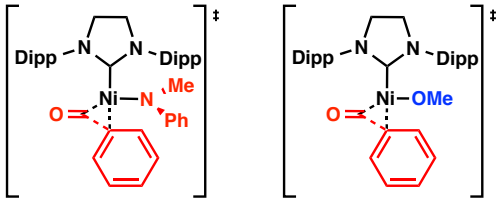


***5.88***
**28.6 kcal/mol**

***5.89***
**24.1 kcal/mol**

### 5.7.4.3 Comparison of Acyl C–N and Aryl C–N Bond Activation Pathway

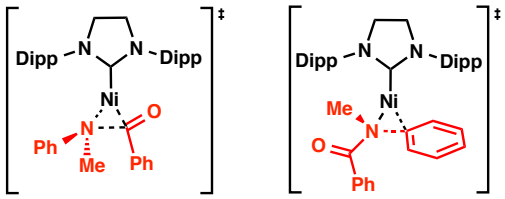


***5.11***
**26.0 kcal/mol**

***5.90***
**35.3 kcal/mol**

*Calculations were performed on the competing aryl C–N bond cleavage transition state. Transition state **5.90** was found to be 9.3 kcal/mol higher compared to the barrier for acyl C–N bond cleavage, via **5.11**.*

### 5.7.4.4 Analysis of Amides Derived from Alkyl Carboxylic Acids

***Table 5.6.*** Comparison of Aryl vs. Alkyl Amide Substrates

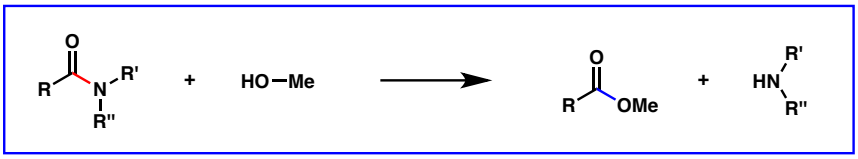


| *Entry* | *Amide* | | *Calculated ΔG (kcal/mol)* | *Calculated oxidative addition barrier with Ni /SIPr (kcal/mol)* |
|---|---|---|---|---|
| 1 | 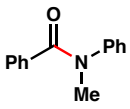 | *5.7g* | –6.8 | 26.0 (see 5.11) |
| 2 | 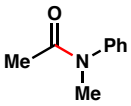 | *5.91* | –3.6 | 31.8 (see 5.92) |
| 3 | 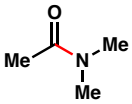 | *5.93* | +2.3 | 36.7 (see 5.94) |

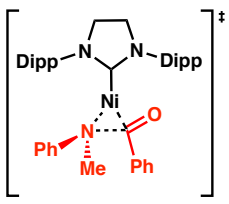


***5.11***
**26.0 kcal/mol**

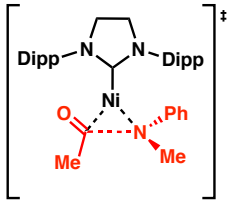


***5.92***
**31.8 kcal/mol**

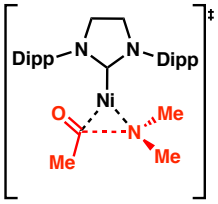


***5.94***
**36.7 kcal/mol**

We have performed computations involving two additional substrates: *N*-Me-*N*-phenylacetamide (**5.91**) and *N*,*N*-dimethylacetamide (**5.93**). In the case of *N*-Me-*N*-phenylacetamide, the oxidative addition barrier (transition state **5.92**) was found to be 31.8 kcal/mol with respect to the $Ni(SIPr)_2$ resting state. Similarly, for *N*,*N*-dimethylacetamide, the oxidative addition barrier (transition state **5.94**) was found to be 36.7 kcal/mol with respect to the $Ni(SIPr)_2$ resting state. These high kinetic barriers are likely responsible for the inability of alkyl

carboxylic acids to participate in our nickel-catalyzed esterifications. Also, in the case of substrate **5.93**, the amide to methyl ester conversion is not energetically favorable.

### 5.7.4.5 Analysis of *N*-Me,Boc Amide Esterification

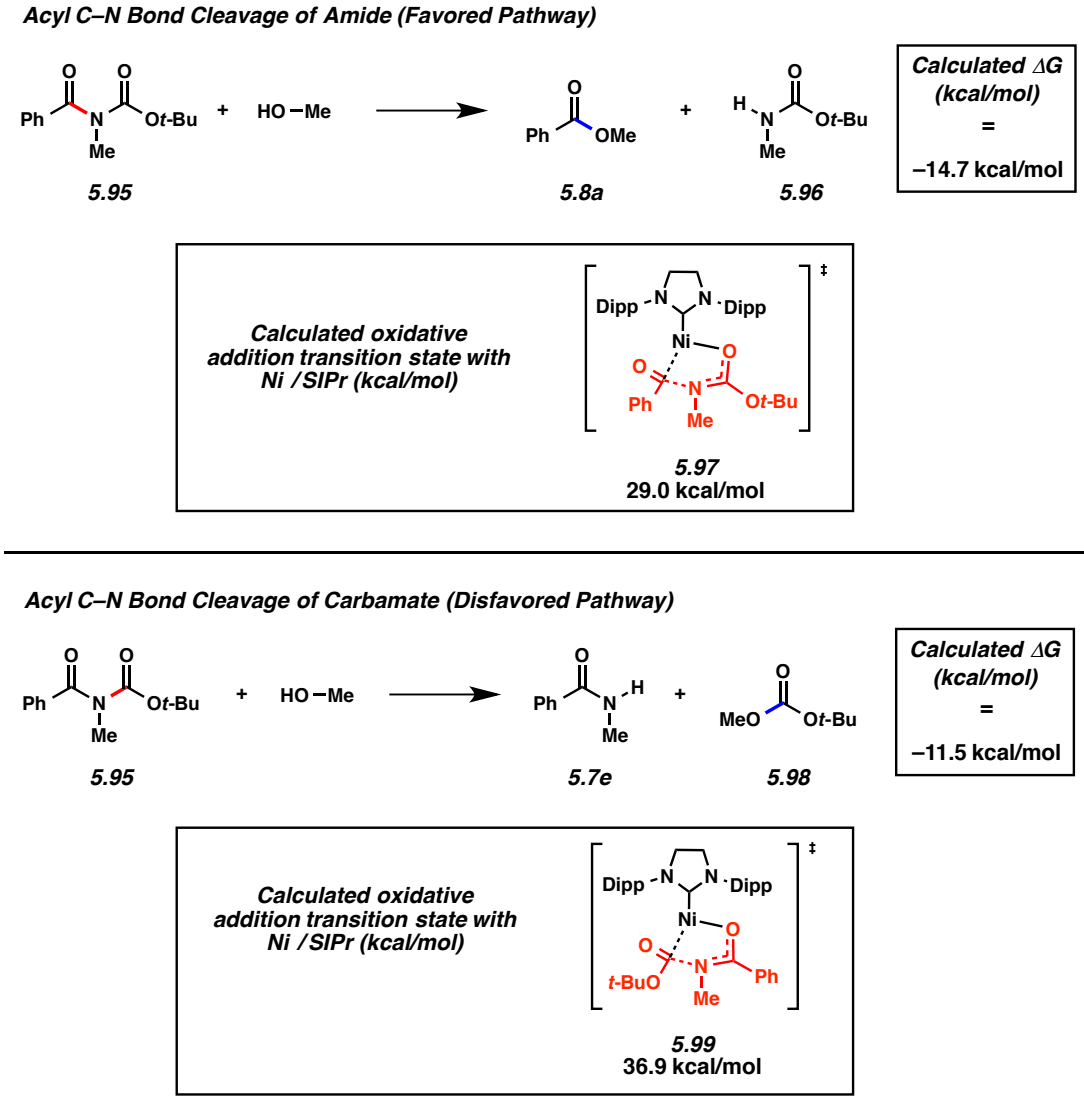


***Figure 5.4.*** Analysis of Competing Pathways for Esterification of *N*-Me,Boc Substrate **5.95**

The calculations show that the desired esterification of substrate **5.95** with MeOH is thermodynamically favorable by 14.7 kcal/mol. The oxidative addition transition state (transition

state **5.97**) was found to be 29.0 kcal/mol with respect to the $Ni(SIPr)_2$ resting state. We have also performed computations of a plausible competitive process involving cleavage of the carbamate acyl C–N bond. This transformation is also thermodynamically favorable (11.5 kcal/mol). However, the oxidative addition barrier (transition state **5.99**) was found to be 36.9 kcal/mol with respect to the $Ni(SIPr)_2$ resting state. Accordingly, carbamate C–N bond cleavage is not observed and the desired esterification occurs smoothly.

### 5.7.4.6 Free Energy and Enthalpy of Amide and Ester Formation

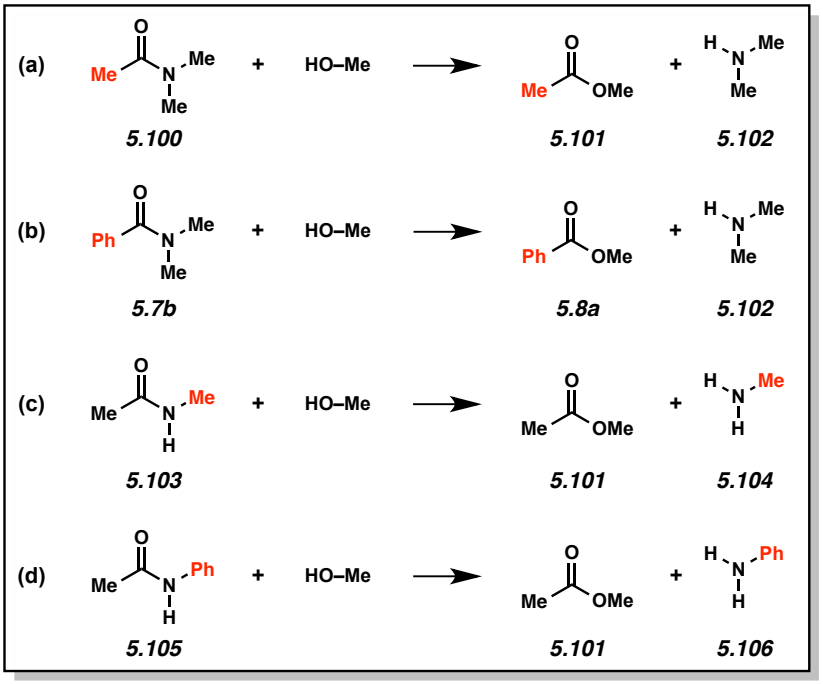


| Reaction | $\Delta_rH$(gas)[a] | $\Delta_rH$(cond.)[d] | $\Delta_rH$(methanol)[e] | $\Delta_rG$(methanol)[f] | $\Delta_rH$(calc.)[g] | $\Delta_rG$(calc.)[g] |
|---|---|---|---|---|---|---|
| (a) | +5.3[b] | +11.4 | | | +2.3 | +2.3 |
| (b) | -0.3 | +10.6 | +3.6 | +3.3 | 0.0 | 0.0 |
| (c) | +3.8 | +14.0 | | | +3.4 | +3.9 |
| (d) | +0.2[c] | +8.0 | | | -3.0 | -2.6 |

[a] Yields were determined by $^1$H NMR analysis using hexamethylbenzene as an internal standard. [a] Reaction enthalpy calculated using gas phase standard enthalpy of formation data.[56] [b] Gas phase enthalpy of formation for the amide **5.100** is calculated from liquid phase standard enthalpy of formation and enthalpy of vaporization.[56] [c] Gas phase enthalpy of formation for the amide **5.105** is calculated from solid phase standard enthalpy of formation and enthalpy of sublimation.[56] [d] Reaction enthalpy calculated using condensed phase standard enthalpy of formation data. Solid phase enthalpies of formation were used for amides **5.7b** and **5.105**. Liquid phase enthalpies of formation were used for other compounds.[56] [e] Reaction enthalpy calculated from enthalpies of reaction and solution.[57] [f] Reaction free energy derived from the equilibrium constant of ester aminolysis in methanol.[57] [g] Energies are calculated with M06/6-311+G(d,p)/SMD(toluene)//B3LYP/6-31G(d). [h] All energies are in kcal/mol.

***Figure 5.5.*** Substitution Effects on Equilibrium of Amide Esterification

Figure 5.5 shows how substituents effect the equilibrium of amide esterification. We performed DFT calculations on the reaction enthalpies and free energies of the esterification of four amides, for which the experimental enthalpy of formation data are available. The enthalpies of reaction are also calculated using experimental enthalpy of formation data in the gas phase

($\Delta_r H$(gas)) and in the condensed phase ($\Delta_r H$(cond.)).[56] Interestingly, the esterification reaction is significantly more endothermic if condensed phase enthalpy of formation data were used. One of the major factors that contribute to this deviation is the greater intermolecular stabilizing forces in neat methanol liquid. The equilibrium of reaction (b) in methanol has been investigated by Guthrie *et al*.[57] The standard free energy of reaction derived from equilibrium constant ($\Delta_r G$(methanol)) and the standard enthalpy of reaction in methanol solution derived from enthalpies of solution data both indicate the amide esterification is less endothermic than the prediction by $\Delta_r H$(cond.). Based on these considerations, we postulate that the gas phase thermodynamic data ($\Delta_r H$(gas)) would better represent the experimental conditions with the non-polar toluene solvent. Unfortunately, the gas phase enthalpies of formation for amides **5.100** and **5.105** are not available, and were derived from liquid and solid phase enthalpies of formation and enthalpies of vaporization and sublimation, respectively. Thus, larger experimental errors are expected for $\Delta_r H$(gas) of reactions (a) and (d).

The DFT calculations with the SMD solvation model in toluene (1.0 M, 298 K) predicted very close reaction enthalpies compared to $\Delta_r H$(gas) for reactions (b) and (c). Larger deviations from $\Delta_r H$(gas) were obtained for (a) and (d), which may be attributed to the greater experimental error as described above. Thus, the DFT predicted enthalpies of reactions ($\Delta_r H$(calc)) are used to analyze the substituent effects. Phenyl substitution at the carbonyl and N position significantly favors the esterification (a vs. b and c vs. d), while the esterification of *N*-methylacetamide is much less favorable than that of *N,N*-dimethylacetamide. This further confirms the expectation that mostly the reverse reaction (i.e. amidation) should be favorable, but the judicious use of varied substrates can perturb the equilibrium.

### 5.7.4.7 Energies, Enthalpies, and Free Energy of the Calculated Structures

***Table 5.7.*** Energies, enthalpies, and free energies of the structures calculated at the M06/SDD, 6-311+G(d,p)(SMD$^{toluene}$)//B3LYP/LANL2DZ,6-31G(d)

| Structures | ZPE | DE | DH | DG | E | H | G | Imaginary | DDG |
|---|---|---|---|---|---|---|---|---|---|
| **MeOH** | 0.051473 | 0.054761 | 0.055705 | 0.028756 | -115.691065 | -115.63536 | -115.662309 | — | — |
| **5.4a** | 0.130353 | 0.135268 | 0.136212 | 0.102291 | -212.479801 | -212.343589 | -212.377510 | — | — |
| **5.4b** | 0.093028 | 0.097390 | 0.098334 | 0.067601 | -135.098988 | -135.000654 | -135.031387 | — | — |
| **5.4c** | 0.135967 | 0.141254 | 0.142199 | 0.107525 | -287.686445 | -287.544246 | -287.578920 | — | — |
| **5.4d** | 0.097148 | 0.102641 | 0.103585 | 0.069012 | -210.253121 | -210.149536 | -210.184109 | — | — |
| **5.4e** | 0.064450 | 0.067831 | 0.068775 | 0.041555 | -95.816309 | -95.747534 | -95.774754 | — | — |
| **5.4f** | 0.117436 | 0.123214 | 0.124158 | 0.088289 | -287.465710 | -287.341552 | -287.377421 | — | — |
| **5.4g** | 0.145946 | 0.153153 | 0.154097 | 0.114653 | -326.747411 | -326.593314 | -326.632758 | — | — |
| **5.7a** | 0.221898 | 0.232888 | 0.233832 | 0.184277 | -556.741196 | -556.507364 | -556.556919 | — | — |
| **5.7b** | 0.184539 | 0.195044 | 0.195988 | 0.148064 | -479.354994 | -479.159006 | -479.206930 | — | — |
| **5.7c** | 0.227243 | 0.238874 | 0.239819 | 0.188374 | -631.941051 | -631.701232 | -631.752677 | — | — |
| **5.7d** | 0.188279 | 0.199798 | 0.200742 | 0.150388 | -554.500325 | -554.299583 | -554.349937 | — | — |
| **5.7e** | 0.156359 | 0.165575 | 0.166519 | 0.121160 | -440.076464 | -439.909945 | -439.955304 | — | — |
| **5.7f** | 0.209470 | 0.221355 | 0.222299 | 0.169869 | -631.715959 | -631.493660 | -631.546090 | — | — |
| **5.7g** | 0.237383 | 0.250756 | 0.2517 | 0.195805 | -670.987803 | -670.736103 | -670.791998 | — | — |
| **5.7a_TS** | 0.817159 | 0.862147 | 0.863091 | 0.73669 | -1888.379615 | -1887.516524 | -1887.642925 | -221.285 | **36.8** |
| **5.7b_TS** | 0.779705 | 0.824113 | 0.825057 | 0.700324 | -1810.994261 | -1810.169204 | -1810.293937 | -243.236 | **36.2** |
| **5.7c_TS** | 0.822386 | 0.868066 | 0.869011 | 0.741075 | -1963.584228 | -1962.715217 | -1962.843153 | -192.983 | **34.0** |
| **5.7d_TS** | 0.78317 | 0.828976 | 0.82992 | 0.701265 | -1886.145139 | -1885.315219 | -1885.443874 | -144.322 | **31.9** |
| **5.7e_TS** | 0.751675 | 0.79476 | 0.795704 | 0.673483 | -1771.711376 | -1770.915672 | -1771.037893 | -265.940 | **39.0** |
| **5.7f_TS** | 0.805092 | 0.850906 | 0.85185 | 0.722942 | -1963.364955 | -1962.513105 | -1962.642013 | -234.989 | **30.6** |
| **5.7g_TS (5.11)** | 0.832519 | 0.880023 | 0.880968 | 0.749155 | -2002.644449 | -2001.763481 | -2001.895294 | -226.879 | **26.0** |
| **5.8a** | 0.144145 | 0.152933 | 0.153878 | 0.109776 | -459.947621 | -459.793743 | -459.837845 | — | — |
| **5.9** | 1.194703 | 1.259623 | 1.260567 | 1.092339 | -2492.357024 | -2491.096457 | -2491.264685 | — | **0.0** |
| **5.10** | 0.834665 | 0.882315 | 0.883259 | 0.750844 | -2002.668552 | -2001.785293 | -2001.917708 | — | **12.0** |
| **5.11** | 0.832519 | 0.880023 | 0.880968 | 0.749155 | -2002.644449 | -2001.763481 | -2001.895294 | -226.879 | **26.0** |
| **5.12** | 0.833357 | 0.881423 | 0.882367 | 0.749078 | -2002.661012 | -2001.778645 | -2001.911934 | — | **15.6** |
| **5.13** | 0.887528 | 0.939803 | 0.940747 | 0.797540 | -2118.365280 | -2117.424533 | -2117.567740 | — | **19.6** |
| **5.14** | 0.884746 | 0.935623 | 0.936567 | 0.799931 | -2118.359517 | -2117.422950 | -2117.559586 | -880.974 | **24.8** |
| **5.15** | 0.890480 | 0.941197 | 0.942141 | 0.806427 | -2118.370107 | -2117.427966 | -2117.563680 | — | **22.2** |
| **5.16** | 0.740176 | 0.783680 | 0.784625 | 0.661525 | -1791.602890 | -1790.818265 | -1790.941365 | — | **15.7** |
| **5.17** | 0.740041 | 0.782667 | 0.783611 | 0.662388 | -1791.591727 | -1790.808116 | -1790.929339 | -178.698 | **23.2** |
| **5.18** | 0.741023 | 0.784452 | 0.785396 | 0.661905 | -1791.625676 | -1790.840280 | -1790.963771 | — | **1.6** |
| **5.88** | 0.831324 | 0.878890 | 0.879834 | 0.749575 | -2002.640735 | -2001.760901 | -2001.891160 | 24.100 | **28.6** |

| | | | | | | | | | |
|---|---|---|---|---|---|---|---|---|---|
| **5.89** | 0.738576 | 0.781652 | 0.782596 | 0.660871 | -1791.588769 | -1790.806173 | -1790.927898 | -141.606 | **24.1** |
| **5.90** | 0.832584 | 0.880133 | 0.881077 | 0.747983 | -2000.935468 | -2000.934524 | -2001.067618 | -285.50 | **35.3** |
| **5.92** | 0.780187 | 0.824315 | 0.825259 | 0.702244 | -1810.187123 | -1810.186179 | -1810.309194 | -262.54 | **31.8** |
| **5.94** | 0.726324 | 0.767748 | 0.768692 | 0.651647 | -1617.596856 | -1617.595911 | -1617.712957 | -261.49 | **36.7** |
| **5.95** | 0.283512 | 0.300766 | 0.30171 | 0.237711 | -785.774018 | -785.472308 | -785.536307 | — | — |
| **5.96** | 0.192446 | 0.203738 | 0.204682 | 0.15551 | -441.544868 | -441.340186 | -441.389358 | — | — |
| **5.97** | 0.878983 | 0.930354 | 0.931298 | 0.791429 | -2117.431420 | -2116.500122 | -2116.639991 | -127.940 | **29.0** |
| **5.98** | 0.180461 | 0.191201 | 0.192146 | 0.144843 | -461.411697 | -461.219551 | -461.266854 | — | — |
| **5.99** | 0.879394 | 0.930259 | 0.931203 | 0.793358 | -2117.420778 | -2116.489575 | -2116.627420 | -181.425 | **36.9** |

### 5.7.4.8 Cartesian Coordinates for the Optimized Structures.

Cartesian coordinates for the optimized structures have been previously reported.[58]

## 5.8 Spectra Relevant to Chapter Five:

**Conversion of Amides to Esters by the Nickel-Catalyzed Activation of Amide C–N Bonds**

Liana Hie, Noah F. Fine Nathel, Tejas K. Shah, Emma L. Baker, Xin Hong,

Yun-Fang Yang, Peng Liu, K. N. Houk & Neil K. Garg

*Nature* **2015**, *524*, 79–83.

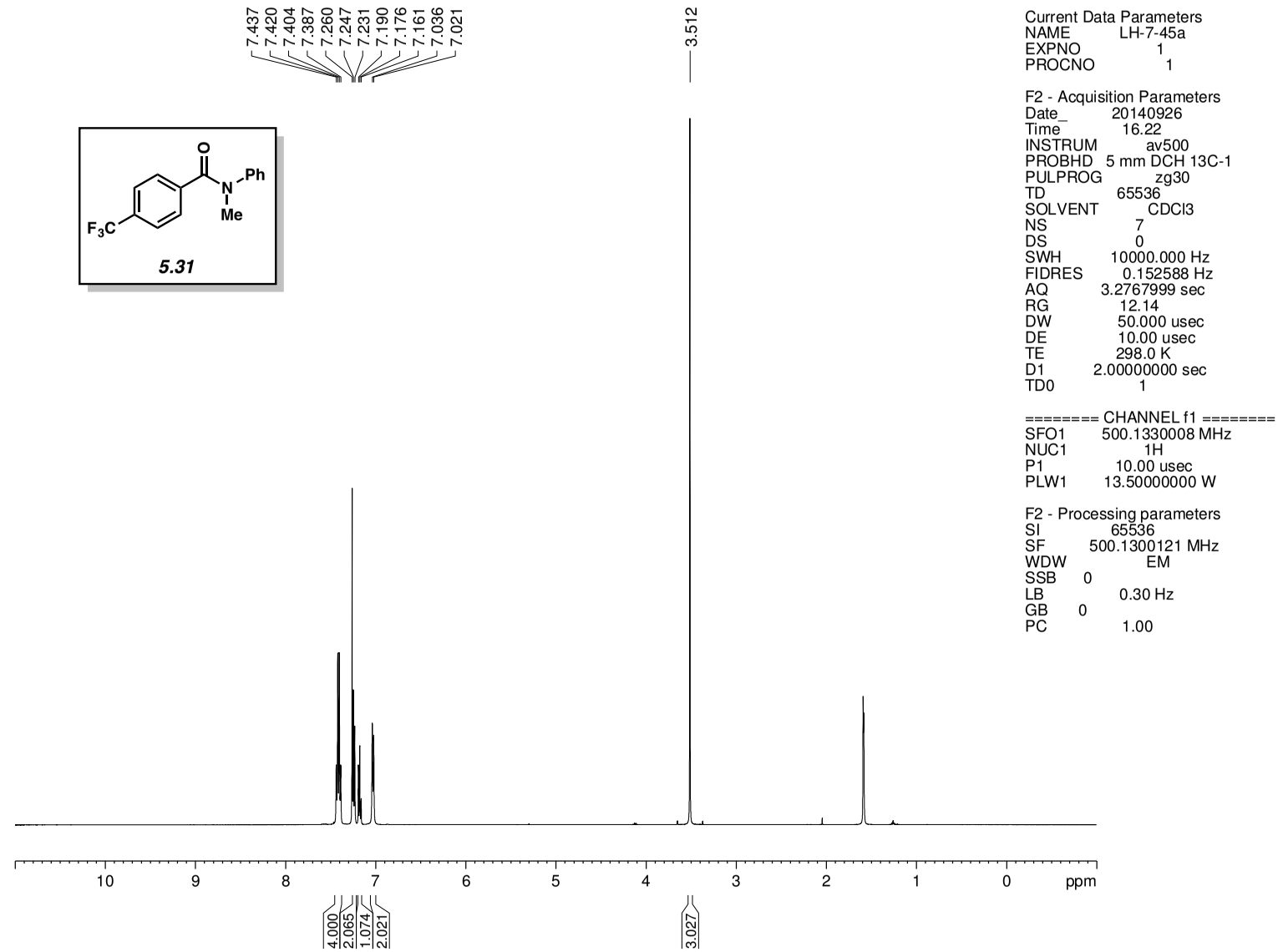


***Figure A5.6.*** $^{1}$H NMR (500 MHz, $CDCl_3$) of compound **5.31**

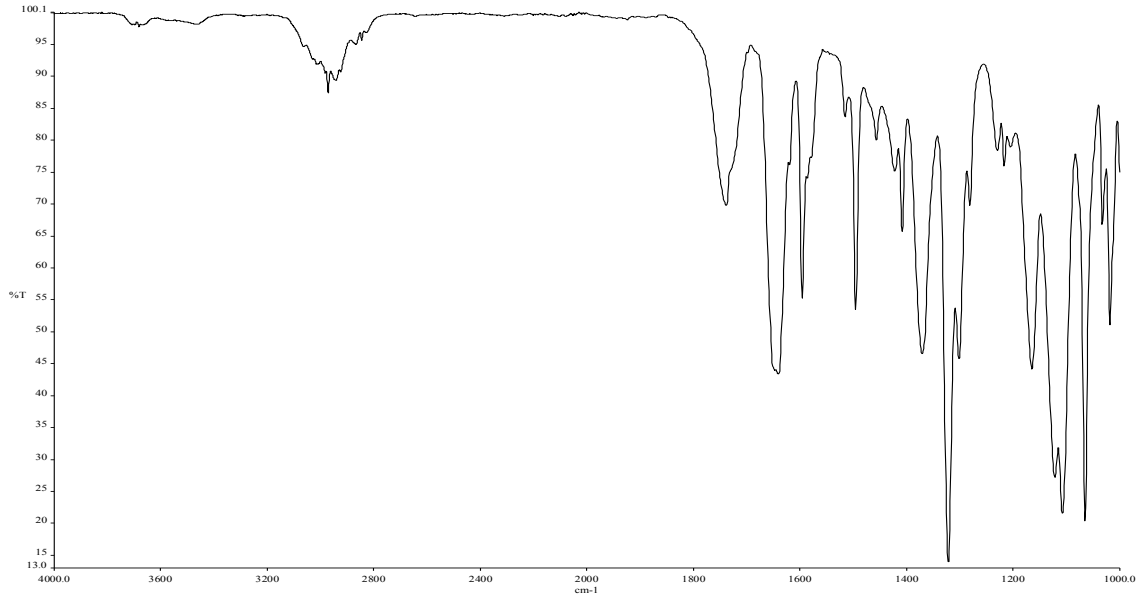


***Figure A5.7.*** Infrared spectrum of compound **5.31**

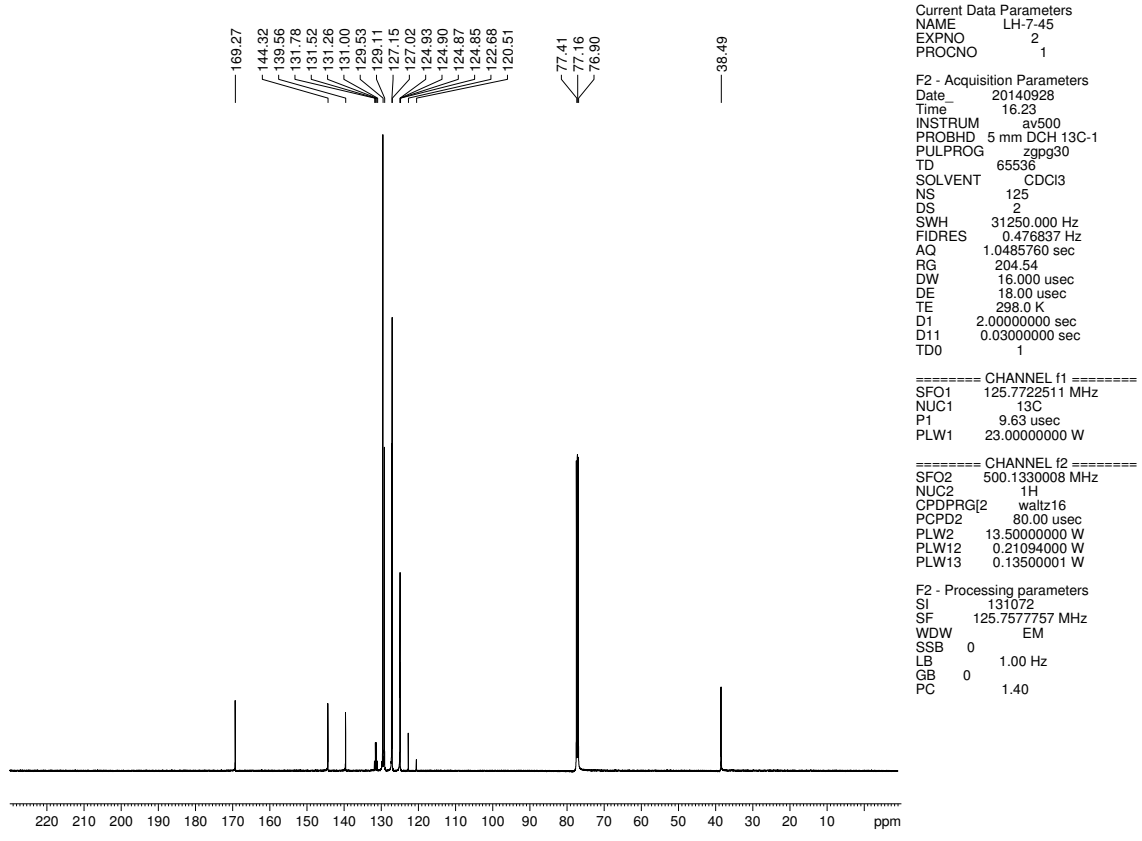


***Figure A5.8.*** $^{13}$C NMR (125 MHz, $CDCl_3$) of compound **5.31**

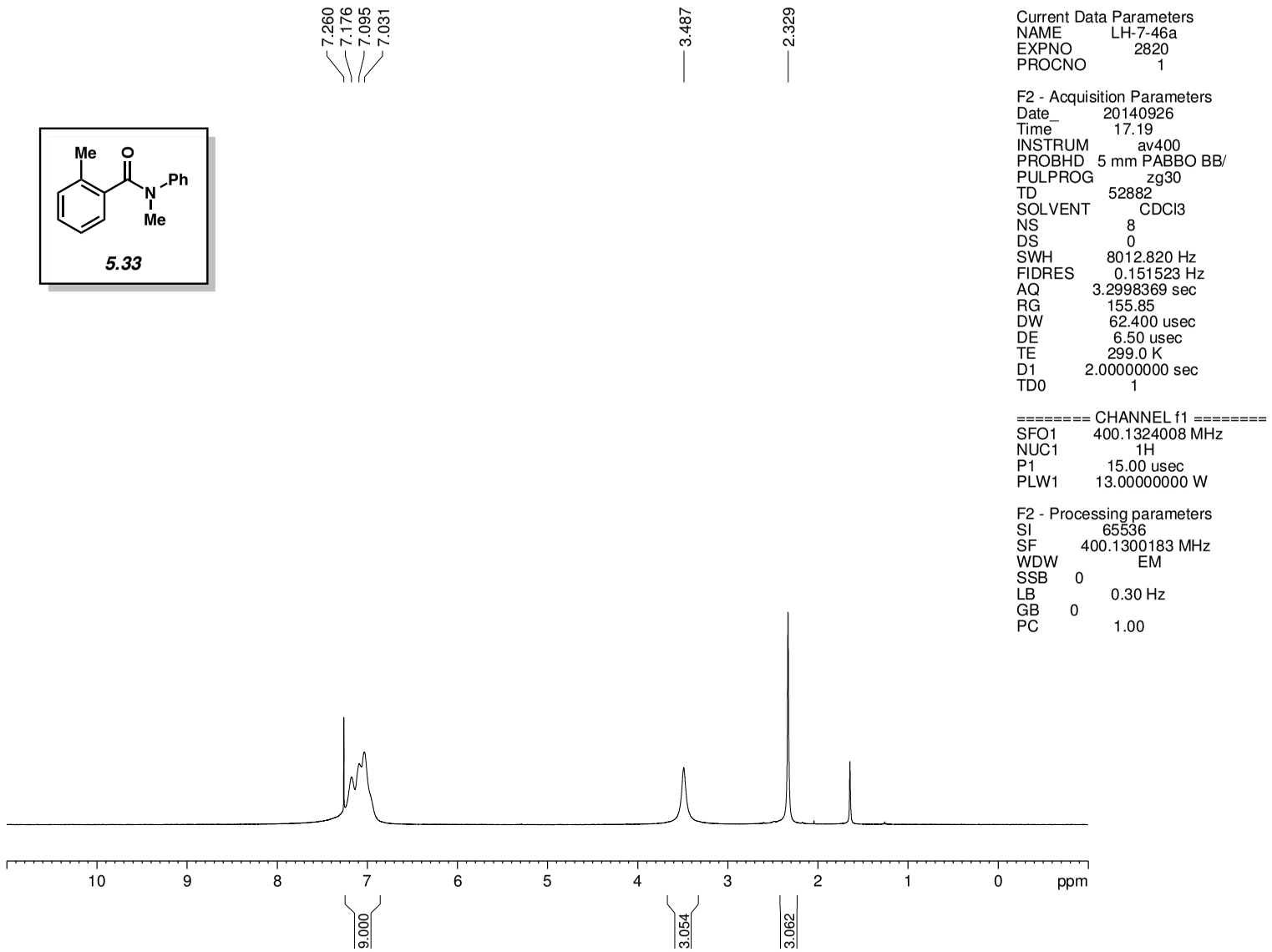


***Figure A5.9.*** $^{1}$H NMR (400 MHz, $CDCl_3$) of compound **5.33**

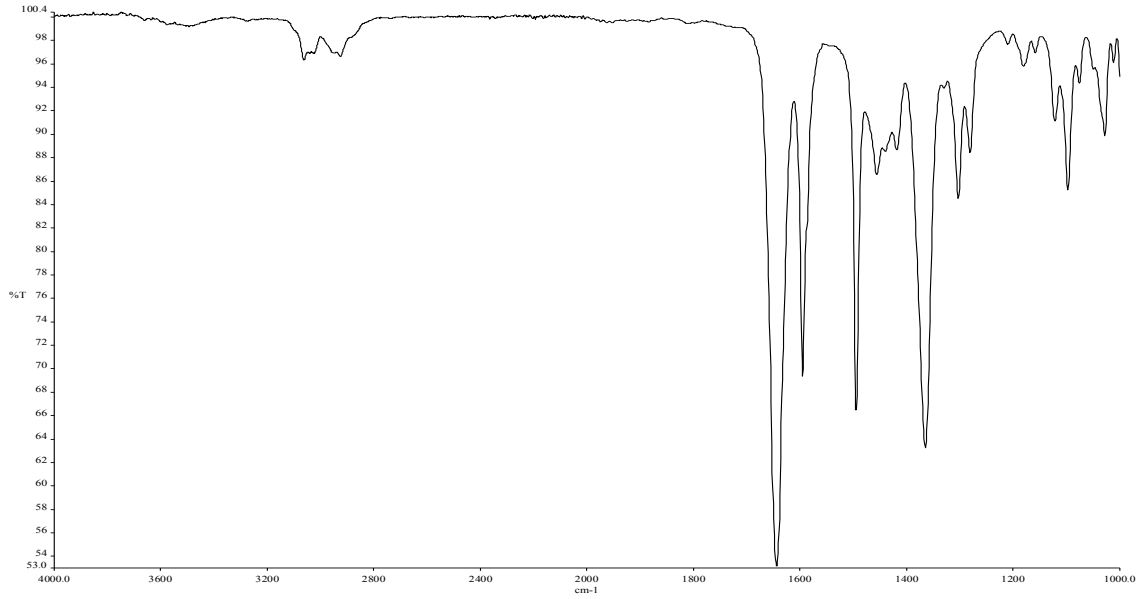


***Figure A5.10.*** Infrared spectrum of compound **5.33**

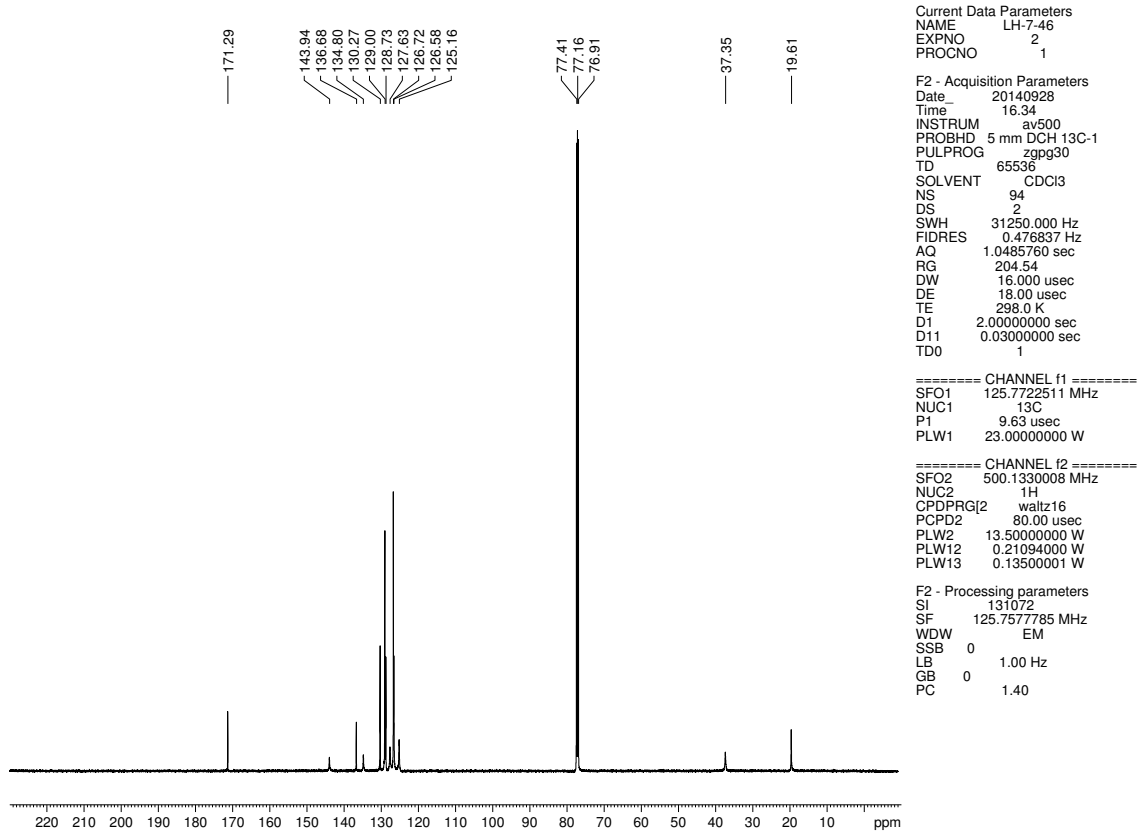


***Figure A5.11.*** $^{13}$C NMR (125 MHz, $CDCl_3$) of compound **5.33**

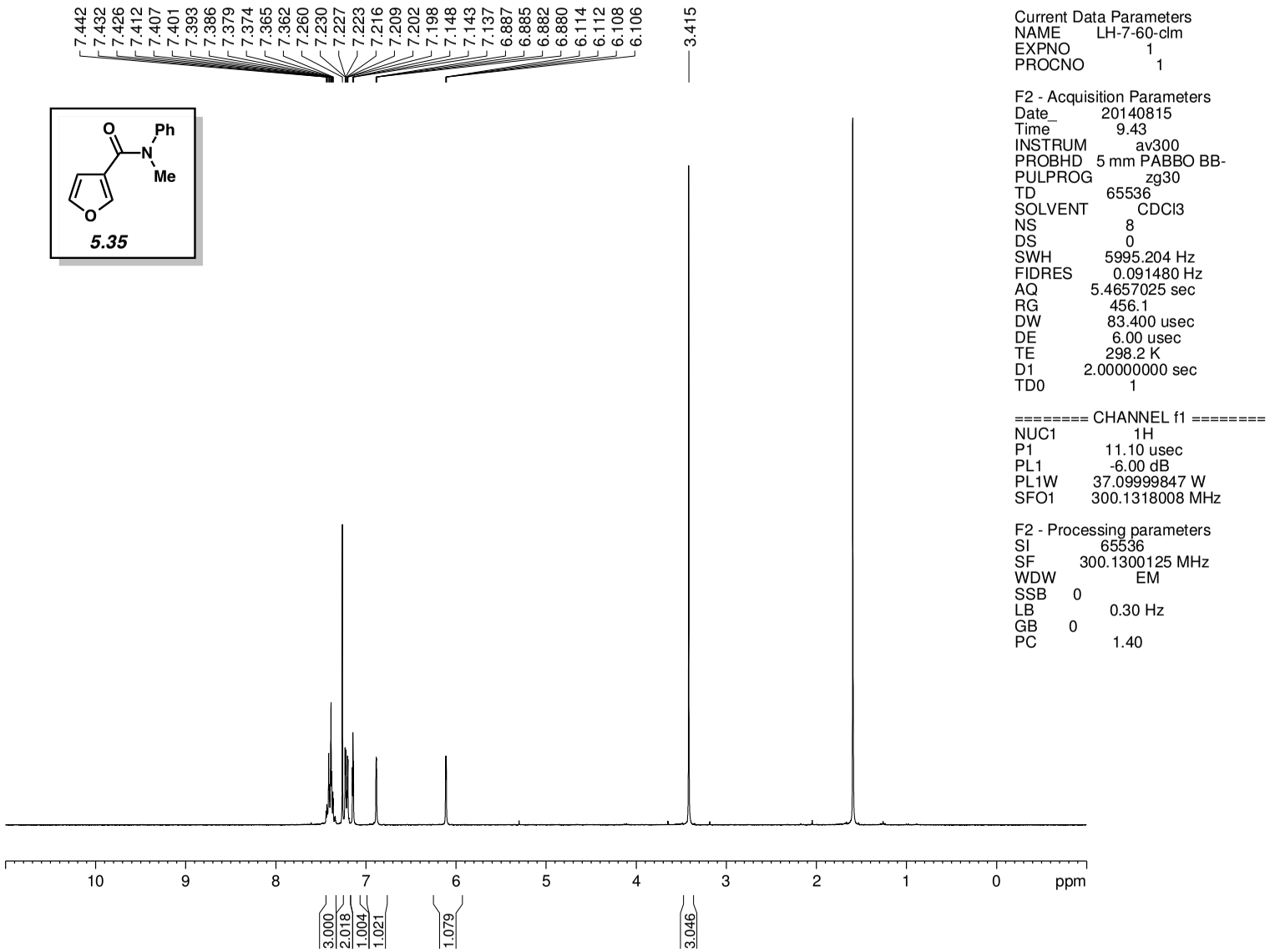


***Figure A5.12.*** $^{1}$H NMR (300 MHz, $CDCl_3$) of compound **5.35**

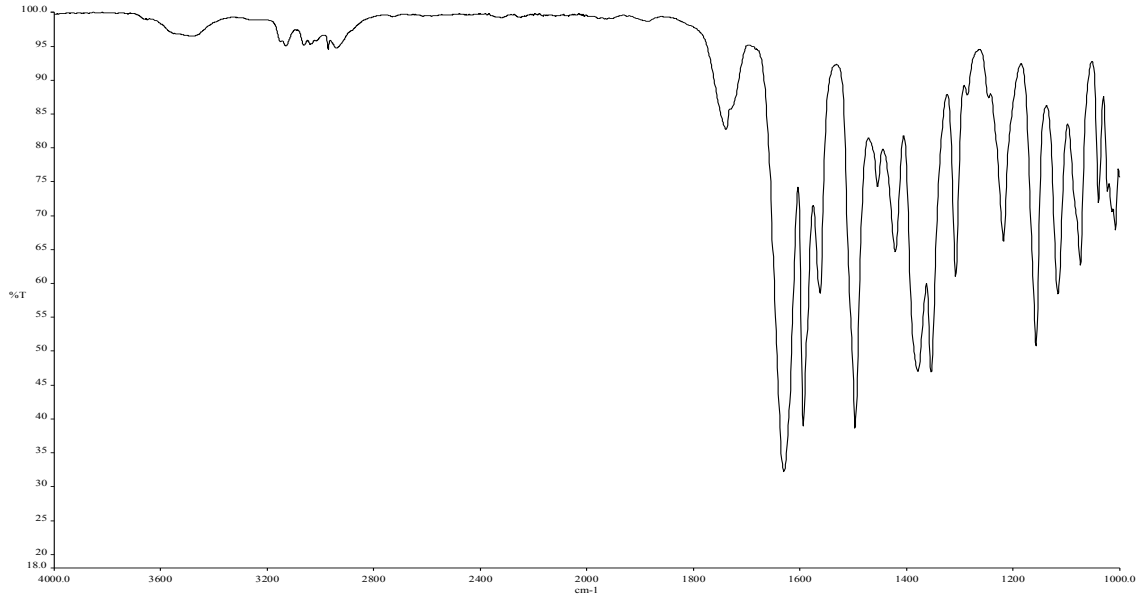


***Figure A5.13.*** Infrared spectrum of compound **5.35**

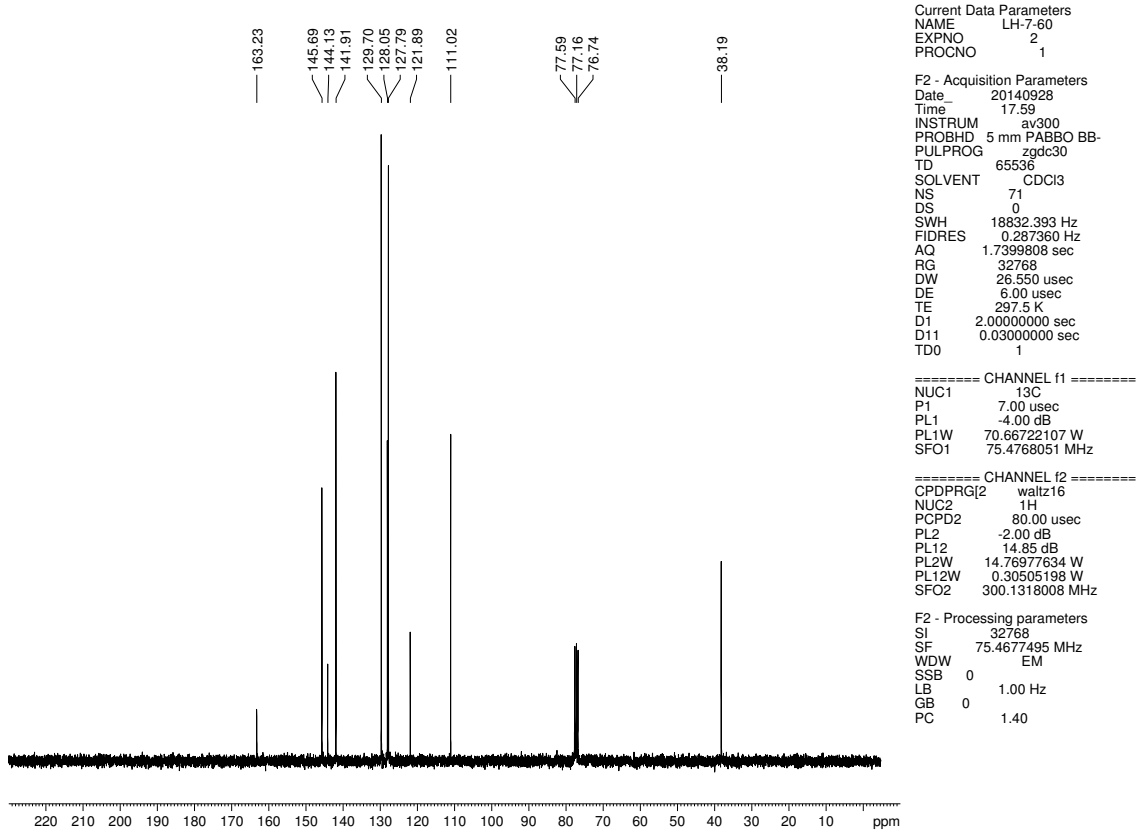


***Figure A5.14.*** $^{13}C$ NMR (75 MHz, $CDCl_3$) of compound **5.35**

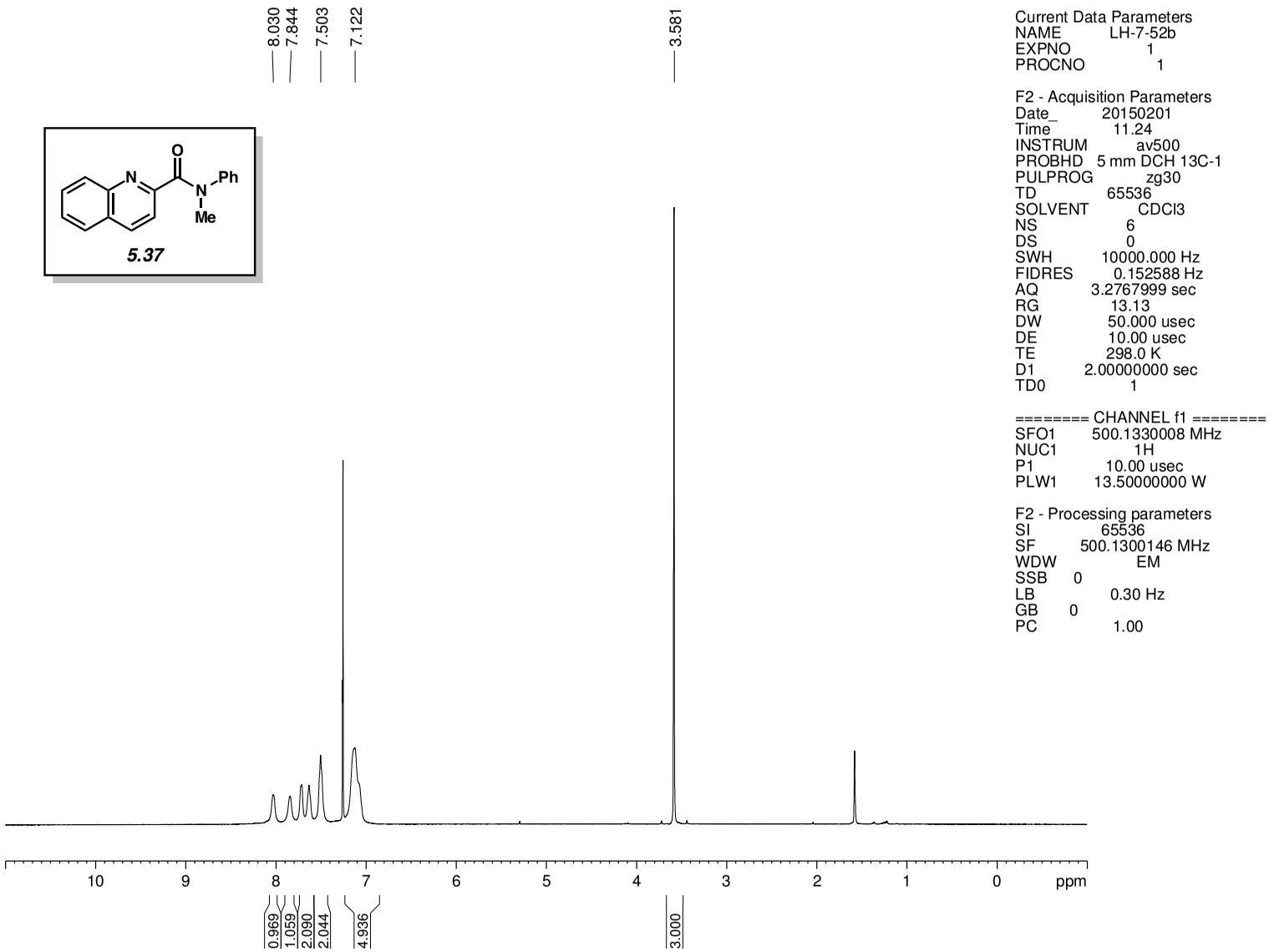


***Figure A5.15.*** $^{1}$H NMR (500 MHz, $CDCl_3$) of compound **5.37**

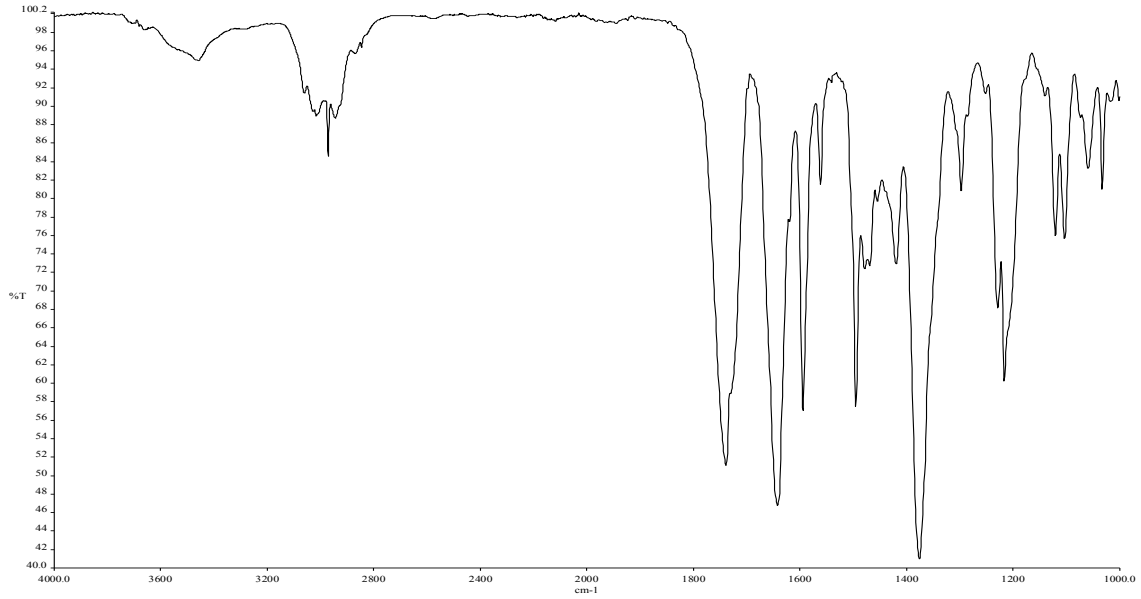


***Figure A5.16.*** Infrared spectrum of compound **5.37**

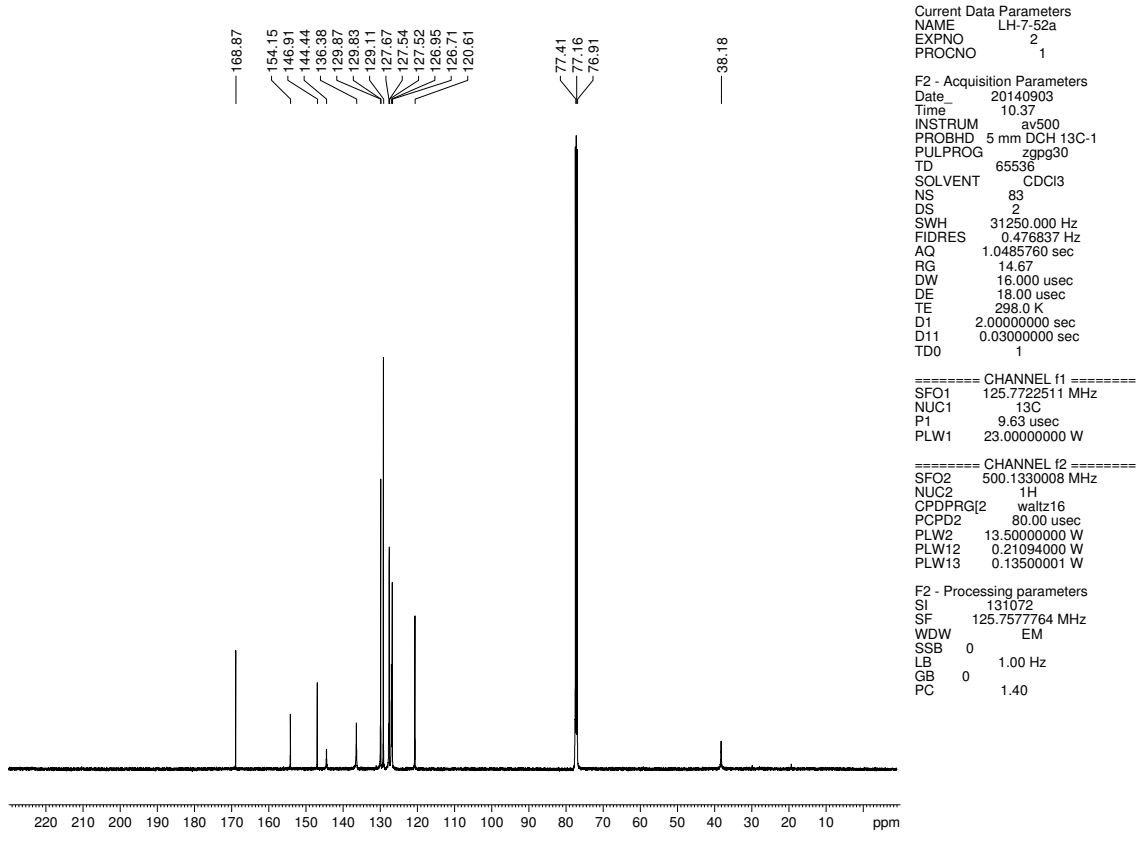


***Figure A5.17.*** $^{13}$C NMR (125 MHz, $CDCl_3$) of compound **5.37**

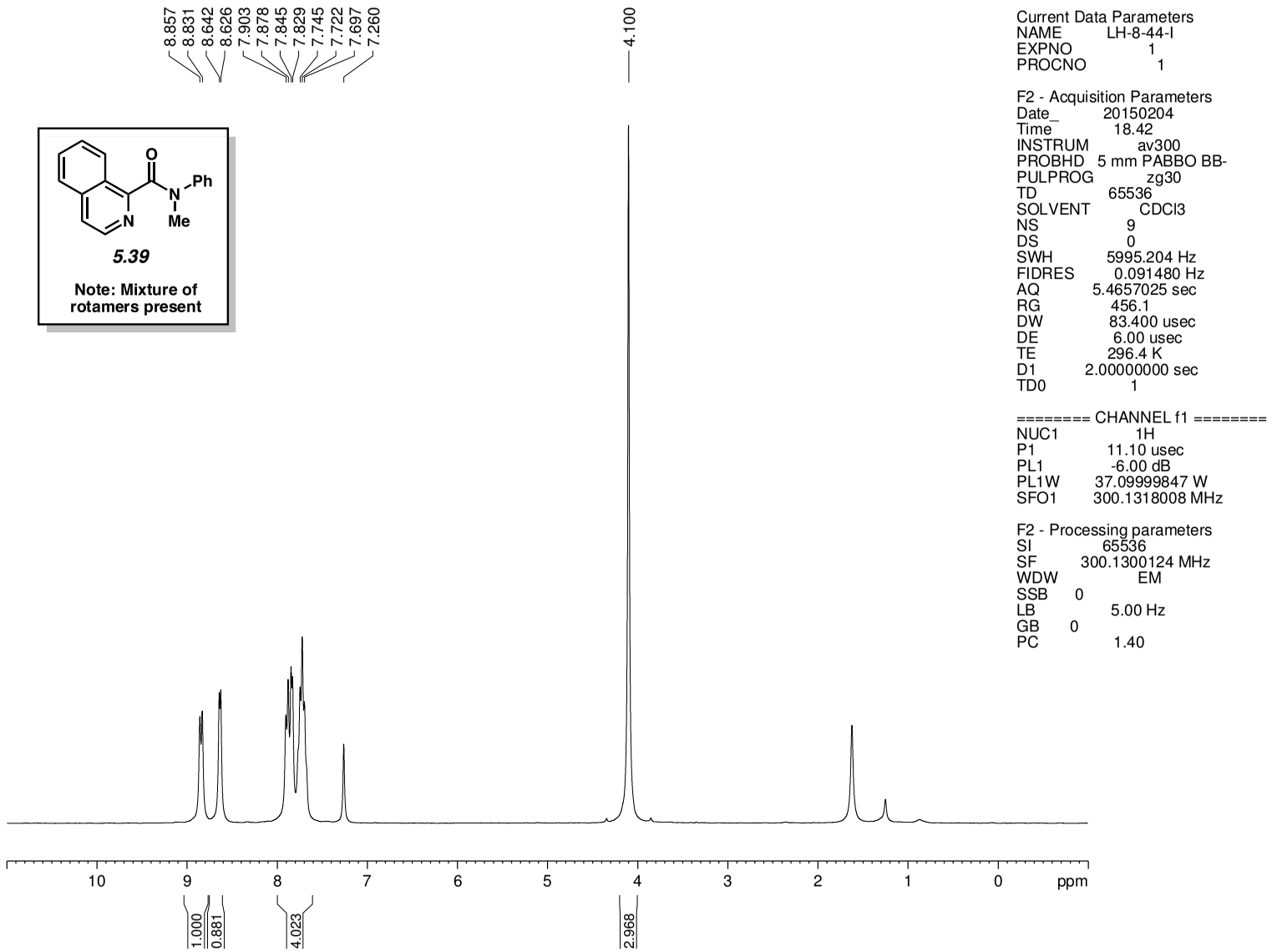


***Figure A5.18.*** $^{1}$H NMR (300 MHz, $CDCl_3$) of compound **5.39**

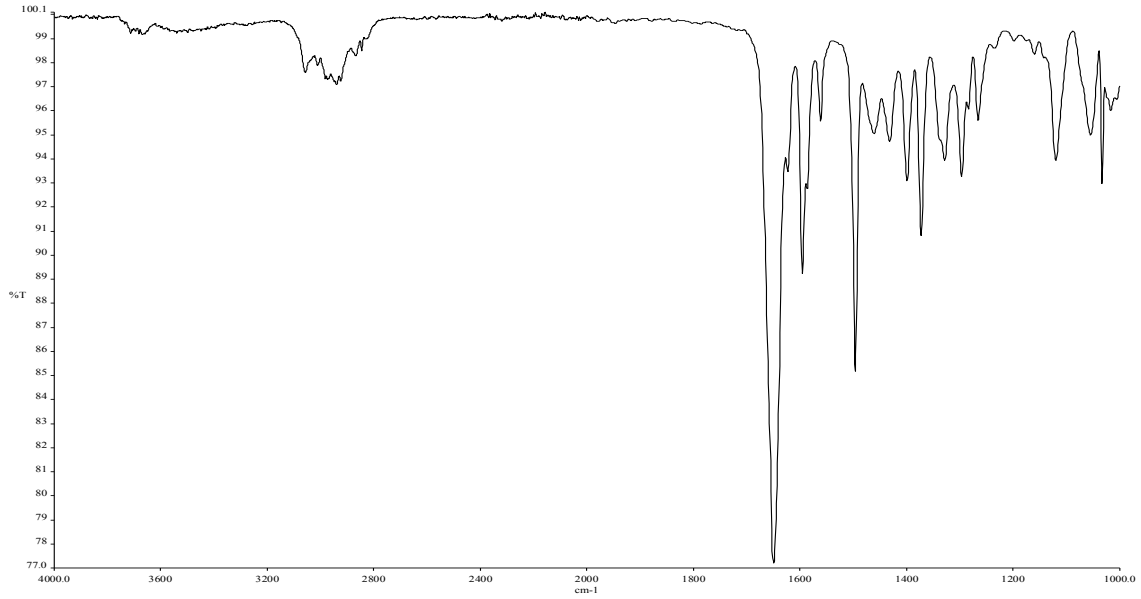


***Figure A5.19.*** Infrared spectrum of compound **5.39**

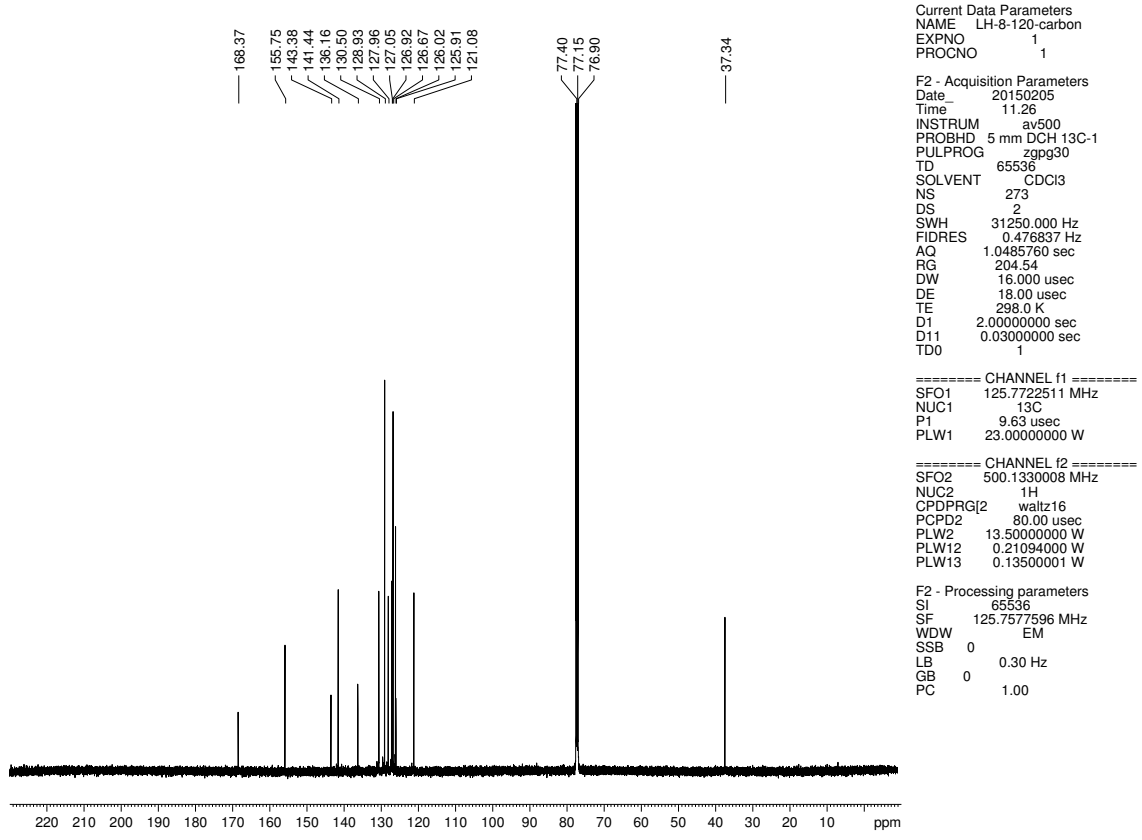


***Figure A5.20.*** $^{13}$C NMR (125 MHz, $CDCl_3$) of compound **5.39**

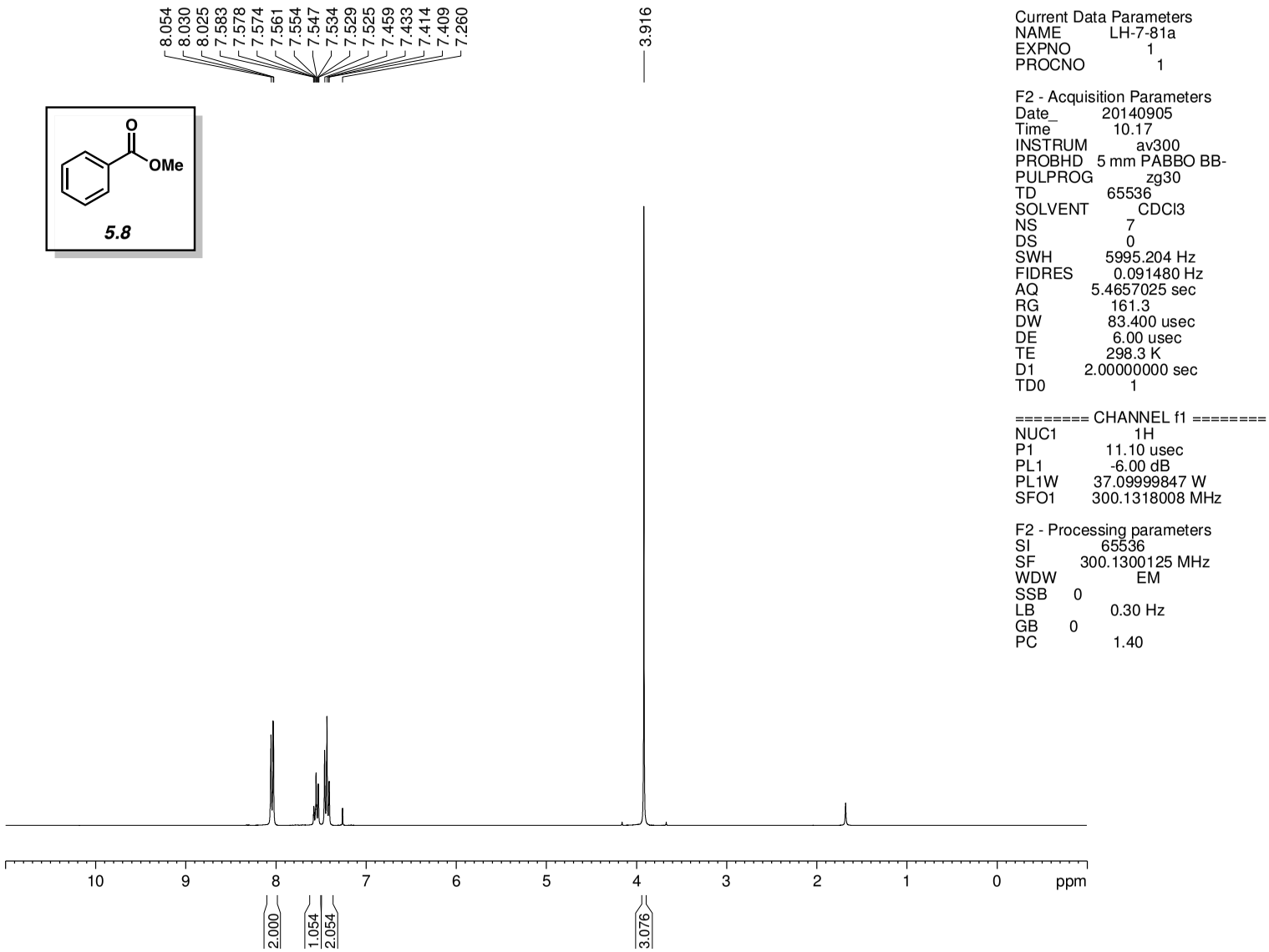


***Figure A5.21.*** $^{1}$H NMR (300 MHz, $CDCl_3$) of compound **5.8**

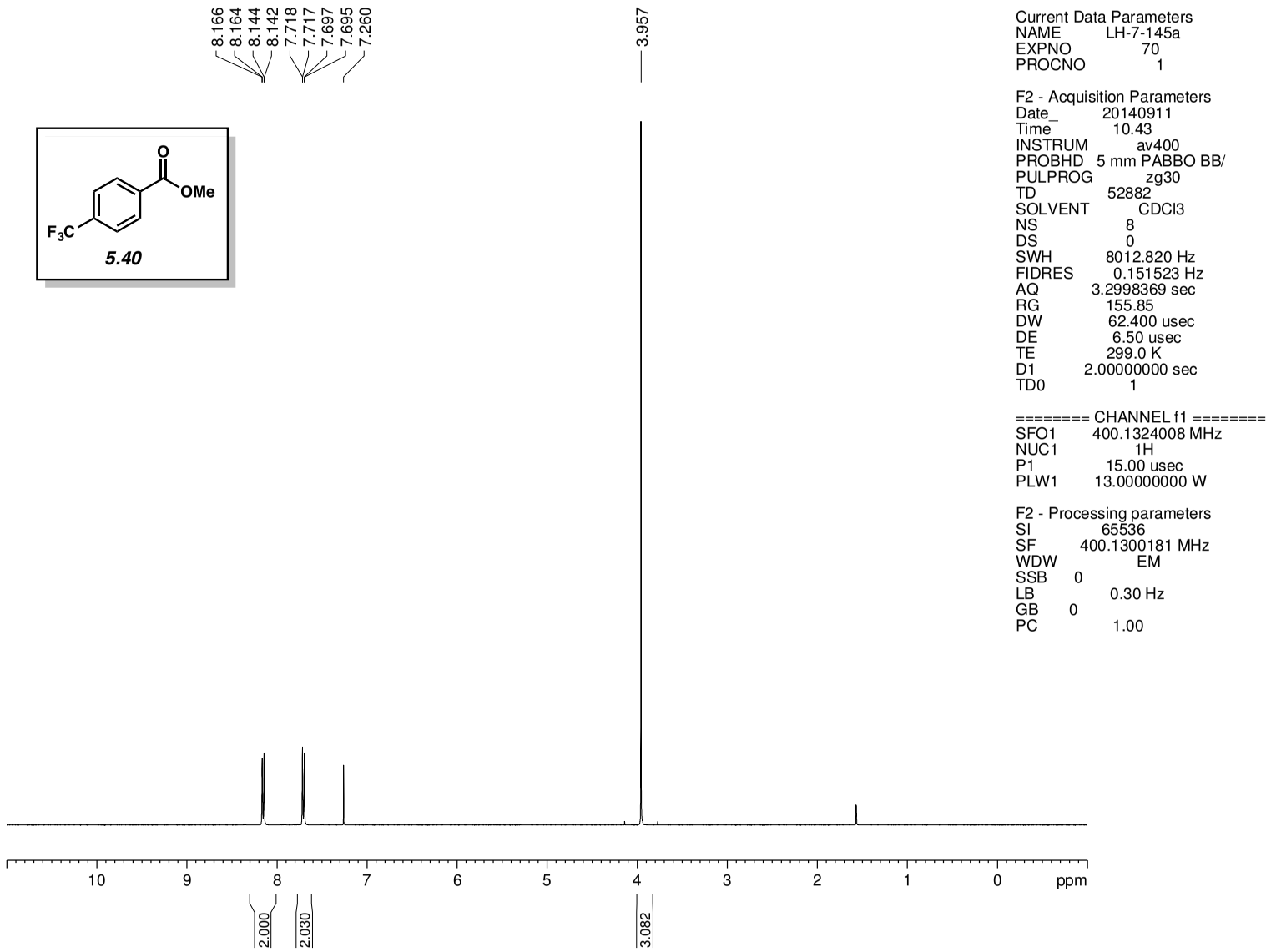


***Figure A5.22.*** $^{1}$H NMR (400 MHz, $CDCl_3$) of compound **5.40**

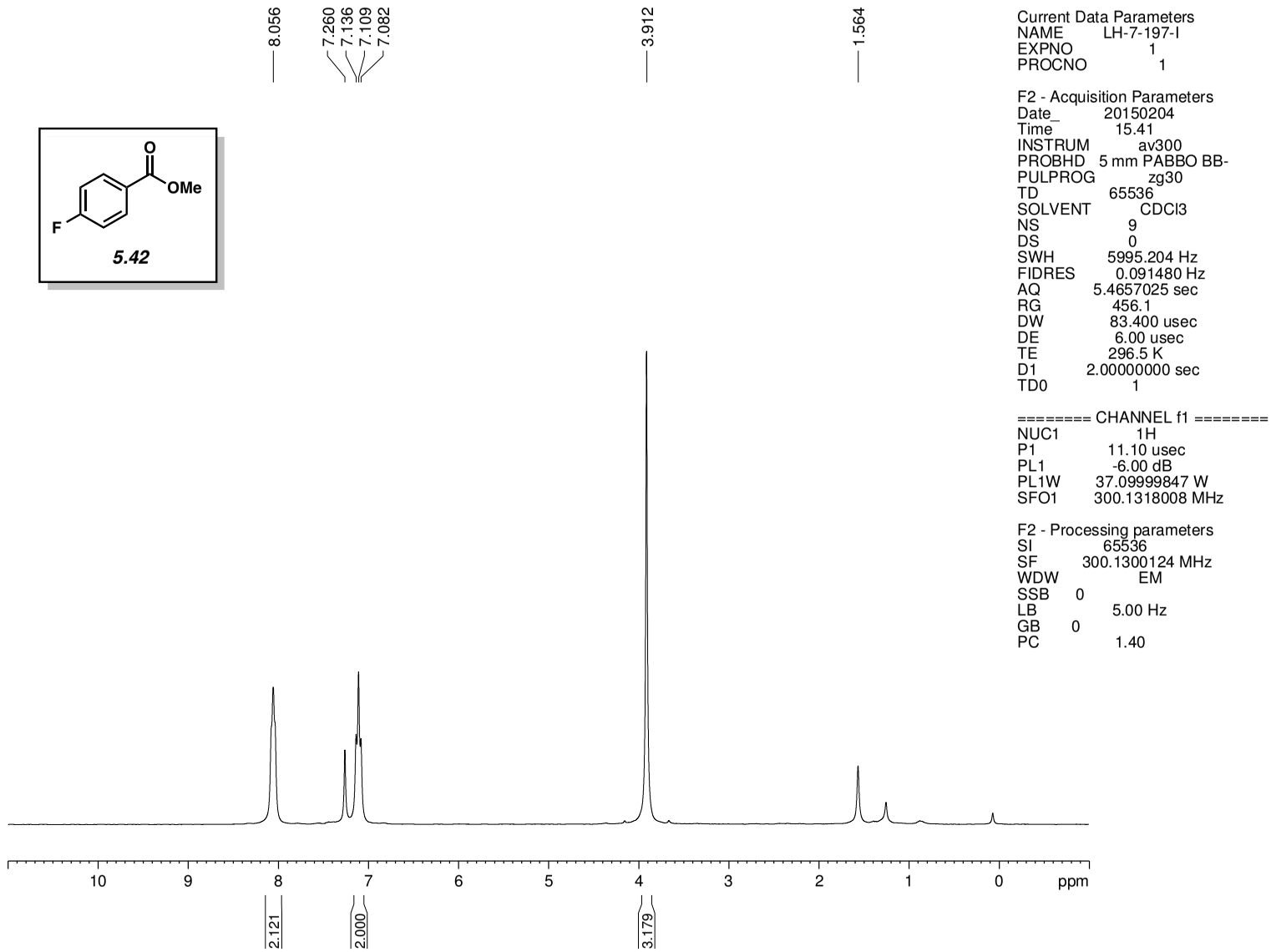


***Figure A5.23.*** $^{1}$H NMR (300 MHz, $CDCl_3$) of compound **5.42**

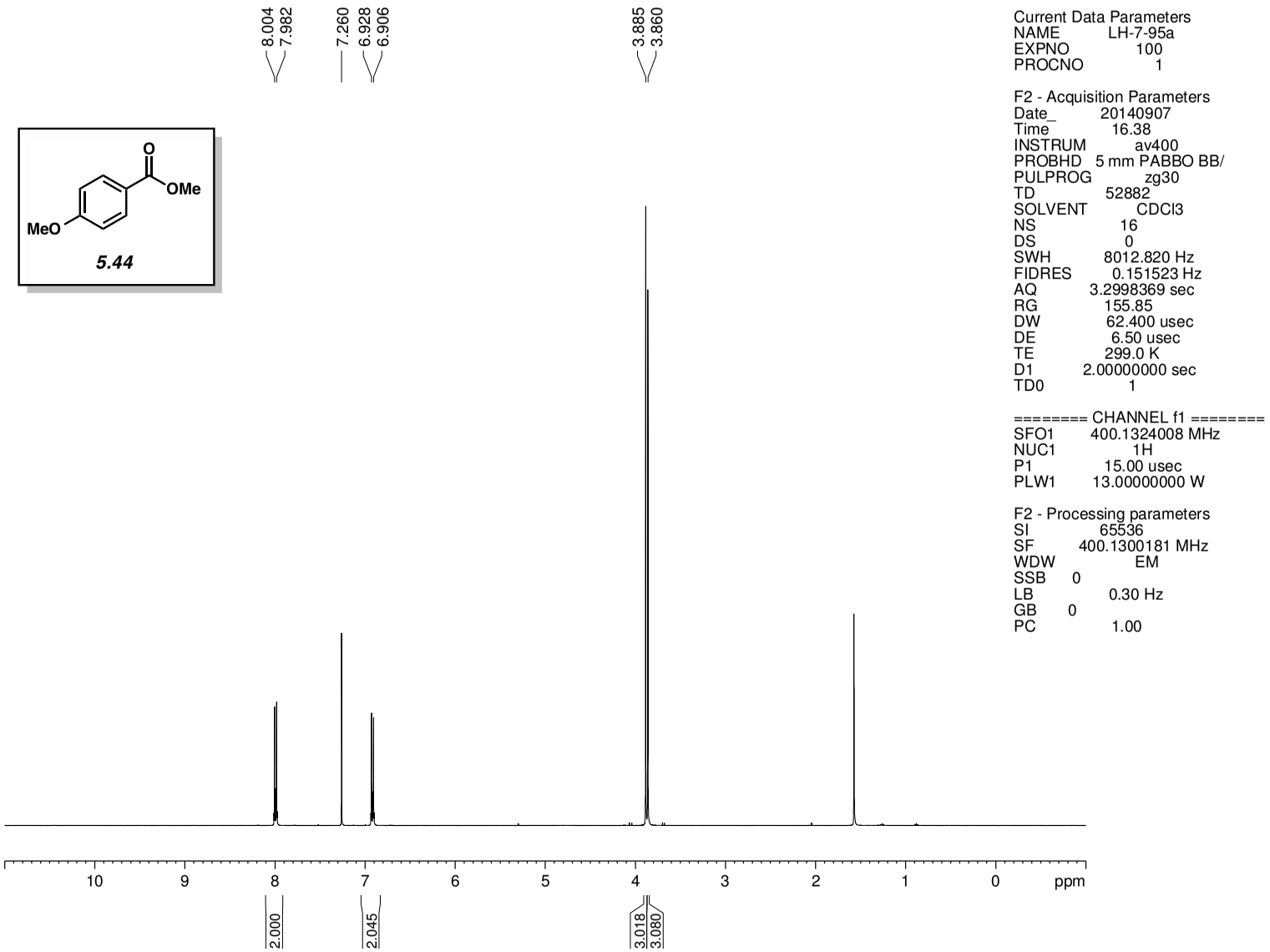


***Figure A5.24.*** $^{1}$H NMR (400 MHz, $CDCl_3$) of compound **5.44**

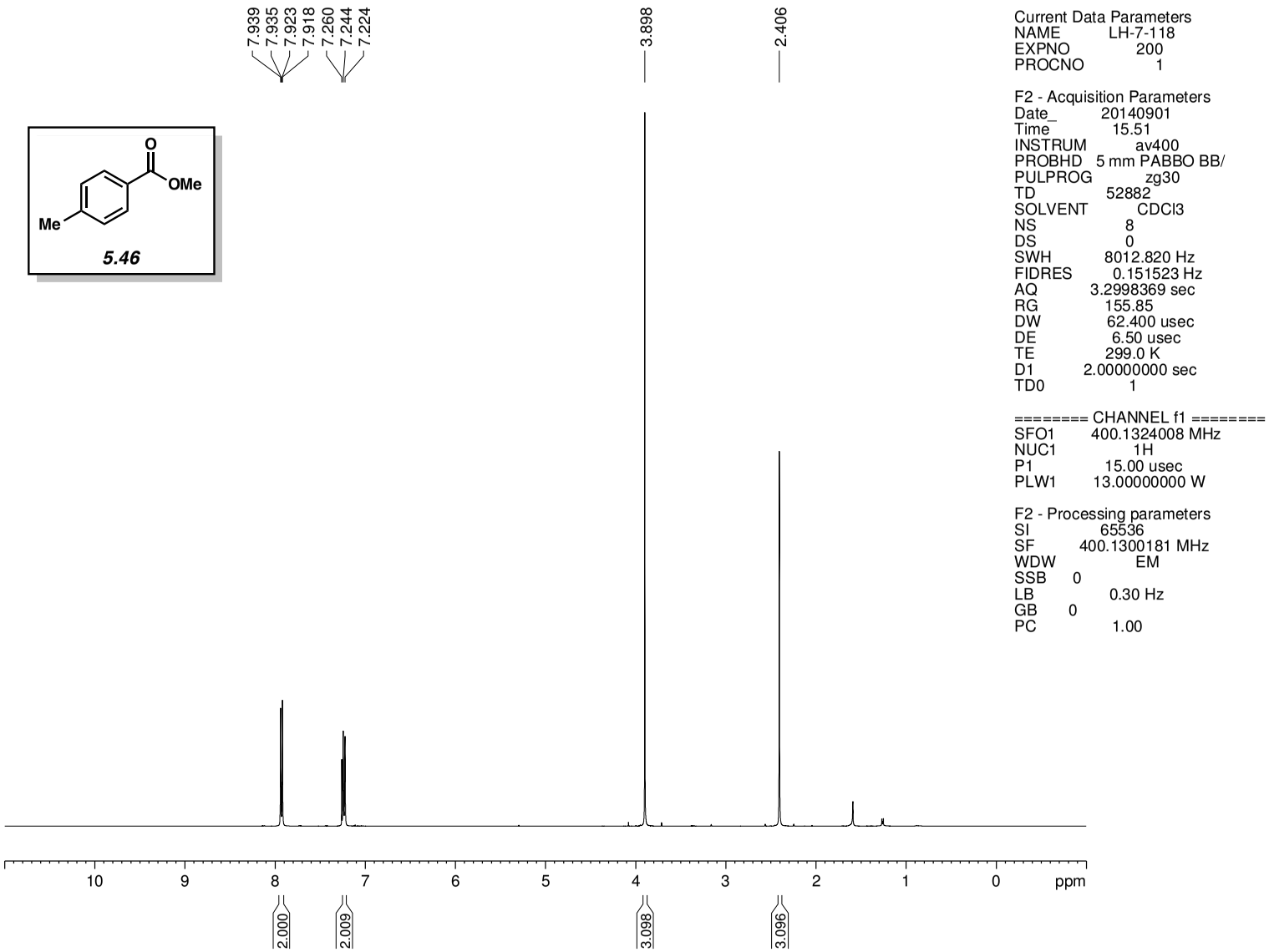


***Figure A5.25.*** $^{1}$H NMR (400 MHz, $CDCl_3$) of compound **5.46**

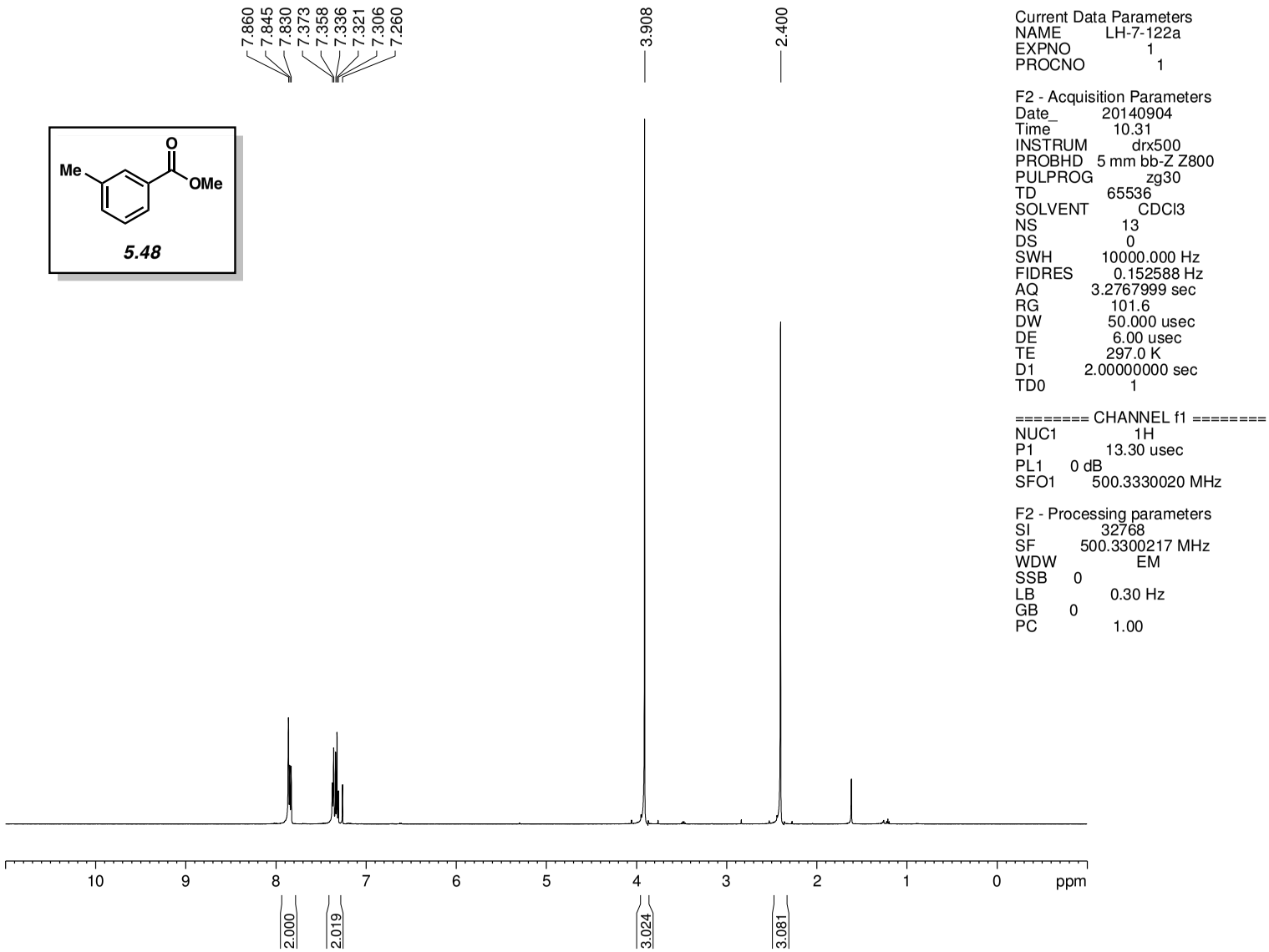


***Figure A5.26.*** $^{1}$H NMR (500 MHz, $CDCl_3$) of compound **5.48**

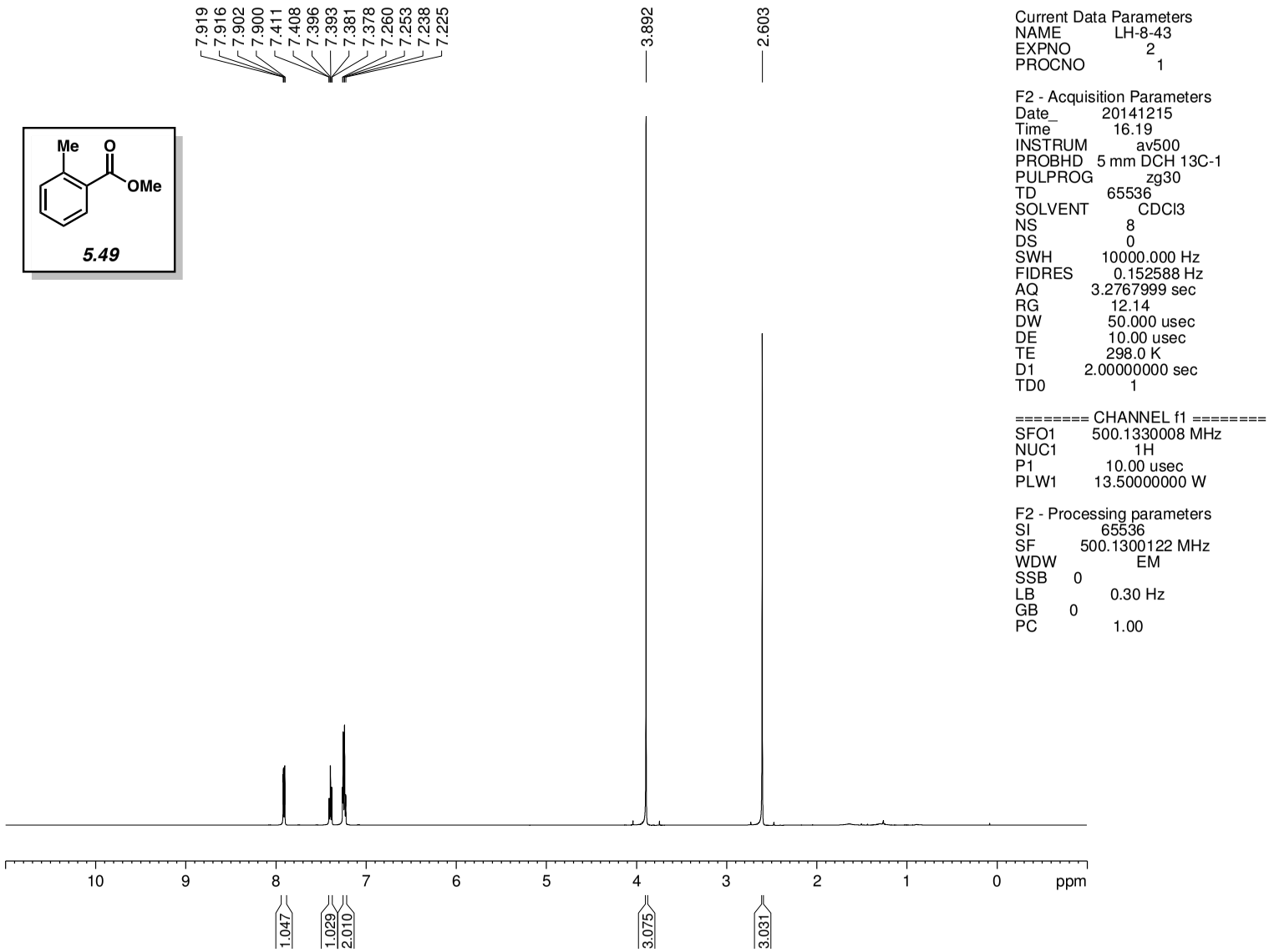


***Figure A5.27.*** $^{1}$H NMR (500 MHz, $CDCl_3$) of compound **5.49**

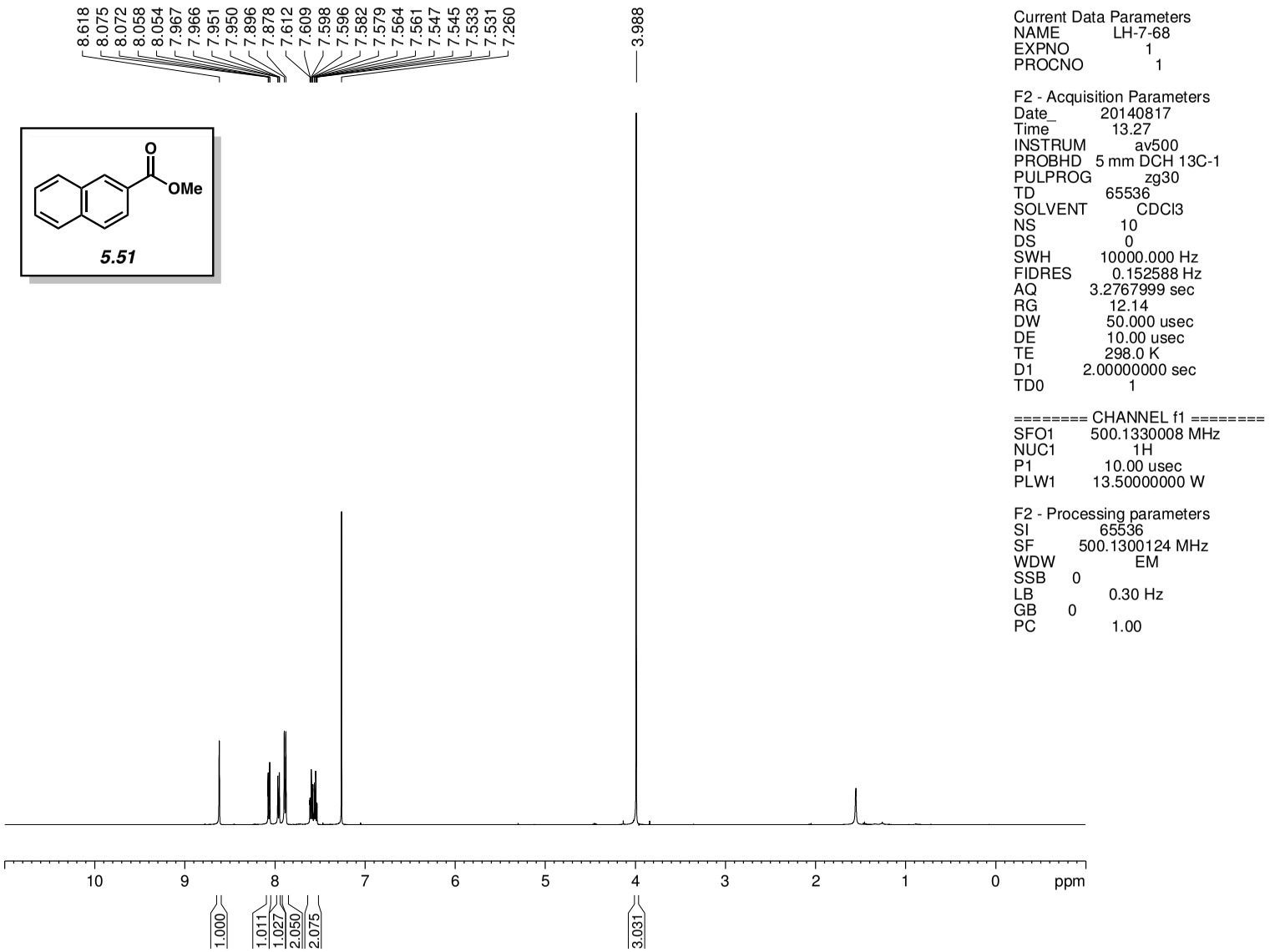


***Figure A5.28.*** $^{1}$H NMR (500 MHz, $CDCl_3$) of compound **5.51**

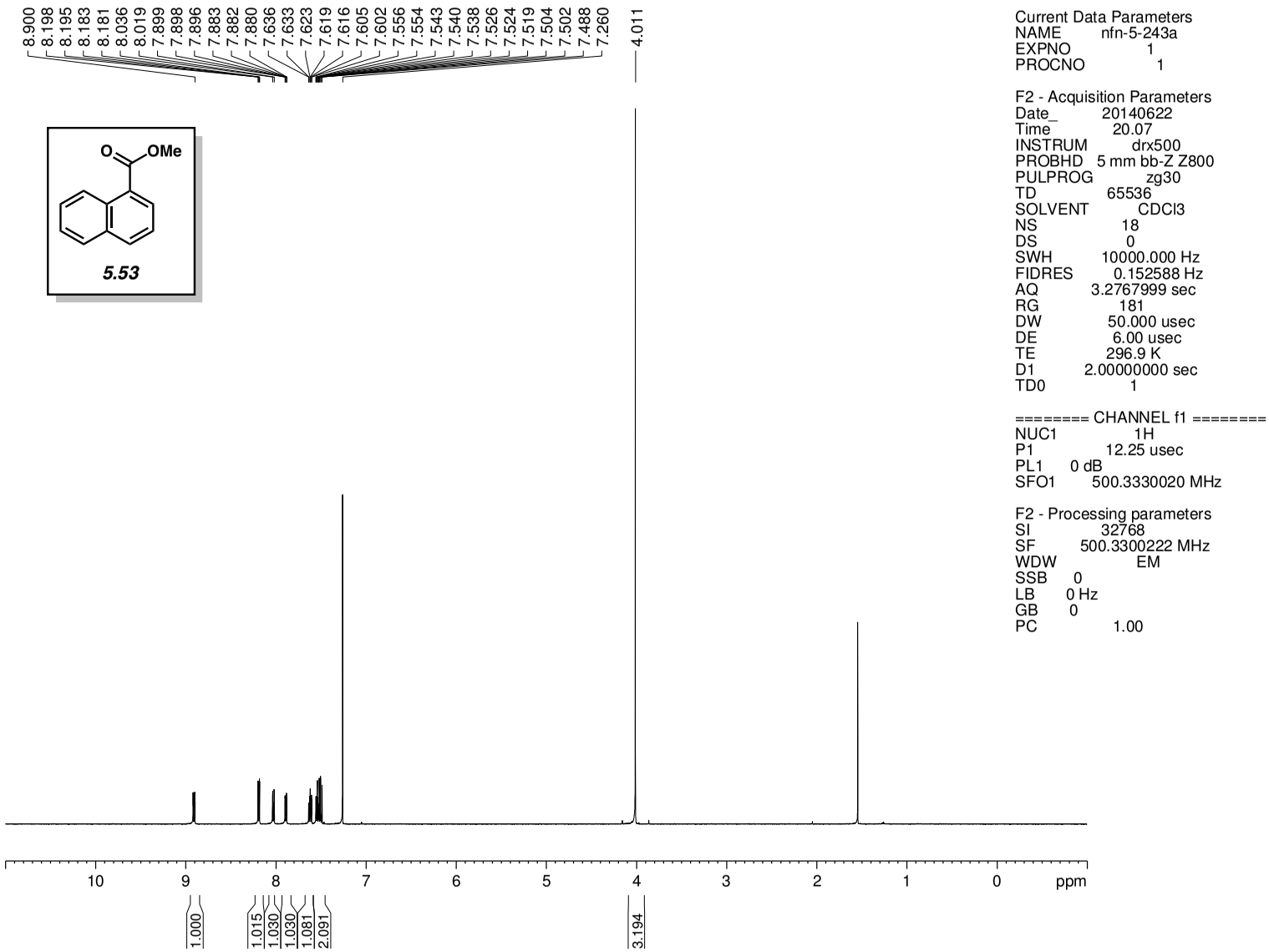


***Figure A5.29.*** $^{1}$H NMR (500 MHz, $CDCl_3$) of compound **5.53**

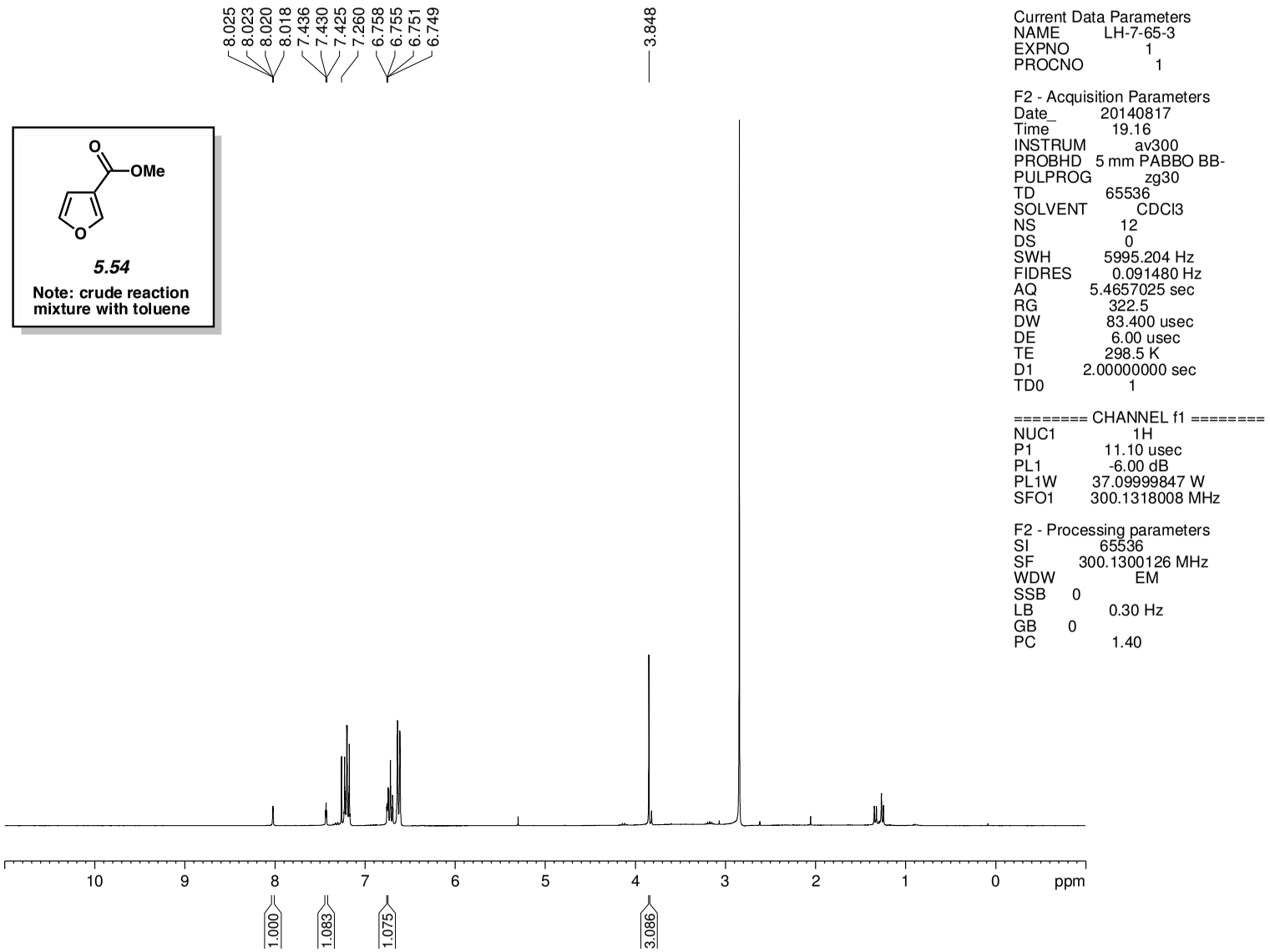


***Figure A5.30.*** $^{1}$H NMR (300 MHz, $CDCl_3$) of compound **5.54**

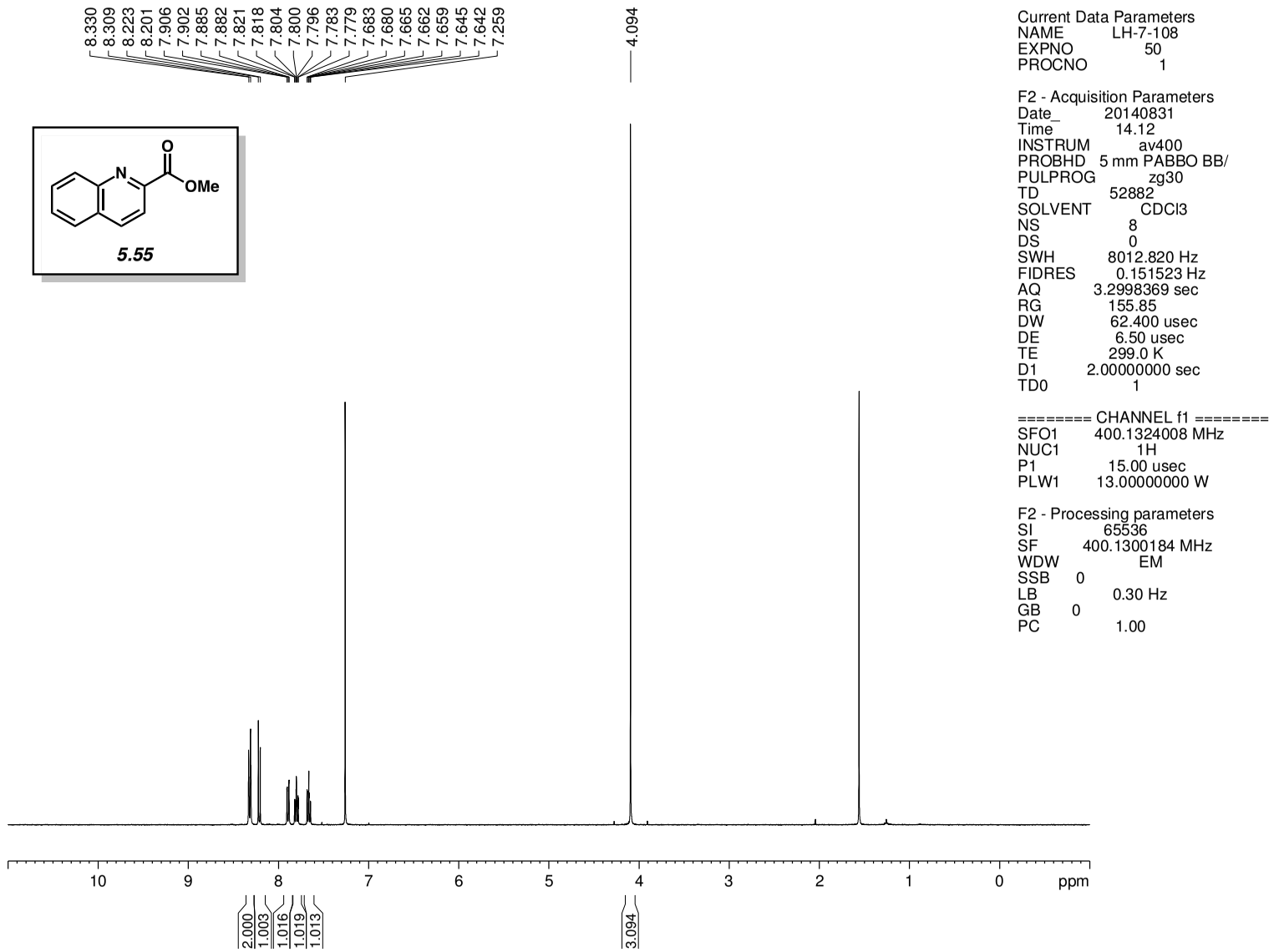


***Figure A5.31.*** $^{1}$H NMR (400 MHz, $CDCl_3$) of compound **5.55**

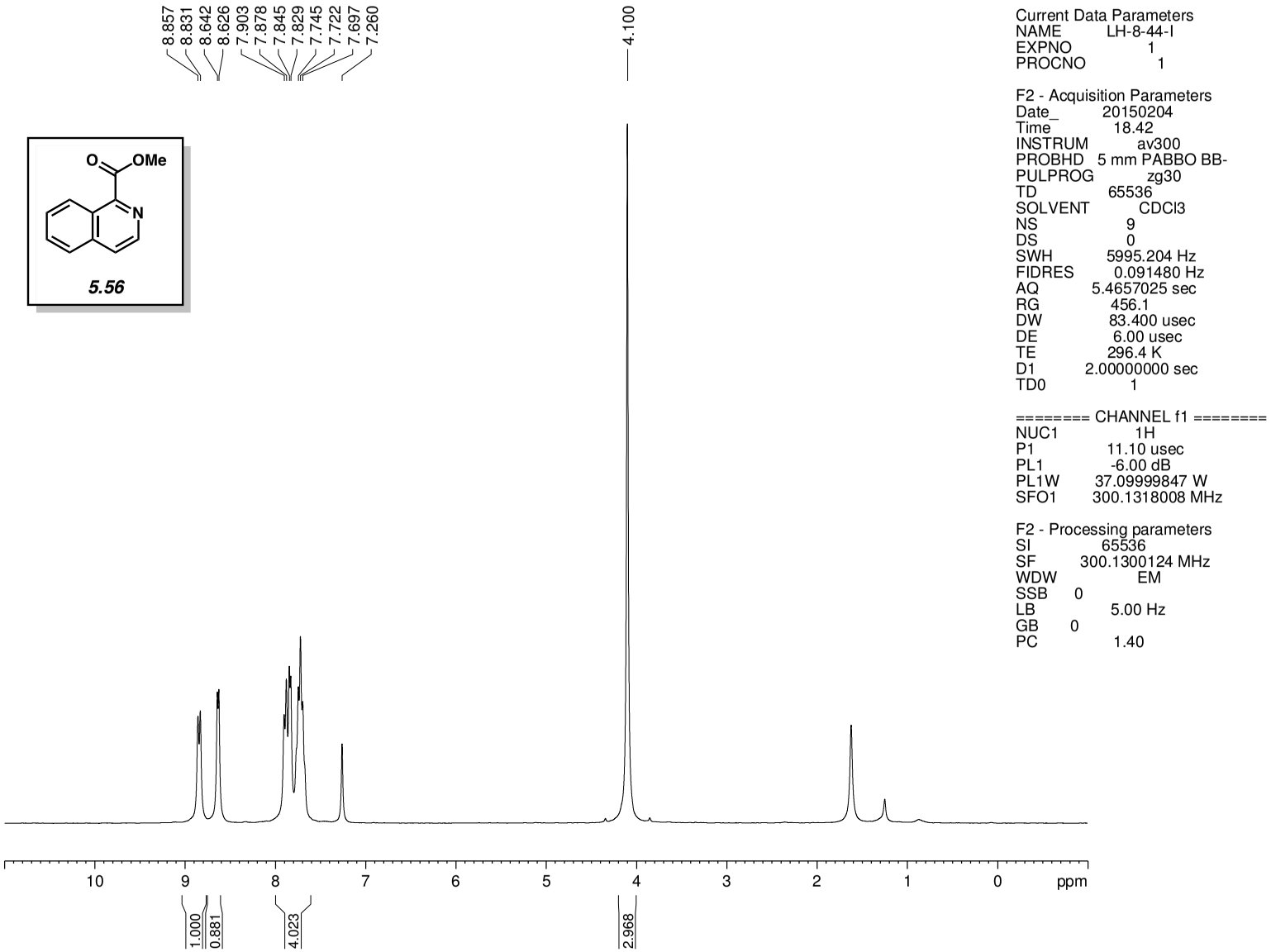


***Figure A5.32.*** $^{1}$H NMR (300 MHz, $CDCl_3$) of compound **5.56**

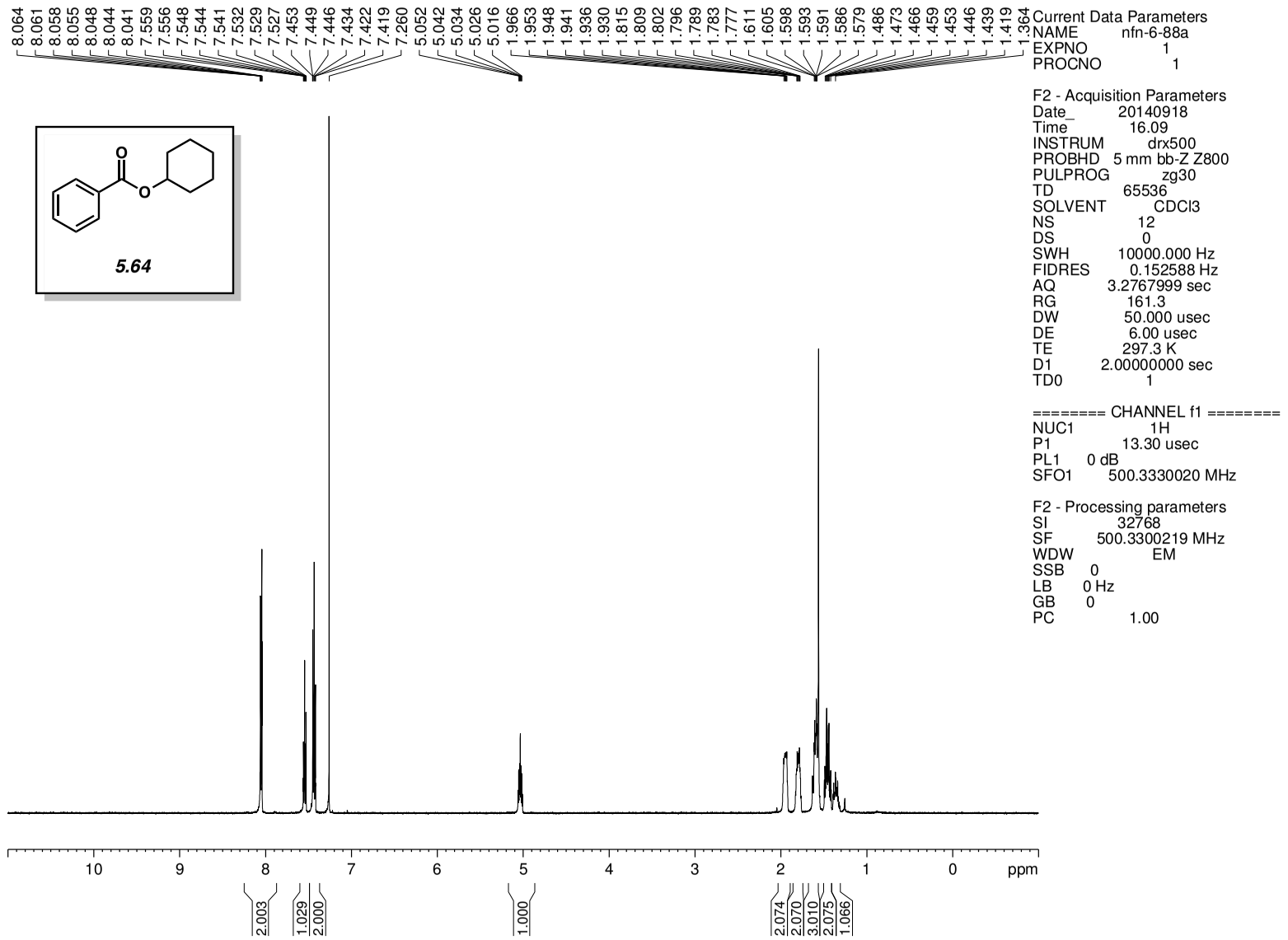


***Figure A5.33.*** $^{1}$H NMR (500 MHz, $CDCl_3$) of compound **5.64**

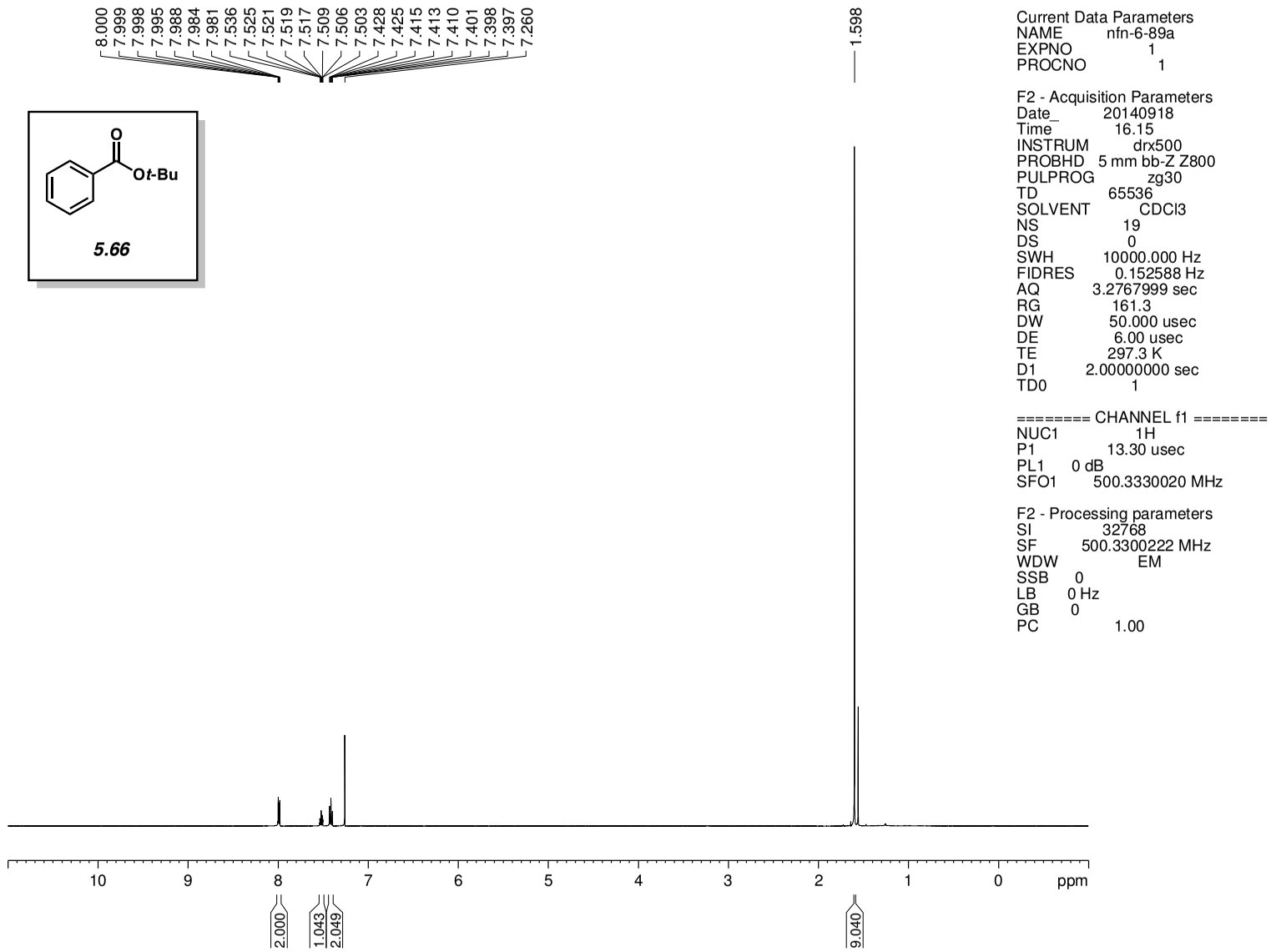


***Figure A5.34.*** $^{1}$H NMR (500 MHz, $CDCl_3$) of compound **5.66**

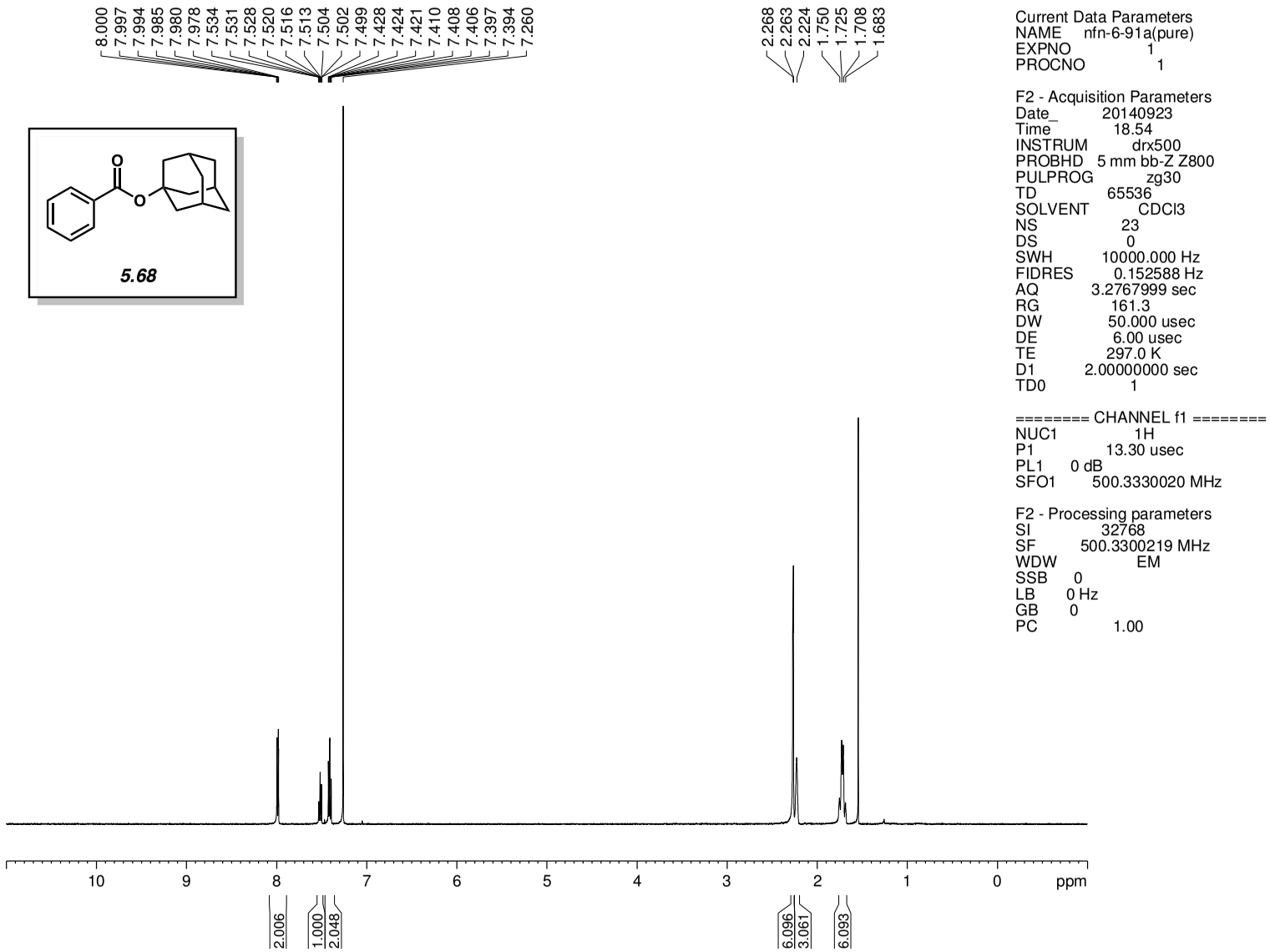


***Figure A5.35.*** $^{1}$H NMR (500 MHz, $CDCl_3$) of compound **5.68**

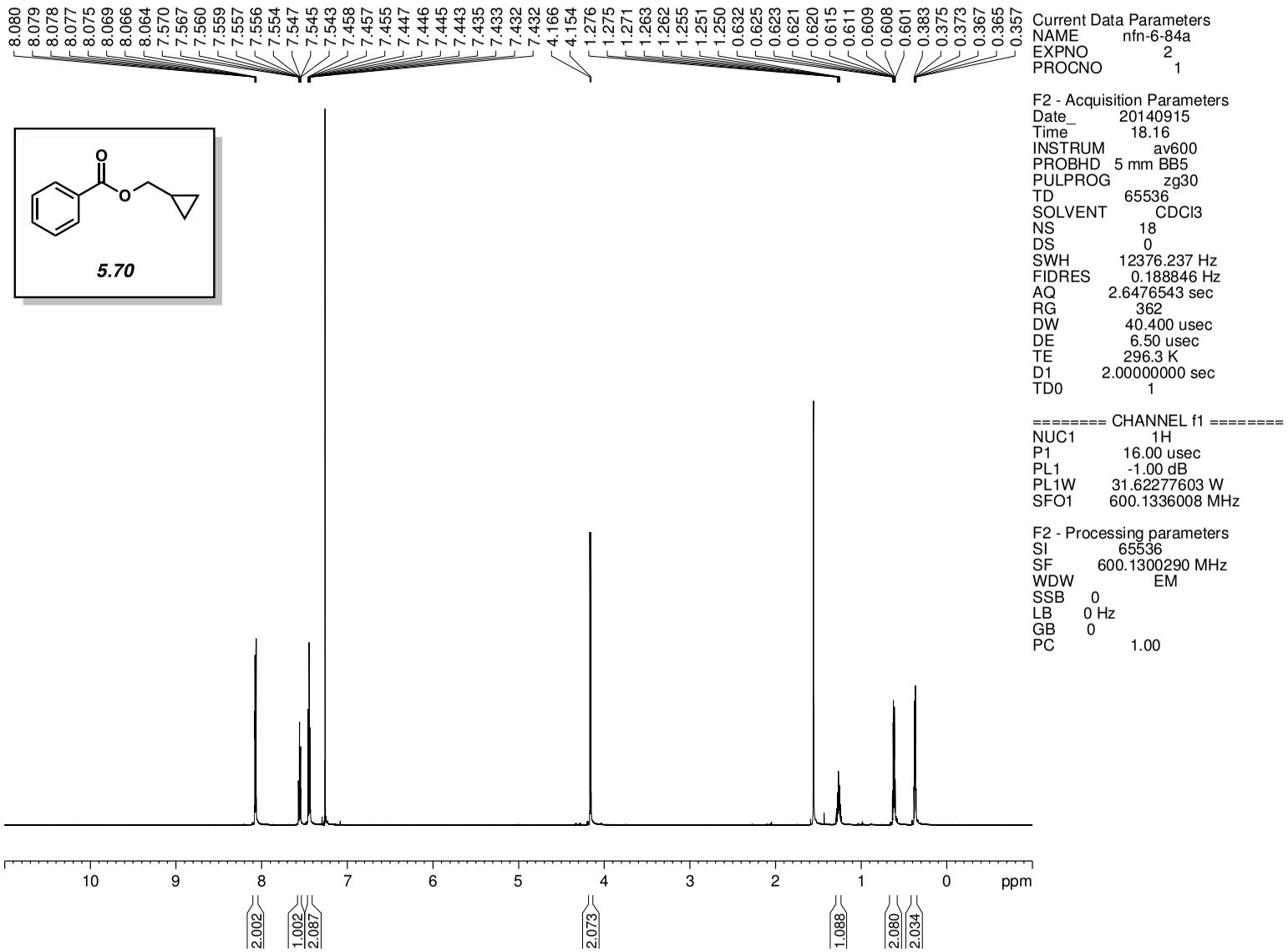


***Figure A5.36.*** $^{1}$H NMR (600 MHz, $CDCl_3$) of compound **5.70**

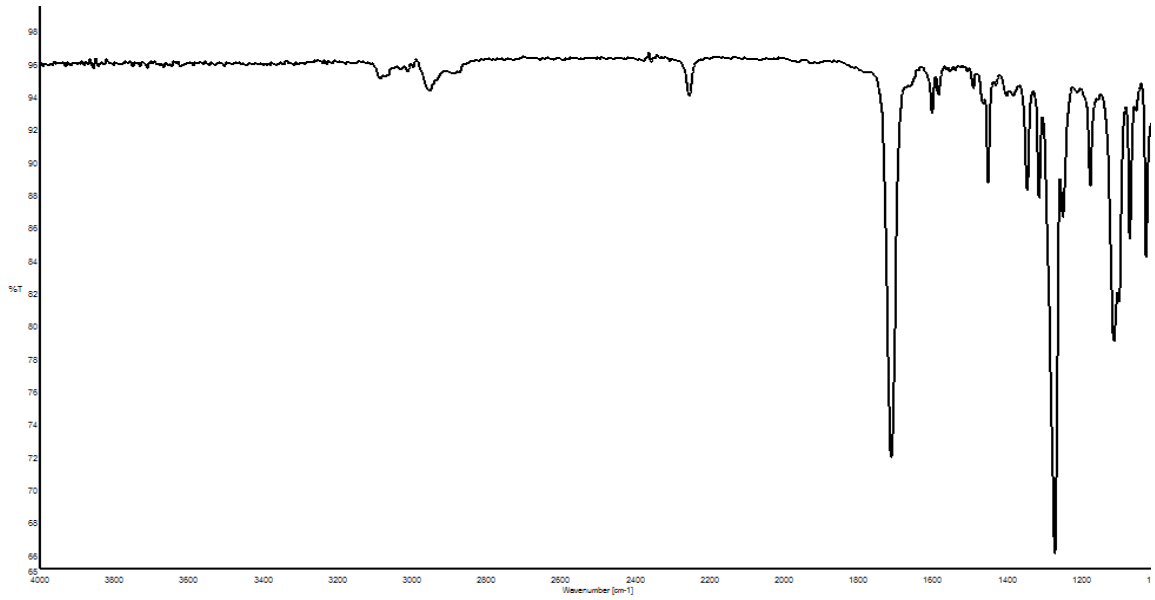


***Figure A5.37.*** Infrared spectrum of compound **5.70**

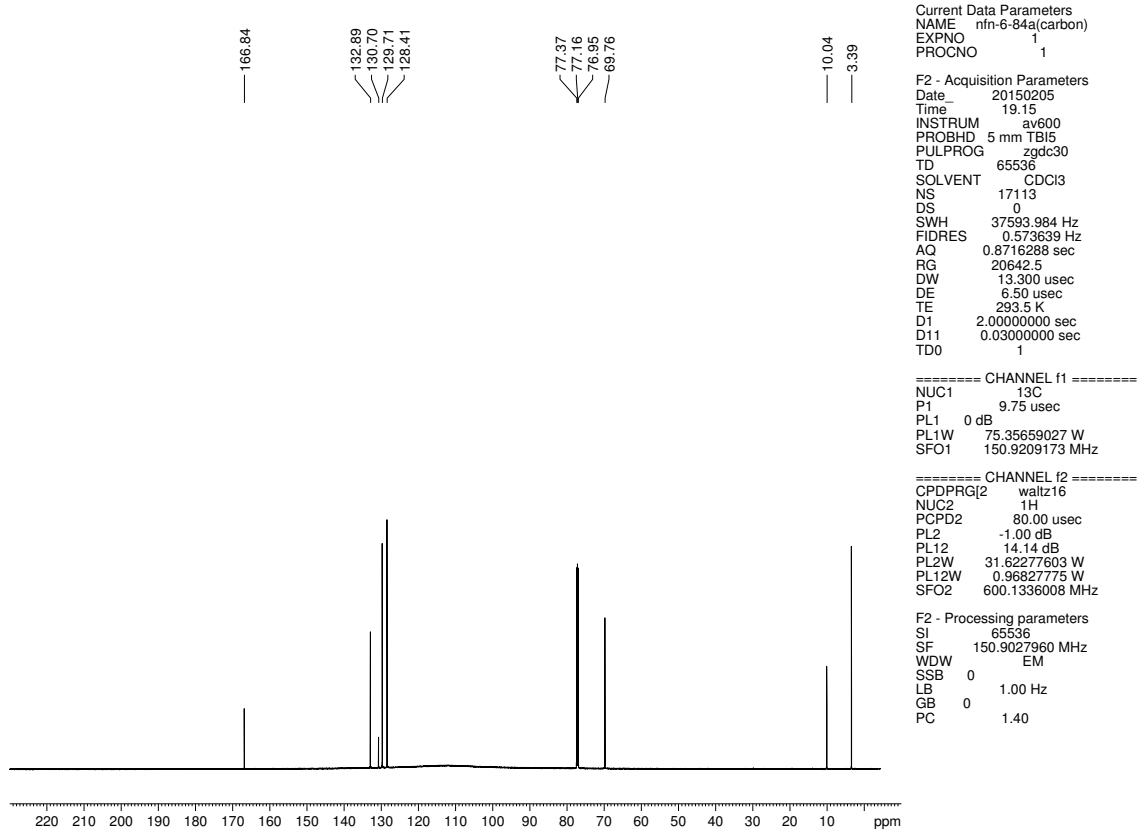


***Figure A5.38.*** $^{13}C$ NMR (150 MHz, $CDCl_3$) of compound **5.70**

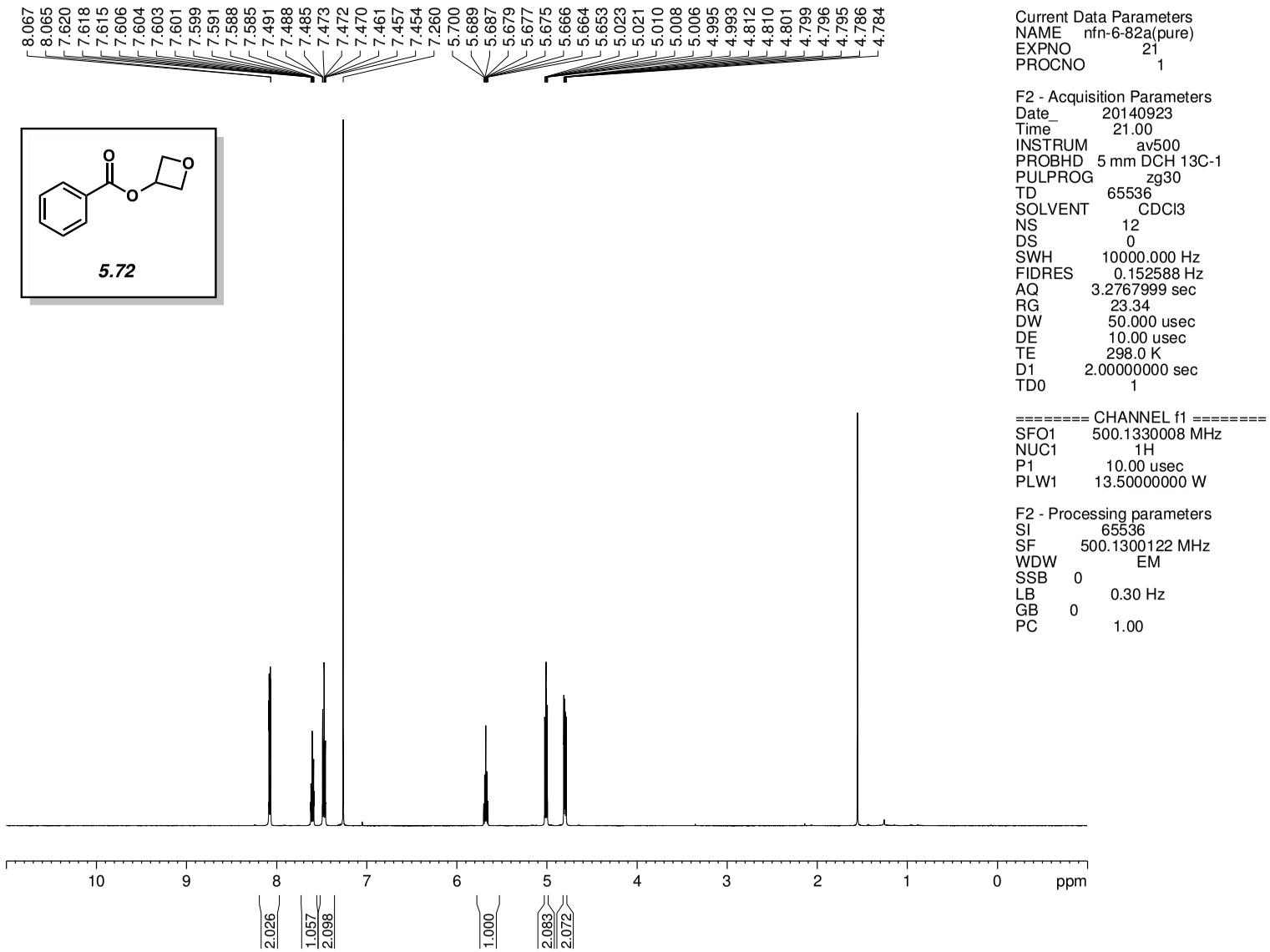


***Figure A5.39.*** $^{1}$H NMR (500 MHz, $CDCl_3$) of compound **5.72**

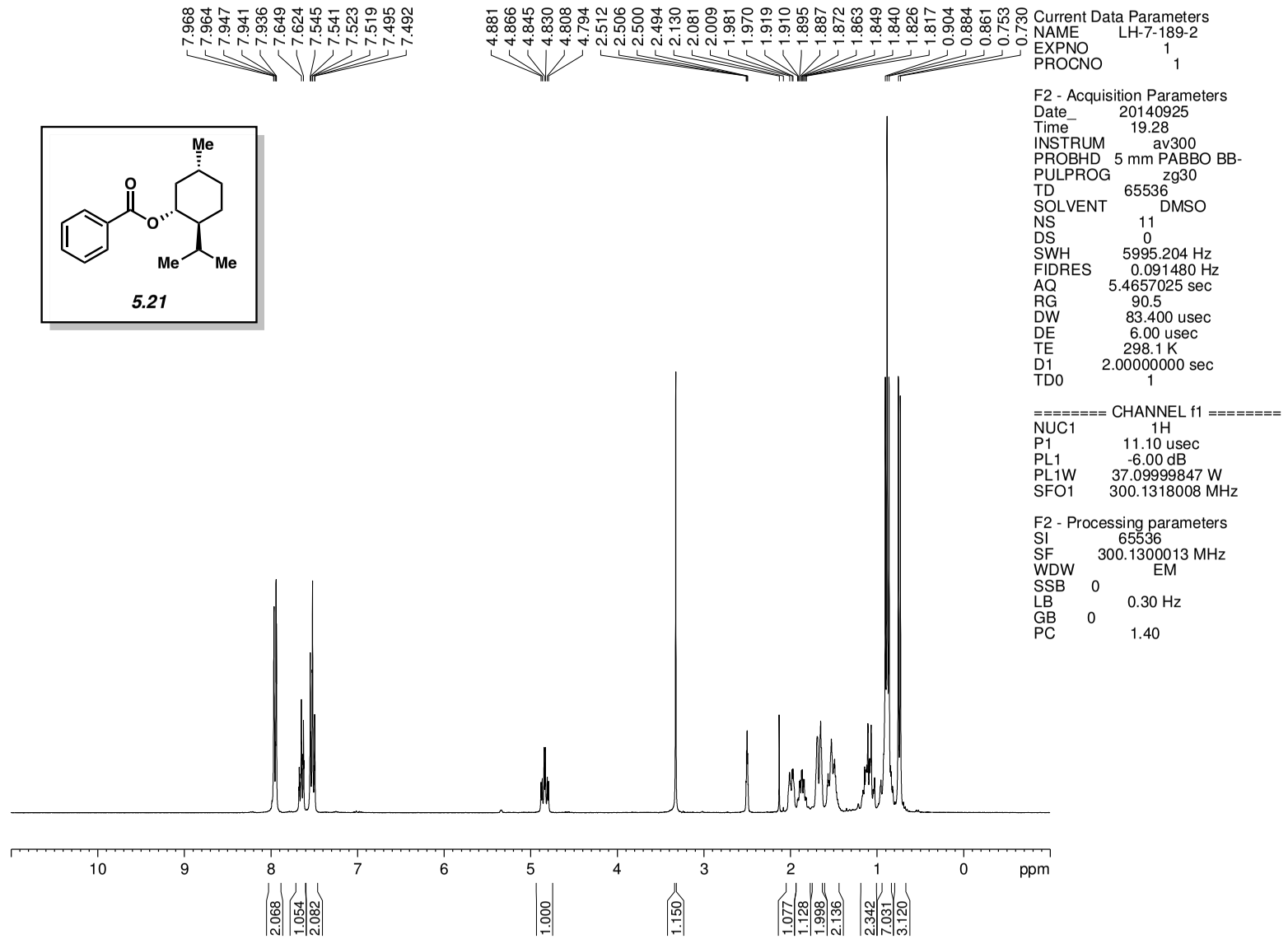


***Figure A5.40.*** $^{1}$H NMR (300 MHz, $(CD_3)_2SO$) of compound

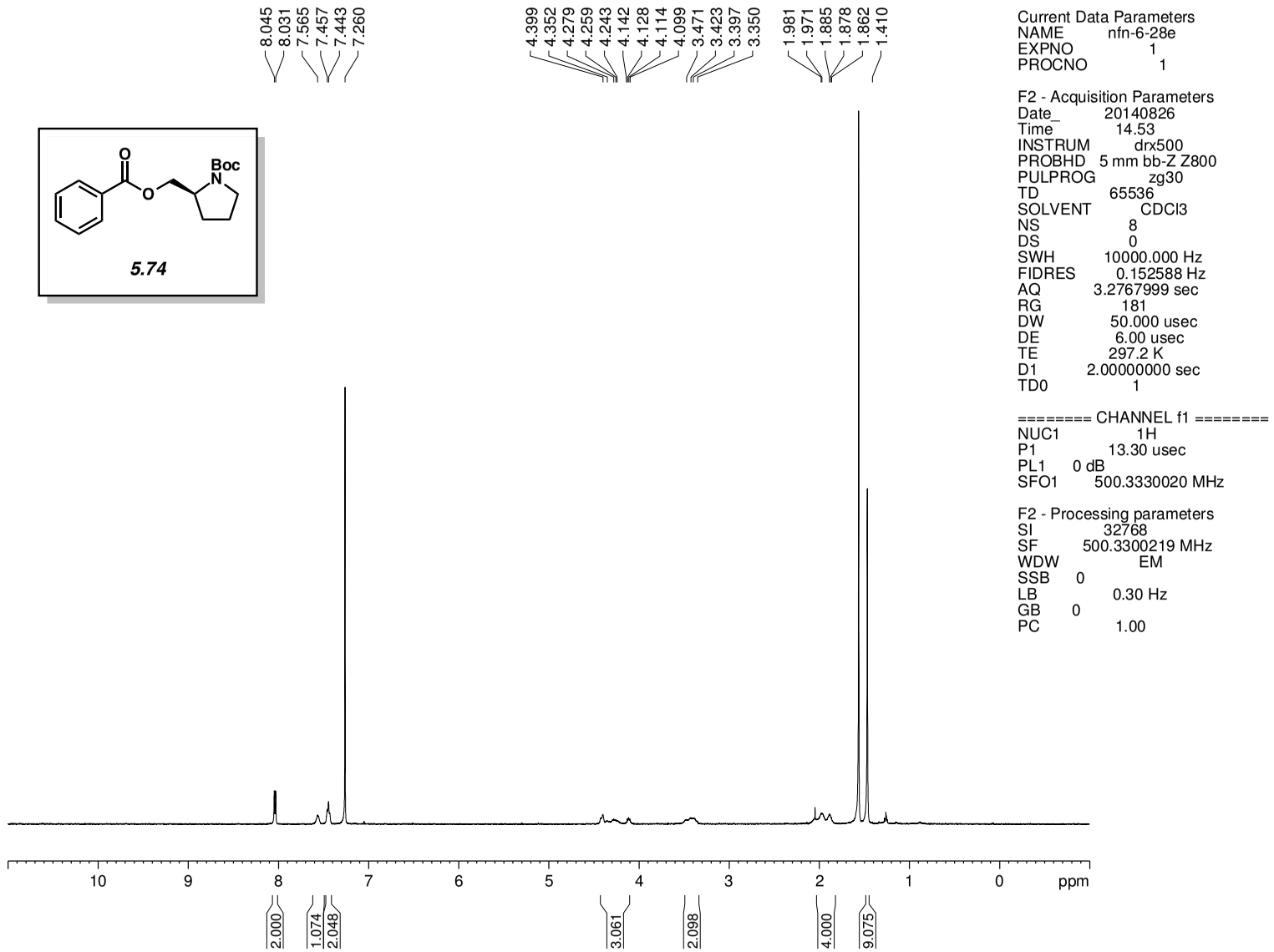


***Figure A5.41.*** $^{1}$H NMR (500 MHz, $CDCl_3$) of compound **5.74**

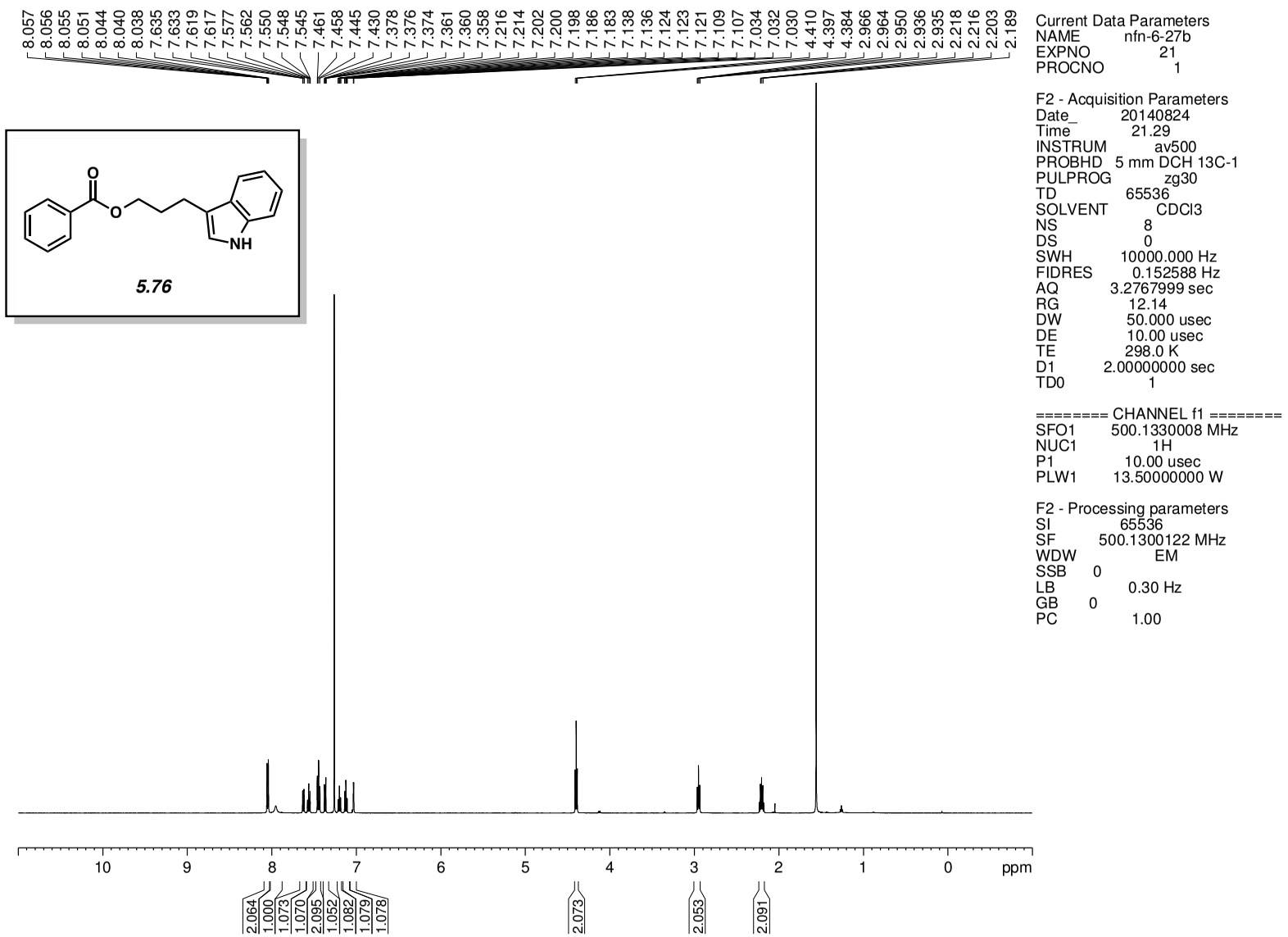


***Figure A5.42.*** $^{1}$H NMR (500 MHz, $CDCl_3$) of compound **5.76**

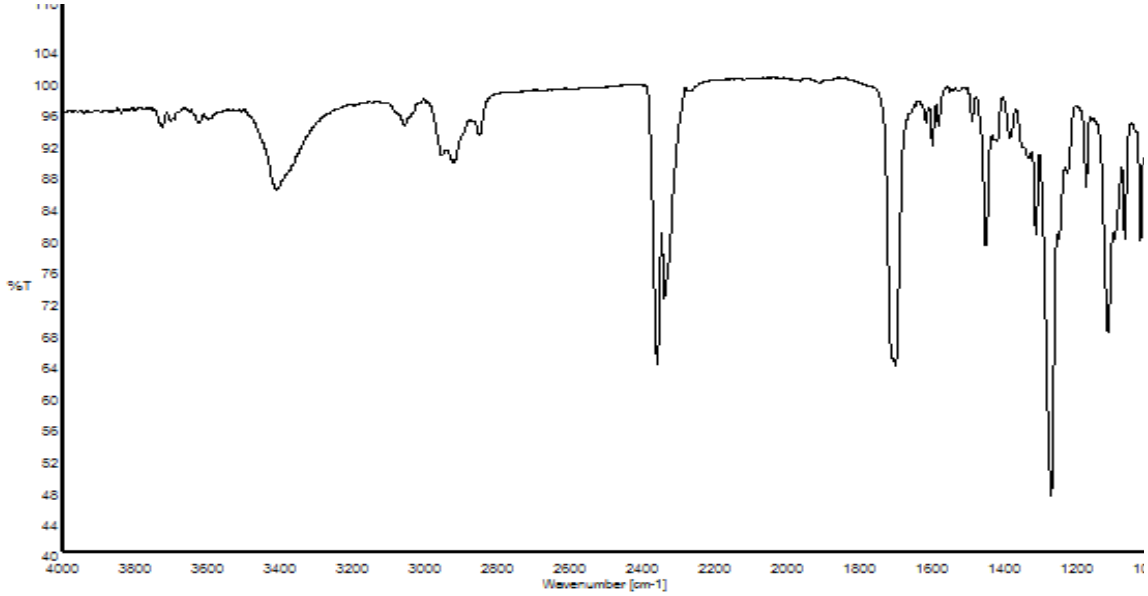


***Figure A5.43.*** Infrared spectrum of compound **5.76**

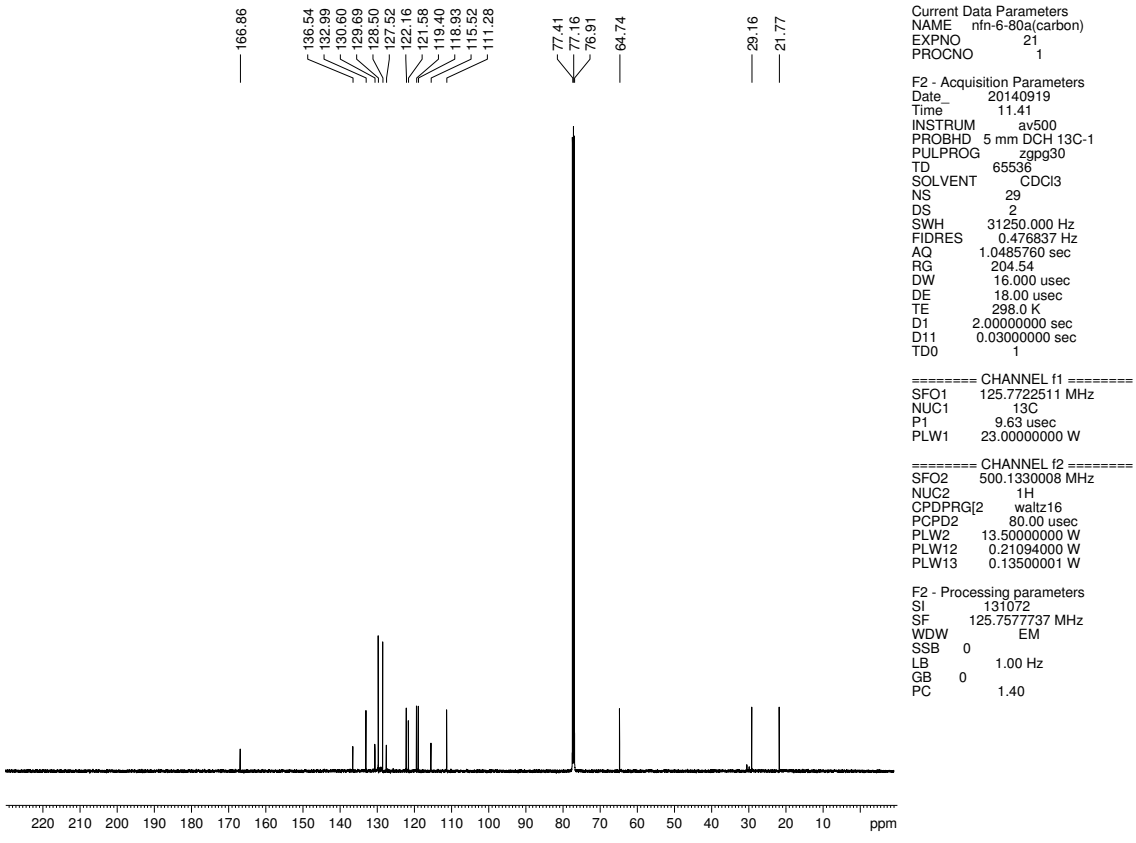


***Figure A5.44.*** $^{13}C$ NMR (125 MHz, $CDCl_3$) of compound **5.76**

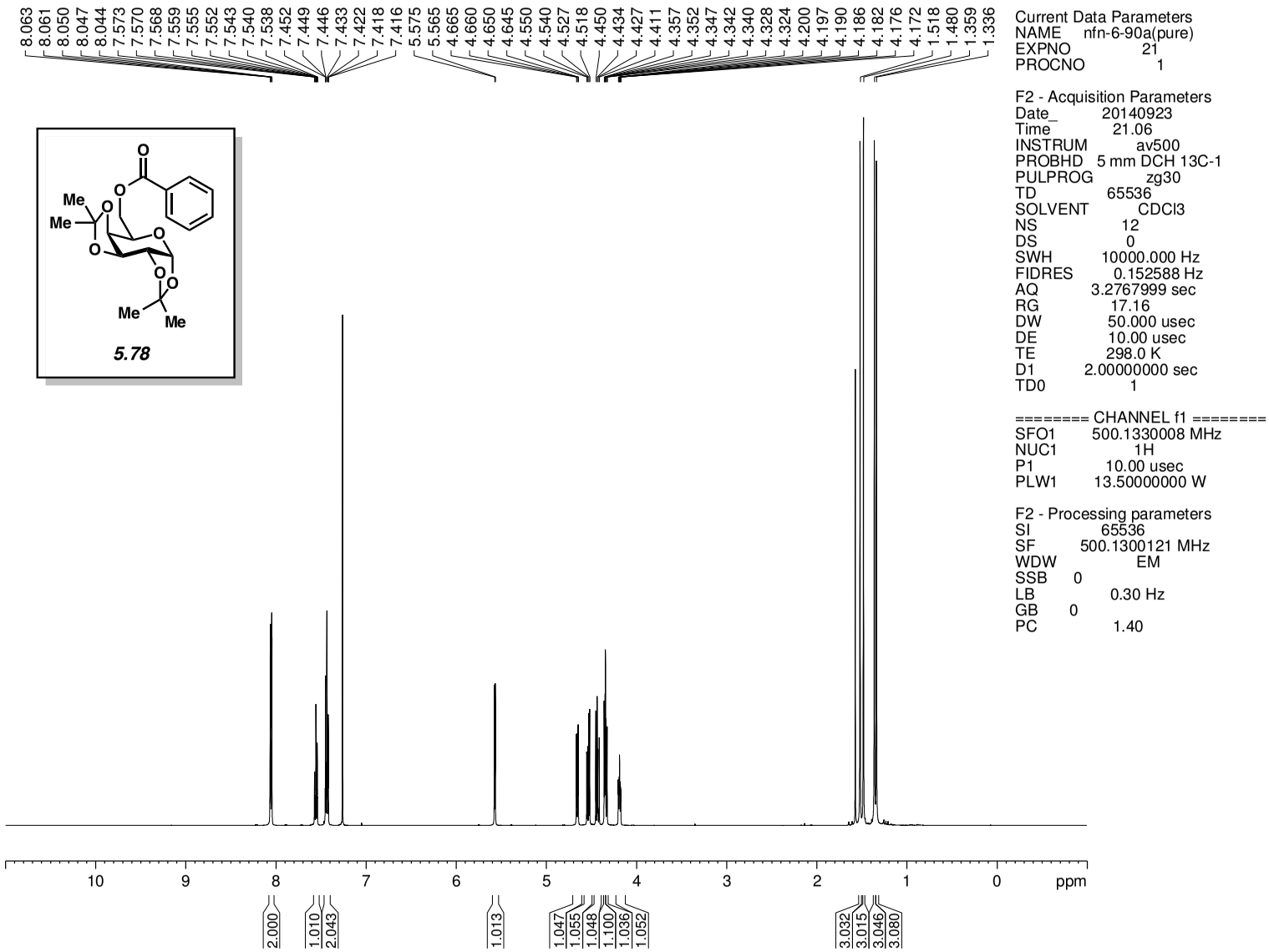


***Figure A5.45.*** $^{1}$H NMR (500 MHz, $CDCl_3$) of compound **5.78**

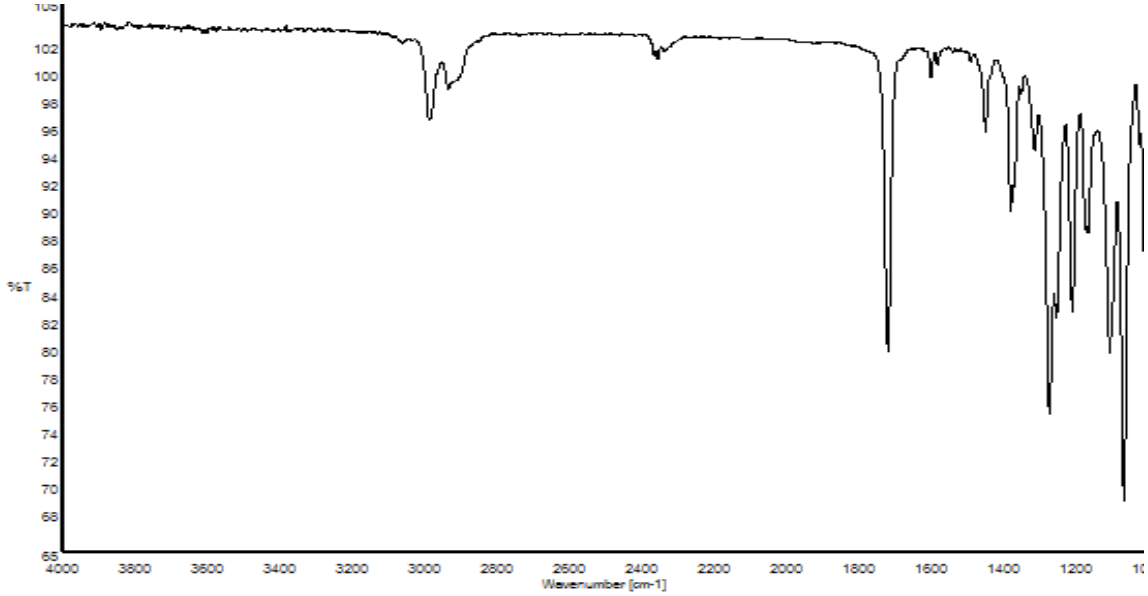


***Figure A5.46.*** Infrared spectrum of compound **5.78**

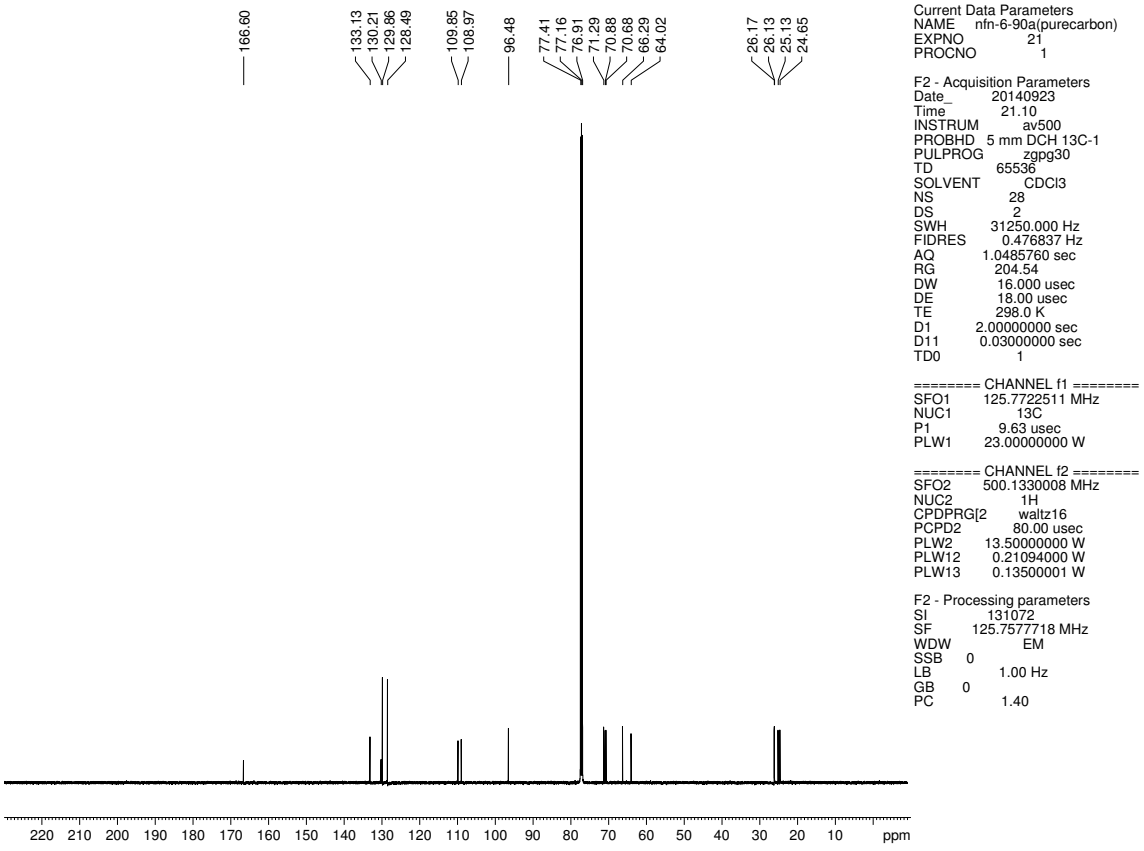


***Figure A5.47.*** $^{13}$C NMR (125 MHz, $CDCl_3$) of compound **5.78**

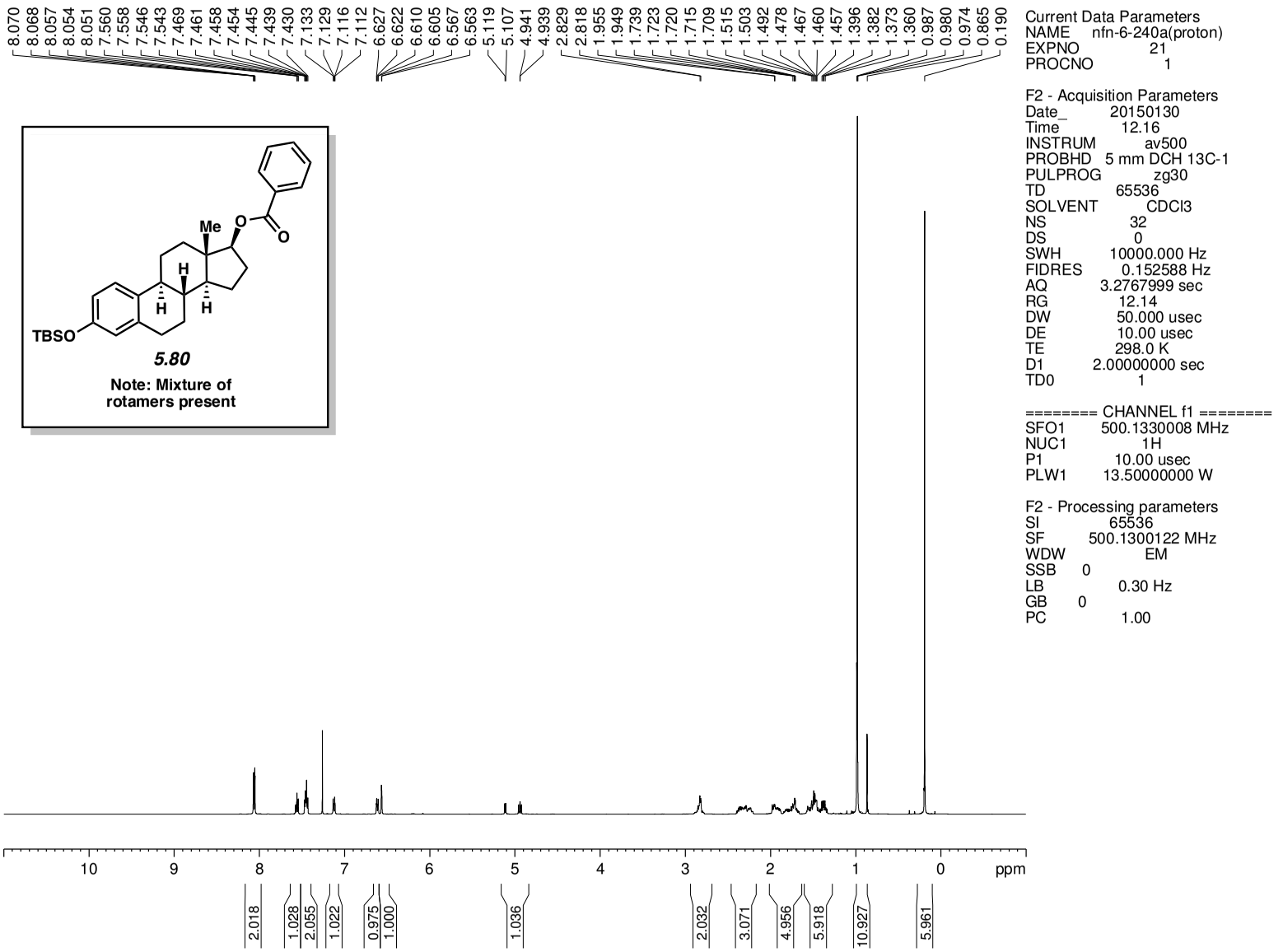


***Figure A5.48.*** $^{1}$H NMR (500 MHz, $CDCl_3$) of compound **5.80**

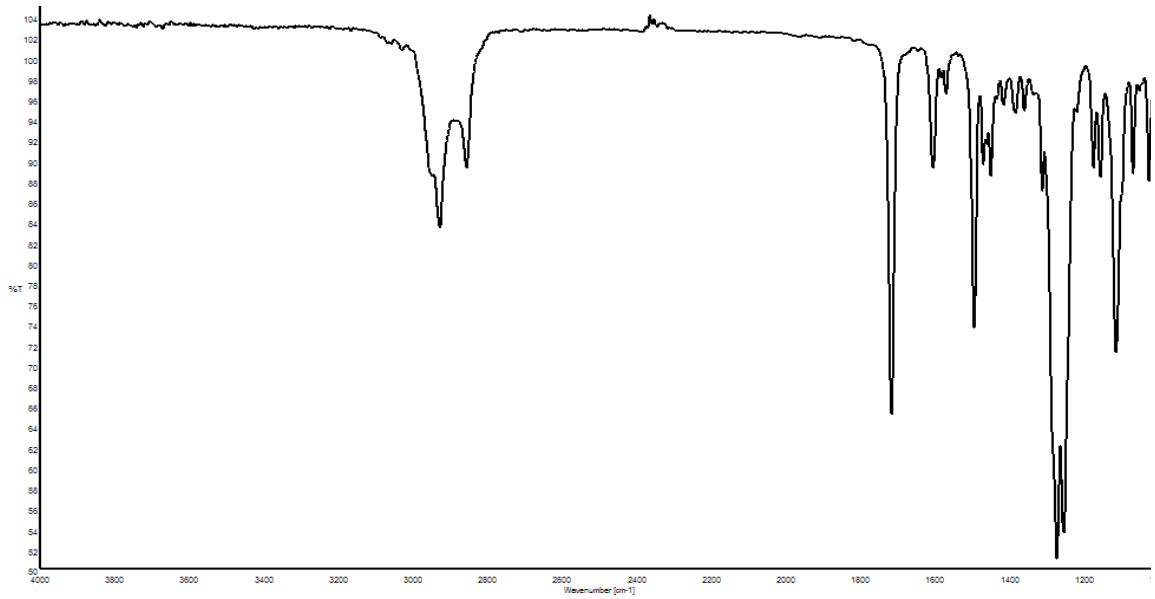


***Figure A5.49.*** Infrared spectrum of compound **5.80**

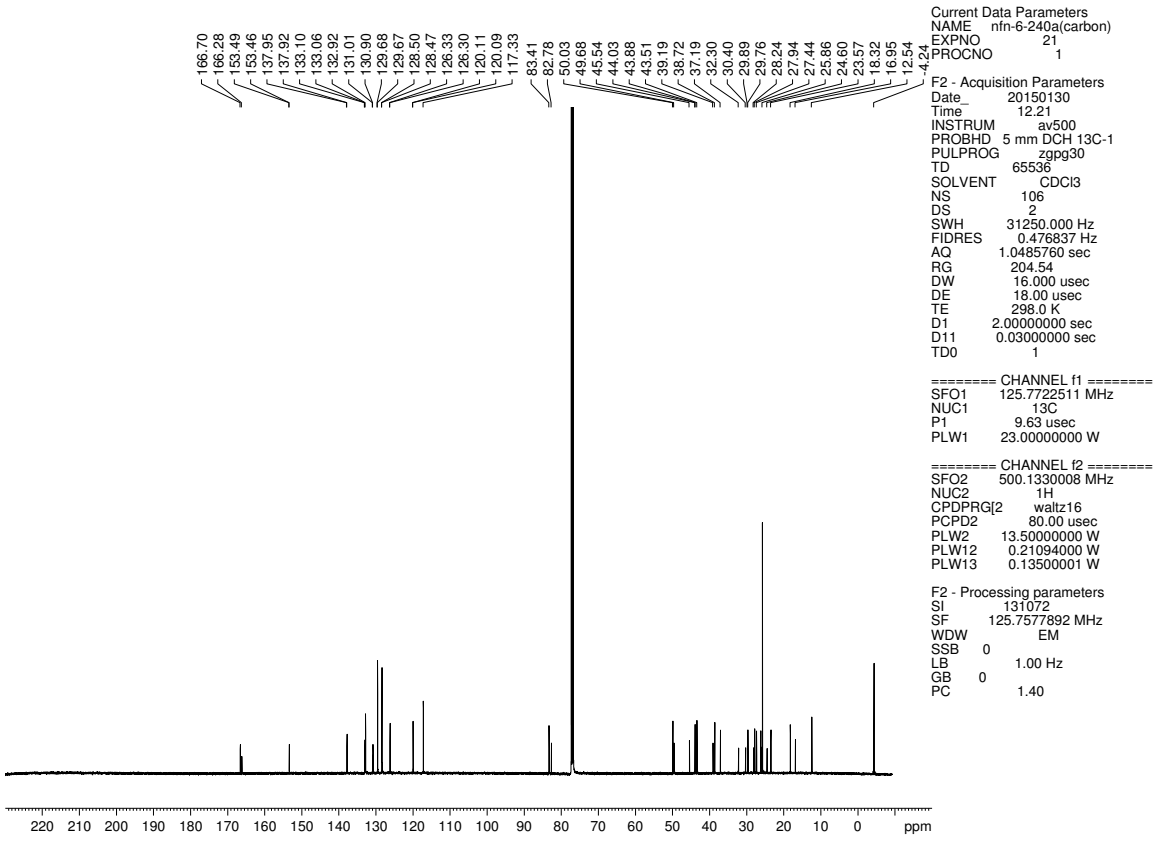


***Figure A5.50.*** $^{13}$C NMR (125 MHz, $CDCl_3$) of compound **5.80**

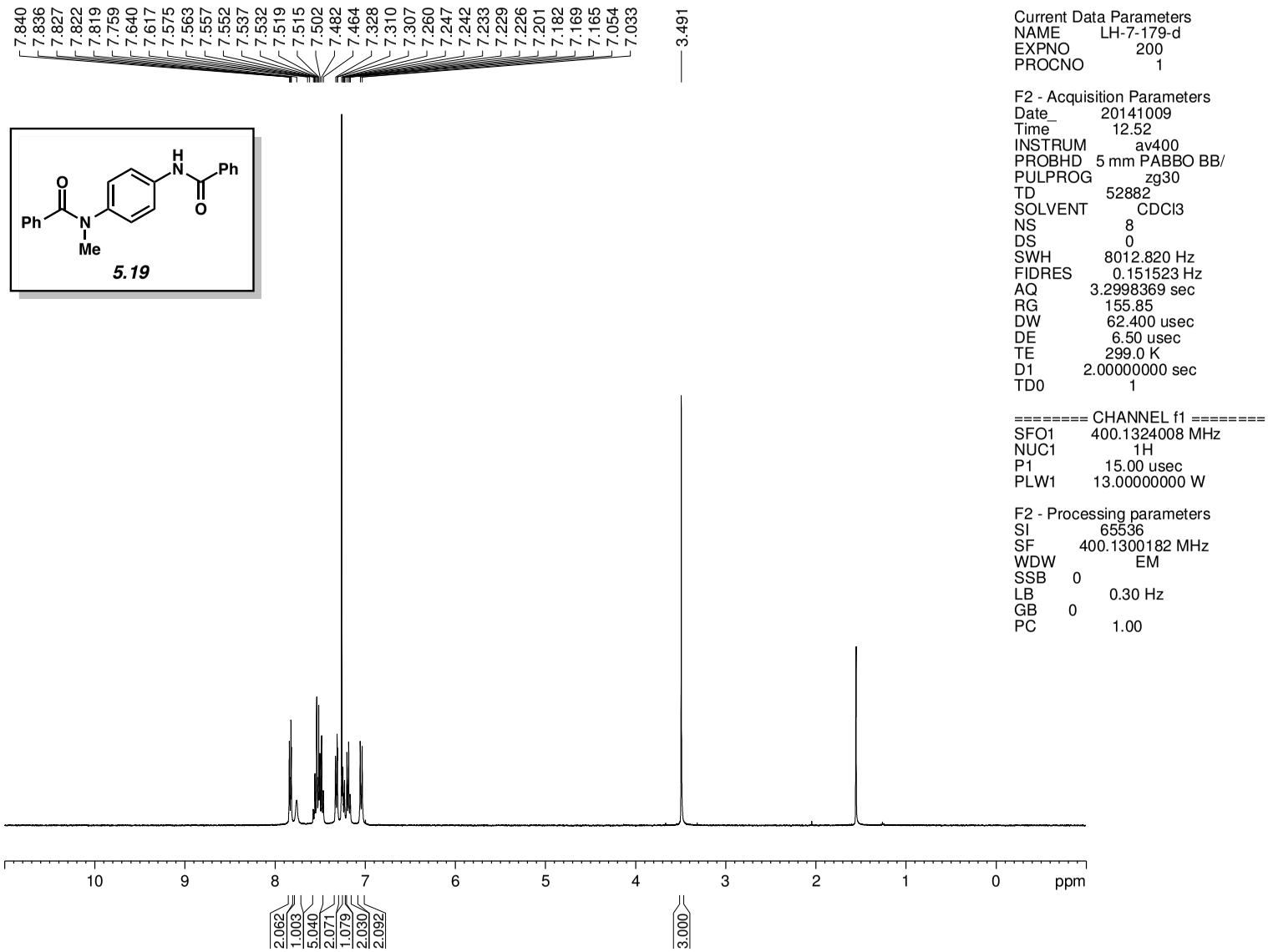


***Figure A5.51.*** $^{1}$H NMR (400 MHz, $CDCl_3$) of compound **5.19**

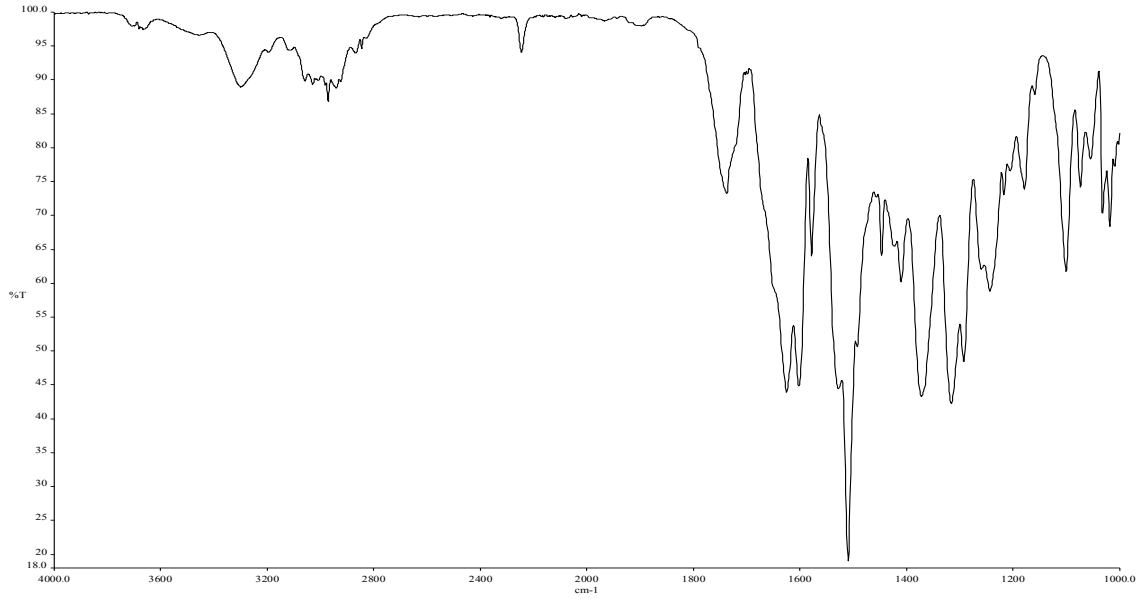


***Figure A5.52.*** Infrared spectrum of compound **5.19**

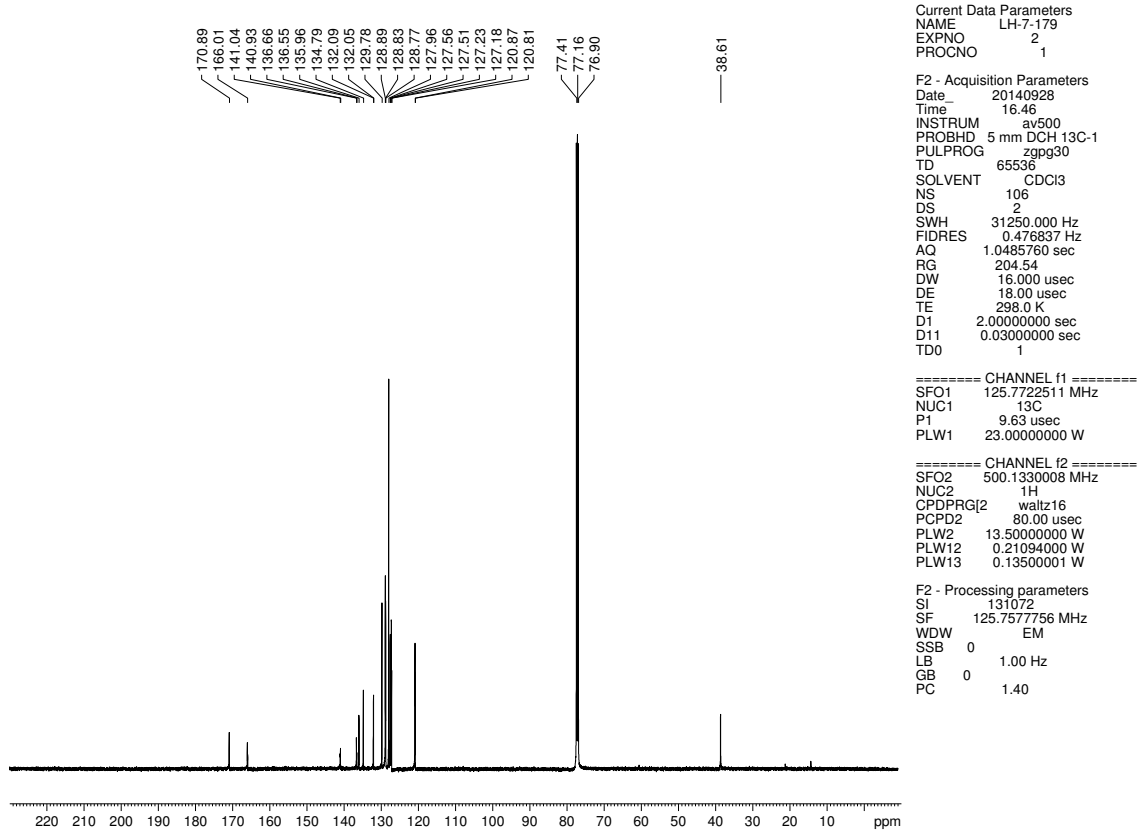


***Figure A5.53.*** $^{13}$C NMR (125 MHz, $CDCl_3$) of compound **5.19**

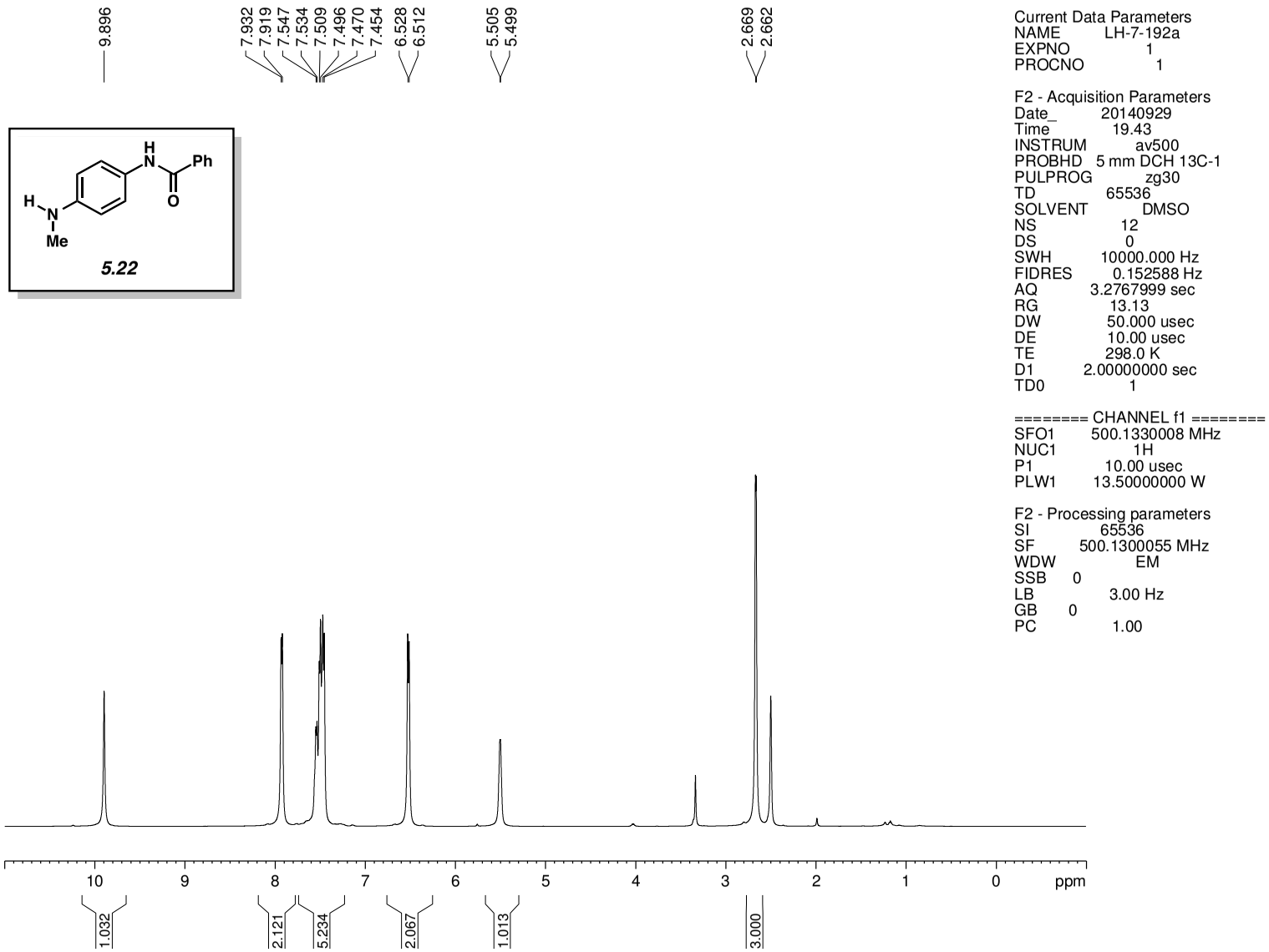


***Figure A5.54.*** $^{1}$H NMR (500 MHz, $(CD_3)_2SO$) of compound **5.22**

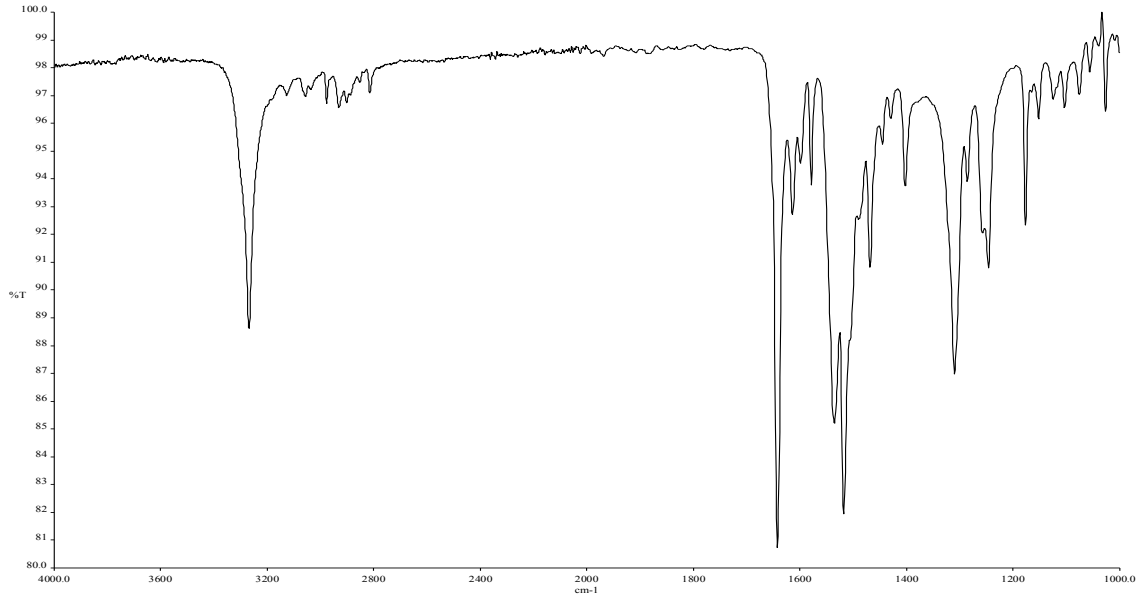


***Figure A5.55.*** Infrared spectrum of compound **5.22**

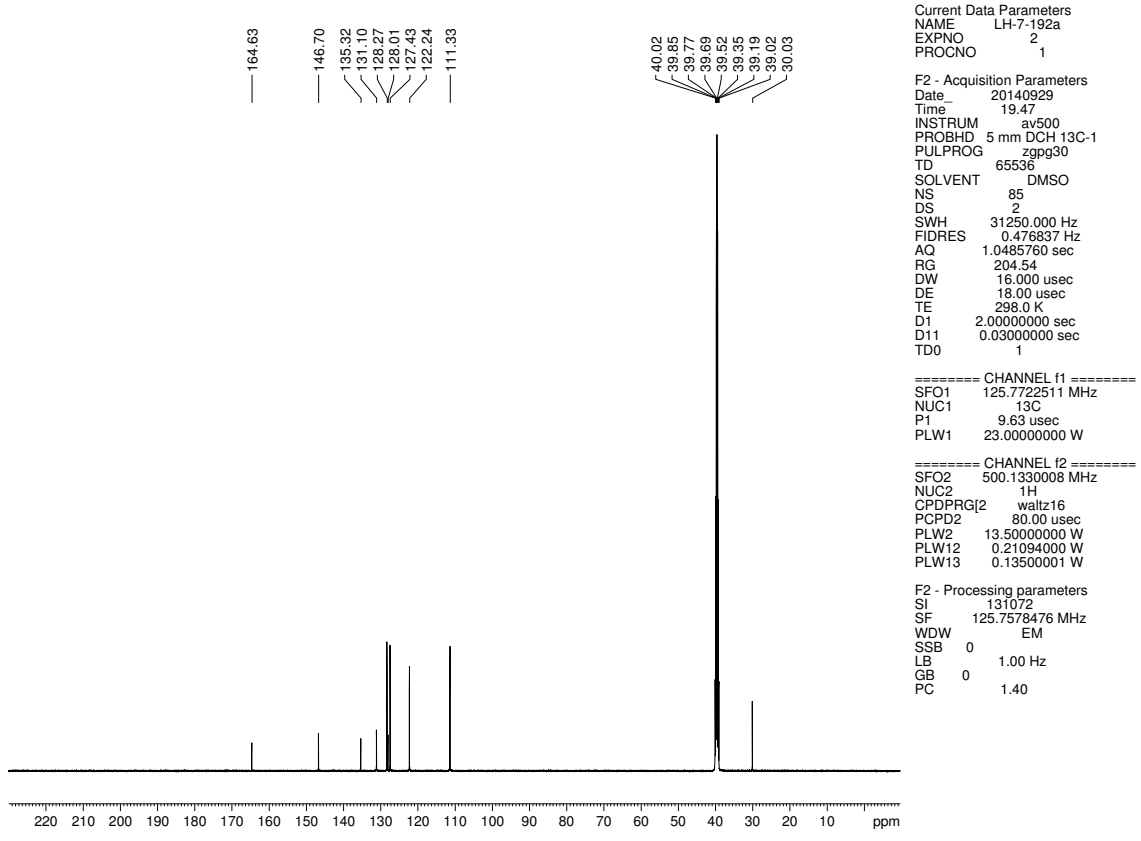


***Figure A5.56.*** $^{13}$C NMR (125 MHz, $(CD_3)_2SO$) of compound **5.22**

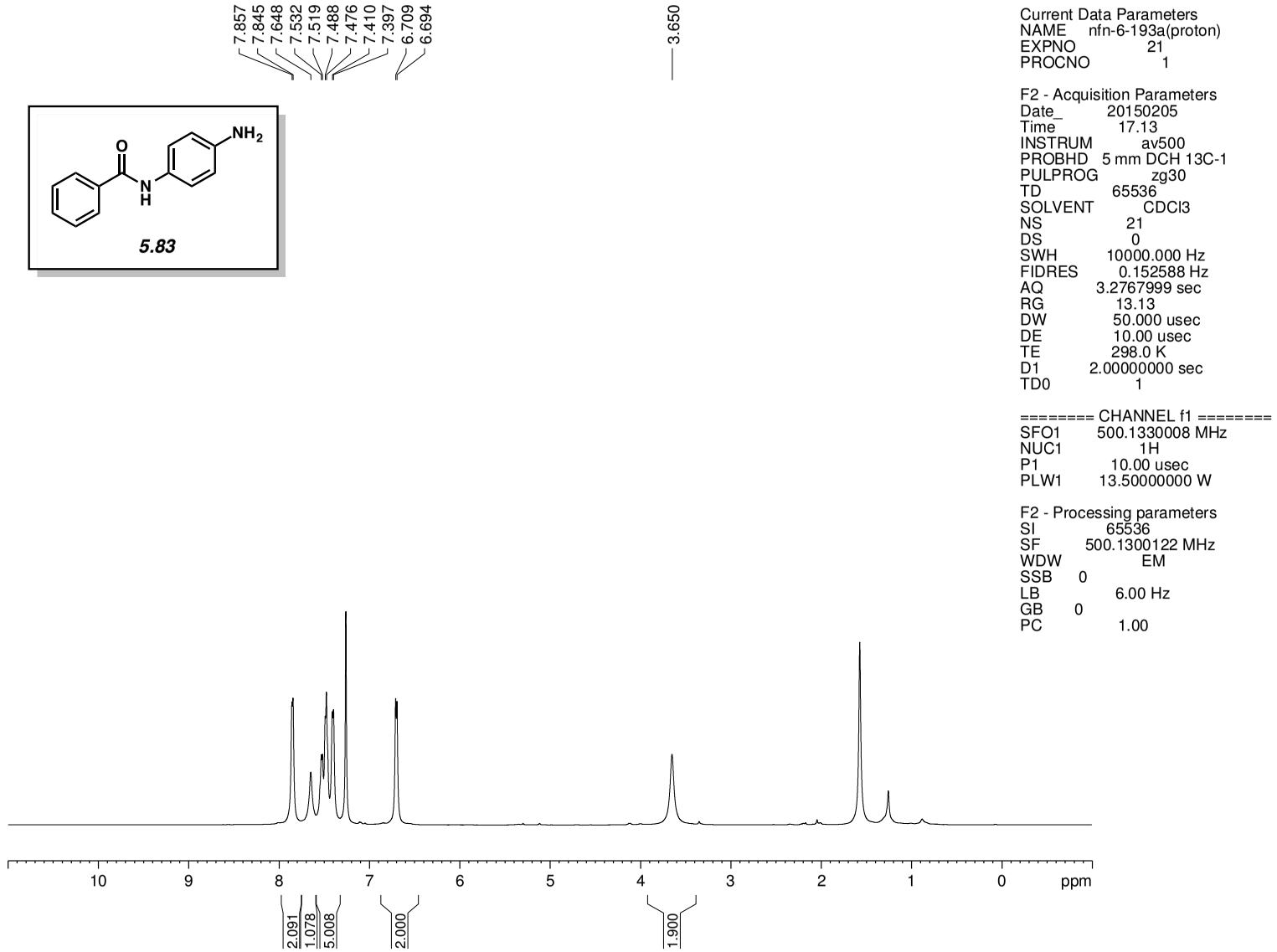


***Figure A5.57.*** $^{1}$H NMR (500 MHz, $CDCl_3$) of compound **5.83**

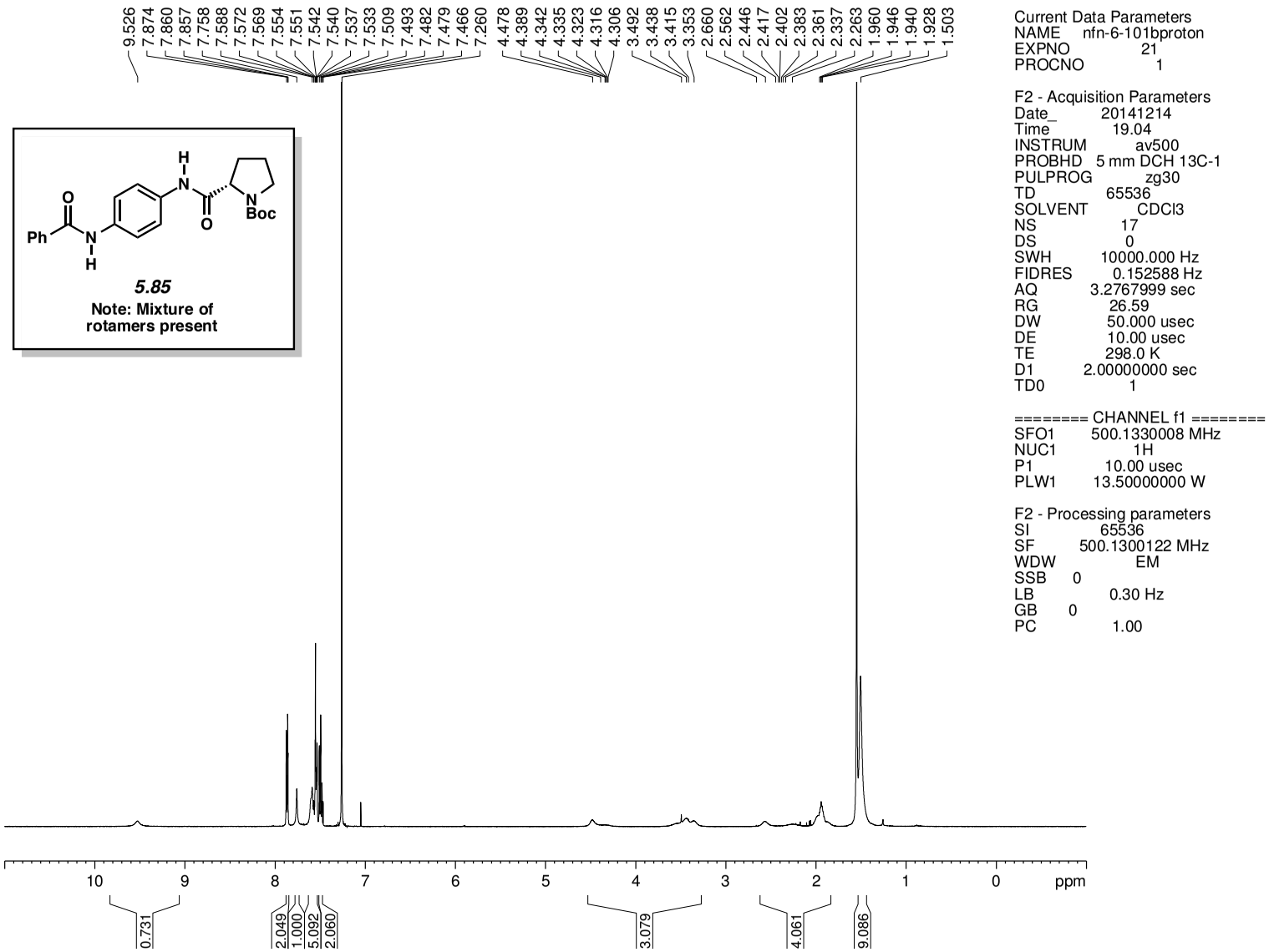


***Figure A5.58.*** $^{1}$H NMR (500 MHz, $CDCl_3$) of compound **5.85**

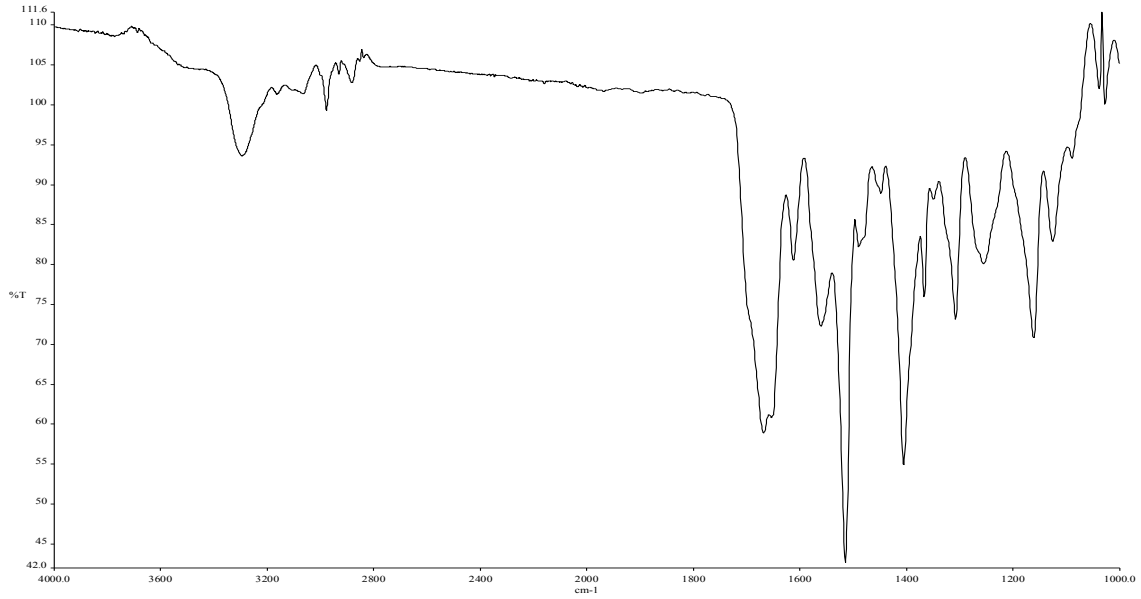


***Figure A5.59.*** Infrared spectrum of compound **5.85**

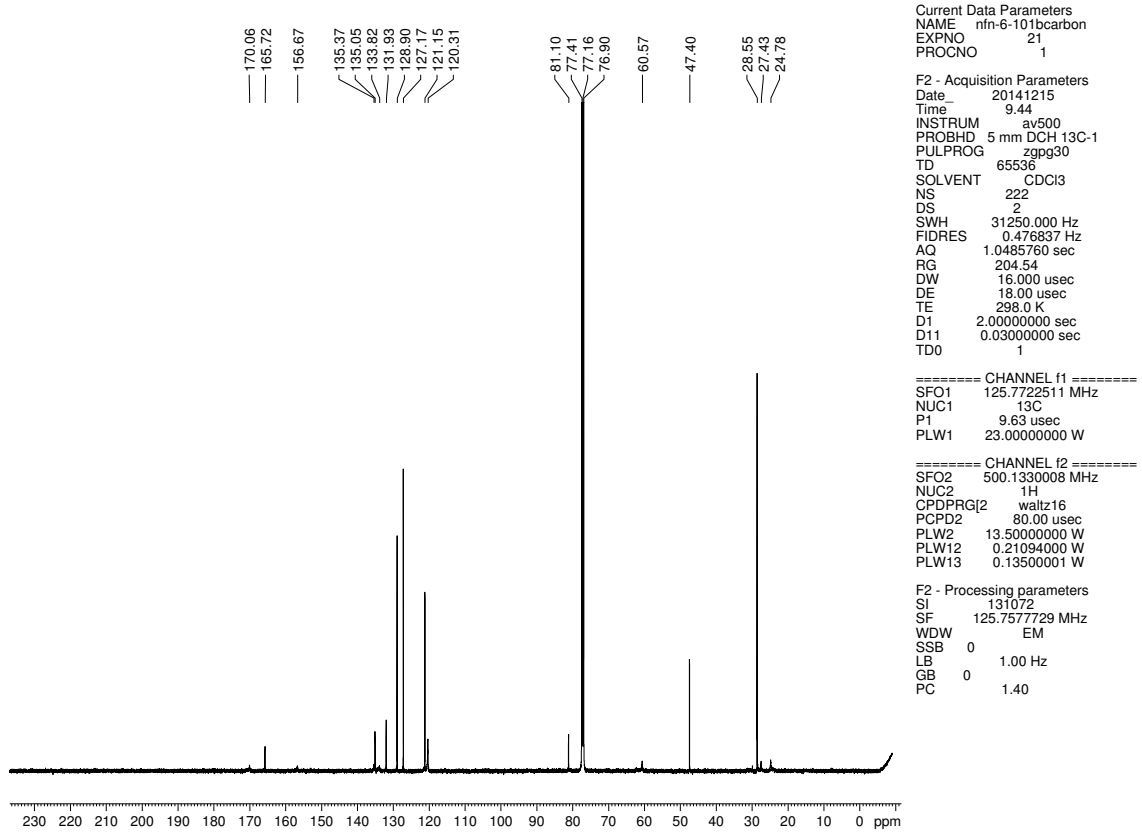


***Figure A5.60.*** $^{13}$C NMR (125 MHz, $CDCl_3$) of compound **5.85**

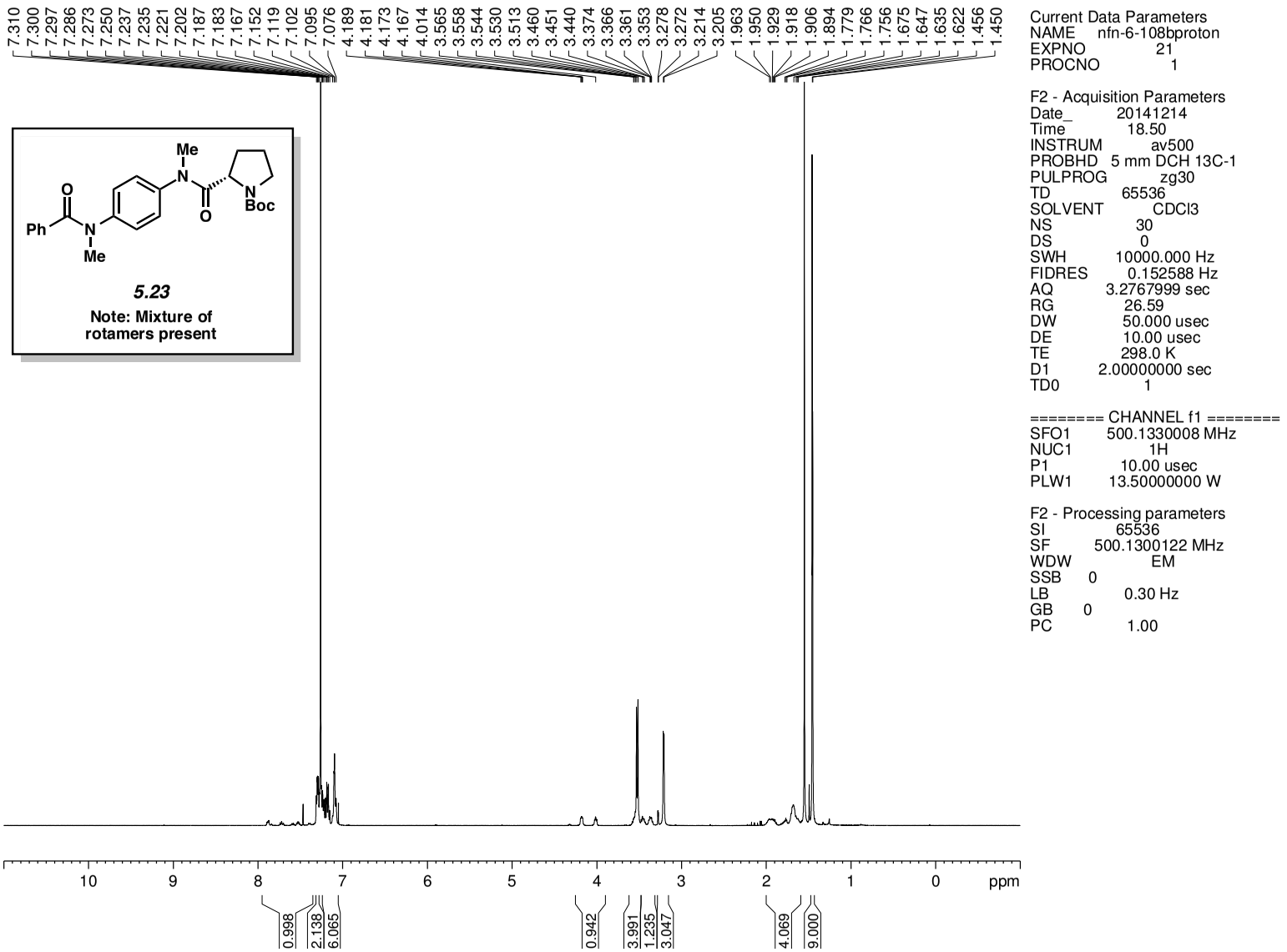


***Figure A5.61.*** $^{1}$H NMR (500 MHz, $CDCl_3$) of compound **5.23**

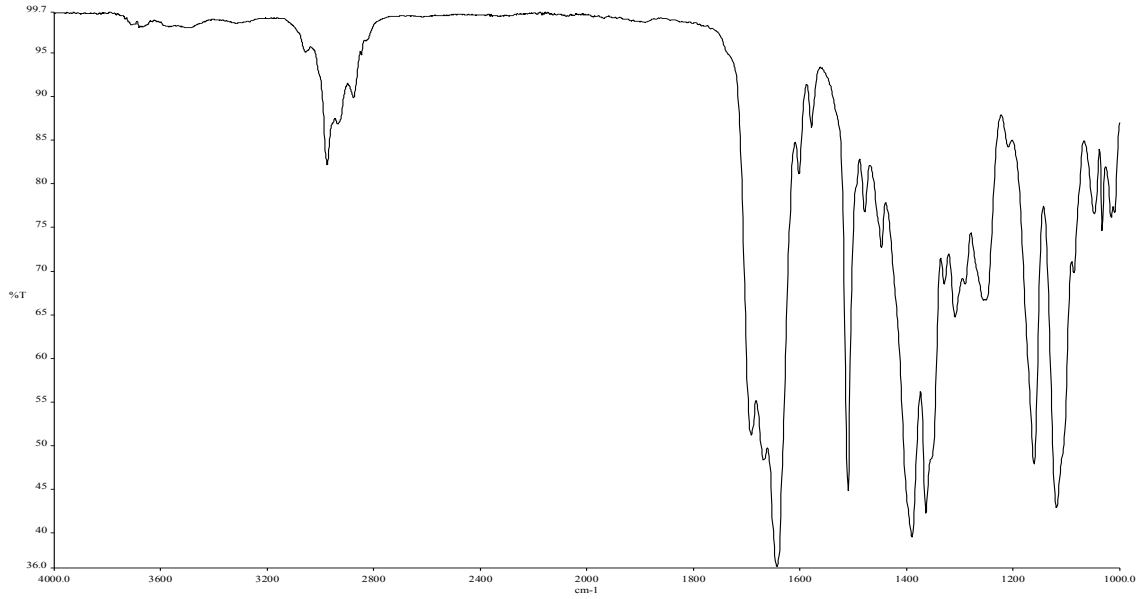


***Figure A5.62.*** Infrared spectrum of compound **5.23**

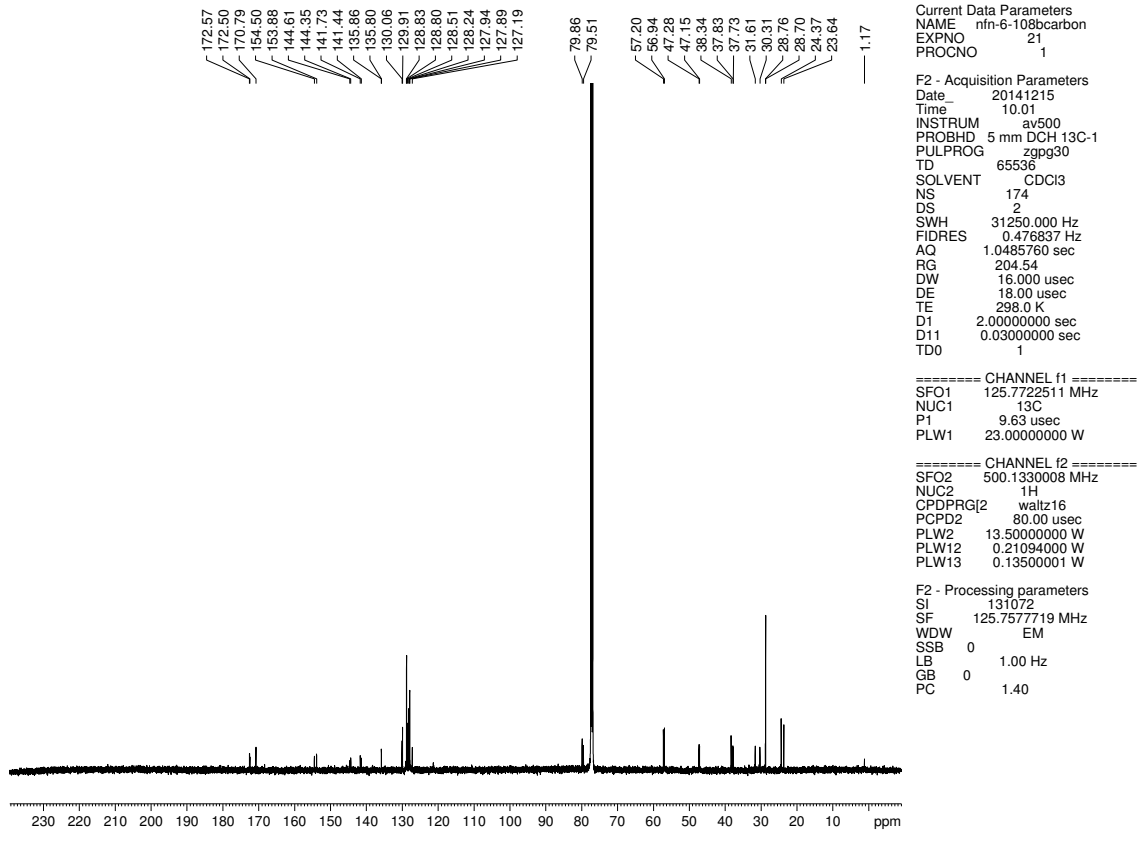


***Figure A5.63.*** $^{13}$C NMR (125 MHz, $CDCl_3$) of compound **5.23**

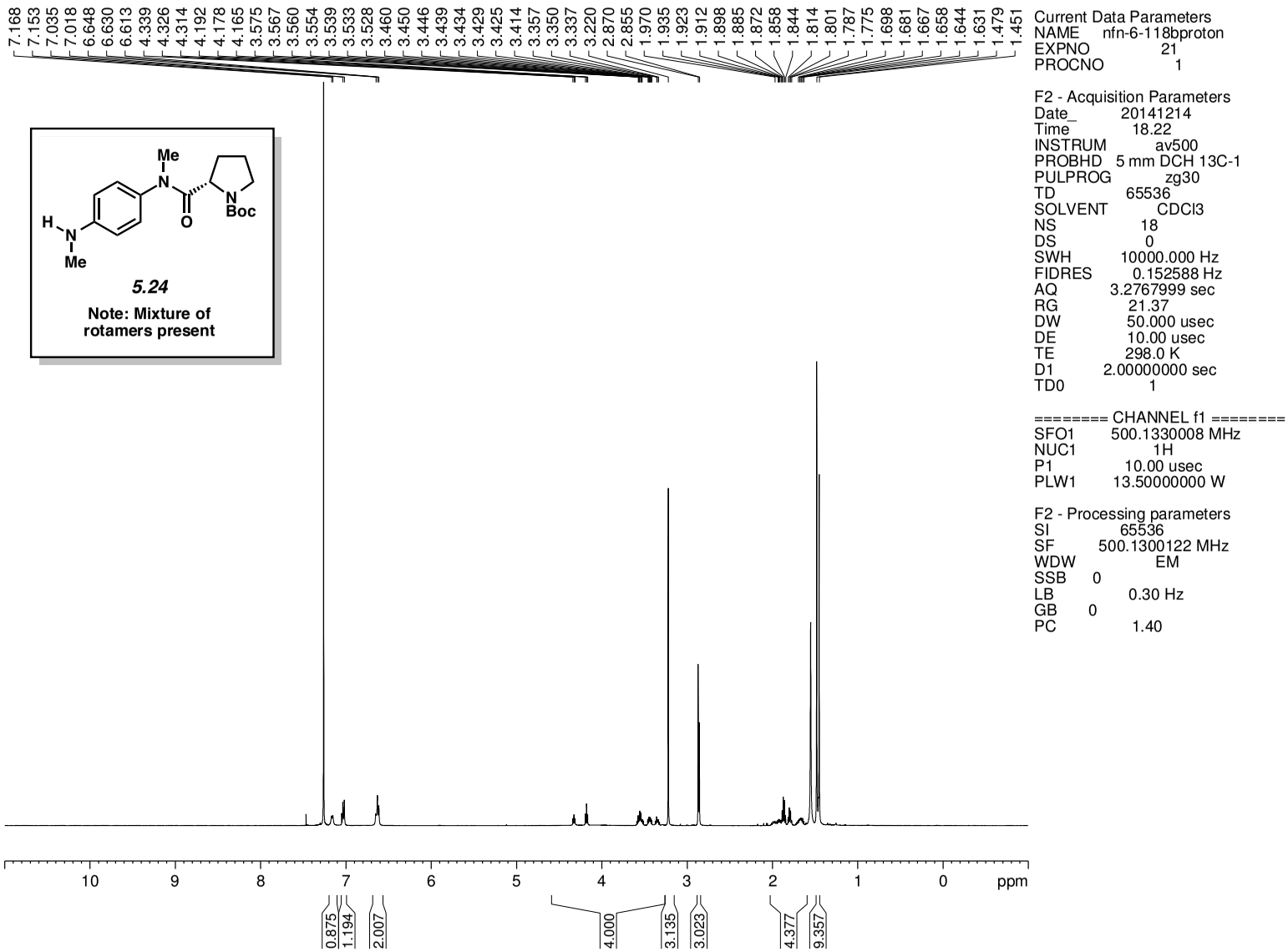


***Figure A5.64.*** $^{1}$H NMR (500 MHz, $CDCl_3$) of compound **5.24**

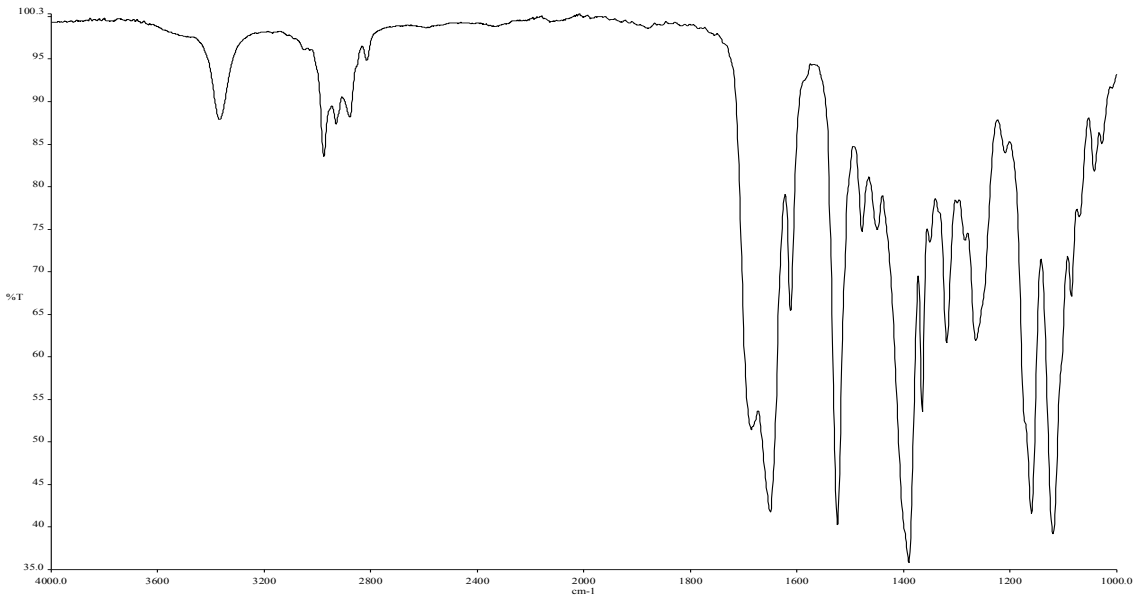


***Figure A5.65.*** Infrared spectrum of compound **5.24**

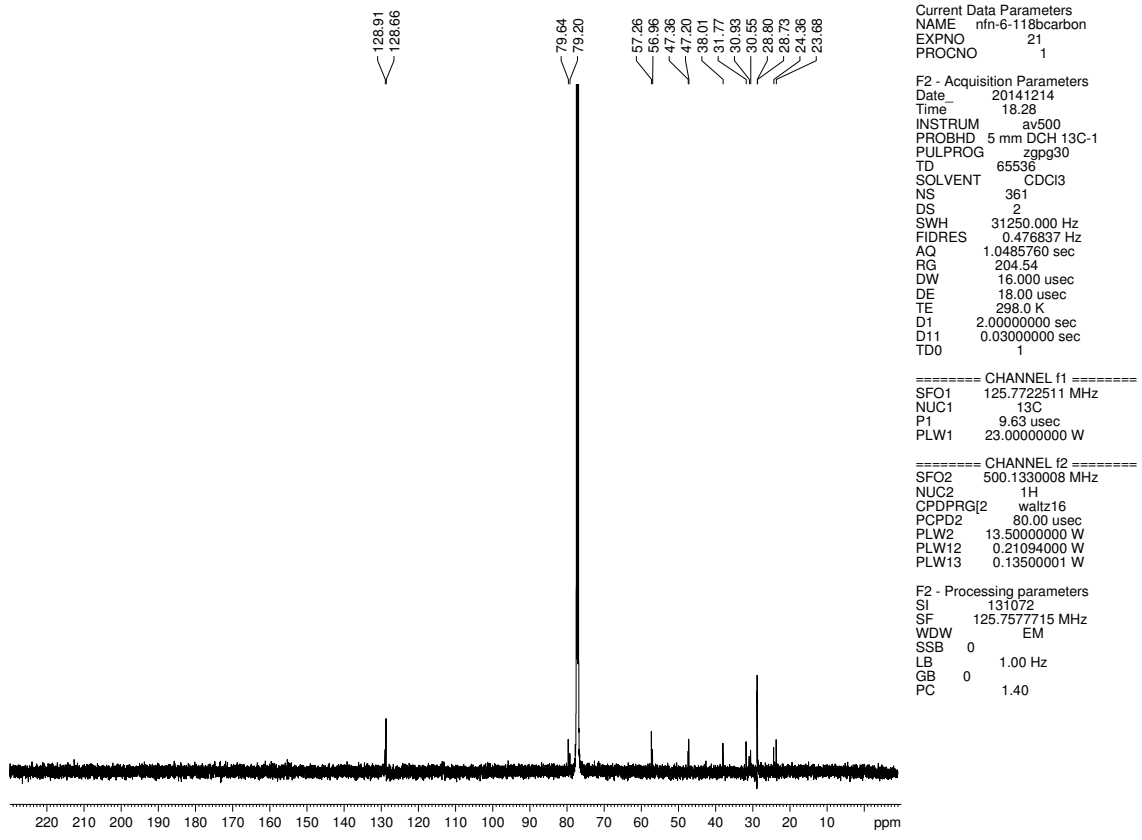


***Figure A5.66.*** $^{13}$C NMR (125 MHz, $CDCl_3$) of compound **5.24**

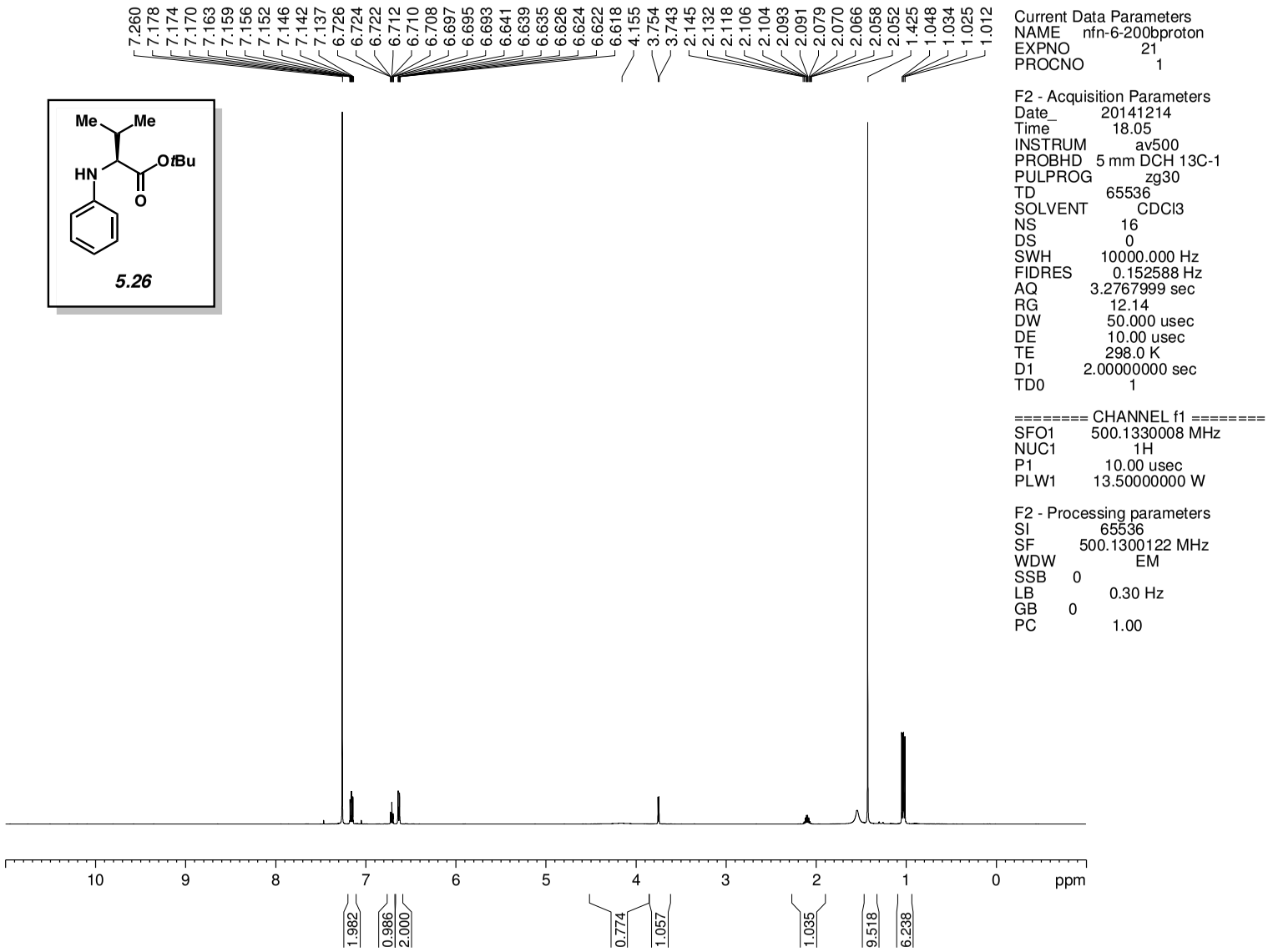


***Figure A5.67.*** $^{1}$H NMR (500 MHz, $CDCl_3$) of compound **5.26**

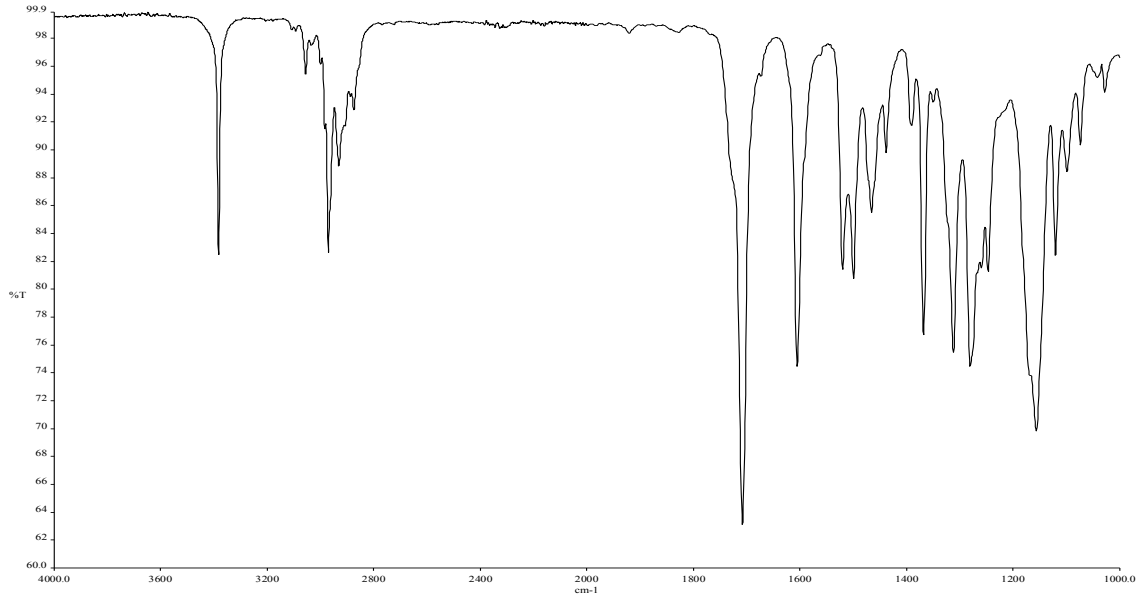


***Figure A5.68.*** Infrared spectrum of compound **5.26**

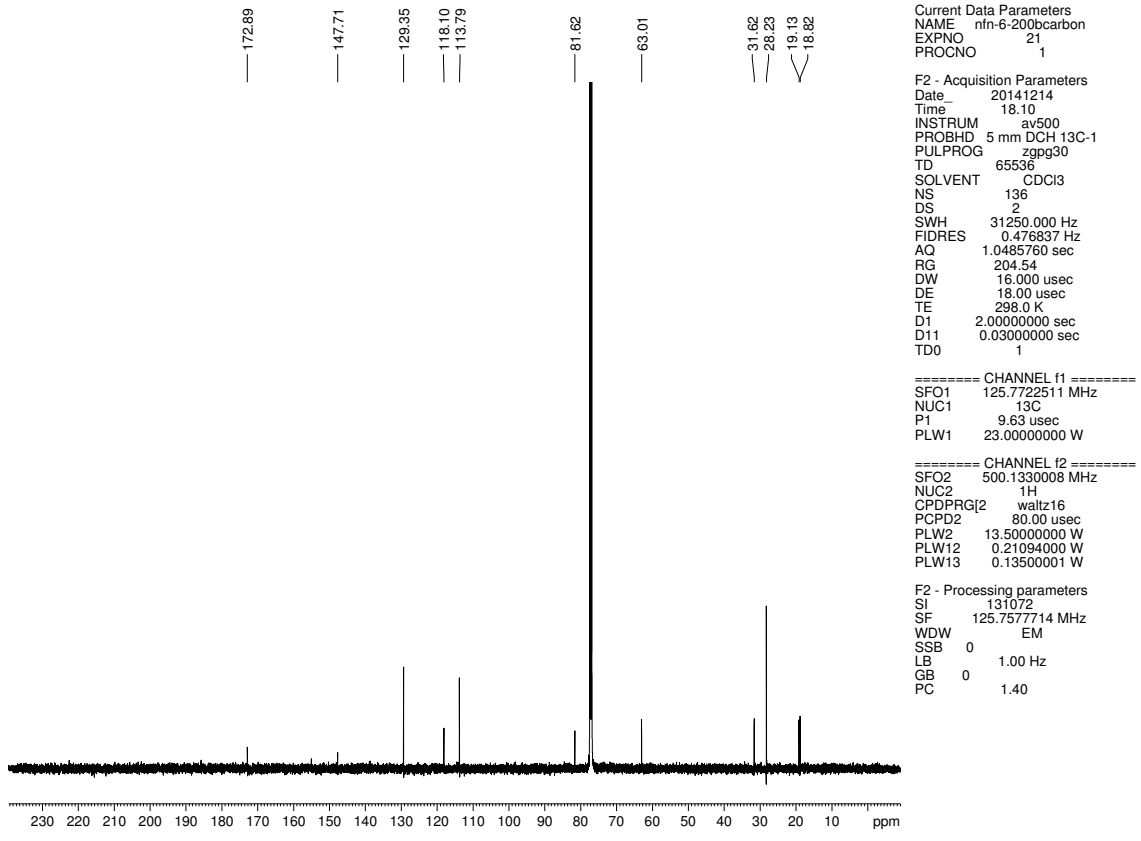


***Figure A5.69.*** $^{13}$C NMR (125 MHz, $CDCl_3$) of compound **5.26**

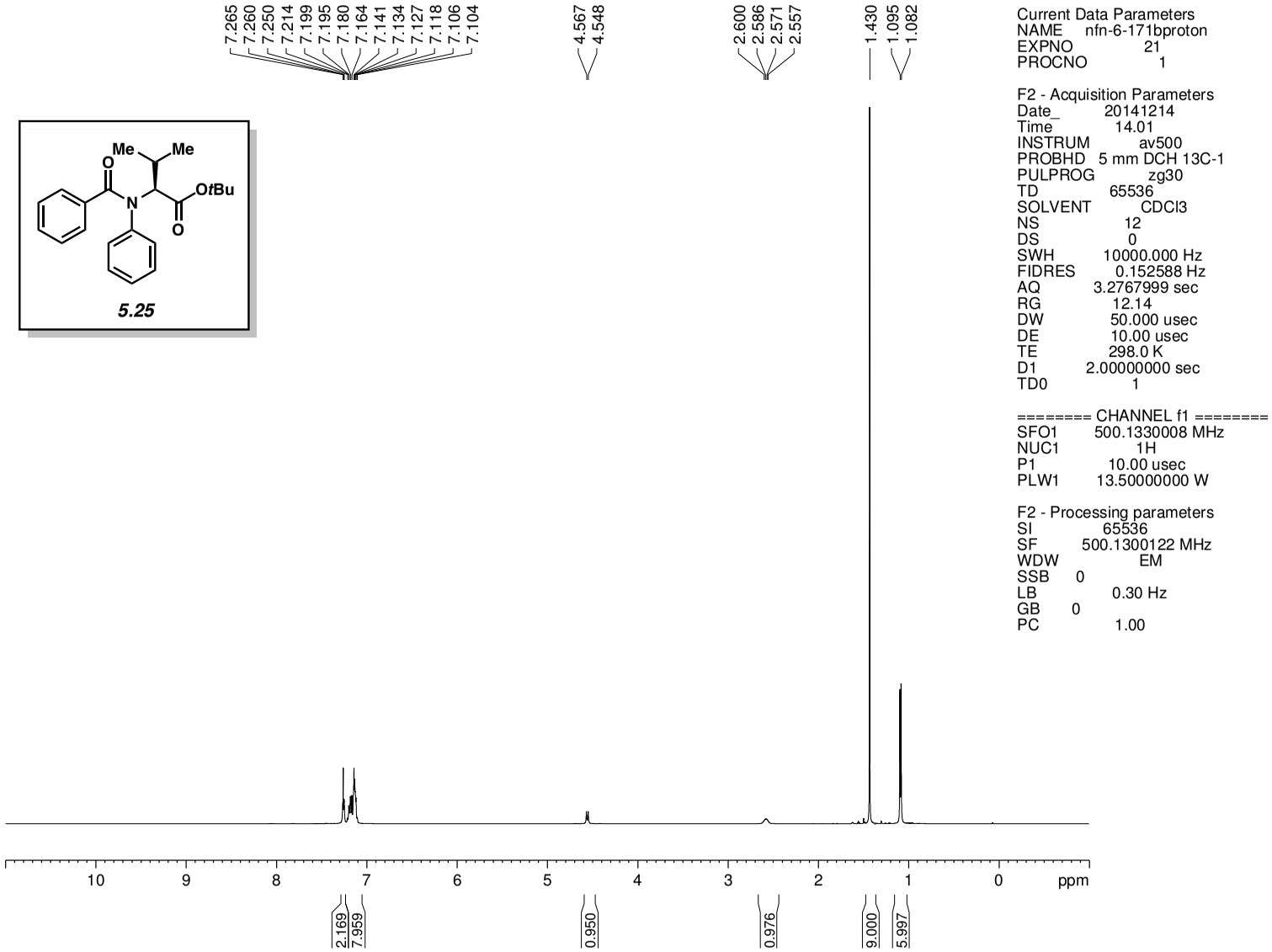


***Figure A5.70.*** $^{1}$H NMR (500 MHz, $CDCl_3$) of compound **5.25**

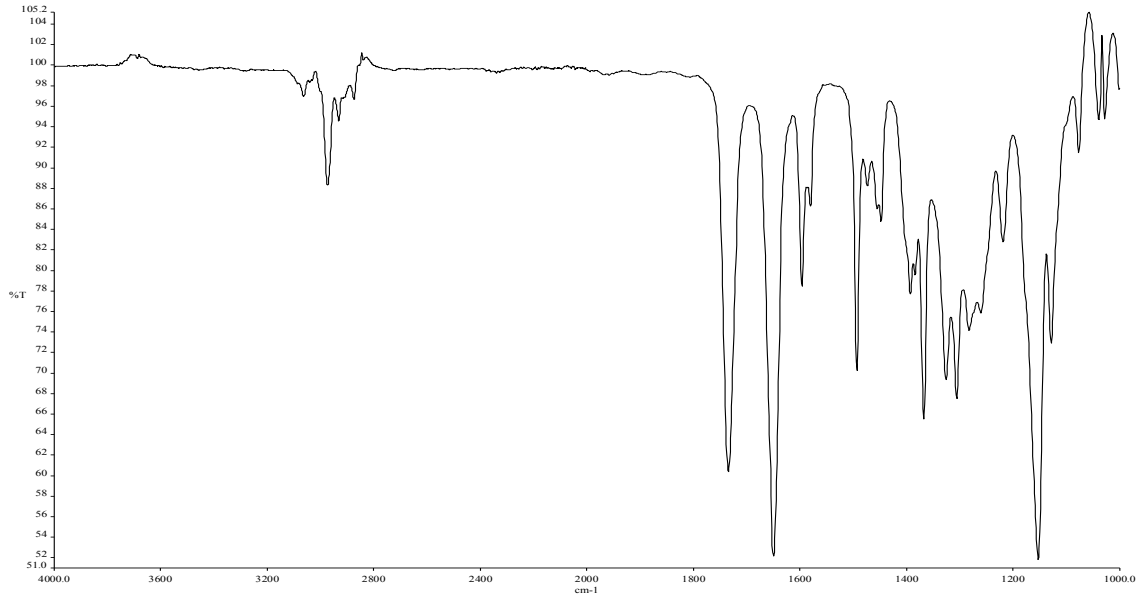


***Figure A5.71.*** Infrared spectrum of compound **5.25**

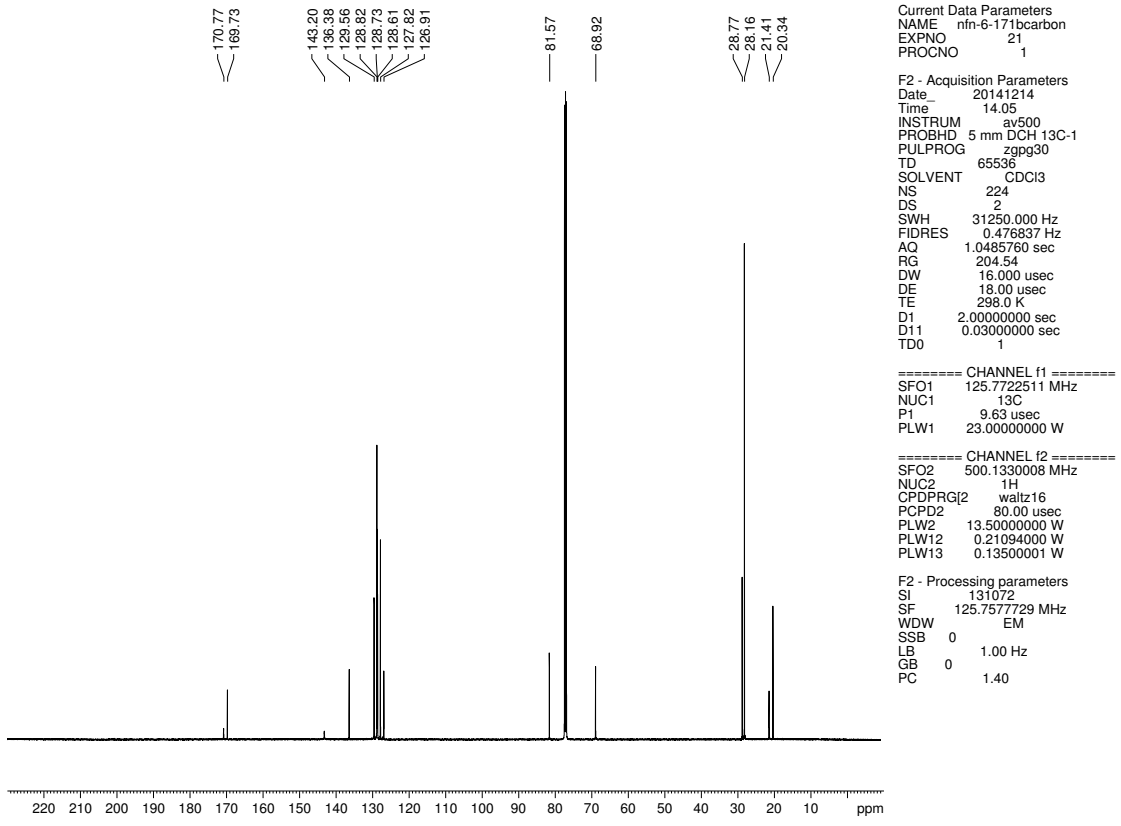


***Figure A5.72.*** $^{13}$C NMR (125 MHz, $CDCl_3$) of compound **5.25**

## 5.9 Notes and References


[1] Greenberg, A., Breneman, C. M., Liebman, J. F., Eds. *The Amide Linkage: Structural Significance in Chemistry, Biochemistry, and Materials Science*; Wiley-Interscience, 2003.

[2] Pauling, L.; Corey, R. B.; Branson, H. R. *Proc. Natl Acad. Sci. USA* **1951**, *37*, 205–211.

[3] Brix, K., Stöcker, W., Eds. *Proteases: Structure and Function*; Springer, 2013.

[4] Corey, E. J.; Cheng, X.-M. *The Logic of Chemical Synthesis*; Wiley, 1995.

[5] Hudlicky, T.; Reed, J. W. *The Way of Synthesis: Evolution of Design and Methods for Natural Products*; Wiley, 2007.

[6] Van Vranken, D.L.; Weiss, G. A. *Introduction to Bioorganic Chemistry and Chemical Biology*; Garland Science, 2013.

[7] Spletstoser, J. T.; White, J. M.; Tunoori, A. R.; Georg, G. I. *J. Am. Chem. Soc.* **2007**, *129*, 3408–3419.

[8] Nahm, S.; Weinreb, S. M. *Tetrahedron Lett.* **1981**, *22*, 3815–3818.

[9] Blangetti, M.; Rosso, H.; Prandi, C.; Deagostino, A.; Venturello, P. *Molecules* **2013**, *18*, 1188–1213.

[10] Tatamidani, H.; Kakiuchi, F.; Chatani, N. *Org. Lett.* **2004**, *6*, 3597–3599.

[11] Dineen, T. A.; Zajac, M. A.; Myers, A. G. *J. Am. Chem. Soc.* **2006**, *128*, 16406–16409.

[12] Stephenson, N. A.; Zhu, J.; Gellman, S. H.; Stahl, S. S. *J. Am. Chem. Soc.* **2009**, *131*, 10003–10008.

[13] Keck, G. E.; McLaws, M. D.; Wager, T. T. *Tetrahedron* **2000**, *56*, 9875–9883.

[14] Nishimoto, S.-i.; Izukawa, T.; Kagiya, T. *Bull. Chem. Soc. Jpn* **1982**, *55*, 1484–1488.

[15] White, E. H. *J. Am. Chem. Soc.* **1955**, *77*, 6011–6014.

[16] Guthrie, J. P.; Pike, D. C.; Lee, Y.-C. *Can. J. Chem.* **1992**, *70*, 1671–1683.

[17] Tasker, S. Z.; Standley, E. A.; Jamison, T. F. *Nature* **2014**, *509*, 299–309.

[18] Mesganaw, T.; Garg, N. K. *Org. Process Res. Dev.* **2013**, *17*, 29–39.

[19] Rosen, B. M. *et al. Chem. Rev.* **2011**, *111*, 1346–1416.

[20] Blakey, S. B.; MacMillan, D. W. C. *J. Am. Chem. Soc.* **2003**, *125*, 6046–6047.

[21] Zhang, X.-Q.; Wang, Z.-X. *Org. Biomol. Chem.* **2014**, *12*, 1448–1453.

[22] Tobisu, M.; Nakamura, K.; Chatani, N. *J. Am. Chem. Soc.* **2014**, *136*, 5587–5590.

[23] Shiba, T., Kurahashi, T. & Matsubara, S. *J. Am. Chem. Soc.* **2013**, *135*, 13636–13639.

[24] Quasdorf, K. W. *et al. J. Am. Chem. Soc.* **2011**, *133*, 6352–6363.

[25] Mesganaw, T. *et al. Chem. Sci.* **2011**, *2*, 1766–1771.

[26] Hong, X.; Liang, Y.; Houk, K. N. *J. Am. Chem. Soc.* **2014**, *136*, 2017–2025.

[27] Lu, Q.; Yu, H.; Fu, Y. *J. Am. Chem. Soc.* **2014**, *136*, 8252–8260.

[28] Xu, H. *et al. J. Am. Chem. Soc.* **2014**, *136*, 14834–14844.

[29] Yamamoto, T.; Ishizu, J.; Kohara, T.; Komiya, S.; Yamamoto, A. *J. Am. Chem. Soc.* **1980**, *102*, 3758–3764.

[30] Amaike, K.; Muto, K.; Yamaguchi, J.; Itami, K. *J. Am. Chem. Soc.* **2012**, *134*, 13573–13576.

[31] (a) Rao, Y.; Li, X.; Danishefsky, S. J. *J. Am. Chem. Soc*. **2009**, *131*, 12924–12926. (b) Oldenhuis, N. J.; Dong, V. M.; Guan, Az. *Tetrahedron* **2014**, *70*, 4213–4218. (c) Friel, D. K.; Snapper, M. L.; Hoveyda, A. H. *J. Am. Chem. Soc*. **2008**, *130*, 9942–9951. (d) Ueda, S.; Nagasawa, H. *J. Org. Chem*. **2009**, *74*, 4272–4277. (e) Li, Y.; Jia, F.; Li, Z. *Chem. Eur. J.* **2013**, *19*, 82–86. (f) Wang, S.; Wang, J.; Guo, R.; Wang, G.; Chen, S.-Y.; Yu, X.-Q. *Tetrahedron Lett*. **2013**, *54*, 6233–6236. (h) Baroudi, A.; Alicea, J.; Flack, P.; Kirincich, J.;

Alabugin, I. V. *J. Org. Chem*. **2011**, *76*, 1521–1537. (h) Fang, W.; Deng, Q.; Xu, M.; Tu, T. *Org. Lett*. **2013**, *15*, 3678–3681. (i) Ganton, M. D.; Kerr. M. A. *Org. Lett*. **2005**, *7*, 4777–4779. (j) Yates, M. H.; Kallman, N. J.; Ley, C. P.; Wei, J. N. *Org. Process. Rev. Dev*. **2009**, *13*, 255–262. (k) Oishi, S.; Saito, S. *Angew. Chem. Int. Ed*. **2012**, *51*, 5395–5399. (l) Johnson II, D. C.; Widlanski, T. S. *Tetrahedron Lett*. **2004**, *45*, 8483–8487.

[32] Zhang, C.; Feng, P.; Jiao, N. *J. Am. Chem. Soc*. **2013**, *135*, 15257–15262.

[33] Ye, Y.; Sanford, M. S. *J. Am. Chem. Soc*. **2012**, *134*, 9034–9037.

[34] Tschaen, B. A.; Schmink, J. R.; Molander, G. A. *Org. Lett*. **2013**, *15*, 500–503.

[35] Powell, A. B.; Stahl, S. S. *Org. Lett*. **2013**, *15*, 5072–5075.

[36] Dohi, S.; Moriyama, K.; Togo, H. *Eur. J. Org. Chem*. **2013**, *34*, 7815–7822.

[37] Correa, A.; Leon, T.; Martin, R. *J. Am. Chem. Soc*. **2014**, *136*, 1062–1069.

[38] Hirashima, S.-I.; Nobuta, T.; Tada, N.; Miura, T.; Itoh, A. *Org. Lett*. **2010**, *12*, 3645–3647.

[39] Harrar, K.; Reiser, O. *Chem. Commun*. **2013**, *48*, 3457–3459.

[40] Heller, S. T.; Sarpong, R. *Org. Lett*. **2010**, *12*, 4572–4575.

[41] Dong, J.; Shi, X.-X.; Yan, J.-J.; Xing, J.; Xhang, Q.; Xiao, S. *Eur. J. Org. Chem*. **2010**, *36*, 6987–6992.

[42] Hanato, M.; Furuya, Y.; Shimmura, T.; Moriyama, K.; Kamiya, S.; Maki, T.; Ishihara, K. *Org. Lett*. **2011**, *13*, 426–429.

[43] Zhou, W.; Li, H.; Wang, L. *Org. Lett*. **2012**, *14*, 4594–4597.

[44] Liu, Z.; Ma, Q.; Liu, Y.; Wang, Q. *Org. Lett*. **2014**, *16*, 236–239.

[45] Kanoh, S.; Naka, M.; Nishimura, T.; Motoi, M. *Tetrahedron* **2002**, *58*, 7049–7064.

[46] Ueda, T.; Konishi, H.; Manabe, K. *Org. Lett*. **2013**, *15*, 5370–5373.

[47] Holan, M.; Jahn, U. *Org. Lett*. **2014**, *16*, 58–61.

[48] Wang, J.; Yin, X.; Wu, J.; Wu, D.; Pan, Y. *Tetrahedron* **2013**, *69*, 10463–10469.

[49] (a) Becke, A. D. *J. Chem. Phys.* **1993**, *98*, 5648–5652. (b) Lee, C.; Yang W.; Parr, R. G. *Phys. Rev. B* **1988**, *37*, 785–789. (c) Becke, A. D. *J. Chem. Phys.* **1993**, *98*, 1372–1377. (d) Stephens, P. J.; Devlin, F. J.; Chabalowski, C. F.; Frisch, M. J. *J. Phys. Chem.* **1994**, *98*, 1623–1627.

[50] (a) Hay, P. J.; Wadt, W. R. *J. Chem. Phys.* **1985**, *82*, 299–310. (b) Roy, L. E.; Hay, P. J.; Martin, R. L. *J. Chem. Theory Comput.* **2008**, *4*, 1029–1031. (c) Ehlers, A. W.; Böhme, M.; Dapprich, S.; Gobbi, A.; Höllwarth, A.; Jonas, V.; Köhler, K. F.; Stegmann, R.; Veldkamp, A.; Frenking, G. *Chem. Phys. Lett.* **1993**, *208*, 111–114.

[51] (a) Ditchfield, R.; Hehre, W. J.; Pople, J. A. *J. Chem. Phys.* **1971**, *54*, 724–728. (b) Hehre, W. J.; Ditchfield, R.; Pople, J. A. *J. Chem. Phys.* **1971**, *54*, 2257–2261. (c) Hariharan, P. C.; Pople, J. A. *Theor. Chim. Acta.* **1973**, *28*, 213–222.

[52] Zhao, Y.; Truhlar, D. G. *Theor. Chem. Acc.* **2008**, *120*, 215–241.

[53] (a) Dolg, M.; Wedig, U.; Stoll, H.; Preuss, H. *J. Chem. Phys.* **1987**, *86*, 866–872. (b) Andrae, D.; Häußermann, U.; Dolg, M.; Stoll, H.; Preuß, H. *Theor. Chem. Acc.* **1990**, *77*, 123–141.

[54] Marenich, A. V.; Cramer, C. J.; Truhlar, D. G. *J. Phys. Chem. B* **2009**, *113*, 6378–6396.

[55] Legault, C. Y. CYLView, 1.0b; Université de Sherbrooke, Canada, **2009**; http://www.cylview.org.

[56] W.E. Acree, Jr., J.S. Chickos, "Phase Transition Enthalpy Measurements of Organic and Organometallic Compounds" in NIST Chemistry WebBook, **NIST Standard Reference Database Number 69**, Eds. P.J. Linstrom and W.G. Mallard, National Institute of Standards

and Technology, Gaithersburg MD, 20899, http://webbook.nist.gov, (retrieved March 27, 2015).

[57] Guthrie, J. P.; Pike, D. C.; Lee, Y.-C. *Can. J. Chem.* **1992**, *70*, 1671–1683.

[58] See the Supporting Information in: Hie, L.; Fine Nathel, N. F.; Shah, T. K.; Baker, E. L.; Xin Hong, Yang, Y.-F.; Liu, P.; Houk, K. N.; Garg, N. K. *Nature* **2015**, *524*, 79–83.